

Analytical and statistical properties of local depth functions motivated by clustering applications

Giacomo Francisci¹, Claudio Agostinelli², Alicia Nieto-Reyes³, and Anand N. Vidyashankar¹

¹*Department of Statistics, George Mason University, Fairfax, Virginia*

²*Dipartimento di Matematica, Università di Trento, Trento, Italy*

³*Departamento de Matemáticas, Estadística y Computación, Universidad de Cantabria, Santander, Spain*

April 26, 2022

Abstract

General local depth functions (*LGD*) are used for describing the local geometric features and mode(s) in multivariate distributions. In this paper, we undertake a rigorous systematic study of *LGD* and establish several analytical and statistical properties. First, we show that, when the underlying probability distribution is absolutely continuous with density $f(\cdot)$, the scaled version of *LGD* (referred to as τ -approximation) converges, uniformly and in $L^d(\mathbb{R}^p)$ to $f(\cdot)$ when τ converges to zero. Second, we establish that, as the sample size diverges to infinity the centered and scaled sample *LGD* converge in distribution to a centered Gaussian process uniformly in the space of bounded functions on \mathcal{H}_G , a class of functions yielding *LGD*. Third, using the sample version of the τ -approximation (*S τ A*) and the gradient system analysis, we develop a new clustering algorithm. The validity of this algorithm requires several results concerning the uniform finite difference approximation of the gradient system associated with *S τ A*. For this reason, we establish *Bernstein*-type inequality for deviations between the centered and scaled sample *LGD*, which is also of independent interest. Finally, invoking the above results, we establish consistency of the clustering algorithm. Applications of the proposed methods to mode estimation and upper level set estimation are also provided. Finite sample performance of the methodology are evaluated using numerical experiments and data analysis.

Key Words: Local depth, extreme localization, Hoeffding’s decomposition, sample local depth, uniform central limit theorem, clustering, modes, gradient system, Lyapunov’s stability Theorem

1 Introduction

Investigation of data depths is gaining momentum due to its applicability in a variety of machine learning problems such as non-parametric classification and clustering. This concept, formalized in Liu [1990] and Zuo and Serfling [2000a], serves to identify a center for multivariate distributions and a multidimensional center-outward order similar to that of a real line. The ordering enables a description of quantiles of multivariate distributions (see Zuo and Serfling [2000b]) and aids in using depth functions (DFs) for clustering. The current paper develops the intuitive notion that local depths possess properties that help in identifying peaks and valleys, and hence clustering based on such identification can improve the quality and stability of the clustering algorithm.

The notion of local depth [Agostinelli and Romanazzi, 2011] provides a framework to describe the local multidimensional features of multivariate distributions. Recently Chandler and Polonik [2021] use it to analyze supervised classification methods for non-Euclidean data. Section 2 of this paper provides a detailed study of local depth functions (LDFs) and their scaled versions, referred to as τ -approximation. Specifically, let $h_\tau^{(G)}(\cdot; \cdot)$ denote a bounded non-negative function satisfying the symmetry conditions

$$h_\tau^{(G)}(x + v; x_1 + v, \dots, x_{k_G} + v) = h_\tau^{(G)}(x; x_1, \dots, x_{k_G}), \quad v \in \mathbb{R}^p$$

and $h_\tau^{(G)}(-x; -x_1, \dots, -x_{k_G}) = h_\tau^{(G)}(x; x_1, \dots, x_{k_G}).$

Then the general local depth function is given by (see below for a precise definition)

$$LGD(x, \tau, P) = \int h_\tau^{(G)}(x; x_1, \dots, x_k) dP(x_1) \dots dP(x_k)$$

and τ is referred to as the *localizing parameter*. This integral representation provides a unified treatment and analyses of several local depth functions available in the literature. We denote by $\mathcal{H}_G = \{h_\tau^{(G)}(x; \cdot) : x \in \mathbb{R}^p, \tau \in [0, \infty]\}$ the class of functions yielding LGD . Typically studied LDFs can be obtained by taking $h_\tau^{(G)}(\cdot; \cdot)$ to be indicators of appropriate Borel sets; that is,

$$h_\tau^{(G)}(x; \cdot) = \mathbf{I}(\cdot \in Z_\tau^G(x)), \quad \text{where}$$

$Z_\tau^G(x)$ is referred to as the local set. The local set associated with lens depth [Liu and Modarres, 2011], denoted by LLD (G in LGD is replaced by L), is

$$Z_\tau^L(x) = \{(x_1, x_2) \in (\mathbb{R}^p)^2 : \max_{i=1,2} \|x - x_i\| \leq \|x_1 - x_2\| \leq \tau\},$$

while that for the spherical depth [Elmore et al., 2006] is given by

$$Z_\tau^B(x) = \{(x_1, x_2) \in (\mathbb{R}^p)^2 : \|2x - (x_1 + x_2)\| \leq \|x_1 - x_2\| \leq \tau\}.$$

The set for the β -skeleton depth [Yang and Modarres, 2018] is given by

$$Z_\tau^{K_\beta}(x) = \{(x_1, x_2) \in (\mathbb{R}^p)^2 : \max_{(i,j) \in \{(1,2), (2,1)\}} \|x_i + (2/\beta - 1)x_j - 2/\beta x\| \leq \|x_1 - x_2\| \leq \tau\},$$

while that for the simplicial depth [Liu, 1990] is

$$Z_\tau^S(x) = \{(x_1, \dots, x_{p+1}) \in (\mathbb{R}^p)^{(p+1)} : x \in \Delta[x_1, \dots, x_{p+1}], \max_{\substack{i,j=1, \dots, p+1 \\ i > j}} \|x_i - x_j\| \leq \tau\},$$

where $\Delta[x_1, \dots, x_{p+1}]$ is the closed simplex with vertices $x_1, \dots, x_{p+1} \in \mathbb{R}^p$. While the definitions of LLD and LSD were available in the literature, the definitions of LBD and LKD , as defined here, seem new. Of course, β -skeleton depth reduces to spherical depth and lens depth for $\beta = 1$ and $\beta = 2$, respectively. Also, when $p = 1$ all of the above four local depths coincide. Finally, taking $\tau = \infty$ in the above, one obtains the general depth function

$$GD(x, P) = \int_{(\mathbb{R}^p)^k} h_\infty^{(G)}(x; x_1, \dots, x_k) dP(x_1) \dots dP(x_k)$$

studied in Zuo and Serfling [2000a] and referred to as *Type A* DFs. Accordingly, we refer to the class of LDFs above as *Type A* LDFs. When there is no scope for confusion, we suppress P in $GD(x, P)$ and $LGD(x, \tau, P)$ and use the notation $GD(x)$ and $LGD(x, \tau)$.

A useful and important aspect of local depth is its behavior under *extreme localization*, *i.e.* when $\tau \rightarrow 0^+$. When P is absolutely continuous with respect to (w.r.t.) the Lebesgue measure with density $f(\cdot)$, LDFs investigated in this paper, under appropriate scaling, converge to a power of $f(\cdot)$. The scaled LDFs are referred to as τ -approximation and denoted by $f_\tau(\cdot)$. Under additional conditions, one obtains convergence to the derivatives of $f(\cdot)$ which facilitates an inquiry into the modes of the density *via* a gradient system analysis. This, in turn, allows one to characterize the related *stable manifolds* paving the way for cluster analysis. Related ideas about clustering appear in Chazal et al. [2013]. Our methodology differs from the existing literature in that we take advantage of the local depth notion, specifically the τ -approximation $f_\tau(\cdot)$ and its properties, developed in

Sections 2 and 3 below, as an approximation to the density. For a detailed discussion on the choice of τ see Remark 2.6 and Subsection 3.3.

Statistical inquiry about local depth requires an investigation into their sample versions, specifically of sample local depth and sample τ -approximation ($S\tau A$), $f_{\tau,n}(\cdot)$. Borrowing tools from empirical process theory, we establish that, when \mathcal{H}_G is a VC-subgraph class, the sample local depth is uniformly consistent. We also obtain a related limit distribution in the class \mathcal{H}_G . Additionally, we develop a *Bernstein* type inequality for sample local depth. These results rely on the Hoeffding’s decomposition of U-statistics representation of the local depth, which incidentally is a critical component of our analysis. A technical challenge to the above development is that the space of bounded functions on \mathcal{H}_G is not separable and it is here that the VC-subgraph property of the class \mathcal{H}_G plays an important role. These results are described in Section 2. It is worth noticing that when performing classification using geometric features, one may encounter arbitrary values of τ at different points $x \in \mathbb{R}^p$ (see for example the cone used in Chandler and Polonik [2021]). In these cases the above technical results facilitate identifying sample sizes required for a given probability content without dependence on x and τ .

The above developments allow further applications to clustering, mode estimation, upper level set estimation, and robust inference based on divergences. Potential other applications include classification based on Neyman-Pearson lemma where plug-in estimators of density and their uniform convergence are used. Our next focus is on the application of the above described methods to clustering. To this end, we recall from dynamical systems that the stable manifold generated by a mode m of a “smooth” density $f(\cdot)$ is given by

$$C(m) := \{x \in S_f : \lim_{t \rightarrow \infty} u_x(t) = m\},$$

where S_f is the interior of the support of $f(\cdot)$ and $u_x(t)$ is the solution at time t of the gradient system

$$u'(t) = \nabla f(u(t))$$

with initial value $u(0) = x$ and $\nabla f(\cdot)$ represents the gradient of $f(\cdot)$. If m_1, \dots, m_M are the modes of $f(\cdot)$, then the clusters associated with $f(\cdot)$ are given by $C(m_1), \dots, C(m_M)$ [Chacón, 2015], where the sets have a non-zero Lebesgue measure. In real applications, $f(\cdot)$ is unknown and is replaced by its estimate $f_{\tau,n}(\cdot)$. For every fixed τ , by previously mentioned results $f_{\tau,n}(\cdot)$ converges to $f_\tau(\cdot)$. This raises the question concerning the convergence of clusters associated with $f_\tau(\cdot)$ to that of $f(\cdot)$. Of course, to get the clusters associated with $f(\cdot)$ we would prefer to replace τ by τ_n so that the $S\tau A$, $f_{\tau_n,n}(\cdot)$, converges to $f(\cdot)$. Hence, to use the gradient system above, it is natural to replace the derivatives by their finite difference approximations. In Section 3 of the paper, we execute this strategy

wherein we not only establish the convergence of population clusters but also that of the empirical clusters. These require uniform convergence of empirical finite difference approximations to the appropriate derivatives which is established using the *Bernstein*-type inequality described previously.

In Section 3.2 we establish the convergence of our clustering method. Specifically, we establish that given a point $x \in \mathbb{R}^p$ our algorithm will assign x to the correct cluster with probability tending to one as the sample size diverges to infinity. A similar idea was recently used in Arias-Castro et al. [2016] for establishing the clustering method based on the mean shift algorithm. As in that paper we also refer to this as consistency of the clustering method. However, it is worth pointing out that the technical details in the proof of consistency are much more delicate than in the mean shift algorithm. Specifically, the algorithm described in this paper can be applied to non-differentiable kernels and LDFs. The procedure is data-driven in the sense that given any initial point the algorithm moves strictly within the data cloud. Our procedure also helps avoiding small peaks that arise in the data.

The consistency proof of the clustering method requires additional analyses via the use of discrete Grönwall lemma and subtle arguments involving the density of data points. The use of $S\tau$ As require a specification of τ . While in some cases, such as β -skeleton depths, one can choose τ to be an appropriate quantile, care is required for other DFs. A natural approach to choosing τ for clustering is via cross-validation as suggested by Wang [2010]. We develop this idea in Subsection 3.3. Finally, we note here that since the method described above is based on mode(s) of the density and upper level sets, the sample τ -approximation can also be used for mode estimation and upper level set estimation. While Section 3 includes mode estimation, upper level set estimation is studied in Appendix D which also has a brief discussion concerning applications to divergence based inference.

While the proofs of our main results require techniques from empirical processes theory, the convergence of the clustering algorithm requires a careful “real analysis” argument involving delicate probability bounds and path-tracing of the solution of the gradient system. These are described in Section 4. Numerical results and data analyses related to clustering algorithm are in Subsection 3.4 and 3.5. We end this introduction section with a comment about the notations used in the paper. We assume that $(\mathbb{R}^p)^{k_G}$ is equipped with $\mathcal{B}((\mathbb{R}^p)^{k_G})$, where $\mathcal{B}(\mathcal{X})$ is the family of Borel subsets of a topological space \mathcal{X} . We denote by S^{p-1} the unit sphere in \mathbb{R}^p and by $\|\cdot\|$ the Euclidean norm on \mathbb{R}^p . For a Borel measure μ on \mathbb{R}^p , $\mu^{\otimes k}$ is the k -fold product measure, $\lambda(\cdot)$ the Lebesgue measure on \mathbb{R}^p . We use *a.e.* to mean almost everywhere with respect to the Lebesgue measure on \mathbb{R}^p and *a.s.* to mean almost surely with respect to a probability measure P on \mathbb{R}^p . The

support of a function $g(\cdot)$ and its interior are denoted by \bar{S}_g and S_g , respectively. Finally, we denote by $B_r(x)$ and $\bar{B}_r(x)$ be the open and closed ball in \mathbb{R}^p with radius $r \geq 0$ and center $x \in \mathbb{R}^p$.

2 Local depth and extreme localization

2.1 Analytic properties

We begin by describing in detail local notions of *Type A* depth functions studied in Zuo and Serfling [2000a]. Let \mathcal{G} denote the class of kernel functions $G(\cdot) : (\mathbb{R}^p)^{k_G} \rightarrow [0, \infty)$ satisfying the properties **(P1)-(P4)** below. Since the index G in $Z_\tau^G(x)$ and the kernel function $G(\cdot) = \mathbf{I}(\cdot \in Z_1^G(0))$ are used to express the same quantity, we use the same notation for both. The *Type A* local depth function is defined as follows:

Definition 2.1 Let $G \in \mathcal{G}$, $\tau \in [0, \infty]$, and let $h_\tau^{(G)} : \mathbb{R}^p \times (\mathbb{R}^p)^{k_G} \rightarrow [0, \infty)$ be given by

$$h_\tau^{(G)}(x; x_1, \dots, x_{k_G}) := \begin{cases} G((x_1 - x)/\tau, \dots, (x_{k_G} - x)/\tau) & \text{if } \tau \in (0, \infty) \\ \lim_{\tau \rightarrow 0^+} G((x_1 - x)/\tau, \dots, (x_{k_G} - x)/\tau) & \text{if } \tau = 0 \\ \lim_{\tau \rightarrow \infty} G((x_1 - x)/\tau, \dots, (x_{k_G} - x)/\tau) & \text{if } \tau = \infty. \end{cases} \quad (2.1)$$

(i) The general local depth at localization level $\tau \in [0, \infty]$ of a point $x \in \mathbb{R}^p$ with respect to P is given by

$$LGD(x, \tau, P) := \int h_\tau^{(G)}(x; x_1, \dots, x_k) dP(x_1) \dots dP(x_k). \quad (2.2)$$

(ii) The general depth of a point $x \in \mathbb{R}^p$ with respect to a probability measure P is given by

$$GD(x, P) := LGD(x, \infty, P). \quad (2.3)$$

Properties of the Kernel $G(\cdot)$:

(P1) $G(\cdot)$ is a non-negative and Borel measurable function satisfying

$$\Lambda_1^{(G)} := \int G(x_1, \dots, x_{k_G}) dx_1 \dots dx_{k_G} < \infty.$$

(P2) $G(\cdot)$ is symmetric and non-increasing along any ray from the origin in $(\mathbb{R}^p)^{k_G}$; that is, for any scalar $\alpha \geq 0$ and $v \in (\mathbb{R}^p)^{k_G}$, $G(v) = G(-v)$ and $G(\alpha v)$ is non-increasing in α .

(P3) $G(x_1, \dots, x_{k_G}) \rightarrow 0$ as $\max_{i=1, \dots, k_G} \|x_i\| \rightarrow \infty$.

(P4) For any $\epsilon > 0$, there exist $0 < \delta \leq \epsilon$ and $c_G > 0$ such that $\lambda((\overline{B}_\delta(0))^{k_G} \cap S_G) > 0$ and $G(\cdot) \geq c_G$ in $(\overline{B}_\delta(0))^{k_G} \cap S_G$.

See Appendix A for a discussion of other depth functions. In typical examples studied in the literature, such as simplicial, lens, and spherical depth, $G(\cdot)$ will have bounded support implying (P3); i.e., for some $\rho > 0$,

$$\overline{S}_G \subset (\overline{B}_\rho(0))^k. \quad (2.4)$$

Additionally we assume, without loss of generality (w.l.o.g.), that functions in \mathcal{G} are permutation invariant (see Appendix A for details). From the discussion in Appendix A it follows that if P is absolutely continuous with respect to the Lebesgue measure on \mathbb{R}^p with density $f(\cdot)$, then

$$LGD(x, \tau, P) = (h_\tau^{(G)}(0; \cdot) * f^{(k)}(\cdot))(x, \dots, x), \quad x \in \mathbb{R}^p, \tau \in [0, \infty], \quad (2.5)$$

where $*$ is the convolution operator and $f^{(k)}(x_1, \dots, x_k) = f(x_1) \dots f(x_k)$. When there is no scope for confusion we suppress the subscript or superscript G . Hence, we also write e.g. k for k_G , $h_{(\cdot)}(\cdot; \cdot)$ for $h_{(\cdot)}^{(G)}(\cdot; \cdot)$, Λ_1 for $\Lambda_1^{(G)}$. Since P is fixed in the following, we write $GD(x)$ for $GD(x, P)$ and $LGD(x, \tau)$ for $LGD(x, \tau, P)$. Also, for $j = 1, \dots, p$, we denote by $\partial_j g(\cdot)$ the partial derivative of the function $g : \mathbb{R}^p \rightarrow \mathbb{R}$ with respect to its j -component. Our first proposition summarizes several continuity and differentiability properties of the LDFs. Specifically, the behavior of the LDFs when $\tau \rightarrow 0^+$ and $\tau \rightarrow \infty$ are provided.

Proposition 2.1 (i) For all $x \in \mathbb{R}^p$, $LGD(x, \cdot)$ is monotonically non-decreasing with

$$\lim_{\tau \rightarrow 0^+} LGD(x, \tau) = G(0, \dots, 0)P^k(\{x\}) \text{ and } \lim_{\tau \rightarrow \infty} LGD(x, \tau) = GD(x).$$

- (ii) For $\tau \in [0, \infty)$, $\lim_{r \rightarrow \infty} \sup_{x \in \mathbb{R}^p \setminus B_r(0)} LGD(x, \tau) = 0$.
- (iii) If P is absolutely continuous with respect to the Lebesgue measure, then, for each $\tau \in [0, \infty)$, $LGD(\cdot, \tau)$ is bounded and continuous.
- (iv) Under assumption (2.4), if P is absolutely continuous with respect to the Lebesgue measure, with m -times continuously differentiable density $f(\cdot)$, then, for each $\tau \in [0, \infty)$, $LGD(\cdot, \tau)$ is m -times continuously differentiable and, for $i_1, \dots, i_m \in \{1, \dots, p\}$,

$$\partial_{i_m} \dots \partial_{i_1} LGD(x, \tau) = (h_\tau(0; \cdot) * (\partial_{i_m} \dots \partial_{i_1} f^{(k)}(\cdot)))(x, \dots, x). \quad (2.6)$$

When $\tau = \infty$, part (ii) does not hold in general. For instance, if P is absolutely continuous with respect to the Lebesgue measure with density function $f(\cdot)$, $k = 1$, and $G(\cdot) =$

$\exp(-\|\cdot\|^2/2)$, then $h_\infty(\cdot; \cdot) \equiv 1$ and (ii) holds for $LGD(\cdot, \infty)$ if and only if it holds for $f(\cdot)$ (see also Zuo and Serfling [2000a]).

Our next result is concerned with the convergence of scaled versions of LDFs in spaces of integrable functions, under extreme localization. To this end, let $L^d((\mathbb{R}^p)^k) = L^d((\mathbb{R}^p)^k, \lambda^{\otimes k})$, $1 \leq d < \infty$, denote the space of Lebesgue measurable functions $g : (\mathbb{R}^p)^k \rightarrow \mathbb{R}$ for which $g^d(\cdot)$ is absolutely integrable, and $L^\infty((\mathbb{R}^p)^k) = L^\infty((\mathbb{R}^p)^k, \lambda^{\otimes k})$ be the space of Lebesgue measurable functions $g : (\mathbb{R}^p)^k \rightarrow \mathbb{R}$ that are essentially bounded.

Theorem 2.1 *Let P be absolutely continuous with respect to the Lebesgue measure on \mathbb{R}^p , with density $f(\cdot)$.*

(i) *Under assumption (2.4) at every point of continuity of $f(\cdot)$, it holds that*

$$\lim_{\tau \rightarrow 0^+} \tau^{-kp} \Lambda_1^{-1} LGD(\cdot, \tau) = f^k(\cdot). \quad (2.7)$$

Furthermore, (2.7) holds uniformly on any set where $f(\cdot)$ is uniformly continuous.

(ii) *If $f(\cdot) \in L^\infty(\mathbb{R}^p)$, then (2.7) holds at every point of continuity of $f(\cdot)$ and the convergence in (2.7) is uniform on any set where $f(\cdot)$ is uniformly continuous.*

(iii) *Let $f(\cdot)$ be twice continuously differentiable. Then, under assumption (2.4), there exists a non-trivial function $R(\cdot)$ such that, for all $x \in S_f$,*

$$\lim_{\tau \rightarrow 0^+} \tau^{-2} (\tau^{-kp} LGD(x, \tau) - \Lambda_1 f^k(x)) = R(x).$$

(iv) *If $f^k(\cdot) \in L^d(\mathbb{R}^p)$, $1 \leq d < \infty$, then $\tau^{-kp} \Lambda_1^{-1} LGD(\cdot, \tau)$ converges in $L^d(\mathbb{R}^p)$ to $f^k(\cdot)$.*

We observe that (iii) provides the rate of convergence of the local depth to the k -th power of the density under extreme localization. An explicit formula for $R(\cdot)$ is provided in Appendix A. It is worth noticing that, under the assumption (2.4), for all $x \in \mathbb{R}^p \setminus \overline{S}_f$, $f^k(x) = 0$ and $\frac{1}{\tau^{kp}} LGD(x, \tau) = 0$ for small values of τ .

Using (2.7) one can express $f(\cdot)$ in terms of the limit of LDFs, for a given choice of $G(\cdot)$. This leads to an important idea, namely the τ -approximation. Our next proposition provides a uniform approximation of the density and its derivatives using the τ -approximation. The sample version of this approximation and its properties are provided in Proposition 2.3. This approximation is useful since in applications it enables one to provide alternative approaches for density estimation. We will illustrate this idea in three distinct but related contexts; *viz.* clustering, estimation of mode, and estimation of upper level sets (see Section 3 and Appendix D).

Definition 2.2 (τ -approximation) *For any $\tau > 0$,*

$$f_\tau^{(G)}(x) := \left(\frac{LGD(x, \tau)}{\tau^{kp} \Lambda_1} \right)^{1/k}. \quad (2.8)$$

Remark 2.1 From Proposition 2.1 (iii), it follows that when P has a density $f(\cdot)$ then, $f_\tau^{(G)}(\cdot)$ is continuous. Additionally, Proposition 2.1 (iv) implies that $f_\tau^{(G)}(\cdot)$ is m -times continuously differentiable in $S_{f_\tau^{(G)}}$.

Remark 2.2 Evidently, when $k = 1$ the τ -approximation reduces to the classical kernel density estimator (KDE) in \mathbb{R}^p where the kernel is given by the function $G(\cdot)$. We will return to this issue in the sections below.

Our next result establishes that the analytical properties of $LGD(\cdot, \cdot)$ are inherited by its τ -approximation $f_\tau^{(G)}(\cdot)$.

Proposition 2.2 Let P be absolutely continuous with respect to the Lebesgue measure on \mathbb{R}^p with density $f(\cdot)$. Then the following hold:

(i) If $f(\cdot)$ is uniformly continuous, then

$$\lim_{\tau \rightarrow 0^+} \sup_{x \in \mathbb{R}^p} |f_\tau^{(G)}(x) - f(x)| = 0. \quad (2.9)$$

(ii) If $f(\cdot)$ is continuous, then for all compact sets $K \subset \mathbb{R}^p$

$$\lim_{\tau \rightarrow 0^+} \sup_{x \in K} |f_\tau^{(G)}(x) - f(x)| = 0.$$

In particular, for all $x \in \mathbb{R}^p$, $\lim_{\tau, \epsilon \rightarrow 0^+} \sup_{y \in \overline{B}_\epsilon(x)} |f_\tau^{(G)}(y) - f(x)| = 0$.

(iii) If $f(\cdot) \in L^{kGd}(\mathbb{R}^p)$, $d \geq 1$, then $f_\tau^{(G)}(\cdot)$ converges in $L^{kGd}(\mathbb{R}^p)$ to $f(\cdot)$.

(iv) Suppose (2.4) holds and $f(\cdot)$ is m -times continuously differentiable, then, for all compact sets $K \subset S_f$ and $i_1, \dots, i_m \in \{1, \dots, p\}$,

$$\lim_{\tau \rightarrow 0^+} \sup_{x \in K} |\partial_{i_m} \dots \partial_{i_1} f_\tau(x) - \partial_{i_m} \dots \partial_{i_1} f(x)| = 0.$$

Remark 2.3 The above proposition implies that the τ -approximation converges uniformly to the density under extreme localization. We also note that continuity is not enough in Proposition 2.2 (i) (see Appendix H for a counterexample). (iv) of the Proposition provides a uniform approximation to the partial derivatives of the τ -approximation and plays a critical role in the properties of clustering investigated in the Section 3.

2.2 Sample local depth

Let $\{X_1, \dots, X_n\}$ be independent and identically distributed (i.i.d.) random variables from P on \mathbb{R}^p ; then the estimate of LGD, called sample local depth, is the U-statistics of order k [Korolyuk and Borovskich, 2013]

$$LGD_n(x, \tau) := \binom{n}{k}^{-1} \sum_{1 \leq i_1 < \dots < i_k \leq n} h_\tau^{(G)}(x; X_{i_1}, \dots, X_{i_k}), \quad (2.10)$$

where $x \in \mathbb{R}^p$ and $\tau \in [0, \infty]$. In particular, $GD(x)$ is estimated by setting $GD_n(x) := LGD_n(x, \infty)$. For $1 \leq j \leq k$, let $h_\tau^{(G,j)}(x; x_1, \dots, x_j) := E[h_\tau^{(G)}(x; x_1, \dots, x_j, X_{j+1}, \dots, X_k)]$ and $\tilde{h}_\tau^{(G,j)}(x; x_1, \dots, x_j) := h_\tau^{(G,j)}(x; x_1, \dots, x_j) - LGD(x, \tau)$. When there is no scope for confusion we also write $h_\tau^{(j)}(\cdot; \cdot)$ for $h_\tau^{(G,j)}(\cdot; \cdot)$ and $\tilde{h}_\tau^{(j)}(\cdot; \cdot)$ for $\tilde{h}_\tau^{(G,j)}(\cdot; \cdot)$. Using (1.1.34) in Korolyuk and Borovskich [2013], we have that

$$Var[LGD_n(x, \tau)] = \binom{n}{k}^{-1} \sum_{j=1}^k \binom{k}{j} \binom{n-k}{k-j} E[(\tilde{h}_\tau^{(G,j)}(x; X_1, \dots, X_j))^2]. \quad (2.11)$$

It follows that, for all $n \in \mathbb{N}$,

$$\begin{aligned} Var[\sqrt{n}LGD_n(x, \tau)] &= nk \binom{n}{k}^{-1} \binom{n-k}{k-1} E[(\tilde{h}_\tau^{(G,1)}(x; X_1))^2] + O\left(\frac{1}{n}\right) \\ &\xrightarrow[n \rightarrow \infty]{} k^2 E[(\tilde{h}_\tau^{(G,1)}(x; X_1))^2]. \end{aligned}$$

The above calculation yields that LGD_n is a consistent estimator of LGD even though this holds under much weaker conditions on $G(\cdot)$. In typical applications, the choice of x , τ , and G vary and in exploratory analyses, different choices of x , τ and G may be investigated. Our next result shows that the LGD_n is uniformly consistent over x and τ . The proof relies on the size of the class $\mathcal{H}_G := \{h_\tau^{(G)}(x; \cdot) : x \in \mathbb{R}^p, \tau \in [0, \infty]\}$ which can be characterized using VC-theory. We impose a very weak condition on the class \mathcal{H}_G , namely that it is a VC-subgraph class (see Definition 3.6.8 of Giné and Nickl [2016]). We show that this assumption holds in several examples studied in the literature. These details are described in Appendix C.

Theorem 2.2 *Let \mathcal{H}_G be a VC-subgraph class of functions. Then*

$$\sup_{\substack{x \in \mathbb{R}^p \\ \tau \in [0, \infty]}} |LGD_n(x, \tau) - LGD(x, \tau)| \xrightarrow[n \rightarrow \infty]{} 0 \text{ a.s.}$$

In some examples, it is possible that $G =: G_\theta \in \mathcal{G}$ is indexed by a parameter $\theta \in \Theta \subset \mathbb{R}$, as is the case for β -skeletons. In such cases, one can strengthen the above Theorem 2.2 to obtain uniformity in the indexing parameter under additional assumptions as described in the Assumption A.1 in Appendix A. That is,

$$\sup_{\theta \in \Theta} \sup_{\substack{x \in \mathbb{R}^p \\ \tau \in [0, \infty]}} |LG_\theta D_n(x, \tau) - LG_\theta D(x, \tau)| \xrightarrow[n \rightarrow \infty]{} 0 \text{ a.s.} \quad (2.12)$$

The details for the β -skeleton are also provided in Appendix C.

Remark 2.4 Returning to Remark 2.2, under the additional assumption that $G(\cdot)$ is a product of kernels, one can obtain our estimator as a U-statistic with a product kernel with the same bandwidth. When the kernel is indexed by $\theta \in \Theta$ as in (2.12), one can obtain as a corollary uniform convergence in θ of these KDEs in \mathbb{R}^p . This result seems new even in the KDE literature. Finally, computational issues for large k are addressed in Appendix G.

We now turn to the uniform central limit theorem for LGD_n over a suitable subset T of $\mathbb{R}^p \times [0, \infty]$. Let $\ell^\infty(T)$ denote the space of all bounded functions $\bar{g}(\cdot) : T \rightarrow \mathbb{R}$. To study the convergence in distribution in $\ell^\infty(T)$, one needs to address the measurability problems that are encountered due to the non-separability of $\ell^\infty(T)$. We address this using Theorem 4.9 in Arcones and Giné [1993]. In their paper they handle the issue by requiring \mathcal{F} (not defined here) to be a “measurable” class, where measurable was described on page 1497. Indeed, in our proof, and as also stated in their paper, we address this issue by establishing that the class of kernels related to the U-statistics is image admissible Suslin (see Dudley [2014]) and (1.9) of their paper holds. In the following, convergence in distribution in $\ell^\infty(T)$ is in the sense of Hoffmann-Jørgensen [Giné and Nickl, 2016, Definition 3.7.22].

Theorem 2.3 Let $T \subset \mathbb{R}^p \times [0, \infty]$ such that $E[(\tilde{h}_\tau^{(1)}(x; X_1))^2] > 0$, for all $(x, \tau) \in T$, and suppose that \mathcal{H}_G is a VC-subgraph class of functions. Then

$$\sqrt{n}(LGD_n(\cdot, \cdot) - LGD(\cdot, \cdot)) \xrightarrow[n \rightarrow \infty]{d} kW(\cdot, \cdot) \text{ in } \ell^\infty(T)$$

where $\{W(x, \tau)\}_{(x, \tau) \in T}$ is a centered Gaussian process with covariance function $\gamma : T \times T \rightarrow \mathbb{R}$ given by

$$\gamma((x, \tau), (y, \nu)) = \int h_\tau^{(1)}(x; x_1)h_\nu^{(1)}(y; x_1)dP(x_1) - LGD(x, \tau)LGD(y, \nu). \quad (2.13)$$

Remark 2.5 Notice that, for $(x, \tau) \in T$, the variance of $W(x, \tau)$ is $\gamma((x, \tau), (x, \tau)) = E[(\tilde{h}_\tau^{(1)}(x; X_1))^2] > 0$ and, in the examples, $T \neq \emptyset$. This implies that the U-statistics (2.10) is non-degenerate, i.e. $\tilde{h}_\tau^{(1)}(x; \cdot) \neq 0$ [Korolyuk and Borovskich, 2013]. Furthermore, if P is absolutely continuous with respect to the Lebesgue measure, $x \in S_P$ (the interior of the support of P), and $\tau > 0$, then since $E[(\tilde{h}_\tau^{(1)}(x; X_1))^2] > 0$, T can be taken to be “large”.

In the clustering applications discussed below, we will establish the consistency of the sample clustering algorithm. This will involve approximating the τ -approximations of the depth functions and their derivatives via their sample versions. The quality of this approximation will play a critical role in the consistency arguments. Our next result

enables this study by establishing the following *Bernstein*-type inequality for local depth functions. Before we state this result, notice that, by Jensen's inequality and (A.1),

$$\sigma_G^2 := \sup_{\substack{x \in \mathbb{R}^p \\ \tau \in [0, \infty]}} E[(\tilde{h}_\tau^{(G,1)}(x; X_1))^2] \leq \sup_{\substack{x \in \mathbb{R}^p \\ \tau \in [0, \infty]}} E[(\tilde{h}_\tau^{(G,k)}(x; X_1, \dots, X_k))^2] \leq l_G^2,$$

where $l_G := G(0, \dots, 0)$.

Theorem 2.4 *Let \mathcal{H}_G be a VC-subgraph class of functions. Then, there are constants $1 < C_{G,0}, C_{G,1}, C_{G,2} < \infty$ such that, for all $t \geq \max(2^3\sigma_G, 2^4C_{G,0})$,*

$$P^{\otimes n}(\sqrt{n} \sup_{\substack{x \in \mathbb{R}^p \\ \tau \in [0, \infty]}} |LGD_n(x, \tau) - LGD(x, \tau)| \geq t) \leq D_G(n, t) := \sum_{j=1}^3 D_{G,j}(n, t), \quad (2.14)$$

where

$$\begin{aligned} D_{G,1}(n, t) &:= 8 \exp\left(-\frac{t^2 \sqrt{n}}{2^{15} k_G^2 (\sigma_G^2 \sqrt{n} + tl_G)}\right), \\ D_{G,2}(n, t) &:= 8C_{G,1}^{2C_{G,2}} \left(\sigma_G^2 + \frac{2tl_G}{\sqrt{n}}\right)^{-C_{G,2}} \exp\left(-\left(\frac{n\sigma_G^2}{2l_G^2} + \frac{\sqrt{nt}}{4l_G}\right)\right), \quad \text{and} \\ D_{G,3}(n, t) &:= 2 \exp\left(-\frac{t^2 \sqrt{n}}{2^{6+k_G} k_G^{k_G+1} l_G C_{G,0} (\sigma_G^2 \sqrt{n} + tl_G)}\right). \end{aligned}$$

We now turn to the $S\tau A$ for estimating the density. To this end, let P be absolutely continuous with respect to the Lebesgue measure with density $f(\cdot)$. The plug-in estimator of $f_\tau^{(G)}(\cdot)$ is given by

$$f_{\tau,n}^{(G)}(x) := \left(\frac{LGD_n(x, \tau)}{\tau^{kp} \Lambda_1}\right)^{1/k}, \quad (2.15)$$

where we recall that we have suppressed G in k_G . Our first result uses Proposition 2.2 and Theorem 2.4 to establish the uniform convergence of $f_{\tau,n}^{(G)}(\cdot)$ to $f(\cdot)$.

Proposition 2.3 *Let \mathcal{H}_G be a VC-subgraph class of functions and suppose that P is absolutely continuous with respect to the Lebesgue measure on \mathbb{R}^p with density $f(\cdot)$. Let $\{\tau_n\}_{n=1}^\infty$ and $\{\epsilon_n\}_{n=1}^\infty$ be sequences of positive scalars converging to zero with $\lim_{n \rightarrow \infty} \frac{n}{\log(n)} \tau_n^{2kp} = \infty$. Then the following hold:*

(i) *If $f(\cdot)$ is uniformly continuous, then*

$$\lim_{n \rightarrow \infty} \sup_{x \in \mathbb{R}^p} |f_{\tau_n,n}^{(G)}(x) - f(x)| = 0 \text{ a.s.}$$

(ii) *If $f(\cdot)$ is continuous, then for all compact sets $K \subset \mathbb{R}^p$*

$$\lim_{n \rightarrow \infty} \sup_{x \in K} |f_{\tau_n,n}^{(G)}(x) - f(x)| = 0 \text{ a.s.}$$

In particular, for all $x \in \mathbb{R}^p$, $\lim_{n \rightarrow \infty} \sup_{y \in \overline{B}_{\epsilon_n}(x)} |f_{\tau_n,n}^{(G)}(y) - f(x)| = 0$ a.s.

Remark 2.6 Under the additional assumption that $\psi^{(G)}(\cdot)$ is integrable in $(\mathbb{R}^p)^k$, where $\psi^{(G)}(w) := \sup_{v \in (\mathbb{R}^p)^k : \|v-w\| \leq 1} G(v)$ (norm in $(\mathbb{R}^p)^k$), it follows from Bertrand-Retali [1978] that consistency can be proved under the weaker condition $\lim_{n \rightarrow \infty} \frac{n}{\log(n)} \tau_n^{kp} = \infty$.

The asymptotic limit distribution of the $S\tau A$ is provided in Appendix B. Examples and verification of the VC-subgraph property are provided in Appendix C. We now turn to discuss clustering application. Appendix D contains applications to estimation of upper level sets of the density and divergence based inference.

3 Clustering

In this section, we describe a new methodology for clustering multivariate data using the theory of dynamical systems. As explained in the Introduction, this involves three distinct but connected steps. In the first step, one constructs cluster(s) in the population as stable manifold(s) generated by the mode(s). Next, the behavior of the gradient system when $f(\cdot)$ is replaced by its τ -approximation is studied and its convergence established under extreme localization. Finally, one replaces the τ -approximated density by its $S\tau A$, $f_{\tau_n, n}(\cdot)$, to obtain the empirical clusters and establish their convergence.

The following discussion is reliant on Assumption 3.1 below concerning the smoothness properties of $f(\cdot)$. Recall that the clusters are defined as the stable manifolds generated by the mode and are obtained using the limiting trajectory of the gradient system. Specifically, for any $\mu \in S_f$, the stable manifold generated by μ is given by

$$C(\mu) := \{x \in S_f : \lim_{t \rightarrow \infty} u_x(t) = \mu\}, \quad (3.1)$$

where $u_x(t)$ is the solution at time t of the gradient system

$$u'(t) = \nabla f(u(t)) \quad (3.2)$$

with initial value $u(0) = x$. For any choice of μ , it is not required for the stable manifold so-defined to be non-trivial; i.e. the Lebesgue measure of $C(\mu)$ can be zero. However, if μ is chosen as a mode of $f(\cdot)$, then, one can verify that the resulting manifold has a positive Lebesgue measure. We next turn to define the stationary points type, and, in particular, the mode. Before we state the assumption, we introduce one more notation: the Hessian matrix associated with any function $g(\cdot)$ is denoted by H_g and $\langle \cdot, \cdot \rangle$ denotes the inner product on \mathbb{R}^p .

Definition 3.1 A stationary point $\mu \in S_f$ of $f(\cdot)$ is said to be of type l , $0 \leq l \leq p$, if $H_f(\mu)$ has l negative and $p - l$ positive eigenvalues. In particular, $m \in S_f$ is said to be a

mode (resp. an antimode) for $f(\cdot)$ if it is a stationary point of $f(\cdot)$ and $H_f(m)$ has only negative (resp. positive) eigenvalues, that is, m is a local maximum (resp. minimum) for $f(\cdot)$. If m_1, \dots, m_M are the modes of $f(\cdot)$, then the clusters induced by m_1, \dots, m_M are the stable manifolds $C(m_1), \dots, C(m_M)$.

Let m_1, \dots, m_M be the modes and μ_1, \dots, μ_L the other stationary points of $f(\cdot)$. We verify in Appendix E that the clusters $C(m_1), \dots, C(m_M)$ are well-defined, non-trivial and disjoint using Lyapunov's theory in dynamical systems. Some aspects of this are well-known in both dynamical systems and Morse theory literature [Hirsch et al., 1974, Matsumoto, 2002, Teschl, 2012]. Additionally, we establish that

$$S_f = \bigcup_{i=1}^M C(m_i) \cup \bigcup_{l=1}^L C(\mu_l).$$

Hence, $C(m_1), \dots, C(m_M), C(\mu_1), \dots, C(\mu_L)$ form a partition of S_f . Also, the set $S_f \setminus (\bigcup_{i=1}^M C(m_i)) = \bigcup_{l=1}^L C(\mu_l)$ has (topological) dimension smaller than p . Proposition E.1 provides a characterization of the boundaries of $C(m_1), \dots, C(m_M)$. In particular, it shows that the clusters $C(m_1), \dots, C(m_M)$ are separated in S_f by the lower dimensional stable manifolds $C(\mu_1), \dots, C(\mu_L)$. This completes the first step. The second step is described in Subsection 3.1 where we describe step-by-step analytical tools to fill in the gap between local depths and stable manifolds generated by the modes. The third step is described in Subsection 3.2. The algorithm is provided in Appendix G.

3.1 Identification of stationary points and convergence of the gradient system under extreme localization

We replace $f(\cdot)$ by $f_\tau(\cdot)$ in (3.2) and consider the gradient system

$$u'(t) = \nabla f_\tau(u(t)). \quad (3.3)$$

The domain of this new system is S_{f_τ} . We summarize the main properties of (3.3) as $\tau \rightarrow 0^+$. We begin with the properties of S_{f_τ} .

Lemma 3.1 *For all $0 < \tau_1 \leq \tau_2$, we have that $S_{f_{\tau_1}} \subset S_{f_{\tau_2}}$. Additionally, if $f(\cdot)$ is continuous, then, for all $\tau > 0$, $S_f \subset S_{f_\tau}$ and $\lim_{\tau \rightarrow 0^+} S_{f_\tau} \supseteq S_f$. Under assumption (2.4), $\lim_{\tau \rightarrow 0^+} S_{f_\tau} \subset \overline{S_f}$.*

We observe that the assumption (2.4) is essential in the last part of Lemma 3.1. Indeed, if $G(\cdot)$ is the Gaussian kernel, then $S_{f_\tau} = \mathbb{R}^p$, for all $\tau > 0$, implying $\lim_{\tau \rightarrow 0^+} S_{f_\tau} = \mathbb{R}^p$. Also, since ∂S_f and S_G have arbitrary shape, it is unclear if $x \in \partial S_f$ belongs to $\lim_{\tau \rightarrow 0^+} S_{f_\tau}$ or

not. Under Assumption 3.1 below, Proposition 2.2 (iv) shows that the gradient and the Hessian matrix of $f_\tau(\cdot)$ converge to those of $f(\cdot)$. Recall that, by Remark (2.1), if $f(\cdot)$ is m -times continuously differentiable, then, $f_\tau(\cdot)$ is m -times continuously differentiable in S_{f_τ} . Additionally, if $f(\cdot)$ is τ -symmetric about a stationary point μ (that is, $f(\mu+x) = f(\mu-x)$, for all $x \in \mathbb{R}^p$ with $\|x\| \leq \tau$), then it is easy to see that the stationary points of $f(\cdot)$ are also the stationary points of $f_\tau(\cdot)$. However, the assumption of τ -symmetry may be harder to verify in applications. For this reason, we *do not make this assumption in the developments below* even though in Appendix F we provide sufficient conditions under which the stationary points (resp. modes, antimodes) of $f(\cdot)$ are *exactly* the stationary points (resp. modes, antimodes) of $f_\tau(\cdot)$ for $\tau > 0$ when τ -symmetry obtains.

Next, to characterize the stationary points of $f_\tau(\cdot)$ without the τ -symmetry condition, notice that for small τ , the first and second order derivatives are close (Proposition 2.2). Hence, one can pick a hypercube, centered at the stationary point with directions provided by eigenvectors of Hessian matrix, so that $f(\cdot)$ and $f_\tau(\cdot)$ share similar properties within the hypercube. This idea is made precise in the following theorem.

Theorem 3.1 *Suppose (2.4) holds true. The following hold:*

- (i) *If $f(\cdot)$ has is continuously differentiable in $\overline{B}_{\rho\tau}(\mu) \subset S_f$, $\tau > 0$, then $\nabla f_\tau(\mu) = 0$ if and only if*

$$\int h_\tau(0; x_1, \dots, x_k) \nabla f(\mu + x_1) f(\mu + x_2) \dots f(\mu + x_k) dx_1 \dots dx_k = 0, \quad (3.4)$$

where the integral of a vector is the vector of the integrals.

- (ii) *If $f(\cdot)$ is twice continuously differentiable in $\overline{B}_\delta(\mu) \subset S_f$, $\delta > 0$, and μ is a stationary point of $f(\cdot)$ of type l , then there exists $h^*, \tau^* > 0$ and a closed hypercube $F_{h^*}(\mu) \subset \overline{B}_\delta(\mu)$ with side length $3/2h^*$ such that, for $0 < \tau \leq \tau^*$, $f_\tau(\cdot)$ has a unique stationary point μ_τ in $\overset{\circ}{F}_{h^*}(\mu)$ and μ_τ is of type l . Moreover, $\|\mu_\tau - \mu\| \xrightarrow[\tau \rightarrow 0^+]{} 0$.*
- (iii) *If $f(\cdot)$ is three times continuously differentiable, then $\|\mu_\tau - \mu\| = O(\tau^2)$.*

We now state the main assumptions required for convergence of clusters obtained using (2.8).

Assumption 3.1 *$f(\cdot)$ is a probability density function on \mathbb{R}^p that is twice continuously differentiable with a finite number of stationary points in S_f . Additionally, the Hessian matrix H_f has non-zero eigenvalues at its stationary points. Also, let $R^\alpha := \{x \in \mathbb{R}^p : f(x) \geq \alpha\}$ be a bounded set for every $\alpha > 0$.*

By continuity of $f(\cdot)$, R^α is compact. We notice that R^α is bounded if $f(\cdot)$ vanishes at infinity, that is, $\sup_{x \in \mathbb{R}^p: \|x\| \geq c} f(x) \rightarrow 0$ as $c \rightarrow \infty$, which is satisfied, for example, if

S_f is bounded. We study next the relationship between the gradient systems (3.3) and (3.2) under extreme localization. To this aim, notice that the sets $\{S_{f_\tau}\}_{\tau>0}$ contain S_f by Lemma 3.1. If it exists, we denote by $u_{x,\tau}(t)$ the solution of (3.3) with initial point $u_{x,\tau}(0) = x$. Since $f_\tau(\cdot)$ is continuous, for $\alpha > 0$, the sets $R_\tau^\alpha := \{x \in \mathbb{R}^p : f_\tau(x) \geq \alpha\} = f_\tau^{-1}([\alpha, \infty))$ are closed. Lemma A.6 in Appendix A shows that they are also bounded. As shown in Appendix E, for the gradient system (3.2), Lemma A.6 along with the boundedness of R^α for all $\alpha > 0$, implies that for all $x \in S_f$ $u_{x,\tau}(\cdot)$ exists and is unique in a maximal time interval (a, ∞) , for some $-\infty \leq a < 0$. For a stationary point $\mu_\tau \in S_f$ of $f_\tau(\cdot)$, the stable manifold generated by μ_τ is

$$C_\tau(\mu_\tau) := \{x \in S_f : \lim_{t \rightarrow \infty} u_{x,\tau}(t) = \mu_\tau\}.$$

We next exploit the differentiability properties of $f_\tau(\cdot)$ to show that the solutions of the gradient system (3.3) converge for $\tau \rightarrow 0^+$ to those of the gradient system (3.2). This is described in Appendix A, Proposition A.2. We now turn to the convergence of the clusters $C_\tau(\mu_\tau)$ under extreme localization. To this end, let $N_f := \{m_1, \dots, m_M, \mu_1, \dots, \mu_L\}$ denote the set of stationary points of $f(\cdot)$.

Theorem 3.2 *Suppose that (2.4) and Assumption 3.1 hold true, and $f(\cdot)$ is three times continuously differentiable. Let $\{\tau_j\}_{j=1}^\infty$ be a sequence of positive scalars converging to 0. Then, for all $\mu \in N_f$, there exists $\tau^* > 0$ and $\{\mu_{\tau_j}\}_{j=1, \tau_j \leq \tau^*}^\infty$ such that $\|\mu_{\tau_j} - \mu\| = O(\tau_j^2)$, where, for each τ_j , μ_{τ_j} is a stationary points of $f_{\tau_j}(\cdot)$ and is of the same type as μ satisfying $\lim_{j \rightarrow \infty} C_{\tau_j}(\mu_{\tau_j}) = C(\mu)$.*

3.2 Algorithm and consistency of empirical clusters

In this section, we describe the algorithm for the numerical approximation of the clusters induced by the system (3.3) and establish its consistency.

Since the sample τ -approximation is, in general, not differentiable in x , we use a finite difference approximation that converges to the directional derivative. The directional derivative of $g(\cdot)$, in the direction of $v \in S^{p-1}$ (the unit sphere in \mathbb{R}^p), is denoted by $\nabla_v g(\cdot) = \langle \nabla g(\cdot), v \rangle$. To this end, for $x \in \mathbb{R}^p$, $\tau > 0$, $n \in \mathbb{N}$, $h > 0$ and a unit vector $v \in \mathbb{R}^p$, the finite difference approximations of the directional derivatives of $f_\tau(\cdot)$ and $f_{\tau,n}(\cdot)$ along v are given by

$$\nabla_v^h f_\tau(x) = \frac{f_\tau(x + hv) - f_\tau(x)}{h} \quad \text{and} \quad \nabla_v^h f_{\tau,n}(x) = \frac{f_{\tau,n}(x + hv) - f_{\tau,n}(x)}{h}.$$

Our first result shows that under the condition $\lim_{n \rightarrow \infty} nh_n^{2k} \tau_n^{2kp} = \infty$, the finite difference approximation to the directional derivative converges uniformly on compact sets, in probability.

Theorem 3.3 Suppose (2.4) holds true. Let K be a compact subset of S_f , $\{h_n\}_{n=1}^\infty$ and $\{\tau_n\}_{n=1}^\infty$ sequences of positive scalars converging to 0 and $\{v_n\}_{n=1}^\infty$ be a sequence in S^{p-1} converging to $v \in S^{p-1}$. (i) If $f(\cdot)$ is continuously differentiable, then

$$\lim_{n \rightarrow \infty} \sup_{x \in K} |\nabla_{v_n}^{h_n} f_{\tau_n}(x) - \nabla_v f(x)| = 0.$$

(ii) If, additionally, \mathcal{H}_G is a VC-subgraph class of functions and $\lim_{n \rightarrow \infty} nh_n^{2k} \tau_n^{2kp} = \infty$, then, for all $\epsilon > 0$,

$$\lim_{n \rightarrow \infty} P^{\otimes n} \left(\sup_{x \in K} |\nabla_{v_n}^{h_n} f_{\tau_n, n}(x) - \nabla_v f(x)| \geq \epsilon \right) = 0.$$

The first step towards identifying the modes, is finding a local maximum of a function. To this end, we use the steepest ascent or gradient ascent idea; that is, starting from a point in the space, the next point is chosen in the direction given by the gradient of the function at that point. This procedure is repeated until convergence to a local maximum is achieved. When clustering using modes, this procedure is often combined with kernel density estimators to find the modes of the density underlying the given data points, and the clusters associated with them [Fukunaga and Hostetler, 1975, Menardi, 2016]. In the following, we propose a similar technique (using instead $S\tau A$), which does not require existence of gradients, and considers data as potential candidate points for the next move. This yields a computationally efficient procedure (see Theorem 3.4 below).

Turning to the consistency result, we need arguments that allows one to approximate uniformly the directional derivative of points over (i) a compact set, (ii) the step-size, and (iii) directions. The next lemma addresses this issue and critically uses the *Bernstein*-type inequality developed in Theorem 2.4. Part (iii) of the lemma below also provides a upper bound on the uniform approximation mentioned above. We need the following notation: for $\delta > 0$, $(A)^{+\delta} := \{x \in \mathbb{R}^p : \inf_{y \in A} \|x - y\| \leq \delta\}$ and $(A)^{-\delta} := \mathbb{R}^p \setminus (\mathbb{R}^p \setminus A)^{+\delta} = \{x \in \mathbb{R}^p : \inf_{y \in \mathbb{R}^p \setminus A} \|x - y\| > \delta\}$.

Lemma 3.2 Suppose (2.4) holds true. Let K be a compact subset of S_f and let $h^* > 0$ be such that $(K)^{+h^*} \subset S_f$. Also, let $\{\tau_n\}_{n=1}^\infty$ and $\{h_n\}_{n=1}^\infty$ be sequences of positive scalars converging to 0. Assume also that $f(\cdot)$ is three times continuously differentiable. Then (i) the finite difference approximation of the directional derivative of $f_\tau(\cdot)$ converges uniformly to that of $f(\cdot)$. That is,

$$\lim_{n \rightarrow \infty} \sup_{h \in [h_n, h^*]} \sup_{v \in S^{p-1}} \sup_{x \in K} |\nabla_v^h f_{\tau_n}(x) - \nabla_v^h f(x)| = 0.$$

(ii) If, additionally, \mathcal{H}_G is a VC-subgraph class of functions and $\lim_{n \rightarrow \infty} nh_n^{2k} \tau_n^{2kp} = \infty$, then, for all $\epsilon > 0$,

$$\lim_{n \rightarrow \infty} P^{\otimes n} \left(\sup_{h \in [h_n, h^*]} \sup_{v \in S^{p-1}} \sup_{x \in K} |\nabla_v^h f_{\tau_n, n}(x) - \nabla_v^h f(x)| \geq \epsilon \right) = 0.$$

(iii) Let $\lim_{n \rightarrow \infty} \frac{n}{\log(n)} h_n^{2k} \tau_n^{2kp} = \infty$ and \mathcal{H}_G be a VC-subgraph class of functions. Then, for all $\epsilon > 0$, there are constants $0 < \tilde{C} < \infty$ and $\tilde{n} \in \mathbb{N}$ such that, for all $n \geq \tilde{n}$,

$$P^{\otimes n} \left(\sup_{h \in [h_n, h^*]} \sup_{v \in S^{p-1}} \sup_{x \in K} |\nabla_v^h f_{\tau_n, n}(x) - \nabla_v^h f(x)| \geq \epsilon \right) \leq \frac{\tilde{C}}{n^2}.$$

We are now ready to state the main result of this section, namely, consistency of the empirically chosen clusters.

Theorem 3.4 Suppose that \mathcal{H}_G is a VC-subgraph class of functions, Assumption 3.1 and (2.4) hold true and $f(\cdot)$ is three times continuously differentiable. Let $\mathcal{X}_n := \{X_1, \dots, X_n\}$ be a sample of i.i.d. random variables from P with density $f(\cdot)$ and $\{h_n\}_{n=1}^\infty$ and $\{\tau_n\}_{n=1}^\infty$ be sequences of positive scalars converging to zero with $\lim_{n \rightarrow \infty} nh_n^{2k} \tau_n^{2kp} = \infty$. For $x \in S_f$ and $r > 0$, define

$$\mathcal{X}_{n,r}(x) := \{X \in \mathcal{X}_n : h_n \leq \|X - x\| \leq r\},$$

$Y_{n,r,0} := x$ and, recursively, if

$$\max_{X \in \mathcal{X}_{n,r}(Y_{n,r,j}) \cup \{Y_{n,r,j}\}} f_{\tau_n, n}(X) - f_{\tau_n, n}(Y_{n,r,j}) > 0, \quad (3.5)$$

then

$$Y_{n,r,j+1} := \operatorname{argmax}_{X \in \mathcal{X}_{n,r}(Y_{n,r,j})} \frac{f_{\tau_n, n}(X) - f_{\tau_n, n}(Y_{n,r,j})}{\|X - Y_{n,r,j}\|}; \quad (3.6)$$

else stop and let $j^* := j$. It holds that $j^* \leq n$. Furthermore, if $x \in C(m_i)$, and given $0 < \eta \leq 1$, $\alpha^* \leq \alpha < f(m_i)$, and $0 < r \leq r^*$, for some $\alpha^*, r^* > 0$, then there exist $n^* \in \mathbb{N}$ such that, with probability at least $1 - \eta$, $Y_{n,r,j^*} \in R^\alpha \cap C(m_i)$, for all $n \geq n^*$.

Using the above theorem, one can estimate the mode using the last iterate, namely, Y_{n,r,j^*} . The Corollary 3.1 below provides strong consistency of this estimate. Turning to the proof of Theorem 3.4, it is divided into four distinct but connected steps. For the first step, let j^* be a non-negative integer and define $\{y_{r,j}\}$ recursively as follows: let $y_{r,0} = x$ and

$$y_{r,j+1} = y_{r,j} + h_j v_j, \quad 0 \leq j \leq (j^* - 1),$$

where $0 < h_j \leq r$ for some small $r > 0$, and where v_j is “close” to the normalized gradient of $f(\cdot)$ at $y_{r,j}$. We show that the sequence $\{y_{r,j}\}$ is close to the solution $u_x(\cdot)$ of (3.2).

This is achieved, using version of the discrete Grönwall lemma (Lemma A.7 in Appendix A). Next, we show that $\{Y_{n,r,j}\}$ in (3.6) behaves like the sequence $\{y_{r,j}\}$ described in Step 1, with probability $(1 - \eta)$. This is achieved in Step 2 using Lemma 3.2. The proof of this step requires the existence of sufficient number of data points in a small neighborhood of all points in the direction of the normalized gradient. We establish that this is indeed the case using compactness arguments in Step 3. Finally, we apply the results of Step 1 to $\{Y_{n,r,j}\}_{j=0}^{j^*}$ yielding that this sequence is close to the solution $u_x(\cdot)$. Since for all points that are not close to a mode, there exists, by Step 3, data points yielding a positive finite difference approximation of the directional derivative, (3.5) occurs with the desired probability. This observation allows to conclude, in Step 4, that Y_{n,r,j^*} is close to the mode.

As a consequence of the above theorem, setting $J_n := \mathbf{I}(Y_{n,r,j^*} \notin R^\alpha \cap C(m_i))$, $\delta \in (0, 1]$, and $\{\eta_n\}_{n=1}^\infty$ be a sequence of scalars in $(0, 1]$ with $\lim_{n \rightarrow \infty} \eta_n = 0$ one can show by Theorem 3.4 that

$$\lim_{n \rightarrow \infty} P^{\otimes n}(J_n \geq \delta) = \lim_{n \rightarrow \infty} P^{\otimes n}(J_n = 1) \leq \lim_{n \rightarrow \infty} \eta_n = 0,$$

implying that J_n converges in probability to zero. Since Y_{n,r,j^*} is the estimate of the mode, we obtain weak consistency of the mode. Furthermore, using (iii) of Lemma 3.2, one can strengthen the conclusion to almost sure convergence. We summarize this observation as a corollary.

Corollary 3.1 *Suppose that $\lim_{n \rightarrow \infty} \frac{n}{\log(n)} h_n^{2k} \tau_n^{2kp} = \infty$ and the assumptions of Theorem 3.4 hold. Then $J_n \xrightarrow[n \rightarrow \infty]{} 0$ a.s..*

It is important to note that one can weaken some of the conditions in the above Theorem. Specifically, in Lemma I.1 in Appendix I we show that, for $p \geq 6k + 1$, the conditions involving $\{h_n\}_{n=1}^\infty$ can be removed provided that the sequence $\{\tau_n\}_{n=1}^\infty$ does not converge to zero “too fast”; for instance, one could choose $\tau_n = n^{-\delta/(2kp)}$ for some $0 < \delta < 1 - \frac{6k}{p}$. To see this, notice from the lemma that h_n can be replaced by $\tilde{h}_n := \min_{y,z \in \mathcal{X}_n \cup \{x\}, y \neq z} \|y - z\|$, which implies that $\mathcal{X}_{n,r}(x) = \{X \in \mathcal{X}_n : h_n \leq \|X - x\| \leq r\}$ can be replaced by $\tilde{\mathcal{X}}_{n,r}(x) = \{X \in \mathcal{X}_n : \|X - x\| \leq r, X \neq x\}$.

3.3 Choice of τ

A key issue in the use of LDFs for clustering is that it requires a value of τ . Theorem 3.4 suggests that τ should decrease slowly with n , namely $\tau = \tau_n = o(n^{-1/(2kp)})$. However, it does not provide an optimal value of τ when n is small. In this subsection, we develop an

alternative data-driven procedure for choosing τ for a fixed sample size n . Wang [2010] proposes to choose among different clustering algorithms the algorithm that minimizes clustering instability in the sense that clusters vary as little as possible when applying the algorithm to different samples. If only one sample is available clustering instability can be evaluated using crossvalidation. For this, the dataset is divided into three parts: the first and second part are used to build two different clusterings of the sample and the third part is used for evaluating instability based on the two clustering. This procedure is repeated multiple times and the average instability is computed. Finally, the algorithm yielding the smallest average instability is chosen. To make this idea precise, let $\mathcal{X}_n = \{X_1, \dots, X_n\}$ be a sample of i.i.d. random variables from P . We represent the output of the clustering algorithm by a function $\psi : \mathbb{R}^p \times \mathcal{P}(\mathcal{X}_n) \times [0, \infty) \rightarrow \mathbb{N}$, which assigns to every $x \in \mathbb{R}^p$, subsample $\mathcal{X} \subset \mathcal{X}_n$, and $\tau \in [0, \infty)$ a cluster labeled by the natural number $\psi(x, \mathcal{X}, \tau)$. Let $m = \lfloor n/3 \rfloor$ be the biggest integer not larger than $n/3$, $\mathcal{X}_{i_1, \dots, i_m} := \{X_{i_1}, \dots, X_{i_m}\}$, and $\mathcal{X}_{i_{m+1}, \dots, i_{2m}} := \{X_{i_{m+1}}, \dots, X_{i_{2m}}\}$ for some permutation (i_1, i_2, \dots, i_n) of $(1, 2, \dots, n)$. The stability of the clustering algorithm with localization parameter τ w.r.t. the permutation $\mathcal{X}_{i_1, \dots, i_n} := \{X_{i_1}, \dots, X_{i_n}\}$ of \mathcal{X}_n is given by the empirical Hamming distance [Ben-David et al., 2006]

$$\begin{aligned} \mathbf{S}(\mathcal{X}_{i_1, \dots, i_n}, \tau) &= \binom{n-2m}{2}^{-1} \sum_{2m+1 \leq i < j \leq n} \mathbf{I}(\mathbf{I}(\psi(X_i, \mathcal{X}_{i_1, \dots, i_m}, \tau) = \psi(X_j, \mathcal{X}_{i_1, \dots, i_m}, \tau)) \\ &\quad + \mathbf{I}(\psi(X_i, \mathcal{X}_{i_{m+1}, \dots, i_{2m}}, \tau) = \psi(X_j, \mathcal{X}_{i_{m+1}, \dots, i_{2m}}, \tau)) = 1). \end{aligned}$$

Finally, the stability of the clustering algorithm with localization parameter τ w.r.t. the sample \mathcal{X}_n is evaluated by taking the average of $\mathbf{S}(\mathcal{X}_{i_1, \dots, i_n}, \tau)$ over C permutations (i_1, i_2, \dots, i_n) of $(1, 2, \dots, n)$. We refer to this average instability as CV (cross-validation) index. We repeat the above procedure for a several values of $\tau \in [T_1, T_2]$, where $0 < T_1 < T_2 < \infty$, and choose the value that minimizes CV index. In our numerical experiments we choose $n = 500, 1000$, $C = 100$, and draw 100 different samples.

As for β -skeleton and simplicial depths the parameter τ can be chosen as a quantile of the distances between the observations. For more details we refer to Appendix G.

3.4 Numerical results

In this subsection, we describe several numerical experiments to evaluate the performance of the clustering algorithm. We use as a metric the proportion of times the correct number of clusters are identified. Additional metrics are described in Appendix J. We consider the following distributions studied in the literature [Wand and Jones, 1993, Chacón, 2015]

in two dimensions: (H) Bimodal IV, (K) Trimodal III, #10 Fountain. We also study the behavior in dimension five (Mult. Bimodal and Mult. Quadrifocal) and for circular distributions (Circular Bimodal I-IV and Circular Quadrifocal I-II), where additional complexities arise for identifying the true clusters.

We next turn to the choice of τ for lens depth. As explained previously, we choose τ to be a quantile. To be more precise, let $\mathcal{X}_n = \{X_1, \dots, X_n\}$ be a sample of i.i.d. random variables with distribution P . We notice that choosing the parameter τ for LLD is equivalent to choose a quantile q for the pairwise distances $\|X_i - X_j\|$, $i > j$, $i, j \in \{1, 2, \dots, n\}$. Similar considerations hold for LSD (see Appendix G). Thus, we choose q following the discussion in Subsection 3.3. Specifically, let $q \in [Q_1, Q_2]$ for some suitable $0 < Q_1 < Q_2 < 1$. Since the CV index achieves its minimum at the boundary points $q = 0$ and $q = 1$, we choose Q_1 and Q_2 to be far away from these boundary points. We now illustrate this idea when P is the Mult. Quadrifocal distribution and the sample size is $n = 1000$. Figure 1 shows the CV index (top-left) and number of clusters (top-center) as a function of q . We plot dotted vertical lines at $q = 0.05, 0.35, 0.4, 0.5, 0.6$. On the top-right we show the CV index as a function of the number of clusters. The bottom-left plot is a zoom of the top-left plot over the interval $[Q_1, Q_2]$, where $Q_1 = 0.01$ and $Q_2 = 0.2$. The bottom-center plot shows the boxplot of optimal value of q over that range and the bottom-right plot displays the number of clusters detected when q is the optimal quantile order. Based on this preliminary analysis we conclude that the optimal value of q for LLD lies between 0.01 and 0.1. Thus, we restrict our numerical experiments to values of q in that range (cf. Appendix J and K). Additional analysis shows that some circular distributions require values of q higher than 0.1 (see Figure 4 in Appendix J.2).

Next, we compare LLD and LSD using the clustering algorithm in Theorem 3.4 with KDE using both the above clustering algorithm and mean shift algorithm of Fukunaga and Hostetler [1975] abbreviated as KDE-“ms”. We emphasize here that by KDE we mean implementation with our algorithm. We also compare with two recent clustering algorithms, which are a combination of mixture model clustering [Fraley and Raftery, 2002] and modal clustering [Chacón, 2015]: (i) mixture model modal merging (M MMM) and (ii) mixture model modal clustering (M MMC). For more details we refer to Chacón [2019] or Appendix J.2. Our simulation results are based on a sample size of 1000 and 100 numerical experiments. For more details on the numerical implementation and the experimental setting we refer to Appendices G, J, and K.

Number of times the true clusters are detected correctly			
	(H) Bimodal IV	(K) Trimodal III	#10 Fountain

MMMM	(0) 100 (0)	(0) 100 (0)	(0) 99 (1)
MMMC	(0) 100 (0)	(0) 100 (0)	(0) 99 (1)
KDE	(0) 100 (0)	(21) 73 (6)	(0) 100 (0)
KDE-" ms "	(0) 99 (1)	(15) 77 (8)	(0) 79 (21)
LLD	(0) 83 (17)	(14) 79 (7)	(0) 100 (0)
LSD	(0) 85 (15)	(13) 75 (12)	(0) 100 (0)
	Bimodal	Mult. Bimodal	Mult. Quadrinodal
MMMM	(0) 100 (0)	(0) 100 (0)	(0) 100 (0)
MMMC	(0) 100 (0)	(0) 100 (0)	(0) 100 (0)
KDE	(0) 99 (1)	(0) 61 (39)	(1) 61 (38)
KDE-" ms "	(0) 97 (3)	(0) 18 (82)	(0) 25 (75)
LLD	(0) 99 (1)	(0) 99 (1)	(0) 100 (0)
LSD	(0) 100 (0)	(12) 63 (25)	(77) 18 (5)
	Circular Bimodal I	Circular Bimodal II	Circular Bimodal III
MMMM	(0) 0 (100)	(0) 0 (100)	(0) 0 (100)
MMMC	(0) 0 (100)	(0) 0 (100)	(0) 0 (100)
KDE	(0) 55 (45)	(0) 9 (91)	(0) 17 (83)
KDE-" ms "	(0) 18 (82)	(0) 0 (100)	(0) 4 (96)
LLD	(0) 74 (26)	(0) 43 (57)	(0) 43 (57)
LSD	(0) 95 (5)	(0) 74 (26)	(0) 73 (27)
	Circular Bimodal IV	Circular Quadrinodal I	Circular Quadrinodal II
MMMM	(0) 0 (100)	(99) 1 (0)	(0) 0 (100)
MMMC	(0) 0 (100)	(99) 1 (0)	(0) 0 (100)
KDE	(0) 2 (98)	(83) 14 (3)	(85) 12 (3)
KDE-" ms "	(0) 0 (100)	(68) 20 (12)	(63) 24 (13)
LLD	(0) 0 (100)	(6) 18 (76)	(7) 16 (77)
LSD	(0) 1 (99)	(65) 32 (3)	(80) 17 (3)

Table 1: Number of times that the procedure identifies the true number of clusters for the densities (H) Bimodal IV, (K) Trimodal III , #10 Fountain, Bimodal, Mult. Bimodal, Mult. Quadrinodal, Circular Bimodal I-IV, and Circular Quadrimodal I-II. In parentheses the number of times the procedure identifies a lower number of clusters (on the left) and a higher number of clusters (on the right).

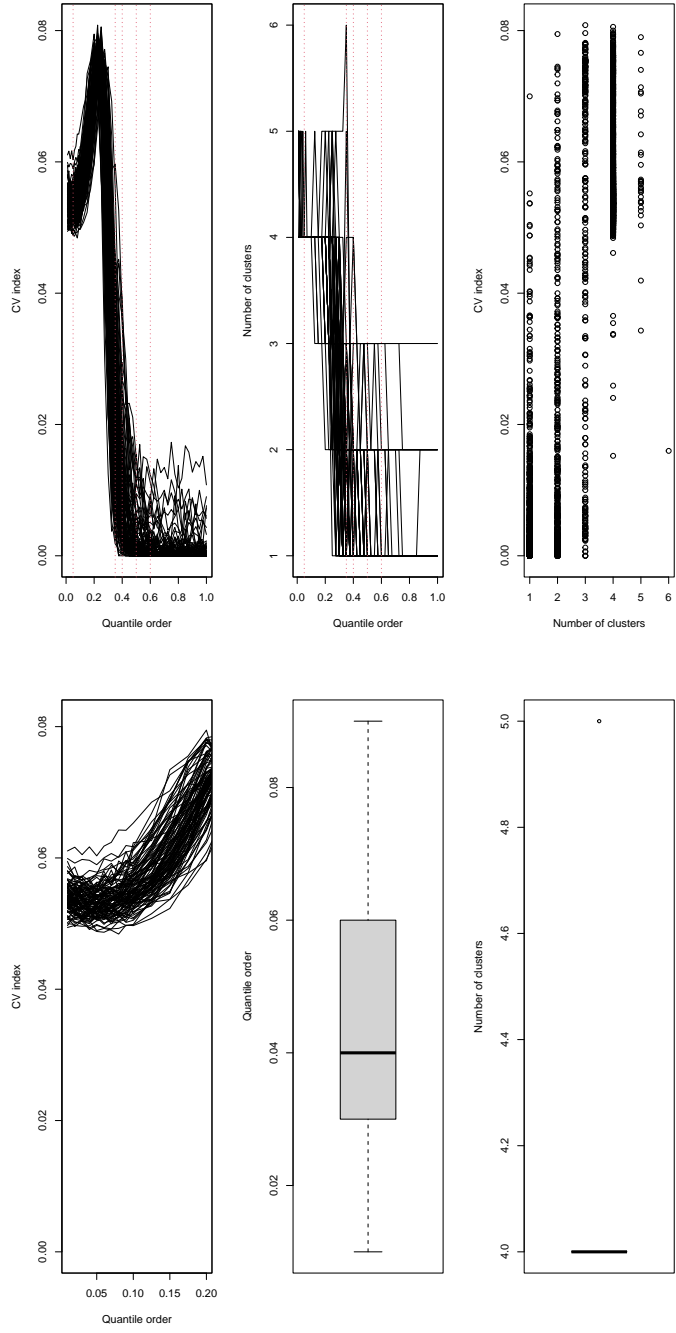


Figure 1: For 100 replications with $n = 1000$ samples for the Mult. Quadrimodal distribution and LLD we plot (i) CV index as a function of the quantile order q (top-left), (ii) number of clusters as a function of q (top-center), (iii) CV index as a function of the number of clusters (top-right), (iv) CV index as a function of $q \in [0.01, 0.2]$ (bottom-left), (v) boxplot of the optimal quantile q in the range $[0.01, 0.2]$ (bottom-center), and (vi) boxplot of the number of clusters for the optimal q (bottom-right).

Based on the results, we notice that our clustering algorithm performs adequately and outperforms in some cases compared with KDE-"`ms`". As expected, MMMM and MMMC are the best for mixture densities. However, they perform poorly for circular densities. More extensive numerical experiments are included in Appendices J and K. Description of the R code used for simulations is included in Appendix J.1.

3.5 Data analysis

We evaluate the performance of our methodology on Iris dataset and Seeds dataset, both available from the UCI machine learning repository (<http://archive.ics.uci.edu/ml/>). In the Iris dataset the sample size is $n = 150$ and there are three classes (Iris Setosa, Iris Versicolour, and Iris Virginica) with four measurements each (sepal length, sepal width, petal length, and petal width). Our algorithm using LDFs and KDE correctly identifies the true number of clusters while KDE-"`ms`" overestimates the number of clusters. Next, turning to Seeds dataset, the sample size is $n = 210$ and there are three clusters relating to three varieties of wheat (Kama, Rosa and Canadian). The data are in seven dimensions representing geometric parameters (continuous) of wheat kernels. Our algorithm correctly identified the three clusters while KDE-"`ms`" (with built-in bandwidth) overestimated the number of clusters. Evaluation of the algorithm on these data sets with respect to other metrics are in Appendix J.

4 Proofs

In this section, we provide detailed proofs of Theorems 2.2-2.4 and Theorem 3.4. The proofs of preliminary results and Theorem 2.1 are given in Appendix A.

Proof of Theorem 2.2. Recall that $\mathcal{H}_G = \{h_\tau^{(G)}(x; \cdot) : x \in \mathbb{R}^p, \tau \in [0, \infty]\}$ and let $\mathcal{H}_{G,1} := \{h_\tau^{(G,1)}(x; \cdot) : x \in \mathbb{R}^p, \tau \in [0, \infty]\}$. We will show that

$$\sup_{h^{(G)} \in \mathcal{H}_G} \left| \int h^{(G)}(x_1, \dots, x_{k_G}) dP(x_1) \dots dP(x_{k_G}) - \binom{n}{k_G}^{-1} \sum_{1 \leq i_1 < \dots < i_{k_G} \leq n} h^{(G)}(X_{i_1}, \dots, X_{i_{k_G}}) \right|$$

converges to 0 with probability one. To this end, we use Corollary 3.3 of Arcones and Giné [1993]. Since \mathcal{H}_G is a VC-subgraph class by hypothesis it is enough to verify that (i) $\sup_{h^{(G)} \in \mathcal{H}_G} |h^{(G)}(\cdot)| < \infty$ and $\sup_{h^{(G,1)} \in \mathcal{H}_{G,1}} |h^{(G,1)}(\cdot)| < \infty$ and (ii) \mathcal{H}_G is image admissible Suslin [Dudley, 2014, p. 186]. This then shows that \mathcal{H}_G is a measurable class [Arcones and Giné, 1993, p. 1497] with a bounded envelope. To this end, by (A.1), $\sup_{h^{(G)} \in \mathcal{H}_G} |h^{(G)}(\cdot)| \leq l_G$, $\sup_{h^{(G,1)} \in \mathcal{H}_{G,1}} |h^{(G,1)}(\cdot)| \leq l_G$, and hence (i) holds. Turning to (ii), we show that the

function $\mathbf{i}_G : [0, \infty] \times \mathbb{R}^p \times (\mathbb{R}^p)^{k_G} \rightarrow \mathbb{R}$ given by $\mathbf{i}_G(\tau; x; x_1, \dots, x_{k_G}) = h_\tau^{(G)}(x; x_1, \dots, x_{k_G})$ is Borel measurable. To see this, let $F_G : (0, \infty) \times \mathbb{R}^p \times (\mathbb{R}^p)^{k_G} \rightarrow (\mathbb{R}^p)^{k_G}$ be given by $F_G(\tau; x; x_1, \dots, x_{k_G}) = \left(\frac{x_1 - x}{\tau}, \dots, \frac{x_{k_G} - x}{\tau} \right)^\top$. Since $G(\cdot)$ is Borel measurable and $F_G(\cdot)$ is continuous, $h_{(\cdot)}^{(G)}(\cdot; \cdot) = G(F_G(\cdot))$ is Borel measurable. In particular, $h_\tau^{(G)}(\cdot; \cdot)$ is Borel measurable for all $\tau \in (0, \infty)$ and $h_0^{(G)}(\cdot; \cdot)$ and $h_\infty^{(G)}(\cdot; \cdot)$ are Borel measurable because they are limit of Borel measurable functions. It follows that, for all $A \in \mathcal{B}(\mathbb{R})$,

$$\begin{aligned} \mathbf{i}_G^{-1}(A) &= (F_G^{-1}(G^{-1}(A)) \cup (\{0\} \times (h_0^{(G)})^{-1}(A)) \cup (\{\infty\} \times (h_\infty^{(G)})^{-1}(A)) \\ &\in \mathcal{B}([0, \infty]) \times \mathcal{B}(\mathbb{R}^p) \times \mathcal{B}((\mathbb{R}^p)^{k_G}) = \mathcal{B}([0, \infty] \times \mathbb{R}^p \times (\mathbb{R}^p)^{k_G}), \end{aligned}$$

that is, $\mathbf{i}_G(\cdot)$ is Borel measurable. Hence, by Dudley [2014, p. 186], the class \mathcal{H}_G is image admissible Suslin via the onto Borel measurable map $\mathbf{e}_G : [0, \infty] \times \mathbb{R}^p \rightarrow \mathcal{H}_G$ given by $\mathbf{e}_G(\tau; x) = h_\tau^{(G)}(x; \cdot)$. \blacksquare

Before proving Theorem 2.3 and Theorem 2.4, we recall that, given a pseudometric space (\mathcal{H}, d) , the ϵ -covering number of \mathcal{H} w.r.t. the pseudodistance d , $N(\mathcal{H}, d, \epsilon)$, is the minimum number of balls with radius at most ϵ required to cover \mathcal{H} .

Proof of Theorem 2.3. To prove Theorem 2.3, we will verify the conditions of Theorem 4.9 in Arcones and Giné [1993]. To this end, first let $\mathcal{H}_G^{(T)} := \{h_\tau^{(G)}(x; \cdot) : (x, \tau) \in T\} \subset \mathcal{H}_G$ and $\mathcal{H}_{G,1}^{(T)} := \{h_\tau^{(G,j)}(x; \cdot) : (x, \tau) \in T\} \subset \mathcal{H}_{G,1}$. As in the proof of Theorem 2.2 where $[0, \infty] \times \mathbb{R}^p$ is replaced by T with the corresponding subspace topology, we see that $\mathcal{H}_G^{(T)}$ is image admissible Suslin [Dudley, 2014, p. 186]. Also, using (A.1), it holds that $\sup_{h \in \mathcal{H}_G^{(T)}} |h(\cdot)| \leq l_G$ and $\sup_{h^{(1)} \in \mathcal{H}_{G,1}^{(T)}} |h^{(1)}(\cdot)| \leq l_G$. This then shows that $\mathcal{H}_G^{(T)}$ is a measurable class with a bounded envelope and (ii) of Theorem 4.9 in Arcones and Giné [1993] holds. To verify (iii) in Arcones and Giné [1993] we appeal to Lemma 4.4 and (4.2) in Alexander [1987] concerning the covering number $N(\mathcal{H}_G^{(T)}, d_{L^2(\mathcal{H}_G^{(T)}, P)}, \cdot)$ of $\mathcal{H}_G^{(T)}$ with respect to the L^2 -distance, $d_{L^2(\mathcal{H}_G^{(T)}, P)}$, given by

$$d_{L^2(\mathcal{H}_G^{(T)}, P)}^2((x, \tau), (y, \nu)) = \int (h_\tau^{(G)}(x; x_1, \dots, x_k) - h_\nu^{(G)}(y; x_1, \dots, x_k))^2 \prod_{i=1}^k dP(x_i).$$

For this, we observe that $\mathcal{H}_G^{(T)}$ is a VC-subgraph class of functions. Thus to complete the proof, we need to verify (i) in Arcones and Giné [1993]. To this end, we need to show: (a) the finite dimensional distributions of $\sqrt{n}(LGD_n(x, \tau, P) - LGD(x, \tau, P))$ converge to a multivariate normal distribution and (b) for each (x, τ) , the limiting normal random variable $\{W(x, \tau)\}_{(x, \tau) \in T}$ admits a version whose sample paths are all bounded and uniformly

continuous with respect to the distance $d_{\mathcal{H}_{G,1}^{(T)}, P}^2$ on $\mathcal{H}_{G,1}^{(T)}$ given by

$$d_{\mathcal{H}_{G,1}^{(T)}, P}^2((x, \tau), (y, \nu)) = \int (h_\tau(x; x_1) - h_\nu(y; x_1))^2 dP(x_1) - (LGD(x, \tau) - LGD(y, \nu))^2,$$

where we identify a function $h_\tau(x; \cdot)$ for $(x, \tau) \in T$ with its parameter (x, τ) . In this sense, $d_{\mathcal{H}_{G,1}^{(T)}, P}^2$ is a metric on T . Since $W(x, \tau)$ is Gaussian, we can apply Giné and Nickl [2016, Theorem 2.3.7] with $T = T$ and $d = d_{\mathcal{H}_{G,1}^{(T)}, P}^2$. First, note that $\{W(x, \tau)\}_{(x, \tau) \in T}$ is a sub-Gaussian process relative to $d_{\mathcal{H}_{G,1}^{(T)}, P}^2$. Indeed, using Proposition A.1 in Appendix A, for $(x, \tau), (y, \nu) \in T$, $(W(x, \tau), W(y, \nu))^\top$ has a bivariate normal distribution with mean $(0, 0)^\top$ and covariance matrix

$$\begin{pmatrix} E[(\tilde{h}_\tau^{(G,1)}(x; X_1))^2] & \gamma((x, \tau), (y, \nu)) \\ \gamma((y, \nu), (x, \tau)) & E[(\tilde{h}_\nu^{(G,1)}(y; X_1))^2] \end{pmatrix}.$$

It follows that $W(x, \tau) - W(y, \nu)$ is normally distributed with mean 0 and variance $E[(\tilde{h}_\tau^{(G,1)}(x; X_1))^2] + E[(\tilde{h}_\nu^{(G,1)}(y; X_1))^2] - 2\gamma((x, \tau), (y, \nu)) = d_{\mathcal{H}_{G,1}^{(T)}, P}^2((x, \tau), (y, \nu))$. Therefore, for all $\alpha \in \mathbb{R}$

$$E\left[\exp\left(\alpha(W(x, \tau) - W(y, \nu))\right)\right] = \exp\left(\frac{\alpha^2}{2} d_{\mathcal{H}_{G,1}^{(T)}, P}^2((x, \tau), (y, \nu))\right)$$

and the process $\{W(x, \tau)\}_{(x, \tau) \in T}$ is sub-Gaussian with respect to $d_{\mathcal{H}_{G,1}^{(T)}, P}^2$. We next verify the integrability condition for the metric entropy. To this end, notice that, for $(x, \tau), (y, \nu) \in T$, the L^2 -distance on $\mathcal{H}_{G,1}^{(T)}$, $d_{L^2(\mathcal{H}_{G,1}^{(T)}, P)}$ is given by

$$d_{L^2(\mathcal{H}_{G,1}^{(T)}, P)}^2((x, \tau), (y, \nu)) = \int (h_\tau^{(G,1)}(x; x_1) - h_\nu^{(G,1)}(y; x_1))^2 dP(x_1).$$

Now using yet another application of Lemma 4.4 of Alexander [1987], it follows that there are constants $C_1, C_2 > 1$ such that

$$N(\mathcal{H}_G^{(T)}, d_{L^2(\mathcal{H}_G^{(T)}, P)}, \sqrt{\epsilon}) \leq \left(\frac{C_1}{\sqrt{\epsilon}}\right)^{C_2}.$$

By Jensen's inequality, it follows that

$$d_{L^2(\mathcal{H}_{G,1}^{(T)}, P)}((x, \tau), (y, \nu)) \leq d_{L^2(\mathcal{H}_G^{(T)}, P)}((x, \tau), (y, \nu)),$$

which in turn, implies that

$$N(\mathcal{H}_{G,1}^{(T)}, d_{L^2(\mathcal{H}_{G,1}^{(T)}, P)}, \sqrt{\epsilon}) \leq N(\mathcal{H}_G^{(T)}, d_{L^2(\mathcal{H}_G^{(T)}, P)}, \sqrt{\epsilon}) \leq \left(\frac{C_1}{\sqrt{\epsilon}}\right)^{C_2}.$$

Thus, for any $0 < \epsilon \leq 1$,

$$\begin{aligned} N(\mathcal{H}_{G,1}^{(T)}, d_{\mathcal{H}_{G,1}^{(T)}, P}^2, \epsilon) &\leq N(\mathcal{H}_{G,1}^{(T)}, d_{L^2(\mathcal{H}_{G,1}^{(T)}, P)}^2, \epsilon) = N(\mathcal{H}_{G,1}^{(T)}, d_{L^2(\mathcal{H}_{G,1}^{(T)}, P)}, \sqrt{\epsilon}) \\ &\leq \left(\frac{C_1}{\sqrt{\epsilon}}\right)^{C_2} \leq \left(\frac{C_1}{\epsilon}\right)^{C_2}. \end{aligned} \quad (4.1)$$

It follows that

$$\int_0^1 \sqrt{\log(N(\mathcal{H}_{G,1}^{(T)}, d_{\mathcal{H}_{G,1}^{(T)}, P}^2, \epsilon)))} d\epsilon \leq \sqrt{C_2} \int_0^1 \sqrt{\log(C_1) - \log(\epsilon)} d\epsilon$$

Now, using $a, b \geq 0$, $\sqrt{a+b} \leq \sqrt{a} + \sqrt{b}$, it follows that the left hand side (LHS) is bounded above by $\sqrt{C_2}$ times

$$\begin{aligned} \sqrt{\log(C_1)} + \int_0^{e^{-1}} \sqrt{-\log(\epsilon)} d\epsilon + \int_{e^{-1}}^1 \sqrt{-\log(\epsilon)} d\epsilon &\leq \sqrt{\log(C_1)} - \int_0^{e^{-1}} \log(\epsilon) d\epsilon + 1 - e^{-1} \\ &= \sqrt{\log(C_1)} + e^{-1} + 1 < \infty. \end{aligned}$$

The proof finally follows from Proposition A.1 in Appendix A. ■

Proof of Theorem 2.4. We will show that there are constants $1 < C_{G,0}, C_{G,1}, C_{G,2} < \infty$ such that

$$P^{\otimes n}(\sqrt{n}M_{G,n} \geq t) \leq D_G(n, t),$$

where

$$M_{G,n} := \sup_{h^{(G)} \in \mathcal{H}_G} \left| \int h(x_1, \dots, x_{k_G}) \prod_{j=1}^{k_G} dP(x_j) - \binom{n}{k_G}^{-1} \sum_{1 \leq i_1 < \dots < i_{k_G} \leq n} h^{(G)}(X_{i_1}, \dots, X_{i_{k_G}}) \right|.$$

To this end, we verify the conditions of Theorem 5 in Arcones [1995]. By (i)-(ii) in the proof of Theorem 2.2, it follows that \mathcal{H}_G is a uniformly bounded, measurable [Arcones and Giné, 1993, p. 1497], VC-subgraph class, where the bounding constant is l_G . We show that this implies conditions (i)-(iii) of Theorem 5 in Arcones [1995]. Condition (i) is clear. Let

$$d_{L^2(\mathcal{H}_G, P)}^2((x, \tau), (y, \nu)) = \int (h_\tau^{(G)}(x; x_1, \dots, x_{k_G}) - h_\nu^{(G)}(y; x_1, \dots, x_{k_G}))^2 \prod_{j=1}^{k_G} dP(x_j)$$

and

$$d_{L^2(\mathcal{H}_{G,1}, P)}^2((x, \tau), (y, \nu)) = \int (h_\tau^{(G,1)}(x; x_1) - h_\nu^{(G,1)}(y; x_1))^2 dP(x_1).$$

By Jensen's inequality, it holds that

$$d_{L^2(\mathcal{H}_{G,1}, P)}((x, \tau), (y, \nu)) \leq d_{L^2(\mathcal{H}_G, P)}((x, \tau), (y, \nu)).$$

Using Lemma 4.4 and (4.2) in Alexander [1987], we see that there are constants $C_{G,1}, C_{G,2} > 1$ such that

$$N(\mathcal{H}_{G,1}, d_{L^2(\mathcal{H}_{G,1}^{(T)}, P)}, \epsilon) \leq N(\mathcal{H}_G, d_{\mathcal{H}_G}, \epsilon) \leq \left(\frac{C_{G,1}}{\epsilon}\right)^{C_{G,2}}. \quad (4.2)$$

Thus, condition (ii) holds true. Finally, (4.2) and [Arcones, 1995, (3.3) and p. 245] imply that there is a constant $C_{G,0}$ such that (iii) holds true. ■

Proof of Theorem 3.4. First, notice that, for all $j = 1, \dots, j^*$, $Y_{n,r,j} \in \mathcal{X}_n$ and, by (3.5), $Y_{n,r,j} \neq Y_{n,r,l}$, for all $l < j$. Hence, $j^* \leq n$. The proof of the remaining part is divided into four steps. In the first step below we introduce few notations and preliminary calculations.

Step 0. Let $\alpha_1 := f(x)$ and $0 < \alpha_2 < \alpha_1$. We recall from Appendix E that the solution $u_x(t)$ of (3.2) exists for $t \in (a, \infty)$, $a < 0$, and define $G_x := \{u_x(t) : t \in [0, \infty)\}$. Since $x \in R^{\alpha_1}$ and $f(u_x(\cdot))$ is monotonically non-decreasing, we have that $\overline{G}_x = G_x \cup \{m_i\} \subset C(m_i) \cap R^{\alpha_1} \subset C(m_i) \cap \dot{R}^{\alpha_2}$. $C(m_i)$ is open by Proposition E.1 in Appendix E and therefore there exists $\xi_1 > 0$ such that (i) $\alpha_3 := \sup_{y \in (C(m_i) \setminus (C(m_i))^{-2\xi_1})} f(y) < f(m_i)$ and (ii) $(G_x)^{+2\xi_1} \subset (C(m_i) \cap R^{\alpha_2})^{-2\xi_1}$. Let $\max(\alpha_2, \alpha_3) < \alpha^* \leq \alpha < f(m_i)$ and $0 < \xi \leq \xi_1$ such that

$$\overline{B}_{4\xi}(m_i) \subset R^\alpha \cap C(m_i). \quad (4.3)$$

Let $K_\xi := R^{\alpha_2} \cap \overline{(C(m_i))^{-\xi}}$. It holds that $(G_x)^{+\xi} \subset K_\xi$, which implies that, for all $\epsilon > 0$,

$$(G_x)^{+\xi} \setminus B_\epsilon(m_i) \subset K_\xi \setminus B_\epsilon(m_i). \quad (4.4)$$

Also, since $\alpha > \alpha_3$, $R^\alpha \cap C(m_i) = R^\alpha \cap (C(m_i))^{-2\xi_1}$, implying that

$$\overline{B}_{4\xi}(m_i) \subset K_\xi. \quad (4.5)$$

For $z \in \mathbb{R}^p$ with $\nabla f(z) \neq 0$, let

$$w(z) := \nabla f(z) / \|\nabla f(z)\| \quad (4.6)$$

and, for $0 < r \leq \xi$ and $j^* \geq 0$ let

$$\begin{aligned} \tilde{G}_{x,j^*,r} &:= \left\{ \{y_{r,j}\}_{j=0}^{j^*} : y_{r,0} = x \text{ and, recursively, } y_{r,j+1} = y_{r,j} + h_j v_j \right. \\ &\quad \left. \text{for some } (h_j, v_j) \in (0, r] \times (S^{p-1} \cap \overline{B}_r(w(y_{r,j}))) \right\}. \end{aligned} \quad (4.7)$$

Step 1. We show that, for small r , every sequence $\{y_{r,j}\}_{j=0}^{j^*} \in \tilde{G}_{x,j^*,r}$ either remains in $(G_x)^{+\xi} \setminus B_\xi(m_i)$ or, for some $j \in \{0, \dots, j^*\}$, $y_{r,j} \in \overline{B}_{4\xi}(m_i)$. To this end, we suppose w.l.o.g. that

$$\|x - m_i\| > 2\xi. \quad (4.8)$$

If (4.8) does not hold, then $y_{r,0} = x \in \overline{B}_{2\xi}(m_i) \subset \overline{B}_{4\xi}(m_i)$. We now define some quantities that are used in the proof of this fact. Specifically, let $t_0 := 0$ and, recursively, $t_{j+1} = \sum_{l=0}^j h_l / \|\nabla f(y_{r,l})\|$. Also, let $0 < \alpha_4(\xi) < f(m_i)$ such that $R^{\alpha_4(\xi)} \cap C(m_i) \subset B_\xi(m_i)$, $t^*(\xi) := \inf\{t \in [0, \infty) : u_x(t) \in R^{\alpha_4(\xi)}\}$, $\tilde{t}^*(\xi) := \inf\{t \in [0, t^*(\xi)] : u_x(t) \in \overline{B}_{2\xi}(m_i)\}$, $\tilde{K}_\xi := K_\xi \setminus \dot{R}^{\alpha_4(\xi)}$, $c_1(\xi) := \inf_{y \in \tilde{K}_\xi} \|\nabla f(y)\| > 0$ and $c_2(\xi) := \sup_{y \in \tilde{K}_\xi} \|\nabla f(y)\| > 0$. Since $\nabla f(\cdot)$ is differentiable, it is locally Lipschitz; hence, Lipschitz in \tilde{K}_ξ . Denote by L the Lipschitz constant. Let $\tilde{j}^* := \max\{j \in \{0, \dots, j^*\} : t_j \leq \tilde{t}^*(\xi)\}$ and, using the continuity of $u_x(\cdot)$, let $0 < r_1 \leq \xi$, such that

$$r_1 \tilde{t}^*(\xi) \left(c_2(\xi) + \sup_{t \in [0, \tilde{t}^*(\xi)]} \|u''_x(t)\| / (2c_1(\xi)) \right) \exp(L\tilde{t}^*(\xi)) \leq \xi \quad (4.9)$$

and, for all $0 < r \leq r_1$,

$$\|u_x(\tilde{t}(\xi) - r/c_1(\xi)) - u_x(\tilde{t}(\xi))\| \leq \xi. \quad (4.10)$$

We show that, for all $j = 0, \dots, \tilde{j}^*$ and $0 < r \leq r_1$, $y_{r,j} \in (G_x)^{+\xi} \setminus B_\xi(m_i)$. We recall that, by (4.4), since $R^{\alpha_4(\xi)} \cap C(m_i) \subset B_\xi(m_i)$, $(G_x)^{+\xi} \setminus B_\xi(m_i) \subset \tilde{K}_\xi$. First, notice that $u_x(t_0) = x$ and, by (4.8), it holds that $y_{r,0} = x \in (G_x)^{+\xi} \setminus B_\xi(m_i)$. We now suppose by induction that, for $j \geq 1$, $y_{r,j-1} \in (G_x)^{+\xi} \setminus B_\xi(m_i)$ and show that $y_{r,j} \in (G_x)^{+\xi} \setminus B_\xi(m_i)$, thus proving the statement. Since $u'_x(t) = \nabla f(u_x(t))$ and $f(\cdot)$ is three times continuously differentiable, then so is $u_x(\cdot)$. By Taylor theorem with Lagrange's form of remainder, there exists $t_{j-1} \leq \tilde{t}_{j-1} \leq t_j$ such that

$$u_x(t_j) = u_x(t_{j-1}) + \frac{h_{j-1}}{\|\nabla f(y_{r,j-1})\|} \nabla f(u_x(t_{j-1})) + \frac{h_{j-1}^2}{2 \|\nabla f(y_{r,j-1})\|^2} u''_x(\tilde{t}_{j-1}).$$

It follows that

$$\begin{aligned} (y_{r,j} - u_x(t_j)) &= (y_{r,j-1} - u_x(t_{j-1})) + h_{j-1}(v_{j-1} - w(y_{r,j-1})) \\ &\quad + \frac{h_{j-1}}{\|\nabla f(y_{r,j-1})\|} (\nabla f(y_{r,j-1}) - \nabla f(u_x(t_{j-1}))) \\ &\quad - \frac{h_{j-1}^2}{2 \|\nabla f(y_{r,j-1})\|^2} u''_x(\tilde{t}_{j-1}). \end{aligned}$$

Now, we use the Lipschitz property of $\nabla f(\cdot)$ and get

$$\begin{aligned} \|y_{r,j} - u_x(t_j)\| &\leq \left(1 + \frac{h_{j-1}L}{\|\nabla f(y_{r,j-1})\|}\right) \|y_{r,j-1} - u_x(t_{j-1})\| + r_1 h_{j-1} \\ &\quad + \frac{h_{j-1}^2}{2 \|\nabla f(y_{r,j-1})\|^2} \sup_{t \in [0, \tilde{t}^*(\xi)]} \|u''_x(t)\|. \end{aligned}$$

We now apply Lemma A.7 in Appendix A with $a_j = \|y_{r,j} - u_x(t_j)\|$,

$$b_j = r_1 h_j + \frac{h_j^2}{2 \|\nabla f(y_{r,j})\|^2} \sup_{t \in [0, \tilde{t}^*(\xi)]} \|u''_x(t)\|,$$

$c_j = \frac{h_j L}{\|\nabla f(y_{r,j})\|}$ and, using (4.9) and $t_j \leq \tilde{t}^*(\xi)$, we get that $\|y_{r,j} - u_x(t_j)\|$ is bounded above by

$$\begin{aligned} &\left(r_1 \sum_{l=0}^{j-1} h_l + \sum_{l=0}^{j-1} \frac{h_l^2}{2 \|\nabla f(y_{r,l})\|^2} \sup_{t \in [0, \tilde{t}^*(\xi)]} \|u''_x(t)\|\right) \exp\left(L \sum_{l=1}^{j-1} \frac{h_l}{\|\nabla f(y_{r,l})\|}\right) \\ &\leq r_1 t_j \left(c_2(\xi) + \sup_{t \in [0, \tilde{t}^*(\xi)]} \|u''_x(t)\| / (2c_1(\xi))\right) \exp(Lt_j) \leq \xi. \end{aligned}$$

It follows that $y_{r,j} \in (G_x)^{+\xi}$. Moreover, $t_j \leq \tilde{t}^*(\xi)$ implies that $\|m_i - u_x(t_j)\| \geq 2\xi$. Hence,

$$\|m_i - y_{r,j}\| \geq \|m_i - u_x(t_j)\| - \|u_x(t_j) - y_{r,j}\| \geq \xi,$$

that is, $y_{r,j} \notin B_\xi(m_i)$. In particular, if $\tilde{j}^* = j^*$, then $y_{r,j} \in (G_x)^{+\xi} \setminus B_\xi(m_i)$ for all $j = 0, \dots, j^*$. Next, we show that, if $\tilde{j}^* < j^*$, then $y_{r,\tilde{j}^*} \in \overline{B}_{4\xi}(m_i)$. Since $\tilde{t}^*(\xi) - r_1/c_1(\xi) < t_{\tilde{j}^*+1} - r_1/c_1(\xi) \leq t_{\tilde{j}^*} \leq \tilde{t}^*(\xi)$, by (4.10) it holds that $\|u_x(t_{\tilde{j}^*}) - u_x(\tilde{t}_\xi^*)\| \leq \xi$. Since $u_x(\tilde{t}^*(\xi)) \in \partial B_{2\xi}(m_i)$, we conclude that

$$\|y_{r,\tilde{j}^*} - m_i\| \leq \|y_{r,\tilde{j}^*} - u_x(t_{\tilde{j}^*})\| + \|u_x(t_{\tilde{j}^*}) - u_x(\tilde{t}_\xi^*)\| + \|u_x(\tilde{t}_\xi^*) - m_i\| \leq 4\xi.$$

Step 2. Notice that $\tilde{K}_\xi \cap N_f = \emptyset$. We apply Lemma A.8 in Appendix A with $K = \tilde{K}_\xi$ and get constants $r^* := \min(r_1, r(\tilde{K}_\xi)) > 0$ and $c^* := c(\tilde{K}_\xi) > 0$ such that, for all $x \in \tilde{K}_\xi$ and $(h, v) \in (0, r^*] \times (S^{p-1} \cap \overline{B}_{r^*}(w(x)))$,

$$\nabla_v^h f(x) \geq c^*. \tag{4.11}$$

For $X \in \mathcal{X}_n$ and $x \in S_f$ let $h_{X,x} = \|X - x\|$ and $v_{X,x} = (X - x)/h_{X,x}$. We show the existence of $0 < r_2 \leq r^*$ such that, for all $0 < r \leq r_2$, there exist $n_1, n_2 \in \mathbb{N}$ such that, with probability at least $1 - \eta$, for $n \geq \max(n_1, n_2)$ and $x \in \tilde{K}_\xi$, we have that $\mathcal{X}_{n,r}(x) \neq \emptyset$,

$$\max_{X \in \mathcal{X}_{n,r}(x) \cup \{x\}} f_{\tau_n,n}(X) - f_{\tau_n,n}(x) > 0 \tag{4.12}$$

and

$$X^*(x) := \operatorname{argmax}_{X \in \mathcal{X}_{n,r}(x)} \frac{f_{\tau_n,n}(X) - f_{\tau_n,n}(x)}{\|X - x\|} = \operatorname{argmax}_{X \in \mathcal{X}_{n,r}(x)} \nabla_{v_{X^*(x),x}}^{h_{X^*(x),x}} f_{\tau_n,n}(x)$$

satisfies

$$(h_{X^*(x),x}, v_{X^*(x),x}) \in [h_n, r] \times (S^{p-1} \cap \overline{B}_{r^*}(w(x))). \quad (4.13)$$

To this end, suppose w.l.o.g. that $r^* \leq 1$. Let $d(r^*) := \inf_{y \in \tilde{K}_\xi} \inf_{v \in S^{p-1} \setminus \overline{B}_{r^*}(w(y))} \langle w(y) - v, \nabla f(y) \rangle > 0$ and choose $0 < d^* < d(r^*) / (5 \max_{y \in \tilde{K}_\xi} \|\nabla f(y)\|)$. Notice that, since $d(r^*) \leq \min_{y \in \tilde{K}_\xi} \|\nabla f(y)\| r^*$, we have $d^* < r^*/5 \leq 1/5$. By the mean value theorem, there exists $0 \leq c \leq 1$ such that $\nabla_v^h f(x) = \langle v, \nabla f(x + chv) \rangle$, $x \in \tilde{K}_\xi$. Next, by the uniform continuity of $\nabla f(\cdot)$ over compact sets, we have that $\nabla_v^h f(x)$ converges to $\nabla_v f(x)$ uniformly over $v \in S^{p-1}$ and $x \in \tilde{K}_\xi$. Let $r_3 > 0$ be such that, for all $h \in (0, r_3]$, $v \in S^{p-1}$, and $x \in \tilde{K}_\xi$,

$$|\nabla_v^h f(x) - \nabla_v f(x)| \leq \min_{y \in \tilde{K}_\xi} \|\nabla f(y)\| d^*.$$

Then, for all $x \in \tilde{K}_\xi$ and $v \in S^{p-1} \cap \overline{B}_{d^*}(w(x))$, it holds that

$$\nabla_v f(x) \geq \|\nabla f(x)\| (1 - \|w(x) - v\|) \geq \|\nabla f(x)\| (1 - d^*), \quad (4.14)$$

which implies that, for all $x \in \tilde{K}_\xi$, $h \in (0, r_3]$, and $v \in S^{p-1} \cap \overline{B}_{d^*}(w(x))$,

$$\nabla_v^h f(x) \geq \nabla_v f(x) - \min_{y \in \tilde{K}_\xi} \|\nabla f(y)\| d^* \geq \|\nabla f(x)\| (1 - 2d^*). \quad (4.15)$$

On the other hand, by definition of d^* , we have that, for all $x \in \tilde{K}_\xi$, and $v \in S^{p-1} \setminus \overline{B}_{r^*}(w(x))$,

$$\nabla_v f(x) \leq (1 - 5d^*) \|\nabla f(x)\|,$$

which implies that, for all $x \in \tilde{K}_\xi$, $h \in (0, r_3]$, and $v \in S^{p-1} \setminus \overline{B}_{r^*}(w(x))$,

$$\nabla_v^h f(x) \leq \nabla_v f(x) + \min_{y \in \tilde{K}_\xi} \|\nabla f(y)\| d^* \leq \|\nabla f(x)\| (1 - 4d^*).$$

Now, let $r_2 := \min(r_3, d^*) < r^*$ and $0 < r \leq r_2$. Notice that $(K)^{+r} \subset (K)^{+r^*} \subset (K)^{+r(\tilde{K}_\xi)} \subset S_f$. Using Lemma 3.2 (ii) with $K = \tilde{K}_\xi$ and $h^* = r$, we choose $n_2 \in \mathbb{N}$ such that, for all $n \geq n_2$, with probability at least $1 - \eta/2$,

$$\sup_{h \in [h_n, r]} \sup_{v \in S^{p-1}} \sup_{x \in \tilde{K}_\xi} |\nabla_v^h f_{\tau_n,n}(x) - \nabla_v^h f(x)| < d^* \min_{y \in \tilde{K}_\xi} \|\nabla f(y)\|. \quad (4.16)$$

It follows from (4.15), (4.14), and (4.16) that, with probability at least $1 - \eta/2$, for all $x \in \tilde{K}_\xi$, $h \in [h_n, r]$, and $v \in S^{p-1} \cap \overline{B}_r(w(x))$,

$$\nabla_v^h f_{\tau_n,n}(x) > (1 - 2d^*) \|\nabla f(x)\| - d^* \min_{y \in \tilde{K}_\xi} \|\nabla f(y)\| \geq (1 - 3d^*) \|\nabla f(x)\|, \quad (4.17)$$

and, for all $x \in \tilde{K}_\xi$, $h \in [h_n, r]$, and $v \in S^{p-1} \setminus \overline{B}_{r^*}(w(x))$,

$$\nabla_v^h f_{\tau_n, n}(x) < (1 - 4d^*) \|\nabla f(x)\| + d^* \min_{y \in \tilde{K}_\xi} \|\nabla f(y)\| \leq (1 - 3d^*) \|\nabla f(x)\|. \quad (4.18)$$

Since $d^* < 1/5$, $(1 - 3d^*) \|\nabla f(x)\| > 0$ for all $x \in \tilde{K}_\xi$. We show in **Step 3** below that there exists a constant n_1 such that, with probability at least $1 - \eta/2$, for all $x \in \tilde{K}_\xi$ and $n \geq n_1$, there exists $X \in \mathcal{X}_{n,r}(x)$ such that

$$(h_{X,x}, v_{X,x}) \in [h_n, r] \times (S^{p-1} \cap \overline{B}_r(w(x))). \quad (4.19)$$

In particular, since $P(A \cap B) \geq P(A) + P(B) - 1$ for all $n \geq \max(n_1, n_2)$, (4.16) and (4.19) hold simultaneously with probability at least $1 - \eta$. It follows from (4.17) and (4.18) that, with probability at least $1 - \eta$, for all $x \in \tilde{K}_\xi$,

$$\sup_{(h,v) \in [h_n, r] \times S^{p-1} \setminus \overline{B}_{r^*}(w(x))} \nabla_v^h f_{\tau_n, n}(x) < \nabla_{v_{X,x}}^{h_{X,x}} f_{\tau_n, n}(x) \leq \sup_{(h,v) \in [h_n, r] \times S^{p-1} \cap \overline{B}_r(w(x))} \nabla_v^h f_{\tau_n, n}(x).$$

Thus, we have shown that the finite difference approximation of $f_{\tau_n, n}(\cdot)$ with step $h_{X,x}$ and direction $v_{X,x}$ is larger than all finite difference approximations with step $h \in [h_n, r]$ and directions $v \in S^{p-1} \setminus \overline{B}_{r^*}(w(x))$. (4.13) follows. Also, (4.17) and (4.19) imply (4.12).

Step 3. We show (4.19). To this end, let $0 < s_1 < s_2 < r$ and n_3 be such that $h_n < s_1$ for all $n \geq n_3$. It is enough to show that there exists $n_1 \geq n_3$ such that, for all $n \geq n_1$,

$$P^{\otimes n}([\mathcal{X}_n \cap D_{s_1, s_2}(x) \neq \emptyset \ \forall x \in \tilde{K}_\xi]) \geq 1 - \eta/2,$$

where $D_{s_1, s_2}(x) := A_{s_1, s_2}(x) \cap C_{s_2}(x)$, $A_{s_1, s_2}(x) := \overline{B}_{s_2}(x) \setminus B_{s_1}(x)$, and

$$C_{s_2}(x) := \left\{ y \in \mathbb{R}^p \setminus \{x\} : \left\| \frac{y - x}{\|y - x\|} - w(x) \right\| \leq s_2 \right\}.$$

Let $0 < \epsilon_1 < \frac{s_2 - s_1}{2}$. We first notice that

$$A_{s_1 + \epsilon_1, s_2 - \epsilon_1}(x) \subset \cap_{z \in B_{\epsilon_1}(x)} A_{s_1, s_2}(z). \quad (4.20)$$

Indeed, $y \in A_{s_1 + \epsilon_1, s_2 - \epsilon_1}(x)$ satisfies $s_1 + \epsilon_1 \leq \|y - x\| \leq s_2 - \epsilon_1$. Therefore, for all $z \in B_{\epsilon_1}(x)$, it holds that

$$s_1 \leq \|y - x\| - \|x - z\| \leq \|y - z\| \leq \|y - x\| + \|x - z\| \leq s_2,$$

that is, $y \in A_{s_1, s_2}(z)$. Now, let $h^* > 0$ such that $(\tilde{K}_\xi)^{+h^*}$ does not contain stationary points of $f(\cdot)$. Since $w(\cdot)$ is uniformly continuous in $(\tilde{K}_\xi)^{+h^*}$, there exists $\epsilon_2 \in (0, h^*]$ such that, for all $x \in K$,

$$\sup_{y \in B_{\epsilon_2}(x)} \|w(x) - w(y)\| \leq \epsilon_1/2. \quad (4.21)$$

Suppose w.l.o.g. that $\epsilon_2 \leq \min(1, \frac{s_1+\epsilon_1}{4})\epsilon_1$. We show that

$$D_{s_1+\epsilon_1, s_2-\epsilon_1}(x) \subset \cap_{z \in B_{\epsilon_2}(x)} D_{s_1, s_2}(z). \quad (4.22)$$

To this end, let $y \in D_{s_1+\epsilon_1, s_2-\epsilon_1}(z)$. By (4.20), it holds that $y \in \cap_{z \in B_{\epsilon_2}(x)} A_{s_1, s_2}(z)$. We need to show that $y \in \cap_{z \in B_{\epsilon_2}(x)} C_{s_2}(z)$. Since, for all $z \in B_{\epsilon_2}(x)$,

$$\left\| \frac{y-z}{\|y-z\|} - \frac{y-x}{\|y-x\|} \right\| \leq 2 \frac{\|z-x\|}{\|y-z\|} \leq \frac{2\epsilon_2}{s_1 + \epsilon_1} \leq \epsilon_1/2,$$

using the triangle inequality and (4.21), we have that

$$\left\| \frac{y-z}{\|y-z\|} - w(z) \right\| \leq \left\| \frac{y-z}{\|y-z\|} - \frac{y-x}{\|y-x\|} \right\| + \left\| \frac{y-x}{\|y-x\|} - w(x) \right\| + \|w(x) - w(z)\| \leq s_2.$$

(4.22) follows. Notice that, for all $x \in \tilde{K}_\xi$, $\lambda(D_{s_1+\epsilon_1, s_2-\epsilon_1}(x)) = \lambda(D_{s_1+\epsilon_1, s_2-\epsilon_1}(0)) =: \tilde{\Lambda} > 0$. Now, by the compactness of $\tilde{K}_\xi \subset \cup_{x \in \tilde{K}_\xi} B_{\epsilon_2}(x)$, there exist $x_1, \dots, x_q \in \tilde{K}_\xi$ such that $\tilde{K}_\xi \subset \cup_{l=1}^q B_{\epsilon_2}(x_l)$. It follows from (4.22) that, for all $z \in \tilde{K}_\xi$, there exists x_l such that $z \in B_{\epsilon_2}(x_l)$ and $D_{s_1+\epsilon_1, s_2-\epsilon_1}(x_l) \subset D_{s_1, s_2}(z)$. Therefore, it is enough to show that there exists $n_1 \geq n_3$ such that, for all $n \geq n_1$,

$$P^{\otimes n}([\mathcal{X}_n \cap D_{s_1+\epsilon_1, s_2-\epsilon_1}(x_l) \neq \emptyset \ \forall l \in \{1, \dots, q\}]) \geq 1 - \eta/2.$$

To this end, notice that $\cup_{l=1}^q D_{s_1+\epsilon_1, s_2-\epsilon_1}(x_l) \subset (\tilde{K}_\xi)^{+r} \subset S_f$ and let $\alpha_0 := \min_{y \in (\tilde{K}_\xi)^{+r}} f(y)$. Then, $p_l := P(D_{s_1+\epsilon_1, s_2-\epsilon_1}(x_l)) \geq \alpha_0 \tilde{\Lambda} > 0$. Observe that

$$\begin{aligned} P^{\otimes n}(\cap_{l=1}^q [\mathcal{X}_n \cap D_{s_1+\epsilon_1, s_2-\epsilon_1}(x_l) \neq \emptyset]) &= 1 - P^{\otimes n}(\cup_{l=1}^q [\mathcal{X}_n \cap D_{s_1+\epsilon_1, s_2-\epsilon_1}(x_l) = \emptyset]) \\ &\geq 1 - \sum_{l=1}^q P^{\otimes n}([\mathcal{X}_n \cap D_{s_1+\epsilon_1, s_2-\epsilon_1}(x_l) = \emptyset]). \end{aligned}$$

Let G_l have the geometric distribution with parameter p_l . Since $\{X_l\}$ are independent, it holds that

$$P^{\otimes n}([\mathcal{X}_n \cap D_{s_1+\epsilon_1, s_2-\epsilon_1}(x_l) = \emptyset]) = P(G_l > n) = \sum_{j=n}^{\infty} (1-p_l)^j p_l = (1-p_l)^n,$$

which implies that

$$P^{\otimes n}(\cap_{l=1}^q [\mathcal{X}_n \cap D_{s_1+\epsilon_1, s_2-\epsilon_1}(x_l) \neq \emptyset]) \geq 1 - \sum_{l=1}^q (1-p_l)^n \geq 1 - q(1-\alpha_0 \tilde{\Lambda})^n. \quad (4.23)$$

The statement follows by taking $n_1 \geq n_3$ such that $\eta/2 \geq q(1-\alpha_0 \tilde{\Lambda})^{n_1}$.

Step 4. Let $n^* := \max(n_1, n_2)$ and $n \geq n^*$. Notice that, by **Step 2**, $\{Y_{n,r,j}\}_{j=0}^{j^*} \in \tilde{G}_{x,j^*,r^*}$ with probability at least $1 - \eta$. Since, $r \leq r^* \leq r_1 \leq \xi$, by **Step 1**, either (i) $\{Y_{n,r,j}\}_{j=0}^{j^*}$ remains in $(G_x)^{+\xi} \setminus B_\xi(m_i)$ or (ii) $Y_{n,r^*,j} \in \overline{B}_{4\xi}(m_i)$ for some $j \in \{0, \dots, j^*\}$. We show that (i) is not possible. Indeed, if $Y_{n,r,j^*} \in (G_x)^{+\xi} \setminus B_\xi(m_i) \subset \tilde{K}_\xi$, then, by (4.12), there exists $X^*(Y_{n,r,j^*}) \in \mathcal{X}_{n,r}(Y_{n,r,j^*})$ such that $f_{\tau_n,n}(X^*(Y_{n,r,j^*})) > f_{\tau_n,n}(Y_{n,r,j^*})$. However, since j^* is the last iterate by (3.5) it holds that $f_{\tau_n,n}(Y_{n,r,j^*}) \geq \max_{X \in \mathcal{X}_{n,r}(Y_{n,r,j^*}) \cup \{Y_{n,r,j^*}\}} f_{\tau_n,n}(X)$. Let $j_0 = \min\{j \in \{0, \dots, j^*\} : Y_{n,r,j} \in \overline{B}_{4\xi}(m_i)\}$. By (4.3), $Y_{n,r,j_0} \in R^\alpha \cap C(m_i)$. We show by induction that $Y_{n,r,j} \in R^\alpha \cap C(m_i)$, for all $j_0 \leq j \leq j^*$. First, notice that, if $Y_{n,r,j} \in R^{\alpha_4(\xi)} \cap C(m_i)$, then $Y_{n,r,j+1} \in B_{\xi+r}(m_i) \subset B_{2\xi}(m_i) \subset R^\alpha \cap C(m_i)$. Second, if $Y_{n,r,j} \in B_{4\xi}(m_i) \setminus (R^{\alpha_4(\xi)} \cap C(m_i))$, then by (4.5) $Y_{n,r,j} \in \tilde{K}_\xi$ and by (4.11) it holds that $f(Y_{n,r,j+1}) > f(Y_{n,r,j})$. Using the induction hypothesis, we conclude that $Y_{n,r,j+1} \in R^\alpha \cap C(m_i)$. This completes the proof of consistency of the algorithm. ■

5 Concluding Remarks

In this paper, we developed the notions of local depth for general *Type A* DFs and established its analytic and statistical properties. Specifically, we established the uniform convergence of sample local depth and related asymptotic limit distribution in $\ell^\infty(T)$ spaces. These results are then used to derive new approaches to clustering, mode estimation, and upper level set estimation. Specifically, we developed a modal clustering approach (via a gradient system) where the density is replaced by the population approximation. Convergence results show that the approximated approach provides, in the limit, the same clusters as those given by the true density. In particular, we have shown that, our approximated approach correctly detects the true modes. We proposed a computationally efficient algorithm for the numerical computation of the clusters at sample level. Additionally and importantly, we established consistency of the sample clustering algorithm and provide details for choosing parameters that arise when implementing the algorithm.

Acknowledgements

For A.N.-R., this research was funded by the Spanish Ministerio de Ciencia, Innovación y Universidades grant number MTM2017-86061-C2-2-P.

References

- Claudio Agostinelli and Mario Romanazzi. Local depth. *Journal of Statistical Planning and Inference*, 141(2):817–830, 2011.
- Kenneth S. Alexander. The central limit theorem for empirical processes on Vapnik-Cervonenkis classes. *The Annals of Probability*, 15(1):178–203, 1987.
- Miguel A. Arcones. A Bernstein-type inequality for U-statistics and U-processes. *Statistics & probability letters*, 22(3):239–247, 1995.
- Miguel A. Arcones and Evarist Giné. Limit theorems for U-processes. *The Annals of Probability*, 21(3):1494–1542, 1993.
- Ery Arias-Castro, David Mason, and Bruno Pelletier. On the estimation of the gradient lines of a density and the consistency of the mean-shift algorithm. *Journal of Machine Learning Research*, 17(1):1487–1514, 2016.
- Shai Ben-David, Ulrike von Luxburg, and Dávid Pál. A sober look at clustering stability. In *International conference on computational learning theory*, pages 5–19, 2006.
- M. Bertrand-Retali. Convergence uniforme d’un estimateur de la densité par la méthode de noyau. *Revue Roumaine de Mathématiques Pures et Appliquées*, 23:361–385, 1978.
- José E. Chacón. A population background for nonparametric density-based clustering. *Statistical Science*, 30(4):518–532, 2015.
- José E. Chacón. Mixture model modal clustering. *Adv. Data Anal. Classif.*, 13(2):379–404, 2019.
- Gabriel Chandler and Wolfgang Polonik. Multiscale geometric feature extraction for high-dimensional and non-euclidean data with applications. *The Annals of Statistics*, 49(2):988–1010, 2021.
- Frédéric Chazal, Leonidas J. Guibas, Steve Y. Oudot, and Primoz Skraba. Persistence-based clustering in riemannian manifolds. *Journal of the ACM*, 60(6), 2013.
- Richard M. Dudley. *Uniform central limit theorems*, volume 142. Cambridge university press, 2014.
- Ryan T. Elmore, Thomas P. Hettmansperger, and Fengjuan Xuan. Spherical data depth and a multivariate median. *DIMACS Series in Discrete Mathematics and Theoretical Computer Science*, 72:87, 2006.

Chris Fraley and Adrian E. Raftery. Model-based clustering, discriminant analysis, and density estimation. *Journal of the American Statistical Association*, 97(458):611–631, 2002.

Keinosuke Fukunaga and Larry Hostetler. The estimation of the gradient of a density function, with applications in pattern recognition. *IEEE Transactions on information theory*, 21(1):32–40, 1975.

Evarist Giné and Richard Nickl. *Mathematical foundations of infinite-dimensional statistical models*, volume 40. Cambridge University Press, 2016.

Vladimir S. Korolyuk and Yu V. Borovskich. *Theory of U-statistics*, volume 273. Springer Science & Business Media, 2013.

Morris W. Hirsch, Robert L. Devaney, and Stephen Smale. *Differential equations, dynamical systems, and linear algebra*, volume 60. Academic press, 1974.

Regina Y. Liu. On a notion of data depth based on random simplices. *The Annals of Statistics*, 18(1):405–414, 1990.

Zhenyu Liu and Reza Modarres. Lens data depth and median. *Journal of Nonparametric Statistics*, 23(4):1063–1074, 2011.

Yukio Matsumoto. *An introduction to Morse theory*, volume 208. American Mathematical Soc., 2002.

Giovanna Menardi. A review on modal clustering. *International Statistical Review*, 84(3):413–433, 2016.

Gerald Teschl. *Ordinary differential equations and dynamical systems*, volume 140. American Mathematical Society, 2012.

Matt P. Wand and M. Chris Jones. Comparison of smoothing parameterizations in bivariate kernel density estimation. *Journal of the American Statistical Association*, 88(422):520–528, 1993.

Junhui Wang. Consistent selection of the number of clusters via crossvalidation. *Biometrika*, 97(4):893–904, 2010.

Mengta Yang and Reza Modarres. β -skeleton depth functions and medians. *Communications in Statistics- Theory and Methods*, 47(20):5127–5143, 2018.

Yijun Zuo and Robert Serfling. General notions of statistical depth function. *Annals of statistics*, pages 461–482, 2000a.

Yijun Zuo and Robert Serfling. Structural properties and convergence results for contours of sample statistical depth functions. *The Annals of Statistics*, 28(2):483–499, 2000b.

A Discussion and additional proofs

A.1 Useful properties of local depth functions

We begin with a brief discussion concerning the properties of local depth functions that are used in the proofs and discussions in the main paper. We first observe, using **(P2)**, that $h_0^{(G)}(x; \cdot) = l_G \mathbf{I}(\cdot \in \{(x, \dots, x)\})$, where $l_G = G(0, \dots, 0)$. Also, by Definition 2.1, and by **(P1)**, **(P2)**, $h_1^{(G)}(0; \cdot) = G(\cdot)$ and

$$0 \leq h_{(\cdot)}^{(G)}(\cdot; \cdot) \leq l_G. \quad (\text{A.1})$$

Furthermore, **(P4)** ensures that $h_\tau(0; \cdot)$ is non-trivial for all $\tau > 0$, since there is a region including the origin of $(\mathbb{R}^d)^{k_G}$ and having positive Lebesgue measure where $h_\tau(0; \cdot)$ is positive. We note that **(P4)** is satisfied whenever $l_G > 0$ and $G(\cdot)$ is continuous in $(0, \dots, 0)$. We will further suppose without loss of generality (w.l.o.g.) that $G(x_1, \dots, x_{k_G}) = G(x_{i_1}, \dots, x_{i_{k_G}})$, for every permutation (i_1, \dots, i_{k_G}) of $(1, \dots, k_G)$ yielding

$$h_\tau^{(G)}(x; x_1, \dots, x_{k_G}) = h_\tau^{(G)}(x; x_{i_1}, \dots, x_{i_{k_G}}); \quad (\text{A.2})$$

since otherwise, one can replace $G(\cdot)$ by $\bar{G}(\cdot)$, where, for $(x_1, \dots, x_{k_G}) \in (\mathbb{R}^p)^{k_G}$,

$$\bar{G}(x_1, \dots, x_{k_G}) = \frac{1}{k_G!} \sum G(x_{i_1}, \dots, x_{i_{k_G}}),$$

and the summation is over all $k_G!$ permutations (i_1, \dots, i_{k_G}) of $(1, \dots, k_G)$. Also, notice that

$$h_\tau^{(G)}(x + v; x_1 + v, \dots, x_{k_G} + v) = h_\tau^{(G)}(x; x_1, \dots, x_{k_G}), \quad v \in \mathbb{R}^p \quad (\text{A.3})$$

$$\text{and } h_\tau^{(G)}(-x; -x_1, \dots, -x_{k_G}) = h_\tau^{(G)}(x; x_1, \dots, x_{k_G}). \quad (\text{A.4})$$

If P is absolutely continuous with respect to the Lebesgue measure on \mathbb{R}^p with density $f(\cdot)$, then, by (A.3) and (A.4), for all $x \in \mathbb{R}^p$ and $\tau \in [0, \infty]$, it holds that

$$\begin{aligned} LGD(x, \tau, P) &= \int h_\tau(0; x - x_1, \dots, x - x_k) f(x_1) \dots f(x_k) dx_1 \dots dx_k \\ &= (h_\tau(0; \cdot) * f^{(k)}(\cdot))(x, \dots, x), \end{aligned}$$

where $*$ is the convolution operator and $f^{(k)}(x_1, \dots, x_k) = f(x_1) \dots f(x_k)$. Thus, (2.5) holds.

Zuo [1998] give two further conditions on $h_\infty(\cdot; \cdot)$ that, along with (A.1), (A.3), and (A.4) with $\tau = \infty$, ensure that $GD(\cdot, \cdot)$ is a statistical depth function in the sense of Zuo and Serfling [2000a]. Notice that *Type A* depth functions (2.3) are the expectation of a bounded and non-negative function $h_\infty^{(G)}(x; \cdot)$. Zuo and Serfling [2000a] also define *Type B* depth functions as the inverse of one plus the expectation of an unbounded and non-negative function $\bar{h}_\infty^{(G)}(x; \cdot)$. That is,

$$GD(x, P) = \left(1 + \int \bar{h}_\infty^{(G)}(x; x_1, \dots, x_k) dP(x_1) \dots dP(x_k) \right)^{-1}.$$

Notice that *Type B* depth functions can be converted into a *Type A* DF by considering the expectation of $g(\bar{h}_\infty^{(G)}(x; \cdot))$, for some decreasing function $g : [0, \infty) \rightarrow [0, \infty)$ with $\lim_{t \rightarrow \infty} g(t) = 0$. Next, turning to *Type C* DFs, again following Zuo and Serfling [2000a], they are given as the inverse of an "outlyingness measure"; that is,

$$GD(x, P) = \left(1 + O(x, P) \right)^{-1},$$

where $O(x, P)$ is a general outlyingness measure of $x \in \mathbb{R}^p$ w.r.t. P . An example of outlyingness measure is $E[\bar{h}_\infty^{(G)}(x; X_1, \dots, X_k)]$ and hence, in this case, *Type C* reduces to *Type B*. Finally, the only instance of *Type D* depth functions is the half-space depth, which is the infimum of probabilities of half-spaces; that is,

$$GD(x, P) = \inf_{u \in S^{p-1}} P(H_{x,u}), \quad \text{where}$$

$$H_{x,u} = \{y \in \mathbb{R}^p : \langle u, y \rangle \leq \langle u, x \rangle\}$$

is the closed half-space with boundary point x and outer normal u , and $\langle \cdot, \cdot \rangle$ is the inner product in \mathbb{R}^p .

A.2 Additional proofs

In the following we will use the following notations: $\{e_i\}_{i=1}^p$ is the standard basis of \mathbb{R}^p and the coordinates of a vector $x \in \mathbb{R}^p$ are given by $x^{(i)} := \langle x, e_i \rangle$, $i = 1, \dots, p$.

Proof of Proposition 2.1. We start by proving (i). For the monotonicity, observe that, by Definition 2.1 and **(P2)**, for all $x \in \mathbb{R}^p$, $(x_1, \dots, x_k) \in (\mathbb{R}^p)^k$ and $0 \leq \tau_1 \leq \tau_2 \leq \infty$, $h_{\tau_1}(x; x_1, \dots, x_k) \leq h_{\tau_2}(x; x_1, \dots, x_k)$ and therefore $LGD(x, \tau_1) \leq LGD(x, \tau_2)$. Using Lebesgue dominated convergence Theorem (LDCT) and Definition 2.1, we get that

$$\lim_{\tau \rightarrow 0^+} LGD(x, \tau) = \int \lim_{\tau \rightarrow 0^+} h_\tau(x; x_1, \dots, x_k) dP(x_1) \dots dP(x_k) = l_G P^k(\{x\})$$

and

$$\lim_{\tau \rightarrow \infty} LGD(x, \tau) = \int \lim_{\tau \rightarrow \infty} h_\tau(x; x_1, \dots, x_k) dP(x_1) \dots dP(x_k) = GD(x).$$

For (ii) observe that, since every probability measure on \mathbb{R}^p is tight [Billingsley, 1999, Theorem 1.3], for all $0 < \epsilon < 1$, there exists $r_1 > 0$ such that $P(\overline{B}_{r_1}(0)) \geq 1 - \epsilon$. Let $\tau \in [0, \infty)$. By **(P3)**, there exists $r^* > 0$ such that, if $x_1 \in \mathbb{R}^p \setminus \overline{B}_{\tau r^*}(x)$, then $h_\tau(x; x_1, \dots, x_k) \leq \epsilon$, for all $x \in \mathbb{R}^p$ and $(x_2, \dots, x_k) \in (\mathbb{R}^p)^{k-1}$. Since, for $r_2 > \tau r^*$ and $x \in \mathbb{R}^p \setminus \overline{B}_{r_1+r_2}(0)$, it holds that $\overline{B}_{\tau r^*}(x) \subset \mathbb{R}^p \setminus \overline{B}_{r_1}(0)$, using (A.1), we have that, for $r \geq r_1 + r_2$, $\sup_{x \in \mathbb{R}^p \setminus \overline{B}_r(0)} LGD(x, \tau)$ is bounded above by

$$\begin{aligned} & \sup_{x \in \mathbb{R}^p \setminus \overline{B}_{r_1+r_2}(0)} \int_{\overline{B}_{\tau r^*}(x) \times (\mathbb{R}^p)^{k-1}} h_\tau(x; x_1, \dots, x_k) dP(x_1) \dots dP(x_k) \\ & + \sup_{x \in \mathbb{R}^p \setminus \overline{B}_{r_1+r_2}(0)} \int_{(\mathbb{R}^p \setminus \overline{B}_{\tau r^*}(x)) \times (\mathbb{R}^p)^{k-1}} h_\tau(x; x_1, \dots, x_k) dP(x_1) \dots dP(x_k) \\ & \leq l \sup_{x \in \mathbb{R}^p \setminus \overline{B}_{r_1+r_2}(0)} P(\overline{B}_{\tau r^*}(x)) + \epsilon \leq l P(\mathbb{R}^p \setminus \overline{B}_{r_1}(0)) + \epsilon \\ & \leq (l+1)\epsilon. \end{aligned}$$

We now prove (iii). Let $f(\cdot)$ be the density function of P with respect to λ . By (A.1), we have that

$$LGD(x, \tau) \leq l \int f(x_1), \dots, f(x_k) dx_1 \dots dx_k = l,$$

which shows that $LGD(\cdot, \tau)$ is bounded. Furthermore, by (2.5) and (A.3), it holds that

$$\begin{aligned} |LGD(y, \tau) - LGD(x, \tau)| &= \left| \int h_\tau(0; x_1, \dots, x_k) \prod_{j=1}^k f(y - x_j) dx_1 \dots dx_k \right. \\ &\quad \left. - \int h_\tau(0; x_1, \dots, x_k) \prod_{j=1}^k f(x - x_j) dx_1 \dots dx_k \right| \\ &\leq l \int \left| \prod_{j=1}^k f(y - x_j) - \prod_{j=1}^k f(x - x_j) \right| dx_1 \dots dx_k. \end{aligned}$$

By Theorem 8.19 in Wheeden and Zygmund [2015], it follows that $|LGD(y, \tau) - LGD(x, \tau)|$ converges to 0 as $\|y - x\| \rightarrow 0$.

We turn to the proof of (iv). We first observe that, by (iii) and (2.5), (iv) holds when $m = 0$. Also, if $\tau = 0$ then $LGD(x, \tau) = 0$ for all $x \in \mathbb{R}^p$ and the statement is trivial. Let $\tau > 0$ and $m \geq 1$. We will show that, for all $0 \leq j \leq m$, the partial derivatives of $LGD(\cdot, \tau)$ up to order j exist and are given by

$$\partial_{i_j} \dots \partial_{i_1} LGD(x, \tau) = (h_\tau(0; \cdot) * (g_{i_j, \dots, i_1}(\cdot)))(x, \dots, x), \quad (\text{A.5})$$

where, for $(x_1, \dots, x_k) \in (\mathbb{R}^p)^k$, $g_{i_j, \dots, i_1}(x_1, \dots, x_k) := \partial_{i_j} \dots \partial_{i_1} f(x_1) \dots f(x_k)$. In particular, since $f(\cdot)$ is m -times continuously differentiable, $g_{i_j, \dots, i_1}(\cdot)$ is $(m-j)$ -times continuously differentiable. For $h > 0$ and $i \in \{1, \dots, p\}$, we define the i^{th} partial finite difference of a function $\tilde{g} : \mathbb{R}^p \rightarrow \mathbb{R}$ by

$$\partial_i^h \tilde{g}(x) = \frac{\tilde{g}(x + he_i) - \tilde{g}(x)}{h}.$$

Suppose by induction that the partial derivatives of the local depth up to order $j-1$ ($1 \leq j \leq m$) exist and, for some choice of indices $i_1, \dots, i_{j-1} \in \{1, \dots, p\}$ are given by (A.5). Let $i_j \in \{1, \dots, p\}$. Then by (A.5) and the mean value theorem, there exists $0 \leq c \leq 1$, such that

$$\begin{aligned} & \partial_{i_j}^h \partial_{i_{j-1}} \dots \partial_{i_1} LGD(x, \tau) \\ &= \int h_\tau(0; x_1, \dots, x_k) \partial_{i_j}^h g_{i_{j-1}, \dots, i_1}(x - x_1, \dots, x - x_k) dx_1 \dots dx_k \\ &= \int h_\tau(0; x_1, \dots, x_k) \partial_{i_j} g_{i_{j-1}, \dots, i_1}(x - x_1, \dots, x + che_{i_j} - x_{i_j}, \dots, x - x_k) dx_1 \dots dx_k. \end{aligned} \tag{A.6}$$

Notice that by (2.4) it follows that $\overline{S}_{h_\tau(0; \cdot)} \subset (\overline{B}_{\tau\rho}(0))^k$; by (A.1), $h_\tau(0; \cdot)$ is bounded; and finally $\partial_{i_j} g_{i_{j-1}, \dots, i_1}(\cdot) = g_{i_j, \dots, i_1}(\cdot)$ is $(m-j)$ -times continuously differentiable (in particular, continuous). By taking the limit for $h \rightarrow 0^+$ in (A.6) and using LDCT, we get (A.5). By induction, (2.6) follows. To conclude, we show that $\partial_{i_m} \dots \partial_{i_1} LGD(\cdot, \tau)$ is continuous. By (A.3) and (A.1), we have that, for $x, y \in \mathbb{R}^p$,

$$\begin{aligned} & |\partial_{i_m} \dots \partial_{i_1} LGD(y, \tau) - \partial_{i_m} \dots \partial_{i_1} LGD(x, \tau)| \\ &= \left| \int h_\tau(0; x_1, \dots, x_k) g_{i_m, \dots, i_1}(y - x_1, \dots, y - x_k) dx_1 \dots dx_k \right. \\ &\quad \left. - \int h_\tau(0; x_1, \dots, x_k) g_{i_m, \dots, i_1}(x - x_1, \dots, x - x_k) dx_1 \dots dx_k \right| \\ &\leq l \int_{\overline{S}_{h_\tau(0; \cdot)}} |g_{i_m, \dots, i_1}(y - x_1, \dots, y - x_k) - g_{i_m, \dots, i_1}(x - x_1, \dots, x - x_k)| dx_1 \dots dx_k. \end{aligned}$$

Since $\overline{S}_{h_\tau(0; \cdot)}$ is compact by (2.4), the continuity follows from the uniform continuity of $g_{i_m, \dots, i_1}(\cdot)$ over compact sets. ■

Before we prove Theorem 2.1 we recall the following results on the approximation of the identity, for the function $G(\cdot)$ (see Section 9.2 in Wheeden and Zygmund [2015] and Section XIII.2 in Torchinsky [1995]) whose proof is part of standard text-book material.

Lemma A.1 Let $\tilde{G}_\tau(\cdot) := \frac{h_\tau(0; \cdot)}{\Lambda_1 \tau^{kp}}$. Then the following hold:

- (i) $\int \tilde{G}_\tau(x_1, \dots, x_k) dx_1 \dots dx_k = 1.$
- (ii) For all $\delta > 0$, $\lim_{\tau \rightarrow 0^+} \int_{(\mathbb{R}^p)^k \setminus (\overline{B}_\delta(0))^k} \tilde{G}_\tau(y_1, \dots, y_k) dy_1 \dots dy_k = 0.$

(iii) Additionally, let $\tilde{f} : (\mathbb{R}^p)^k \rightarrow \mathbb{R}^p$ and suppose that assumption (2.4) holds true. Then, at every point $(x_1, \dots, x_k) \in (\mathbb{R}^p)^k$ of continuity of $\tilde{f}(\cdot)$

$$\lim_{\tau \rightarrow 0^+} (\tilde{G}_\tau * \tilde{f})(x_1, \dots, x_k) = \tilde{f}(x_1, \dots, x_k). \quad (\text{A.7})$$

Furthermore, (A.7) holds uniformly on any set $A \subset (\mathbb{R}^p)^k$ where $\tilde{f}(\cdot)$ is uniformly continuous.

Proof of Theorem 2.1. We begin by proving (i). To this end, notice that, if $f(\cdot)$ is continuous at $x \in \mathbb{R}^p$, then $\tilde{f}(\cdot, \dots, \cdot) := f(\cdot) \dots f(\cdot)$ is continuous at $(x, \dots, x) \in (\mathbb{R}^p)^k$. Similarly, if $f(\cdot)$ is uniformly continuous in $A \subset \mathbb{R}^p$, then $\tilde{f}(\cdot, \dots, \cdot)$ is uniformly continuous in $(A)^k \subset (\mathbb{R}^p)^k$. Now, the result follows from (2.5) and Lemma A.1 (iii).

We now prove (ii). We first notice that, since $f(\cdot) \in L^\infty(\mathbb{R}^p)$, there exists a constant $1 \leq c_\infty < \infty$ such that $f(\cdot) \leq c_\infty$ a.e. In particular, for all $1 \leq q < \infty$, it holds that $f^q(\cdot) \leq c_\infty^q$ a.e., implying that $f^q(\cdot) \in L^\infty(\mathbb{R}^p)$. Then, we compute

$$\begin{aligned} \left| \frac{LGD(x, \tau)}{\Lambda_1 \tau^{kp}} - f^k(x) \right| &= \left| \int \tilde{G}_\tau(x_1, \dots, x_k) \prod_{j=1}^k f(x - x_j) dx_1 \dots dx_k - f^k(x) \right| \\ &\leq \int \left| \prod_{j=1}^k f(x - x_j) - f^k(x) \right| \tilde{G}_\tau(x_1, \dots, x_k) dx_1 \dots dx_k. \end{aligned} \quad (\text{A.8})$$

Next, we recursively apply the triangle inequality and obtain

$$\begin{aligned} \left| \prod_{j=1}^k f(x - x_j) - f^k(x) \right| &= \left| \sum_{i=1}^k \prod_{j=1}^{i-1} f(x - x_j) (f(x - x_i) - f(x)) f^{k-i}(x) \right| \\ &\leq \sum_{i=1}^k \prod_{j=1}^{i-1} f(x - x_j) |f(x - x_i) - f(x)| f^{k-i}(x), \end{aligned} \quad (\text{A.9})$$

thus implying that the right hand side (RHS) of (A.8) is bounded above by

$$\begin{aligned} &\sum_{i=1}^k \int \prod_{j=1}^{i-1} f(x - x_j) |f(x - x_i) - f(x)| f^{k-i}(x) \tilde{G}_\tau(x_1, \dots, x_k) dx_1 \dots dx_k \\ &\leq c_\infty^{k-1} \sum_{i=1}^k \int |f(x - x_i) - f(x)| \tilde{G}_\tau(x_1, \dots, x_k) dx_1 \dots dx_k. \end{aligned}$$

Now, by Lemma A.1 (ii), for all $\delta > 0$ there exists $\tilde{\tau}(\delta) > 0$ such that, for all $0 < \tau \leq \tilde{\tau}(\delta)$,

$$\int_{(\mathbb{R}^p)^k \setminus (\overline{B}_\delta(0))^k} \tilde{G}_\tau(x_1, \dots, x_k) dx_1 \dots x_k \leq \epsilon. \quad (\text{A.10})$$

If $x \in \mathbb{R}^p$ is a continuity point for $f(\cdot)$, then for all $\epsilon > 0$, there exists $\delta > 0$ such that

$$|f(x - y) - f(x)| \leq \epsilon, \quad (\text{A.11})$$

for all $y \in \overline{B}_\delta(0)$. Using Lemma A.1(i), (A.10), and (A.11), we have that, for all $0 < \tau \leq \tilde{\tau}(\delta)$, $\left| \frac{LGD(x, \tau)}{\Lambda_1 \tau^{kp}} - f^k(x) \right|$ is bounded above by

$$\begin{aligned} & c_\infty^{k-1} \sum_{i=1}^k \int_{(\overline{B}_\delta(0))^k} |f(x - x_i) - f(x)| \tilde{G}_\tau(x_1, \dots, x_k) dx_1 \dots dx_k \\ & + c_\infty^{k-1} \sum_{i=1}^k \int_{(\mathbb{R}^p)^k \setminus (\overline{B}_\delta(0))^k} |f(x - x_i) - f(x)| \tilde{G}_\tau(x_1, \dots, x_k) dx_1 \dots dx_k \\ & \leq k c_\infty^{k-1} (1 + 2c_\infty) \epsilon. \end{aligned} \quad (\text{A.12})$$

Finally, if $f(\cdot)$ is uniformly continuous on $A \subset \mathbb{R}^p$, then (A.11) and (A.12) hold for all $x \in A$.

For (iii), notice that, by (A.4) and a change of variable in (2.5),

$$\frac{1}{\tau^{kp}} LGD(x, \tau) - \Lambda_1 f^k(x) = \int h_1(0; x_1, \dots, x_k) \left[\prod_{j=1}^k f(x - \tau x_j) - f^k(x) \right] dx_1 dx_2. \quad (\text{A.13})$$

Since $f(\cdot)$ is twice continuously differentiable, by multivariate Taylor's theorem with integral remainder, for $i = 1, \dots, k$,

$$f(x + \tau x_i) = f(x) + \tau \langle \nabla f(x), x_i \rangle + \tau^2 \int_0^1 (1-z) x_i^\top H_f(x + z \tau x_i) x_i dz.$$

Therefore,

$$\begin{aligned} f(x + \tau x_1) \dots f(x + \tau x_k) &= f^k(x) + \tau f^{k-1}(x) \langle \nabla f(x), \sum_{i=1}^k x_i \rangle \\ &+ \tau^2 f^{k-1}(x) \sum_{i=1}^k \int_0^1 (1-z) x_i^\top H_f(x + z \tau x_i) x_i dz \\ &+ \tau^2 f^{k-2}(x) \sum_{i=1}^k \sum_{j=i+1}^k \langle \nabla f(x), x_i \rangle \langle \nabla f(x), x_j \rangle + O(\tau^2). \end{aligned} \quad (\text{A.14})$$

Since S_f is open, there exist $\tau^* > 0$ such that, for all $\tau \in [0, \tau^*]$, $(x_1, \dots, x_k) \in \overline{S}_{h_1(0, \cdot)}$ and $z \in [0, 1]$, $x + z\tau x_i \in S_f$. The continuity of the second order partial derivatives implies that, for $\tau \in [0, \tau^*]$, the functions

$$(x_1, \dots, x_k) \mapsto \int_0^1 (1-z)x_i^\top H_f(x + z\tau x_i)x_i dz$$

are continuous (and uniformly bounded for all $\tau \in [0, \tau^*]$) with

$$\lim_{\tau \rightarrow 0^+} \int_0^1 (1-z)x_i^\top H_f(x + z\tau x_i)x_i dz = \frac{1}{2}x_i^\top H_f(x)x_i. \quad (\text{A.15})$$

Similarly, the remainder $O(\tau^2)$ is uniformly bounded for all $\tau \in [0, \tau^*]$ and continuous with respect to (x_1, \dots, x_k) . By substituting (A.14) in (A.13), we see that

$$\begin{aligned} & \frac{1}{\tau^{kp}} LGD(x, \tau) - \Lambda_1 f^k(x) \\ &= \tau f^{k-1}(x) \int h_1(0; x_1, \dots, x_k) \langle \nabla f(x), \sum_{i=1}^k x_i \rangle dx_1 \dots dx_k \\ &+ \tau^2 f^{k-1}(x) \int h_1(0; x_1, \dots, x_k) \left[\sum_{i=1}^k \int_0^1 (1-z)x_i^\top H_f(x + z\tau x_i)x_i dz \right] dx_1 \dots dx_k \\ &+ \tau^2 f^{k-2}(x) \int h_1(0; x_1, \dots, x_k) \left[\sum_{i=1}^k \sum_{j=i+1}^k \langle \nabla f(x), x_i \rangle \langle \nabla f(x), x_j \rangle \right] dx_1 \dots dx_k \\ &+ O(\tau^2). \end{aligned}$$

By (A.4) and the change of variable $-(x_1, \dots, x_k)$ for (x_1, \dots, x_k) , it follows that

$$\begin{aligned} & \int h_1(0; x_1, \dots, x_k) \langle \nabla f(x), \sum_{i=1}^k x_i \rangle dx_1 \dots dx_k \\ &= - \int h_1(0; x_1, \dots, x_k) \langle \nabla f(x), \sum_{i=1}^k x_i \rangle dx_1 \dots dx_k. \end{aligned}$$

Therefore,

$$\int h_1(0; x_1, \dots, x_k) \langle \nabla f(x), \sum_{i=1}^k x_i \rangle dx_1 \dots dx_k = 0.$$

Now, (A.2) implies that

$$\begin{aligned} & \int h_1(0; x_1, \dots, x_k) \left[\sum_{i=1}^k \int_0^1 (1-z)x_i^\top H_f(x + z\tau x_i)x_i dz \right] dx_1 \dots dx_k \\ &= k \int h_1(0; x_1, \dots, x_k) \left[\int_0^1 (1-z)x_1^\top H_f(x + z\tau x_1)x_1 dz \right] dx_1 \dots dx_k \end{aligned}$$

and

$$\begin{aligned} & \int h_1(0; x_1, \dots, x_k) \left[\sum_{i=1}^k \sum_{j=i+1}^k \langle \nabla f(x), x_i \rangle \langle \nabla f(x), x_j \rangle \right] dx_1 \dots dx_k \\ &= \frac{k(k-1)}{2} f^{k-2}(x) \int h_1(0; x_1, \dots, x_k) \langle \nabla f(x), x_1 \rangle \langle \nabla f(x), x_2 \rangle dx_1 \dots dx_k. \end{aligned}$$

By (A.15) and LDCT, we conclude that

$$\lim_{\tau \rightarrow 0^+} \frac{1}{\tau^2} \left(\frac{1}{\tau^{kp}} LGD(x, \tau) - \Lambda_1 f^k(x) \right) = R(x),$$

where $R(x) = R_1(x) + R_2(x)$ and

$$\begin{aligned} R_1(x) &:= \frac{k}{2} f^{k-1}(x) \int h_1(0; x_1, \dots, x_k) x_1^\top H_f(x) x_1 dx_1 \dots dx_k, \\ R_2(x) &:= \frac{k(k-1)}{2} f^{k-2}(x) \int h_1(0; x_1, \dots, x_k) \langle \nabla f(x), x_1 \rangle \langle \nabla f(x), x_2 \rangle dx_1 \dots dx_k. \end{aligned}$$

We now prove (iv). We first notice that, since $f(\cdot) \in L^1(\mathbb{R}^p) \cap L^{kd}(\mathbb{R}^p)$, then $f(\cdot) \in L^q(\mathbb{R}^p)$, for all $1 \leq q \leq kd$. Indeed, it holds that

$$\begin{aligned} \int_{\mathbb{R}^p} f^q(x) dx &= \int_{\{y \in \mathbb{R}^p : f(y) < 1\}} f^q(x) dx + \int_{\{y \in \mathbb{R}^p : f(y) \geq 1\}} f^q(x) dx \\ &\leq \int_{\{y \in \mathbb{R}^p : f(y) < 1\}} f(x) dx + \int_{\{y \in \mathbb{R}^p : f(y) \geq 1\}} f^{kd}(x) dx < \infty. \end{aligned}$$

Next, we write in (A.8) $\tilde{G}_\tau(x_1, \dots, x_k) = \tilde{G}_\tau^{1/d}(x_1, \dots, x_k) \tilde{G}_\tau^{1/\tilde{d}}(x_1, \dots, x_k)$, where $\tilde{d} \in (1, \infty]$ satisfies $1/d + 1/\tilde{d} = 1$ ($\tilde{d} = \infty$ if $d = 1$), apply Hölder inequality with exponents d and \tilde{d} and Lemma A.1 (i), thus obtaining

$$\left| \frac{LGD(x, \tau)}{\Lambda_1 \tau^{kp}} - f^k(x) \right|^d \leq \int \left| \prod_{j=1}^k f(x - x_j) - f^k(x) \right|^d \tilde{G}_\tau(x_1, \dots, x_k) dx_1 \dots dx_k.$$

Now, Jensen's inequality yields that $(\sum_{i=1}^k a_i)^d \leq k^{d-1} \sum_{i=1}^k a_i^d$ for $a_i \geq 0$. Using this and (A.9), we obtain that

$$\int \left| \frac{LGD(x, \tau)}{\Lambda_1 \tau^{kp}} - f^k(x) \right|^d dx \leq k^{d-1} \sum_{i=1}^k I_{\tau,i},$$

where

$$I_{\tau,i} := \int \left(\int \left(\prod_{j=1}^{i-1} f^d(x - x_j) |f(x - x_i) - f(x)|^d f^{(k-i)d}(x) \right) \tilde{G}_\tau(x_1, \dots, x_k) dx_1 \dots dx_k \right) dx.$$

Notice that $I_{\tau,i}$ are finite since $f(\cdot) \in L^q(\mathbb{R}^p)$, $1 \leq q \leq kd$, and, by (A.1), $0 \leq \tilde{G}_\tau(\cdot) \leq l/\Lambda_1 \tau^{kp}$. By Fubini's theorem, we have that

$$I_{\tau,i} = \int J_{\tau,i}(x_1, \dots, x_k) \tilde{G}_\tau(x_1, \dots, x_k) dx_1 \dots dx_k,$$

where

$$J_{\tau,i}(x_1, \dots, x_k) := \int \prod_{j=1}^{i-1} f^d(x - x_j) |f(x - x_i) - f(x)|^d f^{(k-i)d}(x) dx.$$

Now, we apply again Hölder inequality with exponents $s = k/(k-1)$ and $t = k$, and see that

$$\begin{aligned} J_{\tau,i}(x_1, \dots, x_k) &\leq \left[\int \prod_{j=1}^{i-1} f^{sd}(x - x_j) f^{(k-i)sd}(x) dx \right]^{1/s} \left[\int |f(x - x_i) - f(x)|^{td} dx \right]^{1/t} \\ &\leq c_1 K(x_1, \dots, x_k), \end{aligned}$$

where

$$c_1 := \max_{i=1, \dots, p} \left[\int \prod_{j=1}^{i-1} f^{sd}(x - x_j) f^{(k-i)sd}(x) dx \right]^{1/s}$$

and

$$K(x_1, \dots, x_k) := \max_{i=1, \dots, p} \left[\int |f(x - x_i) - f(x)|^{td} dx \right]^{1/t}.$$

Notice that

$$K(x_1, \dots, x_k) \leq c_2 := 2^d \left[\int f(x)^{td} dx \right]^{1/t} < \infty, \quad (\text{A.16})$$

and, for all $\epsilon > 0$, by Theorem 8.19 in Wheeden and Zygmund [2015], there exists $\delta > 0$ such that, for all $(x_1, \dots, x_k) \in (\overline{B}_\delta(0))^k$,

$$K(x_1, \dots, x_k) \leq \epsilon. \quad (\text{A.17})$$

Using Lemma A.1 (i), (A.16), (A.17), and (A.10), we conclude that, for all $0 < \tau \leq \tilde{\tau}(\delta)$,

$$\begin{aligned} \int \left| \frac{LGD(x, \tau)}{\Lambda_1 \tau^{kp}} - f^k(x) \right|^d dx &\leq c_1 k^d \int K(x_1, \dots, x_k) \tilde{G}_\tau(x_1, \dots, x_k) dx_1 \dots dx_k \\ &\leq c_1 (1 + c_2) k^d \epsilon. \end{aligned}$$

■

Before proving Proposition 2.2 we establish useful inequalities in the following lemma.

Lemma A.2 *Let $s, t \geq 0$. The following hold: (i) $|t^a - s^a| \leq |t - s|^a$, for all $0 < a \leq 1$, and (ii) $|t^a - s^a| \geq |t - s|^a$, for all $a > 1$.*

Proof. It is enough to prove the statement for $0 < s < t$. Let $\varphi : (0, \infty] \rightarrow \mathbb{R}$ be given by $\varphi(a) = (1 - s/t)^a - 1 + (s/t)^a$. Notice that, $\lim_{a \rightarrow 0^+} \varphi(a) = 1$, $\lim_{a \rightarrow \infty} \varphi(a) = -1$ and

$$\varphi'(a) = \log(1 - s/t)(1 - s/t)^a + \log(s/t)(s/t)^a < 0.$$

Then, the equality $\varphi(1) = 0$ shows that $\varphi(a) \geq 0$, for $0 < a \leq 1$, and $\varphi(a) < 0$, for $a > 1$. The same inequalities hold for $t^a \varphi(a)$ and the result follows. \blacksquare

Proof of Proposition 2.2. We start by proving (i). By Lemma A.2, for $\tau > 0$,

$$\begin{aligned} \sup_{x \in \mathbb{R}^p} |f_\tau^{(G)}(x) - f(x)| &= \sup_{x \in \mathbb{R}^p} \left| \left(\frac{LGD(x, \tau)}{\tau^{k_G p} \Lambda_1^{(G)}} \right)^{1/k_G} - (f^{k_G}(x))^{1/k_G} \right| \\ &\leq \sup_{x \in \mathbb{R}^p} \left| \frac{LGD(x, \tau)}{\tau^{k_G p} \Lambda_1^{(G)}} - f^{k_G}(x) \right|^{1/k_G} \\ &= \sup_{x \in \mathbb{R}^p} F_\tau^{(G)}(x)^{1/k_G}, \end{aligned}$$

where

$$F_\tau^{(G)}(x) := \left| \frac{1}{\Lambda_1^{(G)}} \int h_1^{(G)}(0; x_1, \dots, x_{k_G}) \left[\prod_{j=1}^{k_G} f(x + \tau x_j) - f^{k_G}(x) \right] dx_1 \dots dx_{k_G} \right|.$$

Since the k_G^{th} root is a continuous and increasing function, we have that

$$\sup_{x \in \mathbb{R}^p} F_\tau^{(G)}(x)^{1/k_G} = (\sup_{x \in \mathbb{R}^p} F_\tau^{(G)}(x))^{1/k_G}. \quad (\text{A.18})$$

Hence, (2.9) follows, if we show that

$$\lim_{\tau \rightarrow 0^+} \sup_{x \in \mathbb{R}^p} F_\tau^{(G)}(x) = 0. \quad (\text{A.19})$$

For this, observe that $\sup_{x \in \mathbb{R}^p} F_\tau^{(G)}(x)$ is bounded above by

$$\int h_1^{(G)}(0; x_1, \dots, x_{k_G}) \sup_{x \in \mathbb{R}^p} \left| \prod_{j=1}^{k_G} f(x + \tau x_j) - f^{k_G}(x) \right| dx_1 \dots dx_{k_G}.$$

Since $f(\cdot)$ is uniformly continuous, for all $(x_1, \dots, x_{k_G}) \in (\mathbb{R}^p)^{k_G}$, it holds that

$$\lim_{\tau \rightarrow 0^+} \sup_{x \in \mathbb{R}^p} \left| \prod_{j=1}^{k_G} f(x + \tau x_j) - f^{k_G}(x) \right| = 0.$$

(A.19) now follows from LDCT, since $h_1^{(G)}(0; \cdot) \in L^1((\mathbb{R}^p)^{k_G})$ and the supremum is bounded because $f(\cdot)$ is bounded (see Appendix H).

Since a continuous function is uniformly continuous on a compact set, the proof of the first part of (ii) follows from the proof of (i) with \mathbb{R}^p replaced by K . For the second part of (ii), notice that

$$\sup_{y \in \overline{B}_\epsilon(x)} |f_\tau^{(G)}(y) - f(x)| \leq \sup_{y \in \overline{B}_\epsilon(x)} |f_\tau^{(G)}(y) - f(y)| + \sup_{y \in \overline{B}_\epsilon(x)} |f(y) - f(x)|.$$

The result now follows from the first part of (ii) and continuity of $f(\cdot)$. Finally, for (iii), notice that, by Lemma A.2 and Theorem 2.1 (iv),

$$\int |f_\tau^{(G)}(y) - f(y)|^{k_G d} dy \leq \int |(f_\tau^{(G)})^{k_G}(y) - f^{k_G}(y)|^d dy \xrightarrow{\tau \rightarrow 0^+} 0.$$

Before we prove Proposition (iv) we state without proof a result concerning the partial derivatives of the composition of two functions (Proposition 1 in Hardy [2006]). For any set R , we denote by $\#R$ the cardinality of R .

Claim A.1 *Let $\varphi : \mathbb{R}^p \rightarrow \mathbb{R}$ and $\psi : \mathbb{R} \rightarrow \mathbb{R}$ be m -times continuously differentiable in $A \subset \mathbb{R}^p$ and $\varphi(A) \subset \mathbb{R}$, respectively. Then, $\psi(\varphi(\cdot))$ is m -times continuously differentiable in A and, for $x \in A$ and $i_1, \dots, i_m \in \{1, \dots, p\}$, it holds that*

$$\partial_{i_m} \dots \partial_{i_1} \psi(\varphi(x)) = \sum_{R \in \mathcal{R}_m} [\partial^{[\#R]} \psi](\varphi(x)) \prod_{\{i_{j_l}, \dots, i_{j_1}\} \in R} \partial_{i_{j_l}} \dots \partial_{i_{j_1}} \varphi(x),$$

where \mathcal{R}_m is the set of all partitions of $\{1, \dots, m\}$ and $\partial^{[l]}$ denotes the (unidimensional) l^{th} derivative.

The following lemma, which is standard, is required for completing the proof of the proposition. We include its proof to make the paper self-contained.

Lemma A.3 *Let $\varphi_n : \mathbb{R}^p \rightarrow \mathbb{R}$, $\phi_n : \mathbb{R}^p \rightarrow \mathbb{R}$ and $A \subset \mathbb{R}^p$. Suppose that $\varphi_n(\cdot)$ and $\phi_n(\cdot)$ converge uniformly on A to $\varphi(\cdot)$ and $\phi(\cdot)$, respectively. It holds that (i) $(\varphi_n + \phi_n)(\cdot)$ converges uniformly on A to $(\varphi + \phi)(\cdot)$ and (ii) if $\varphi_n(\cdot)$ and $\phi_n(\cdot)$ are bounded on A , then $(\varphi_n \phi_n)(\cdot)$ converges uniformly on A to $(\varphi \phi)(\cdot)$.*

Proof of (i) is standard. For (ii) let $c_1 := \sup_{x \in A} |\varphi(x)|$ and $c_2 := \sup_{x \in A} |\phi(x)|$. For $0 < \epsilon \leq 1$ there exists $n^* \in \mathbb{N}$ such that for all $n \geq n^*$ $\sup_{x \in A} |\varphi_n(x) - \varphi(x)| \leq \epsilon$ and $\sup_{x \in A} |\phi_n(x) - \phi(x)| \leq \epsilon$. It follows that

$$\begin{aligned} \sup_{x \in A} |\varphi_n(x)\phi_n(x) - \varphi(x)\phi(x)| &\leq \sup_{x \in A} |\varphi_n(x)| |\phi_n(x) - \phi(x)| + \sup_{x \in A} |\phi(x)| |\varphi_n(x) - \varphi(x)| \\ &\leq (1 + c_1 + c_2)\epsilon. \end{aligned}$$

This completes the proof of the lemma.

We now turn to the proof of (iv). We first notice that, by Proposition 2.1 (iv) and Remark 2.1, $LGD(\cdot, \tau)$ and $f_\tau(\cdot)$ are m -times continuously differentiable in S_f . Since $K \subset S_f$, $c_1 := \min_{x \in K} f^k(x) > 0$ and $c_2 := \max_{x \in K} f^k(x) < \infty$. By Theorem 2.1 (i), there exists $\tau^* > 0$ such that, for all $0 < \tau \leq \tau^*$, $\sup_{x \in K} |f_\tau^k(x) - f^k(x)| \leq c_1/2$, implying that $f_\tau^k(x) \in [c_3, c_4]$, where $c_3 := c_1/2$ and $c_4 := c_2 + c_1/2$. Next, we apply Lemma A.1 with $\varphi(\cdot) = f^k(\cdot)$ and $\psi(\cdot) = (\cdot)^{1/k}$, and obtain that

$$\partial_{i_m} \dots \partial_{i_1} f(x) = \partial_{i_m} \dots \partial_{i_1} \psi(\varphi(x)) = \sum_{R \in \mathcal{R}_m} [\partial^{[R]} \psi](\varphi(x)) \prod_{\{i_{j_l}, \dots, i_{j_1}\} \in R} \partial_{i_{j_l}} \dots \partial_{i_{j_1}} \varphi(x). \quad (\text{A.20})$$

Similarly, with $\varphi_\tau(\cdot) := f_\tau^k(\cdot)$, we have that

$$\partial_{i_m} \dots \partial_{i_1} f_\tau(x) = \partial_{i_m} \dots \partial_{i_1} \psi(\varphi_\tau(x)) = \sum_{R \in \mathcal{R}_m} [\partial^{[R]} \psi](\varphi_\tau(x)) \prod_{\{i_{j_l}, \dots, i_{j_1}\} \in R} \partial_{i_{j_l}} \dots \partial_{i_{j_1}} \varphi_\tau(x). \quad (\text{A.21})$$

By Proposition 2.1 (iv), it holds that $\partial_{i_{j_l}} \dots \partial_{i_{j_1}} \varphi_\tau(x) = (\tilde{G}_\tau(\cdot) * (\partial_{i_{j_l}} \dots \partial_{i_{j_1}} f^k(\cdot)))(x, \dots, x)$. We apply Lemma A.1 (iii) with $\tilde{f}(\cdot, \dots, \cdot) = \partial_{i_{j_l}} \dots \partial_{i_{j_1}} (f(\cdot) \dots f(\cdot))$ and $A = (K)^k$, and obtain that $\partial_{i_{j_l}} \dots \partial_{i_{j_1}} \varphi_\tau(\cdot)$ converges uniformly on K to $\partial_{i_{j_l}} \dots \partial_{i_{j_1}} \varphi(\cdot)$. Next, notice that, for all $j \in \{1, \dots, m\}$, $\partial^{[j]} \psi(\cdot)$ is uniformly continuous on $[c_3, c_4]$: for all $\epsilon > 0$, there exists $\delta > 0$ such that $\sup_{s, t \in [c_3, c_4]: |s-t| \leq \delta} |\partial^{[j]} \psi(s) - \partial^{[j]} \psi(t)| \leq \epsilon$. By Theorem 2.1 (i), there exists $0 < \tau^{**} \leq \tau^*$, such that, for all $0 < \tau \leq \tau^{**}$, $\sup_{x \in K} |f_\tau^k(x) - f^k(x)| \leq \delta$. Therefore, we have that, for all $0 < \tau \leq \tau^{**}$, $\sup_{x \in K} |[\partial^{[j]} \psi](\varphi_\tau(x)) - [\partial^{[j]} \psi](\varphi(x))| \leq \epsilon$; that is, $[\partial^{[j]} \psi](\varphi_\tau(\cdot))$ converges uniformly on K to $[\partial^{[j]} \psi](\varphi(\cdot))$. Now, the result follows from (A.20), (A.21), and Lemma A.3 with $A = K$. ■

We now return to the proof of Theorem 2.2 over an additional parameter space Θ uniformly over an additional parameter space Θ .

Assumption A.1 for (2.12): *We need the following assumptions on $G_\theta(\cdot)$.*

(A1) $G_\theta(\cdot)$ satisfies (P1)-(P4), where $k_{G_\theta} = k_{G_\Theta}$ is independent of θ .

(A2) $\mathcal{H}_{G_\Theta} = \cup_{\theta \in \Theta} \mathcal{H}_{G_\theta}$ is a VC-subgraph class.

(A3) $\sup_{\theta \in \Theta} G_\theta(\cdot) \leq l_{G_\Theta}$.

(A4) $G(\cdot)(\cdot)$ is jointly Borel measurable.

Proof of (2.12). The proof follows essentially as in Section 4 with minor changes. We include an argument for completeness. To this end, first note that that $\mathcal{H}_{G_\theta} = \{h_\tau^{(G_\theta)}(x; \cdot) : x \in \mathbb{R}^p, \tau \in [0, \infty]\}$ and $\mathcal{H}_{G_{\theta,1}} := \{h_\tau^{(G_{\theta,1})}(x; \cdot) : x \in \mathbb{R}^p, \tau \in [0, \infty]\}$. We verify (i) and (ii)

in the proof of Theorem 2.2 for the class \mathcal{H}_{G_Θ} . For (i), notice that, in view of **(A3)**, both $\sup_{\theta \in \Theta} \sup_{h^{(G_\theta)} \in \mathcal{H}_{G_\theta}} |h^{(G_\theta)}(\cdot)|$ and $\sup_{\theta \in \Theta} \sup_{h^{(G_{\theta,1})} \in \mathcal{H}_{G_{\theta,1}}} |h^{(G_{\theta,1})}(\cdot)|$ are bounded above by $l_{G,\Theta}$. We now turn to (ii). Let $i_{G_\Theta} : [0, \infty] \times \Theta \times \mathbb{R}^p \times (\mathbb{R}^p)^{k_{G_\Theta}} \rightarrow \mathbb{R}$ be given by $i_{G_\Theta}(\tau; \theta; x; x_1, \dots, x_{k_{G_\Theta}}) = h_\tau^{(G_\theta)}(x; x_1, \dots, x_{k_{G_\Theta}})$ and $F_{G_\Theta} : (0, \infty) \times \Theta \times \mathbb{R}^p \times (\mathbb{R}^p)^{k_{G_\Theta}} \rightarrow (\mathbb{R}^p)^{k_{G_\Theta}}$ be given by $F_{G_\Theta}(\tau; \theta; x; x_1, \dots, x_{k_{G_\Theta}}) = \left(\theta, \frac{x_1 - x}{\tau}, \dots, \frac{x_{k_{G_\Theta}} - x}{\tau} \right)^\top$. For simplicity, let $H_\tau^{(G_\Theta)}(\theta; \cdot, \cdot) = h_\tau^{(G_\theta)}(\cdot; \cdot)$, $\tau \in \{0, \infty\}$, and $G_*(\theta; \cdot) = G_\theta(\cdot)$, yielding $h_\tau^{(G_\Theta)}(\cdot; \cdot) = G_*(F_{G_\Theta}(\tau; \theta; \cdot; \cdot))$, $\theta \in \Theta$, $\tau \in (0, \infty)$. It follows from **(A4)** that $G_*(F_{G_\Theta}(\cdot; \cdot; \cdot; \cdot))$, $H_0^{G_\Theta}(\cdot; \cdot, \cdot)$, and $H_\infty^{G_\Theta}(\cdot; \cdot, \cdot)$ are Borel measurable. Therefore, for all $A \in \mathcal{B}(\mathbb{R})$,

$$\begin{aligned} i_{G_\Theta}^{-1}(A) &= (F_{G_\Theta}^{-1}(G_*^{-1}(A)) \cup (\{0\} \times (H_0^{(G_\Theta)})^{-1}(A)) \cup (\{\infty\} \times (H_\infty^{(G_\Theta)})^{-1}(A)) \\ &\in \mathcal{B}([0, \infty] \times \Theta \times \mathbb{R}^p \times (\mathbb{R}^p)^{k_{G_\Theta}}). \end{aligned}$$

We conclude that $i_{G_\Theta}(\cdot)$ is Borel measurable and the class \mathcal{H}_{G_Θ} is image admissible Suslin via $e_{G_\Theta} : [0, \infty] \times \Theta \times \mathbb{R}^p \rightarrow \mathcal{H}_{G_\Theta}$ given by $e_{G_\Theta}(\tau; \theta; x) = h_\tau^{(G_\theta)}(x; \cdot)$. ■

Before we state Proposition A.1, which is used in the proof of Theorem 2.3, we recall that T is a subset of $\mathbb{R}^p \times [0, \infty]$ such that, for $(x, \tau) \in T$, $E[(\tilde{h}_\tau^{(1)}(x; X_1))^2] > 0$. For $m \geq 1$ and $(x_1, \tau_1), \dots, (x_m, \tau_m) \in T$, we also use the notations

$$\mathbf{LGD}_n(x_l, \tau_l) := (LGD_n(x_1, \tau_1), \dots, LGD_n(x_m, \tau_m))^\top,$$

$$\mathbf{LGD}(x_l, \tau_l) := (LGD(x_1, \tau_1), \dots, LGD(x_m, \tau_m))^\top,$$

and, for $j = 1, \dots, k$ and $y_1, \dots, y_j \in \mathbb{R}^p$,

$$\mathbf{h}_{\tau_l}^{(j)}(x_l; y_1, \dots, y_j) := (h_{\tau_1}^{(j)}(x_1; y_1, \dots, y_j), \dots, h_{\tau_m}^{(j)}(x_m; y_1, \dots, y_j))^\top.$$

Proposition A.1 *For $(x_1, \tau_1), \dots, (x_m, \tau_m) \in T$, $\sqrt{n}(\mathbf{LGD}_n(x_l, \tau_l) - \mathbf{LGD}(x_l, \tau_l))$ converges in distribution to a m -variate normal distribution with mean 0 and covariance matrix whose $(l_1, l_2)^{th}$ element is given by $k^2 \gamma((x_{l_1}, \tau_{l_1}), (x_{l_2}, \tau_{l_2}))$, where $l_1, l_2 = 1, \dots, m$.*

Proof of Proposition A.1. Using Hoeffding's decomposition of U-statistics (see (1.1.22) in Korolyuk and Borovskich [2013]), it follows that, for all $(x, \tau) \in T$,

$$LGD_n(x, \tau) - LGD(x, \tau) = \sum_{j=1}^k \binom{k}{j} \binom{n}{j}^{-1} \sum_{1 \leq i_1 < \dots < i_j \leq n} g_\tau^{(j)}(x; X_{i_1}, \dots, X_{i_j}), \quad (\text{A.22})$$

where, for $j = 1, \dots, k$, $g_\tau^{(j)}(x; \cdot)$ is defined recursively by

$$g_\tau^{(j)}(x; x_1, \dots, x_j) := h_\tau^{(j)}(x; x_1, \dots, x_j) - LGD(x, \tau) - \sum_{s=1}^{j-1} \sum_{1 \leq i_1 < \dots < i_s \leq j} g_\tau^{(s-1)}(x; x_{i_1}, \dots, x_{i_s}).$$

In particular, $g_\tau^{(j)}(x; \cdot)$ is completely degenerate (see (1.1.8) in Korolyuk and Borovskich [2013]), that is,

$$E[g_\tau^{(j)}(x; x_1, \dots, x_{j-1}, X_j)] = 0. \quad (\text{A.23})$$

For $j = 1, \dots, k$ and $y_1, \dots, y_j \in \mathbb{R}^p$, let

$$\mathbf{g}_{\tau_l}^{(j)}(x_l; y_1, \dots, y_j) := (g_{\tau_1}^{(j)}(x_1; y_1, \dots, y_j), \dots, g_{\tau_m}^{(j)}(x_m; y_1, \dots, y_j))^\top.$$

For $m \geq 1$ and $(x_1, \tau_1), \dots, (x_m, \tau_m) \in T$, it follows that

$$\mathbf{LGD}_n(x_l, \tau_l) - \mathbf{LGD}(x_l, \tau_l) = \frac{k}{n} \sum_{i=1}^n [\mathbf{h}_{\tau_l}^{(1)}(x_l; X_i) - \mathbf{LGD}(x_l, \tau_l)] + \sum_{j=2}^k \mathbf{R}_n^{(j)},$$

where, for $j = 2, \dots, k$,

$$\mathbf{R}_n^{(j)} = \mathbf{R}_n^{(j)}(X_1, \dots, X_n) := \binom{k}{j} \binom{n}{j}^{-1} \sum_{1 \leq i_1 < \dots < i_j \leq n} \mathbf{g}_{\tau_l}^{(j)}(x_l; X_{i_1}, \dots, X_{i_j}).$$

Now applying Cheybchev's inequality, for all $\epsilon > 0$,

$$P^{\otimes n}(\sqrt{n} \|\mathbf{R}_n^{(j)}\| > \epsilon) \leq \frac{n}{\epsilon^2} \binom{k}{j}^2 \binom{n}{j}^{-2} \sum_{l=1}^m E\left[\left(\sum_{1 \leq i_1 < \dots < i_j \leq n} \mathbf{g}_{\tau_l}^{(j)}(x_l; X_{i_1}, \dots, X_{i_j})\right)^2\right].$$

Observe that, for $l = 1, \dots, m$,

$$\begin{aligned} E\left[\left(\sum_{1 \leq i_1 < \dots < i_j \leq n} g_{\tau_l}^{(j)}(x_l; X_{i_1}, \dots, X_{i_j})\right)^2\right] &= \sum_{1 \leq i_1 < \dots < i_j \leq n} E\left[\left(g_{\tau_l}^{(j)}(x_l; X_{i_1}, \dots, X_{i_j})\right)^2\right] \\ &+ \sum_{1 \leq i_1 < \dots < i_j \leq n} \sum_{\substack{1 \leq s_1 < \dots < s_j \leq n \\ \exists l \in \{i_1, \dots, i_j\}: s_1, \dots, s_j \neq l}} E\left[g_{\tau_l}^{(j)}(x_l; X_{i_1}, \dots, X_{i_j}) g_{\tau_l}^{(j)}(x_l; X_{s_1}, \dots, X_{s_j})\right]. \end{aligned}$$

By conditioning on all $X_{i_1}, \dots, X_{i_j}, X_{s_1}, \dots, X_{s_j}$ but X_l and using (A.23), we see that

$$E\left[g_{\tau_l}^{(j)}(x_l; X_{i_1}, \dots, X_{i_j}) g_{\tau_l}^{(j)}(x_l; X_{s_1}, \dots, X_{s_j})\right] = 0.$$

It follows that

$$E\left[\left(\sum_{1 \leq i_1 < \dots < i_j \leq n} g_{\tau_l}^{(j)}(x_l; X_{i_1}, \dots, X_{i_j})\right)^2\right] = \binom{n}{j} E\left[\left(g_{\tau_l}^{(j)}(x_l; X_1, \dots, X_j)\right)^2\right].$$

Hence,

$$P^{\otimes n}(\sqrt{n} \|\mathbf{R}_n^{(j)}\| > \epsilon) \leq \frac{n}{\epsilon^2} \binom{k}{j}^2 \binom{n}{j}^{-1} \sum_{l=1}^m E\left[\left(g_{\tau_l}^{(j)}(x_l; X_1, \dots, X_j)\right)^2\right] \quad (\text{A.24})$$

and this converges to 0 as $n \rightarrow \infty$, which implies that, for all $j \geq 2$, $\mathbf{R}_n^{(j)}$ converges to 0 in probability. Next, observe that $\frac{1}{n} \sum_{i=1}^n [\mathbf{h}_{\tau_l}^{(1)}(x_l; X_i) - \mathbf{LGD}(x_l, \tau_l)]$ is an average of i.i.d. random variables with mean 0 and covariance matrix whose $(l_1, l_2)^{\text{th}}$ element is given by

$$E \left[\left(h_{\tau_{l_1}}^{(1)}(x_{l_1}; X_i) - LGD(x_{l_1}, \tau_{l_1}) \right) \left(h_{\tau_{l_2}}^{(1)}(x_{l_2}; X_i) - LGD(x_{l_2}, \tau_{l_2}) \right) \right],$$

which is the same as $\gamma((x_{l_1}, \tau_{l_1}), (x_{l_2}, \tau_{l_2}))$. Therefore, by the multivariate central limit theorem, as $n \rightarrow \infty$,

$$\sqrt{n} \frac{1}{n} \sum_{i=1}^n [\mathbf{h}_{\tau_l}^{(1)}(x_l; X_i) - \mathbf{LGD}(x_l, \tau_l)]$$

converges in distribution to a multivariate normal distribution with mean 0 and covariance matrix given by $\gamma((x_{l_1}, \tau_{l_1}), (x_{l_2}, \tau_{l_2}))$. \blacksquare

An immediate consequence of Proposition A.1 is the following corollary.

Corollary A.1 *If $x \in \mathbb{R}^p$ and $\tau \in (0, \infty]$ satisfy $E[(\tilde{h}_{\tau}^{(1)}(x; X_1))^2] > 0$, then*

$$\sqrt{n} (LGD_n(x, \tau) - LGD(x, \tau)) \xrightarrow[n \rightarrow \infty]{d} N(0, k^2 E[(\tilde{h}_{\tau}^{(1)}(x; X_1))^2]). \quad (\text{A.25})$$

Next, we state and prove a result concerning the quantity $D_G(\cdot, \cdot)$ in (2.14) that will be used for the proof of Proposition 2.3.

Lemma A.4 *Let $D_G(\cdot, \cdot)$, σ_G , and $C_{G,0}$ be as in Theorem 2.4, $\{a_n\}_{n=1}^{\infty}$ be a sequence of positive scalars converging to zero with $\lim_{n \rightarrow \infty} \frac{n}{\log(n)} a_n^2 = \infty$, $b > 0$, and $t_n := \sqrt{n}a_n b$. Then, there are constants $0 < \tilde{C}_G < \infty$ and $\tilde{n} \in \mathbb{N}$ such that, for all $n \geq \tilde{n}$, $t_n \geq \max(2^3 \sigma_G, 2^4 C_{G,0})$ and*

$$D_G(n, t_n) \leq \frac{\tilde{C}_G}{n^2}.$$

Proof of Lemma A.4. Since $\lim_{n \rightarrow \infty} t_n = \infty$ and $\lim_{n \rightarrow \infty} a_n = 0$, there is $n_1 \in \mathbb{N}$, such that, for all $n \geq n_1$, $t_n \geq \max(2^3 \sigma_G, 2^4 C_{G,0})$ and $t_n/\sqrt{n} = a_n b \leq 1$. Then, for all $n \geq n_1$, it holds that

$$\begin{aligned} D_G(n, t_n) &\leq 8 \exp \left(-\frac{t_n^2}{2^{15} k_G^2 (\sigma_G^2 + l_G)} \right) + 2 \exp \left(-\frac{t_n^2}{2^{6+k_G} k_G^{k_G+1} l_G C_{G,0} (\sigma_G^2 + l_G)} \right) \\ &\quad + 8 C_{G,1}^{2C_{G,2}} (\sigma_G^2 + 2a_n b l_G)^{-C_{G,2}} \exp \left(-\left(\frac{n \sigma_G^2}{2l_G^2} + \frac{\sqrt{n} t_n}{4l_G} \right) \right) \\ &\leq 16 \exp \left(-\frac{t_n^2}{C_{G,3}} \right) + C_{G,4} a_n^{-C_{G,2}} \exp \left(-\frac{\sqrt{n} t_n}{C_{G,5}} \right), \end{aligned}$$

where $C_{G,3} := (\sigma_G^2 + l_G) \max(2^{15} k_G^2, 2^{6+k_G} k_G^{k_G+1} l_G C_{G,0})$, $C_{G,4} := 8C_{G,1}^{2C_{G,2}} (2bl_G)^{-C_{G,2}}$, and $C_{G,5} := 4l_G$. Next, we use that $\lim_{n \rightarrow \infty} \frac{n}{\log(n)} a_n^2 = \infty$ to show that

$$\lim_{n \rightarrow \infty} n^2 \exp\left(-\frac{t_n^2}{C_{G,3}}\right) = \lim_{n \rightarrow \infty} \exp\left(-\left(\frac{\log(n)}{C_{G,3}}\right)\left(\frac{t_n^2}{\log(n)} - 2C_{G,3}\right)\right) = 0.$$

In particular, there is $n_2 \in \mathbb{N}$, such that, for all $n \geq n_2$, $\exp\left(-\frac{t_n^2}{C_{G,3}}\right) \leq \frac{1}{n^2}$. Next, notice that

$$\begin{aligned} n^2 a_n^{-C_{G,2}} \exp\left(-\frac{\sqrt{n}t_n}{C_{G,5}}\right) &= \exp\left(2\log(n) - \frac{na_n b}{2C_{G,5}}\right) \exp\left(-C_{G,2} \log(a_n) - \frac{na_n b}{2C_{G,5}}\right) \\ &= \exp\left(-\log(n)\left(\frac{b}{2C_{G,5}} \frac{na_n}{\log(n)} - 2\right)\right) \\ &\quad \exp\left(-\frac{b}{2C_{G,5}} na_n \left(1 + \frac{2C_{G,2}C_{G,5}}{b} \frac{\log(a_n)}{na_n}\right)\right). \end{aligned}$$

Now, $\lim_{n \rightarrow \infty} \frac{na_n^2}{\log(n)} = \infty$ implies that $\lim_{n \rightarrow \infty} \frac{na_n}{\log(n)} = \infty$ and $\lim_{n \rightarrow \infty} na_n = \infty$ yielding that

$$\lim_{n \rightarrow \infty} n^2 a_n^{-C_{G,2}} \exp\left(-\frac{\sqrt{n}t_n}{C_{G,5}}\right) = 0.$$

This show that there is $n_3 \in \mathbb{N}$ such that $a_n^{-C_{G,2}} \exp\left(-\frac{\sqrt{n}t_n}{C_{G,5}}\right) \leq \frac{1}{n^2}$ for all $n \geq n_3$. Let $\tilde{n} = \max_{i=1,\dots,3} n_i$. Then, for all $n \geq \tilde{n}$, it holds that

$$D_G(n, t_n) \leq \frac{16 + C_{G,4}}{n^2},$$

and the result follows by setting $\tilde{C}_G := 16 + C_{G,4}$. ■

Proof of Proposition 2.3. For (i), observe that

$$\sup_{x \in \mathbb{R}^p} |f_{\tau_n, n}^{(G)}(x) - f(x)| \leq \sup_{x \in \mathbb{R}^p} |f_{\tau_n, n}^{(G)}(x) - f_{\tau_n}^{(G)}(x)| + \sup_{x \in \mathbb{R}^p} |f_{\tau_n}^{(G)}(x) - f(x)|$$

and, by Proposition 2.2 (i), it is enough to show that

$$\lim_{n \rightarrow \infty} \sup_{x \in \mathbb{R}^p} |f_{\tau_n, n}^{(G)}(x) - f_{\tau_n}^{(G)}(x)| = 0 \text{ a.s.} \tag{A.26}$$

Now, using Lemma A.2, we see that

$$\sup_{x \in \mathbb{R}^p} |f_{\tau_n, n}^{(G)}(x) - f_{\tau_n}^{(G)}(x)| \leq \sup_{\substack{x \in \mathbb{R}^p \\ \tau \in [0, \infty]}} \left| \frac{LGD_n(x, \tau) - LGD(x, \tau)}{\Lambda_1^{(G)} \tau_n^{k_G p}} \right|^{1/k_G}.$$

Let $\epsilon > 0$, $t_n := \sqrt{n} \tau_n^{k_{GP}} \Lambda_1^{(G)} \epsilon^{k_G}$ and notice that, since $\lim_{n \rightarrow \infty} n \tau_n^{2k_{GP}} = \infty$, $\lim_{n \rightarrow \infty} t_n = \infty$. It follows from Theorem 2.4 and Lemma A.4 with $a_n = \tau_n^{k_{GP}}$ and $b = \Lambda_1^{(G)} \epsilon^{k_G}$ that there are constants $1 < C_{G,0} < \infty$, $0 < \tilde{C}_G < \infty$, and $\tilde{n} \in \mathbb{N}$ such that, for all $n \geq \tilde{n}$, $t_n \geq \max(2^3 \sigma_G, 2^4 C_{G,0})$ and

$$\begin{aligned} P^{\otimes n} \left(\sup_{x \in \mathbb{R}^p} |f_{\tau_n, n}^{(G)}(x) - f_{\tau_n}^{(G)}(x)| \geq \epsilon \right) &= P^{\otimes n} \left(\sqrt{n} \sup_{\substack{x \in \mathbb{R}^p \\ \tau \in [0, \infty]}} |LGD_n(x, \tau) - LGD(x, \tau)| \geq t_n \right) \\ &\leq D_G(n, t_n) \leq \frac{\tilde{C}_G}{n^2}. \end{aligned}$$

Therefore, we obtain that

$$\begin{aligned} \sum_{n=1}^{\infty} P^{\otimes n} \left(\sup_{x \in \mathbb{R}^p} |f_{\tau_n, n}^{(G)}(x) - f_{\tau_n}^{(G)}(x)| \geq \epsilon \right) &\leq \tilde{n} - 1 + \sum_{n=\tilde{n}}^{\infty} D_G(n, t_n) \\ &\leq \tilde{n} - 1 + \sum_{n=\tilde{n}}^{\infty} \frac{\tilde{C}_G}{n^2} < \infty. \end{aligned}$$

Now, (A.26) follows from Borel-Cantelli lemma. The proof of the first part of (ii) follows from the inequality

$$\sup_{x \in K} |f_{\tau_n, n}^{(G)}(x) - f(x)| \leq \sup_{x \in \mathbb{R}^p} |f_{\tau_n, n}^{(G)}(x) - f_{\tau_n}^{(G)}(x)| + \sup_{x \in K} |f_{\tau_n}^{(G)}(x) - f(x)|,$$

(A.26), and Proposition 2.2 (ii). For the second part of (ii), let $\epsilon^* > 0$ and $n^* \in \mathbb{N}$ such that $\epsilon_n \leq \epsilon^*$ for all $n \geq n^*$. Then, for all $n \geq n^*$ and $x \in \mathbb{R}^p$,

$$\sup_{y \in \overline{B}_{\epsilon_n}(x)} |f_{\tau_n, n}^{(G)}(y) - f(x)| \leq \sup_{y \in \overline{B}_{\epsilon^*}(x)} |f_{\tau_n, n}^{(G)}(y) - f_{\tau_n}^{(G)}(y)| + \sup_{y \in \overline{B}_{\epsilon_n}(x)} |f_{\tau_n}^{(G)}(y) - f(x)|.$$

Now, using the compactness of $\overline{B}_{\epsilon^*}(x)$ and the first part of (ii), we have that

$$\lim_{n \rightarrow \infty} \sup_{y \in \overline{B}_{\epsilon^*}(x)} |f_{\tau_n, n}^{(G)}(y) - f_{\tau_n}^{(G)}(y)| = 0 \text{ a.s.}$$

Finally, Proposition 2.2 (ii) implies that

$$\lim_{n \rightarrow \infty} \sup_{y \in \overline{B}_{\epsilon_n}(x)} |f_{\tau_n}^{(G)}(y) - f(x)| = 0.$$

■

We next turn to the proof of Lemma 3.1. First, we recall the definition of limits of sets below. The limit inferior and superior of a sequence of sets $\{A_n\}_{n=1}^{\infty}$ are $\liminf_{n \rightarrow \infty} A_n = \bigcup_{n=1}^{\infty} \bigcap_{l=n}^{\infty} A_l$ and $\limsup_{n \rightarrow \infty} A_n = \bigcap_{n=1}^{\infty} \bigcup_{l=n}^{\infty} A_l$. If they are equal we say that the

sequence $\{A_n\}_{n=1}^\infty$ converges and write $A = \lim_{n \rightarrow \infty} A_n$, where $A := \liminf_{n \rightarrow \infty} A_n = \limsup_{n \rightarrow \infty} A_n$.

Proof of Lemma 3.1. We first observe that $x \in S_{f_\tau}$ if and only if $f_\tau(x) > 0$ if and only if $LGD(x, \tau) > 0$. Proposition 2.1 (i) implies that for $x \in \mathbb{R}^p$, $LGD(x, \tau_1) \leq LGD(x, \tau_2)$, from which it follows that $S_{f_{\tau_1}} \subset S_{f_{\tau_2}}$. Next, suppose that $f(\cdot)$ is continuous and let $x \in S_f$ and $\tau > 0$. Since $f(\cdot)$ is continuous, S_f is open and there exists $\epsilon > 0$ such that $\overline{B}_{\tau\epsilon}(x) \subset S_f$. By (P4), there exist $0 < \delta \leq \tau\epsilon$ and $c > 0$ such that $\lambda((\overline{B}_\delta(x))^k \cap S_{h_\tau(x; \cdot)}) > 0$ and $h_\tau(x; \cdot) \geq c$ in $(\overline{B}_\delta(x))^k \cap S_{h_\tau(x; \cdot)}$. It follows that

$$\begin{aligned} LGD(x, \tau) &= \int h_\tau(x; x_1, \dots, x_k) f(x_1) \dots f(x_k) dx_1 \dots dx_k \\ &\geq c \int_{(\overline{B}_\delta(x))^k \cap S_{h_\tau(x; \cdot)}} f(x_1) \dots f(x_k) dx_1 \dots dx_k > 0. \end{aligned}$$

Thus $x \in S_{f_\tau}$ and $S_f \subset S_{f_\tau}$. Since the sets $\{S_{f_\tau}\}_{\tau > 0}$ are monotonically decreasing with τ , we have that $\lim_{\tau \rightarrow 0^+} S_{f_\tau} = \cap_{\tau > 0} S_{f_\tau} \supset S_f$. For the last part, let $x \in \mathbb{R}^p \setminus \overline{S}_f$. Since $\mathbb{R}^p \setminus \overline{S}_f$ is open, there exists $\epsilon > 0$ such that $\overline{B}_\epsilon(x) \subset \mathbb{R}^p \setminus \overline{S}_f$. Let $0 < \tau \leq \epsilon/\rho$. By (2.4) it follows that $S_{h_\tau(x; \cdot)} \subset (\overline{B}_{\rho\tau}(x))^k \subset (\overline{B}_\epsilon(x))^k$ implying that $LGD(x, \tau) = 0$. Therefore, $x \notin \cap_{\tau > 0} S_{f_\tau}$ and $\cap_{\tau > 0} S_{f_\tau} \subset \overline{S}_f$. \blacksquare

The next lemma is used in the proof of Theorem 3.1 (iii), Proposition A.2 (ii), and Lemma 3.2 (i) and provides a uniform approximation of $f_\tau(\cdot)$ in compact sets.

Lemma A.5 Suppose (2.4) holds true and $f(\cdot)$ is three times continuously differentiable. Let K be a compact subset of S_f . Then, there are constants $\tau(K), c_1(K), c_2(K) > 0$ and a continuously differentiable function $\tilde{R}_\tau : K \rightarrow \mathbb{R}$ such that, for all $x \in K$ and $0 < \tau \leq \tau(K)$, $|\tilde{R}_\tau(x)| \leq c_1(K)$, $\|\nabla \tilde{R}_\tau(x)\| \leq c_2(K)$, and

$$f_\tau(x) = f(x) + \tilde{R}_\tau(x)\tau^2.$$

Proof of Lemma A.5. Notice that, since $K \subset S_f$, K is closed and S_f is open, there is $\delta, h^* > 0$ such that $(K)^{+(\delta+h^*)} \subset S_f$. Let $\tau_1 := \delta/\rho$ and $K^* = K^{+h^*}$. Then, for $\tau \in (0, \tau_1]$, we have that $(K^*)^{+\rho\tau} \subset (K)^{+(\delta+h^*)}$ and, by Remark 2.1, $f_\tau(\cdot)$ is three times continuously differentiable in K^* . Since $f(\cdot)$ is three times continuously differentiable, by Theorem 2.1 (iii), we have that, for $x \in K^*$,

$$f_\tau^k(x) - f^k(x) = Q_\tau(x)\tau^2,$$

where, for all $\tau \in [0, \tau_1]$, $Q_\tau(x) := R(x)/\Lambda_1 + o(\tau)$ is well-defined and continuously differentiable with uniformly bounded derivatives in K^* . Let

$$c_3(K^*) := \sup_{y \in K^*} \sup_{\tau \in [0, \tau_1]} |Q_\tau(y)/f^k(y)|$$

and $\tau(K) \in (0, \min(1, \tau_1, c_3^{-1/2}(K^*), c_3^{-2}(K^*)))$. It follows from Newton's generalized binomial theorem that, for $\tau \in (0, \tau(K)]$,

$$\begin{aligned} f_\tau(x) &= f(x) \left(1 + Q_\tau(x)/f^k(x)\tau^2\right)^{1/k} \\ &= f(x) + 1/kQ_\tau(x)/f^{k-1}(x)\tau^2 + \tau^3\tilde{Q}_\tau(x), \end{aligned}$$

here $\tilde{Q}_\tau(x) := 1/\tau^3 f(x) \sum_{j=2}^{\infty} \binom{1/k}{j} (Q_\tau(x)/f^k(x)\tau^2)^j$ and $\binom{1/k}{j} = (1/k \dots (1/k-j+1))/j!$.

Now, since $\tau \leq \tau(K) < 1$, we obtain that

$$\begin{aligned} |\tilde{Q}_\tau(x)| &\leq f(x) \left| \sum_{l=2}^{\infty} \binom{1/k}{l} (\tau^{1/2}Q_\tau(x)/f^k(x))^l \right| \\ &= f(x) \left(1 + 1/k\tau^{1/2}Q_\tau(x)/f^k(x) - (1 + \tau^{1/2}Q_\tau(x)/f^k(x))^{1/k}\right). \end{aligned}$$

Hence, $c_4(K^*) := \sup_{y \in K^*} \sup_{\tau \in [0, \tau(K)]} |\tilde{Q}_\tau(y)| < \infty$. Let $\tilde{R}_\tau(x) := 1/kQ_\tau(x)/f^{k-1}(x) + \tau\tilde{Q}_\tau(x)$. We need to show that, for all $\tau \in (0, \tau(K)]$, $\tilde{Q}_\tau(\cdot)$ is continuously differentiable in K with uniformly bounded derivatives. To this end, let $T_{\tau,l}(x) := \binom{1/k}{l} (Q_\tau(x)/f^k(x)\tau^2)^l$, $\tilde{T}_{\tau,l}^{(i)}(x) := \binom{1/k}{l} l(Q_\tau(x)/f^k(x)\tau^2)^{l-1} \partial_i(Q_\tau(x)/f^k(x)\tau^2)$, $S_{\tau,j}(x) := \sum_{l=2}^j T_{\tau,l}(x)$ and $\tilde{S}_{\tau,j}^{(i)}(x) := \sum_{l=2}^j \tilde{T}_{\tau,l}^{(i)}(x)$. Notice that $\partial_i S_{\tau,j}(x) = \tilde{S}_{\tau,j}^{(i)}(x)$. Let

$$c_5(K^*) := \sup_{y \in K^*} \sup_{\tau \in [0, \tau(K)]} \|\nabla Q_\tau(y)/f^k(y)\|.$$

We compute

$$\begin{aligned} \sup_{y \in K^*} \sup_{\tau \in [0, \tau(K)]} |S_{\tau,\infty}(y) - S_{\tau,j}(y)| &\leq \sum_{l=j+1}^{\infty} (c_3(K^*)\tau^2(K))^l \\ &= \frac{(c_3(K^*)\tau^2(K))^{j+1}}{1 - c_3(K^*)\tau^2(K)} \xrightarrow{j \rightarrow \infty} 0 \end{aligned}$$

and

$$\begin{aligned} \sup_{y \in K^*} \sup_{\tau \in [0, \tau(K)]} |\tilde{S}_{\tau,j}^{(i)}(y) - \tilde{S}_{\tau,j}^{(i)}(y)| &\leq c_4(K^*)\tau^2(K) \sum_{l=j}^{\infty} (c_3(K^*)\tau^2(K))^l \\ &= c_4(K^*)\tau^2(K) \frac{(c_3(K^*)\tau^2(K))^j}{1 - c_3(K^*)\tau^2(K)} \xrightarrow{j \rightarrow \infty} 0. \end{aligned}$$

Hence, the series $S_{\tau,j}(\cdot)$ and $\tilde{S}_{\tau,j}^{(i)}(\cdot)$ converge uniformly to $S_{\tau,\infty}(\cdot)$ and $\tilde{S}_{\tau,\infty}^{(i)}(\cdot)$. By the fundamental theorem of calculus (FTC), the uniform convergence of $\tilde{S}_{\tau,\infty}^{(i)}(\cdot)$, and LDCT, we have that, for all $x \in K$ and $0 < h \leq h^*$,

$$\begin{aligned} S_{\tau,\infty}(x + he_i) - S_{\tau,\infty}(x) &= \sum_{l=2}^{\infty} (T_{\tau,l}(x + he_i) - T_{\tau,l}(x)) \\ &= \sum_{l=2}^{\infty} \int_0^h \tilde{T}_{\tau,l}^{(i)}(x + te_i) dt = \int_0^h \tilde{S}_{\tau,\infty}^{(i)}(x + te_i) dt. \end{aligned}$$

Now, using again FTC, we have that

$$\partial_i S_{\tau,\infty}(x) = \lim_{h \rightarrow 0^+} \frac{S_{\tau,\infty}(x + he_i) - S_{\tau,\infty}(x)}{h} = \lim_{h \rightarrow 0^+} 1/h \int_0^h \tilde{S}_{\tau,\infty}^{(i)}(x + te_i) dt = \tilde{S}_{\tau,\infty}^{(i)}(x)$$

and

$$\begin{aligned} \nabla S_{\tau,\infty}(x) &= (\tilde{S}_{\tau,\infty}^{(1)}(x), \dots, \tilde{S}_{\tau,\infty}^{(p)}(x))^\top \\ &= \sum_{l=2}^{\infty} \binom{1/k}{l} l(Q_\tau(x)/f^k(x)\tau^2)^{l-1} \nabla(Q_\tau(x)/f^k(x)\tau^2). \end{aligned}$$

Hence, $\tilde{Q}_\tau(\cdot)$ is continuously differentiable in K and

$$\nabla \tilde{Q}_\tau(x) = \nabla f(x)(S_{\tau,\infty}(x)/\tau^3) + f(x)\nabla S_{\tau,\infty}(x)/\tau^3.$$

Since $\left| \binom{1/k}{l} l \right| \leq 1$ and $c_3(K^*)\tau^{1/2}(K) < 1$ we obtain that

$$\sup_{y \in K} \sup_{\tau \in [0, \tau(K)]} |S_{\tau,\infty}(x)/\tau^3| \leq \sum_{l=2}^{\infty} (c_3(K^*)\tau^{1/2}(K))^l < \infty$$

and

$$\sup_{y \in K} \sup_{\tau \in [0, \tau(K)]} \|\nabla S_{\tau,\infty}(x)/\tau^3\| \leq c_5(K^*) \sum_{l=1}^{\infty} (c_3(K^*)\tau^{1/2}(K))^l < \infty.$$

Thus, $c_6(K) := \sup_{y \in K} \sup_{\tau \in [0, \tau(K)]} \|\nabla \tilde{Q}_\tau(x)\| < \infty$. Let

$$c_7(K) := \sup_{y \in K} \sup_{\tau \in [0, \tau(K)]} |(Q_\tau(y)/f^{k-1}(y))|$$

and

$$c_8(K) := \sup_{y \in K^*} \sup_{\tau \in [0, \tau(K)]} \|\nabla(Q_\tau(y)/f^{k-1}(y))\|.$$

Then, we conclude that

$$\sup_{x \in K} \sup_{\tau \in [0, \tau(K)]} |\tilde{R}_\tau(x)| \leq c_1(K) := c_7(K)/k + \tau(K)c_4(K^*) < \infty$$

and

$$\sup_{x \in K} \sup_{\tau \in [0, \tau(K)]} \|\nabla \tilde{R}_\tau(x)\| \leq c_2(K) := c_8(K)/k + \tau^2(K)c_6(K) < \infty.$$

■

We now turn to the proof of Theorem 3.1. To this end, we introduce few additional notations. The norm of a $p \times p$ matrix A is given by $\|A\|_{\mathcal{M}} := \sup_{y \in \mathbb{R}^p, y \neq 0} \|Ay\| / \|y\|$ and

the spectrum of A , that is, the set of all the eigenvalues of A is denoted by $\sigma(A)$. Finally, the sign function $\text{sgn} : \mathbb{R} \rightarrow \mathbb{R}$ is given by

$$\text{sgn}(t) = \begin{cases} -1 & \text{if } t < 0 \\ 0 & \text{if } t = 0 \\ 1 & \text{if } t > 0. \end{cases}$$

Before the proof, we provide a brief description of the idea. Proof of (i) is standard and allows for a characterization of the stationary points of $f_\tau(\cdot)$ when τ -symmetry prevails. As for the proof part (ii), note that for each stationary point μ of $f(\cdot)$, first a closed hypercube centered at μ with directions given by the orthogonal eigenvectors of $H_f(\mu)$ is constructed. The side lengths of the hypercube are such that, for small enough τ and all points in the hypercube (i) the eigenvalues of $H_{f_\tau}(\cdot)$ and $H_f(\cdot)$ corresponding to the same eigenvector have the same sign and (ii) points on opposite “hyperfaces” have directional derivatives (w.r.t. the eigenvector that is orthogonal to the two “hyperfaces”) of opposite sign. This follows using the convergence of first and second order derivatives of $f_\tau(\cdot)$ to those of $f(\cdot)$. Now, (ii) implies that every straight line connecting the two “hyperfaces” contains a point having zero directional derivative. Thus, by intersecting all such sets of points along every direction, we find a point μ_τ having zero directional derivative w.r.t. all eigenvectors. Since these are orthogonal, the gradient of μ_τ is zero, that is, μ_τ is a stationary point of $f_\tau(\cdot)$. Next, using (i), we conclude that μ_τ and μ are of the same type. Finally, the convergence $\mu_\tau \rightarrow \mu$ follows by letting the side length of the hypercube converge to zero. For part (iii), we use Lemma A.5 to show that, in a compact set, $|\nabla f_\tau(\cdot) - \nabla f(\cdot)| = o(\tau^2)$. We then infer the same order of convergence for μ_τ to μ .

Proof of Theorem 3.1. We start by proving (i). Notice that, if $f(\cdot)$ is continuously differentiable in $\overline{B}_{\rho\tau}(x) \subset S_f$, then, for $j = 1, \dots, p$,

$$\partial_j f_\tau(x) = \frac{1}{k} (f_\tau(x))^{1-k} \frac{\partial_j LGD(x, \tau)}{\tau^{kp} \Lambda_1}, \quad (\text{A.27})$$

where, by Proposition 2.1, (A.2) and (A.4),

$$\begin{aligned} \partial_j LGD(x, \tau) &= \int h_\tau(0; x_1, \dots, x_k) \partial_j (f(x - x_1) \dots f(x - x_k)) dx_1 \dots dx_k \\ &= k \int h_\tau(0; x_1, \dots, x_k) \partial_j f(x + x_1) f(x + x_2) \dots f(x + x_k) dx_1 \dots dx_k. \end{aligned}$$

Hence, $\partial_j f_\tau(\mu) = 0$ if and only if

$$\int h_\tau(0; x_1, \dots, x_k) \partial_j f(\mu + x_1) f(\mu + x_2) \dots f(\mu + x_k) dx_1 \dots dx_k = 0, \quad (\text{A.28})$$

and hence (3.4) holds. We next turn to the proof of (ii). Since $H_f(\mu)$ is symmetric, it has orthonormal eigenvectors v_i associated with eigenvalues λ_i , $i = 1, \dots, p$. Notice that, since μ is of type l , l eigenvalues are negative and $p - l$ are positive. In particular,

$$\min_{i=1,\dots,p} |\lambda_i| > 0. \quad (\text{A.29})$$

Let $0 < \tau \leq \tau_1$, where $\tau_1 := \delta/(2(1 + \rho))$, and $x \in \overline{B}_{\tau_1}(\mu)$. Since $x \in \overline{B}_{\delta/2}(\mu)$, $(\overline{B}_{\tau_1}(x))^{+\rho\tau} \subset \overline{B}_{\delta/2}(x) \subset \overline{B}_\delta(\mu)$. It follows that $f_\tau(\cdot)$ is twice continuously differentiable in $\overline{B}_{\tau_1}(x)$ and its first order partial derivatives are given by (A.27). By uniform continuity of the second order partial derivatives of $f(\cdot)$ in $\overline{B}_\delta(\mu)$ and Proposition 2.2 (iv), it follows that, for $i, j = 1, \dots, p$,

$$\sup_{y \in \overline{B}_\delta(\mu)} |\partial_i \partial_j f(y) - \partial_i \partial_j f(\mu)| \xrightarrow[\delta \rightarrow 0^+]{} 0. \quad (\text{A.30})$$

and, for $0 < \tilde{\tau}_1, \tilde{\tau}_2 \leq \tau_1$,

$$\begin{aligned} \sup_{0 < \tau \leq \tilde{\tau}_2} \sup_{y \in \overline{B}_{\tilde{\tau}_1}(\mu)} |\partial_i \partial_j f_\tau(y) - \partial_i \partial_j f(y)| &\leq \sup_{0 < \tau \leq \tilde{\tau}_2} \sup_{y \in \overline{B}_{\tau_1}(\mu)} |\partial_i \partial_j f_\tau(y) - \partial_i \partial_j f(y)| \\ &\quad + \sup_{y \in \overline{B}_{\tilde{\tau}_1}(\mu)} |\partial_i \partial_j f(y) - \partial_i \partial_j f(y)| \xrightarrow[\tilde{\tau}_1, \tilde{\tau}_2 \rightarrow 0^+]{} 0. \end{aligned} \quad (\text{A.31})$$

For $y_1, \dots, y_p \in \overline{B}_\delta(0)$, let

$$H_f(\mu; y_1, \dots, y_p) := \begin{pmatrix} (\nabla \partial_1 f(x + y_1))^\top \\ \vdots \\ (\nabla \partial_p f(x + y_p))^\top \end{pmatrix}^\top$$

and, for $y_1, \dots, y_p \in \overline{B}_{\tau_1}(0)$,

$$H_{f_\tau}(\mu; y_1, \dots, y_p) := \begin{pmatrix} (\nabla \partial_1 f_\tau(x + y_1))^\top \\ \vdots \\ (\nabla \partial_p f_\tau(x + y_p))^\top \end{pmatrix}^\top.$$

(A.30) and (A.31) show that,

$$\sup_{y_1, \dots, y_p \in \overline{B}_\delta(0)} \|H_f(\mu; y_1, \dots, y_p) - H_f(\mu)\|_{\mathcal{M}} \xrightarrow[\delta \rightarrow 0^+]{} 0 \quad (\text{A.32})$$

and

$$\sup_{0 < \tau \leq \tilde{\tau}_2} \sup_{y_1, \dots, y_p \in \overline{B}_{\tilde{\tau}_1}(0)} \|H_{f_\tau}(\mu; y_1, \dots, y_p) - H_f(\mu)\|_{\mathcal{M}} \xrightarrow[\tilde{\tau}_1, \tilde{\tau}_2 \rightarrow 0^+]{} 0. \quad (\text{A.33})$$

In particular, (A.32) implies that, for $i = 1, \dots, p$,

$$\sup_{y_1, \dots, y_p \in \overline{B}_\delta(0)} \|H_f(\mu; y_1, \dots, y_p)v_i - \lambda_i v_i\| \xrightarrow[\delta \rightarrow 0^+]{} 0.$$

and, for $t_i \in \mathbb{R}$,

$$\sup_{y_1, \dots, y_p \in \overline{B}_\delta(0)} \left| \langle H_f(\mu; y_1, \dots, y_p) \left(v_i + \sum_{j=1, j \neq i}^p t_j v_j \right), v_i \rangle - \lambda_i \right| \xrightarrow[\delta \rightarrow 0^+]{} 0.$$

By (A.29), there exists $0 < \delta_2 \leq \delta$ such that, for $i = 1, \dots, p$,

$$\operatorname{sgn} \left(\langle H_f(\mu; y_1, \dots, y_p) \left(v_i + \sum_{j=1, j \neq i}^p t_j v_j \right), v_i \rangle \right) = \operatorname{sgn}(\lambda_i), \quad (\text{A.34})$$

for all $y_1, \dots, y_p \in \overline{B}_{\delta_2}(0)$. Similarly, by (A.33), we see that

$$\sup_{0 < \tau \leq \tilde{\tau}_2} \sup_{y_1, \dots, y_p \in \overline{B}_{\tilde{\tau}_1}(0)} \|H_{f_\tau}(\mu; y_1, \dots, y_p)v_i - \lambda_i v_i\| \xrightarrow[\tilde{\tau}_1, \tilde{\tau}_2 \rightarrow 0^+]{} 0,$$

which implies that

$$\sup_{0 < \tau \leq \tilde{\tau}_2} \sup_{y_1, \dots, y_p \in \overline{B}_{\tilde{\tau}_1}(0)} |\langle H_{f_\tau}(\mu; y_1, \dots, y_p)v_i, v_i \rangle - \lambda_i| \xrightarrow[\tilde{\tau}_1, \tilde{\tau}_2 \rightarrow 0^+]{} 0. \quad (\text{A.35})$$

Moreover, by Bauer–Fike theorem (Theorem 2.1 in Eisenstat and Ipsen [1998]), for all $\tilde{\lambda}_\tau(\mu; y_1, \dots, y_p) \in \sigma(H_{f_\tau}(\mu; y_1, \dots, y_p))$, we have that

$$\min_{i=1, \dots, p} |\tilde{\lambda}_\tau(\mu; y_1, \dots, y_p) - \lambda_i| \leq \|H_{f_\tau}(\mu; y_1, \dots, y_p) - H_f(\mu)\|_{\mathcal{M}}. \quad (\text{A.36})$$

By (A.29), (A.35), (A.36) and (A.33), it follows that, there exists $0 < \tau_2 \leq \tau_1$ such that, for all $0 < \tau \leq \tau_2$ and $y_1, \dots, y_p \in \overline{B}_{\tau_2}(0)$,

$$\operatorname{sgn} (\langle H_{f_\tau}(\mu; y_1, \dots, y_p)v_i, v_i \rangle) = \operatorname{sgn}(\lambda_i) \quad (\text{A.37})$$

and $\sigma(H_{f_\tau}(\mu; y_1, \dots, y_p)) = \{\tilde{\lambda}_{\tau,1}(\mu; y_1, \dots, y_p), \dots, \tilde{\lambda}_{\tau,p}(\mu; y_1, \dots, y_p)\}$ with

$$\operatorname{sgn}(\tilde{\lambda}_{\tau,i}(\mu; y_1, \dots, y_p)) = \operatorname{sgn}(\lambda_i). \quad (\text{A.38})$$

Now, let $0 < \tau \leq \tau_2$, $0 < h \leq h^*$, where $h^* := \min(\delta_2, \tau_2)/(2\sqrt{p})$, and $t_i \in [-2h, 2h]$. By the mean value theorem, there exist $0 \leq c_{i,j} \leq 1$ such that

$$\nabla f(\mu \pm hv_i + \sum_{j=1, j \neq i}^p t_j v_j) = H_f(\mu; y_1, \dots, y_p) \left(\pm hv_i + \sum_{j=1, j \neq i}^p t_j v_j \right),$$

where $y_j = c_{i,j} \left(\pm h v_i + \sum_{j=1, j \neq i} t_j v_j \right)$, implying that

$$\frac{1}{h} \langle \nabla f(\mu \pm h v_i + \sum_{j=1, j \neq i} t_j v_j), v_i \rangle = \pm \langle H_f(\mu; y_1, \dots, y_p) \left(v_i \pm \sum_{j=1, j \neq i}^p t_j / h v_j \right), v_i \rangle.$$

Since $\|y_j\| \leq 2\sqrt{p}h^* \leq \delta_2$, by (A.34),

$$\operatorname{sgn} \left(\langle \nabla f(\mu \pm h v_i + \sum_{j=1, j \neq i} t_j v_j), v_i \rangle \right) = \operatorname{sgn}(\pm \lambda_i). \quad (\text{A.39})$$

Now, let us define the hypercube $F_{h^*}(\mu)$ with center μ by

$$F_{h^*}(\mu) := \left\{ \mu + \sum_{j=1}^p t_j v_j, t_j \in [-3/4h^*, 3/4h^*] \right\}$$

and its “hyperfaces” by

$$F_{h^*,i}^\pm(\mu) := \left\{ \mu \pm 3/4h^* v_i + \sum_{j=1, j \neq i}^p t_j v_j, t_j \in [-3/4h^*, 3/4h^*] \right\}.$$

Since, by (2.4), for $0 < \tau \leq \tau^*$, where $\tau^* := \min(\tau_2, h^*/(4\rho))$,

$$\overline{S}_{h_\tau(0; \cdot, x_2, \dots, x_k)} \subset \overline{B}_{\rho\tau}(0) \subset \left\{ \sum_{j=1}^p s_j v_j : s_j \in [-h^*/4, h^*/4] \right\},$$

we have that, for $\mu_i^\pm \in F_{h^*,i}^\pm(\mu)$ and $x_1 \in \overline{S}_{h_\tau(0; \cdot, x_2, \dots, x_k)}$,

$$\mu_i^\pm + x_1 \in \mu + \left\{ \pm h v_i + \sum_{j=1, j \neq i}^p s_j v_j : h \in [h^*/2, h^*], s_j \in [-h^*, h^*] \right\}.$$

Now, by (A.39),

$$\operatorname{sgn} (\langle \nabla f(\mu_i^\pm + x_1), v_i \rangle) = \operatorname{sgn}(\pm \lambda_i),$$

for all $x_1 \in \overline{S}_{h_\tau(0; \cdot, x_2, \dots, x_k)}$ and $t_j \in [-3/4h^*, 3/4h^*]$. It follows from (A.27) that

$$\operatorname{sgn} (\langle \nabla f_\tau(\mu_i^\pm), v_i \rangle) = \operatorname{sgn}(\pm \lambda_i).$$

In particular, for all $\mu_i^+ \in F_{h^*,i}^+(\mu)$ and $\mu_i^- \in F_{h^*,i}^-(\mu)$,

$$\operatorname{sgn} (\langle \nabla f_\tau(\mu_i^+), v_i \rangle) = -\operatorname{sgn} (\langle \nabla f_\tau(\mu_i^-), v_i \rangle) \neq 0. \quad (\text{A.40})$$

Notice that $\mu_i^+ \in F_{h^*,i}^+(\mu)$ if and only if $\mu_i^+ - 3/2h^* v_i \in F_{h^*,i}^-(\mu)$ and let $\alpha_i : F_{h^*,i}^+(\mu) \times [0, 1] \rightarrow F_{h^*}(\mu)$ be given by

$$\alpha_i(y, t) = (1-t)y + t(y - 3/2h^* v_i) = y - 3/2h^* t v_i.$$

Since $\nabla f_\tau(\cdot)$ is continuous, by (A.40), for all $\mu_i^+ \in F_{h^*,i}^+(\mu)$, there exists $0 < t_1 < 1$ such that $\langle \nabla f_\tau(\alpha_i(\mu_i^+, t_1)), v_i \rangle = 0$. Next, we show that t_1 is unique. To this end, let $0 < t_2 < 1$ be such that $\langle \nabla f_\tau(\alpha_i(\mu_i^+, t_2)), v_i \rangle = 0$. By the mean value theorem, there exist $0 \leq c_j \leq 1$ such that

$$\nabla f_\tau(\alpha_i(\mu_i^+, t_2)) = \nabla f_\tau(\alpha_i(\mu_i^+, t_1)) + H_{f_\tau}(\mu; y_1, \dots, y_p)^\top (\alpha_i(\mu_i^+, t_2) - \alpha_i(\mu_i^+, t_1)),$$

where $y_j = (1 - c_j)\alpha_i(\mu_i^+, t_2) + c_j\alpha_i(\mu_i^+, t_1) - \mu$, implying that

$$3/2h^*(t_2 - t_1)\langle H_{f_\tau}(\mu; y_1, \dots, y_p)v_i, v_i \rangle = 0.$$

By (A.37), it follows that $t_2 = t_1$. Let, for $i = 1, \dots, p$,

$$Z_{\tau,i}(\mu) := \{\alpha_i(y, t) : \langle \nabla f_\tau(\alpha_i(y, t)), v_i \rangle = 0, y \in F_i^+(\mu), t \in [0, 1]\}.$$

Notice that $Z_{\tau,i}(\mu)$ are closed subsets of the hypercube $F_{h^*}(\mu)$ with dimension $p - 1$ that divide $F_{h^*}(\mu)$ into two parts with only the faces $F_{h^*,i}^+(\mu)$ and $F_{h^*,i}^-(\mu)$ entirely contained in the same part. It follows that $\cap_{i=1}^p Z_{\tau,i}(\mu) = \{\mu_\tau\}$, where μ_τ satisfies $\langle \nabla f_\tau(\mu_\tau), v_i \rangle = 0$, for all $i = 1, \dots, p$, implying that $\nabla f_\tau(\mu_\tau) = 0$. Finally, by (A.38) and $\|\mu_\tau - \mu\| \leq 3/4\sqrt{ph^*} \leq \tau_2$, it follows that μ_τ is of type l . Also, by letting $\tau_2 \rightarrow 0^+$, we see that $\|\mu_\tau - \mu\| \rightarrow 0$.

Finally, we prove (iii). Since $H_f(\mu)^{-1}$ is symmetric, it holds that

$$\xi := \|H_f(\mu)^{-1}\|_{\mathcal{M}} = \max_{i=1, \dots, p} 1/|\lambda_i| > 0.$$

By (A.33), there exists $0 < \tau_3 \leq \tau_1$, such that, for all $0 < \tau \leq \tau_3$ and $y_j \in \overline{B}_{\tau_3}(0)$, $j = 1, \dots, p$,

$$\|H_{f_\tau}(\mu; y_1, \dots, y_p) - H_f(\mu)\|_{\mathcal{M}} \leq 1/(2\xi). \quad (\text{A.41})$$

It follows from (A.41) and the triangle inequality that, for all $v \in \mathbb{R}^p$,

$$\begin{aligned} \|v\| &\leq 2\xi (\|H_f(\mu)v\| - 1/(2\xi) \|v\|) \\ &\leq 2\xi (\|H_f(\mu)v\| - \|(H_{f_\tau}(\mu; y_1, \dots, y_p) - H_f(\mu))v\|) \\ &\leq 2\xi \|H_{f_\tau}(\mu; y_1, \dots, y_p)\|. \end{aligned}$$

By setting $w = H_{f_\tau}(\mu; y_1, \dots, y_p)v$, we see that $\|w\| \geq 1/(2\xi) \|H_{f_\tau}(\mu; y_1, \dots, y_p)w\|$ implying that

$$\|H_{f_\tau}(\mu; y_1, \dots, y_p)^{-1}\|_{\mathcal{M}} \leq 2\xi. \quad (\text{A.42})$$

Moreover, by the mean value theorem, there exist $0 \leq \tilde{c}_j \leq 1$, $j = 1, \dots, p$, such that,

$$\nabla f_\tau(\mu) = \nabla f_\tau(\mu) - \nabla f_\tau(\mu_\tau) = H_{f_\tau}(\mu; y_1, \dots, y_p)(\mu - \mu_\tau),$$

where $y_j = \tilde{c}_j\mu + (1 - \tilde{c}_j)\mu_\tau - \mu = (1 - \tilde{c}_j)(\mu - \mu_\tau)$. Since $\|y_j\| \leq \|\mu - \mu_\tau\| \leq \tau_2$, by (A.38) $H_{f_\tau}(\mu; y_1, \dots, y_p)$ is invertible. We now apply Lemma A.5 with $K = \overline{B}_\delta(\mu)$ and get constants $\tau(K), c_2(K) > 0$ such that, for all $y \in K$ and $0 < \tau \leq \min(\tau_2, \tau(K))$,

$$\|\nabla f_\tau(y) - \nabla f(y)\| \leq c_2(K)\tau^2. \quad (\text{A.43})$$

Using (A.42) and (A.43), we conclude that, for all $0 < \tau \leq \min(\tau_2, \tau(K))$,

$$\|\mu - \mu_\tau\| \leq \|H_{f_\tau}(\mu; y_1, \dots, y_p)^{-1}\|_{\mathcal{M}} \|\nabla f_\tau(\mu) - \nabla f(\mu)\| \leq 2\xi c_2(K)\tau^2.$$

■

We study next the relationship between the gradient systems (3.3) and (3.2) under extreme localization. To this aim, notice that the sets $\{S_{f_\tau}\}_{\tau>0}$ contain S_f by Lemma 3.1. Furthermore, because of Remark 2.1 and Proposition 2.2 (iv), $f_\tau(\cdot)$ is twice continuously differentiable in S_{f_τ} and its gradient and Hessian matrix converge to those of $f(\cdot)$ in S_f . If it exists, we denote by $u_{x,\tau}(t)$ the solution of (3.3) with initial point $u_{x,\tau}(0) = x$. Since $f_\tau(\cdot)$ is continuous, for $\alpha > 0$, the sets $R_\tau^\alpha = \{x \in \mathbb{R}^p : f_\tau(x) \geq \alpha\} = f_\tau^{-1}([\alpha, \infty))$ are closed. The next lemma shows that they are also bounded.

Lemma A.6 *Under assumption (2.4), $(R^\alpha)^{-\rho\tau} \subset R_\tau^\alpha \subset (R^\alpha)^{+\rho\tau}$, for all $\tau > 0$ and $\alpha > 0$. In particular, if R^α is bounded for $\alpha > 0$, then R_τ^α is also bounded for any $\tau > 0$.*

Proof of Lemma A.6. Since $x \in (R^\alpha)^{-\rho\tau}$ satisfies $\inf_{y \in \mathbb{R}^p \setminus R^\alpha} \|x - y\| > \rho\tau$, we have that $\overline{B}_{\rho\tau}(x) \subset R^\alpha$. By (A.3) and (2.4), we also have that $S_{h_\tau(x;\cdot)} \subset (\overline{B}_{\rho\tau}(x))^k \subset (R^\alpha)^k$. It follows that

$$f_\tau(x) = \left(\int \frac{h_\tau(x; x_1, \dots, x_k)}{\tau^{kp}\Lambda_1} f(x_1) \dots f(x_k) dx_1 \dots dx_k \right)^{1/k} \geq \alpha, \quad (\text{A.44})$$

and therefore $x \in R_\tau^\alpha$. Next, let $x \in R_\tau^\alpha$. Then, there exists $(x_1, \dots, x_k) \in S_{h_\tau(x;\cdot)}$ such that $f(x_1) \dots f(x_k) \geq \alpha^k$. In particular, since $S_{h_\tau(x;\cdot)} \subset (\overline{B}_{\rho\tau}(x))^k$, there exists a point $z \in \overline{B}_{\rho\tau}(x)$ with $f(z) \geq \alpha$. Hence $z \in R^\alpha$, and since $z \in \overline{B}_{\rho\tau}(x)$, $\|x - z\| \leq \rho\tau$, implying that $x \in (R^\alpha)^{+\rho\tau}$. Finally, suppose that for $\alpha > 0$, R^α is bounded. Then, there exists $r > 0$ such that $R^\alpha \subset \overline{B}_r(0)$. It follows that, for $\tau > 0$, $x \in R_\tau^\alpha \subset (R^\alpha)^{+\rho\tau}$ satisfies $\|x\| \leq \inf_{y \in R^\alpha} (\|y\| + \|y - x\|) \leq r + \inf_{y \in R^\alpha} \|y - x\| \leq r + \rho\tau$. Hence $R_\tau^\alpha \subset \overline{B}_{r+\rho\tau}(0)$ is bounded. ■

The next proposition is required in the proof of Theorem 3.2 and its proof is based on (iv) Proposition 2.9, Grönwall's inequality, and Lemma A.5.

Proposition A.2 Suppose that (2.4) holds true. (i) If $f(\cdot)$ is continuously differentiable in \mathbb{R}^p and, for all $\alpha > 0$, R^α is compact, then, for all $t \geq 0$ and $x \in S_f$,

$$\lim_{\tau \rightarrow 0^+} u_{x,\tau}(t) = u_x(t).$$

(ii) If, additionally, $f(\cdot)$ is three times continuously differentiable, then, for $x \in S_f$,

$$\lim_{\tau \rightarrow 0^+} \sup_{t \in [0, \infty)} |u_{x,\tau}(t) - u_x(t)| = 0.$$

Proof of Proposition A.2. Fix $x \in S_f$ and let $\alpha > 0$ be such that $x \in R^\alpha$. Since $R^\alpha \subset S_f$ is compact, $\mathbb{R}^p \setminus S_f$ is closed and these two sets are disjoint, we have that $\text{dist}(R^\alpha, \mathbb{R}^p \setminus S_f) > 0$. Let $\delta := \text{dist}(R^\alpha, \mathbb{R}^p \setminus S_f)/(3\rho)$ and notice that by definition

$$\begin{aligned} \text{dist}((R^\alpha)^{+\delta}, \mathbb{R}^p \setminus S_f) &= \inf_{y \in \mathbb{R}^p \setminus S_f, z \in (R^\alpha)^{+\delta}} \|y - z\| \\ &= \inf_{y \in \mathbb{R}^p \setminus S_f} \inf_{z \in \mathbb{R}^p : \inf_{w \in R^\alpha} \|w - z\| \leq \delta} \|y - z\|. \end{aligned}$$

By the triangle inequality, we have that for $w \in R^\alpha$

$$\|y - z\| \geq \|y - w\| - \|w - z\| \geq \|y - w\| - \delta.$$

It follows that

$$\text{dist}((R^\alpha)^{+\delta}, \mathbb{R}^p \setminus S_f) \geq \text{dist}(R^\alpha, \mathbb{R}^p \setminus S_f) - \delta = 2\delta > 0. \quad (\text{A.45})$$

Lemma A.6 implies that for all $0 < \tau \leq \delta/\rho$, $R_\tau^\alpha \subset (R^\alpha)^{+\rho\tau} \subset (R^\alpha)^{+\delta} \subset S_f$. In the rest of the proof, we suppose that $0 < \tau \leq \delta/\rho$. Also, for all $s \geq 0$, $u_x(s) \in R^\alpha$ and $u_{x,\tau}(s) \in R_\tau^\alpha$; as shown in Appendix E, the solutions of the gradient system (3.2) cannot leave the regions R^α , and the same is true for the gradient system (3.3) and R_τ^α . In particular, for all $s \geq 0$, $u_x(s), u_{x,\tau}(s) \in K$, where $K := (R^\alpha)^{+\delta}$ is a compact subset of S_f . Now, noticing that the integral of a vector is the vector of the integrals of its components, we obtain, for $t \geq 0$,

$$u_{x,\tau}(t) - u_x(t) = \int_0^t \nabla f_\tau(u_{x,\tau}(s)) - \nabla f(u_x(s)) ds.$$

Next by adding and subtracting $\nabla f_\tau(u_x(s))$ inside the integral and taking the Euclidean norm on both sides we see that

$$\begin{aligned} \|u_{x,\tau}(t) - u_x(t)\| &\leq \int_0^t \|\nabla f_\tau(u_{x,\tau}(s)) - \nabla f_\tau(u_x(s))\| ds \\ &\quad + \int_0^t \|\nabla f_\tau(u_x(s)) - \nabla f(u_x(s))\| ds. \end{aligned}$$

Since $\nabla f_\tau(\cdot)$ is locally Lipschitz in S_f , it is Lipschitz in the compact subset K ; that is, there exists a constant $L_\tau < \infty$ such that for all $y, z \in K$

$$\|\nabla f_\tau(y) - \nabla f_\tau(z)\| \leq L_\tau \|y - z\|. \quad (\text{A.46})$$

It follows that

$$\|u_{x,\tau}(t) - u_x(t)\| \leq L_\tau \int_0^t \|u_{x,\tau}(s) - u_x(s)\| ds + \int_0^t \|\nabla f_\tau(u_x(s)) - \nabla f(u_x(s))\| ds.$$

We now apply Grönwall's inequality [Hale, 1980][Corollary 6.6] with $a = 0$, $\beta(s) = L_\tau$, $0 \leq s \leq t$, $\alpha = \int_0^t \|\nabla f_\tau(u_x(s)) - \nabla f(u_x(s))\| ds$ and $\varphi(t) = \|u_{x,\tau}(t) - u_x(t)\|$, and obtain that

$$\|u_{x,\tau}(t) - u_x(t)\| \leq e^{L_\tau} \int_0^t \|\nabla f_\tau(u_x(s)) - \nabla f(u_x(s))\| ds. \quad (\text{A.47})$$

To prove (i) we need to show that this converges to 0 as $\tau \rightarrow 0^+$. To this end, since $\nabla f(\cdot)$ is also locally Lipschitz in S_f , there exists a constant $L < \infty$ such that, for all $y, z \in K$

$$\|\nabla f(y) - \nabla f(z)\| \leq L \|y - z\|. \quad (\text{A.48})$$

By (A.48) and Proposition 2.2 (iv), it follows that, for all $y, z \in K$ with $y \neq z$,

$$\lim_{\tau \rightarrow 0^+} \frac{\|\nabla f_\tau(y) - \nabla f_\tau(z)\|}{\|y - z\|} = \frac{\|\nabla f(y) - \nabla f(z)\|}{\|y - z\|} \leq L. \quad (\text{A.49})$$

Hence, $\{L_\tau\}_{0 < \tau \leq \delta/\rho}$ in (A.46) can be chosen in such a way that $\lim_{\tau \rightarrow 0^+} L_\tau = L$. In particular, there exists $0 < \tau^* \leq \delta/\rho$, such that

$$L_\tau \leq L + 1, \quad (\text{A.50})$$

for all $0 < \tau \leq \tau^*$. Therefore, from (A.47), it follows that

$$\lim_{\tau \rightarrow 0^+} \|u_{x,\tau}(t) - u_x(t)\| = 0,$$

if we can show that

$$\int_0^t \|\nabla f_\tau(u_x(s)) - \nabla f(u_x(s))\| ds \xrightarrow[\tau \rightarrow 0^+]{} 0. \quad (\text{A.51})$$

To show this, we first enlarge the compact set K by δ in such a way that it is still contained in S_f by considering the set $(K)^{+\delta} \subset (R^\alpha)^{+2\delta}$. As in (A.45), we see that

$$\text{dist}((R^\alpha)^{+2\delta}, \mathbb{R}^p \setminus S_f) \geq \text{dist}(R^\alpha, \mathbb{R}^p \setminus S_f) - 2\delta = \delta > 0,$$

and $(K)^{+\delta}$ is indeed a compact subset of S_f . Furthermore, for all $y \in K$, $\overline{B}_{\rho\tau}(y) \subset \overline{B}_\delta(y) \subset (K)^{+\delta} \subset S_f$, and, in particular, by (A.3) and (2.4), $\overline{S}_{h_\tau(y,\cdot)} \subset (\overline{B}_\delta(y))^k \subset (S_f)^k$. Now, by (A.27), we see that for $y \in K$, the j^{th} partial derivative of $f_\tau(\cdot)$ at y is given by

$$\partial_j f_\tau(y) = \frac{1}{k} (f_\tau(y))^{1-k} \left(\int \frac{h_\tau(y; x_1, \dots, x_k)}{\tau^{kp} \Lambda_1} \partial_j(f(x_1) \dots f(x_k)) dx_1 \dots dx_k \right)$$

and

$$|\partial_j f_\tau(y)| \leq \left(\frac{\alpha_0}{\beta_0} \right)^{k-1} \alpha_1^{(j)} < \infty,$$

where $\alpha_0 := \max_{z \in (K)^{+\delta}} f(z)$, $\beta_0 := \min_{z \in (K)^{+\delta}} f(z)$ and $\alpha_1^{(j)} := \max_{z \in (K)^{+\delta}} \partial_j f(z)$ satisfy $0 < \alpha_0, \beta_0, \alpha_1^{(j)} < \infty$. It follows that, for $y \in K$,

$$\|\nabla f_\tau(y) - \nabla f(y)\| \leq \|\nabla f_\tau(y)\| + \|\nabla f(y)\| \leq \left(1 + \left(\frac{\alpha_0}{\beta_0} \right)^{k-1} \right) \|(\alpha_1^{(1)}, \dots, \alpha_1^{(p)})^\top\| < \infty.$$

Therefore, for all $0 \leq s \leq t$, $\|\nabla f_\tau(u_x(s)) - \nabla f(u_x(s))\|$ is bounded and by Proposition 2.2 (iv), for all $0 \leq s \leq t$, $\|\nabla f_\tau(u_x(s)) - \nabla f(u_x(s))\| \xrightarrow[\tau \rightarrow 0^+]{} 0$. Now, (A.51) follows using LDCT completing the proof of (i). We now prove (ii). By Lemma A.5, there are constants $\tau(K), c_2(K) > 0$ such that, for all $y \in K$ and $0 < \tau \leq \min(\delta, \tau(K))$,

$$\|\nabla f_\tau(y) - \nabla f(y)\| \leq c_2(K) \tau^2. \quad (\text{A.52})$$

By (A.47), (A.50) and (A.52), we conclude that

$$\begin{aligned} \lim_{\tau \rightarrow 0^+} \sup_{t \in [0, \infty)} |u_{x,\tau}(t) - u_x(t)| &\leq e^{L+1} \lim_{\tau \rightarrow 0^+} \sup_{t \in [0, 1/\tau]} \int_0^t \|\nabla f_\tau(u_x(s)) - \nabla f(u_x(s))\| ds \\ &\leq e^{L+1} \lim_{\tau \rightarrow 0^+} c_2(K) \tau = 0. \end{aligned}$$

This completes the proof of the proposition. ■

We now prove the convergence of clusters based on τ -approximation to that based on $f(\cdot)$.

Proof of Theorem 3.2. Let $\alpha := \min_{\nu \in N_f} f(\nu)/2$, $\delta := \text{dist}(R^{2\alpha}, \mathbb{R}^p \setminus R^\alpha)/(1 + \rho)$, $\{\alpha_n\}_{n=1}^\infty$ be a sequences of positive scalars converging monotonically to 0 with $\alpha_1 < \alpha$ and $\delta_n := \min(\text{dist}(R^{2\alpha}, \mathbb{R}^p \setminus R^\alpha), \text{dist}(R^{\alpha_n}, \mathbb{R}^p \setminus S_f))/(1 + \rho)$. We see that

$$N_f \subset R^{2\alpha} \subset (R^\alpha)^{-\delta} \subset (R^\alpha)^{-\delta_n} \subset (R^{\alpha_n})^{-\delta_n}, \quad (\text{A.53})$$

with

$$\begin{aligned} \text{dist}(N_f, \mathbb{R}^p \setminus (R^{\alpha_n})^{-\delta_n}) &\geq \text{dist}(R^{2\alpha}, \mathbb{R}^p \setminus (R^\alpha)^{-\delta}) = \text{dist}(R^{2\alpha}, (\mathbb{R}^p \setminus R^\alpha)^{+\delta}) \\ &\geq \text{dist}(R^{2\alpha}, \mathbb{R}^p \setminus R^\alpha) - \delta \geq \delta \geq \delta_n. \end{aligned} \quad (\text{A.54})$$

Furthermore, by Lemma A.6, for $0 < \tau \leq \delta_n$,

$$(R^{\alpha_n})^{-\delta_n} \subset (R^{\alpha_n})^{-\rho\tau} \subset R_{\tau}^{\alpha_n} \subset (R^{\alpha_n})^{+\rho\tau} \subset (R^{\alpha_n})^{+\delta_n} \subset S_f. \quad (\text{A.55})$$

We notice that, by Assumption 3.1, $(R^{\alpha_n})^{-\delta_n}$ is bounded. Moreover, by Lemma 3.1 and Remark 2.1, $f_{\tau}(\cdot)$ is twice continuously differentiable in $S_f \subset S_{f_{\tau}}$. Now, by Theorem 3.1 (ii), there exist $h^*, \tau^* > 0$ and closed hypercubes $F_{h^*}(\mu)$, $\mu \in N_f$, with side length $3/2h^*$, such that, for $0 < \tau_j \leq \tau^*$, $f_{\tau_j}(\cdot)$ has a unique stationary point μ_{τ_j} in $\dot{F}_{h^*}(\mu)$ and μ_{τ_j} is, for $\tau_j \leq \tau^*$, of the same type as μ , and $\lim_{j \rightarrow \infty} \|\mu_{\tau_j} - \mu\| = 0$. We can suppose without loss of generality that $3/2h^* \leq \delta/\sqrt{p}$, that is $F_{h^*}(\mu) \subset \overline{B}_{\delta}(\mu)$. By (A.53) and (A.54), it follows that $F_{h^*}(\mu) \subset (R^{\alpha_n})^{-\delta_n}$ and $K_n := (R^{\alpha_n})^{+\delta_n} \setminus \cup_{\nu \in N_f} \dot{F}_{h^*}(\nu)$ is compact. Let $\eta_n := \min_{y \in K_n} \|\nabla f(y)\| > 0$. By Proposition 2.2 (iv), there exists $0 < \tau_n^* \leq \min(\tau^*, \delta_n)$ such that $\|\nabla f_{\tau}(y) - \nabla f(y)\| < \eta_n$, for all $y \in (R^{\alpha_n})^{+\delta_n}$ and $0 < \tau \leq \tau_n^*$. Hence,

$$\|\nabla f_{\tau}(y)\| \geq \|\nabla f(y)\| - \|\nabla f_{\tau}(y) - \nabla f(y)\| > 0.$$

It follows that $\{\nu_{\tau_j}\}_{\nu \in N_f}$ are the only stationary points of $f_{\tau_j}(\cdot)$ in $(R^{\alpha_n})^{+\delta_n}$. Now, by (A.55), $(R^{\alpha_n})^{-\delta_n} \subset R_{\tau_j}^{\alpha_n} \subset (R^{\alpha_n})^{+\delta_n}$, which implies that the solutions of (3.3) starting in $(R^{\alpha_n})^{-\delta_n}$ cannot leave the set to reach another possible stationary point of $f_{\tau_j}(\cdot)$ outside $R_{\tau_j}^{\alpha_n}$. Therefore, for $0 < \tau_j \leq \tau_n^*$, we can partition $(R^{\alpha_n})^{-\delta_n}$ as

$$\cup_{\nu \in N_f} (C(\nu) \cap (R^{\alpha_n})^{-\delta_n}) = (R^{\alpha_n})^{-\delta_n} = \cup_{\nu \in N_f} (C_{\tau_j}(\nu_{\tau_j}) \cap (R^{\alpha_n})^{-\delta_n}). \quad (\text{A.56})$$

Next, we show that $(R^{\alpha_n})^{-\delta_n} \uparrow_{n \rightarrow \infty} S_f$. To this end, let $x \in S_f$. Clearly, $x \in R^{f(x)} \subset \dot{R}^{f(x)/2}$. Since $\alpha_n, \delta_n \xrightarrow{n \rightarrow \infty} 0$, there exists n^* such that, for all $n \geq n^*$, $\alpha_n < f(x)/2$ and $\delta_n < \text{dist}(R^{f(x)}, \mathbb{R}^p \setminus \dot{R}^{f(x)/2})/2$. Then, $x \in (R^{f(x)/2})^{-\delta_n} \subset (R^{\alpha_n})^{-\delta_n}$. We recall that the symmetric difference between two subsets A and B of \mathbb{R}^p is $A \Delta B = ((\mathbb{R}^p \setminus A) \cap B) \cup (A \cap (\mathbb{R}^p \setminus B))$. For $\mu \in N_f$, using Corollary L.1 (v), it holds that

$$\begin{aligned} \limsup_{j \rightarrow \infty} C_{\tau_j}(\mu_{\tau_j}) \Delta C(\mu) &= (\lim_{n \rightarrow \infty} (R^{\alpha_n})^{-\delta_n}) \cap (\limsup_{j \rightarrow \infty} C_{\tau_j}(\mu_{\tau_j}) \Delta C(\mu)) \\ &= \lim_{n \rightarrow \infty} ((R^{\alpha_n})^{-\delta_n} \cap (\limsup_{j \rightarrow \infty} C_{\tau_j}(\mu_{\tau_j}) \Delta C(\mu))). \end{aligned}$$

Using (A.56), we have that $(R^{\alpha_n})^{-\delta_n} \cap (\limsup_{j \rightarrow \infty} C_{\tau_j}(\mu_{\tau_j}) \Delta C(\mu))$ is a subset of

$$(R^{\alpha_n})^{-\delta_n} \cap (\cap_{j=1, \tau_j \leq \tau_n^*}^{\infty} \cup_{l=j}^{\infty} C_{\tau_l}(\mu_{\tau_j}) \Delta C(\mu)),$$

which is equal to

$$\begin{aligned} &((R^{\alpha_n})^{-\delta_n} \cap (\cap_{j=1, \tau_j \leq \tau_n^*}^{\infty} \cup_{l=j}^{\infty} C_{\tau_l}(\mu))) \cap (\cup_{\nu \in N_f, \nu \neq \mu} C(\nu)) \\ &\cup ((R^{\alpha_n})^{-\delta_n} \cap C(\mu) \cap (\cup_{\nu \in N_f, \nu \neq \mu} (\cap_{j=1, \tau_j \leq \tau_n^*}^{\infty} \cup_{l=j}^{\infty} C_{\tau_l}(\nu_{\tau_j}))). \end{aligned}$$

The above union is contained in

$$(R^{\alpha_n})^{-\delta_n} \cap (\cup_{\mu \in N_f} \cup_{\nu \in N_f, \nu \neq \mu} C(\mu) \cap (\cap_{j=1, \tau_j \leq \tau_n^*} \cup_{l=j}^\infty C_{\tau_l}(\nu_{\tau_l}))).$$

It follows that $\limsup_{j \rightarrow \infty} C_{\tau_j}(\mu_{\tau_j}) \Delta C(\mu)$ is contained in

$$\lim_{n \rightarrow \infty} (R^{\alpha_n})^{-\delta_n} \cap (\cup_{\mu \in N_f} \cup_{\nu \in N_f, \nu \neq \mu} C(\mu) \cap (\cap_{j=1, \tau_j \leq \tau_n^*} \cup_{l=j}^\infty C_{\tau_l}(\nu_{\tau_l}))).$$

Now, using Corollary L.1 (v)-(vi), this is equal to

$$\cup_{\mu \in N_f} \cup_{\nu \in N_f, \nu \neq \mu} \lim_{n \rightarrow \infty} ((R^{\alpha_n})^{-\delta_n} \cap C(\mu) \cap (\cap_{j=1, \tau_j \leq \tau_n^*} \cup_{l=j}^\infty C_{\tau_l}(\nu_{\tau_l}))).$$

Now, let

$$x \in (R^{\alpha_n})^{-\delta_n} \cap C(\mu) \cap (\cap_{j=1, \tau_j \leq \tau_n^*} \cup_{l=j}^\infty C_{\tau_l}(\nu_{\tau_l})).$$

Then, there exists a subsequence $\{\tilde{\tau}_j\}_{j=1}^\infty$ of $\{\tau_j\}_{j=1}^\infty$ such that $\lim_{t \rightarrow \infty} u_{x, \tilde{\tau}_j}(t) = \nu_{\tilde{\tau}_j}$. In particular, $\lim_{j \rightarrow \infty} \lim_{t \rightarrow \infty} u_{x, \tilde{\tau}_j}(t) = \nu$. On the other hand, by Proposition A.2 (ii), $u_{x, \tilde{\tau}_j}(\cdot)$ converges uniformly on $[0, \infty)$ to $u_x(\cdot)$, as $j \rightarrow \infty$. Therefore,

$$\lim_{t \rightarrow \infty} \lim_{j \rightarrow \infty} u_{x, \tilde{\tau}_j}(t) = \lim_{t \rightarrow \infty} u_x(t) = \mu.$$

By Moore-Osgood theorem (see Theorem 7.11 in Rudin [1976]), it follows that $\nu = \lim_{j \rightarrow \infty} \lim_{t \rightarrow \infty} u_{x, \tilde{\tau}_j}(t) = \lim_{t \rightarrow \infty} \lim_{j \rightarrow \infty} u_{x, \tilde{\tau}_j}(t) = \mu$. We conclude that

$$\cup_{\mu \in N_f} \cup_{\nu \in N_f, \nu \neq \mu} \lim_{n \rightarrow \infty} ((R^{\alpha_n})^{-\delta_n} \cap C(\mu) \cap (\cap_{j=1, \tau_j \leq \tau_n^*} \cup_{l=j}^\infty C_{\tau_l}(\nu_{\tau_l}))) = \emptyset,$$

implying that $\lim_{j \rightarrow \infty} C_{\tau_j}(\mu_{\tau_j}) \Delta C(\mu) = \limsup_{j \rightarrow \infty} C_{\tau_j}(\mu_{\tau_j}) \Delta C(\mu) = \emptyset$. Finally, Lemma L.3 in Appendix L with $A_j = C_{\tau_j}(\mu_{\tau_j})$ and $A = C(\mu)$ implies that $\lim_{j \rightarrow \infty} C_{\tau_j}(\mu_{\tau_j}) = C(\mu)$.

■

As an application of Lemma L.4, we also have that $\lim_{j \rightarrow \infty} (C_{\tau_j}(\mu_{\tau_j}))^{+\xi} = (C(\mu))^{+\xi}$, for all $\xi > 0$ and $\lim_{j \rightarrow \infty} \overline{C_{\tau_j}(\mu_{\tau_j})} = \overline{C(\mu)}$.

Proof of Theorem 3.3. We begin by proving (i). Let $h^*, n^* > 0$ be such that $(K)^{+h^*} \subset S_f$ and $0 < h_n \leq h^*$, for all $n \geq n^*$. Notice that $f_{\tau_n}(\cdot)$ is continuously differentiable in $(K)^{+h^*}$ (see Remark 2.1). By the mean value theorem, there exist $0 \leq c_{1,n}, c_{2,n} \leq 1$ such that

$$f(x + h_n v_n) - f(x) = h_n \langle \nabla f(x + c_{1,n} h_n v_n), v_n \rangle \quad (\text{A.57})$$

and

$$f_{\tau_n}(x + h_n v_n) - f_{\tau_n}(x) = h_n \langle \nabla f_{\tau_n}(x + c_{2,n} h_n v_n), v_n \rangle. \quad (\text{A.58})$$

Using the triangle inequality, we have that

$$\sup_{x \in K} |\nabla_{v_n}^{h_n} f_{\tau_n}(x) - \nabla_v f(x)| \leq \sup_{x \in K} |\nabla_{v_n}^{h_n} f_{\tau_n}(x) - \nabla_{v_n}^{h_n} f(x)| + \sup_{x \in K} |\nabla_{v_n}^{h_n} f(x) - \nabla_v f(x)|.$$

We show that each term converges to 0 as $n \rightarrow \infty$. First, by (A.57), the uniform continuity of $\nabla f(\cdot)$ in $(K)^{+h^*}$ and $\lim_{n \rightarrow \infty} \|v_n - v\| = 0$, it follows that

$$\begin{aligned} \lim_{n \rightarrow \infty} \sup_{x \in K} |\nabla_{v_n}^{h_n} f(x) - \nabla_v f(x)| &= \lim_{n \rightarrow \infty} \sup_{x \in K} |\langle \nabla f(x + c_{1,n} h_n v_n), v_n \rangle - \langle \nabla f(x), v \rangle| \\ &\leq \lim_{n \rightarrow \infty} \sup_{x \in K} |\langle \nabla f(x + c_{1,n} h_n v_n), v_n - v \rangle| \\ &\quad + \lim_{n \rightarrow \infty} \sup_{x \in K} |\langle \nabla f(x + c_{1,n} h_n v_n) - \nabla f(x), v \rangle| \\ &\leq \sup_{y \in (K)^{+h^*}} \|\nabla f(y)\| \lim_{n \rightarrow \infty} \|v_n - v\| \\ &\quad + \lim_{n \rightarrow \infty} \sup_{x \in K} \|\nabla f(x + c_{1,n} h_n v_n) - \nabla f(x)\| = 0. \end{aligned}$$

Also, by (A.57) and (A.58), it holds that

$$\begin{aligned} \sup_{x \in K} |\nabla_{v_n}^{h_n} f_{\tau_n}(x) - \nabla_{v_n}^{h_n} f(x)| &= \sup_{x \in K} |\langle \nabla f_{\tau_n}(x + c_{2,n} h_n v_n) - \nabla f(x + c_{1,n} h_n v_n), v_n \rangle| \\ &\leq \sup_{x \in K} \|\nabla f_{\tau_n}(x + c_{2,n} h_n v_n) - \nabla f(x + c_{1,n} h_n v_n)\|. \end{aligned}$$

Finally, Proposition 2.2 (iv) and the uniform continuity of $\nabla f(\cdot)$ in $(K)^{+h^*}$ imply that

$$\begin{aligned} \lim_{n \rightarrow \infty} \sup_{x \in K} |\nabla_{v_n}^{h_n} f_{\tau_n}(x) - \nabla_{v_n}^{h_n} f(x)| &\leq \lim_{n \rightarrow \infty} \sup_{x \in K} \|\nabla f_{\tau_n}(x + c_{2,n} h_n v_n) - \nabla f(x + c_{2,n} h_n v_n)\| \\ &\quad + \lim_{n \rightarrow \infty} \sup_{x \in K} \|\nabla f(x + c_{2,n} h_n v_n) - \nabla f(x + c_{1,n} h_n v_n)\| \\ &\leq \lim_{n \rightarrow \infty} \sup_{y \in (K)^{+h^*}} \|\nabla f_{\tau_n}(y) - \nabla f(y)\| \\ &\quad + \sup_{y \in (K)^{+h^*}} \lim_{n \rightarrow \infty} \sup_{z \in \overline{B}_{h_n}(y) \cap (K)^{+h^*}} \|\nabla f(y) - \nabla f(z)\| = 0. \end{aligned}$$

We now prove (ii). Since

$$\sup_{x \in K} |\nabla_{v_n}^{h_n} f_{\tau_n,n}(x) - \nabla_v f(x)| \leq \sup_{x \in K} |\nabla_{v_n}^{h_n} f_{\tau_n,n}(x) - \nabla_{v_n}^{h_n} f_{\tau_n}(x)| + \sup_{x \in K} |\nabla_{v_n}^{h_n} f_{\tau_n}(x) - \nabla_v f(x)|,$$

using (i), it is enough to show that

$$\lim_{n \rightarrow \infty} P^{\otimes n} \left(\sup_{x \in K} |\nabla_{v_n}^{h_n} f_{\tau_n,n}(x) - \nabla_{v_n}^{h_n} f_{\tau_n}(x)| \geq \frac{\epsilon}{2} \right) = 0.$$

Notice that, by Lemma A.2,

$$\begin{aligned} \sup_{x \in K} |\nabla_{v_n}^{h_n} f_{\tau_n, n}(x) - \nabla_{v_n}^{h_n} f_{\tau_n}(x)| &= \sup_{x \in K} \left| \frac{f_{\tau_n, n}(x + h_n v_n) - f_{\tau_n}(x + h_n v_n)}{h_n} - \frac{f_{\tau_n, n}(x) - f_{\tau_n}(x)}{h_n} \right| \\ &\leq \sup_{x \in K} \left| \frac{LGD_n(x + h_n v_n, \tau_n) - LGD(x + h_n v_n, \tau_n)}{h_n^k \tau_n^{kp} \Lambda_1} \right|^{1/k} \\ &\quad + \sup_{x \in K} \left| \frac{LGD_n(x, \tau_n) - LGD(x, \tau_n)}{h_n^k \tau_n^{kp} \Lambda_1} \right|^{1/k}. \end{aligned}$$

We now use that $\lim_{n \rightarrow \infty} \sqrt{n} h_n^k \tau_n^{kp} = \infty$ and apply Theorem 2.4 with $t = t_n := \sqrt{n} h_n^k \tau_n^{kp} \Lambda_1 (\epsilon/4)^k$. It follows that there are constants $\sigma_G \geq 0$, $1 < C_{G,0}, C_{G,1}, C_{G,2} < \infty$, and $n^{**} \in \mathbb{N}$ such that, for all $n \geq n^{**}$, $t_n \geq \max(2^3 \sigma_G, 2^4 C_{G,0})$ and

$$\begin{aligned} P^{\otimes n} \left(\sup_{x \in K} |\nabla_{v_n}^{h_n} f_{\tau_n, n}(x) - \nabla_{v_n}^{h_n} f_{\tau_n}(x)| > \frac{\epsilon}{2} \right) &\leq P^{\otimes n} \left(\sup_{\substack{x \in \mathbb{R}^p \\ \tau \in [0, \infty]}} \left| \frac{LGD_n(x, \tau) - LGD(x, \tau)}{h_n^k \tau_n^{kp} \Lambda_1} \right|^{1/k} \geq \frac{\epsilon}{4} \right) \\ &= P^{\otimes n} \left(\sqrt{n} \sup_{\substack{x \in \mathbb{R}^p \\ \tau \in [0, \infty]}} |LGD_n(x, \tau) - LGD(x, \tau)| \geq t_n \right) \\ &\leq D_G(n, t_n), \end{aligned}$$

where $D_G(\cdot, \cdot)$ is defined in (2.14). Now, the result follows from $\lim_{n \rightarrow \infty} D_G(n, t_n) = 0$. ■

Proof of Lemma 3.2. We begin by proving (i). By Lemma A.5 there are constants $\tau((K)^{+h^*}), c_2((K)^{+h^*}) > 0$ such that, for all $y \in (K)^{+h^*}$ and $0 < \tau \leq \tau((K)^{+h^*})$,

$$f_\tau(y) = f(y) + \tilde{R}_\tau(y) \tau^2$$

and $\|\nabla \tilde{R}_\tau(y)\| \leq c_2((K)^{+h^*})$. Let $n^* \in \mathbb{N}$ such that $\tau_n \leq \tau((K)^{+h^*})$ for all $n \geq n^*$. It holds that, for all $n \geq n^*$,

$$\nabla_v^h f_{\tau_n}(x) - \nabla_v^h f(x) = \frac{\tilde{R}_{\tau_n}(x + hv) - \tilde{R}_{\tau_n}(x)}{h} \tau_n^2.$$

Now, by the mean value theorem, there are constants $0 \leq \tilde{c}_n \leq 1$ such that

$$\frac{\tilde{R}_{\tau_n}(x + hv) - \tilde{R}_{\tau_n}(x)}{h} = \langle \nabla \tilde{R}_{\tau_n}(x + \tilde{c}_n hv), v \rangle,$$

implying that

$$\left| \frac{\tilde{R}_{\tau_n}(x + hv) - \tilde{R}_{\tau_n}(x)}{h} \right| \leq \|\nabla \tilde{R}_{\tau_n}(x + \tilde{c}_n hv)\| \leq c_2((K)^{+h^*}).$$

It follows that

$$\lim_{n \rightarrow \infty} \sup_{h \in [h_n, h^*]} \sup_{v \in S^{p-1}} \sup_{x \in K} |\nabla_v^h f_{\tau_n}(x) - \nabla_v^h f(x)| \leq c_2((K)^{+h^*}) \lim_{n \rightarrow \infty} \tau_n^2 = 0.$$

We now prove (ii). By (i), it is enough to show that

$$\lim_{n \rightarrow \infty} P^{\otimes n} \left(\sup_{h \in [h_n, h^*]} \sup_{v \in S^{p-1}} \sup_{x \in K} |\nabla_v^h f_{\tau_n, n}(x) - \nabla_v^h f_{\tau_n}(x)| \geq \frac{\epsilon}{2} \right) = 0.$$

Notice that, by Lemma A.2,

$$\begin{aligned} |\nabla_v^h f_{\tau_n, n}(x) - \nabla_v^h f_{\tau_n}(x)| &= \left| \frac{f_{\tau_n, n}(x + hv) - f_{\tau_n}(x + hv)}{h} - \frac{f_{\tau_n, n}(x) - f_{\tau_n}(x)}{h} \right| \\ &\leq \left| \frac{LGD_n(x + hv, \tau_n) - LGD(x + hv, \tau_n)}{h_n^k \tau_n^{kp} \Lambda_1} \right|^{1/k} \\ &\quad + \left| \frac{LGD_n(x, \tau_n) - LGD(x, \tau_n)}{h_n^k \tau_n^{kp} \Lambda_1} \right|^{1/k} \\ &\leq 2 \sup_{\substack{x \in \mathbb{R}^p \\ \tau \in [0, \infty]}} \left| \frac{LGD_n(x, \tau) - LGD(x, \tau)}{h_n^k \tau_n^{kp} \Lambda_1} \right|^{1/k}. \end{aligned}$$

We apply again Theorem 2.4 with $t = t_n := \sqrt{n} h_n^k \tau_n^{kp} \Lambda_1 (\epsilon/4)^k$. Then, there are constants $1 < C_{G,0}, C_{G,1}, C_{G,2} < \infty$ such that, for large enough n ,

$$\begin{aligned} &P^{\otimes n} \left(\sup_{h \in [h_n, h^*]} \sup_{v \in S^{p-1}} \sup_{x \in K} |\nabla_v^h f_{\tau_n, n}(x) - \nabla_v^h f_{\tau_n}(x)| \geq \frac{\epsilon}{2} \right) \\ &\leq P^{\otimes n} \left(\sqrt{n} \sup_{\substack{x \in \mathbb{R}^p \\ \tau \in [0, \infty]}} |LGD_n(x, \tau) - LGD(x, \tau)| \geq t_n \right) \\ &\leq D_G(n, t_n), \end{aligned}$$

where $D_G(\cdot, \cdot)$ is defined in (2.14). Since $\lim_{n \rightarrow \infty} t_n = \infty$, $\lim_{n \rightarrow \infty} h_n = 0$, and $\lim_{n \rightarrow \infty} \tau_n = 0$, we conclude that $\lim_{n \rightarrow \infty} D_G(n, t_n) = 0$. Finally, for (iii), we apply Lemma A.4 with $a_n = h_n^k \tau_n^{kp}$ and $b = \Lambda_1 (\epsilon/4)^k$ and get constants $0 < \tilde{C} < \infty$ and $\tilde{n} \in \mathbb{N}$ such that, for all $n \geq \tilde{n}$,

$$D_G(n, t_n) \leq \frac{\tilde{C}}{n^2}.$$

■

A version of discrete Grönwall lemma (see e.g. Holte [2009]) is needed in Theorem 3.4 to evaluate the difference between the sequence $\{y_{n,r,j}\}_{j=1}^{J^*}$ (defined in the proof) and the solution $u_x(\cdot)$ of (3.2). Discrete Grönwall lemma is a suitable tool for this scope. Indeed, it is often used to compare the solution of ordinary differential equations with the approximation given by Euler method (see e.g. Theorem 2.4 in Atkinson et al. [2009]).

Lemma A.7 (Discrete Grönwall lemma) *Let $\{a_n\}_{n=0}^\infty$, $\{b_n\}_{n=0}^\infty$ and $\{c_n\}_{n=0}^\infty$ be non-negative sequences. If $a_0 = 0$ and $a_n \leq (1 + c_{n-1})a_{n-1} + b_{n-1}$ for all $n \geq 1$, then, $a_n \leq (\sum_{j=0}^{n-1} b_j) \exp(\sum_{j=1}^{n-1} c_j)$.*

Proof of Lemma A.7. By applying recursively the inequality for $\{a_n\}_{n=0}^\infty$ and using $a_0 = 0$, we see that

$$a_n \leq \sum_{j=0}^{n-1} b_j \prod_{l=j+1}^{n-1} (1 + c_l).$$

Now, using $1 + s \leq e^s$ with $s = c_l$, we get that

$$a_n \leq \sum_{j=0}^{n-1} b_j \exp\left(\sum_{l=j+1}^{n-1} c_l\right) \leq \left(\sum_{j=0}^{n-1} b_j\right) \exp\left(\sum_{j=1}^{n-1} c_j\right).$$

■

Lemma A.8 *Suppose that $f(\cdot)$ is continuously differentiable and K is a compact subset of S_f with $K \cap N_f = \emptyset$. Then, there exist $r(K), c(K) > 0$ such that $(K)^{+r(K)} \subset S_f$ and, for all $x \in K$ and $(h, v) \in (0, r(K)] \times (S^{p-1} \cap \overline{B}_{r(K)}(w(x))), \nabla_v^h f(x) \geq c(K)$.*

Proof of Lemma A.8. Recall (4.6) and let $g : [0, \infty) \rightarrow \mathbb{R}$ be given by

$$g(h) = \min_{y \in K} (f(y + hw(y)) - f(y)).$$

By the mean value theorem, it holds that $g(h) = h \min_{y \in K} \langle \nabla f(y + chw(y)), w(y) \rangle$, for some $0 \leq c \leq 1$. Let $h(K) > 0$ such that $(K)^{+h(K)} \subset S_f$. Since, by Remark 2.1, $\nabla f(\cdot)$ is uniformly continuous in $(K)^{+h(K)}$, we have that

$$g'(0) = \lim_{h \rightarrow 0^+} g(h)/h = \min_{y \in K} \|\nabla f(y)\|. \quad (\text{A.59})$$

Now, by multivariate Taylor's theorem with integral remainder, we have that, for $v \in S^{p-1}$ and $h > 0$,

$$\begin{aligned} f(x + hv) &= f(x + hw(x)) + h \langle \nabla f(x + hw(x)), v - w(x) \rangle \\ &\quad + h^2 \int_0^1 (1-s)(v - w(x))^\top H_f(x + hs(v - w(x)))(v - w(x)) ds. \end{aligned}$$

It follows that, for $0 < h \leq h(K)/2$,

$$\begin{aligned}
f(x + hv) &\geq f(x) + g(h) + h \langle \nabla f(x + hw(x)), v - w(x) \rangle \\
&\quad + h^2 \int_0^1 (1-s)(v-w(x))^\top H_f(x + hs(v-w(x)))(v-w(x)) ds \\
&\geq f(x) + g(h) - h \|v - w(x)\| \|\nabla f(x + hw(x))\| \\
&\quad - h^2 \|v - w(x)\|^2 \int_0^1 (1-s) \|H_f(x + hs(v-w(x)))\|_{\mathcal{M}} ds \\
&\geq f(x) + g(h) - h \|v - w(x)\| c_1 - h^2 \|v - w(x)\|^2 c_2/2,
\end{aligned}$$

where

$$c_1 := \max_{y \in (K)^{+h(K)/2}} \|\nabla f(y)\|$$

and

$$c_2 := \max_{y \in (K)^{+h(K)}} \|H_f(y)\|_{\mathcal{M}}.$$

Therefore, we have that

$$\nabla_v^h f(x) \geq \tilde{g}(h) := g(h)/h - \|v - w(x)\| c_1 - h \|v - w(x)\|^2 c_2/2.$$

Since $f(\cdot)$ has no stationary points in K , $\min_{y \in K} \|\nabla f(y)\| > 0$, and the result follows from (A.59). \blacksquare

Proof of Corollary 3.1. Let $\delta > 0$. We show that there exists $n^* \in \mathbb{N}$ and $\{\eta_n\}_{n=1}^\infty$ such that

$$\sum_{n=1}^{\infty} P^{\otimes n}(J_n \geq \delta) \leq n^* - 1 + \sum_{n=n^*}^{\infty} P^{\otimes n}(J_n = 1) \leq n^* - 1 + \sum_{n=n^*}^{\infty} \eta_n < \infty.$$

Then the result follows from Borel-Cantelli lemma. To this end, we explicitly express the constant η in Theorem 3.4 as a function of n and observe the convergence of the series. We first notice that, for $n \geq n_1$, we can choose $\eta_n/2 \geq k(1 - \alpha_0 \Lambda^*)^n$ in (4.23). Next, we apply in (4.16) Lemma 3.2 (iii) with $K = \tilde{K}_\xi$, $h^* = r$, and $\epsilon = d^* \min_{y \in \tilde{K}_\xi} \|\nabla f(y)\|$ and get constants $0 < \tilde{C} < \infty$ and $\tilde{n} \in \mathbb{N}$ such that, for all $n \geq \tilde{n}$,

$$P^{\otimes n} \left(\sup_{h \in [h_n, r]} \sup_{v \in S^{p-1}} \sup_{x \in \tilde{K}_\xi} |\nabla_v^h f_{\tau_n, n}(x) - \nabla_v^h f(x)| < d^* \min_{y \in \tilde{K}_\xi} \|\nabla f(y)\| \right) \leq 1 - \frac{\tilde{C}}{n^2}.$$

Therefore, for all $n \geq n^* := \max(n_1, \tilde{n})$, we can choose

$$\eta_n/2 = \max(k(1 - \alpha_0 \Lambda^*)^n, \tilde{C}/n^2),$$

yielding $\sum_{n=n^*}^{\infty} \eta_n < \infty$. \blacksquare

B Central limit results for sample τ -approximations

It is well known that extreme localization is an important concept in depth analysis, however, the fluctuations of $f_{\tau,n}(\cdot)$ are unknown. Our main result in this section characterizes the asymptotic variance and establishes a related limit distribution. To this end, let

$$\Lambda_1^{*2} := \int \Lambda_1^2(x_1) dx_1,$$

where, for $x_1 \in \mathbb{R}^p$,

$$\Lambda_1(x_1) := \int h_1(0; x_1, \dots, x_p) dx_2 \dots dx_p.$$

Theorem B.1 *Let P be absolutely continuous with respect to the Lebesgue measure on \mathbb{R}^p with continuous density $f(\cdot)$. Let $x \in S_f$ and $\{\tau_n\}_{n=1}^\infty$ be a sequence of positive scalars converging to zero. Suppose (2.4) and $E[(\tilde{h}_\tau^{(1)}(x; X_1))^2] > 0$ hold true. If $\sqrt{n}\tau_n^{((2k-1)p)/2} \xrightarrow[n \rightarrow \infty]{d} \infty$, then*

$$\sqrt{n}\tau_n^{p/2} (f_{\tau_n,n}(x) - f_{\tau_n}(x)) \xrightarrow[n \rightarrow \infty]{d} N\left(0, \frac{\Lambda_1^{*2}}{\Lambda_1^2} f(x)\right).$$

Remark B.1 *We notice that, for $k > 1$, the limit distribution in Theorem B.1 with $f_{\tau_n}(\cdot)$ replaced by $f(\cdot)$ cannot hold. In fact, the deterministic term $f_{\tau_n}(x) - f(x)$ is, by Lemma A.5, of order $O(\tau_n^2)$, while the term $f_{\tau_n,n}(x) - f_{\tau_n}(x)$ converges to a normal distribution at rate $1/(\sqrt{n}\tau_n^{p/2})$. Since, necessarily, $\sqrt{n}\tau_n^{((2k-1)p)/2} \xrightarrow[n \rightarrow \infty]{d} \infty$, $f_{\tau_n}(x) - f(x)$ is the dominant term. On the other hand, if $k = 1$, $\sqrt{n}\tau_n^{p/2} \xrightarrow[n \rightarrow \infty]{d} \infty$ and $\sqrt{n}\tau_n^{p/2+2} \xrightarrow[n \rightarrow \infty]{d} 0$, then, by Lemma A.5, $\sqrt{n}\tau_n^{p/2} (f_{\tau_n}(x) - f(x)) \xrightarrow[n \rightarrow \infty]{d} 0$. Hence,*

$$\sqrt{n}\tau_n^{p/2} (f_{\tau_n,n}(x) - f(x)) \xrightarrow[n \rightarrow \infty]{d} N\left(0, \frac{\Lambda_1^{*2}}{\Lambda_1^2} f(x)\right).$$

In the examples with uniform kernel, the constant Λ_1 appearing in the limiting variance in Theorem B.1 can be calculated numerically using (2.4) by computing the percentage of uniformly distributed random points in $(\bar{B}_\rho(0))^k$ that lie in $Z_1^G(0)$ (e.g., for $G = K_\beta$, $k = 2$ and $\rho = \sqrt{2} \min(1, \beta/2)$) and multiplying the result by its volume $((\pi^{p/2} \rho^p)/\Gamma(pk/2+1))^k$, where $\Gamma(\cdot)$ is the gamma function. Similarly, the constant Λ_1^{*2} can be calculated by approximating the integral with a sum. An alternative form for Theorem B.1 without the factor $f(x)$ in the variance term is given in the following corollary.

Before proving Theorem B.1, we provide a lemma concerning the order of convergence of $E[(\tilde{h}_\tau^{(1)}(x; X_1))^2]$ to 0, as $\tau \rightarrow 0^+$.

Lemma B.1 Suppose (2.4) holds true. If $f(\cdot)$ is continuous, then

$$\lim_{\tau \rightarrow 0^+} \frac{E[(\tilde{h}_\tau^{(1)}(x; X_1))^2]}{\tau^{(2k-1)p}} = \Lambda_1^{*2} f^{2k-1}(x),$$

where

$$\Lambda_1^{*2} = \int \left(\int h_1(0; x_1, \dots, x_k) dx_2 \dots dx_k \right)^2 dx_1.$$

Proof of Lemma B.1. Let $\tau > 0$. We compute

$$\frac{E[(\tilde{h}_\tau^{(1)}(x; X_1))^2]}{\tau^{(2k-1)p}} = \frac{E[(h_\tau^{(1)}(x; X_1))^2]}{\tau^{(2k-1)p}} - \left(\frac{LGD(x, \tau)}{\tau^{(k-1/2)p}} \right)^2, \quad (\text{B.1})$$

where, by Theorem 2.1 (i),

$$\frac{LGD(x, \tau)}{\tau^{kp}} \xrightarrow[\tau \rightarrow 0^+]{ } \Lambda_1 f^k(x) \quad \text{and} \quad \frac{LGD(x, \tau)}{\tau^{(k-1/2)p}} \xrightarrow[\tau \rightarrow 0^+]{ } 0.$$

We now focus on the first term in (B.1). By changing variables twice, we note that

$$\begin{aligned} \frac{E[(h_\tau^{(1)}(x; X_1))^2]}{\tau^{(2k-1)p}} &= \frac{1}{\tau^{(2k-1)p}} \int \left(\int h_\tau(x; x_1, \dots, x_k) \prod_{j=2}^k f(x_j) dx_2 \dots dx_k \right)^2 f(x_1) dx_1 \\ &= \frac{1}{\tau^{2(k-1)p}} \int \left(\int h_1 \left(0; x_1, \frac{x_2 - x}{\tau}, \dots, \frac{x_k - x}{\tau} \right) \prod_{j=2}^k f(x_j) dx_2 \dots dx_k \right)^2 f(x + \tau x_1) dx_1 \\ &= \int \left(\int h_1(0; x_1, \dots, x_k) \prod_{j=2}^k f(x + \tau x_j) dx_2 \dots dx_k \right)^2 f(x + \tau x_1) dx_1. \end{aligned}$$

Since $f(\cdot)$ is continuous, it follows from the boundeness of $h_1(\cdot; \cdot)$, (2.4) and LDCT that

$$\begin{aligned} \lim_{\tau \rightarrow 0^+} \int h_1(0; x_1, \dots, x_k) \prod_{j=2}^k f(x + \tau x_j) dx_2 \dots dx_k \\ = f^{k-1}(x) \int h_1(0; x_1, \dots, x_k) dx_2 \dots dx_k \end{aligned}$$

and

$$\begin{aligned} \lim_{\tau \rightarrow 0^+} \int \left(\int h_1(0; x_1, \dots, x_k) \prod_{j=2}^k f(x + \tau x_j) dx_2 \dots dx_k \right)^2 f(x + \tau x_1) dx_1 \\ = f^{2k-1}(x) \int \left(\int h_1(0; x_1, \dots, x_k) dx_2 \dots dx_k \right)^2 dx_1 \end{aligned}$$

■

Proof of Theorem B.1. Using Hoeffding's decomposition of U-statistics ((A.22) with τ replaced by τ_n), it follows that

$$\begin{aligned} LGD_n(x, \tau_n) - LGD(x, \tau_n) &= \frac{k}{n} \sum_{i=1}^n [h_{\tau_n}^{(1)}(x; X_i) - LGD(x, \tau_n)] \\ &\quad + \sum_{j=2}^k \binom{k}{j} \binom{n}{j}^{-1} \sum_{1 \leq i_1 < \dots < i_j \leq n} g_{\tau_n}^{(j)}(x; X_{i_1}, \dots, X_{i_j}). \end{aligned} \quad (\text{B.2})$$

Notice that, by Remark 2.5, $E[(\tilde{h}_{\tau_n}^{(1)}(x; X_1))^2] > 0$. Now, applying Lindeberg-Levy Theorem for triangular arrays [Billingsley, 2012, Theorem 27.2] with

$$r_n = n, \quad s_n = \sqrt{n}(E[(\tilde{h}_{\tau_n}^{(1)}(x; X_1))^2])^{1/2}, \quad \text{and} \quad S_n = \sum_{i=1}^n [h_{\tau_n}^{(1)}(x; X_i) - LGD(x, \tau_n)],$$

it follows that

$$\sqrt{n} \frac{1}{n} \sum_{i=1}^n [h_{\tau_n}^{(1)}(x; X_i) - LGD(x, \tau_n)] / (E[(\tilde{h}_{\tau_n}^{(1)}(x; X_1))^2])^{1/2} \xrightarrow[n \rightarrow \infty]{d} N(0, 1), \quad (\text{B.3})$$

provided the Lindeberg condition [Billingsley, 2012, Equation (27.8)]

$$\lim_{n \rightarrow \infty} \frac{1}{E[(\tilde{h}_{\tau_n}^{(1)}(x; X_1))^2]} \int_{A_{n,\epsilon}} (h_{\tau_n}(x; x_1) - LGD(x, \tau_n))^2 f(x_1) dx_1 = 0 \quad (\text{B.4})$$

holds for all $\epsilon > 0$, where

$$A_{n,\epsilon} := \{x_1 \in \mathbb{R}^p : (h_{\tau_n}(x; x_1) - LGD(x, \tau_n))^2 \geq \epsilon^2 n E[(\tilde{h}_{\tau_n}^{(1)}(x; X_1))^2]\}.$$

Using (A.1), it holds that $(h_{\tau_n}(x; x_1) - LGD(x, \tau_n))^2 \leq l^2$, for all $x, x_1 \in \mathbb{R}^p$. Also, due to $x \in S_f$ and $n \tau_n^{(2k-1)p} \xrightarrow[n \rightarrow \infty]{d} \infty$, Lemma B.1 implies that $n E[(\tilde{h}_{\tau_n}^{(1)}(x; X_1))^2] \xrightarrow[n \rightarrow \infty]{d} \infty$. Let $n^* \in \mathbb{N}$ be such that for all $n \geq n^*$, $l^2 < \epsilon^2 n E[(\tilde{h}_{\tau_n}^{(1)}(x; X_1))^2]$. It follows that $A_{n,\epsilon} = \emptyset$ for all $n \geq n^*$. Thus, (B.4) holds true and we obtain (B.3). Finally, for $j = 2, \dots, k$, let

$$R_n^{(j)} = R_n^{(j)}(X_1, \dots, X_n) := \binom{k}{j} \binom{n}{j}^{-1} \sum_{1 \leq i_1 < \dots < i_j \leq n} g_{\tau_n}^{(j)}(x; X_{i_1}, \dots, X_{i_j}).$$

By (A.24) with $m = 1$, $\mathbf{R}_n^{(j)} = R_n^{(j)}$, x_1 replaced by x and τ_1 replaced by τ_n ,

$$P^{\otimes n}(\sqrt{n} |R_n^{(j)}| > \epsilon) \leq \frac{n}{\epsilon^2} \binom{k}{j}^2 \binom{n}{j}^{-1} E \left[\left(g_{\tau_n}^{(j)}(x; X_1, \dots, X_j) \right)^2 \right],$$

which implies that

$$P^{\otimes n} \left(\sqrt{n} \frac{|R_n^{(j)}|}{(E[(\tilde{h}_{\tau_n}^{(1)}(x; X_1))^2])^{1/2}} > \epsilon \right) \leq \frac{n \binom{k}{j}^2 \binom{n}{j}^{-1}}{\epsilon^2 E[(\tilde{h}_{\tau_n}^{(1)}(x; X_1))^2]} E \left[\left(g_{\tau_n}^{(j)}(x; X_1, \dots, X_j) \right)^2 \right].$$

Since $j \geq 2$ and $nE[(\tilde{h}_{\tau_n}^{(1)}(x; X_1))^2] \xrightarrow[n \rightarrow \infty]{} \infty$,

$$P^{\otimes n} \left(\sqrt{n} |R_n^{(j)}| / (E[(\tilde{h}_{\tau_n}^{(1)}(x; X_1))^2])^{1/2} > \epsilon \right) \xrightarrow[n \rightarrow \infty]{} 0. \quad (\text{B.5})$$

From (B.2), (B.3), and (B.5), it follows that

$$\sqrt{n} \frac{LGD_n(x, \tau_n) - LGD(x, \tau_n)}{k(E[(\tilde{h}_{\tau_n}^{(1)}(x; X_1))^2])^{1/2}} \xrightarrow[n \rightarrow \infty]{d} N(0, 1). \quad (\text{B.6})$$

Now, using the delta method we obtain

$$\sqrt{n} \frac{(LGD(x, \tau_n))^{1-1/k}}{(E[(\tilde{h}_{\tau_n}^{(1)}(x; X_1))^2])^{1/2}} ((LGD_n(x, \tau_n))^{1/k} - (LGD(x, \tau_n))^{1/k}) \xrightarrow[n \rightarrow \infty]{d} N(0, 1);$$

equivalently,

$$Z_n := \sqrt{n} \frac{\tau_n^{kp} \Lambda_1 f_{\tau_n}^{k-1}(x)}{(E[(\tilde{h}_{\tau_n}^{(1)}(x; X_1))^2])^{1/2}} (f_{\tau_n, n}(x) - f_{\tau_n}(x)) \xrightarrow[n \rightarrow \infty]{d} N(0, 1). \quad (\text{B.7})$$

To complete the proof, since $x \in S_f$ and $\tau_n > 0$, it holds, by Theorem 2.1 (i), that

$$\frac{f_{\tau_n}^k(x)}{f^k(x)} = \frac{LGD(x, \tau_n)}{\Lambda_1 \tau_n^{kp} f^k(x)} \xrightarrow[n \rightarrow \infty]{} 1 \quad (\text{B.8})$$

and, by Lemma B.1,

$$\frac{(E[(\tilde{h}_{\tau_n}^{(1)}(x; X_1))^2])^{1/2}}{\tau_n^{(k-1/2)p}} \xrightarrow[n \rightarrow \infty]{} \Lambda_1^* f^{k-1/2}(x) > 0. \quad (\text{B.9})$$

(B.8) and (B.9) imply that

$$\begin{aligned} Y_n &:= \frac{(E[(\tilde{h}_{\tau_n}^{(1)}(x; X_1))^2])^{1/2}}{\tau_n^{(k-1/2)p} f_{\tau_n}^{k-1}(x)} \cdot \frac{1}{\Lambda_1^* f^{\frac{1}{2}}(x)} \\ &= \frac{(E[(\tilde{h}_{\tau_n}^{(1)}(x; X_1))^2])^{1/2}}{\tau_n^{(k-1/2)p}} \cdot \frac{1}{\Lambda_1^* f^{k-1/2}(x)} \cdot \frac{f^{k-1}(x)}{f_{\tau_n}^{k-1}(x)} \xrightarrow[n \rightarrow \infty]{} 1. \end{aligned}$$

From (B.7) and Slutsky's Theorem it follows that

$$Y_n Z_n \xrightarrow[n \rightarrow \infty]{d} N(0, 1),$$

completing the proof. ■

Corollary B.1 Under the hypothesis of Theorem B.1,

$$\sqrt{n}\tau_n^{\frac{1}{2}p} \left(\sqrt{f_{\tau_n,n}(x)} - \sqrt{f_{\tau_n}(x)} \right) \xrightarrow[n \rightarrow \infty]{d} N \left(0, \frac{\Lambda_1^{*2}}{4\Lambda_1^2} \right).$$

Proof of Corollary B.1. We will show that

$$\frac{f_{\tau_n,n}(x)}{f_{\tau_n}(x)} = \frac{(LGD_n(x, \tau_n))^{1/k}}{(LGD(x, \tau_n))^{1/k}} \xrightarrow[n \rightarrow \infty]{d} 1. \quad (\text{B.10})$$

For this, it is enough to verify that

$$\frac{LGD_n(x, \tau_n)}{LGD(x, \tau_n)} \xrightarrow[n \rightarrow \infty]{d} 1. \quad (\text{B.11})$$

Notice that

$$\frac{LGD_n(x, \tau_n)}{LGD(x, \tau_n)} = \frac{\tau_n^{kp}}{LGD(x, \tau_n)} \cdot \frac{LGD_n(x, \tau_n) - LGD(x, \tau_n)}{\tau_n^{kp}} + 1,$$

where, by Theorem 2.1 (i),

$$\frac{LGD(x, \tau_n)}{\tau_n^{kp}} \xrightarrow[n \rightarrow \infty]{} \Lambda_1 f^k(x) > 0.$$

On the other hand,

$$\frac{LGD_n(x, \tau_n) - LGD(x, \tau_n)}{\tau_n^{kp}} = \left(\frac{(E[(\tilde{h}_{\tau_n}^{(1)}(x; X_1))^2])^{1/2}}{\tau_n^{(k-1/2)p} \cdot \sqrt{n}\tau_n^{\frac{1}{2}p}} \right) \left(\sqrt{n} \frac{LGD_n(x, \tau_n) - LGD(x, \tau_n)}{(E[(\tilde{h}_{\tau_n}^{(1)}(x; X_1))^2])^{1/2}} \right),$$

where $\sqrt{n}\tau_n^{\frac{1}{2}p} \xrightarrow[n \rightarrow \infty]{} \infty$, by Lemma B.1,

$$\frac{(E[(\tilde{h}_{\tau_n}^{(1)}(x; X_1))^2])^{1/2}}{\tau_n^{(k-1/2)p}} \xrightarrow[n \rightarrow \infty]{} \Lambda_1^* f^{k-1/2}(x) > 0,$$

and by (B.6)

$$\sqrt{n} \frac{LGD_n(x, \tau_n) - LGD(x, \tau_n)}{(E[(\tilde{h}_{\tau_n}^{(1)}(x; X_1))^2])^{1/2}} \xrightarrow[n \rightarrow \infty]{d} N(0, k^2).$$

Now applying Slutsky's Theorem

$$\frac{LGD_n(x, \tau_n) - LGD(x, \tau_n)}{\tau_n^{kp}} \xrightarrow[n \rightarrow \infty]{d} 0,$$

and, hence (B.11) and (B.10) hold. Now, (B.8) and (B.10) imply that

$$\frac{f_{\tau_n,n}(x)}{f(x)} = \frac{f_{\tau_n,n}(x)}{f_{\tau_n}(x)} \cdot \frac{f_{\tau_n}(x)}{f(x)} \xrightarrow[n \rightarrow \infty]{d} 1. \quad (\text{B.12})$$

By Theorem B.1

$$Z_n^* := \sqrt{n} \tau_n^{\frac{1}{2}p} \frac{1}{\sqrt{f(x)}} (f_{\tau_n, n}(x) - f_{\tau_n}(x)) \xrightarrow[n \rightarrow \infty]{d} N\left(0, \frac{\Lambda_1^{*2}}{\Lambda_1^2}\right),$$

where we can write $f_{\tau_n, n}(x) - f_{\tau_n}(x)$ as

$$f_{\tau_n, n}(x) - f_{\tau_n}(x) = \left(\sqrt{f_{\tau_n, n}(x)} - \sqrt{f_{\tau_n}(x)} \right) \left(\sqrt{f_{\tau_n, n}(x)} + \sqrt{f_{\tau_n}(x)} \right).$$

Also, by (B.8) and (B.12)

$$Y_n^* := \frac{\sqrt{f_{\tau_n, n}(x)} + \sqrt{f_{\tau_n}(x)}}{\sqrt{f(x)}} = \sqrt{\frac{f_{\tau_n, n}(x)}{f(x)}} + \sqrt{\frac{f_{\tau_n}(x)}{f(x)}} \xrightarrow[n \rightarrow \infty]{d} 2,$$

and, by another application of Slutsky's Theorem,

$$\frac{Z_n^*}{Y_n^*} \xrightarrow[n \rightarrow \infty]{d} N\left(0, \frac{\Lambda_1^{*2}}{4\Lambda_1^2}\right),$$

proving the Corollary. ■

An extension of Theorem B.1 uniformly over S_f , namely,

$$\sqrt{n} \tau_n^{\frac{1}{2}p} (f_{\tau_n, n}(\cdot) - f_{\tau_n}(\cdot)) \xrightarrow[n \rightarrow \infty]{d} \frac{\Lambda_1^*}{\Lambda_1} W(\cdot) \text{ in } \ell^\infty(S_f),$$

where $\{W(x)\}_{x \in S_f}$ is a centered Gaussian process with the covariance function $\gamma : S_f \times S_f \rightarrow \mathbb{R}$ given by $\gamma(x, y) = \sqrt{f(x)f(y)}$, requires an extension of the results of Arcones and Giné [1993] to triangular arrays and it is beyond the scope of the present paper. A result in this direction, when the kernel is uniform, is given by Schneemeier [1989], but this is not sufficient in this context since the sets $\{Z_{\tau_n}^G(x)\}_{n=1}^\infty$ depend on n and x .

C Examples

In this section of the appendix, we provide additional examples of LDFs and verify that they satisfy the VC-subgraph property.

Example C.1 As in the introduction, let $G(\cdot) = \mathbf{I}(\cdot \in Z_1^G(0))$, for some $k \geq 1$. Then, as before, for $G = L, B, S, K_\beta$, we obtain local lens [Kleindessner and Von Luxburg, 2017], spherical, simplicial [Agostinelli and Romanazzi, 2008], and β -skeleton depth. In particular, $K_1 = B$ and $K_2 = L$. We will now verify that these class of depth functions satisfy the VC-subgraph property. Let $\mathcal{B} := \{\overline{B}_r(x) : x \in \mathbb{R}^p, r > 0\}$ be the class of balls in \mathbb{R}^p and, for $\beta \geq 1$, $\mathcal{K}_\beta := \{\overline{B}_{\frac{\beta}{2}\|x_1-x_2\|}(\frac{\beta}{2}x_1 + (1 - \frac{\beta}{2})x_2) \cap \overline{B}_{\frac{\beta}{2}\|x_1-x_2\|}((1 - \frac{\beta}{2})x_1 + \frac{\beta}{2}x_2) : x_1, x_2 \in \mathbb{R}^p\}$.

$x_1, x_2 \in \mathbb{R}^p\}$ be the class of all β -skeleton sets. By Theorem 1 in Dudley [1979], \mathcal{B} is a VC-class of sets. Applying Proposition 3.6.7 (ii) of Giné and Nickl [2016], it follows that also the intersection $\mathcal{B} \cap \mathcal{B}$ is a VC-class of sets. Since a subset of a VC-class of sets is still a VC-class (see Proposition 3.6.7 (iv) in Giné and Nickl [2016]), it holds that, for all $\beta \geq 1$, $\mathcal{K}_\beta \subset \mathcal{B} \cap \mathcal{B}$ is a VC-class. We finally notice that the function $\mathbf{I}(\cdot \in Z_1^{K(\cdot)}(0))$ is jointly Borel measurable. Similarly, the class of simplices in \mathbb{R}^p , which are given by the intersections of $p+1$ half-spaces, is a VC-class (see Corollary 6.7 of Arcones and Giné [1993]).

In the above discussion, one requires measurability of the sets $Z_\tau^G(x)$. This can be seen by noticing that these sets are closed in $(\mathbb{R}^p)^{k_G}$. We illustrate this for simplicial depth, where the set under consideration is $Z_\infty^S(x)$. To this end, suppose that $(x_1^{(n)}, \dots, x_{p+1}^{(n)})$ belongs to $Z_\infty^S(x)$, for all n , and converges as $n \rightarrow \infty$ to $(x_1, \dots, x_{p+1}) \in (\mathbb{R}^p)^{(p+1)}$. Convergence is equivalent to $\lim_{n \rightarrow \infty} \|x_i^{(n)} - x_i\| = 0$, for all $i = 1, \dots, p+1$. Suppose by contradiction that $(x_1, \dots, x_{p+1}) \notin Z_\infty^S(x)$, that is, $x \notin \Delta[x_1, \dots, x_{p+1}]$. Then, there exists $v \in S^{p-1}$ such that the halfspace $H_{x,v} = \{y \in \mathbb{R}^p : \langle y, v \rangle \geq \langle x, v \rangle\}$ does not contain any of the points x_1, \dots, x_{p+1} . That is, $\langle x_i - x, v \rangle < 0$, for all $i = 1, \dots, p+1$. It follows that there is $n^* \in \mathbb{N}$ such that $\langle x_i^{(n)} - x, v \rangle < 0$, for all $i = 1, \dots, p+1$ and $n \geq n^*$. On the other hand, $x \in \Delta[x_1^{(n)}, \dots, x_{p+1}^{(n)}]$, for all n , implies that for some $i_n \in \{1, \dots, p+1\}$, $\langle x_{i_n} - x, v \rangle \geq 0$. Finally, closeness of $Z_\tau^S(x)$ follows from closeness of

$$Y_\tau^S := \{(x_1, \dots, x_{p+1}) \in (\mathbb{R}^p)^{p+1} : \max_{\substack{i,j=1,\dots,p+1 \\ i>j}} \|x_i - x_j\| \leq \tau\}$$

and the equality $Z_\tau^S(x) = Z_\infty^S(x) \cap Y_\tau^S$.

Example C.2 We turn to the uniform kernel [Devroye and Györfi, 1985] in this example. Again, in this case, $k = 1$ and

$$G(\cdot) := \mathbf{I}(\cdot \in \overline{B}_1(0)).$$

Since closed balls in \mathbb{R}^p form a VC-class of sets by Theorem 1 in Dudley [1979], it follows that $G(\cdot)$ belongs to the VC-subgraph class.

Example C.3 Depth functions can also be developed using kernel density techniques. Specifically, setting $k = 1$ and $G(\cdot) := \exp(-\|\cdot\|^2/2)$, that is a Gaussian kernel with covariance matrix $\tau^2 I$ [Chacón and Duong, 2018], one can obtain “kernel depth functions”. Also, the h -depth [Cuevas et al., 2007], used in functional data, can be obtained by scaling the above Gaussian kernel by τ .

Example C.4 As a last example, we consider LDFs generated using continuous bump functions (see e.g. Section 13 in Tu [2011]). These are non-negative, continuous functions $G : \mathbb{R}^p \rightarrow \mathbb{R}$ (hence, $k_G = 1$) with bounded support. From the continuity and bounded support assumption it follows that $G(\cdot)$ has finite integral. Under the additional assumptions that $G(0) > 0$ and $G(\cdot)$ is non-increasing along any ray from the origin $0 \in \mathbb{R}^p$, we see that **(P2)** and **(P4)** hold. Bump functions can be constructed, for instance, by the following procedure. Let $g_1 : \mathbb{R} \rightarrow \mathbb{R}$ be positive, continuous and increasing with $\lim_{t \rightarrow \infty} g_1(t) = \infty$. Set $g_2(t) := 1/g_1(1/t)$ and

$$g_3(t) := \begin{cases} g_2(1+t)g_2(1-t) & \text{if } |t| < 1 \\ 0 & \text{if } |t| \geq 1. \end{cases}$$

Finally, let $G(x) := g_3(\|x\|)$. Alternative, one can let $G(x)$ be the product $\prod_{i=1}^p g_3(x^{(i)})$. Additional smoothness can be added by requiring that $g_1(\cdot)$ has continuous derivatives of all orders and $\lim_{t \rightarrow \infty} g_1(t)/t^n = \infty$, for all $n \in \mathbb{N}$. This last assumption ensures that $G(\cdot)$ decays quickly to zero near the boundary of its support. For instance, by taking $g_1(t) = e^{t/2}$, we get the classical bump function

$$G(x) := \begin{cases} e^{-1/(1-\|x\|^2)} & \text{if } \|x\| < 1 \\ 0 & \text{if } \|x\| \geq 1, \end{cases}$$

which has continuous derivatives of all orders and decays exponentially fast as $\|x\| \rightarrow 1^-$.

D Density level set estimation

In this section, we provide an application of the theory and methods of the paper to estimate the upper level sets. We briefly describe another application to divergence based inference. We begin with the definition of level sets and upper level sets.

Definition D.1 For $\alpha > 0$, the level sets of $f(\cdot)$ and $f_\tau(\cdot)$ are $L^\alpha = \{x \in \mathbb{R}^p : f(x) = \alpha\}$ and $L_\tau^\alpha = \{x \in \mathbb{R}^p : f_\tau(x) = \alpha\}$, respectively. The upper level sets of $f(\cdot)$, $f_\tau(\cdot)$ and $f_{\tau,n}(\cdot)$ are $R^\alpha := \{x \in \mathbb{R}^p : f(x) \geq \alpha\}$, $R_\tau^\alpha := \{x \in \mathbb{R}^p : f_\tau(x) \geq \alpha\}$ and $R_{\tau,n}^\alpha := \{x \in \mathbb{R}^p : f_{\tau,n}(x) \geq \alpha\}$, respectively.

The next proposition shows that in the limit the upper level sets induced by $f_\tau(\cdot)$ and $f_{\tau,n}(\cdot)$ coincide with those induced by $f(\cdot)$. We use the notation \mathring{A} for the interior of a set A .

Proposition D.1 Suppose that $f(\cdot)$ is uniformly continuous. Let $\{\alpha_n\}_{n=1}^\infty$ and $\{\tau_n\}_{n=1}^\infty$ be sequences of positive scalars converging to $\alpha > 0$ and 0, respectively. It holds that

$$\overset{\circ}{R}{}^\alpha \subset \liminf_{n \rightarrow \infty} R_{\tau_n}^{\alpha_n} \subset \limsup_{n \rightarrow \infty} R_{\tau_n}^{\alpha_n} \subset R^\alpha, \quad (\text{D.1})$$

and, if $\lambda(L^\alpha) = 0$, then

$$\lim_{n \rightarrow \infty} R_{\tau_n}^{\alpha_n} = R^\alpha \text{ a.e.} \quad (\text{D.2})$$

Suppose additionally that \mathcal{H}_G is a VC-subgraph class of functions and $\lim_{n \rightarrow \infty} \frac{n}{\log(n)} \tau_n^{2kp} = \infty$. It holds that

$$\overset{\circ}{R}{}^\alpha \subset \liminf_{n \rightarrow \infty} R_{\tau_n, n}^{\alpha_n} \subset \limsup_{n \rightarrow \infty} R_{\tau_n, n}^{\alpha_n} \subset R^\alpha \text{ a.s.,} \quad (\text{D.3})$$

and, if $\lambda(L^\alpha) = 0$, then

$$\lim_{n \rightarrow \infty} R_{\tau_n, n}^{\alpha_n} = R^\alpha \text{ a.s.} \quad (\text{D.4})$$

Proof of Proposition D.1. Using $\lim_{l \rightarrow \infty} \alpha_l = \alpha$ and Proposition 2.2 (i), we have that, for all $m \in \mathbb{N}$, there exists a constant $n \in \mathbb{N}$ such that $|\alpha_l - \alpha| < \frac{1}{m}$, for all $l \geq n$, and $|f_{\tau_l}(x) - f(x)| < \frac{1}{m}$, for all $l \geq n$ and $x \in \mathbb{R}^p$. It follows that

$$\begin{aligned} \liminf_{n \rightarrow \infty} R_{\tau_n}^{\alpha_n} &= \bigcup_{n=1}^\infty \bigcap_{l=n}^\infty \{x \in \mathbb{R}^p : f_{\tau_l}(x) \geq \alpha_l\} \\ &\supset \{x \in \mathbb{R}^p : f(x) > \alpha + \frac{2}{m}\} = \overset{\circ}{R}{}^{\alpha + \frac{2}{m}} \uparrow_{m \rightarrow \infty} \bigcup_{m=1}^\infty \overset{\circ}{R}{}^{\alpha + \frac{2}{m}} = \overset{\circ}{R}{}^\alpha \end{aligned}$$

and

$$\begin{aligned} \limsup_{n \rightarrow \infty} R_{\tau_n}^{\alpha_n} &= \bigcap_{n=1}^\infty \bigcup_{l=n}^\infty \{x \in \mathbb{R}^p : f_{\tau_l}(x) \geq \alpha_l\} \\ &\subset \{x \in \mathbb{R}^p : f(x) \geq \alpha - \frac{2}{m}\} = R^{\alpha - \frac{2}{m}} \downarrow_{m \rightarrow \infty} \bigcap_{m=1}^\infty R^{\alpha - \frac{2}{m}} = R^\alpha, \end{aligned}$$

establishing (D.1). For the second part, using $R^\alpha = L^\alpha \cup \overset{\circ}{R}{}^\alpha$ and (D.1), it follows that

$$\begin{aligned} \liminf_{n \rightarrow \infty} R_{\tau_n}^{\alpha_n} &= \overset{\circ}{R}{}^\alpha \cup \left(\liminf_{n \rightarrow \infty} R_{\tau_n}^{\alpha_n} \cap L^\alpha \right) \text{ and} \\ \limsup_{n \rightarrow \infty} R_{\tau_n}^{\alpha_n} &= \overset{\circ}{R}{}^\alpha \cup \left(\limsup_{n \rightarrow \infty} R_{\tau_n}^{\alpha_n} \cap L^\alpha \right), \text{ where} \end{aligned}$$

$$\liminf_{n \rightarrow \infty} R_{\tau_n}^{\alpha_n} \cap L^\alpha \subset \limsup_{n \rightarrow \infty} R_{\tau_n}^{\alpha_n} \cap L^\alpha \subset L^\alpha$$

are sets of Lebesgue measure 0. Therefore,

$$\liminf_{n \rightarrow \infty} R_{\tau_n}^{\alpha_n} = \limsup_{n \rightarrow \infty} R_{\tau_n}^{\alpha_n} = R^\alpha$$

except for a set of Lebesgue measure 0 and we obtain (D.2). We now prove (D.3). Let $D_{n,m} := \{x \in \mathbb{R}^p : |f_{\tau_n, n}(x) - f(x)| < \frac{1}{m}\}$. We first show that $\lim_{n \rightarrow \infty} D_{n,m} = \mathbb{R}^p$

a.s. To this end, we use Proposition 2.3 (i) and notice that, almost surely, there exists $n^*(m) \in \mathbb{N}$ (in general, different for different samples) such that, for all $n \geq n^*(m)$, $\sup_{x \in \mathbb{R}^p} |f_{\tau_n, n}(x) - f(x)| < \frac{1}{m}$. It follows that

$$\liminf_{n \rightarrow \infty} D_{n,m} = \lim_{n \rightarrow \infty} \cap_{l=n}^{\infty} D_{l,m} \supset \cap_{l=n^*(m)}^{\infty} D_{l,m} = \mathbb{R}^p \text{ a.s.}$$

Next, using Corollary L.1 (v), we have that, for all $m \in \mathbb{N}$,

$$\begin{aligned} \liminf_{n \rightarrow \infty} R_{\tau_n, n}^{\alpha_n} &\supset \liminf_{n \rightarrow \infty} \{x \in \mathbb{R}^p : f_{\tau_n, n}(x) > \alpha + \frac{1}{m}, |f_{\tau_n, n}(x) - f(x)| < \frac{1}{m}\} \\ &\supset \lim_{n \rightarrow \infty} (\mathring{R}^{\alpha + \frac{2}{m}} \cap D_{n,m}) = \mathring{R}^{\alpha + \frac{2}{m}} \text{ a.s.,} \end{aligned} \quad (\text{D.5})$$

and

$$\begin{aligned} \limsup_{n \rightarrow \infty} R_{\tau_n, n}^{\alpha_n} &\subset \limsup_{n \rightarrow \infty} \{x \in \mathbb{R}^p : f_{\tau_n, n}(x) \geq \alpha - \frac{1}{m}, |f_{\tau_n, n}(x) - f(x)| < \frac{1}{m}\} \\ &\subset \lim_{n \rightarrow \infty} (R^{\alpha - \frac{2}{m}} \cap D_{n,m}) = R^{\alpha - \frac{2}{m}} \text{ a.s.} \end{aligned} \quad (\text{D.6})$$

Using (D.5) and (D.6), we conclude that

$$\mathring{R}^\alpha = \cup_{m=1}^{\infty} \mathring{R}^{\alpha + \frac{2}{m}} \subset \liminf_{n \rightarrow \infty} R_{\tau_n, n}^{\alpha_n} \subset \limsup_{n \rightarrow \infty} R_{\tau_n, n}^{\alpha_n} \subset \cap_{m=1}^{\infty} R^{\alpha - \frac{2}{m}} = R^\alpha \text{ a.s.}$$

Finally, notice that, since P is absolutely continuous with respect to the Lebesgue measure, $\lambda(L^\alpha) = 0$ implies that

$$P(\liminf_{n \rightarrow \infty} R_{\tau_n}^{\alpha_n} \cap L^\alpha) \leq P(\limsup_{n \rightarrow \infty} R_{\tau_n}^{\alpha_n} \cap L^\alpha) \leq P(L^\alpha) = 0.$$

Thus,

$$\liminf_{n \rightarrow \infty} R_{\tau_n, n}^{\alpha_n} = \limsup_{n \rightarrow \infty} R_{\tau_n, n}^{\alpha_n} = R^\alpha \text{ a.s.,}$$

and (D.4) holds. ■

Remark D.1 If we restrict R^α , R_τ^α and $R_{\tau,n}^\alpha$ to a compact subset of \mathbb{R}^p , then, using Propositions 2.2-2.3 (ii), we see that Proposition D.1 also holds for continuous $f(\cdot)$.

Since a common approach in modal clustering is to define clusters as the connected components of the upper level sets R^α for some $\alpha > 0$ [Menardi, 2016], once the connected components are computed, the remaining points may be allocated to one of the clusters by using supervised classification techniques. A common approach is then to study how the clusters change as the parameter α varies, yielding cluster trees.

D.1 Divergence based inference

In this subsection, we provide how the methods can be applied for robust inference. Specifically, let $\{X_n : n \geq 1\}$ denote a collection of i.i.d. random variables with density $f(\cdot)$ and postulated to belong to a parametric family $\mathcal{R}_\Theta = \{r(\cdot; \theta); \theta \in \Theta \subset \mathbb{R}^d\}$. Beran [1977], for the real valued case, defined the minimum Hellinger distance estimator of θ to be the minimizer of

$$\theta_n = \operatorname{argmin}_{\theta \in \Theta} \left\| f_n^{\frac{1}{2}}(\cdot) - r^{\frac{1}{2}}(\cdot; \theta) \right\|_2,$$

where $\|\cdot\|_2$ represents the L^2 norm and $f_n(\cdot)$ is the Kernel density estimator of $f(\cdot)$ and is given by

$$f_n(x) = \frac{1}{n\tau_n^p} \sum_{i=1}^n K\left(\frac{x - X_i}{\tau_n}\right),$$

$K(\cdot)$ is a probability density and $\{\tau_n\}_{n=1}^\infty$ is a sequence of constants (referred to as bandwidth) converging to 0 while $n\tau_n^p \rightarrow \infty$ as $n \rightarrow \infty$. Under appropriate regularity conditions, Beran [1977] establishes consistency and asymptotic normality of $(\theta_n - \theta_f)$, where

$$\theta_f = \operatorname{argmin}_{\theta \in \Theta} \left\| f^{\frac{1}{2}}(\cdot) - r^{\frac{1}{2}}(\cdot; \theta) \right\|_2. \quad (\text{D.7})$$

Extensions of these ideas to multivariate models has been studied in Tamura and Boos [1986]. Lindsay [1994] developed a general framework of divergence based inference and studied the trade-off between efficiency and robustness. Specifically, let $\mathfrak{D}(\cdot)$ denote a three-times continuously differentiable convex function and let

$$\delta_\theta(x) := \frac{f(x) - r(x; \theta)}{r(x; \theta)}$$

denote the Pearson's residuals. The minimum divergence estimator of θ is defined to be

$$\theta_n := \operatorname{argmin}_{\theta \in \Theta} \int_{\mathbb{R}} \mathfrak{D}(\delta_{n,\theta}(x)) r(x; \theta) dx$$

where

$$\delta_{n,\theta}(x) := \frac{f_n(x) - r(x; \theta)}{r(x; \theta)},$$

and $f_n(\cdot)$ is, as before, the KDE. For more details concerning divergence based inference see Basu et al. [2019]. We define the local depth based minimum divergence estimator of θ to be

$$\theta_n^{(G)} := \operatorname{argmin}_{\theta \in \Theta} \int_{\mathbb{R}^p} \mathfrak{D}(\delta_{n,\theta}^{(G)}(x)) r(x; \theta) dx,$$

where $f_n(\cdot)$ is the $S\tau A$. Under the assumption that $r(\cdot; \theta)$ and $f(\cdot)$ has bounded support and other regularity conditions, one can establish using Proposition 2.3 that the resulting estimator is strongly consistent with Gaussian limit distribution whose mean is zero and covariance matrix is Σ_f . Here Σ_f takes into account the trade off between model misspecification and efficiency through the divergence \mathfrak{D} . When the true model coincides with $f(\cdot)$, efficiency follows. The proof of consistency relies on L^1 -convergence of $f_n(\cdot)$ which can be from Proposition 2.3. The limit distribution follows, after a Taylor approximation, from Theorem B.1 and family regularity. We notice here that the assumption of bounded support for the true density is not required for kernel density estimators. We conjecture that this is also true when using $S\tau A$ for estimating $f(\cdot)$ and this holds uniformly over the kernels $G(\cdot) \in \mathcal{G}$. Nevertheless, it follows that our results allow development of robust methodology for densities with bounded support, using a general class of density estimators involving local depth functions.

E Mathematical background for cluster identification

For the discussion in this section, we recall Assumption 3.1 and Definition 3.1 of the main paper. Since the clusters are obtained as limits of trajectories induced by modes, we now summarize relevant properties of the gradient system (3.2) by using results from the theory of ordinary differential equations and dynamical systems [Agarwal and Lakshmikantham, 1993, Hale, 1980, Teschl, 2012, Perko, 2013]. We first note that $u_x(\cdot)$ exists and is unique for t in some maximal time interval (a, b) with $a < 0 < b$, where $a = -\infty$ or $b = \infty$ is allowed. To see this, observe that, as $f(\cdot)$ is twice continuously differentiable, for every $x \in \mathbb{R}^p$ there exists a convex neighborhood $U(x)$ of x in which the second order partial derivatives are bounded. By applying Agarwal and Lakshmikantham [1993][Lemma 3.2.1] to ∇f , it follows that ∇f is Lipschitz in $U(x)$, and therefore ∇f is locally Lipschitz in S_f . Now, applying Picard-Lindelöf Theorem [Teschl, 2012][Theorem 2.2 and 2.5] it follows that $u_x(\cdot)$ exists in some time interval, which can be chosen to be maximal in view of Theorem 2.13 in Teschl [2012].

We now show that, using the boundedness of R^α , the solution $u_x(t)$ exists for all $t \geq 0$ and all $x \in S_f$. Furthermore, the solution starting in R^α cannot leave the set. To this end, notice that the equilibria of (3.2) are the stationary points of $f(\cdot)$. The gradient computed at each point gives the direction of most rapid increase of $f(\cdot)$. Hence, the trajectories $\{u_x(t) : t \in \mathbb{R}\}$ for $x \in S_f$ that are not stationary points are curves of steepest ascent for $f(\cdot)$. More specifically, if $u_x(t) \in L^\alpha$ for some $x \in S_f$ and $t \in \mathbb{R}$, then any vector v tangent to L^α at $u_x(t)$ satisfies $\langle v, u'_x(t) \rangle = 0$ (see Hirsch et al. [1974][Chapter

9 §4 Theorem 2] and Jost [2005][Lemma 6. 4. 2.]). Hence, either $u_x(t) = x$ for all t is a stationary point of the gradient system (3.2) or the trajectory $\{u_x(t) : t \in \mathbb{R}\}$ crosses L^α orthogonally. This also implies that $u_x(t)$ cannot leave R^α for $t \geq 0$. Furthermore, this property shows that, for all $x \in S_f$, the solution $u_x(t)$ exists for all $t \geq 0$, i.e. the maximal time interval in which $u_x(\cdot)$ is defined is (a, ∞) for some $a < 0$, where $a = -\infty$ is possible. To see this, for $x \in S_f$, choose an $\alpha > 0$ such that $x \in R^\alpha$. Since $u_x(t)$ cannot leave R^α for $t \geq 0$ and R^α is compact, the result follows from Teschl [2012][Corollary 2.15]. Recalling that our clusters are the stable manifolds generated by modes, we now link modes to the gradient system. This requires the notion of ω -limit which we now define.

Definition E.1 *The ω -limit of a point $x \in S_f$ is the set of points $y \in S_f$ such that $u_x(t)$ goes to y as $t \rightarrow \infty$, in symbols*

$$\omega(x) := \{y \in S_f : \lim_{t \rightarrow \infty} u_x(t) = y\}.$$

We use the following definition of Hirsch et al. [1974][Chapter 9 §3 Theorem 1] and Teschl [2012][Section 6.6]). For any function $W : U \rightarrow \mathbb{R}$, we use the notation $W'(u_x(t)) = \frac{dW(u_x(t))}{dt}$.

Definition E.2 *Let $\mu \in S_f$ be an equilibrium point for (3.2) and $U \subset S_f$ a neighborhood of μ . A differentiable function $W : U \rightarrow \mathbb{R}$ is a strict Lyapunov function if (i) $W(\mu) = 0$ and $W(u) > 0$ for $u \neq \mu$, and (ii) $W'(u_x(t)) < 0$ when $u_x(t) \in U \setminus \{\mu\}$.*

Let $V(\cdot) := -f(\cdot)$. If m is a mode for $f(\cdot)$, there exists a neighborhood $U(m)$ of m such that, for all $u \in U(m) \setminus \{m\}$, $V(u) - V(m) > 0$ and

$$(V(u) - V(m))' = -(f(u))' = -\langle \nabla f(u), u' \rangle = -\|\nabla f(u)\|^2 < 0.$$

Hence, $V(u) - V(m)$ is a strict Lyapunov function in $U(m)$. By the Lyapunov stability Theorem (see Hirsch et al. [1974][Chapter 9 §3 Theorem 1] and Hale [1980][Chapter X.1 Theorem 1.1]) m is asymptotically stable, that is, there is a neighborhood $U^*(m) \subset U(m)$ of m such that each solution starting from a point $x \in U^*(m)$ converges to m , i.e., for all $x \in U^*(m)$, $\omega(x) = \{m\}$. As we will see below, the set of points that have m as ω -limit, that is, the stable manifold generated by m , is typically much larger than $U^*(m)$. For instance, if $0 < \alpha < f(m)$ is such that $C(m) \cap R^\alpha$ contains no equilibria other than m , then, since each solution of (3.2) starting in $C(m) \cap R^\alpha$ cannot leave $C(m) \cap R^\alpha$, by LaSalle's invariance principle (see Hirsch et al. [1974][Chapter 9 §3 Theorem 2] and Teschl [2012][Theorem 6.14]) applied to the strict Lyapunov function $V(\cdot) - V(m)$, all the points in that component have m as an ω -limit point. On the other hand, if m is an antimode

for $f(\cdot)$, there exists a neighborhood $U(m)$ of m such that for all $u \in U(m) \setminus \{m\}$, $V(m) - V(u) > 0$ and $(V(m) - V(u))' > 0$. This implies that m is unstable [Hale, 1980][Chapter X.1 Theorem 1.2]: for every neighborhood $U^*(m) \subset U(m)$ of m , every solution u_x starting from a point $x \in U^*(m)$ eventually leaves $U^*(m)$. Furthermore, any ω -limit point of gradient system (3.2) is an equilibrium point: that is, a stationary points of $f(\cdot)$ (see Hirsch et al. [1974][Chapter 9 §4 Theorem 4] and Hale [1980][Chapter X.1 Theorem 1.3], and Jost [2005][Lemma 6. 4. 4.] in a different context).

For a stationary point μ of $f(\cdot)$, recall from (3.1) that $C(\mu)$ is the stable manifold induced by μ , that is, the set of points with ω -limit μ . The hypothesis that H_f has non-zero eigenvalues at stationary points and Stable Manifold Theorem (see Section 2.7 in Perko [2013], Section 9 in [Teschl, 2012] and Theorem A, Remark 2.3 in Abbondandolo and Pietro [2006]) indeed imply that the sets $C(\mu)$ are immersed submanifolds of \mathbb{R}^p with (topological) dimension equal to the number of negative eigenvalues of $H_f(\mu)$. As in Definition 3.1, let m_1, \dots, m_M be the modes and μ_1, \dots, μ_L the other stationary points of $f(\cdot)$. We are now ready to verify that the clusters $C(m_1), \dots, C(m_M)$ are non-trivial. We first observe that, by the uniqueness of the limit,

$$C(m_1), \dots, C(m_M), C(\mu_1), \dots, C(\mu_L)$$

are disjoint and, since any ω -limit point of gradient system (3.2) is an equilibrium point,

$$S_f = \bigcup_{i=1}^M C(m_i) \cup \bigcup_{l=1}^L C(\mu_l). \quad (\text{E.1})$$

Hence, $C(m_1), \dots, C(m_M), C(\mu_1), \dots, C(\mu_L)$ form a partition of S_f . Also, the set $S_f \setminus (\bigcup_{i=1}^M C(m_i)) = \bigcup_{l=1}^L C(\mu_l)$ has (topological) dimension smaller than p . The next proposition provides a characterization of the boundaries of $C(m_1), \dots, C(m_M)$. In particular, it shows that the clusters $C(m_1), \dots, C(m_M)$ are divided in S_f by the lower dimensional stable manifolds $C(\mu_1), \dots, C(\mu_L)$.

Proposition E.1 *Suppose that Assumption 3.1 holds true. Then, for all $i = 1, \dots, M$, $C(m_i)$ is open and $\partial C(m_i) \subset \partial S_f \cup \bigcup_{l=1}^L C(\mu_l)$.*

Proof of Proposition E.1. We prove this by contradiction. Suppose that $C(m_i)$ is not open. Then there exists $x \in C(m_i)$ such that, for all $\epsilon > 0$, $\overline{B}_\epsilon(x) \cap (\mathbb{R}^p \setminus C(m_i)) \neq \emptyset$. Using (E.1), we get that

$$(\mathbb{R}^p \setminus C(m_i)) = (\mathbb{R}^p \setminus S_f) \cup \bigcup_{\substack{j=1 \\ i \neq j}}^M C(m_j) \cup \bigcup_{l=1}^L C(\mu_l).$$

Since $x \in S_f$ and S_f is open, there exists $\epsilon^* > 0$ such that $\overline{B}_{\epsilon^*}(x) \cap (\mathbb{R}^p \setminus S_f) = \emptyset$. Hence, for all $0 < \epsilon \leq \epsilon^*$, it holds that

$$\overline{B}_\epsilon(x) \cap (\bigcup_{\substack{j=1 \\ i \neq j}}^M C(m_j) \cup \bigcup_{l=1}^L C(\mu_l)) \neq \emptyset.$$

Therefore, there is a sequence $\{x_l\}_{l=1}^\infty$ in $(\bigcup_{\substack{j=1 \\ i \neq j}}^M C(m_j) \cup \bigcup_{l=1}^L C(\mu_l))$ with $\lim_{l \rightarrow \infty} x_l = x$ and $f(x_l) \geq \alpha$, where $\alpha := f(x)/2$. Notice that, by Assumption 3.1, $f(\cdot)$ is twice continuously differentiable and R^α is compact. In particular, $\nabla f(\cdot)$ is locally Lipschitz. Denote by L the Lipschitz constant of $\nabla f(\cdot)$ on R^α and let $\delta := \text{dist}(\{m_i\}, \mathbb{R}^p \setminus C(m_i))/3$. Recall that $u_x(t)$ exists for all $t \in (a, \infty)$, $a < 0$. Since $x \in C(m_i)$, there exists $t^* \geq 0$ such that, for all $t \geq t^*$, $\|m_i - u_x(t)\| \leq \delta$. By continuity of solutions of ordinary differential equations with respect to the initial value (see Theorem 2.8 and (2.43) in Teschl [2012]), for all $t \geq 0$, it holds that

$$\|u_x(t) - u_{x_l}(t)\| \leq \|x_l - x\| e^{Lt}.$$

Let l^* such that, for all $l \geq l^*$, $\|x_l - x\| e^{Lt^*} \leq \delta$. Then, by the triangle inequality, we have that $\|m_i - u_{x_l}(t^*)\| \leq 2\delta$. Hence, $u_{x_l}(t^*) \in C(m_i)$. By the flow property of autonomous ordinary differential equations (see (6.10) in Teschl [2012]), it holds that $u_{x_l}(t + t^*) = u_{u_{x_l}(t^*)}(t)$, implying that

$$\lim_{t \rightarrow \infty} u_{x_l}(t + t^*) = \lim_{t \rightarrow \infty} u_{u_{x_l}(t^*)}(t) = m_i.$$

But this implies that $x_l \in C(m_i)$. A contradiction. Hence, $C(m_i)$ are open for all $i = 1, \dots, M$. Now, using again (E.1), we have that

$$\partial C(m_i) \subset \partial S_f \cup \bigcup_{\substack{j=1 \\ j \neq i}}^M C(m_j) \cup \bigcup_{l=1}^L C(\mu_l).$$

Since $C(m_i)$ and $C(m_j)$ are open and disjoint for $j \neq i$, we obtain that

$$\partial C(m_i) \subset \overline{C(m_i)} \subset \mathbb{R}^p \setminus C(m_j)$$

yielding that $\partial C(m_i) \cap (\bigcup_{\substack{j=1 \\ j \neq i}}^M C(m_j)) = \emptyset$. ■

Remark E.1 *Since Hausdorff dimension is larger or equal to topological dimension (see Theorem 6.3.10 in Edgar [2007]), the stable manifold $C(\mu_l)$ does not necessarily have Lebesgue measure zero. However, $\lambda(C(\mu_l)) = 0$ whenever topological and Hausdorff dimension coincide; and if they differ, the latter is smaller than n . Osgood curves [Sagan, 1994, Chapter 8] are examples of one-dimensional embedded manifolds in \mathbb{R}^2 with positive Lebesgue measure. These examples also show that, in Proposition D.1, the assumption that the level sets of $f(\cdot)$ have zero Lebesgue measure is, in general, necessary.*

F Exact identification of stationary points and modes

In this section, we further develop the results of Section 3.1 by providing some conditions under which the stationary points (resp. modes, antimodes) of $f(\cdot)$ are *exactly* the stationary points (resp. modes, antimodes) of $f_\tau(\cdot)$ for $\tau > 0$. The key criteria for the identification of the modes is the notion of symmetry proposed below.

Definition F.1 *Given $\tau > 0$, a density function $f(\cdot)$ is said to be τ -centrally symmetric about $\mu \in S_f$ if, for all $x \in \mathbb{R}^p$ with $\|x\| \leq \tau$, $f(\mu + x) = f(\mu - x)$.*

In particular, for $p = 1$, $f(\cdot)$ is τ -centrally symmetric about $\mu \in \mathbb{R}$ if $f(\mu - x) = f(\mu + x)$ for all $x \in [0, \tau]$. If $f(\cdot)$ has a continuous derivative, a direct computation using Corollary H.1 shows that, for $G = L, S, B, K_\beta$, $f'_\tau(\mu) = 0$. Indeed, by (H.1), we see that

$$f_\tau(x) = \frac{1}{\tau} \sqrt{LGD(x, \tau)}$$

where

$$LGD(x, \tau) = 2 \int_{T_{++}^\tau} f(x + x_1)f(x - x_2)dx_1 dx_2$$

and

$$T_{++}^\tau = \{(x_1, x_2) : x_1 \geq 0, x_2 \geq 0, x_1 + x_2 \leq \tau\}.$$

In particular, if $f(\cdot)$ has a continuous derivative, it follows that

$$f'_\tau(x) = \frac{1}{\tau \sqrt{LGD(x, \tau)}} \int_{T_{++}^\tau} f'(x + x_1)f(x - x_2) + f(x + x_1)f'(x - x_2)dx_1 dx_2.$$

Therefore, the sign of $f_\tau(x)$ depends on the sign of $f'(\cdot)$ in the interval $(x - \tau, x + \tau)$. In particular, if $\mu \in \mathbb{R}$ satisfies $f(\mu - x) = f(\mu + x)$ for all $x \in (0, \tau)$, it follows that $f'(\mu - x) = -f'(\mu + x)$, yielding $f'_\tau(\mu) = 0$.

Our next result, which is about the Hessian matrix, gives sufficient conditions for a stationary point μ and a mode m of $f(\cdot)$ to be a stationary point and a mode of $f_\tau(\cdot)$.

Theorem F.1 *Suppose (2.4) holds true and let $\tau > 0$. Then the following hold:*

- (i) *If $f(\cdot)$ has continuous first order partial derivatives in $\overline{B}_\tau(\mu) \subset S_f$ and $f(\cdot)$ is τ -centrally symmetric about the stationary point μ , then μ is a stationary point for $f_\tau(\cdot)$.*
- (ii) *Suppose that $f(\cdot)$ is τ -centrally symmetric about a mode (resp. an antimode) m and has continuous second order partial derivatives in $\overline{B}_\tau(m)$. If, for all $x_1, \dots, x_k \in \overline{B}_\tau(m)$, the matrix*

$$J_f(x_1, \dots, x_k) := H_f(x_1)f(x_2)\dots f(x_k) + (k-1)\nabla f(x_1)\nabla f(x_2)^\top f(x_3)\dots f(x_k)$$

is negative (resp. positive) definite, then m is also a mode (resp. an antimode) for $f_\tau(\cdot)$.

Notice that $J_f(m, \dots, m) = H_f(m)f^{k-1}(m)$ is negative (resp. positive) definite and therefore the last condition of Theorem F.1 is satisfied by $f(\cdot)$, for τ small.

Proof of Theorem F.1. For (i) notice that if $f(\cdot)$ is τ -centrally symmetric about μ , then, for all $y \in \mathbb{R}^p$ with $\|y\| \leq \tau$, $f(\mu + y) = f(\mu - y)$ and $\partial_j f(\mu - y) = -\partial_j f(\mu + y)$. By the change of variable $-(x_1, \dots, x_k)$ for (x_1, \dots, x_k) on the LHS of (3.4) and (A.4) it follows that, for all $1 \leq j \leq p$,

$$\begin{aligned} & \int h_\tau(0; x_1, \dots, x_k) \nabla f(\mu + x_1) f(\mu + x_2) \dots f(\mu + x_k) dx_1 \dots dx_k \\ &= \int h_\tau(0; x_1, \dots, x_k) \nabla f(\mu - x_1) f(\mu + x_2) \dots f(\mu - x_k) dx_1 \dots dx_k \\ &= - \int h_\tau(0; x_1, \dots, x_k) \nabla f(\mu + x_1) f(\mu + x_2) \dots f(\mu + x_k) dx_1 \dots dx_k, \end{aligned}$$

and therefore (3.4) and $\nabla f_\tau(\mu) = 0$.

We now prove (ii). Since $f(\cdot)$ is τ -centrally symmetric about m , by (i),

$$\partial_j f_\tau(m) = 0 \text{ for } j = 1, \dots, p \quad (\text{F.1})$$

and hence m is a stationary point for $f_\tau(\cdot)$. Moreover, (F.1) implies that, for $i, j = 1, \dots, p$,

$$\begin{aligned} \partial_i \partial_j f_\tau(m) &= \frac{1}{k} \left(\frac{1}{k} - 1 \right) (f_\tau(m))^{1-2k} (\partial_i f_\tau^k(m)) (\partial_j f_\tau^k(m)) + \frac{1}{k} (f_\tau(m))^{1-k} (\partial_i \partial_j f_\tau^k(m)) \\ &= \frac{1}{k} (f_\tau(m))^{1-k} (\partial_i \partial_j f_\tau^k(m)), \end{aligned}$$

where, by Proposition 2.1, (A.2) and (A.4),

$$\begin{aligned} \partial_i \partial_j f_\tau^k(m) &= k \int \frac{h_\tau(0; x_1, \dots, x_k)}{\tau^{kp} \Lambda_1} \left[\partial_i \partial_j f(m + x_1) \prod_{l=2}^k f(m + x_l) \right. \\ &\quad \left. + (k-1) \partial_j f(m + x_1) \partial_i f(m + x_2) \prod_{l=3}^k f(m + x_l) \right] dx_1 \dots dx_k. \end{aligned}$$

Noticing that the integral of a matrix is the matrix of the integrals, we get that

$$H_{f_\tau}(m) = \frac{1}{k} (f_\tau(m))^{k-1} \int \frac{h_\tau(0; x_1, \dots, x_k)}{\tau^{kp} \Lambda_1} J_f(m + x_1, \dots, m + x_k) dx_1 \dots dx_k.$$

Since the Hessian is symmetric, there exists an orthogonal matrix Q such that

$$\begin{aligned} D &= Q^\top H_{f_\tau}(m) Q \\ &= \frac{1}{k} (f_\tau(m))^{k-1} \int \frac{h_\tau(0; x_1, \dots, x_k)}{\tau^{kp} \Lambda_1} Q^\top J_f(m + x_1, \dots, m + x_k) Q dx_1 \dots dx_k \end{aligned}$$

is a diagonal matrix. Now, since $J_f(m+x_1, \dots, m+x_k)$ is negative (resp. positive) definite, for all $y \in \mathbb{R}^p \setminus \{0\}$, $y^\top J_f(m+x_1, \dots, m+x_k)y < 0$ (resp. > 0), and therefore the diagonal elements of $Q^\top J_f(m+x_1, \dots, m+x_k)Q$ are negative (resp. positive). It follows that the diagonal elements of D (that is, the eigenvalues of $H_{f_\tau}(m)$) are negative (resp. positive) and m is a mode (resp. an antimode) for $f_\tau(\cdot)$. ■

G Clustering Algorithm

In this section, we provide a detailed description of the algorithm for clustering. As a first step, starting from a point $x \in \mathbb{R}^p$, we search, in a given neighborhood of x , for the point y that yields the largest directional derivative $\nabla_v^h f_{\tau,n}$ with $h = \|y - x\|$ and $v = (y - x)/\|y - x\|$. Since

$$(\tau^{kp}\Lambda_1)^{1/k} \nabla_v^h f_\tau(x) = \frac{(LGD(x + hv, \tau))^{1/k} - (LGD(x, \tau))^{1/k}}{h} \quad \text{and}$$

$$(\tau^{kp}\Lambda_1)^{1/k} \nabla_v^h f_{\tau,n}(x) = \frac{(LGD_n(x + hv, \tau))^{1/k} - (LGD_n(x, \tau))^{1/k}}{h},$$

the constant $(\tau^{kp}\Lambda_1)^{1/k}$ does not influence the choice of the point y which maximizes both finite differences $\nabla_v^h f_\tau(x)$ and $\nabla_v^h f_{\tau,n}(x)$. This allows one to ignore the constant in the specification of the algorithm. That is, the finite difference approximation of the directional derivative of the k^{th} root of the local depth can be computed *avoiding the computation of the constant Λ_1* . We show, in fact, that the constant $(\tau^{kp}\Lambda_1)^{1/k}$ also does not influence the clusters induced by the system (3.3). Since $\tau, \Lambda_1 > 0$, if, for $x \in \mathbb{R}^p$, $u_{x,\tau} : \mathbb{R} \rightarrow \mathbb{R}^p$ is a solution of the system (3.3) with $u_{x,\tau}(0) = x$, then $\tilde{u}_{x,\tau} : \mathbb{R} \rightarrow \mathbb{R}^p$ given by $\tilde{u}_{x,\tau}(t) := u_{x,\tau}((\tau^{kp}\Lambda_1)^{1/k}t)$ also satisfies $\tilde{u}_{x,\tau}(0) = x$ and it is a solution of the system

$$\tilde{u}'(t) = \nabla ((LGD(\tilde{u}(t), \tau))^{1/k}). \quad (\text{G.1})$$

Moreover, since $\lim_{t \rightarrow \infty} u_{x,\tau}(t) = \lim_{t \rightarrow \infty} \tilde{u}_{x,\tau}(t)$ for all $x \in \mathbb{R}^p$, the clusters induced by (3.3) and (G.1) are the same. Hence, for $x, y \in \mathbb{R}^p$ with $y \neq x$ and $h = \|y - x\| \leq r$ small enough, we consider the finite difference approximation of the directional derivatives of $(LGD(x, \tau))^{1/k}$ and $(LGD_n(x, \tau))^{1/k}$ along the direction $v = \frac{y-x}{\|y-x\|}$ given by

$$d_\tau(x; y) := \frac{(LGD(y, \tau))^{1/k} - (LGD(x, \tau))^{1/k}}{\|y - x\|} \quad \text{and} \quad (\text{G.2})$$

$$d_{\tau,n}(x; y) := \frac{(LGD_n(y, \tau))^{1/k} - (LGD_n(x, \tau))^{1/k}}{\|y - x\|}. \quad (\text{G.3})$$

Next, given n data points x_1, \dots, x_n , the localization parameter τ used for the clustering procedure is chosen as the quantile of order q , $0 \leq q \leq 1$, of the empirical distribution of the $\binom{n}{2}$ distances $\|x_i - x_j\|$, $i > j$, $i, j \in \{1, 2, \dots, n\}$ for lens depth, spherical depth, and β -skeleton depth. Detailed methodology for simplicial depth is provided below. We now summarize the procedure for computing the clusters in Algorithm 1.

Algorithm 1: Clustering with general local depth

Input: $\{x_1, \dots, x_n\}, \{y_1, \dots, y_o\}$ (optional), q, s, r

Output: Local maxima for input points: $\{z_1, \dots, z_{n+o}\}$

```

1 Compute the quantile  $\tau$  of order  $q$  of all pairwise distances:  $\|x_i - x_j\|$ ,  $i > j$ ,
    $i, j \in \{1, 2, \dots, n\}$ 
2 Store  $\{x_1, \dots, x_n\}, \{y_1, \dots, y_o\}$  in new variables
  for  $i = 1$  to  $n$  do
    |  $z_i^* := x_i$ 
  end
  for  $i = 1$  to  $o$  do
    |  $z_{i+n}^* := y_i$ 
  end
3 Compute the general local depth with localization parameter  $\tau$  of  $\{z_1^*, \dots, z_{n+o}^*\}$ 
   w.r.t.  $\{x_1, \dots, x_n\}$ 
4 For all points, compute the corresponding local maxima
  for  $i = 1$  to  $n + o$  do
    | repeat
    5   |    $z_i := z_i^*$ 
    6   |   Store the data points (different from  $z_i$ ) at distance from  $z_i$  smaller than
        |    $r$  or the  $s$  closest data points if they are less than  $s$  in new variables
        |    $w_1, \dots, w_l$  ( $l \geq s$ )
    7   |    $z_i^* := \text{argmax}_{v \in \{w_1, \dots, w_l\}} d_{\tau, n}(z_i; v)$ 
    |   until  $LGD_n(z_i^*, \tau) > LGD_n(z_i, \tau)$ 
  end

```

The algorithm requires as input, data points $\{x_1, \dots, x_n\}$, quantile q , and two additional parameters, r and s . Additional points $\{y_1, \dots, y_o\}$ may also be provided as input. Starting from any point $x \in \{x_1, \dots, x_n\} \cup \{y_1, \dots, y_o\}$, based on the finite difference (G.3), the algorithm moves to another data point $y \in \{x_1, \dots, x_n\}$ (hence, except for the initial step, only data points are involved in (G.3)). The parameter r gives a bound on the norm $\|y - x\|$ in (G.3) in order to choose only those points that are close to each

other. The parameter s , representing the minimal number of directions at each step of the algorithm, is exploited to ensure that the number of directional derivatives taken into account is not too small. Based on these choices, the steps 5, 6 and 7 of Algorithm 1 are repeated until the local maximum is achieved. The resulting data points are returned as output.

We now turn to the choice of the parameters r , s , and q . We notice that for a good approximation to the directional derivative, the parameter r cannot be too large. Several exploratory analyses show that, under this condition, the parameter r does not significantly influence the output of Algorithm 1. Hence, we fix $r = 0.05$ in all our numerical work.

Turning to s , it is a good idea to consider a large number of various directions. The parameter s ensures that a sufficient number of directions are evaluated to get close to the maximum (over $v \in S^{p-1}$) of the directional derivative. This is particularly important in regions where data are sparse. The quantity s can also play the role of a smoothing parameter. If q (and hence τ) is small with a small sample size n , then the sample local depth can be noisy and have local peaks with a small basin of attraction that were not present in the original distribution. In this case, the choice of a larger s helps to avoid these local maxima.

We now describe a general method for the choice of s . Let $w(x) = \nabla f(x)/(\|\nabla f(x)\|)$ and V_i , $i = 1, \dots, s$ be independent according to the uniform distribution P_V on the unit sphere S^{p-1} . We take uniform distribution on S^{p-1} because directions of the s data points close to x are, in general, unknown. Then, for a given precision $\epsilon \in (0, 1)$, with probability at least $1 - \eta$ ($\eta \in (0, 1)$), we require that

$$P_V^{\otimes s} \left(\min_{i=1, \dots, s} \|V_i - w(x)\| \leq \epsilon \right) \geq 1 - \eta.$$

Using the independence of V_i s and due to the uniformity on S^{p-1} , we see that this is equivalent to

$$(1 - P_V(\|V_1 - e_p\| \leq \epsilon))^s \leq \eta,$$

where $e_p = (0, \dots, 0, 1)^\top \in \mathbb{R}^p$. Therefore, s can be taken to be the smallest integer greater than or equal to

$$g_p(\eta, \epsilon) := \log_{1-t_p(\epsilon)}(\eta),$$

where $t_p(\epsilon) := P_V(\|V_1 - e_p\| \leq \epsilon)$. Next, we compute the quantity $t_p(\epsilon)$. For $p = 1$, P_V is the Rademacher distribution yielding $t_p(\epsilon) = 1/2$. For $p \geq 2$, $t_p(\epsilon)$ is the probability (i.e. the area) of the hyperspherical cap $C_{1,\epsilon} = S^{p-1} \cap \overline{B}_\epsilon(e_p)$. Li [2011] shows that this is

given by

$$t_p(\epsilon) = \frac{1}{2} I_{r^2(\epsilon)}\left(\frac{p-1}{2}, \frac{1}{2}\right),$$

where $I_z(\alpha, \beta)$ is the cumulative distribution function of a beta probability distribution with parameters $\alpha, \beta > 0$ and $r(\epsilon)$ is the radius of the hyperspherical cap. By Pythagoras theorem,

$$r^2(\epsilon) = 1^2 - (1 - h(\epsilon))^2 = 2h(\epsilon) - h^2(\epsilon),$$

where $h(\epsilon)$ is the height of the hyperspherical cap. To compute $r^2(\epsilon)$, we first compute $h(\epsilon)$. Since every point $x \in C_{1,\epsilon}$ satisfies $\langle x, e_p \rangle = 1 - \epsilon^2/2$, we conclude that $h(\epsilon) = 1 - \langle x, e_p \rangle = \epsilon^2/2$ and $r^2(\epsilon) = \epsilon^2 - \epsilon^4/2$. For $p = 1$, by choosing $\eta = 0.05$ and any $\epsilon \in (0, 1)$, the above procedure yields $s = 5$. For $p = 2$, $\eta = 0.05$, and $\epsilon = 0.3$ (thus $h(\epsilon) = 0.045$), one obtains $s = 30$. Similarly, if $p = 5$, $\eta = 0.05$, and $\epsilon = 0.7$ (thus $h(\epsilon) = 0.245$), then $s = 71$. We notice that, for fixed η and ϵ , $g_p(\eta, \epsilon)$ is increasing in p as $I_{r^2(\epsilon)}\left(\frac{p-1}{2}, \frac{1}{2}\right)$ is decreasing in p . This implies that a larger sample size is required to obtain the same precision in higher dimensions.

We now turn to the parameter q . We notice that choosing q is equivalent to choosing τ . Thus typical values of τ correspond to typical values of q . Now, convergence of the clustering algorithm (cf. Theorem 3.4) requires that $\lim_{n \rightarrow \infty} n\tau_n^{2kp} = \infty$. Thus, we can take $\tau_n = n^{(-1+\delta)/(2kp)}$, for some $\delta > 0$. While for the class of β -skeleton depths q can be taken as the quantile of pairwise distances $\|x_i - x_j\|$, $i > j$, $i, j \in \{1, 2, \dots, n\}$, for the simplicial depth, q can be chosen as a quantile of the $\binom{n}{p+1}$ maxima of the form $\max_{\substack{j,l=1,\dots,p+1 \\ j>l}} \|x_{i_j} - x_{i_l}\|$ for all $\binom{n}{p+1}$ combinations of indices i_1, \dots, i_{p+1} from $\{1, 2, \dots, n\}$. Alternatively, we could choose τ as described in Theorem 3.4 for all depths, that is, τ_n such that $\lim_{n \rightarrow \infty} nh_n^{2k} \tau_n^{2kp} = \infty$.

We now turn to the computational complexity of β -skeleton and simplicial depth. To this end, we recall that $LK_\beta D_n$ is a U-statistics of order 2, while LSD_n is a U-statistics of order $(p+1)$. This means that the computational complexity of $LK_\beta D_n$ is of order $O(\binom{n}{2})$, while the computational complexity of the LSD_n is of order $O(\binom{n}{p+1})$, which makes a significant difference, especially in high dimensions. For large p and n , an approximation to LSD can be made by considering a large number of simplices sampled with replacement amongst all the $\binom{n}{p+1}$ simplices that define LSD_n ; in our simulations (see Appendix J) we sample 10^8 simplices to reduce the computational cost.

H Necessity of conditions in Proposition 2.2

When $p = 1$ certain simplifications occur in Theorem 2.1. Specifically, for $G = L, S, B, K_\beta$, $\Lambda_1 = 1$. This is summarized in the following corollary.

Corollary H.1 *Let $G = L, S, B, K_\beta$, $p = 1$, P be absolutely continuous with respect to the Lebesgue measure on \mathbb{R}^p , with density $f(\cdot)$. It holds that*

$$LGD(x, \tau) = 2 \int_{T_{++}^\tau} f(x + x_1)f(x - x_2)dx_1dx_2, \quad (\text{H.1})$$

where $T_{++}^\tau := \{(x_1, x_2) : x_1 \geq 0, x_2 \geq 0, x_1 + x_2 \leq \tau\}$. Furthermore, we have that (i) at every point of continuity of $f(\cdot)$

$$\lim_{\tau \rightarrow 0^+} \frac{1}{\tau^2} LGD(\cdot, \tau) = f^2(\cdot), \quad (\text{H.2})$$

and (H.2) holds uniformly on any set where $f(\cdot)$ is uniformly continuous.

(ii) If $f(\cdot) \in L^\infty(\mathbb{R})$, then (H.2) holds at every point of continuity of $f(\cdot)$ and the convergence in (H.2) is uniform on any set where $f(\cdot)$ is uniformly continuous.

(iii) If $f(\cdot)$ is twice continuously differentiable, then

$$\lim_{\tau \rightarrow 0^+} \frac{1}{\tau^2} \left(\frac{1}{\tau^2} LGD(x, \tau) - f^2(x) \right) = \frac{1}{12} [2f(x)f''(x) + [f'(x)]^2].$$

(iv) If $f^2(\cdot) \in L^d(\mathbb{R})$, $1 \leq d < \infty$, then $\frac{LGD(\cdot, \tau)}{\tau^2}$ converges in $L^d(\mathbb{R})$ to $f^2(\cdot)$.

Proof of Corollary H.1. By a change of variable, it follows that

$$\begin{aligned} LGD(x, \tau) &= \int_{Z_\tau(x)} f(x_1)f(x_2)dx_1dx_2 \\ &= \int_{Z_\tau^G(0)} f(x + x_1)f(x + x_2)dx_1dx_2. \end{aligned} \quad (\text{H.3})$$

In two dimensions $Z_\tau^G(0)$ can be expressed as the union of two triangles T_{-+}^τ and T_{+-}^τ ; that is,

$$\begin{aligned} T_{-+}^\tau &:= \{(x_1, x_2) \in \mathbb{R}^2 : x_1 \leq 0, x_2 \geq 0, x_2 - x_1 \leq \tau\} \\ T_{+-}^\tau &:= \{(x_1, x_2) \in \mathbb{R}^2 : x_1 \geq 0, x_2 \leq 0, x_1 - x_2 \leq \tau\}. \end{aligned}$$

Now, by a change of variables in the integrals over the triangles it follows that

$$\begin{aligned} LGD(x, \tau) &= \int_{T_{-+}^\tau} f(x + x_1)f(x + x_2) + f(x - x_1)f(x - x_2)dx_1dx_2 \\ &= \int_{T_{++}^\tau} f(x - x_1)f(x + x_2) + f(x + x_1)f(x - x_2)dx_1dx_2 \\ &= 2 \int_{T_{++}^\tau} f(x + x_1)f(x - x_2)dx_1dx_2. \end{aligned}$$

(i), (ii) and (iv) follows directly from Theorem 2.1 (i), (ii) and (iv) and the fact that $Z_1(0)$ is bounded with area $\Lambda_1 = 1$. Finally, (iii) follows from Theorem 2.1 (iii), where $R(x) = R_1(x) + R_2(x)$ with

$$R_1(x) = 2f(x)f''(x) \int_0^1 \int_0^{1-x_1} x_1^2 dx_1 dx_2 = \frac{1}{6}f(x)f''(x), \quad \text{and}$$

$$R_2(x) = 2f'(x)]^2 \int_0^1 \int_0^{1-x_1} x_1 x_2 dx_1 dx_2 = \frac{1}{12}[f'(x)]^2.$$

■

We now show that continuity is not sufficient in Proposition 2.2 (i). For $p = 1$ and $G = L, S, B, K_\beta$, consider the function $\tilde{f} : \mathbb{R} \rightarrow \mathbb{R}$ with interior of the support $\cup_{n=1}^{\infty} (n - \frac{1}{2n^3}, n + \frac{1}{2n^3})$ defined by

$$\tilde{f}(n+x_1) = \tilde{f}(n-x_1) = \begin{cases} 2n^4 \left(\frac{1}{2n^3} - x_1\right) & \text{if } 0 \leq x_1 < \frac{1}{2n^3} \\ 0 & \text{if } \frac{1}{2n^3} \leq x_1 \leq \frac{1}{2}. \end{cases}$$

Notice that, since $\sum_{n=1}^{\infty} \frac{1}{n^2} = \frac{\pi^2}{6}$,

$$\int \tilde{f}(x) dx = \sum_{n=1}^{\infty} \int_{(n - \frac{1}{2n^3}, n + \frac{1}{2n^3})} \tilde{f}(x) dx = \sum_{n=1}^{\infty} \frac{1}{2n^2} = \frac{\pi^2}{12}.$$

Let $c := \frac{\pi^2}{12}$. Then $f : \mathbb{R} \rightarrow \mathbb{R}$ defined by $f(x) = \frac{1}{c}\tilde{f}(x)$ is an unbounded, continuous density function. The τ -approximation of $f(\cdot)$ is given by $f_\tau(x) = \frac{1}{\tau} \sqrt{LGD(x, \tau)}$, where, by Corollary H.1,

$$\begin{aligned} LGD(x, \tau) &= 2 \int_{T_{++}^\tau} f(x+x_1)f(x-x_2) dx_1 dx_2 \\ &= 2 \int_0^\tau \left[\int_0^{\tau-x_1} f(x-x_2) dx_2 \right] f(x+x_1) dx_1. \end{aligned}$$

Notice that $f(\cdot)$ is symmetric about $n \in \mathbb{N}$ and for $\frac{1}{n^3} \leq \tau \leq \frac{1}{2}$

$$\begin{aligned} LGD(n, \tau) &= 2 \int_0^{\min(\tau, \frac{1}{2n^3})} \left[\int_0^{\min(\tau-x_1, \frac{1}{2n^3})} \frac{2n^4}{c} \left(\frac{1}{2n^3} - x_2 \right) dx_2 \right] \frac{2n^4}{c} \left(\frac{1}{2n^3} - x_1 \right) dx_1 \\ &= \frac{2}{c^2} \int_0^{\frac{1}{2n^3}} \left[\int_0^{\frac{1}{2n^3}} 2n^4 \left(\frac{1}{2n^3} - x_2 \right) dx_2 \right] 2n^4 \left(\frac{1}{2n^3} - x_1 \right) dx_1 \\ &= \frac{2}{c^2} \int_0^{\frac{1}{2n^3}} \frac{n^2}{2} \left(\frac{1}{2n^3} - x_1 \right) dx_1 = \frac{1}{8c^2 n^4}. \end{aligned}$$

For all $0 < \tau \leq \frac{1}{2}$ fixed there exists $n \in \mathbb{N}$ such that $\frac{1}{n^2} \leq \tau$, and therefore

$$\begin{aligned} \sup_{x \in \mathbb{R}} |f_\tau^{(G)}(x) - f(x)| &\geq \sup_{n \in \mathbb{N}: \frac{1}{n^2} \leq \tau} |f_\tau^{(G)}(n) - f(n)| = \sup_{n \in \mathbb{N}: \frac{1}{n^2} \leq \tau} \left| \frac{1}{\tau} \frac{1}{2\sqrt{2}cn^2} - n \right| \\ &\geq \sup_{n \in \mathbb{N}: \frac{1}{n^2} \leq \tau} \left| \frac{1}{2\sqrt{2}c} - n \right| = \infty. \end{aligned}$$

Uniform continuity in Proposition 2.2 (i) prevents $f(\cdot)$ to become arbitrarily large implying that the above supremum is bounded. Also, it ensures that the supremum converges to zero, thus allowing to use LDCT and obtain the statement. Indeed, we see below that if $f(\cdot)$ is uniformly continuous then it is also bounded. To this end, suppose by contradiction that $f(\cdot)$ is unbounded. Let $y_0 = 0$. Then, for all $n \in \mathbb{N}$ there exists $y_n \in \mathbb{R}^p$ such that $f(y_n) \geq n$ and $\|y_n\|_2 \geq \|y_{n-1}\|_2 + 1$. Since $f(\cdot)$ is uniformly continuous, there exists $\delta \in (0, 1/2)$ such that $\sup_{z \in \overline{B}_\delta(x)} |f(x) - f(z)| \leq 1$ for all $x \in \mathbb{R}^p$. It follows that $\inf_{z \in \overline{B}_\delta(y_n)} f(z) \geq n - 1$ and

$$\int f(x) dx \geq \sum_{n=2}^{\infty} \int_{\overline{B}_\delta(y_n)} f(x) dx \geq \sum_{n=2}^{\infty} \lambda(\overline{B}_\delta(y_n)) = \infty.$$

I Supplementary results related to Theorem 3.4

As the next Lemma shows, in Theorem 3.4, the minimum distance between all data points and a point $x \in S_f$ (denoted as \tilde{h}_n below) is positive a.s. for all $n \in \mathbb{N}$ and converges to zero a.s. as $n \rightarrow \infty$. However, $p \geq 6k + 1$ is needed for $n\tilde{h}_n^{2k}\tau_n^{2kp} \xrightarrow[n \rightarrow \infty]{} \infty$ a.s., for some sequence of positive scalars $\{\tau_n\}_{n=1}^{\infty}$ converging to zero (by Lemma I.1 (iii) we can take $\tau_n^{2kp} = n^{-\delta}$, for some $0 < \delta < 1 - \frac{6k}{d}$, that is $\tau_n = n^{-\delta/(2kp)}$). This shows that, for $p \geq 6k + 1$, by choosing a suitable sequence $\{\tau_n\}_{n=1}^{\infty}$, we can replace h_n by \tilde{h}_n in Theorem 3.4. In turn, this allows replacement of the set $\mathcal{X}_{n,r}(x) = \{X \in \mathcal{X}_n : h_n \leq \|X - x\| \leq r\}$ by $\tilde{\mathcal{X}}_{n,r}(x) = \{X \in \mathcal{X}_n : \|X - x\| \leq r, X \neq x\}$.

Lemma I.1 *Let $\mathcal{X}_n := \{X_1, \dots, X_n\}$ a sample of i.i.d. random variables from a probability distribution P with continuous and bounded density $f(\cdot)$, $x \in S_f$, and $\tilde{h}_n = \min_{y,z \in \mathcal{X}_n \cup \{x\}, y \neq z} \|y - z\|$. Then, (i) $\tilde{h}_n > 0$ a.s., (ii) $\tilde{h}_n \xrightarrow[n \rightarrow \infty]{} 0$ a.s. and (iii) for $p \geq 6k + 1$ and $0 < \delta < 1 - \frac{6k}{\delta}$, $n^{1-\delta}\tilde{h}_n^{2k} \xrightarrow[n \rightarrow \infty]{} \infty$ a.s.*

Proof of Lemma I.1. We first prove (i). Since P is absolutely continuous w.r.t. the Lebesgue measure, it holds that

$$\begin{aligned} P^{\otimes n}(\tilde{h}_n = 0) &= P^{\otimes n}(\cup_{i=1}^n [\|X_i - x\| = 0] \cup \cup_{i=1}^n \cup_{j=i+1}^n [\|X_i - X_j\| = 0]) \\ &\leq \sum_{i=1}^n P^{\otimes n}(\|X_i - x\| = 0) + \sum_{i=1}^n \sum_{j=i+1}^n P^{\otimes n}(\|X_i - X_j\| = 0) \\ &= nP(\|X_1 - x\| = 0) + \frac{n(n-1)}{2} \int P(\|X_1 - y\| = 0) f(y) dy = 0. \end{aligned}$$

For (ii), observe that, for all $\epsilon > 0$,

$$P^{\otimes n}(\tilde{h}_n \geq \epsilon) \leq P^{\otimes n}(\min_{i=1,\dots,n} \|X_i - x\| \geq \epsilon) = P(\|X_1 - x\| \geq \epsilon)^n.$$

Since $x \in S_f$ and $f(\cdot)$ is continuous, it holds that $P(\|X_1 - x\| \geq \epsilon) < 1$ and

$$\sum_{n=2}^{\infty} P^{\otimes n}(\tilde{h}_n \geq \epsilon) \leq \sum_{n=2}^{\infty} P(\|X_1 - x\| \geq \epsilon)^n < \infty.$$

By Borel-Cantelli lemma, it follows that $\tilde{h}_n \xrightarrow[n \rightarrow \infty]{} 0$ a.s. We now prove (iii). To this end, let $M > 0$ and notice that $P^{\otimes n}(n^{1-\delta}\tilde{h}_n^{2k} \leq M^{2k})$ is equal to

$$P^{\otimes n}(\cup_{i=1}^n [\|X_i - x\| \leq Mn^{-(1-\delta)/(2k)}] \cup \cup_{i=1}^n \cup_{j=i+1}^n [\|X_i - X_j\| \leq Mn^{-(1-\delta)/(2k)}]),$$

which is bounded above by

$$\begin{aligned} &\sum_{i=1}^n P^{\otimes n}(\|X_i - x\| \leq Mn^{-(1-\delta)/(2k)}) + \sum_{i=1}^n \sum_{j=i+1}^n P^{\otimes n}(\|X_i - X_j\| \leq Mn^{-(1-\delta)/(2k)}) \\ &= nP(B_{Mn^{-(1-\delta)/(2k)}}(x)) + \frac{n(n-1)}{2} \int P(B_{Mn^{-(1-\delta)/(2k)}}(y)) f(y) dy. \end{aligned} \tag{I.1}$$

Now, since $f(\cdot)$ is bounded, we have that $\alpha := \sup_{y \in \mathbb{R}^p} f(y) < \infty$. For $y \in \mathbb{R}^p$, it holds that

$$P(B_{Mn^{-(1-\delta)/(2k)}}(y)) \leq \alpha \lambda(\overline{B}_{Mn^{-(1-\delta)/(2k)}}(x)) = \alpha C n^{-p(1-\delta)/(2k)}, \tag{I.2}$$

where $C = M^p \pi^{p/2} / \Gamma(p/2 + 1)$. Using (I.2) in (I.1), we obtain that

$$P^{\otimes n}(n^{1-\delta}\tilde{h}_n^{2k} \leq M^{2k}) \leq \alpha C n^{2-p(1-\delta)/(2k)}.$$

Therefore, using $p \geq 6k + 1$ and $0 < \delta < 1 - \frac{6k}{p}$, we have that

$$\sum_{n=1}^{\infty} P^{\otimes n}(n^{1-\delta}\tilde{h}_n^{2k} \leq M^{2k}) \leq \alpha C \sum_{n=1}^{\infty} n^{2-p(1-\delta)/(2k)} < \infty.$$

By another application of Borel-Cantelli lemma and Theorem 5.2 in Billingsley [2012], we conclude that $n^{1-\delta} \tilde{h}_n^{2k} \xrightarrow[n \rightarrow \infty]{} \infty$ a.s. ■

The next result shows that, the normalized gradient of $f_\tau(\cdot)$ converges uniformly to the normalized gradient of $f(\cdot)$ in a compact set not containing the stationary points of $f(\cdot)$.

Lemma I.2 *Suppose that $f(\cdot)$ is continuously differentiable and (2.4) holds true. Let $K \subset S_f$ be a compact set with $K \cap N_f = \emptyset$. Recall (4.6) and, for $\tau > 0$ and $z \in \mathbb{R}^p$ with $\nabla f_\tau(z) \neq 0$, let $w_\tau(z) := \nabla f_\tau(z) / \|\nabla f_\tau(z)\|$. Then,*

$$\lim_{\tau \rightarrow 0^+} \sup_{x \in K} \|w_\tau(x) - w(x)\| = 0. \quad (\text{I.3})$$

Proof of Lemma I.2. We use Proposition 2.2 (iv), which shows that, as $\tau \rightarrow 0^+$, $\nabla f_\tau(\cdot)$ converges uniformly in K to $\nabla f(\cdot)$. Since $K \cap N_f = \emptyset$, there exists τ^* such that $\min_{x \in K} \|\nabla f_\tau(x)\| \geq c/2$ for all $0 < \tau \leq \tau^*$, where $c := \min_{x \in K} \|\nabla f(x)\|$. Then, using triangle inequality, we see that

$$\sup_{x \in K} \|w_\tau(x) - w(x)\| \leq 4/c \sup_{x \in K} \|\nabla f_\tau(x) - \nabla f(x)\|,$$

which gives (I.3). ■

J Simulations and data analysis

J.1 Illustrative examples

We begin this section with a one-dimensional example showing the flexibility of the τ -approximation for different values of τ . As described in Section 2, for small values of τ , $f_\tau(\cdot)$ “resembles” the underlying density, while for larger τ it becomes unimodal, as DFs are decreasing from the median of the distribution. We take this univariate distribution to be a mixture of four normal distributions with means $-2, 0, 3, 4$, standard deviations $0.5, 0.8, 0.5, 0.2$ and weights $0.25, 0.5, 0.15$ and 0.1 , respectively. The resulting density is quadrimodal and is depicted in Fig 2 along with its sample τ -approximation for $\tau = 0.5, 1, 2, 4$. For reproducibility, we use the seed 1234 for all figures that are based on one-sample and appearing in Appendix J and Appendix K respectively. As can be seen from the Fig 2 for $\tau = 0.5$ the approximation has a similar shape to the density with approximately the same number of modes. For $\tau = 1$, the clusters corresponding to the modes at $x = 3$ and $x = 4$ merge yielding only three clusters. As we increase τ from 1 to

2, we notice that one can still identify two clusters, while, for $\tau = 4$, the τ -approximation has a unimodal shape.

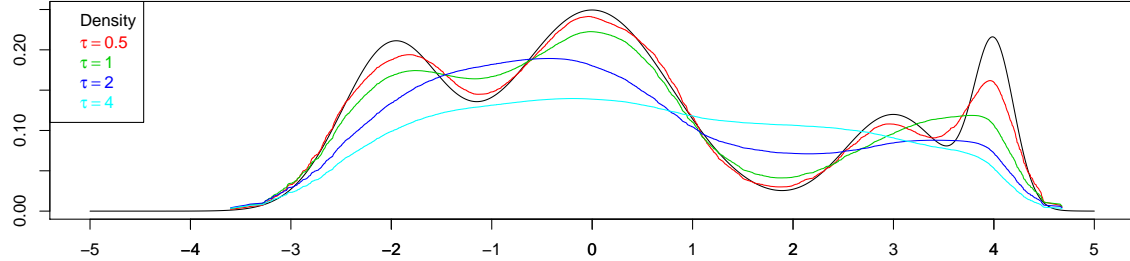


Figure 2: In black the quadrimodal mixture density and in red, green, blue and cyan its sample τ -approximation $f_{\tau,n}(\cdot)$ for $\tau = 0.5, 1, 2, 4$, respectively, and $n = 6000$.

Turning to bivariate examples studied in the literature (see Chacón [2015]), we consider mixtures of bivariate normal distributions with the following characteristics: (i) two-mixture with equal weights (Bimodal) and identity covariance matrix and (ii) the mixtures investigated in Wand and Jones [1993] and Chacón [2009] referred to as (H) Bimodal IV, (K) Trimodal III and #10 Fountain (see Fig 3, first row, (K) Trimodal III is in Appendix K.2). Their analytical expression and the associated *true clusters* are given in Appendix K.1. We apply our algorithm to analyze these models and identify clusters; these results are displayed in Fig 3 (second row). A comparison of our results with the clusters obtained using the kernel density estimator are provided in Fig 3 (third row). Specifically, clusters are obtained via the kernel mean shift algorithm as implemented by the function `kms` in the R package `ks` [Duong, 2018]. We set maximum number of iterations to 5000 and tolerance to 10^{-8} . The plug-in estimator of the bandwidth matrix is given by the function `Hpi` with pilot option "dunconstr" and derivatives of order one. The bandwidth matrix is obtained via minimization of the asymptotic mean integrated squared error (AMISE) of the gradient of the estimated density. For more details on the bandwidth matrix selection procedure see Sections 3.6 and 5.6.4 in Chacón and Duong [2018]. For more details on the mean shift clustering algorithm see Section 6.2.2 of Chacón and Duong [2018]. By a visual inspection of Fig 3, LLD performs a better clustering estimation than KDE. A more detailed analysis of these and other distributions under extreme localization is provided in Appendix K.2.

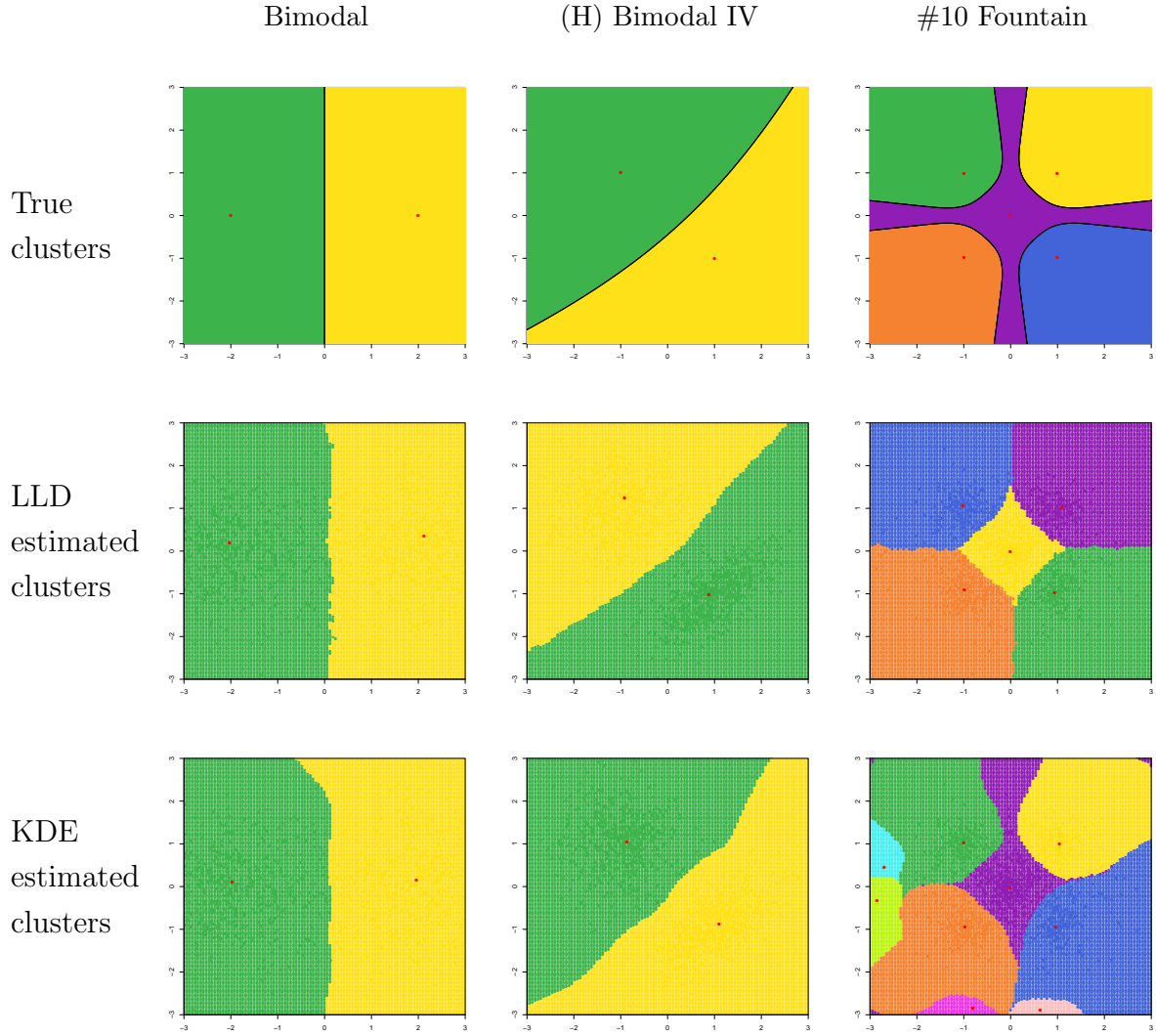


Figure 3: Clusters associated with the Bimodal (left), (H) Bimodal IV (middle) and #10 Fountain (right) densities. True clusters (first row). Local depth clustering based on $n = 1000$ samples from these densities and parameters $q = 0.05$, $s = 50$ and $r = 0.05$ (second row). Kernel density estimator clustering (third row). The true modes (first row) and the predicted modes (second and third rows) are plotted in red.

J.2 Numerical experiments

In this subsection, we describe additional metrics and simulation results of our method for identification of clusters. For the sake of completeness and ease of comparisons, we retain the results described in the main paper. Specifically, we evaluate the performance in three different ways: (i) true number of clusters identified by the algorithm, (ii) empirical Hausdorff distance between the “true” cluster and the estimated cluster, and (iii) empirical probability distance (see Chacón [2015], for instance). We recall that the symmetric difference between two subsets A and B of \mathbb{R}^p is $A\Delta B = ((\mathbb{R}^p \setminus A) \cap B) \cup (A \cap (\mathbb{R}^p \setminus B))$. Let X_1, \dots, X_n be i.i.d. samples from some probability distribution P . The empirical probability distance between the clusterings $\mathcal{C} = \{C_1, \dots, C_l\}$ and $\mathcal{D} = \{D_1, \dots, D_s\}$ with $l < s$ is given by

$$\hat{d}_{P,\eta}(\mathcal{C}, \mathcal{D}) = \frac{1}{2n} \min_{\pi \in \mathcal{P}_s} \left(\sum_{i=1}^l \sum_{j=1}^n \mathbf{I}(X_j \in C_i \Delta D_{\pi(i)}) + \eta \sum_{i=l+1}^s \sum_{j=1}^n \mathbf{I}(X_j \in D_{\pi(i)}) \right),$$

where \mathcal{P}_s is the set of all permutations of $\{1, \dots, s\}$ and $\eta \geq 0$ is a penalization coefficient for clusters that do not match with any other. If $l = s$ the second term in the above expression is zero. In our numerical experiments, we choose $\eta = 1$. Additional results for other values of η are provided in Appendix K.3.

The empirical Hausdorff distance $\hat{d}_H(\mathcal{C}, \mathcal{D})$ is given by

$$\frac{1}{n} \max \left(\max_{i \in \{1, \dots, t\}} \min_{j \in \{1, \dots, s\}} \sum_{l=1}^n \mathbf{I}(X_l \in C_i \Delta D_j), \max_{j \in \{1, \dots, s\}} \min_{i \in \{1, \dots, t\}} \sum_{l=1}^n \mathbf{I}(X_l \in C_i \Delta D_j) \right).$$

In numerical experiments and data analysis, \mathcal{C} is taken to be the set of true clusters while \mathcal{D} is the set of estimated clusters, produced by the algorithm. If the estimated clusters coincide with the true clusters, then both these distances, *viz.* the *clustering errors*, are zero. Thus, small values of these distances suggest a good performance. In this manuscript, as explained before, we consider the following distributions commonly used in the literature: Bimodal, (H) Bimodal IV, (K) Trimodal III and #10 Fountain. To test the performance of our methodology in multivariate models, we consider a bimodal and a quadrimodal density in dimension five. We refer to these distributions as Mult. Bimodal and Mult. Quadrimodal. Additionally, we also study seven circular distributions, which we refer to as Circular Bimodal I-V and Circular Quadrimodal I-II. These are described in Appendix K.1. As before, our simulation results are based on a sample size of 1000 and 100 numerical experiments and we choose τ so that the corresponding quantiles q are given by 0.01, 0.05 and 0.1 (see Algorithm 1). We compare our results based on LLD and LSD, with hierarchical clustering (Hclust) and Kernel density estimator (KDE) using both

Algorithm 1 and mean shift algorithm [Fukunaga and Hostetler, 1975]. In the last case, we use the abbreviation KDE-"**ms**". For more details about the numerical implementation and the quantiles for LSD we refer to Appendix G. Further simulation results for these and other distributions are provided in Appendix K.3. The hierarchical clustering requires a pre-specification of the number of clusters while the other methods do not, and it is reported here since it is one of the widely used methods for clustering. Thus, we compute it making use of the true number of clusters, which implies that the obtained results are not comparable with those of the other methodologies. Specifically, we use the R function **hclust** based on the Euclidean distance between the observations and the default complete linkage method, i.e. the clusters distance is the maximum distance between the points in each cluster. Next, we apply the function **cutree**, based on the true number of clusters, to the output of **hclust**, yielding the final clusters. We also apply two other recent clustering algorithms [Chacón, 2019], which are a combination of mixture model clustering [Fraley and Raftery, 2002] and modal clustering [Chacón, 2015] procedures. Both algorithms start by fitting a normal mixture density $\hat{f}(x) = \sum_{t=1}^{\hat{T}} \hat{\pi}_t \phi(x|\hat{\mu}_t, \hat{\Sigma}_t)$, where $\hat{\pi}_t \geq 0$, $\sum_{t=1}^{\hat{T}} \hat{\pi}_t = 1$, and $\phi(\cdot|\mu, \Sigma)$ is the density of a p -variate normal distribution with mean μ and covariance matrix Σ . This is done using the expectation maximization (EM) algorithm implemented in the function **Mclust** from the R package **mclust** [Scrucca et al., 2016]. In the above, \hat{T} is the value of $T \in \{1, \dots, 9\}$ that minimizes the Bayesian information criterion (BIC) for fitting $\hat{f}_T(x) = \sum_{t=1}^T \hat{\pi}_t \phi(x|\hat{\mu}_t, \hat{\Sigma}_t)$. Mixture model clusters are then the sets given by

$$\hat{C}_t := \{x \in \mathbb{R}^p : \hat{\pi}_t \phi(x|\hat{\mu}_t, \hat{\Sigma}_t) > \max_{\substack{j=1, \dots, \hat{T}, \\ j \neq t}} \hat{\pi}_j \phi(x|\hat{\mu}_j, \hat{\Sigma}_j)\}$$

for $t = 1, \dots, \hat{T}$. The first clustering algorithm is called mixture model modal merging (MMMM) and relies on the idea that mixture components are likely to be more than the number modes. Thus, one would like to merge mixture components whose points converge to the same mode into a single cluster. Following this idea, one applies mean shift algorithm starting from the estimated mixture means $\hat{\mu}_1, \dots, \hat{\mu}_{\hat{T}}$ and merges those clusters whose estimated means converge to the same mode, yielding clusters $\tilde{C}_1, \dots, \tilde{C}_{\hat{U}}$ where $\hat{U} \leq \hat{T}$. The second clustering algorithm is called mixture model modal clustering (MMMC) and is based on a direct computation of the stable manifolds generated by $\hat{f}(\cdot)$. An algorithm for this is provided in Section 3.1 of Chacón [2019]. Turing to LLD, exploratory analysis suggests that some circular distributions require values of q higher than 0.1. To see this, let P be the Curved Bimodal II distribution and draw 100 samples from P . Figure 4 shows the CV index over $C = 100$ subsamples (top-left) and number of clusters (top-center) as a function of q . We plot dotted vertical lines at

$q = 0.05, 0.15, 0.2, 0.3, 0.35, 0.4, 0.5, 0.6$. On the top-right we show the CV index as a function of the number of clusters. The bottom-left plot is a zoom of the top-left plot over the interval $[Q_1, Q_2]$, where $Q_1 = 0.225$ and $Q_2 = 0.6$. The bottom-center plot shows the boxplot of optimal value of q over that range and the bottom-right plot displays the number of clusters detected when q is the optimal quantile order. Thus, for circular distributions we let q run up to 0.2. Figures 14-127 in Appendix K.3 shows clustering errors for all the distributions in Appendix K.1 and all values of q .

Table 2 provides clustering errors based on the Hausdorff distance and the probability distance. The best results are highlighted in bold. From these results we see that clustering errors based on the KDE, KDE-"**ms**", LLD, LSD, and Hclust are similar for the distributions (H) Bimodal IV, (K) Trimodal III, #10 Fountain, and Bimodal. However, LLD outperforms KDE, KDE-"**ms**", and LSD for the distribution in dimension five as can be seen from the columns Mult. Bimodal and Mult. Quadrifocal. Since all these distributions are mixture of normal densities, as expected, MMMM and MMC yield the smallest error apart from the #10 Fountain distribution. However, these methods perform poorly for the circular distributions Circular Bimodal I-V and Circular Quadrifocal I-II. Among the density based methods, that is, excluding Hclust, LSD performs best for the Circular Bimodal I, II, and III densities. For the Circular Bimodal IV densities, clustering errors are similar, although KDE is slightly preferable. It is worth recalling here that by KDE we mean KDE using the Algorithm 1. Turning to the Circular Quadrifocal I and Circular Quadrifocal II densities, LLD and KDE-"**ms**" yield the smallest Hausdorff and probability distance, respectively. Table 3 (Table 1 in the main paper) provides a comparison of the number of times the correct number of clusters is detected. The number of times the procedure identifies a lower number of clusters (on the left) and a higher number of clusters (on the right) is also provided. We notice that MMMM and MMC always identify the correct number of clusters for (H) Bimodal IV, (K) Trimodal III, Bimodal, Mult. Bimodal, and Mult. Quadrifocal distributions. However they overestimate the number of clusters 100 times out of 100 for the distributions Circular Bimodal I-IV and underestimate it for the distributions Circular Quadrifocal I-II. The proposed methods perform better than KDE-"**ms**" for the Circular Bimodal I-III distributions, whereas KDE-"**ms**" is preferable for the distributions Circular Quadrifocal I-II. It is possible to improve the performance of LSD for distributions in dimension 5 by choosing smaller values of q , as described in Subsection J.3.

Clustering errors (Hausdorff distance)			
	(H) Bimodal IV	(K) Trimodal III	#10 Fountain

MMMM	0.00 (0.00)	0.03 (0.01)	0.22 (0.03)
MMMC	0.00 (0.00)	0.02 (0.01)	0.09 (0.02)
KDE ^a	0.00 (0.00)	0.12 (0.17)	0.06 (0.01)
KDE-" ms " ^d	0.00 (0.03)	0.10 (0.15)	0.08 (0.05)
LLD ¹	0.05 (0.10)	0.10 (0.15)	0.06 (0.01)
LSD ²	0.05 (0.11)	0.10 (0.15)	0.06 (0.01)
Hclust *	0.05 (0.09)	0.15 (0.09)	0.29 (0.05)
	Bimodal	Mult. Bimodal	Mult. Quadrimodal
MMMM	0.00 (0.00)	0.00 (0.00)	0.00 (0.00)
MMMC	0.00 (0.00)	0.00 (0.00)	0.00 (0.00)
KDE ^a	0.01 (0.03)	0.15 (0.17)	0.10 (0.08)
KDE-" ms " ^d	0.01 (0.05)	0.38 (0.17)	0.16 (0.08)
LLD ³	0.01 (0.03)	0.01 (0.04)	0.02 (0.01)
LSD ⁴	0.00 (0.00)	0.23 (0.18)	0.38 (0.18)
Hclust *	0.06 (0.05)	0.05 (0.03)	0.07 (0.03)
	Circular Bimodal I	Circular Bimodal II	Circular Bimodal III
MMMM	0.44 (0.03)	0.55 (0.04)	0.54 (0.04)
MMMC	0.46 (0.03)	0.53 (0.05)	0.52 (0.05)
KDE ^c	0.17 (0.16)	0.40 (0.13)	0.38 (0.16)
KDE-" ms " ^d	0.37 (0.17)	0.44 (0.07)	0.42 (0.10)
LLD ⁵	0.10 (0.12)	0.27 (0.21)	0.26 (0.21)
LSD ⁶	0.05 (0.07)	0.13 (0.17)	0.13 (0.18)
Hclust *	0.36 (0.09)	0.34 (0.10)	0.03 (0.02)
	Circular Bimodal IV	Circular Quadrimodal I	Circular Quadrimodal II
MMMM	0.24 (0.08)	0.72 (0.11)	0.75 (0.06)
MMMC	0.25 (0.07)	0.73 (0.11)	0.75 (0.05)
KDE ^b	0.21 (0.03)	0.31 (0.11)	0.35 (0.14)
KDE-" ms " ^e	0.24 (0.03)	0.29 (0.09)	0.33 (0.13)
LLD ⁴	0.32 (0.12)	0.22 (0.05)	0.23 (0.06)
LSD ²	0.23 (0.07)	0.26 (0.13)	0.29 (0.14)
Hclust *	0.33 (0.11)	0.31 (0.14)	0.37 (0.13)
Clustering errors (distance in probability)			

	(H) Bimodal IV	(K) Trimodal III	#10 Fountain
MMMM	0.00 (0.00)	0.03 (0.01)	0.23 (0.07)
MMMC	0.00 (0.00)	0.02 (0.01)	0.10 (0.07)
KDE ^a	0.00 (0.00)	0.06 (0.07)	0.06 (0.01)
KDE-" ms " ^d	0.01 (0.07)	0.06 (0.08)	0.21 (0.31)
LLD ¹	0.13 (0.28)	0.06 (0.07)	0.06 (0.01)
LSD ²	0.12 (0.27)	0.07 (0.09)	0.06 (0.01)
Hclust *	0.05 (0.09)	0.16 (0.09)	0.35 (0.07)
	Bimodal	Mult. Bimodal	Mult. Quadrinodal
MMMM	0.00 (0.00)	0.00 (0.00)	0.01 (0.00)
MMMC	0.00 (0.00)	0.00 (0.00)	0.01 (0.00)
KDE ^a	0.01 (0.02)	0.09 (0.13)	0.34 (0.37)
KDE-" ms " ^d	0.01 (0.04)	0.12 (0.13)	0.57 (0.33)
LLD ³	0.01 (0.02)	0.01 (0.01)	0.03 (0.01)
LSD ⁴	0.00 (0.00)	0.20 (0.17)	0.45 (0.17)
Hclust *	0.06 (0.05)	0.05 (0.03)	0.10 (0.04)
	Circular Bimodal I	Circular Bimodal II	Circular Bimodal III
MMMM	0.32 (0.06)	0.55 (0.05)	0.55 (0.04)
MMMC	0.29 (0.05)	0.53 (0.05)	0.52 (0.05)
KDE ^c	0.18 (0.19)	0.34 (0.11)	0.30 (0.14)
KDE-" ms " ^d	0.14 (0.11)	0.38 (0.12)	0.30 (0.14)
LLD ⁵	0.09 (0.10)	0.21 (0.17)	0.21 (0.17)
LSD ⁶	0.04 (0.05)	0.11 (0.14)	0.12 (0.15)
Hclust *	0.18 (0.05)	0.17 (0.05)	0.01 (0.01)
	Circular Bimodal IV	Circular Quadri-modal I	Circular Quadri-modal II
MMMM	0.19 (0.12)	0.70 (0.09)	0.72 (0.06)
MMMC	0.22 (0.18)	0.71 (0.08)	0.73 (0.04)
KDE ^b	0.23 (0.18)	0.15 (0.10)	0.18 (0.11)
KDE-" ms " ^e	0.20 (0.11)	0.39 (0.13)	0.42 (0.14)
LLD ⁴	0.34 (0.21)	0.51 (0.19)	0.50 (0.16)
LSD ²	0.25 (0.21)	0.32 (0.15)	0.35 (0.15)
Hclust *	0.17 (0.05)	0.02 (0.02)	0.04 (0.03)

^a pilot="dunconstr", s = 30 ^b pilot="dscalar", s = 30
^c pilot="dunconstr", s = 50
^d pilot="dunconstr", mean shift algorithm ^e pilot="dscalar", mean
shift algorithm ¹ q = 0.1, s = 30. ² q = 0.01, s = 30.
³ q = 0.1, s = 50. ⁴ q = 0.05, s = 30. ⁵ q = 0.2, s = 50.
⁶ q = 0.05, s = 50. * The true number of clusters is given in input.

Table 2: Mean of the clustering errors based on the Hausdorff distance and the distance in probability for the densities (H) Bimodal IV, (K) Trimodal III, #10 Fountain, Bimodal, Mult. Bimodal, Mult. Quadrifocal, Circular Bimodal I-IV, and Circular Quadrifocal I-II. In parentheses the standard deviation. The true number of clusters is specified as input for the hierarchical clustering algorithm.

Number of times the true clusters are detected correctly			
	(H) Bimodal IV	(K) Trimodal III	#10 Fountain
MMMM	(0) 100 (0)	(0) 100 (0)	(0) 99 (1)
MMMC	(0) 100 (0)	(0) 100 (0)	(0) 99 (1)
KDE ^a	(0) 100 (0)	(21) 73 (6)	(0) 100 (0)
KDE-" ms " ^d	(0) 99 (1)	(15) 77 (8)	(0) 79 (21)
LLD ¹	(0) 83 (17)	(14) 79 (7)	(0) 100 (0)
LSD ²	(0) 85 (15)	(13) 75 (12)	(0) 100 (0)
	Bimodal	Mult. Bimodal	Mult. Quadrifocal
MMMM	(0) 100 (0)	(0) 100 (0)	(0) 100 (0)
MMMC	(0) 100 (0)	(0) 100 (0)	(0) 100 (0)
KDE ^a	(0) 99 (1)	(0) 61 (39)	(1) 61 (38)
KDE-" ms " ^d	(0) 97 (3)	(0) 18 (82)	(0) 25 (75)
LLD ³	(0) 99 (1)	(0) 99 (1)	(0) 100 (0)
LSD ⁴	(0) 100 (0)	(12) 63 (25)	(77) 18 (5)
	Circular Bimodal I	Circular Bimodal II	Circular Bimodal III
MMMM	(0) 0 (100)	(0) 0 (100)	(0) 0 (100)
MMMC	(0) 0 (100)	(0) 0 (100)	(0) 0 (100)
KDE ^c	(0) 55 (45)	(0) 9 (91)	(0) 17 (83)
KDE-" ms " ^d	(0) 18 (82)	(0) 0 (100)	(0) 4 (96)
LLD ⁵	(0) 74 (26)	(0) 43 (57)	(0) 43 (57)

LSD ⁶	(0) 95 (5)	(0) 74 (26)	(0) 73 (27)
	Circular Bimodal IV	Circular Quadrimodal I	Circular Quadrimodal II
MMMM	(0) 0 (100)	(99) 1 (0)	(100) 0 (0)
MMMC	(0) 0 (100)	(99) 1 (0)	(100) 0 (0)
KDE ^b	(0) 2 (98)	(83) 14 (3)	(85) 12 (3)
KDE-" ms " ^e	(0) 0 (100)	(68) 20 (12)	(63) 24 (13)
LLD ⁴	(0) 0 (100)	(6) 18 (76)	(7) 16 (77)
LSD ²	(0) 1 (99)	(65) 32 (3)	(80) 17 (3)

Table 3: Number of times that the procedure identifies the true number of clusters for the densities (H) Bimodal IV, (K) Trimodal III , #10 Fountain, Bimodal, Mult. Bimodal, Mult. Quadrinodal, Circular Bimodal I-IV, and Circular Quadrinodal I-II. In parentheses the number of times the procedure identifies a lower number of clusters (on the left) and a higher number of clusters (on the right).

J.3 Data analysis

In this section, we revisit the data analysis with more details. As explained in the main paper, we evaluate the performance of our methodology on two datasets taken from the UCI machine learning repository (<http://archive.ics.uci.edu/ml/>), namely, the Iris dataset and the Seeds dataset. For the sake of completeness we provide more details concerning the data sets. The Iris dataset consists of $n = 150$ observations from three classes (Iris Setosa, Iris Versicolour, and Iris Virginica) with four measurements each (sepal length, sepal width, petal length, and petal width). We compare our results to those based on KDE (with built-in bandwidth) and Hclust. Our algorithm, based on both lens and simplicial depth, correctly identifies all three clusters (see Table 4); furthermore, the Hausdorff distance and probability distance from our algorithm are smaller than those of the competitors.

Seeds dataset consists of $n = 210$ observations concerning three varieties of wheat; namely, Kama, Rosa and Canadian. High quality visualization of the internal kernel structure was detected using a soft X-ray technique and seven geometric parameters of wheat kernels were recorded. They are area, perimeter, compactness, length of kernel, width of kernel, asymmetry coefficient, and length of kernel groove. All of these geometric parameters were continuous and real-valued. Table 4 contains the results of our analysis. The best results are highlighted in bold and correspond to LLD. We notice that both

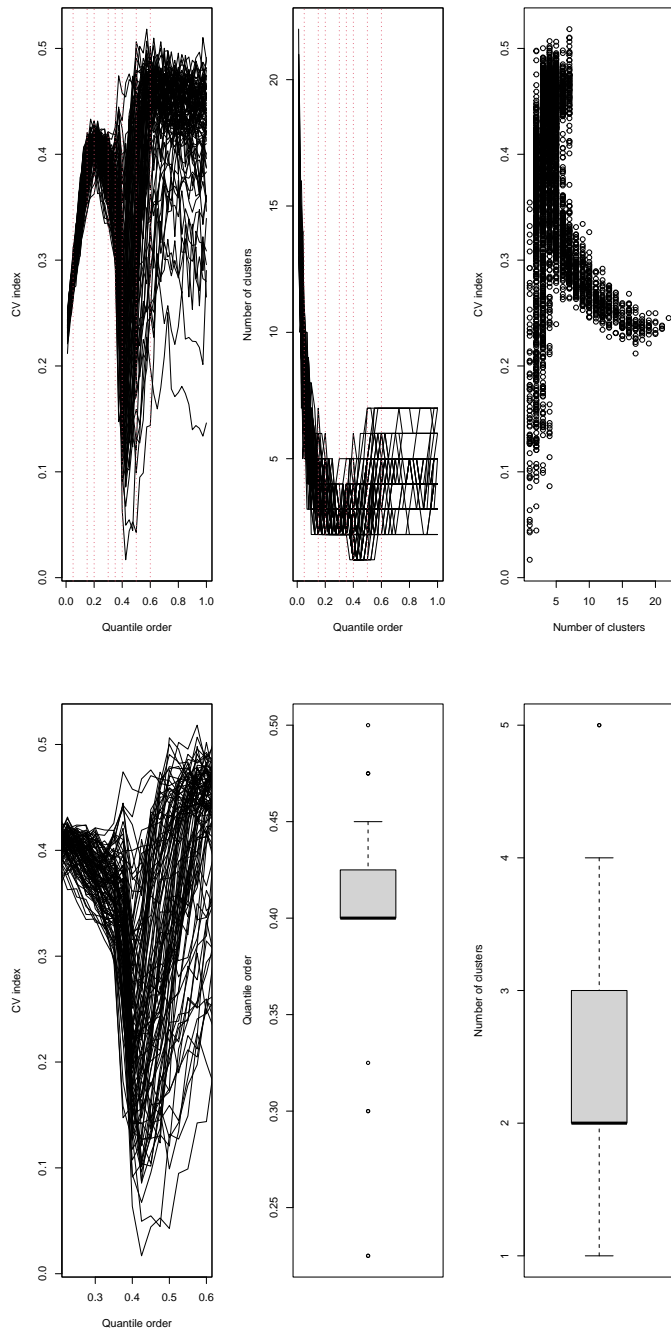


Figure 4: For 100 replications with $n = 1000$ samples for the Curved Bimodal II distribution and LLD with $s = 30$ we plot (i) CV index as a function of the quantile order q (top-left), (ii) number of clusters as a function of q (top-center), (iii) CV index as a function of the number of clusters (top-right), (iv) CV index as a function of $q \in [0.225, 0.6]$ (bottom-left), (v) boxplot of the optimal quantile q in the range $[0.225, 0.6]$ (bottom-center), and (vi) boxplot of the number of clusters for the optimal quantile q (bottom-right).

of our methods, LLD and LSD, as well as KDE, correctly identify the true number of clusters.

It is worth mentioning here that Hclust was given as input the true number of clusters, three, as required by this methodology. However, the Hausdorff distance and probability distance of our proposed methods are smaller than those of Hclust. KDE-"**ms**", in both the examples, overestimates the true number of clusters.

Clustering errors for Iris data			
	Number of clusters	Distance in prob.	Hausdorff distance
KDE ^a	3	0.03	0.03
KDE-" ms " ^d	7	0.37	0.31
LLD ⁴	3	0.10	0.10
LSD ⁵	3	0.10	0.10
Hclust [*]		0.16	0.16
Clustering errors for Seeds data			
	Number of clusters	Distance in prob.	Hausdorff distance
KDE ^a	3	0.16	0.16
KDE-" ms " ^d	25	0.75	0.33
LLD ⁴	3	0.10	0.10
LSD ⁶	3	0.17	0.17
Hclust [*]		0.20	0.20

⁵ $q = 10^{-4}$, $s = 20$. ⁶ $q = 10^{-5}$, $s = 20$.

Table 4: Mean of the clustering errors based on the Hausdorff distance and distance in probability for the Iris and Seeds data. The true number of clusters is specified as input for the hierarchical clustering algorithm.

K Additional simulations

K.1 True clusters

In this subsection we provide the analytical expression for the distributions Bimodal, (H) Bimodal IV, (K) Trimodal III, #10 Fountain, Mult. Bimodal, and Mult. Quadrinodal considered in Section J and the corresponding true clusters. We also consider two additional distributions: one is (L) Quadrinodal distribution in Wand and Jones [1993] and a four-mixture, which is defined below, and referred to as Quadrinodal (without (L)). We now describe these distributions.

- (i) The Bimodal density is a two-mixture of normal distributions with equal weights, identity covariance matrix and means $(-2, 0)$ and $(2, 0)$.
- (ii) The Quadrinodal density is a mixture of four normal distributions with means $(-2, 2)$, $(-2, -2)$, $(2, -2)$ and $(2, 2)$, and again equal weights and identity covariance matrix.
- (iii) The (H) Bimodal IV density is a mixture of two normal distributions with equal weights, means $\mu_1 = (1, -1)^\top$, $\mu_2 = (-1, 1)^\top$ and covariances

$$\Sigma_1 = \frac{4}{9} \begin{pmatrix} 1 & \frac{7}{10} \\ \frac{7}{10} & 1 \end{pmatrix} \quad \text{and} \quad \Sigma_2 = \frac{4}{9} \begin{pmatrix} 1 & 0 \\ 0 & 1 \end{pmatrix}.$$

- (iv) The (K) Trimodal III density is a mixture of three normal distributions with weights $w_1 = w_2 = \frac{3}{7}$ and $w_3 = \frac{1}{7}$; means $\mu_1 = (-1, 0)^\top$, $\mu_2 = (1, 2 \cdot \frac{\sqrt{3}}{3})^\top$ and $\mu_3 = (1, -2 \cdot \frac{\sqrt{3}}{3})^\top$; and covariances

$$\Sigma_1 = \begin{pmatrix} \frac{9}{25} & \frac{7}{10} \cdot \frac{9}{25} \\ \frac{7}{10} \cdot \frac{9}{25} & \frac{49}{100} \end{pmatrix} \quad \text{and} \quad \Sigma_2 = \Sigma_3 = \begin{pmatrix} \frac{9}{25} & 0 \\ 0 & \frac{49}{100} \end{pmatrix}.$$

- (v) The (L) Quadrinodal density is a mixture of four normal distributions with weights $w_1 = w_3 = \frac{1}{8}$ and $w_2 = w_4 = \frac{3}{8}$; means $\mu_1 = (-1, 1)^\top$, $\mu_2 = (-1, -1)^\top$, $\mu_3 = (1, -1)^\top$ and $\mu_4 = (1, 1)^\top$; and covariances

$$\begin{aligned} \Sigma_1 &= \begin{pmatrix} \frac{4}{9} & \frac{2}{5} \cdot \frac{4}{9} \\ \frac{2}{5} \cdot \frac{4}{9} & \frac{4}{9} \end{pmatrix}, & \Sigma_2 &= \begin{pmatrix} \frac{4}{9} & \frac{3}{5} \cdot \frac{4}{9} \\ \frac{3}{5} \cdot \frac{4}{9} & \frac{4}{9} \end{pmatrix}, \\ \Sigma_3 &= \begin{pmatrix} \frac{4}{9} & -\frac{7}{10} \cdot \frac{4}{9} \\ -\frac{7}{10} \cdot \frac{4}{9} & \frac{4}{9} \end{pmatrix} & \text{and} & \Sigma_4 = \begin{pmatrix} \frac{4}{9} & -\frac{1}{2} \cdot \frac{4}{9} \\ -\frac{1}{2} \cdot \frac{4}{9} & \frac{4}{9} \end{pmatrix}. \end{aligned}$$

- (vi) The #10 Fountain density is a mixture of six normal distributions with weights $w_1 = \frac{1}{2}$ and $w_2 = w_3 = w_4 = w_5 = w_6 = \frac{1}{10}$; means $\mu_1 = \mu_2 = (0, 0)^\top$, $\mu_3 = (-1, 1)^\top$, $\mu_4 = (-1, -1)^\top$, $\mu_5 = (1, -1)^\top$ and $\mu_6 = (1, 1)^\top$; and covariances

$$\Sigma_1 = \begin{pmatrix} 1 & 0 \\ 0 & 1 \end{pmatrix}, \quad \Sigma_2 = \Sigma_3 = \Sigma_4 = \Sigma_5 = \Sigma_6 = \begin{pmatrix} \frac{1}{16} & 0 \\ 0 & \frac{1}{16} \end{pmatrix}.$$

The true clusters corresponding to these densities are in Fig 3 (first row) and Fig 7 (first row), in Appendix K.2. They are constructed as follows. First, we compute the gradient of the densities. Next, we use the R package `deSolve` to solve the (negative) gradient system

$$u'(t) = -\nabla f(u(t))$$

with initial value very close to the saddle points of $f(\cdot)$ (see Chacón [2015]). In this way, we build the "borders" of the clusters (i.e. the curves in black). Finally, we plot modes in red and draw each cluster with a different color.

The Mult. Bimodal and Mult. Quadrifocal densities are obtained as mixtures of normal densities with identity covariance matrix and equal weights. In particular, (vii) the Mult. Bimodal density is a mixture of two normal distributions with means $(-2, 0, 0, 0, 0)$ and $(2, 0, 0, 0, 0)$ and (viii) the Mult. Quadrifocal density is a mixture of four normal distributions with means $(-2, 2, 0, 0, 0)$, $(-2, -2, 0, 0, 0)$, $(2, -2, 0, 0, 0)$ and $(2, 2, 0, 0, 0)$. The true clusters for these distributions can be deduced from those of the Bimodal and Quadrifocal densities, respectively.

In Section K.3 we perform additional simulations on four more challenging circular densities, referred to as Circular 2, Circular 2 Cauchy, Circular 3 and Circular 4 Cauchy. They have densities proportional to $f_1(\cdot)$, $f_2(\cdot)$, $f_3(\cdot)$ and $f_4(\cdot)$ (respectively), where

$$\begin{aligned} f_1(x) &= 0.5 \exp(-12.5(-2 + \|x\|)^2) \left(1.1 - \frac{x^{(1)}}{\|x\|} \right) \\ &\quad + 0.5 \exp(-12.5(-0.5 + \|x\|)^2) \left(1.1 + \frac{x^{(1)}}{\|x\|} \right), \\ f_2(x) &= \left(0.5 \left(1.1 + \frac{x^{(1)}}{\|x\|} \right) \right) / (1 + 25(-2 + \|x\|)^2) \\ &\quad + \left(0.5 \left(1.1 + \frac{x^{(1)}}{\|x\|} \right) \right) / (1 + 25(-0.5 + \|x\|)^2), \\ f_3(x) &= 0.3 \exp\left(-\frac{200}{9}(-1.5 + \|x\|)^2\right) \left(1.1 - \frac{x^{(1)}}{\|x\|} \right) \\ &\quad + 0.15 \exp\left(-\frac{200}{9}(-2.5 + \|x\|)^2\right) \left(1.1 + \frac{x^{(1)}}{\|x\|} \right) \\ &\quad + 0.55 \exp\left(-\frac{200}{9}(-0.5 + \|x\|)^2\right) \left(1.1 + \frac{x^{(1)}}{\|x\|} \right), \\ f_4(x) &= \left(2 + \cos\left(4 \arccos\left(\frac{x^{(1)}}{\|x\|}\right)\right) \right) / (1 + (-2 + \|x\|)^2). \end{aligned}$$

Fig 5 shows the functions $f_1(\cdot)$, $f_2(\cdot)$, $f_3(\cdot)$ and $f_4(\cdot)$. The true clusters associated with these densities are shown in Fig 6. Although the density Circular 4 Cauchy has a circular structure, it does not have clusters of a circular form, which makes it easier to identify the true clusters in the simulations.

We also consider seven additional circular distributions. Five of them are bimodal distributions and are called Circular Bimodal I, II, III, IV, and V, and two of them are quadrifocal distributions and are called Circular Quadrifocal I and II. We now describe these distributions.

(i) The Circular Bimodal I distribution is a mixture with equal weights of the distri-

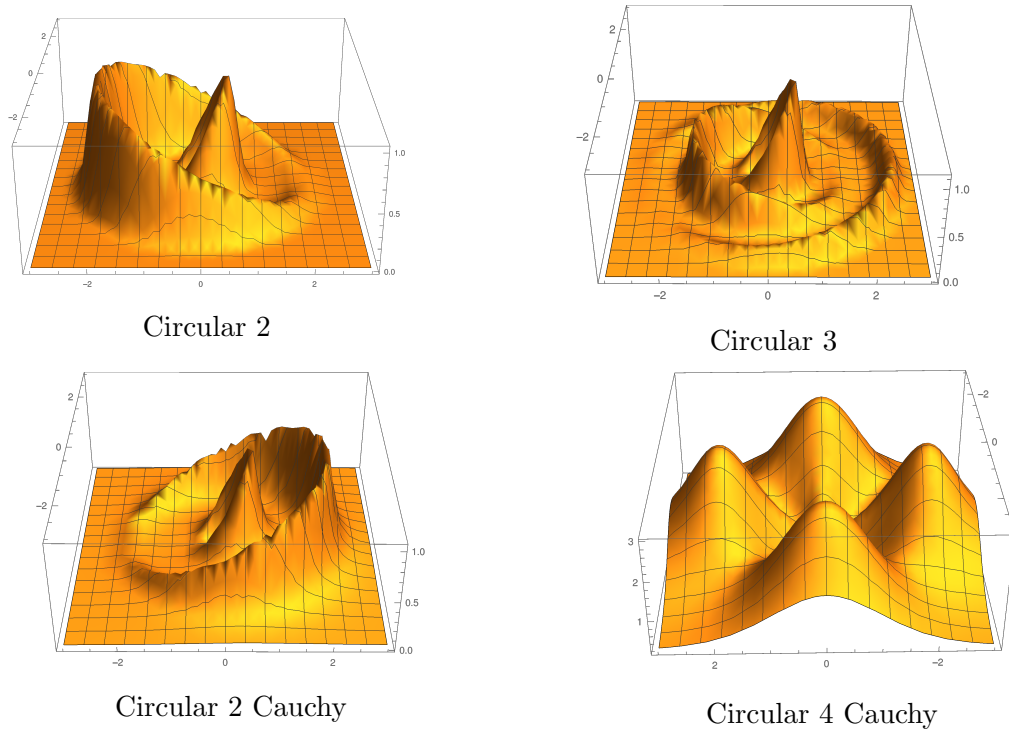
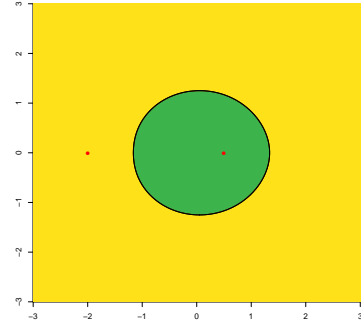
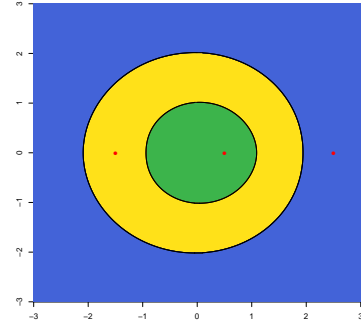


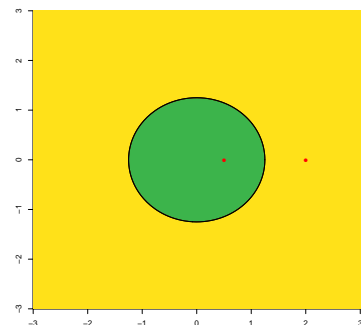
Figure 5: Plots of the functions $f_1(\cdot)$, $f_2(\cdot)$, $f_3(\cdot)$ and $f_4(\cdot)$ proportional to the Circular 2, Circular 2 Cauchy, Circular 3 and Circular 4 Cauchy densities, respectively.



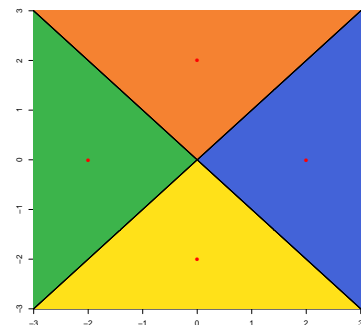
Circular 2



Circular 3



Circular 2 Cauchy



Circular 4 Cauchy

Figure 6: True clusters associated with the Circular 2, Circular 2 Cauchy, Circular 3 and Circular 4 Cauchy densities. The modes are plotted in red.

bution $(X_1^{(1)} \sin(X_1^{(2)}), X_1^{(1)} \cos(X_1^{(2)}))$, where X_1 is normal with mean $\mu_1 = (2\pi, 0)^T$ and covariance matrix

$$\Sigma_1 = \begin{pmatrix} 0.2 & 0 \\ 0 & 0.5 \end{pmatrix}$$

and a center normal distribution with covariance matrix $\Sigma_2 = 3I$.

(ii) The Circular Bimodal II distribution is a mixture with weights $w_1 = 3/4$ and $w_2 = 1/4$ of the distribution $(X_2^{(1)} \sin(X_2^{(2)}), X_2^{(1)} \cos(X_2^{(2)}))$, where X_2 is normal with mean $\mu_1 = (2\pi, 0)^T$ and covariance matrix

$$\Sigma_1 = \begin{pmatrix} 0.2 & 0 \\ 0 & 1 \end{pmatrix}$$

and a center normal distribution with covariance matrix $\Sigma_2 = 2I$.

(iii) The Circular Bimodal III distribution is a mixture with weights $w_1 = 3/4$ and $w_2 = 1/4$ of the distribution $(X_3^{(1)} \sin(X_3^{(2)}), X_3^{(1)} \cos(X_3^{(2)}))$, where X_3 is normal with mean $\mu_1 = (2\pi, 0)^T$ and covariance matrix

$$\Sigma_1 = \begin{pmatrix} 0.2 & 0 \\ 0 & 1 \end{pmatrix}$$

and a normal distribution with mean $\mu_2 = (0, -2\pi)^T$ and covariance matrix $\Sigma_2 = 2I$.

(iv) The Circular Bimodal IV distribution is a mixture with weights $w_1 = 1/4$ and $w_2 = 3/4$ of the distribution $(X_4^{(1)} \sin(X_4^{(2)}), X_4^{(1)} \cos(X_4^{(2)}))$, where X_4 is normal with mean $\mu_1 = (2\pi, 0)^T$ and covariance matrix

$$\Sigma_1 = \begin{pmatrix} 0.2 & 0 \\ 0 & 1 \end{pmatrix}$$

and a centered normal distribution with covariance matrix $\Sigma_2 = 2I$.

(v) The Circular Bimodal V distribution is a mixture with weights $w_1 = 1/4$ and $w_2 = 3/4$ of the distribution $(X_5^{(1)} \sin(X_5^{(2)}), X_5^{(1)} \cos(X_5^{(2)}))$, where X_5 is normal with mean $\mu_1 = (2\pi, 0)^T$ and covariance matrix

$$\Sigma_1 = \begin{pmatrix} 0.2 & 0 \\ 0 & 1 \end{pmatrix}$$

and a normal distribution with mean $\mu_2 = (0, -2\pi)^T$ and covariance matrix $\Sigma_2 = 2I$.

(vi) The Circular Quadrinormal I density is a mixture of four multivariate skew-normal distributions [Azzalini and Capitanio, 1999] with weights $w_1 = w_2 = w_3 = w_4 = 1/4$, location parameters $\mu_1 = (0.3, 0)^T$, $\mu_2 = (-0.3, 0)^T$, $\mu_3 = (0, 0.3)^T$, and $\mu_4 = (0, -0.3)^T$; matrices

$$\Omega_1 = \Omega_2 = \begin{pmatrix} 2 & 0 \\ 0 & 1/4 \end{pmatrix} \quad \text{and} \quad \Omega_3 = \Omega_4 = \begin{pmatrix} 1/4 & 0 \\ 0 & 2 \end{pmatrix};$$

and slant vectors $\alpha_1 = (10, 0)^\top$, $\alpha_2 = (-10, 0)^\top$, $\alpha_3 = (0, 10)^\top$, and $\alpha_4 = (0, -10)^\top$.

(vii) The Circular Quadrimodal II density is a mixture of four multivariate skew-normal distributions with weights $w_1 = w_2 = w_3 = w_4 = 1/4$, location parameters $\mu_1 = (1/4, 0)^\top$, $\mu_2 = (-1/4, 0)^\top$, $\mu_3 = (0, 1/4)^\top$, and $\mu_4 = (0, -1/4)^\top$; matrices

$$\Omega_1 = \Omega_2 = \begin{pmatrix} 2 & 0 \\ 0 & 1/4 \end{pmatrix} \quad \text{and} \quad \Omega_3 = \Omega_4 = \begin{pmatrix} 1/4 & 0 \\ 0 & 2 \end{pmatrix};$$

and slant vectors $\alpha_1 = (20, 0)^\top$, $\alpha_2 = (-20, 0)^\top$, $\alpha_3 = (0, 20)^\top$, and $\alpha_4 = (0, -20)^\top$.

For the distributions Circular Bimodal I-V and Circular Quadrimodal I-II, we evaluate, for simplicity, the clustering algorithm on the basis of the appartenence to the correct mixture components and not on the basis of the appartenence to the true underlying clusters, that is, the stable manifolds associated to the gradient system (3.2).

K.2 Illustrative examples

In this subsection, we provide additional illustrations of clustering (as in Fig 3, Appendix J), by considering the distributions (K) Trimodal III, Quadrimodal, and (L) Quadrimodal. For this, we compare the second and the third row in Fig 7 with the true clusters in the first row. Based on this comparison, we observe that the cluster estimates based on the proposed LLD method (second row) are better than those based on KDE (third row). Also, Figs 8 through 13 provide further illustrations of clustering for different choices of s and q , similar to the second rows of Fig 3 and Fig 7. These may be regarded as the bivariate analogue of Fig 2 for the densities Bimodal, (H) Bimodal IV, (K) Trimodal III, Quadrimodal, (L) Quadrimodal and #10 Fountain. Since the parameter r does not affect the output of Algorithm 1, we leave it fixed at $r = 0.05$. However, the choice of q affects the estimated clusters and a recommendation on its choice is given in Section 3.

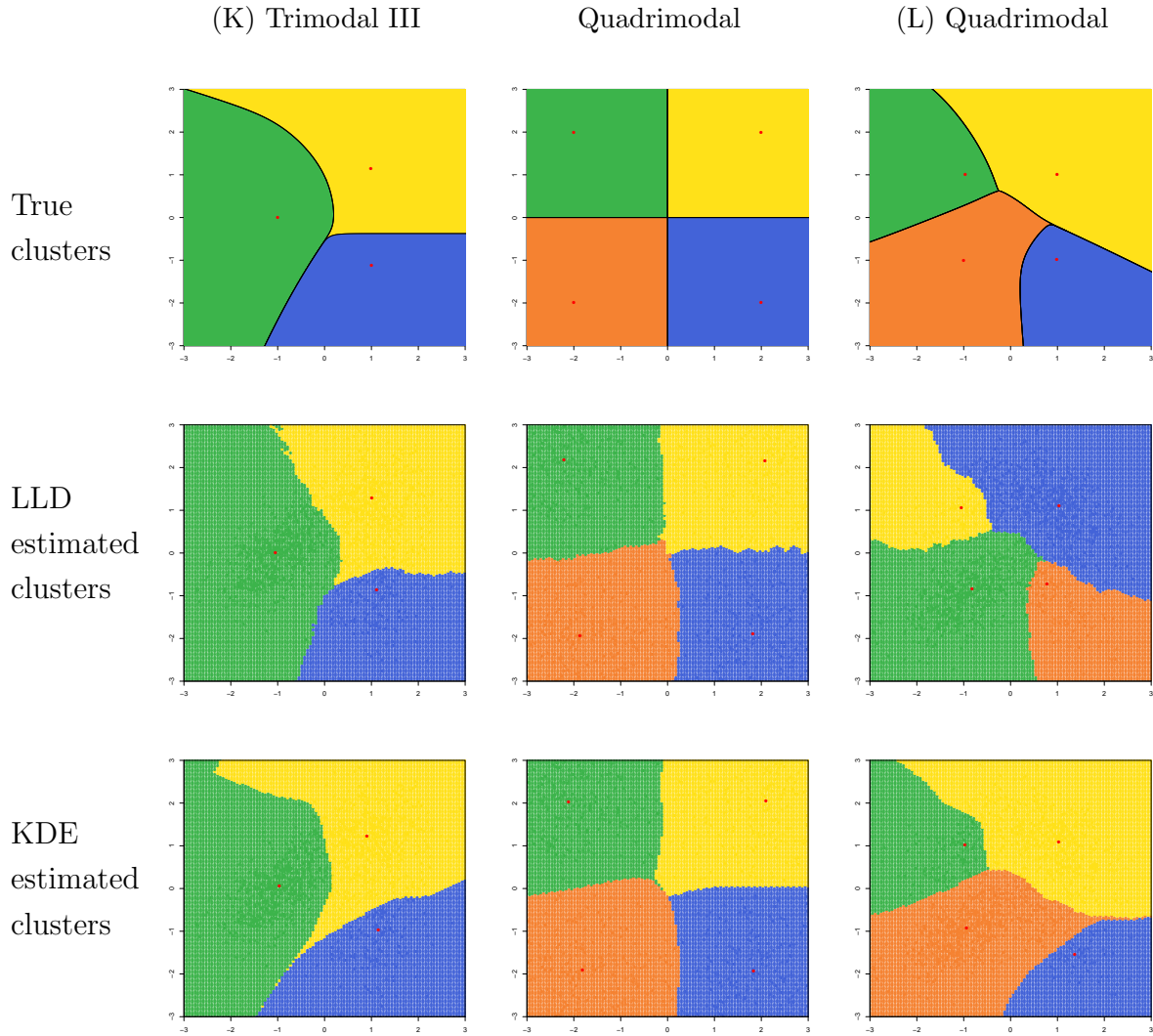


Figure 7: Clusters associated with the (K) Trimodal III (left), Quadrifocal (middle) and (L) Quadrifocal (right) densities. True clusters (first row). Local depth clustering based on $n = 1000$ samples from these densities and parameters $q = 0.05$, $s = 50$ and $r = 0.05$ (second row). Kernel density estimator clustering (third row). The true modes (first row) and the predicted modes (second and third rows) are plotted in red.

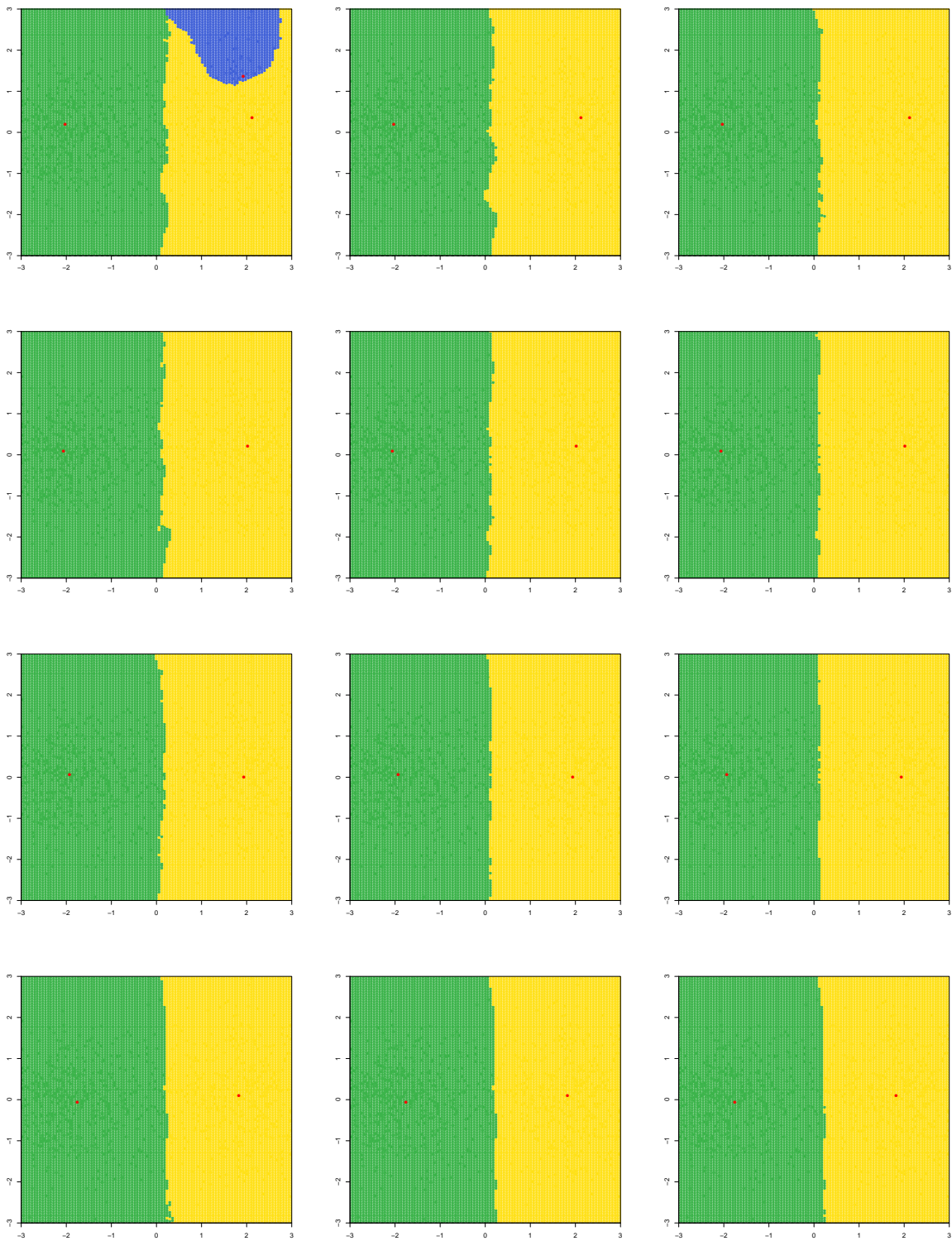


Figure 8: Local depth clustering of $n = 1000$ samples from the Bimodal density. The predicted local maxima are plotted in red. The parameters are $r = 0.05, s = 10, 30, 50$ in each column (from left to right) and $q = 0.05, 0.10, 0.25, 0.50$ in each row (from the top down).

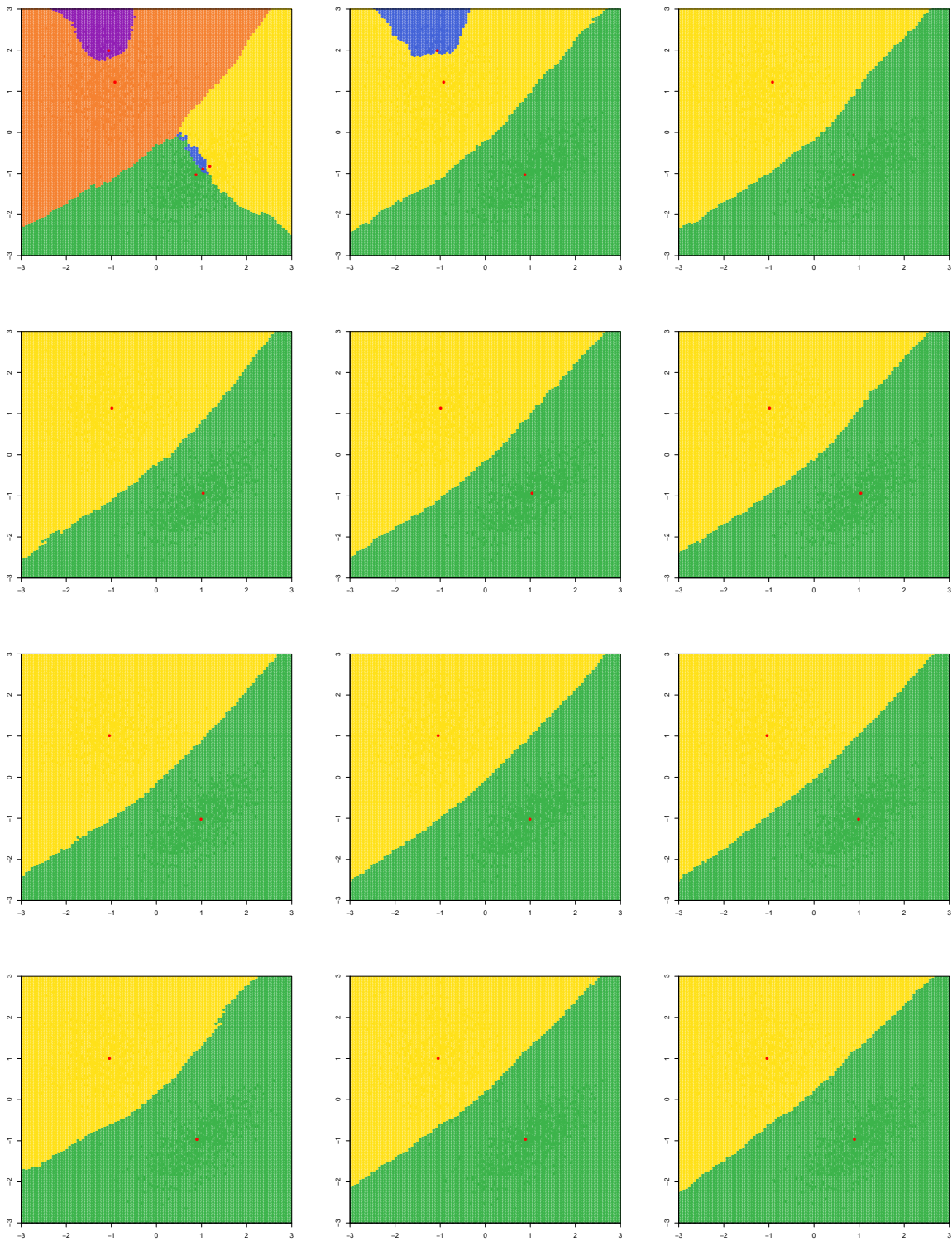


Figure 9: Local depth clustering of $n = 1000$ samples from the (H) Bimodal IV density. The predicted local maxima are plotted in red. The parameters are $r = 0.05, 10, 30, 50$ in each column (from left to right) and $q = 0.05, 0.10, 0.25, 0.50$ in each row (from the top down).

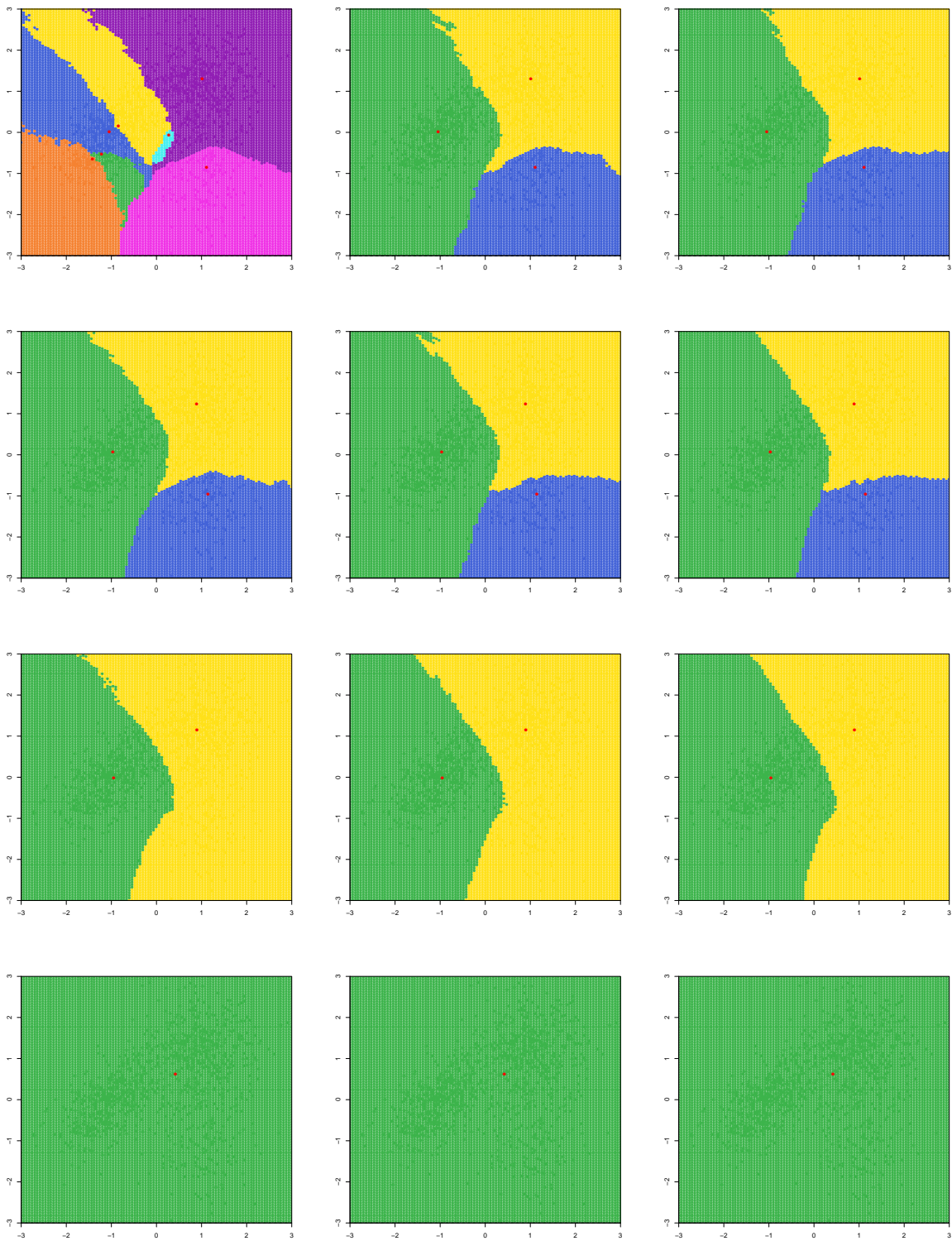


Figure 10: Local depth clustering of $n = 1000$ samples from the (K) Trimodal III density. The predicted local maxima are plotted in red. The parameters are $r = 0.05, 10, 30, 50$ in each column (from left to right) and $q = 0.05, 0.10, 0.25, 0.50$ in each row (from the top down).

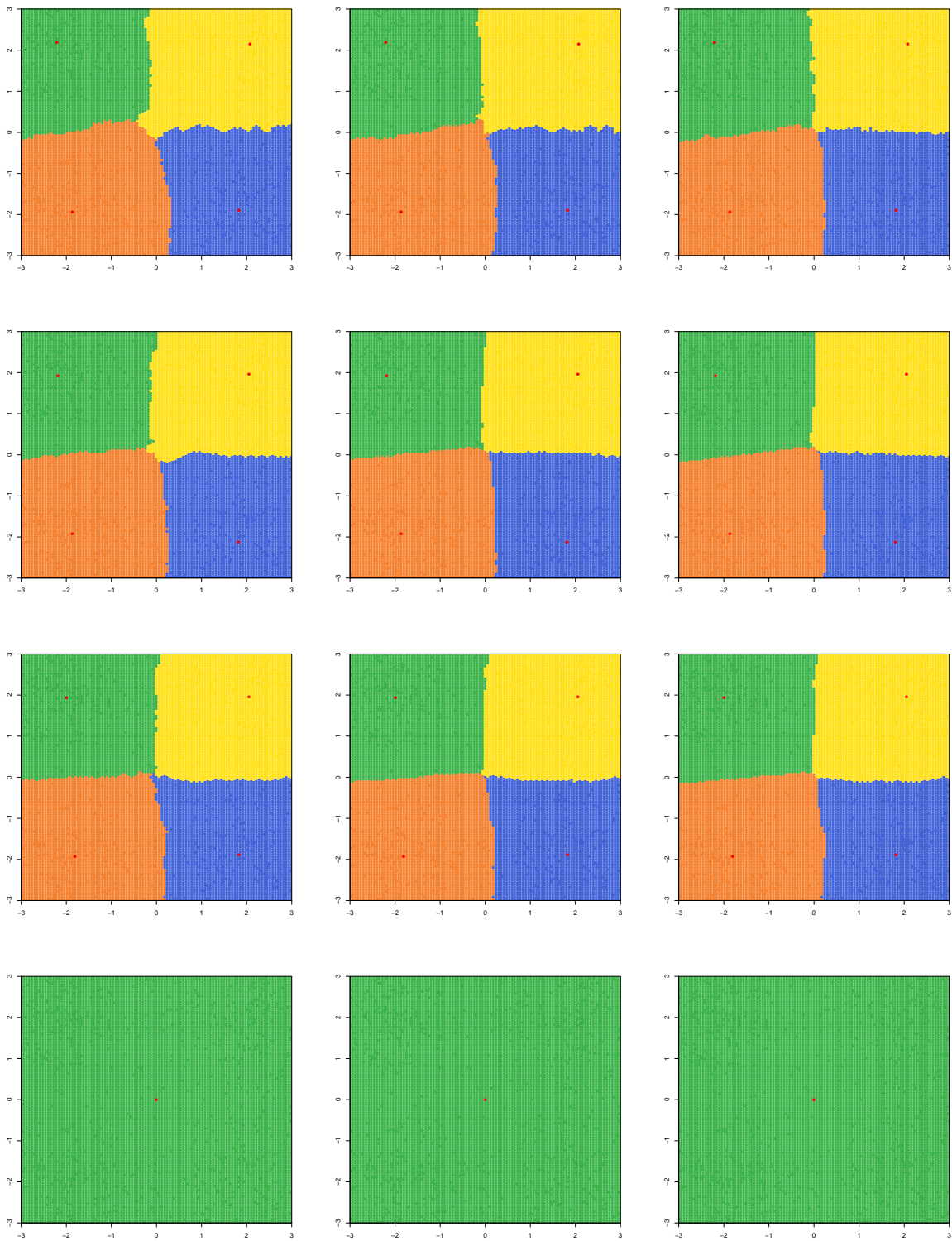


Figure 11: Local depth clustering of $n = 1000$ samples from the Quadrimodal density. The predicted local maxima are plotted in red. The parameters are $r = 0.05, 10, 30, 50$ in each column (from left to right) and $q = 0.05, 0.10, 0.25, 0.50$ in each row (from the top down).

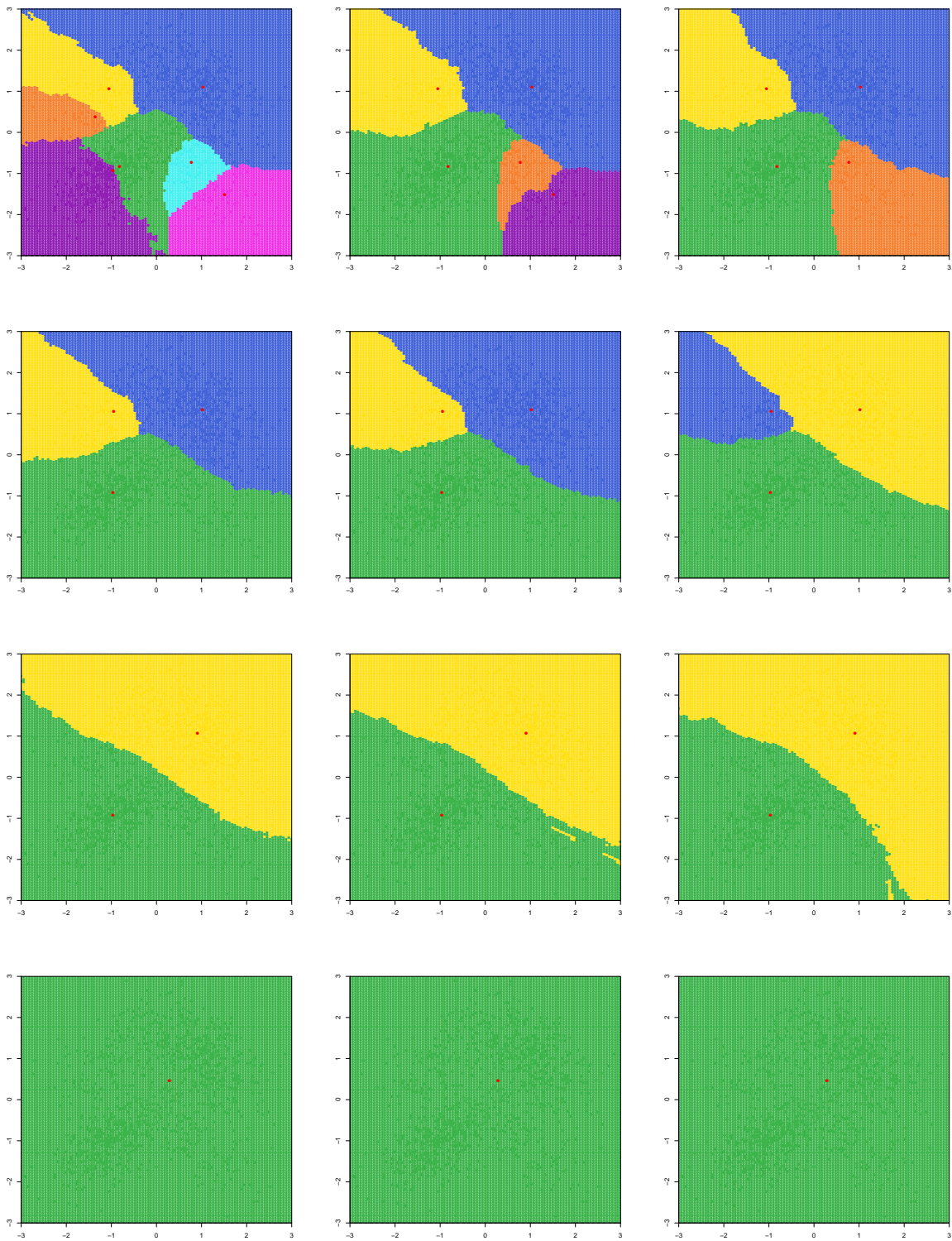


Figure 12: Local depth clustering of $n = 1000$ samples from the (L) Quadrimodal density. The predicted local maxima are plotted in red. The parameters are $r = 0.05, 0.30, 0.50$ in each column (from left to right) and $q = 0.05, 0.10, 0.25, 0.50$ in each row (from the top down).

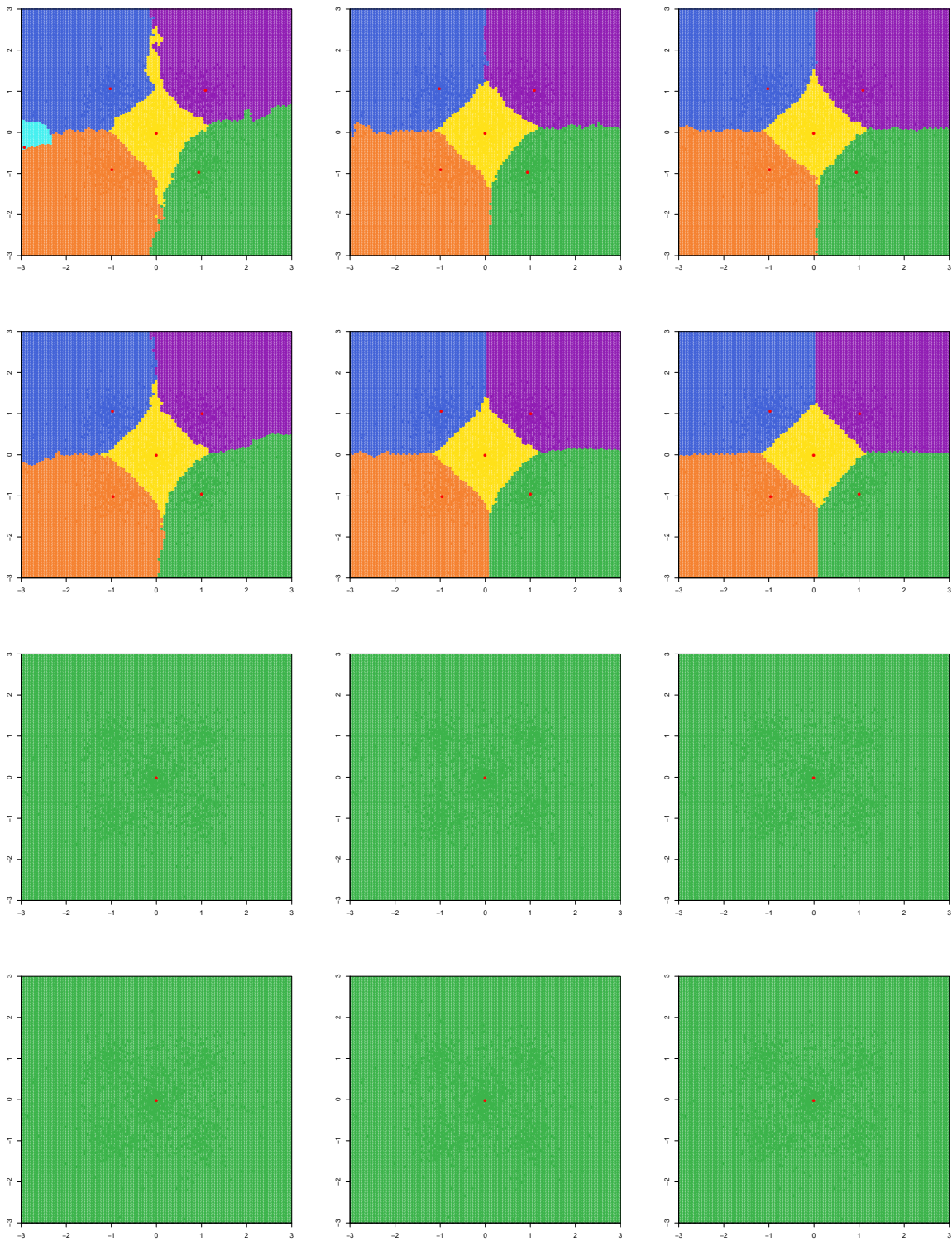


Figure 13: Local depth clustering of $n = 1000$ samples from the #10 Fountain density. The predicted local maxima are plotted in red. The parameters are $r = 0.05, s = 10, 30, 50$ in each column (from left to right) and $q = 0.05, 0.10, 0.25, 0.50$ in each row (from the top down).

K.3 Numerical experiments

In this subsection, we provide additional simulation results complementing those of the main paper and Section J. Tables 5 through 10 contain results for all the distributions in Appendix K.1 for several choices of q and s beyond what is described in the main paper. Since the parameter r does not affect the output of Algorithm 1, we leave it fixed at $r = 0.05$. The expressions LLD- q - s and LSD- q - s refer to LLD and LSD with parameters q and s . To investigate the effect of sample size, in Tables 11 through 16 n is set at 500, instead of 1000. In the second part of Tables 5 through 7 and 11 through 13, the first row refers to the case $\eta = 0$ and the second row to the case $\eta = 1$. From these two values, it is possible to compute the distance in probability for all values of η . In all the tables the best results are in bold face. For the probability distance, the best results are bolded only for the case $\eta = 1$.

For KDE we use the R function `kms` from the R-package `ks` [Duong, 2018], in which the bandwidth matrix is estimated using the function `Hpi` with derivative order one and pilot options "`dunconstr`" or "`dscalar`". In the first case, the starting matrix is obtained via minimization of asymptotic mean squared error (AMSE) while, in the second case, a diagonal pilot bandwidth matrix is used to estimate the final (full) bandwidth matrix. Finally, we set maximum number of iterations to 5000 and tolerance to 10^{-8} . For more details on the bandwidth selection procedure see Sections 3.6 and 5.6.4 in Chacón and Duong [2018]. In the tables, the expressions KDE-"`dun`"- s and KDE-"`dsc`"- s refer to KDE with Algorithm 1 and parameter s ; and pilot options "`dunconstr`" and "`dscalar`", respectively. Similarly, the expressions KDE-"`dun`"-"`ms`" and KDE-"`dsc`"-"`ms`" refer to KDE with mean shift algorithm and pilot options "`dunconstr`" and "`dscalar`".

From the tables, we observe that for mixture of normal distributions, the best results are always obtained by MMMM and MMMC. Among other methods, LLD yields the best results for the distributions Mult. Bimodal and Mult. Quadrimodal, see Tables 7, 10, 13 and 16. For the distributions (H) Bimodal IV, (K) Trimodal III, (L) Quadrimodal, Bimodal, and Quadrimodal, KDE, LLD, and LSD all yield similar results. Turning to the circular densities, we notice that for Circular 2 and Circular 2 Cauchy, KDE, LLD and LSD outperform all the other procedures, as can be seen from Tables 5, 6, 10, 11, 12 and 16. From the tables, it also clear that the best clustering results for the distributions #10 Fountain, Circular 2, Circular 2 Cauchy, Circular 3, and Circular 4 Cauchy, are shared by KDE, LLD and LSD. Furthermore, LSD outperforms all the competitors for the distributions Circular Bimodal I-III, as can be seen from Tables 8, 10, 14, and 16. These tables and Tables 9 and 15 show that the smallest clustering errors and highest frequency with which the true number of clusters are detected for the distributions Circular Bimodal

IV-V and Circular Quadrinodal I-II are shared by KDE, LLD, and LSD. Finally, we notice that the merging algorithm in Chazal et al. [2013] may be used to improve the results of KDE, LLD, and LSD for the circular densities in Tables 6, 10, 12 and 16. As explained previously in Subsection J.2, one can improve the performance of LSD using smaller values of q .

Figures 14-127 show, for all the distributions in Appendix K.1, how Hausdorff distance, probability distance, and frequency of correctly detected number of clusters vary as a function of the localization parameter or quantile order. Specifically, Figures 14-32 and Figures 71-89 refer to Hausdorff distance and the sample sizes $n = 1000$ and $n = 500$, respectively. Similarly, Figures 33-51 and Figures 90-108 show the probability distance for $n = 1000$ and $n = 500$. Finally, Figures 52-70 ($n = 1000$) and Figures 109-127 ($n = 500$) display the frequency of correctly detected number of clusters. The first row contains the results for MMMM (left) and MMMC (right). For KDE-"`dun`"- s , KDE-"`dsc`"- s , KDE-"`dun`"-"`ms`", and KDE-"`dsc`"-"`ms`", we multiply the estimated bandwidth matrix by a localization parameter with values between 0.02 and 2 and plot the clustering error as a function of the localization parameter. The second row shows the results for KDE-"`dun`"-30 (left) and KDE-"`dsc`"-30 (right), the third row displays the results for KDE-"`dun`"-50 (left) and KDE-"`dsc`"-50 (right), and the fourth row shows the results for KDE-"`dun`"-"`ms`", and KDE-"`dsc`"-"`ms`". Finally, the fifth row contains the clustering errors for LLD- q -30 (left) and LLD- q -50 (right) as a function of the quantile order q .

Clustering errors (Hausdorff distance)				
	(H) Bimodal IV	(K) Trimodal III	(L) Quadri-modal	#10 Fountain
MMMC	0.00 (0.00)	0.03 (0.01)	0.07 (0.08)	0.22 (0.03)
MMMC	0.00 (0.00)	0.02 (0.01)	0.06 (0.07)	0.09 (0.02)
KDE-" <code>dun</code> "-30	0.00 (0.00)	0.12 (0.17)	0.23 (0.16)	0.06 (0.01)
KDE-" <code>dun</code> "-50	0.00 (0.00)	0.17 (0.20)	0.30 (0.17)	0.06 (0.01)
KDE-" <code>dsc</code> "-30	0.04 (0.10)	0.09 (0.14)	0.18 (0.14)	0.06 (0.01)
KDE-" <code>dsc</code> "-50	0.04 (0.09)	0.14 (0.18)	0.24 (0.16)	0.06 (0.01)
KDE-" <code>dun</code> "-" <code>ms</code> "	0.00 (0.03)	0.10 (0.15)	0.19 (0.15)	0.08 (0.05)
KDE-" <code>dsc</code> "-" <code>ms</code> "	0.05 (0.11)	0.07 (0.11)	0.14 (0.11)	0.11 (0.06)
LLD-0.05-30	0.27 (0.17)	0.18 (0.10)	0.15 (0.08)	0.06 (0.02)
LLD-0.05-50	0.22 (0.17)	0.17 (0.12)	0.16 (0.10)	0.06 (0.01)
LLD-0.1-30	0.05 (0.11)	0.10 (0.15)	0.22 (0.16)	0.06 (0.01)
LLD-0.1-50	0.02 (0.08)	0.12 (0.17)	0.26 (0.16)	0.06 (0.01)

LSD-0.01-30	0.05 (0.11)	0.10 (0.15)	0.20 (0.15)	0.06 (0.01)
LSD-0.01-50	0.04 (0.09)	0.13 (0.17)	0.26 (0.16)	0.06 (0.01)
LSD-0.05-30	0.00 (0.00)	0.25 (0.21)	0.48 (0.02)	0.35 (0.15)
LSD-0.05-50	0.00 (0.00)	0.29 (0.21)	0.48 (0.01)	0.38 (0.15)
Hclust *	0.05 (0.09)	0.15 (0.09)	0.22 (0.08)	0.29 (0.05)
Clustering errors (distance in probability)				
	(H) Bimodal IV	(K) Trimodal III	(L) Quadri-modal	#10 Fountain
MMMM	0.00 (0.00) 0.00 (0.00)	0.03 (0.01) 0.03 (0.01)	0.06 (0.02) 0.07 (0.03)	0.23 (0.06) 0.23 (0.07)
MMMC	0.00 (0.00) 0.00 (0.00)	0.02 (0.01) 0.02 (0.01)	0.03 (0.02) 0.04 (0.04)	0.10 (0.06) 0.10 (0.07)
KDE-"dun"-30	0.00 (0.00) 0.00 (0.00)	0.05 (0.03) 0.06 (0.07)	0.11 (0.10) 0.16 (0.13)	0.06 (0.01) 0.06 (0.01)
KDE-"dun"-50	0.00 (0.00) 0.00 (0.00)	0.05 (0.02) 0.07 (0.05)	0.10 (0.06) 0.17 (0.08)	0.06 (0.01) 0.06 (0.01)
KDE-"dsc"-30	0.07 (0.17) 0.11 (0.26)	0.04 (0.03) 0.06 (0.07)	0.12 (0.13) 0.16 (0.17)	0.06 (0.01) 0.06 (0.01)
KDE-"dsc"-50	0.06 (0.16) 0.09 (0.24)	0.04 (0.02) 0.06 (0.05)	0.12 (0.10) 0.17 (0.13)	0.06 (0.01) 0.06 (0.01)
KDE-"dun"- "ms"	0.01 (0.05) 0.01 (0.07)	0.05 (0.04) 0.06 (0.08)	0.11 (0.12) 0.16 (0.16)	0.19 (0.26) 0.21 (0.31)
KDE-"dsc"- "ms"	0.09 (0.19) 0.13 (0.28)	0.04 (0.04) 0.06 (0.07)	0.17 (0.19) 0.22 (0.25)	0.34 (0.30) 0.41 (0.36)
LLD-0.05-30	0.33 (0.21) 0.53 (0.33)	0.10 (0.07) 0.18 (0.14)	0.31 (0.22) 0.42 (0.30)	0.07 (0.05) 0.07 (0.06)
LLD-0.05-50	0.31 (0.25) 0.47 (0.37)	0.09 (0.07) 0.15 (0.13)	0.21 (0.21) 0.26 (0.26)	0.06 (0.01) 0.06 (0.01)
LLD-0.1-30	0.09 (0.19) 0.13 (0.28)	0.04 (0.04) 0.06 (0.07)	0.09 (0.06) 0.14 (0.08)	0.06 (0.01) 0.06 (0.01)
LLD-0.1-50	0.04 (0.12) 0.05 (0.18)	0.04 (0.03) 0.06 (0.05)	0.10 (0.06) 0.15 (0.08)	0.06 (0.01) 0.06 (0.01)
LSD-0.01-30	0.08 (0.18) 0.12 (0.27)	0.05 (0.06) 0.07 (0.09)	0.10 (0.07) 0.14 (0.10)	0.06 (0.01) 0.06 (0.01)

LSD-0.01-50	0.06 (0.15) 0.08 (0.23)	0.05 (0.03) 0.06 (0.06)	0.10 (0.07) 0.16 (0.09)	0.06 (0.01) 0.06 (0.00)
LSD-0.05-30	0.00 (0.00) 0.00 (0.00)	0.06 (0.02) 0.09 (0.05)	0.11 (0.01) 0.20 (0.01)	0.19 (0.07) 0.32 (0.14)
LSD-0.05-50	0.00 (0.00) 0.00 (0.00)	0.06 (0.02) 0.10 (0.05)	0.11 (0.01) 0.20 (0.01)	0.20 (0.06) 0.35 (0.14)
Hclust *	0.05 (0.09)	0.16 (0.09)	0.29 (0.11)	0.35 (0.07)

Table 5: Mean of the clustering errors based on Hausdorff distance and distance in probability over 100 replications with $n = 1000$ samples for the densities (H) Bimodal IV, (K) Trimodal III, (L) Quadrinodal and #10 Fountain. In parentheses the standard deviation.

Clustering errors (Hausdorff distance)				
	Circular 2	Circular 2 Cauchy	Circular 3	Circular 4 Cauchy
MMMM	0.57 (0.05)	0.61 (0.05)	0.35 (0.02)	0.08 (0.08)
MMMC	0.55 (0.05)	0.58 (0.04)	0.34 (0.02)	0.06 (0.07)
KDE-"dun"-30	0.50 (0.08)	0.42 (0.12)	0.32 (0.02)	0.02 (0.01)
KDE-"dun"-50	0.49 (0.08)	0.39 (0.16)	0.32 (0.04)	0.02 (0.01)
KDE-"dsc"-30	0.55 (0.07)	0.49 (0.08)	0.33 (0.02)	0.02 (0.01)
KDE-"dsc"-50	0.53 (0.07)	0.46 (0.10)	0.33 (0.02)	0.02 (0.01)
KDE-"dun"- "ms"	0.51 (0.08)	0.44 (0.09)	0.31 (0.02)	0.03 (0.06)
KDE-"dsc"- "ms"	0.56 (0.06)	0.53 (0.08)	0.32 (0.01)	0.08 (0.1)
LLD-0.05-30	0.61 (0.05)	0.56 (0.07)	0.33 (0.01)	0.02 (0.03)
LLD-0.05-50	0.59 (0.05)	0.52 (0.07)	0.34 (0.02)	0.02 (0.01)
LLD-0.1-30	0.52 (0.06)	0.45 (0.08)	0.32 (0.02)	0.01 (0.01)
LLD-0.1-50	0.49 (0.07)	0.43 (0.10)	0.31 (0.03)	0.01 (0.01)
LLD-0.15-30	0.43 (0.12)	0.35 (0.20)	0.32 (0.03)	0.02 (0.01)
LLD-0.15-50	0.39 (0.16)	0.30 (0.21)	0.31 (0.04)	0.02 (0.01)
LLD-0.2-30	0.35 (0.19)	0.39 (0.31)	0.34 (0.05)	0.04 (0.05)
LLD-0.2-50	0.28 (0.21)	0.49 (0.34)	0.40 (0.09)	0.04 (0.07)
LSD-0.01-30	0.50 (0.06)	0.43 (0.12)	0.31 (0.03)	0.01 (0.01)
LSD-0.01-50	0.48 (0.08)	0.41 (0.14)	0.31 (0.03)	0.01 (0.01)
LSD-0.05-30	0.26 (0.21)	0.43 (0.31)	0.31 (0.04)	0.04 (0.06)

LSD-0.05-50	0.16 (0.20)	0.49 (0.33)	0.32 (0.07)	0.04 (0.06)
LSD-0.1-30	0.38 (0.15)	0.78 (0.10)	0.36 (0.07)	0.25 (0.20)
LSD-0.1-50	0.20 (0.19)	0.80 (0.07)	0.49 (0.12)	0.28 (0.21)
Hclust *	0.34 (0.12)	0.38 (0.08)	0.37 (0.05)	0.24 (0.06)
Clustering errors (distance in probability)				
	Circular 2	Circular 2 Cauchy	Circular 3	Circular 4 Cauchy
MMMM	0.31 (0.04)	0.41 (0.04)	0.34 (0.05)	0.15 (0.19)
	0.61 (0.07)	0.63 (0.05)	0.62 (0.08)	0.17 (0.24)
MMMC	0.31 (0.04)	0.37 (0.03)	0.32 (0.05)	0.12 (0.20)
	0.62 (0.08)	0.62 (0.06)	0.60 (0.07)	0.15 (0.25)
KDE-"dun"-30	0.30 (0.06)	0.32 (0.13)	0.31 (0.06)	0.02 (0.01)
	0.59 (0.11)	0.55 (0.18)	0.54 (0.12)	0.02 (0.01)
KDE-"dun"-50	0.30 (0.07)	0.30 (0.16)	0.33 (0.08)	0.02 (0.01)
	0.57 (0.12)	0.49 (0.23)	0.52 (0.15)	0.02 (0.01)
KDE-"dsc"-30	0.31 (0.05)	0.32 (0.07)	0.31 (0.04)	0.03 (0.04)
	0.61 (0.09)	0.60 (0.10)	0.57 (0.07)	0.03 (0.05)
KDE-"dsc"-50	0.31 (0.05)	0.32 (0.10)	0.32 (0.05)	0.02 (0.01)
	0.59 (0.10)	0.57 (0.14)	0.56 (0.09)	0.02 (0.01)
KDE-"dun"- "ms"	0.30 (0.05)	0.31 (0.08)	0.28 (0.05)	0.06 (0.14)
	0.59 (0.10)	0.59 (0.15)	0.53 (0.10)	0.07 (0.16)
KDE-"dsc"- "ms"	0.31 (0.04)	0.32 (0.05)	0.29 (0.03)	0.15 (0.23)
	0.61 (0.08)	0.63 (0.10)	0.58 (0.06)	0.19 (0.28)
LLD-0.05-30	0.34 (0.03)	0.32 (0.05)	0.32 (0.03)	0.04 (0.09)
	0.66 (0.07)	0.65 (0.09)	0.59 (0.07)	0.04 (0.11)
LLD-0.05-50	0.33 (0.04)	0.33 (0.07)	0.32 (0.05)	0.03 (0.04)
	0.64 (0.07)	0.62 (0.09)	0.57 (0.08)	0.03 (0.05)
LLD-0.1-30	0.31 (0.06)	0.32 (0.12)	0.32 (0.06)	0.02 (0.01)
	0.59 (0.10)	0.55 (0.15)	0.55 (0.11)	0.02 (0.01)
LLD-0.1-50	0.32 (0.10)	0.33 (0.15)	0.34 (0.08)	0.02 (0.01)
	0.58 (0.12)	0.53 (0.18)	0.54 (0.14)	0.02 (0.01)
LLD-0.15-30	0.30 (0.13)	0.27 (0.20)	0.35 (0.07)	0.02 (0.01)
	0.51 (0.18)	0.40 (0.26)	0.55 (0.11)	0.02 (0.01)
LLD-0.15-50	0.30 (0.18)	0.24 (0.20)	0.38 (0.09)	0.03 (0.01)
	0.47 (0.23)	0.35 (0.26)	0.54 (0.14)	0.03 (0.01)

LLD-0.2-30	0.25 (0.18) 0.40 (0.25)	0.19 (0.19) 0.25 (0.22)	0.41 (0.09) 0.55 (0.10)	0.04 (0.03) 0.04 (0.05)
LLD-0.2-50	0.20 (0.18) 0.30 (0.26)	0.14 (0.15) 0.20 (0.17)	0.46 (0.09) 0.51 (0.10)	0.04 (0.03) 0.05 (0.06)
LSD-0.01-30	0.30 (0.07) 0.57 (0.10)	0.32 (0.14) 0.52 (0.18)	0.31 (0.07) 0.54 (0.12)	0.02 (0.01) 0.02 (0.01)
LSD-0.01-50	0.32 (0.10) 0.56 (0.13)	0.32 (0.16) 0.50 (0.20)	0.33 (0.08) 0.54 (0.14)	0.02 (0.01) 0.02 (0.01)
LSD-0.05-30	0.19 (0.18) 0.29 (0.26)	0.20 (0.18) 0.26 (0.20)	0.38 (0.08) 0.54 (0.13)	0.04 (0.03) 0.05 (0.05)
LSD-0.05-50	0.13 (0.17) 0.18 (0.23)	0.15 (0.15) 0.21 (0.16)	0.40 (0.09) 0.46 (0.13)	0.04 (0.03) 0.05 (0.05)
LSD-0.1-30	0.33 (0.13) 0.57 (0.22)	0.13 (0.11) 0.21 (0.09)	0.44 (0.08) 0.56 (0.11)	0.16 (0.09) 0.28 (0.20)
LSD-0.1-50	0.21 (0.20) 0.31 (0.31)	0.10 (0.06) 0.19 (0.05)	0.43 (0.09) 0.53 (0.08)	0.18 (0.09) 0.32 (0.21)
Hclust *	0.34 (0.12)	0.38 (0.08)	0.43 (0.05)	0.34 (0.09)

Table 6: Mean of the clustering errors based on Hausdorff distance and distance in probability over 100 replications with $n = 1000$ samples for the densities Circular 2, Circular 2 Cauchy, Circular 3 and Circular 4 Cauchy. In parentheses the standard deviation.

Clustering errors (Hausdorff distance)					
	Bimodal	Quadrinodal	Mult. Bi- modal	Bi- modal	Mult. Quadri- modal
MMMM	0.00 (0.00)	0.00 (0.00)	0.00 (0.00)	0.01 (0.00)	
MMMC	0.00 (0.00)	0.00 (0.00)	0.00 (0.00)	0.01 (0.00)	
KDE-"dun"-30	0.01 (0.03)	0.01 (0.00)	0.15 (0.17)	0.10 (0.08)	
KDE-"dun"-50	0.01 (0.03)	0.01 (0.00)	0.07 (0.12)	0.07 (0.07)	
KDE-"dsc"-30	0.04 (0.10)	0.01 (0.00)	0.13 (0.17)	0.09 (0.08)	
KDE-"dsc"-50	0.04 (0.09)	0.01 (0.00)	0.06 (0.11)	0.06 (0.07)	
KDE-"dun"- "ms"	0.01 (0.05)	0.01 (0.00)	0.38 (0.17)	0.16 (0.08)	
KDE-"dsc"- "ms"	0.07 (0.14)	0.01 (0.03)	0.19 (0.21)	0.08 (0.08)	
LLD-0.05-30	0.25 (0.19)	0.04 (0.06)	0.05 (0.11)	0.03 (0.04)	
LLD-0.05-50	0.16 (0.18)	0.02 (0.04)	0.01 (0.04)	0.02 (0.01)	

LLD-0.1-30	0.01 (0.04)	0.01 (0.02)	0.06 (0.13)	0.03 (0.05)
LLD-0.1-50	0.01 (0.03)	0.01 (0.00)	0.01 (0.04)	0.02 (0.01)
LSD-0.01-30	0.02 (0.06)	0.01 (0.00)	0.31 (0.15)	0.55 (0.19)
LSD-0.01-50	0.01 (0.04)	0.01 (0.00)	0.31 (0.18)	0.64 (0.17)
LSD-0.05-30	0.00 (0.00)	0.01 (0.00)	0.23 (0.18)	0.38 (0.18)
LSD-0.05-50	0.00 (0.00)	0.01 (0.00)	0.23 (0.20)	0.48 (0.18)
LSD- 10^{-4} -30	/	/	0.07 (0.13)	0.38 (0.14)
LSD- 10^{-4} -50	/	/	0.02 (0.03)	0.47 (0.20)
LSD- 10^{-5} -30	/	/	0.07 (0.14)	0.10 (0.08)
LSD- 10^{-5} -50	/	/	0.02 (0.06)	0.09 (0.09)
Hclust *	0.06 (0.05)	0.10 (0.05)	0.05 (0.03)	0.07 (0.03)
Clustering errors (distance in probability)				
	Bimodal	Quadrinodal	Mult. Bi-modal	Mult. Quadri-modal
MMMM	0.00 (0.00) 0.00 (0.00)	0.01 (0.00) 0.01 (0.00)	0.00 (0.00) 0.00 (0.00)	0.01 (0.00) 0.01 (0.00)
MMMC	0.00 (0.00) 0.00 (0.00)	0.01 (0.00) 0.01 (0.00)	0.00 (0.00) 0.00 (0.00)	0.01 (0.00) 0.01 (0.00)
KDE-"dun"-30	0.01 (0.01) 0.01 (0.02)	0.01 (0.00) 0.01 (0.00)	0.06 (0.07) 0.09 (0.13)	0.29 (0.31) 0.34 (0.37)
KDE-"dun"-50	0.01 (0.01) 0.01 (0.02)	0.01 (0.00) 0.01 (0.00)	0.04 (0.06) 0.06 (0.11)	0.12 (0.20) 0.14 (0.24)
KDE-"dsc"-30	0.02 (0.03) 0.03 (0.07)	0.01 (0.00) 0.01 (0.00)	0.05 (0.07) 0.08 (0.12)	0.24 (0.30) 0.28 (0.35)
KDE-"dsc"-50	0.01 (0.03) 0.02 (0.06)	0.01 (0.00) 0.01 (0.00)	0.03 (0.06) 0.05 (0.10)	0.10 (0.18) 0.11 (0.21)
KDE-"dun"- "ms"	0.01 (0.02) 0.01 (0.04)	0.01 (0.00) 0.01 (0.00)	0.07 (0.06) 0.12 (0.13)	0.43 (0.27) 0.57 (0.33)
KDE-"dsc"- "ms"	0.03 (0.04) 0.05 (0.08)	0.02 (0.06) 0.03 (0.08)	0.04 (0.05) 0.07 (0.11)	0.24 (0.30) 0.29 (0.36)
LLD-0.05-30	0.06 (0.06) 0.12 (0.12)	0.08 (0.16) 0.11 (0.21)	0.024 (0.06) 0.04 (0.10)	0.08 (0.19) 0.09 (0.22)
LLD-0.05-50	0.05 (0.05) 0.09 (0.11)	0.05 (0.14) 0.06 (0.17)	0.01 (0.01) 0.01 (0.01)	0.03 (0.01) 0.03 (0.01)

LLD-0.1-30	0.01 (0.02) 0.01 (0.03)	0.02 (0.06) 0.02 (0.07)	0.02 (0.06) 0.04 (0.10)	0.08 (0.19) 0.09 (0.22)
LLD-0.1-50	0.01 (0.01) 0.01 (0.02)	0.01 (0.00) 0.01 (0.01)	0.01 (0.01) 0.01 (0.01)	0.03 (0.01) 0.03 (0.01)
LSD-0.01-30	0.01 (0.02) 0.01 (0.04)	0.01 (0.00) 0.01 (0.00)	0.17 (0.07) 0.26 (0.14)	0.32 (0.07) 0.57 (0.15)
LSD-0.01-50	0.01 (0.02) 0.01 (0.03)	0.01 (0.00) 0.01 (0.00)	0.18 (0.07) 0.28 (0.17)	0.33 (0.05) 0.64 (0.13)
LSD-0.05-30	0.00 (0.00) 0.00 (0.00)	0.01 (0.00) 0.01 (0.00)	0.15 (0.11) 0.21 (0.17)	0.29 (0.11) 0.45 (0.17)
LSD-0.05-50	0.00 (0.00) 0.00 (0.00)	0.01 (0.01) 0.01 (0.01)	0.14 (0.10) 0.22 (0.20)	0.28 (0.07) 0.52 (0.16)
LSD- 10^{-4} -30	/ /	/ /	0.03 (0.04) 0.04 (0.08)	0.34 (0.15) 0.5 (0.18)
LSD- 10^{-4} -50	/ /	/ /	0.02 (0.01) 0.02 (0.02)	0.31 (0.1) 0.52 (0.17)
LSD- 10^{-5} -30	/ /	/ /	0.03 (0.04) 0.04 (0.07)	0.24 (0.27) 0.29 (0.33)
LSD- 10^{-5} -50	/ /	/ /	0.02 (0.02) 0.02 (0.04)	0.12 (0.16) 0.15 (0.2)
Hclust *	0.06 (0.05)	0.14 (0.07)	0.05 (0.03)	0.10 (0.04)

Table 7: Mean of the clustering errors based on Hausdorff distance and distance in probability over 100 replications with $n = 1000$ samples for the densities Bimodal, Quadrimodal, Mult. Bimodal and Mult. Quadrimodal. In parentheses the standard deviation.

Clustering errors (Hausdorff distance)				
	Circular Bimodal I	Circular Bimodal II	Circular Bimodal III	Circular Bimodal IV
MMMM	0.44 (0.03)	0.55 (0.04)	0.54 (0.04)	0.24 (0.08)
MMMC	0.46 (0.03)	0.53 (0.05)	0.52 (0.05)	0.25 (0.07)
KDE-"dun"-30	0.21 (0.17)	0.44 (0.07)	0.41 (0.12)	0.20 (0.04)
KDE-"dun"-50	0.17 (0.16)	0.40 (0.13)	0.38 (0.16)	0.16 (0.06)
KDE-"dsc"-30	0.33 (0.14)	0.48 (0.06)	0.47 (0.06)	0.21 (0.03)
KDE-"dsc"-50	0.28 (0.15)	0.46 (0.07)	0.46 (0.08)	0.17 (0.06)

KDE-"dun"- "ms"	0.37 (0.17)	0.44 (0.07)	0.42 (0.10)	0.23 (0.01)
KDE-"dsc"- "ms"	0.45 (0.09)	0.48 (0.07)	0.48 (0.05)	0.24 (0.03)
LLD-0.05-30	0.44 (0.04)	0.55 (0.05)	0.55 (0.05)	0.32 (0.12)
LLD-0.05-50	0.40 (0.08)	0.52 (0.06)	0.52 (0.06)	0.28 (0.13)
LLD-0.1-30	0.33 (0.13)	0.47 (0.07)	0.47 (0.07)	0.22 (0.04)
LLD-0.1-50	0.25 (0.15)	0.45 (0.09)	0.45 (0.09)	0.18 (0.05)
LLD-0.15-30	0.22 (0.16)	0.40 (0.15)	0.40 (0.15)	0.21 (0.05)
LLD-0.15-50	0.16 (0.15)	0.35 (0.18)	0.35 (0.18)	0.17 (0.05)
LLD-0.2-30	0.14 (0.15)	0.34 (0.19)	0.35 (0.18)	0.19 (0.05)
LLD-0.2-50	0.10 (0.12)	0.27 (0.21)	0.26 (0.21)	0.17 (0.05)
LSD-0.01-30	0.29 (0.14)	0.46 (0.06)	0.46 (0.06)	0.23 (0.07)
LSD-0.01-50	0.23 (0.15)	0.45 (0.08)	0.45 (0.07)	0.20 (0.09)
LSD-0.05-30	0.11 (0.14)	0.28 (0.20)	0.27 (0.21)	0.19 (0.05)
LSD-0.05-50	0.05 (0.07)	0.13 (0.17)	0.13 (0.18)	0.16 (0.05)
Hclust *	0.36 (0.09)	0.34 (0.10)	0.03 (0.02)	0.33 (0.11)
Clustering errors (distance in probability)				
	Circular Bimodal I	Circular Bimodal II	Circular Bimodal III	Circular Bimodal IV
MMMM	0.17 (0.03) 0.32 (0.06)	0.28 (0.02) 0.55 (0.05)	0.28 (0.02) 0.55 (0.04)	0.10 (0.06) 0.19 (0.12)
MMMC	0.15 (0.02) 0.29 (0.05)	0.27 (0.02) 0.53 (0.05)	0.27 (0.03) 0.52 (0.05)	0.11 (0.09) 0.22 (0.18)
KDE-"dun"-30	0.08 (0.07) 0.22 (0.19)	0.07 (0.06) 0.36 (0.06)	0.10 (0.08) 0.33 (0.11)	0.02 (0.01) 0.25 (0.18)
KDE-"dun"-50	0.07 (0.07) 0.18 (0.19)	0.10 (0.07) 0.34 (0.11)	0.12 (0.08) 0.30 (0.14)	0.03 (0.02) 0.20 (0.19)
KDE-"dsc"-30	0.10 (0.06) 0.34 (0.14)	0.04 (0.03) 0.37 (0.05)	0.06 (0.05) 0.35 (0.06)	0.02 (0.01) 0.23 (0.18)
KDE-"dsc"-50	0.09 (0.06) 0.30 (0.16)	0.07 (0.05) 0.37 (0.05)	0.08 (0.06) 0.35 (0.07)	0.03 (0.02) 0.23 (0.20)
KDE-"dun"- "ms"	0.08 (0.05) 0.14 (0.11)	0.19 (0.06) 0.38 (0.12)	0.16 (0.07) 0.30 (0.14)	0.10 (0.05) 0.19 (0.11)
KDE-"dsc"- "ms"	0.13 (0.06) 0.25 (0.13)	0.24 (0.05) 0.48 (0.10)	0.23 (0.04) 0.45 (0.09)	0.10 (0.06) 0.20 (0.11)

LLD-0.05-30	0.20 (0.05) 0.40 (0.11)	0.29 (0.03) 0.58 (0.06)	0.29 (0.03) 0.58 (0.06)	0.18 (0.10) 0.34 (0.21)
LLD-0.05-50	0.18 (0.05) 0.34 (0.11)	0.27 (0.04) 0.53 (0.07)	0.27 (0.03) 0.53 (0.07)	0.17 (0.12) 0.31 (0.24)
LLD-0.1-30	0.12 (0.05) 0.23 (0.09)	0.22 (0.05) 0.43 (0.11)	0.22 (0.05) 0.43 (0.10)	0.13 (0.11) 0.23 (0.21)
LLD-0.1-50	0.10 (0.05) 0.18 (0.11)	0.20 (0.06) 0.39 (0.11)	0.21 (0.06) 0.39 (0.12)	0.13 (0.13) 0.22 (0.25)
LLD-0.15-30	0.09 (0.05) 0.15 (0.11)	0.18 (0.07) 0.34 (0.14)	0.18 (0.07) 0.33 (0.15)	0.13 (0.11) 0.23 (0.22)
LLD-0.15-50	0.07 (0.05) 0.12 (0.10)	0.15 (0.08) 0.28 (0.15)	0.15 (0.08) 0.27 (0.15)	0.14 (0.14) 0.23 (0.26)
LLD-0.2-30	0.07 (0.05) 0.12 (0.11)	0.15 (0.08) 0.27 (0.16)	0.15 (0.08) 0.29 (0.16)	0.12 (0.12) 0.22 (0.23)
LLD-0.2-50	0.06 (0.05) 0.09 (0.10)	0.12 (0.08) 0.21 (0.17)	0.12 (0.08) 0.21 (0.17)	0.14 (0.14) 0.23 (0.26)
LSD-0.01-30	0.11 (0.05) 0.20 (0.10)	0.21 (0.05) 0.41 (0.10)	0.22 (0.05) 0.41 (0.10)	0.14 (0.11) 0.25 (0.21)
LSD-0.01-50	0.09 (0.05) 0.16 (0.11)	0.20 (0.06) 0.37 (0.11)	0.20 (0.05) 0.37 (0.11)	0.15 (0.13) 0.25 (0.26)
LSD-0.05-30	0.05 (0.05) 0.09 (0.10)	0.13 (0.08) 0.23 (0.17)	0.12 (0.09) 0.22 (0.17)	0.13 (0.13) 0.22 (0.24)
LSD-0.05-50	0.04 (0.02) 0.04 (0.05)	0.07 (0.07) 0.11 (0.14)	0.07 (0.08) 0.12 (0.15)	0.14 (0.14) 0.23 (0.27)
Hclust *	0.18 (0.05)	0.17 (0.05)	0.01 (0.01)	0.17 (0.05)

Table 8: Mean of the clustering errors based on Hausdorff distance and distance in probability over 100 replications with $n = 1000$ samples for the densities Circular Bimodal I-IV. In parentheses the standard deviation.

Clustering errors (Hausdorff distance)			
	Circular Bimodal V	Circular Quadrinodal I	Circular Quadrinodal II
MMMM	0.24 (0.07)	0.72 (0.11)	0.75 (0.06)

MMMC	0.25 (0.07)	0.73 (0.11)	0.75 (0.05)
KDE-" <i>dun</i> "-30	0.20 (0.04)	0.34 (0.13)	0.42 (0.18)
KDE-" <i>dun</i> "-50	0.16 (0.06)	0.36 (0.13)	0.46 (0.19)
KDE-" <i>dsc</i> "-30	0.21 (0.03)	0.31 (0.11)	0.35 (0.14)
KDE-" <i>dsc</i> "-50	0.18 (0.05)	0.33 (0.11)	0.38 (0.15)
KDE-" <i>dun</i> "-" <i>ms</i> "	0.23 (0.02)	0.32 (0.12)	0.39 (0.17)
KDE-" <i>dsc</i> "-" <i>ms</i> "	0.23 (0.02)	0.29 (0.09)	0.33 (0.13)
LLD-0.05-30	0.31 (0.11)	0.22 (0.05)	0.23 (0.06)
LLD-0.05-50	0.28 (0.13)	0.23 (0.08)	0.25 (0.09)
LLD-0.1-30	0.21 (0.04)	0.25 (0.12)	0.28 (0.17)
LLD-0.1-50	0.17 (0.06)	0.27 (0.11)	0.32 (0.19)
LLD-0.15-30	0.21 (0.05)	0.34 (0.19)	0.64 (0.18)
LLD-0.15-50	0.16 (0.06)	0.38 (0.19)	0.69 (0.16)
LLD-0.2-30	0.19 (0.05)	0.68 (0.16)	0.71 (0.13)
LLD-0.2-50	0.15 (0.06)	0.72 (0.12)	0.76 (0.06)
LSD-0.01-30	0.24 (0.08)	0.26 (0.13)	0.29 (0.14)
LSD-0.01-50	0.18 (0.09)	0.28 (0.13)	0.34 (0.17)
LSD-0.05-30	0.18 (0.05)	0.63 (0.19)	0.72 (0.11)
LSD-0.05-50	0.14 (0.07)	0.65 (0.19)	0.75 (0.06)
Hclust *	0.02 (0.02)	0.31 (0.14)	0.37 (0.13)
Clustering errors (distance in probability)			
	Circular Bimodal V	Circular Quadrifomodal I	Circular Quadrifomodal II
MMMM	0.10 (0.06) 0.19 (0.11)	0.36 (0.03) 0.70 (0.09)	0.36 (0.02) 0.72 (0.06)
MMMC	0.10 (0.06) 0.19 (0.13)	0.36 (0.03) 0.71 (0.08)	0.37 (0.01) 0.73 (0.04)
KDE-" <i>dun</i> "-30	0.02 (0.02) 0.29 (0.19)	0.01 (0.02) 0.20 (0.10)	0.02 (0.04) 0.25 (0.13)
KDE-" <i>dun</i> "-50	0.03 (0.03) 0.28 (0.20)	0.01 (0.02) 0.22 (0.10)	0.03 (0.05) 0.29 (0.13)
KDE-" <i>dsc</i> "-30	0.02 (0.01) 0.28 (0.19)	0.01 (0.02) 0.15 (0.10)	0.01 (0.02) 0.18 (0.11)

KDE-" dsc "-50	0.03 (0.03) 0.31 (0.19)	0.01 (0.02) 0.18 (0.09)	0.01 (0.03) 0.21 (0.11)
KDE-" dun "-" ms "	0.09 (0.06) 0.18 (0.11)	0.23 (0.06) 0.41 (0.13)	0.26 (0.08) 0.46 (0.15)
KDE-" dsc "-" ms "	0.10 (0.06) 0.19 (0.11)	0.27 (0.11) 0.39 (0.13)	0.29 (0.10) 0.42 (0.14)
LLD-0.05-30	0.16 (0.09) 0.31 (0.17)	0.40 (0.15) 0.51 (0.19)	0.37 (0.13) 0.50 (0.16)
LLD-0.05-50	0.14 (0.10) 0.26 (0.19)	0.35 (0.16) 0.42 (0.20)	0.36 (0.16) 0.45 (0.19)
LLD-0.1-30	0.11 (0.08) 0.20 (0.15)	0.21 (0.10) 0.31 (0.15)	0.21 (0.09) 0.33 (0.17)
LLD-0.1-50	0.09 (0.09) 0.16 (0.18)	0.20 (0.05) 0.32 (0.13)	0.21 (0.09) 0.35 (0.18)
LLD-0.15-30	0.10 (0.08) 0.18 (0.16)	0.22 (0.07) 0.38 (0.18)	0.33 (0.06) 0.64 (0.14)
LLD-0.15-50	0.10 (0.12) 0.18 (0.22)	0.24 (0.07) 0.43 (0.17)	0.34 (0.06) 0.68 (0.12)
LLD-0.2-30	0.10 (0.10) 0.18 (0.19)	0.34 (0.05) 0.67 (0.11)	0.22 (0.07) 0.38 (0.18)
LLD-0.2-50	0.10 (0.12) 0.17 (0.21)	0.35 (0.04) 0.70 (0.09)	0.36 (0.01) 0.73 (0.03)
LSD-0.01-30	0.12 (0.08) 0.22 (0.16)	0.21 (0.08) 0.32 (0.15)	0.21 (0.09) 0.35 (0.15)
LSD-0.01-50	0.10 (0.10) 0.18 (0.20)	0.20 (0.05) 0.34 (0.14)	0.23 (0.09) 0.40 (0.17)
LSD-0.05-30	0.10 (0.10) 0.17 (0.19)	0.33 (0.06) 0.64 (0.14)	0.35 (0.04) 0.70 (0.09)
LSD-0.05-50	0.09 (0.12) 0.16 (0.22)	0.33 (0.05) 0.66 (0.12)	0.36 (0.02) 0.72 (0.05)
Hclust *	0.01 (0.01)	0.02 (0.02)	0.04 (0.03)

Table 9: Mean of the clustering errors based on Hausdorff distance and distance in probability over 100 replications with $n = 1000$ samples for the densities Circular Bimodal V and Circular Quadrinodal I-II. In parentheses the standard deviation.

Number of times the true clusters are detected correctly				
	(H) Bimodal IV	(K) Trimodal III	(L) Quadri- modal	#10 Fountain
MMMM	(0) 100 (0)	(0) 100 (0)	(23) 77 (0)	(0) 99 (1)
MMMC	(0) 100 (0)	(0) 100 (0)	(23) 77 (0)	(0) 99 (1)
KDE-"dun"-30	(0) 100 (0)	(21) 73 (6)	(75) 22 (3)	(0) 100 (0)
KDE-"dun"-50	(0) 100 (0)	(34) 66 (0)	(85) 14 (1)	(0) 100 (0)
KDE-"dsc"-30	(0) 86 (14)	(12) 76 (12)	(57) 38 (5)	(0) 100 (0)
KDE-"dsc"-50	(0) 88 (12)	(25) 74 (1)	(73) 24 (3)	(0) 100 (0)
KDE-"dun"- "ms"	(0) 99 (1)	(15) 77 (8)	(62) 31 (7)	(0) 79 (21)
KDE-"dsc"- "ms"	(0) 82 (18)	(6) 72 (22)	(35) 46 (19)	(0) 49 (51)
LLD-0.05-30	(0) 27 (73)	(0) 24 (76)	(7) 32 (61)	(0) 99 (1)
LLD-0.05-50	(0) 38 (62)	(5) 39 (56)	(29) 45 (26)	(0) 100 (0)
LLD-0.1-30	(0) 83 (17)	(14) 79 (7)	(69) 29 (2)	(0) 100 (0)
LLD-0.1-50	(0) 93 (7)	(20) 78 (2)	(82) 16 (2)	(0) 100 (0)
LSD-0.01-30	(0) 85 (15)	(13) 75 (12)	(65) 33 (2)	(0) 100 (0)
LSD-0.01-50	(0) 89 (11)	(21) 74 (5)	(80) 18 (2)	(0) 100 (0)
LSD-0.05-30	(0) 100 (0)	(51) 49 (0)	(100) 0 (0)	(89) 11 (0)
LSD-0.05-50	(0) 100 (0)	(61) 39 (0)	(100) 0 (0)	(94) 6 (0)
	Circular 2	Circular 2 Cauchy	Circular 3	Circular 4 Cauchy
MMMM	(0) 0 (100)	(0) 0 (100)	(0) 0 (100)	(1) 84 (15)
MMMC	(0) 0 (100)	(0) 0 (100)	(0) 0 (100)	(1) 84 (15)
KDE-"dun"-30	(0) 0 (100)	(0) 4 (96)	(0) 0 (100)	(0) 100 (0)
KDE-"dun"-50	(0) 0 (100)	(0) 13 (87)	(0) 2 (98)	(0) 100 (0)
KDE-"dsc"-30	(0) 0 (100)	(0) 0 (100)	(0) 0 (100)	(0) 99 (1)
KDE-"dsc"-50	(0) 0 (100)	(0) 2 (98)	(0) 0 (100)	(0) 100 (0)
KDE-"dun"- "ms"	(0) 0 (100)	(0) 0 (100)	(0) 0 (100)	(0) 92 (8)
KDE-"dsc"- "ms"	(0) 0 (100)	(0) 0 (100)	(0) 0 (100)	(0) 72 (28)
LLD-0.05-30	(0) 0 (100)	(0) 0 (100)	(0) 0 (100)	(0) 97 (3)
LLD-0.05-50	(0) 0 (100)	(0) 0 (100)	(0) 0 (100)	(0) 99 (1)
LLD-0.1-30	(0) 0 (100)	(0) 2 (98)	(0) 0 (100)	(0) 100 (0)
LLD-0.1-50	(0) 0 (100)	(0) 5 (95)	(0) 1 (99)	(0) 100 (0)
LLD-0.15-30	(0) 7 (93)	(0) 27 (73)	(0) 0 (100)	(0) 100 (0)

LLD-0.15-50	(0) 15 (85)	(0) 37 (63)	(0) 1 (99)	(0) 100 (0)
LLD-0.2-30	(0) 24 (76)	(26) 49 (25)	(0) 2 (98)	(4) 96 (0)
LLD-0.2-50	(0) 42 (58)	(46) 41 (13)	(7) 47 (46)	(7) 93 (0)
LSD-0.01-30	(0) 0 (100)	(0) 6 (94)	(0) 0 (100)	(0) 100 (0)
LSD-0.01-50	(0) 1 (99)	(0) 10 (90)	(0) 0 (100)	(0) 100 (0)
LSD-0.05-30	(0) 44 (56)	(30) 47 (23)	(0) 5 (95)	(5) 95 (0)
LSD-0.05-50	(0) 69 (31)	(44) 43 (13)	(4) 51 (45)	(6) 94 (0)
LSD-0.1-30	(0) 5 (95)	(91) 8 (1)	(2) 13 (85)	(64) 36 (0)
LSD-0.1-50	(1) 54 (45)	(97) 3 (0)	(45) 36 (19)	(71) 29 (0)
	Bimodal	Quadrinodal	Mult. Bi- modal	Mult. Quadri- modal
MMMM	(0) 100 (0)	(0) 100 (0)	(0) 100 (0)	(0) 100 (0)
MMMC	(0) 100 (0)	(0) 100 (0)	(0) 100 (0)	(0) 100 (0)
KDE-"dun"-30	(0) 99 (1)	(0) 100 (0)	(0) 61 (39)	(1) 61 (38)
KDE-"dun"-50	(0) 99 (1)	(0) 100 (0)	(0) 81 (19)	(5) 85 (10)
KDE-"dsc"-30	(0) 88 (12)	(0) 100 (0)	(0) 67 (33)	(2) 68 (30)
KDE-"dsc"-50	(0) 90 (10)	(0) 100 (0)	(0) 86 (14)	(5) 89 (6)
KDE-"dun"- "ms"	(0) 97 (3)	(0) 100 (0)	(0) 18 (82)	(0) 25 (75)
KDE-"dsc"- "ms"	(0) 79 (21)	(0) 97 (3)	(0) 57 (43)	(0) 66 (34)
LLD-0.05-30	(0) 36 (64)	(0) 80 (20)	(0) 88 (12)	(0) 92 (8)
LLD-0.05-50	(0) 55 (45)	(0) 91 (9)	(0) 99 (1)	(0) 100 (0)
LLD-0.1-30	(0) 98 (2)	(0) 99 (1)	(0) 85 (15)	(0) 93 (7)
LLD-0.1-50	(0) 99 (1)	(0) 100 (0)	(0) 99 (1)	(0) 100 (0)
LSD-0.01-30	(0) 96 (4)	(0) 100 (0)	(13) 48 (39)	(93) 6 (1)
LSD-0.01-50	(0) 98 (2)	(0) 100 (0)	(32) 49 (19)	(99) 1 (0)
LSD-0.05-30	(0) 100 (0)	(0) 100 (0)	(12) 63 (25)	(77) 18 (5)
LSD-0.05-50	(0) 100 (0)	(0) 100 (0)	(29) 66 (5)	(97) 3 (0)
LSD- 10^{-4} -30	/	/	(0) 84 (16)	(71) 11 (18)
LSD- 10^{-4} -50	/	/	(0) 99 (1)	(86) 11 (3)
LSD- 10^{-5} -30	/	/	(0) 82 (18)	(4) 65 (31)
LSD- 10^{-5} -50	/	/	(0) 97 (3)	(11) 82 (7)
	Circular Bimodal I	Circular Bimodal II	Circular Bimodal III	Circular Bimodal IV
MMMM	(0) 0 (100)	(0) 0 (100)	(0) 0 (100)	(0) 0 (100)

MMMC	(0) 0 (100)	(0) 0 (100)	(0) 0 (100)	(0) 0 (100)
KDE-"dun"-30	(0) 45 (55)	(0) 1 (99)	(0) 8 (92)	(0) 4 (96)
KDE-"dun"-50	(0) 55 (45)	(0) 9 (91)	(0) 17 (83)	(0) 20 (80)
KDE-"dsc"-30	(0) 14 (86)	(0) 0 (100)	(0) 1 (99)	(0) 2 (98)
KDE-"dsc"-50	(0) 23 (77)	(0) 1 (99)	(0) 2 (98)	(0) 15 (85)
KDE-"dun"- "ms"	(0) 18 (82)	(0) 0 (100)	(0) 4 (96)	(0) 0 (100)
KDE-"dsc"- "ms"	(0) 3 (97)	(0) 0 (100)	(0) 0 (100)	(0) 0 (100)
LLD-0.05-30	(0) 0 (100)	(0) 0 (100)	(0) 0 (100)	(0) 0 (100)
LLD-0.05-50	(0) 3 (97)	(0) 0 (100)	(0) 0 (100)	(0) 4 (96)
LLD-0.1-30	(0) 12 (88)	(0) 1 (99)	(0) 1 (99)	(0) 2 (98)
LLD-0.1-50	(0) 30 (70)	(0) 3 (97)	(0) 3 (97)	(0) 8 (92)
LLD-0.15-30	(0) 39 (61)	(0) 12 (88)	(0) 13 (87)	(0) 2 (98)
LLD-0.15-50	(0) 57 (43)	(0) 23 (77)	(0) 22 (78)	(0) 11 (89)
LLD-0.2-30	(0) 59 (41)	(0) 26 (74)	(0) 23 (77)	(0) 6 (94)
LLD-0.2-50	(0) 74 (26)	(0) 43 (57)	(0) 43 (57)	(0) 17 (83)
LSD-0.01-30	(0) 20 (80)	(0) 1 (99)	(0) 1 (99)	(0) 1 (99)
LSD-0.01-50	(0) 35 (65)	(0) 3 (97)	(0) 2 (98)	(0) 9 (91)
LSD-0.05-30	(0) 73 (27)	(0) 39 (61)	(0) 41 (59)	(0) 8 (92)
LSD-0.05-50	(0) 95 (5)	(0) 74 (26)	(0) 73 (27)	(0) 23 (77)
	Circular Bimodal V	Circular Quadrinodal I	Circular Quadrinodal II	/
MMMM	(0) 0 (100)	(99) 1 (0)	(100) 0 (0)	/
MMMC	(0) 0 (100)	(99) 1 (0)	(100) 0 (0)	/
KDE-"dun"-30	(0) 3 (97)	(93) 7 (0)	(96) 4 (0)	/
KDE-"dun"-50	(0) 15 (85)	(97) 3 (0)	(100) 0 (0)	/
KDE-"dsc"-30	(0) 2 (98)	(83) 14 (3)	(85) 12 (3)	/
KDE-"dsc"-50	(0) 7 (93)	(92) 7 (1)	(93) 6 (1)	/
KDE-"dun"- "ms"	(0) 0 (100)	(92) 8 (0)	(89) 10 (1)	/
KDE-"dsc"- "ms"	(0) 0 (100)	(68) 20 (12)	(63) 24 (13)	/
LLD-0.05-30	(0) 0 (100)	(6) 18 (76)	(7) 16 (77)	/
LLD-0.05-50	(0) 4 (96)	(18) 43 (39)	(23) 31 (46)	/
LLD-0.1-30	(0) 1 (99)	(61) 33 (6)	(63) 34 (3)	/
LLD-0.1-50	(0) 10 (90)	(78) 20 (2)	(76) 22 (2)	/

LLD-0.15-30	(0) 2 (98)	(78) 21 (1)	(99) 1 (0)	/
LLD-0.15-50	(0) 12 (88)	(87) 13 (0)	(99) 1 (0)	/
LLD-0.2-30	(0) 4 (96)	(100) 0 (0)	(100) 0 (0)	/
LLD-0.2-50	(0) 17 (83)	(100) 0 (0)	(100) 0 (0)	/
LSD-0.01-30	(0) 0 (100)	(65) 32 (3)	(80) 17 (3)	/
LSD-0.01-50	(0) 10 (90)	(80) 20 (0)	(87) 10 (3)	/
LSD-0.05-30	(0) 6 (94)	(100) 0 (0)	(100) 0 (0)	/
LSD-0.05-50	(0) 23 (77)	(100) 0 (0)	(100) 0 (0)	/

Table 10: Number of times over 100 replications with $n = 1000$ samples that the procedure identifies the true number of clusters for the densities (H) Bimodal IV, (K) Trimodal III, (L) Quadrifocal, #10 Fountain, Circular 2, Circular 2 Cauchy, Circular 3, Circular 4 Cauchy, Bimodal, Quadrifocal, Mult. Bimodal, Mult. Quadrifocal, Circular Bimodal I-V, and Quadrifocal I-II. In parentheses the number of times the procedure identifies a lower number of clusters (on the left) and a higher number of clusters (on the right).

Clustering errors (Hausdorff distance)				
	(H) Bimodal IV	(K) Trimodal III	(L) Quadrifocal	#10 Fountain
MMMM	0.00 (0.00)	0.05 (0.09)	0.11 (0.10)	0.23 (0.05)
MMMC	0.00 (0.00)	0.05 (0.09)	0.09 (0.10)	0.12 (0.05)
KDE-"dun"-30	0.01 (0.03)	0.20 (0.20)	0.37 (0.15)	0.07 (0.01)
KDE-"dun"-50	0.01 (0.03)	0.28 (0.21)	0.44 (0.10)	0.07 (0.01)
KDE-"dsc"-30	0.06 (0.12)	0.14 (0.18)	0.30 (0.16)	0.07 (0.01)
KDE-"dsc"-50	0.04 (0.10)	0.23 (0.20)	0.41 (0.12)	0.07 (0.01)
KDE-"dun"- "ms"	0.01 (0.03)	0.10 (0.14)	0.25 (0.16)	0.09 (0.05)
KDE-"dsc"- "ms"	0.12 (0.16)	0.08 (0.10)	0.16 (0.11)	0.13 (0.05)
LLD-0.05-30	0.30 (0.14)	0.18 (0.11)	0.20 (0.09)	0.07 (0.02)
LLD-0.05-50	0.17 (0.15)	0.20 (0.16)	0.29 (0.14)	0.07 (0.01)
LLD-0.1-30	0.06 (0.11)	0.11 (0.16)	0.29 (0.16)	0.06 (0.01)
LLD-0.1-50	0.03 (0.08)	0.20 (0.20)	0.38 (0.14)	0.07 (0.02)
LSD-0.01-30	0.07 (0.12)	0.14 (0.17)	0.31 (0.16)	0.06 (0.01)
LSD-0.01-50	0.04 (0.10)	0.23 (0.20)	0.40 (0.13)	0.07 (0.03)
LSD-0.05-30	0.01 (0.00)	0.32 (0.20)	0.47 (0.02)	0.47 (0.18)
LSD-0.05-50	0.01 (0.00)	0.40 (0.15)	0.48 (0.02)	0.54 (0.20)

Hclust *	0.03 (0.07)	0.15 (0.09)	0.23 (0.09)	0.27 (0.07)
Clustering errors (distance in probability)				
	(H) Bimodal IV	(K) Trimodal III	(L) Quadri-modal	#10 Fountain
MMMM	0.00 (0.00) 0.00 (0.00)	0.04 (0.05) 0.04 (0.08)	0.07 (0.02) 0.08 (0.04)	0.23 (0.09) 0.24 (0.11)
MMMC	0.00 (0.00) 0.00 (0.00)	0.03 (0.02) 0.03 (0.04)	0.05 (0.04) 0.07 (0.06)	0.12 (0.10) 0.13 (0.12)
KDE-"dun"-30	0.01 (0.05) 0.01 (0.08)	0.06 (0.03) 0.08 (0.05)	0.10 (0.02) 0.18 (0.04)	0.07 (0.01) 0.07 (0.01)
KDE-"dun"-50	0.01 (0.05) 0.01 (0.08)	0.07 (0.02) 0.10 (0.05)	0.10 (0.01) 0.19 (0.03)	0.07 (0.01) 0.07 (0.01)
KDE-"dsc"-30	0.09 (0.19) 0.14 (0.29)	0.05 (0.03) 0.07 (0.06)	0.10 (0.03) 0.16 (0.05)	0.07 (0.01) 0.07 (0.01)
KDE-"dsc"-50	0.07 (0.16) 0.10 (0.24)	0.07 (0.04) 0.10 (0.06)	0.10 (0.02) 0.19 (0.03)	0.07 (0.01) 0.07 (0.01)
KDE-"dun"- "ms"	0.01 (0.05) 0.01 (0.08)	0.04 (0.03) 0.05 (0.05)	0.10 (0.07) 0.16 (0.1)	0.22 (0.27) 0.26 (0.32)
KDE-"dsc"- "ms"	0.18 (0.25) 0.27 (0.37)	0.05 (0.04) 0.06 (0.06)	0.12 (0.11) 0.17 (0.16)	0.42 (0.27) 0.52 (0.33)
LLD-0.05-30	0.11 (0.06) 0.21 (0.13)	0.10 (0.07) 0.17 (0.12)	0.28 (0.20) 0.36 (0.27)	0.07 (0.08) 0.08 (0.09)
LLD-0.05-50	0.06 (0.06) 0.12 (0.12)	0.10 (0.09) 0.14 (0.12)	0.15 (0.13) 0.21 (0.13)	0.07 (0.01) 0.07 (0.01)
LLD-0.1-30	0.02 (0.04) 0.04 (0.08)	0.05 (0.05) 0.07 (0.07)	0.10 (0.05) 0.16 (0.06)	0.06 (0.01) 0.06 (0.01)
LLD-0.1-50	0.01 (0.03) 0.02 (0.06)	0.07 (0.06) 0.09 (0.07)	0.10 (0.03) 0.18 (0.04)	0.07 (0.01) 0.07 (0.02)
LSD-0.01-30	0.10 (0.19) 0.15 (0.30)	0.06 (0.05) 0.08 (0.08)	0.10 (0.03) 0.16 (0.05)	0.06 (0.01) 0.06 (0.01)
LSD-0.01-50	0.06 (0.16) 0.09 (0.24)	0.07 (0.05) 0.10 (0.07)	0.10 (0.02) 0.18 (0.04)	0.07 (0.02) 0.07 (0.02)
LSD-0.05-30	0.00 (0.00) 0.01 (0.00)	0.07 (0.02) 0.11 (0.05)	0.11 (0.01) 0.20 (0.02)	0.24 (0.06) 0.44 (0.15)

LSD-0.05-50	0.01 (0.00)	0.08 (0.02)	0.11 (0.01)	0.26 (0.06)
	0.01 (0.00)	0.13 (0.04)	0.20 (0.02)	0.49 (0.14)
Hclust *	0.03 (0.07)	0.15 (0.09)	0.28 (0.10)	0.34 (0.10)

Table 11: Mean of the clustering errors based on Hausdorff distance and distance in probability over 100 replications with $n = 500$ samples for the densities (H) Bimodal IV, (K) Trimodal III, (L) Quadrinodal and #10 Fountain. In parentheses the standard deviation.

Clustering errors (Hausdorff distance)				
	Circular 2	Circular 2 Cauchy	Circular 3	Circular 4 Cauchy
MMMM	0.57 (0.04)	0.57 (0.06)	0.34 (0.03)	0.09 (0.12)
MMMC	0.55 (0.04)	0.55 (0.06)	0.33 (0.02)	0.13 (0.20)
KDE-"dun"-30	0.48 (0.08)	0.36 (0.16)	0.31 (0.05)	0.03 (0.04)
KDE-"dun"-50	0.45 (0.08)	0.29 (0.19)	0.28 (0.06)	0.05 (0.06)
KDE-"dsc"-30	0.52 (0.07)	0.46 (0.09)	0.34 (0.02)	0.03 (0.03)
KDE-"dsc"-50	0.47 (0.07)	0.42 (0.13)	0.32 (0.05)	0.03 (0.03)
KDE-"dun"- "ms"	0.50 (0.08)	0.41 (0.09)	0.32 (0.02)	0.05 (0.07)
KDE-"dsc"- "ms"	0.55 (0.06)	0.51 (0.08)	0.32 (0.02)	0.09 (0.10)
LLD-0.05-30	0.58 (0.05)	0.53 (0.07)	0.34 (0.02)	0.05 (0.06)
LLD-0.05-50	0.53 (0.06)	0.49 (0.06)	0.33 (0.04)	0.03 (0.03)
LLD-0.1-30	0.51 (0.06)	0.46 (0.09)	0.32 (0.04)	0.03 (0.03)
LLD-0.1-50	0.49 (0.06)	0.41 (0.15)	0.30 (0.05)	0.03 (0.03)
LLD-0.15-30	0.45 (0.10)	0.37 (0.17)	0.32 (0.04)	0.04 (0.04)
LLD-0.15-50	0.40 (0.15)	0.30 (0.20)	0.34 (0.08)	0.05 (0.06)
LLD-0.2-30	0.39 (0.16)	0.51 (0.28)	0.38 (0.08)	0.12 (0.12)
LLD-0.2-50	0.31 (0.19)	0.59 (0.28)	0.50 (0.14)	0.16 (0.13)
LSD-0.01-30	0.50 (0.06)	0.45 (0.08)	0.33 (0.03)	0.03 (0.03)
LSD-0.01-50	0.48 (0.08)	0.43 (0.12)	0.31 (0.06)	0.03 (0.03)
LSD-0.05-30	0.28 (0.21)	0.56 (0.29)	0.36 (0.08)	0.15 (0.14)
LSD-0.05-50	0.20 (0.20)	0.60 (0.27)	0.49 (0.14)	0.19 (0.14)
LSD-0.1-30	0.31 (0.20)	0.77 (0.13)	0.46 (0.10)	0.38 (0.19)
LSD-0.1-50	0.25 (0.26)	0.80 (0.07)	0.65 (0.13)	0.44 (0.20)
Hclust *	0.33 (0.12)	0.37 (0.08)	0.37 (0.06)	0.22 (0.07)

Clustering errors (distance in probability)				
	Circular 2	Circular 2 Cauchy	Circular 3	Circular 4 Cauchy
MMMM	0.30 (0.04)	0.40 (0.04)	0.33 (0.06)	0.11 (0.14)
	0.61 (0.06)	0.61 (0.06)	0.59 (0.08)	0.15 (0.20)
MMMC	0.31 (0.04)	0.37 (0.05)	0.32 (0.05)	0.11 (0.12)
	0.61 (0.08)	0.61 (0.07)	0.59 (0.09)	0.16 (0.22)
KDE-"dun"-30	0.32 (0.08)	0.30 (0.19)	0.35 (0.10)	0.04 (0.02)
	0.57 (0.13)	0.45 (0.25)	0.53 (0.16)	0.04 (0.04)
KDE-"dun"-50	0.33 (0.12)	0.25 (0.19)	0.37 (0.13)	0.05 (0.03)
	0.54 (0.16)	0.36 (0.26)	0.49 (0.20)	0.06 (0.05)
KDE-"dsc"-30	0.32 (0.06)	0.33 (0.11)	0.33 (0.06)	0.04 (0.02)
	0.60 (0.10)	0.57 (0.15)	0.55 (0.11)	0.04 (0.02)
KDE-"dsc"-50	0.32 (0.10)	0.32 (0.16)	0.37 (0.11)	0.04 (0.02)
	0.55 (0.14)	0.50 (0.20)	0.53 (0.15)	0.04 (0.03)
KDE-"dun"- "ms"	0.30 (0.06)	0.30 (0.09)	0.32 (0.06)	0.09 (0.18)
	0.59 (0.11)	0.57 (0.16)	0.55 (0.12)	0.10 (0.20)
KDE-"dsc"- "ms"	0.31 (0.04)	0.31 (0.06)	0.29 (0.03)	0.18 (0.23)
	0.62 (0.08)	0.61 (0.1)	0.56 (0.07)	0.22 (0.28)
LLD-0.05-30	0.34 (0.04)	0.33 (0.07)	0.34 (0.05)	0.09 (0.17)
	0.65 (0.07)	0.62 (0.09)	0.59 (0.09)	0.11 (0.21)
LLD-0.05-50	0.33 (0.07)	0.34 (0.10)	0.37 (0.09)	0.05 (0.07)
	0.59 (0.10)	0.58 (0.10)	0.56 (0.13)	0.05 (0.09)
LLD-0.1-30	0.32 (0.06)	0.34 (0.14)	0.35 (0.08)	0.03 (0.02)
	0.59 (0.10)	0.54 (0.15)	0.54 (0.13)	0.03 (0.02)
LLD-0.1-50	0.34 (0.10)	0.32 (0.17)	0.39 (0.12)	0.04 (0.02)
	0.57 (0.12)	0.48 (0.20)	0.52 (0.18)	0.04 (0.03)
LLD-0.15-30	0.32 (0.12)	0.31 (0.19)	0.38 (0.09)	0.05 (0.03)
	0.54 (0.16)	0.45 (0.24)	0.53 (0.14)	0.05 (0.04)
LLD-0.15-50	0.30 (0.16)	0.25 (0.19)	0.40 (0.09)	0.05 (0.03)
	0.47 (0.22)	0.34 (0.25)	0.46 (0.12)	0.06 (0.04)
LLD-0.2-30	0.29 (0.17)	0.23 (0.19)	0.44 (0.09)	0.09 (0.05)
	0.46 (0.23)	0.30 (0.20)	0.51 (0.10)	0.12 (0.10)
LLD-0.2-50	0.26 (0.20)	0.19 (0.17)	0.37 (0.07)	0.10 (0.06)
	0.37 (0.27)	0.25 (0.16)	0.50 (0.08)	0.16 (0.12)

LSD-0.01-30	0.32 (0.09) 0.58 (0.11)	0.34 (0.13) 0.54 (0.15)	0.34 (0.09) 0.54 (0.13)	0.03 (0.02) 0.04 (0.02)
LSD-0.01-50	0.34 (0.11) 0.56 (0.13)	0.33 (0.16) 0.51 (0.18)	0.37 (0.11) 0.50 (0.17)	0.04 (0.02) 0.04 (0.03)
LSD-0.05-30	0.22 (0.19) 0.33 (0.26)	0.20 (0.18) 0.25 (0.16)	0.43 (0.10) 0.51 (0.13)	0.10 (0.06) 0.16 (0.12)
LSD-0.05-50	0.16 (0.18) 0.22 (0.25)	0.19 (0.17) 0.25 (0.15)	0.36 (0.08) 0.48 (0.08)	0.12 (0.06) 0.19 (0.13)
LSD-0.1-30	0.27 (0.17) 0.41 (0.28)	0.13 (0.11) 0.21 (0.08)	0.48 (0.10) 0.54 (0.10)	0.23 (0.08) 0.43 (0.17)
LSD-0.1-50	0.16 (0.15) 0.22 (0.23)	0.10 (0.06) 0.19 (0.05)	0.34 (0.07) 0.56 (0.06)	0.25 (0.07) 0.49 (0.16)
Hclust *	0.33 (0.12)	0.37 (0.08)	0.44 (0.06)	0.31 (0.11)

Table 12: Mean of the clustering errors based on Hausdorff distance and distance in probability over 100 replications with $n = 500$ samples for the densities Circular 2, Circular 2 Cauchy, Circular 3 and Circular 4 Cauchy. In parentheses the standard deviation.

Clustering errors (Hausdorff distance)					
	Bimodal	Quadrinodal	Mult. Bi- modal	Bi- modal	Mult. Quadri- modal
MMMM	0.00 (0.00)	0.01 (0.00)	0.00 (0.00)	0.01 (0.00)	
MMMC	0.00 (0.00)	0.01 (0.00)	0.00 (0.00)	0.01 (0.00)	
KDE-"dun"-30	0.01 (0.04)	0.01 (0.01)	0.13 (0.16)	0.11 (0.09)	
KDE-"dun"-50	0.01 (0.04)	0.02 (0.01)	0.07 (0.12)	0.14 (0.12)	
KDE-"dsc"-30	0.04 (0.10)	0.02 (0.02)	0.11 (0.15)	0.11 (0.09)	
KDE-"dsc"-50	0.02 (0.06)	0.01 (0.01)	0.07 (0.12)	0.13 (0.11)	
KDE-"dun"- "ms"	0.02 (0.06)	0.01 (0.01)	0.49 (0.01)	0.23 (0.03)	
KDE-"dsc"- "ms"	0.10 (0.16)	0.02 (0.03)	0.45 (0.1)	0.20 (0.06)	
LLD-0.05-30	0.26 (0.17)	0.05 (0.06)	0.03 (0.06)	0.04 (0.03)	
LLD-0.05-50	0.12 (0.16)	0.02 (0.04)	0.02 (0.03)	0.05 (0.06)	
LLD-0.1-30	0.05 (0.10)	0.01 (0.01)	0.03 (0.07)	0.05 (0.06)	
LLD-0.1-50	0.02 (0.06)	0.01 (0.01)	0.02 (0.03)	0.06 (0.08)	
LSD-0.01-30	0.04 (0.09)	0.01 (0.01)	0.40 (0.17)	0.67 (0.15)	
LSD-0.01-50	0.02 (0.07)	0.01 (0.01)	0.46 (0.14)	0.74 (0.10)	

LSD-0.05-30	0.01 (0.00)	0.01 (0.01)	0.35 (0.21)	0.52 (0.19)
LSD-0.05-50	0.01 (0.01)	0.02 (0.03)	0.40 (0.19)	0.62 (0.19)
LSD- 10^{-4} -30	/	/	0.03 (0.07)	0.48 (0.17)
LSD- 10^{-4} -50	/	/	0.04 (0.09)	0.55 (0.17)
LSD- 10^{-5} -30	/	/	0.03 (0.06)	0.20 (0.14)
LSD- 10^{-5} -50	/	/	0.03 (0.05)	0.27 (0.15)
Hclust *	0.08 (0.07)	0.08 (0.05)	0.05 (0.02)	0.07 (0.04)
Clustering errors (distance in probability)				
	Bimodal	Quadrinodal	Mult. Bi-modal	Mult. Quadrinodal
MMMM	0.00 (0.00) 0.00 (0.00)	0.01 (0.00) 0.01 (0.00)	0.00 (0.00) 0.00 (0.00)	0.01 (0.00) 0.01 (0.00)
MMMC	0.00 (0.00) 0.00 (0.00)	0.01 (0.00) 0.01 (0.00)	0.00 (0.00) 0.00 (0.00)	0.01 (0.00) 0.01 (0.00)
KDE-" dun "-30	0.01 (0.02) 0.01 (0.03)	0.02 (0.01) 0.02 (0.01)	0.06 (0.07) 0.09 (0.12)	0.23 (0.26) 0.27 (0.31)
KDE-" dun "-50	0.01 (0.02) 0.01 (0.03)	0.02 (0.01) 0.02 (0.01)	0.05 (0.06) 0.06 (0.10)	0.13 (0.12) 0.17 (0.16)
KDE-" dsc "-30	0.02 (0.04) 0.03 (0.07)	0.02 (0.04) 0.03 (0.06)	0.05 (0.07) 0.08 (0.11)	0.23 (0.27) 0.27 (0.32)
KDE-" dsc "-50	0.01 (0.02) 0.02 (0.04)	0.02 (0.01) 0.02 (0.01)	0.05 (0.07) 0.06 (0.10)	0.12 (0.09) 0.15 (0.13)
KDE-" dun "-" ms "	0.01 (0.02) 0.02 (0.05)	0.02 (0.02) 0.02 (0.03)	0.12 (0.07) 0.21 (0.13)	0.44 (0.13) 0.68 (0.15)
KDE-" dsc "-" ms "	0.03 (0.05) 0.06 (0.09)	0.03 (0.07) 0.04 (0.09)	0.08 (0.07) 0.13 (0.12)	0.52 (0.22) 0.68 (0.27)
LLD-0.05-30	0.08 (0.06) 0.14 (0.11)	0.09 (0.17) 0.12 (0.21)	0.02 (0.02) 0.02 (0.04)	0.04 (0.02) 0.04 (0.02)
LLD-0.05-50	0.04 (0.05) 0.08 (0.11)	0.03 (0.05) 0.04 (0.08)	0.02 (0.01) 0.02 (0.02)	0.06 (0.03) 0.06 (0.06)
LLD-0.1-30	0.02 (0.03) 0.03 (0.07)	0.02 (0.01) 0.02 (0.01)	0.02 (0.03) 0.02 (0.05)	0.05 (0.03) 0.06 (0.06)
LLD-0.1-50	0.01 (0.02) 0.02 (0.04)	0.02 (0.01) 0.02 (0.01)	0.01 (0.01) 0.02 (0.02)	0.06 (0.04) 0.07 (0.07)

LSD-0.01-30	0.02 (0.03) 0.03 (0.07)	0.02 (0.01) 0.02 (0.01)	0.22 (0.06) 0.37 (0.15)	0.34 (0.05) 0.66 (0.10)
LSD-0.01-50	0.01 (0.02) 0.02 (0.05)	0.02 (0.01) 0.02 (0.01)	0.23 (0.05) 0.43 (0.12)	0.36 (0.03) 0.71 (0.06)
LSD-0.05-30	0.01 (0.00) 0.01 (0.00)	0.02 (0.01) 0.02 (0.01)	0.19 (0.08) 0.32 (0.19)	0.30 (0.07) 0.54 (0.15)
LSD-0.05-50	0.01 (0.01) 0.01 (0.01)	0.02 (0.01) 0.02 (0.02)	0.20 (0.07) 0.38 (0.17)	0.32 (0.05) 0.63 (0.12)
LSD- 10^{-4} -30	/ /	/ /	0.03 (0.03) 0.03 (0.06)	0.29 (0.08) 0.52 (0.14)
LSD- 10^{-4} -50	/ /	/ /	0.03 (0.04) 0.04 (0.08)	0.30 (0.06) 0.57 (0.12)
LSD- 10^{-5} -30	/ /	/ /	0.02 (0.02) 0.02 (0.02)	0.17 (0.13) 0.23 (0.18)
LSD- 10^{-5} -50	/ /	/ /	0.02 (0.03) 0.03 (0.05)	0.18 (0.09) 0.29 (0.16)
Hclust *	0.08 (0.07)	0.11 (0.07)	0.05 (0.02)	0.10 (0.05)

Table 13: Mean of the clustering errors based on Hausdorff distance and distance in probability over 100 replications with $n = 500$ samples for the densities Bimodal, Quadrinodal, Mult. Bimodal and Mult. Quadrinodal. In parentheses the standard deviation.

Clustering errors (Hausdorff distance)				
	Circular Bimodal I	Circular Bimodal II	Circular Bimodal III	Circular Bimodal IV
MMMM	0.42 (0.04)	0.53 (0.04)	0.53 (0.04)	0.22 (0.06)
MMMC	0.44 (0.03)	0.52 (0.04)	0.51 (0.04)	0.23 (0.05)
KDE-" <i>dun</i> "-30	0.19 (0.17)	0.42 (0.11)	0.39 (0.15)	0.17 (0.05)
KDE-" <i>dun</i> "-50	0.14 (0.14)	0.35 (0.18)	0.34 (0.19)	0.25 (0.23)
KDE-" <i>dsc</i> "-30	0.29 (0.14)	0.45 (0.06)	0.46 (0.07)	0.18 (0.05)
KDE-" <i>dsc</i> "-50	0.21 (0.16)	0.42 (0.12)	0.44 (0.10)	0.22 (0.20)
KDE-" <i>dun</i> "-" <i>ms</i> "	0.38 (0.16)	0.43 (0.07)	0.42 (0.10)	0.23 (0.02)
KDE-" <i>dsc</i> "-" <i>ms</i> "	0.43 (0.11)	0.47 (0.07)	0.46 (0.07)	0.24 (0.02)
LLD-0.05-30	0.42 (0.05)	0.53 (0.05)	0.53 (0.05)	0.30 (0.13)
LLD-0.05-50	0.34 (0.10)	0.48 (0.04)	0.48 (0.04)	0.22 (0.15)

LLD-0.1-30	0.32 (0.14)	0.47 (0.06)	0.47 (0.06)	0.19 (0.06)
LLD-0.1-50	0.23 (0.16)	0.44 (0.10)	0.44 (0.10)	0.19 (0.17)
LLD-0.15-30	0.24 (0.16)	0.40 (0.15)	0.40 (0.16)	0.17 (0.05)
LLD-0.15-50	0.13 (0.14)	0.35 (0.18)	0.35 (0.19)	0.20 (0.18)
LLD-0.2-30	0.16 (0.15)	0.30 (0.20)	0.31 (0.20)	0.16 (0.05)
LLD-0.2-50	0.08 (0.10)	0.21 (0.20)	0.21 (0.21)	0.28 (0.25)
LSD-0.01-30	0.30 (0.14)	0.46 (0.08)	0.46 (0.09)	0.20 (0.08)
LSD-0.01-50	0.20 (0.15)	0.44 (0.09)	0.43 (0.11)	0.19 (0.16)
LSD-0.05-30	0.10 (0.13)	0.20 (0.20)	0.21 (0.21)	0.16 (0.05)
LSD-0.05-50	0.07 (0.08)	0.12 (0.15)	0.10 (0.15)	0.38 (0.29)
Hclust *	0.36 (0.10)	0.34 (0.12)	0.03 (0.03)	0.29 (0.12)

Clustering errors (distance in probability)

	Circular Bimodal I	Circular Bimodal II	Circular Bimodal III	Circular Bimodal IV
MMMM	0.16 (0.03)	0.29 (0.03)	0.29 (0.03)	0.08 (0.04)
	0.30 (0.06)	0.56 (0.06)	0.56 (0.06)	0.15 (0.08)
MMMC	0.15 (0.05)	0.27 (0.03)	0.28 (0.03)	0.09 (0.08)
	0.29 (0.09)	0.53 (0.05)	0.54 (0.06)	0.17 (0.15)
KDE-"dun"-30	0.06 (0.06)	0.09 (0.07)	0.11 (0.08)	0.04 (0.01)
	0.18 (0.18)	0.33 (0.10)	0.30 (0.13)	0.19 (0.18)
KDE-"dun"-50	0.06 (0.06)	0.11 (0.08)	0.11 (0.08)	0.07 (0.02)
	0.13 (0.17)	0.26 (0.15)	0.25 (0.15)	0.16 (0.17)
KDE-"dsc"-30	0.09 (0.06)	0.06 (0.05)	0.08 (0.07)	0.03 (0.01)
	0.29 (0.16)	0.34 (0.07)	0.34 (0.07)	0.20 (0.18)
KDE-"dsc"-50	0.07 (0.06)	0.10 (0.07)	0.11 (0.07)	0.07 (0.02)
	0.21 (0.18)	0.31 (0.11)	0.32 (0.09)	0.14 (0.16)
KDE-"dun"- "ms"	0.08 (0.06)	0.19 (0.06)	0.16 (0.07)	0.09 (0.04)
	0.15 (0.13)	0.37 (0.11)	0.31 (0.14)	0.18 (0.08)
KDE-"dsc"- "ms"	0.12 (0.06)	0.23 (0.05)	0.22 (0.06)	0.09 (0.04)
	0.24 (0.11)	0.46 (0.10)	0.43 (0.11)	0.19 (0.08)
LLD-0.05-30	0.20 (0.06)	0.28 (0.04)	0.28 (0.04)	0.17 (0.10)
	0.38 (0.12)	0.54 (0.07)	0.54 (0.07)	0.30 (0.21)
LLD-0.05-50	0.15 (0.07)	0.25 (0.05)	0.24 (0.05)	0.18 (0.13)
	0.27 (0.13)	0.47 (0.08)	0.46 (0.09)	0.28 (0.26)

LLD-0.1-30	0.12 (0.07) 0.21 (0.12)	0.23 (0.06) 0.43 (0.11)	0.23 (0.06) 0.43 (0.11)	0.17 (0.15) 0.28 (0.30)
LLD-0.1-50	0.10 (0.07) 0.17 (0.13)	0.21 (0.08) 0.37 (0.13)	0.20 (0.08) 0.36 (0.13)	0.16 (0.12) 0.23 (0.25)
LLD-0.15-30	0.10 (0.07) 0.16 (0.13)	0.19 (0.09) 0.33 (0.16)	0.18 (0.09) 0.32 (0.16)	0.17 (0.16) 0.28 (0.30)
LLD-0.15-50	0.07 (0.06) 0.10 (0.11)	0.16 (0.09) 0.28 (0.16)	0.16 (0.10) 0.27 (0.17)	0.16 (0.09) 0.20 (0.19)
LLD-0.2-30	0.08 (0.07) 0.12 (0.13)	0.14 (0.09) 0.24 (0.17)	0.14 (0.09) 0.24 (0.17)	0.17 (0.16) 0.28 (0.31)
LLD-0.2-50	0.06 (0.04) 0.07 (0.07)	0.11 (0.08) 0.17 (0.15)	0.10 (0.08) 0.16 (0.16)	0.15 (0.05) 0.18 (0.09)
LSD-0.01-30	0.11 (0.07) 0.20 (0.13)	0.22 (0.07) 0.41 (0.12)	0.22 (0.07) 0.41 (0.12)	0.18 (0.15) 0.30 (0.29)
LSD-0.01-50	0.10 (0.08) 0.16 (0.15)	0.20 (0.08) 0.37 (0.13)	0.19 (0.08) 0.35 (0.13)	0.17 (0.12) 0.22 (0.23)
LSD-0.05-30	0.06 (0.04) 0.08 (0.09)	0.10 (0.08) 0.17 (0.16)	0.10 (0.08) 0.17 (0.17)	0.16 (0.14) 0.24 (0.27)
LSD-0.05-50	0.05 (0.03) 0.06 (0.06)	0.07 (0.06) 0.10 (0.12)	0.06 (0.06) 0.09 (0.12)	0.15 (0.07) 0.21 (0.12)
Hclust *	0.18 (0.05)	0.17 (0.06)	0.02 (0.02)	0.15 (0.06)

Table 14: Mean of the clustering errors based on Hausdorff distance and distance in probability over 100 replications with $n = 500$ samples for the densities Circular Bimodal I-IV. In parentheses the standard deviation.

Clustering errors (Hausdorff distance)			
	Circular Bimodal V	Circular Quadrinodal I	Circular Quadrinodal II
MMMM	0.23 (0.07)	0.76 (0.07)	0.77 (0.01)
MMMC	0.24 (0.06)	0.76 (0.07)	0.77 (0.01)
KDE-"dun"-30	0.16 (0.06)	0.46 (0.20)	0.59 (0.20)
KDE-"dun"-50	0.09 (0.06)	0.50 (0.21)	0.64 (0.19)
KDE-"dsc"-30	0.17 (0.05)	0.34 (0.14)	0.45 (0.19)

KDE-" dsc "-50	0.09 (0.07)	0.41 (0.18)	0.50 (0.20)
KDE-" dun "-" ms "	0.23 (0.02)	0.42 (0.18)	0.53 (0.22)
KDE-" dsc "-" ms "	0.23 (0.02)	0.29 (0.12)	0.36 (0.16)
LLD-0.05-30	0.29 (0.13)	0.22 (0.08)	0.23 (0.07)
LLD-0.05-50	0.19 (0.18)	0.26 (0.12)	0.26 (0.11)
LLD-0.1-30	0.17 (0.06)	0.30 (0.13)	0.36 (0.19)
LLD-0.1-50	0.09 (0.08)	0.36 (0.15)	0.43 (0.20)
LLD-0.15-30	0.15 (0.06)	0.45 (0.18)	0.68 (0.16)
LLD-0.15-50	0.08 (0.06)	0.51 (0.20)	0.71 (0.14)
LLD-0.2-30	0.14 (0.07)	0.68 (0.16)	0.75 (0.10)
LLD-0.2-50	0.07 (0.06)	0.72 (0.13)	0.77 (0.05)
LSD-0.01-30	0.19 (0.09)	0.34 (0.13)	0.38 (0.17)
LSD-0.01-50	0.10 (0.10)	0.38 (0.15)	0.46 (0.21)
LSD-0.05-30	0.14 (0.07)	0.69 (0.17)	0.73 (0.11)
LSD-0.05-50	0.07 (0.05)	0.69 (0.16)	0.75 (0.09)
Hclust *	0.01 (0.02)	0.30 (0.13)	0.36 (0.12)
Clustering errors (distance in probability)			
	Circular Bimodal V	Circular Quadriformal I	Circular Quadriformal II
MMMM	0.09 (0.06) 0.17 (0.12)	0.36 (0.03) 0.72 (0.06)	0.36 (0.01) 0.73 (0.01)
MMMC	0.09 (0.07) 0.17 (0.14)	0.36 (0.02) 0.72 (0.05)	0.36 (0.01) 0.73 (0.01)
KDE-" dun "-30	0.04 (0.02) 0.28 (0.19)	0.04 (0.05) 0.29 (0.13)	0.07 (0.05) 0.37 (0.13)
KDE-" dun "-50	0.03 (0.02) 0.13 (0.18)	0.05 (0.05) 0.33 (0.13)	0.08 (0.05) 0.41 (0.12)
KDE-" dsc "-30	0.04 (0.02) 0.31 (0.19)	0.01 (0.03) 0.19 (0.11)	0.03 (0.04) 0.25 (0.13)
KDE-" dsc "-50	0.03 (0.02) 0.14 (0.19)	0.03 (0.04) 0.24 (0.13)	0.05 (0.05) 0.31 (0.14)
KDE-" dun "-" ms "	0.10 (0.07) 0.19 (0.13)	0.27 (0.07) 0.50 (0.14)	0.32 (0.08) 0.58 (0.15)

KDE-" dsc "-" ms "	0.10 (0.06) 0.20 (0.13)	0.28 (0.11) 0.38 (0.14)	0.34 (0.11) 0.45 (0.14)
LLD-0.05-30	0.14 (0.09) 0.27 (0.19)	0.34 (0.17) 0.43 (0.20)	0.36 (0.16) 0.48 (0.18)
LLD-0.05-50	0.09 (0.08) 0.15 (0.15)	0.25 (0.11) 0.34 (0.14)	0.27 (0.13) 0.35 (0.16)
LLD-0.1-30	0.09 (0.10) 0.16 (0.17)	0.22 (0.06) 0.35 (0.14)	0.25 (0.09) 0.40 (0.18)
LLD-0.1-50	0.06 (0.07) 0.08 (0.13)	0.24 (0.06) 0.41 (0.14)	0.26 (0.08) 0.46 (0.18)
LLD-0.15-30	0.08 (0.08) 0.14 (0.15)	0.26 (0.07) 0.48 (0.16)	0.34 (0.05) 0.66 (0.12)
LLD-0.15-50	0.06 (0.08) 0.09 (0.14)	0.29 (0.06) 0.56 (0.14)	0.35 (0.04) 0.69 (0.10)
LLD-0.2-30	0.07 (0.07) 0.12 (0.13)	0.34 (0.05) 0.66 (0.11)	0.36 (0.02) 0.71 (0.05)
LLD-0.2-50	0.06 (0.08) 0.09 (0.14)	0.35 (0.04) 0.70 (0.09)	0.36 (0.01) 0.73 (0.03)
LSD-0.01-30	0.10 (0.09) 0.17 (0.17)	0.23 (0.05) 0.39 (0.13)	0.25 (0.08) 0.43 (0.16)
LSD-0.01-50	0.07 (0.08) 0.10 (0.16)	0.24 (0.05) 0.43 (0.13)	0.27 (0.07) 0.50 (0.17)
LSD-0.05-30	0.07 (0.08) 0.12 (0.15)	0.34 (0.04) 0.68 (0.10)	0.36 (0.03) 0.71 (0.07)
LSD-0.05-50	0.06 (0.05) 0.07 (0.09)	0.34 (0.04) 0.68 (0.10)	0.36 (0.02) 0.72 (0.05)
Hclust *	0.01 (0.01)	0.02 (0.02)	0.03 (0.02)

Table 15: Mean of the clustering errors based on Hausdorff distance and distance in probability over 100 replications with $n = 500$ samples for the densities Circular Bimodal V and Circular Quadrinodal I-II. In parentheses the standard deviation.

Number of times the true clusters are detected correctly				
	(H) Bimodal IV	(K) Trimodal III	(L) Quadri-modal	#10 Fountain

MMMM	(0) 100 (0)	(4) 93 (3)	(37) 63 (0)	(5) 93 (2)
MMMC	(0) 100 (0)	(4) 93 (3)	(37) 62 (1)	(5) 93 (2)
KDE-"dun"-30	(0) 99 (1)	(39) 60 (1)	(97) 3 (0)	(0) 100 (0)
KDE-"dun"-50	(0) 99 (1)	(58) 42 (0)	(100) 0 (0)	(0) 100 (0)
KDE-"dsc"-30	(0) 82 (18)	(22) 73 (5)	(90) 10 (0)	(0) 100 (0)
KDE-"dsc"-50	(0) 88 (12)	(45) 54 (1)	(100) 0 (0)	(0) 100 (0)
KDE-"dun"- "ms"	(0) 99 (1)	(13) 80 (7)	(78) 20 (2)	(0) 72 (28)
KDE-"dsc"- "ms"	(0) 65 (35)	(4) 72 (24)	(54) 35 (11)	(0) 31 (69)
LLD-0.05-30	(0) 15 (85)	(0) 34 (66)	(24) 32 (44)	(0) 99 (1)
LLD-0.05-50	(0) 45 (55)	(17) 50 (33)	(79) 16 (5)	(0) 100 (0)
LLD-0.1-30	(0) 82 (18)	(14) 78 (8)	(88) 11 (1)	(0) 100 (0)
LLD-0.1-50	(0) 92 (8)	(37) 63 (0)	(99) 1 (0)	(1) 99 (0)
LSD-0.01-30	(0) 80 (20)	(18) 69 (13)	(89) 11 (0)	(0) 100 (0)
LSD-0.01-50	(0) 88 (12)	(41) 55 (4)	(100) 0 (0)	(2) 98 (0)
LSD-0.05-30	(0) 100 (0)	(67) 33 (0)	(100) 0 (0)	(96) 4 (0)
LSD-0.05-50	(0) 100 (0)	(84) 16 (0)	(100) 0 (0)	(99) 1 (0)
	Circular 2 Cauchy	Circular 2 Cauchy	Circular 3	Circular 4 Cauchy
MMMM	(0) 0 (100)	(0) 0 (100)	(0) 0 (100)	(13) 76 (4)
MMMC	(0) 0 (100)	(0) 0 (100)	(0) 0 (100)	(19) 77 (4)
KDE-"dun"-30	(0) 0 (100)	(0) 18 (82)	(0) 4 (96)	(2) 98 (0)
KDE-"dun"-50	(0) 1 (99)	(0) 36 (64)	(1) 26 (73)	(5) 95 (0)
KDE-"dsc"-30	(0) 0 (100)	(0) 2 (98)	(0) 0 (100)	(1) 99 (0)
KDE-"dsc"-50	(0) 1 (99)	(0) 8 (92)	(0) 6 (94)	(1) 99 (0)
KDE-"dun"- "ms"	(0) 0 (100)	(0) 0 (100)	(0) 0 (100)	(2) 88 (10)
KDE-"dsc"- "ms"	(0) 0 (100)	(0) 0 (100)	(0) 0 (100)	(1) 65 (34)
LLD-0.05-30	(0) 0 (100)	(0) 0 (100)	(0) 0 (100)	(1) 86 (13)
LLD-0.05-50	(0) 0 (100)	(0) 0 (100)	(0) 1 (99)	(1) 97 (2)
LLD-0.1-30	(0) 0 (100)	(0) 3 (97)	(0) 2 (98)	(1) 99 (0)
LLD-0.1-50	(0) 0 (100)	(0) 13 (87)	(0) 11 (89)	(1) 99 (0)
LLD-0.15-30	(0) 3 (97)	(0) 21 (79)	(0) 7 (93)	(3) 97 (0)
LLD-0.15-50	(0) 15 (85)	(0) 43 (57)	(8) 47 (45)	(4) 96 (0)
LLD-0.2-30	(0) 15 (85)	(35) 38 (27)	(10) 38 (52)	(32) 68 (0)
LLD-0.2-50	(0) 35 (65)	(53) 36 (11)	(71) 24 (5)	(44) 56 (0)

LSD-0.01-30	(0) 0 (100)	(0) 2 (98)	(0) 1 (99)	(1) 99 (0)
LSD-0.01-50	(0) 1 (99)	(0) 8 (92)	(0) 12 (88)	(1) 99 (0)
LSD-0.05-30	(0) 41 (59)	(48) 43 (9)	(9) 35 (56)	(43) 57 (0)
LSD-0.05-50	(0) 63 (37)	(55) 38 (7)	(71) 29 (0)	(54) 46 (0)
LSD-0.1-30	(3) 34 (63)	(89) 11 (0)	(22) 51 (27)	(92) 8 (0)
LSD-0.1-50	(12) 65 (23)	(97) 3 (0)	(94) 6 (0)	(93) 7 (0)
	Bimodal	Quadrinodal	Mult. Bi-modal	Mult. Quadrinodal
MMMM	(0) 100 (0)	(0) 100 (0)	(0) 100 (0)	(0) 100 (0)
MMMC	(0) 100 (0)	(0) 100 (0)	(0) 100 (0)	(0) 100 (0)
KDE-" <i>dun</i> "-30	(0) 98 (2)	(0) 100 (0)	(2) 72 (26)	(8) 70 (22)
KDE-" <i>dun</i> "-50	(0) 98 (2)	(0) 100 (0)	(3) 88 (9)	(28) 69 (3)
KDE-" <i>dsc</i> "-30	(0) 88 (12)	(0) 97 (3)	(2) 78 (20)	(9) 68 (23)
KDE-" <i>dsc</i> "-50	(0) 96 (4)	(0) 100 (0)	(3) 90 (7)	(26) 73 (1)
KDE-" <i>dun</i> "-" <i>ms</i> "	(0) 96 (4)	(0) 99 (1)	(0) 0 (100)	(0) 2 (98)
KDE-" <i>dsc</i> "-" <i>ms</i> "	(0) 74 (26)	(0) 95 (5)	(0) 5 (95)	(0) 13 (87)
LLD-0.05-30	(0) 29 (71)	(0) 78 (22)	(0) 95 (5)	(0) 97 (3)
LLD-0.05-50	(0) 65 (35)	(0) 94 (6)	(0) 99 (1)	(6) 94 (0)
LLD-0.1-30	(0) 87 (13)	(0) 100 (0)	(0) 94 (6)	(6) 94 (0)
LLD-0.1-50	(0) 96 (4)	(0) 100 (0)	(0) 99 (1)	(10) 90 (0)
LSD-0.01-30	(0) 90 (10)	(0) 100 (0)	(61) 36 (3)	(100) 0 (0)
LSD-0.01-50	(0) 95 (5)	(0) 100 (0)	(85) 15 (0)	(100) 0 (0)
LSD-0.05-30	(0) 100 (0)	(0) 100 (0)	(56) 42 (2)	(96) 4 (0)
LSD-0.05-50	(0) 100 (0)	(1) 99 (0)	(73) 27 (0)	(100) 0 (0)
LSD- 10^{-4} -30	/	/	(1) 97 (2)	(94) 5 (1)
LSD- 10^{-4} -50	/	/	(3) 97 (0)	(98) 2 (0)
LSD- 10^{-5} -30	/	/	(0) 97 (3)	(43) 53 (4)
LSD- 10^{-5} -50	/	/	(1) 99 (0)	(67) 32 (1)
	Circular Bimodal I	Circular Bimodal II	Circular Bimodal III	Circular Bimodal IV
MMMM	(0) 0 (100)	(0) 0 (100)	(0) 0 (100)	(0) 0 (100)
MMMC	(0) 0 (100)	(0) 0 (100)	(0) 0 (100)	(0) 0 (100)
KDE-" <i>dun</i> "-30	(0) 51 (49)	(0) 6 (94)	(0) 13 (87)	(0) 20 (80)
KDE-" <i>dun</i> "-50	(0) 67 (33)	(0) 25 (75)	(0) 26 (74)	(16) 71 (13)

KDE-" dsc "-30	(0) 21 (79)	(0) 1 (99)	(0) 2 (98)	(0) 16 (84)
KDE-" dsc "-50	(0) 44 (56)	(0) 8 (92)	(0) 5 (95)	(12) 71 (17)
KDE-" dun "-" ms "	(0) 15 (85)	(0) 0 (100)	(0) 4 (96)	(0) 0 (100)
KDE-" dsc "-" ms "	(0) 5 (95)	(0) 0 (100)	(0) 1 (99)	(0) 0 (100)
LLD-0.05-30	(0) 0 (100)	(0) 0 (100)	(0) 0 (100)	(0) 2 (98)
LLD-0.05-50	(0) 8 (92)	(0) 0 (100)	(0) 0 (100)	(0) 41 (59)
LLD-0.1-30	(0) 16 (84)	(0) 1 (99)	(0) 1 (99)	(0) 8 (92)
LLD-0.1-50	(0) 37 (63)	(0) 5 (95)	(0) 5 (95)	(7) 65 (28)
LLD-0.15-30	(0) 36 (64)	(0) 14 (86)	(0) 15 (85)	(0) 14 (86)
LLD-0.15-50	(0) 71 (29)	(0) 25 (75)	(0) 26 (74)	(9) 75 (16)
LLD-0.2-30	(0) 59 (41)	(0) 36 (64)	(0) 35 (65)	(0) 25 (75)
LLD-0.2-50	(0) 86 (14)	(0) 60 (40)	(0) 58 (42)	(20) 75 (5)
LSD-0.01-30	(0) 19 (81)	(0) 2 (98)	(0) 3 (97)	(0) 8 (92)
LSD-0.01-50	(0) 45 (55)	(0) 4 (96)	(0) 7 (93)	(5) 69 (26)
LSD-0.05-30	(0) 78 (22)	(0) 60 (40)	(0) 57 (43)	(0) 35 (65)
LSD-0.05-50	(0) 90 (10)	(0) 83 (17)	(0) 84 (16)	(37) 59 (4)
	Circular Bimodal V	Circular Quadrinodal I	Circular Quadrinodal II	/
MMMM	(0) 0 (100)	(100) 0 (0)	(100) 0 (0)	/
MMMC	(0) 0 (100)	(100) 0 (0)	(100) 0 (0)	/
KDE-" dun "-30	(0) 15 (85)	(100) 0 (0)	(100) 0 (0)	/
KDE-" dun "-50	(0) 64 (36)	(100) 0 (0)	(100) 0 (0)	/
KDE-" dsc "-30	(0) 8 (92)	(90) 10 (0)	(98) 2 (0)	/
KDE-" dsc "-50	(0) 60 (40)	(98) 2 (0)	(99) 1 (0)	/
KDE-" dun "-" ms "	(0) 0 (100)	(99) 1 (0)	(94) 5 (1)	/
KDE-" dsc "-" ms "	(0) 0 (100)	(61) 32 (7)	(53) 34 (13)	/
LLD-0.05-30	(0) 2 (98)	(19) 36 45	(12) 20 (68)	/
LLD-0.05-50	(0) 44 (56)	(54) 38 (8)	(48) 38 (14)	/
LLD-0.1-30	(0) 8 (92)	(79) 19 (2)	(76) 23 (1)	/
LLD-0.1-50	(0) 62 (38)	(94) 6 (0)	(91) 9 (0)	/
LLD-0.15-30	(0) 14 (86)	(98) 2 (0)	(100) 0 (0)	/
LLD-0.15-50	(0) 68 (32)	(100) 0 (0)	(100) 0 (0)	/
LLD-0.2-30	(0) 24 (76)	(100) 0 (0)	(100) 0 (0)	/

LLD-0.2-50	(0) 72 (28)	(100) 0 (0)	(100) 0 (0)	/
LSD-0.01-30	(0) 7 (93)	(90) 10 (0)	(88) 11 (1)	/
LSD-0.01-50	(0) 59 (41)	(95) 5 (0)	(96) 4 (0)	/
LSD-0.05-30	(0) 27 (73)	(100) 0 (0)	(100) 0 (0)	/
LSD-0.05-50	(0) 75 (25)	(100) 0 (0)	(100) 0 (0)	/

Table 16: Number of times over 100 replications with $n = 500$ samples that the procedure identifies the true number of clusters for the densities (H) Bimodal IV, (K) Trimodal III, (L) Quadrinodal, #10 Fountain, Circular 2, Circular 2 Cauchy, Circular 3, Circular 4 Cauchy, Bimodal, Quadrinodal, Mult. Bimodal, Mult. Quadrinodal, Circular Bimodal I-V, and Quadrinodal I-II. In parentheses the number of times the procedure identifies a lower number of clusters (on the left) and a higher number of clusters (on the right).

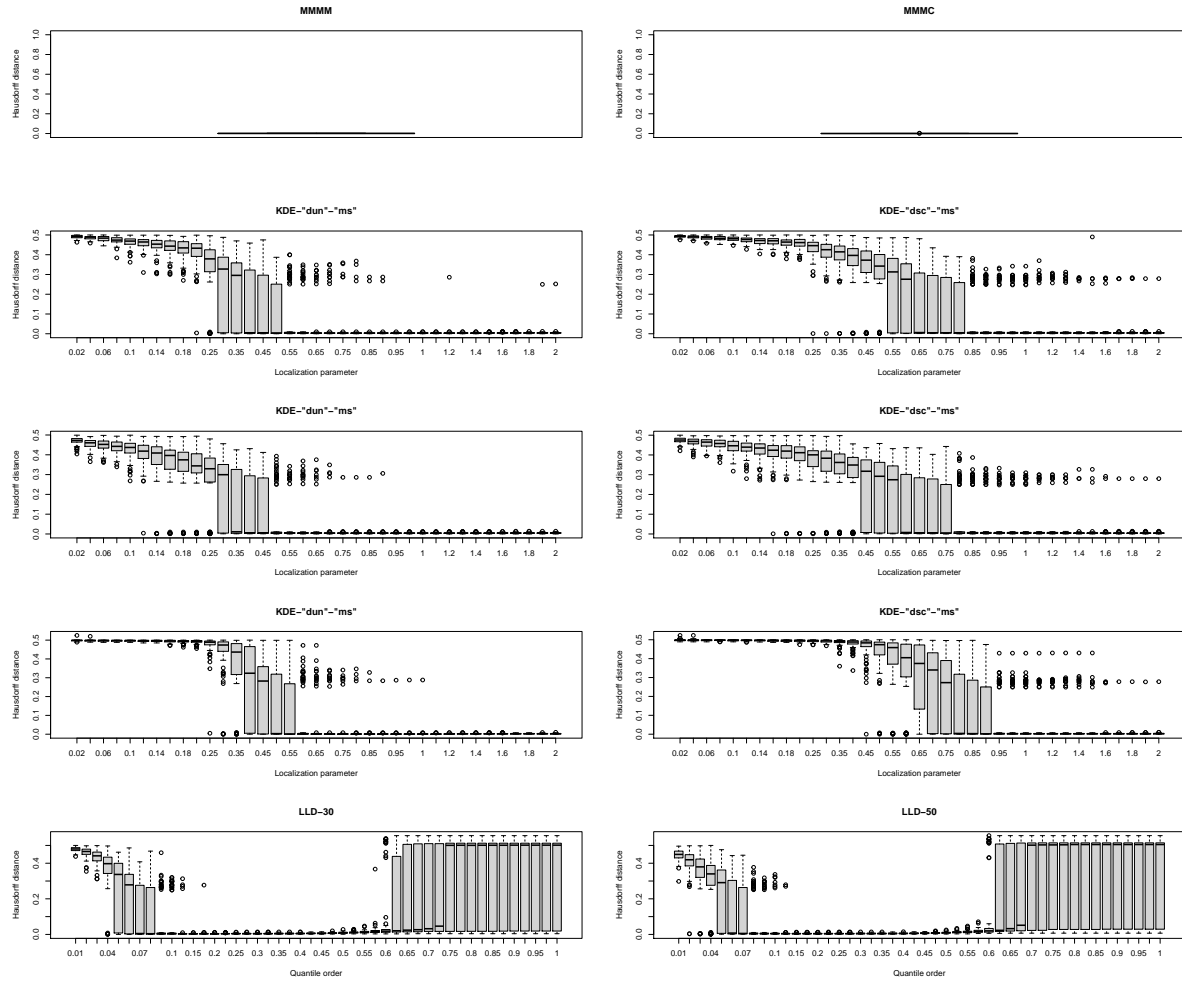


Figure 14: Boxplot of clustering errors based on Hausdorff distance over 100 replications with $n = 1000$ samples for the (H) Bimodal IV density.

L Convergence of sets

In this section, we summarize with proofs various properties concerning the limits of sets.

Lemma L.1 *Let $\{A_n\}_{n=1}^{\infty}$, $\{B_n\}_{n=1}^{\infty}$ be sequences of sets in \mathbb{R}^p . Then, it holds that*

- (i) $\liminf_{n \rightarrow \infty} (A_n \cap B_n) = (\liminf_{n \rightarrow \infty} A_n) \cap (\liminf_{n \rightarrow \infty} B_n)$,
- (ii) $\limsup_{n \rightarrow \infty} (A_n \cap B_n) \subset (\limsup_{n \rightarrow \infty} A_n) \cap (\limsup_{n \rightarrow \infty} B_n)$,
- (iii) $\liminf_{n \rightarrow \infty} (A_n \cup B_n) \supset (\liminf_{n \rightarrow \infty} A_n) \cup (\liminf_{n \rightarrow \infty} B_n)$, and
- (iv) $\limsup_{n \rightarrow \infty} (A_n \cup B_n) = (\limsup_{n \rightarrow \infty} A_n) \cup (\limsup_{n \rightarrow \infty} B_n)$.

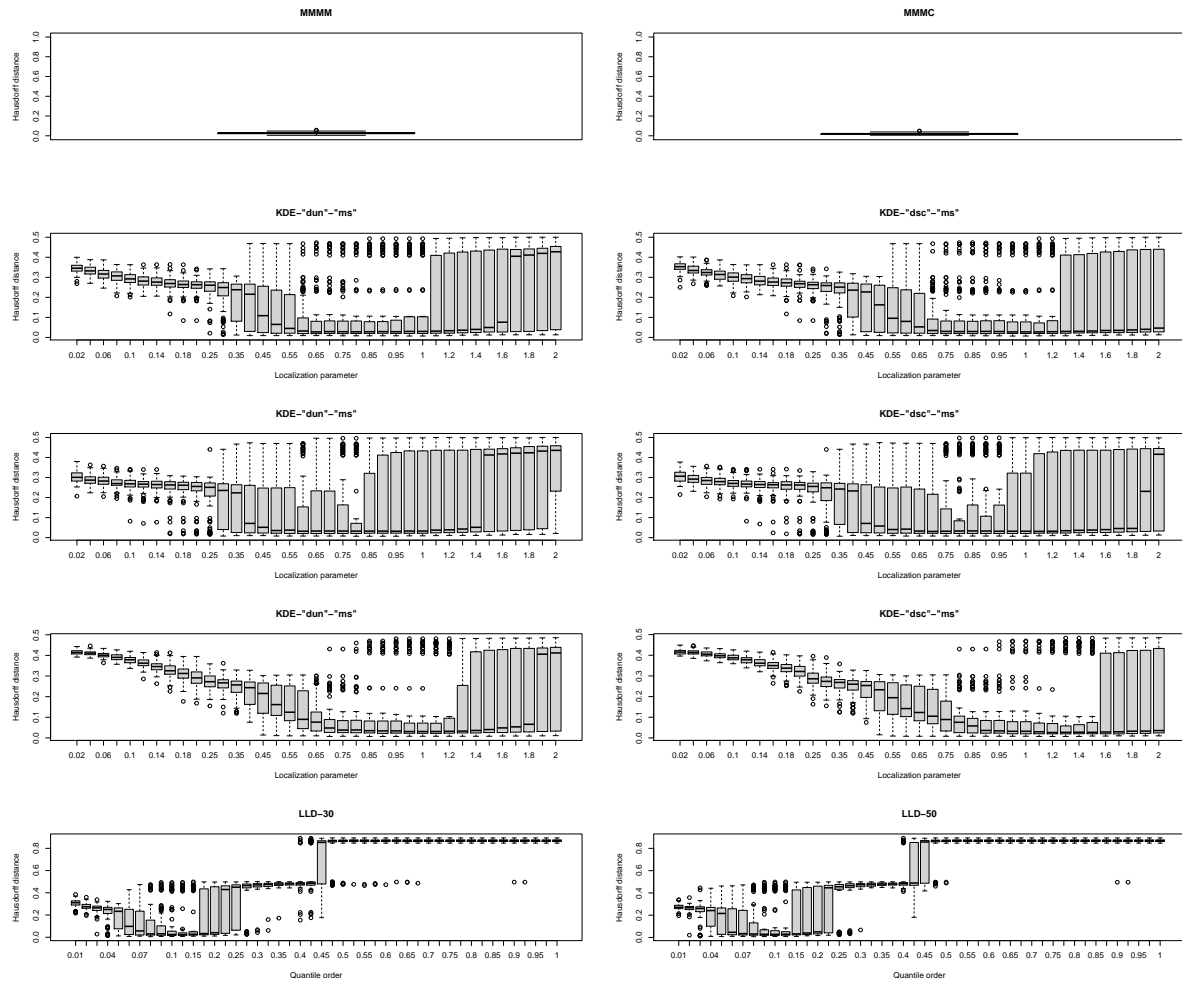


Figure 15: Boxplot of clustering errors based on Hausdorff distance over 100 replications with $n = 1000$ samples for the (K) Trimodal III density.

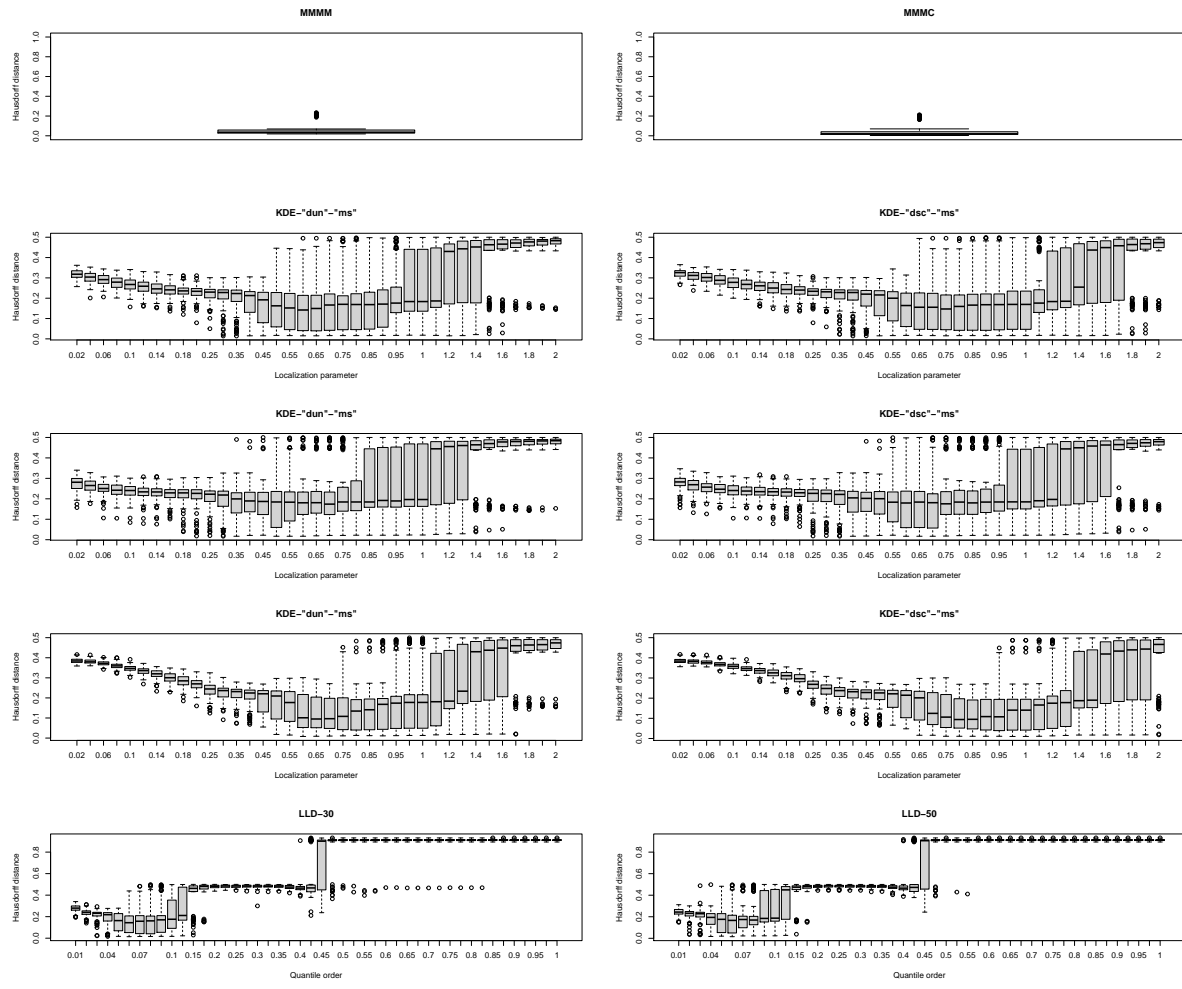


Figure 16: Boxplot of clustering errors based on Hausdorff distance over 100 replications with $n = 1000$ samples for the (L) Quadrimodal density.

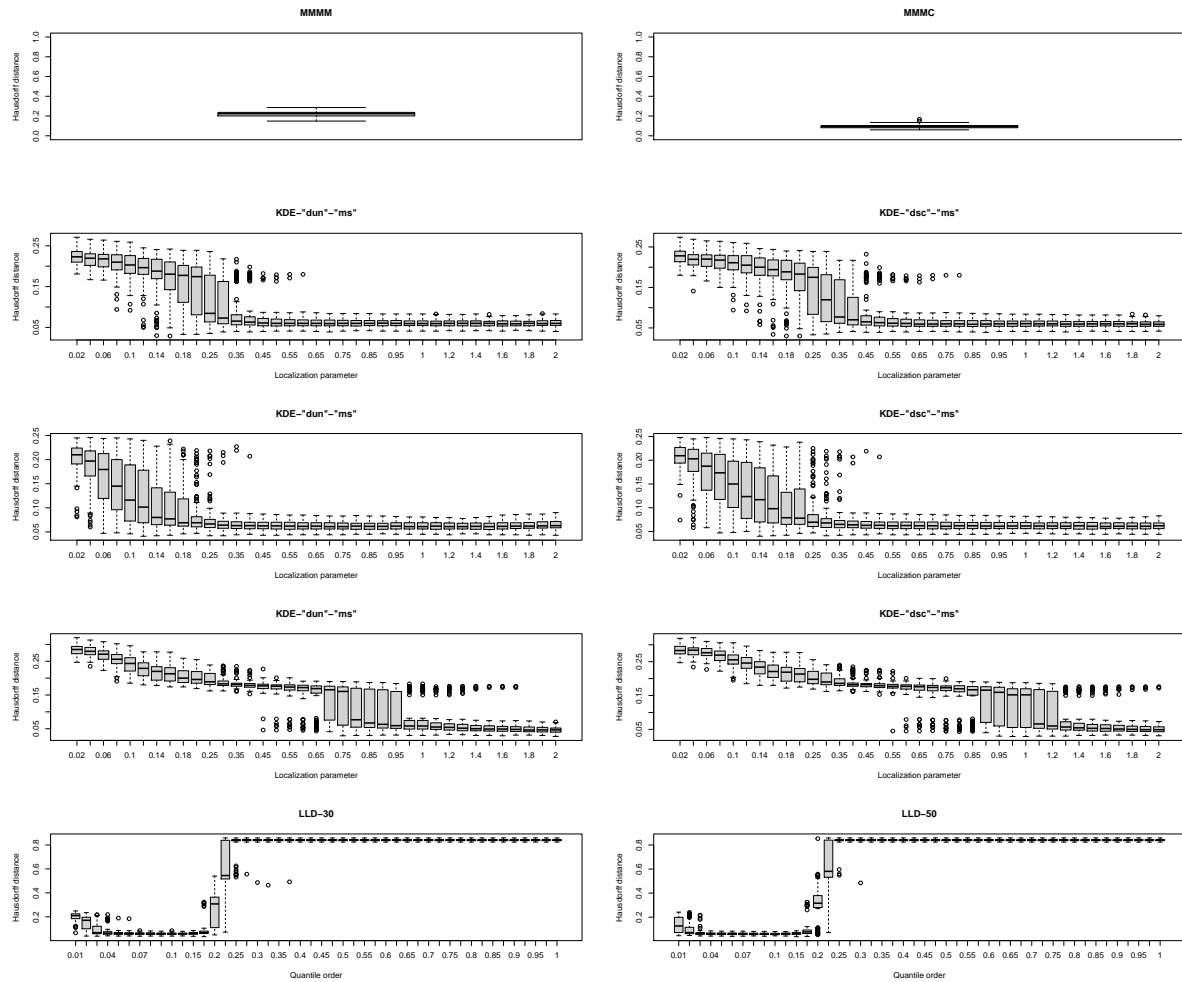


Figure 17: Boxplot of clustering errors based on Hausdorff distance over 100 replications with $n = 1000$ samples for the #10 fountain density.

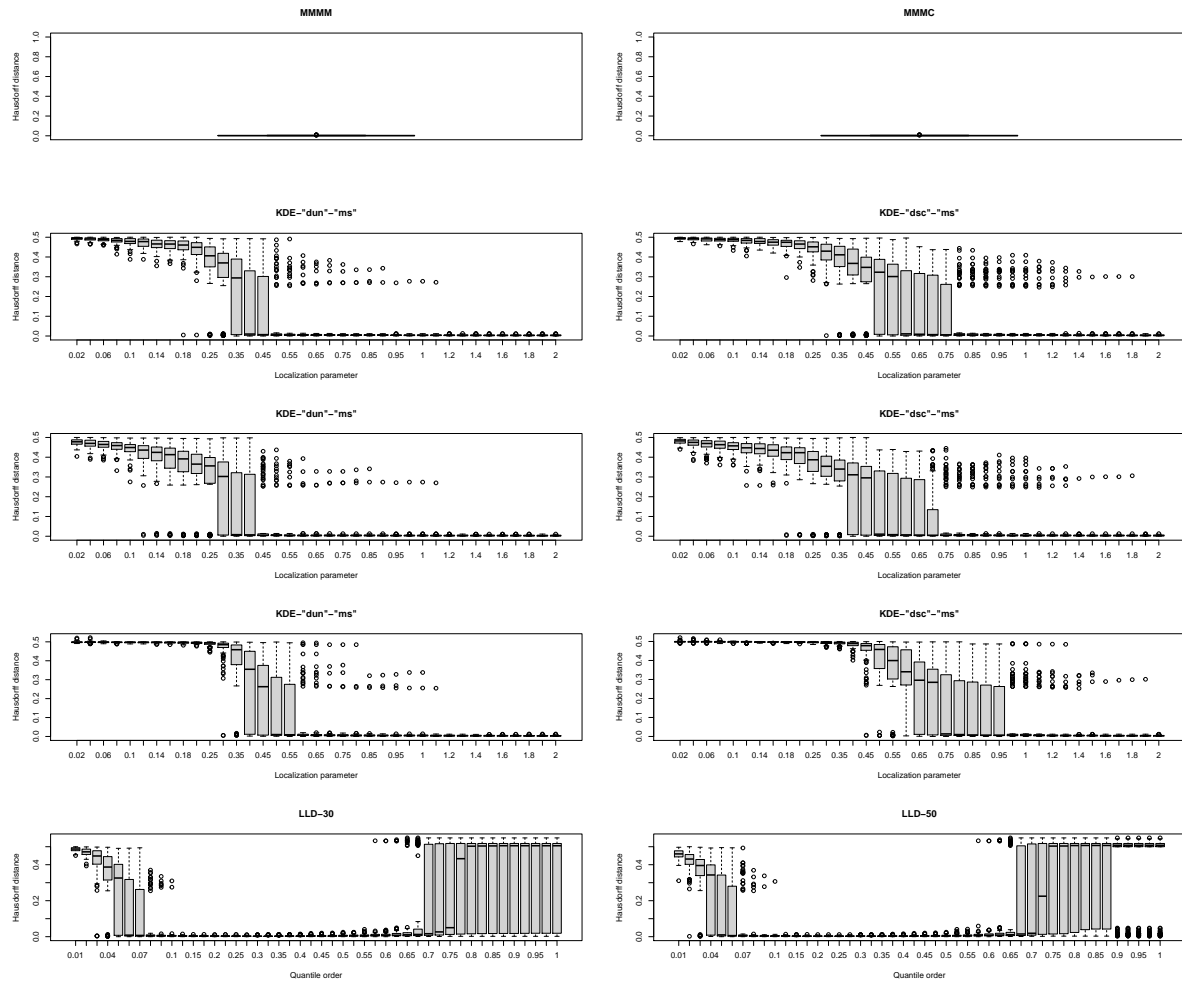


Figure 18: Boxplot of clustering errors based on Hausdorff distance over 100 replications with $n = 1000$ samples for the Bimodal density.

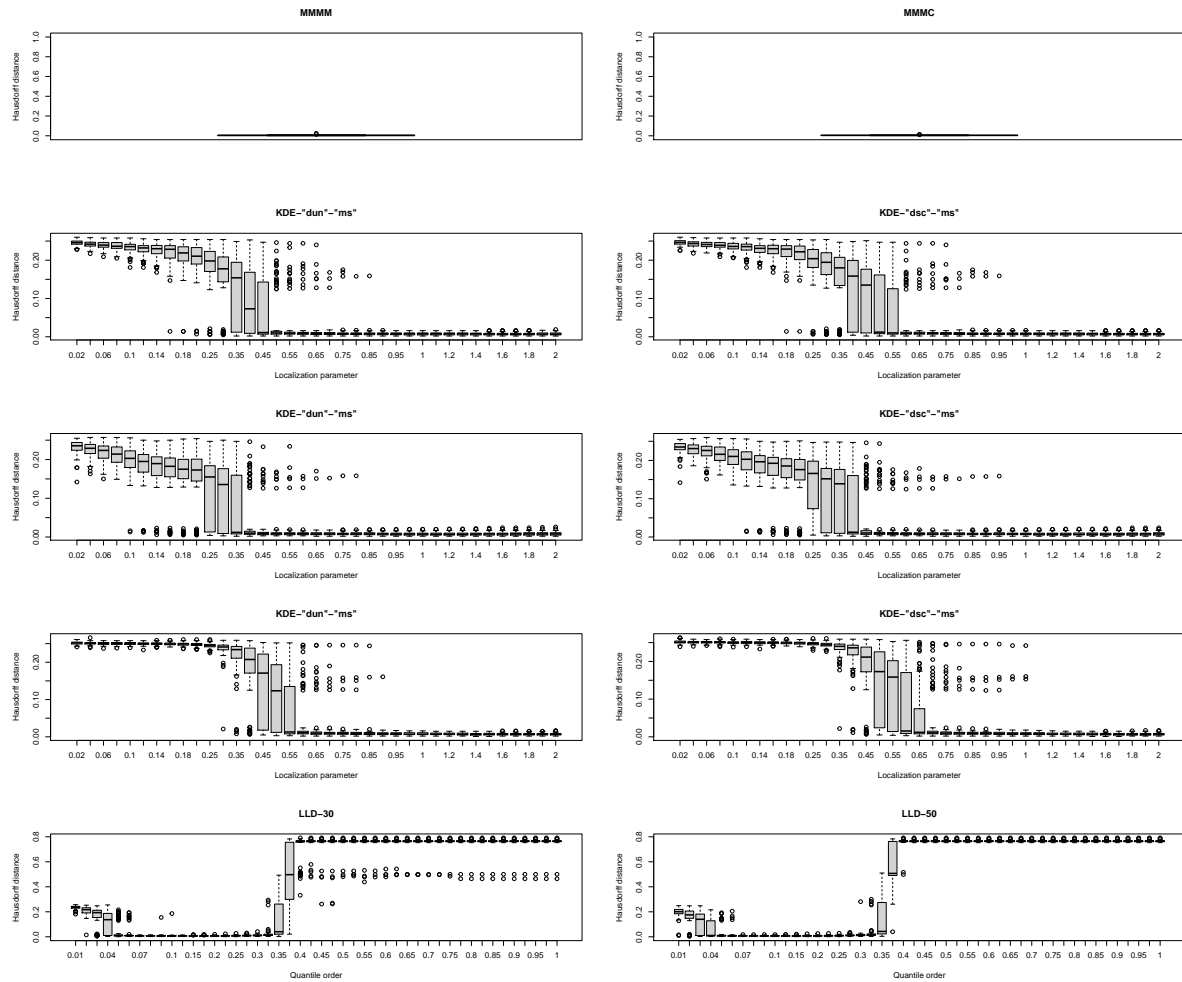


Figure 19: Boxplot of clustering errors based on Hausdorff distance over 100 replications with $n = 1000$ samples for the Quadrimodal density.

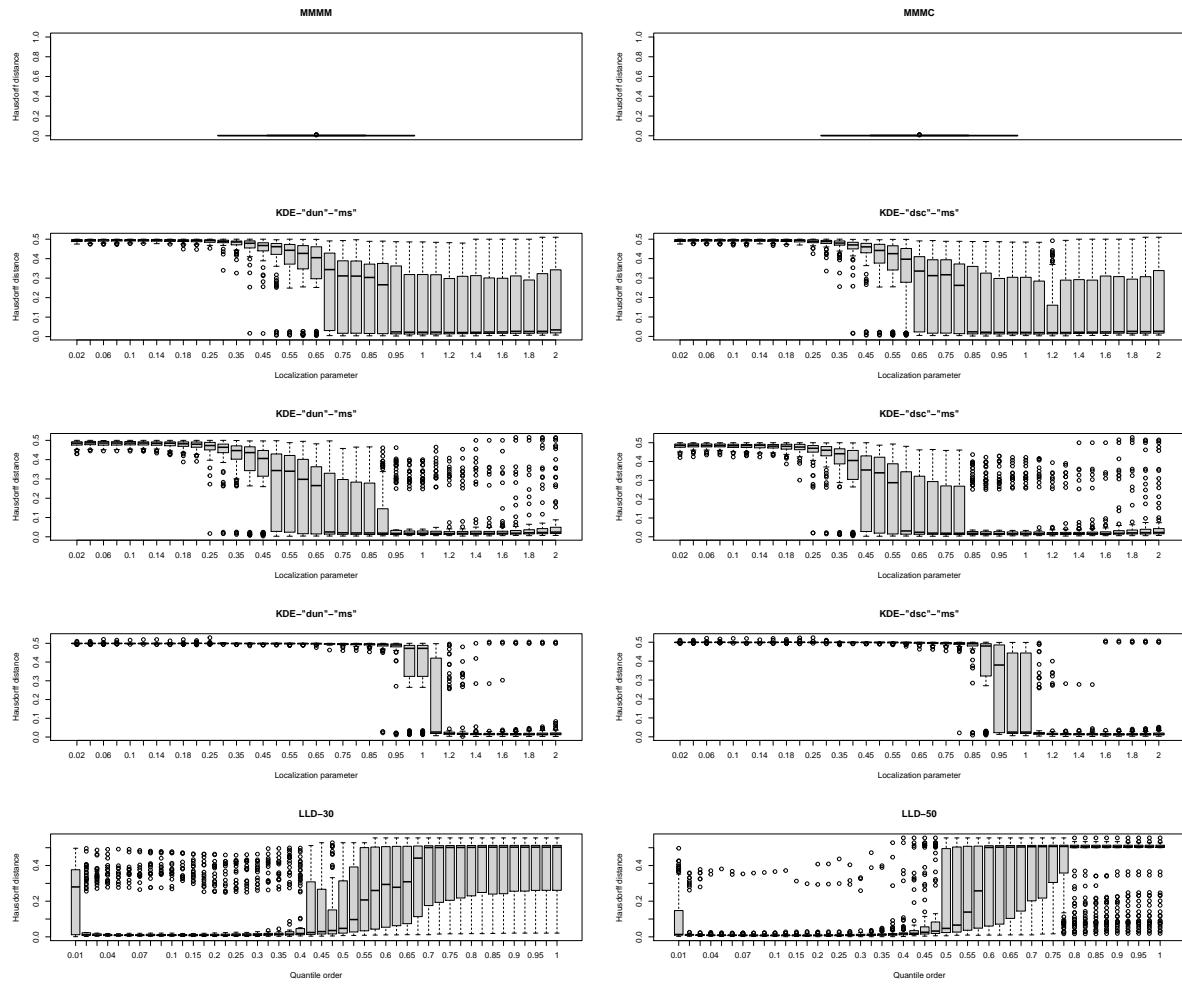


Figure 20: Boxplot of clustering errors based on Hausdorff distance over 100 replications with $n = 1000$ samples for the Mult. Bimodal density.

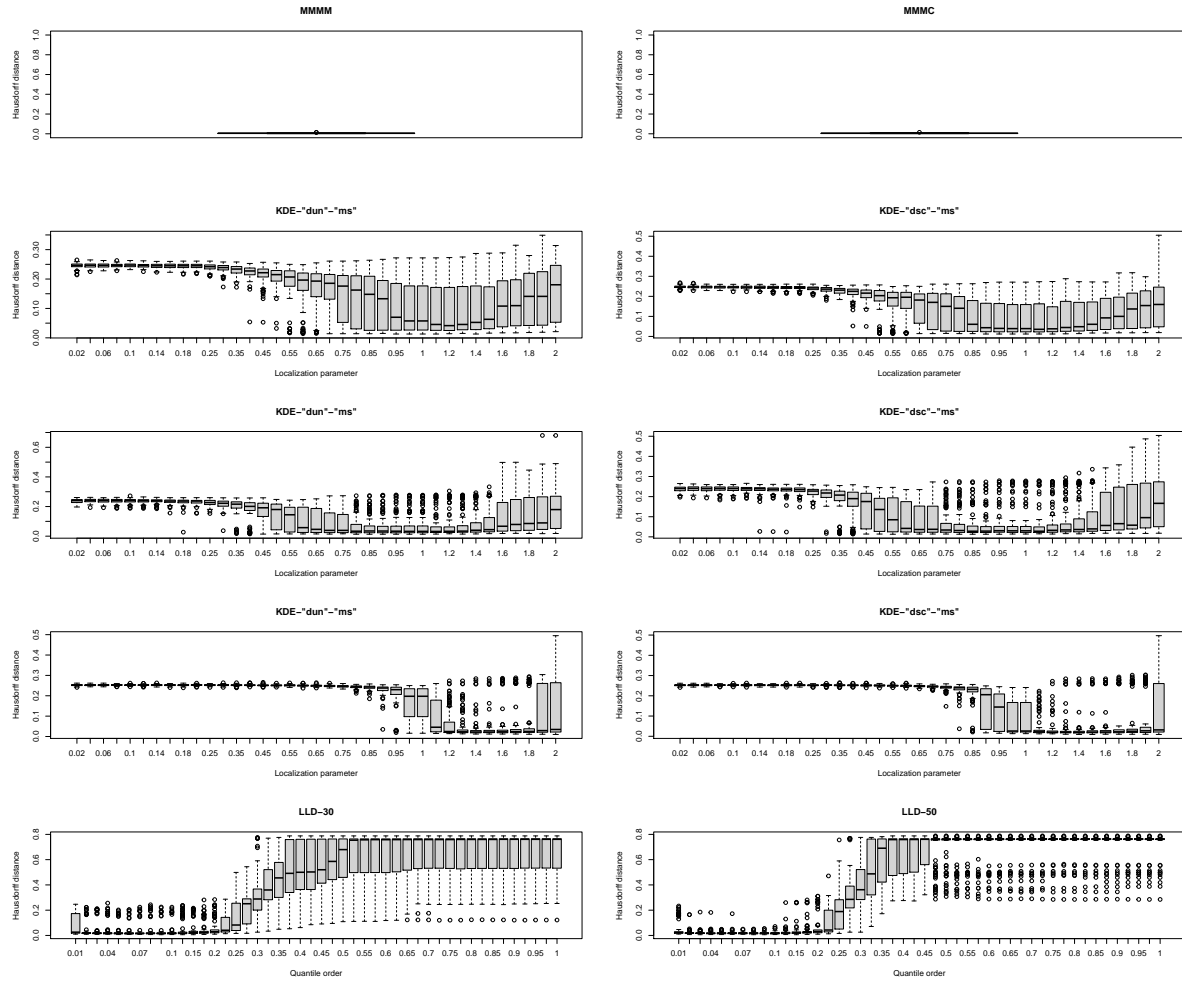


Figure 21: Boxplot of clustering errors based on Hausdorff distance over 100 replications with $n = 1000$ samples for the Mult. Quadrinodal density.

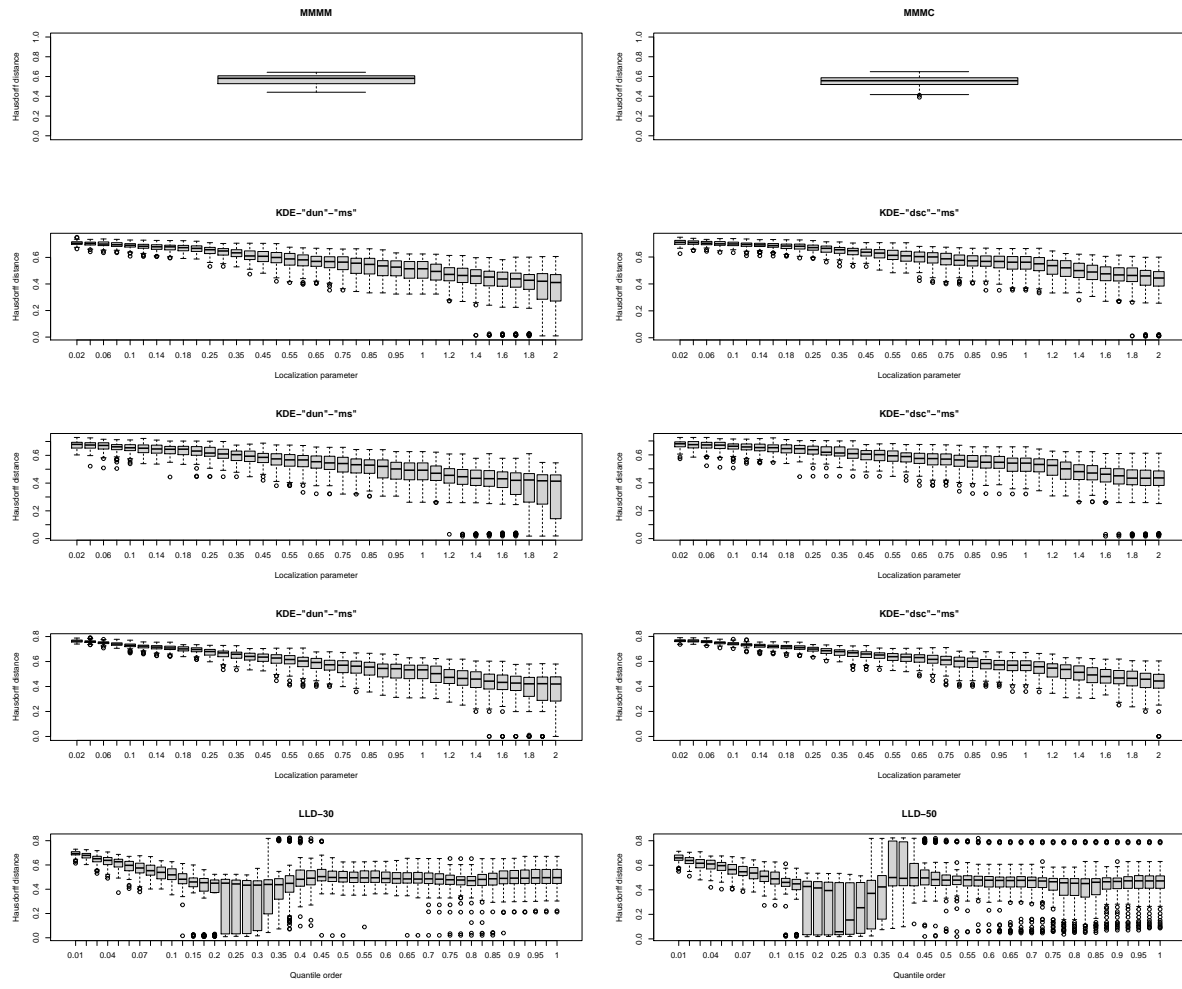


Figure 22: Boxplot of clustering errors based on Hausdorff distance over 100 replications with $n = 1000$ samples for the Circular 2 density.

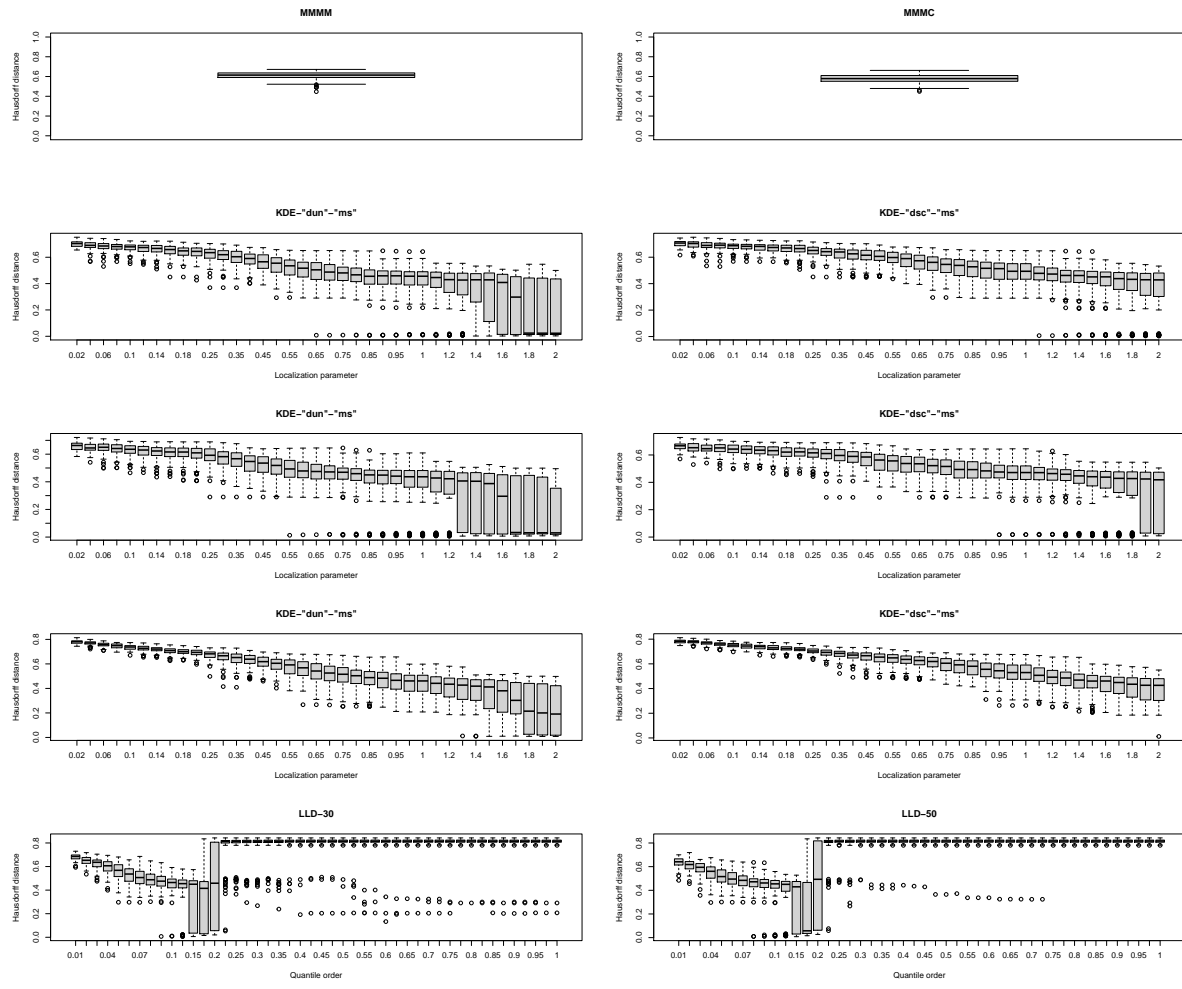


Figure 23: Boxplot of clustering errors based on Hausdorff distance over 100 replications with $n = 1000$ samples for the Circular 2 Cauchy density.

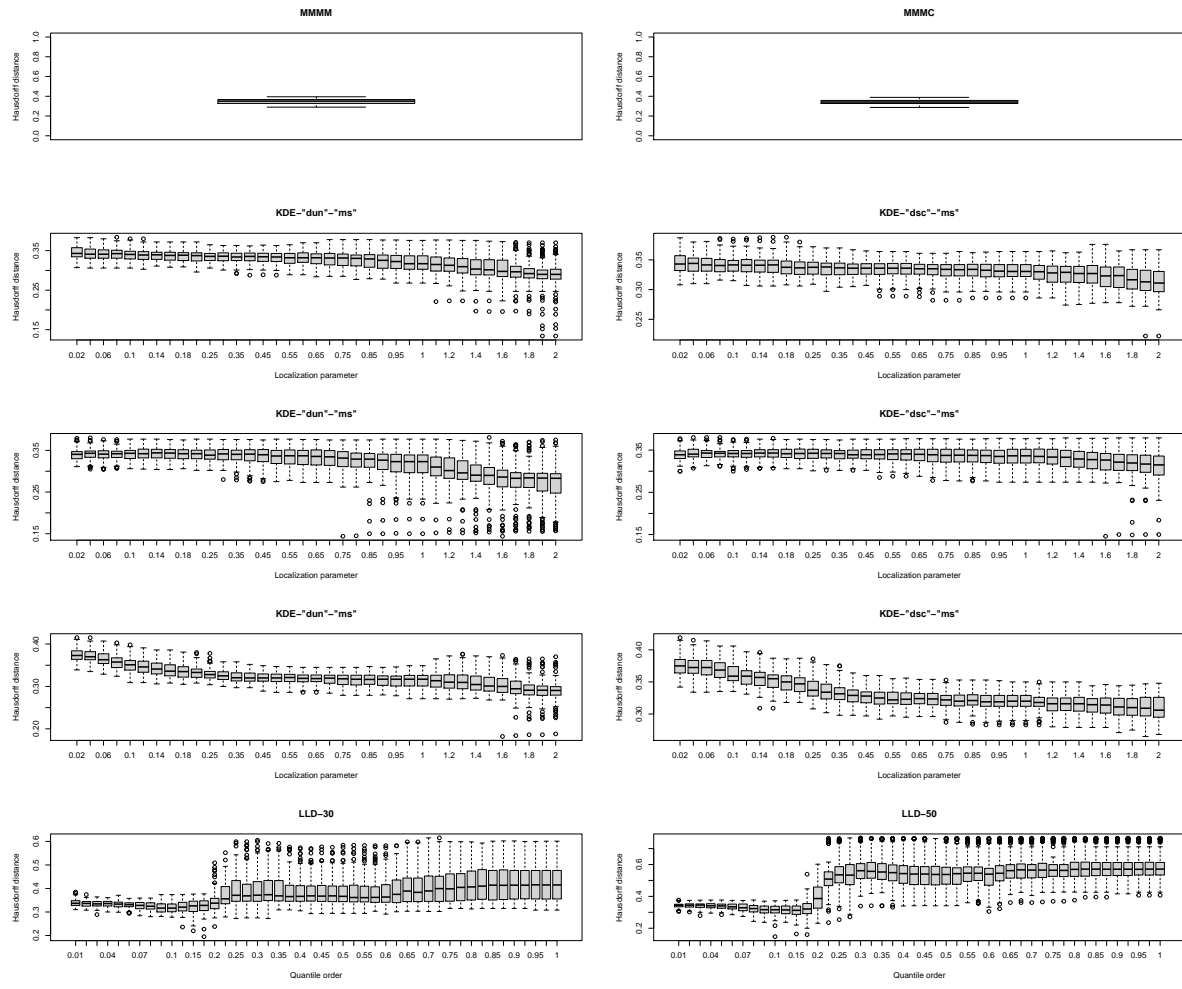


Figure 24: Boxplot of clustering errors based on Hausdorff distance over 100 replications with $n = 1000$ samples for the Circular 3 density.

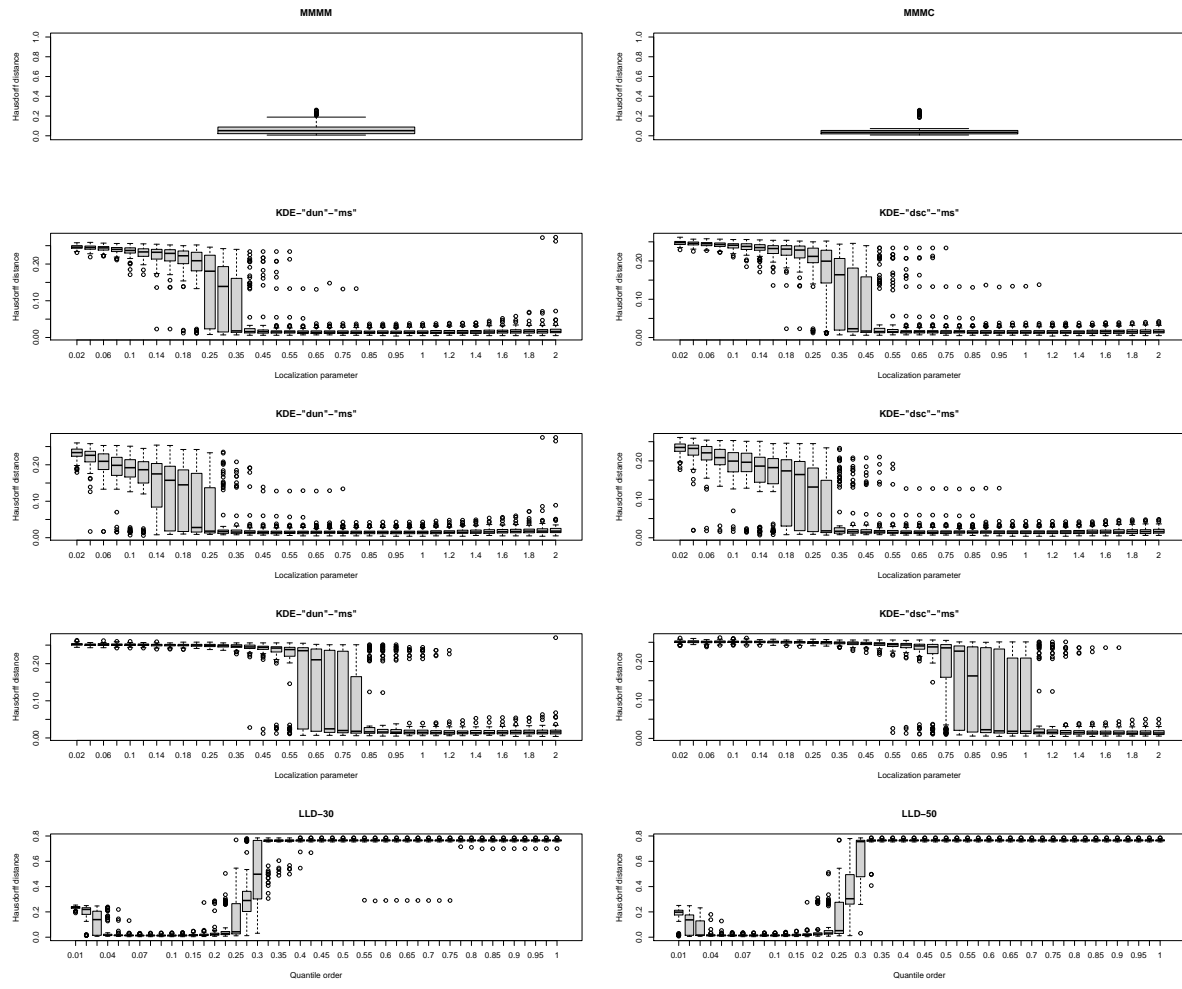


Figure 25: Boxplot of clustering errors based on Hausdorff distance over 100 replications with $n = 1000$ samples for the Circular 4 Cauchy density.

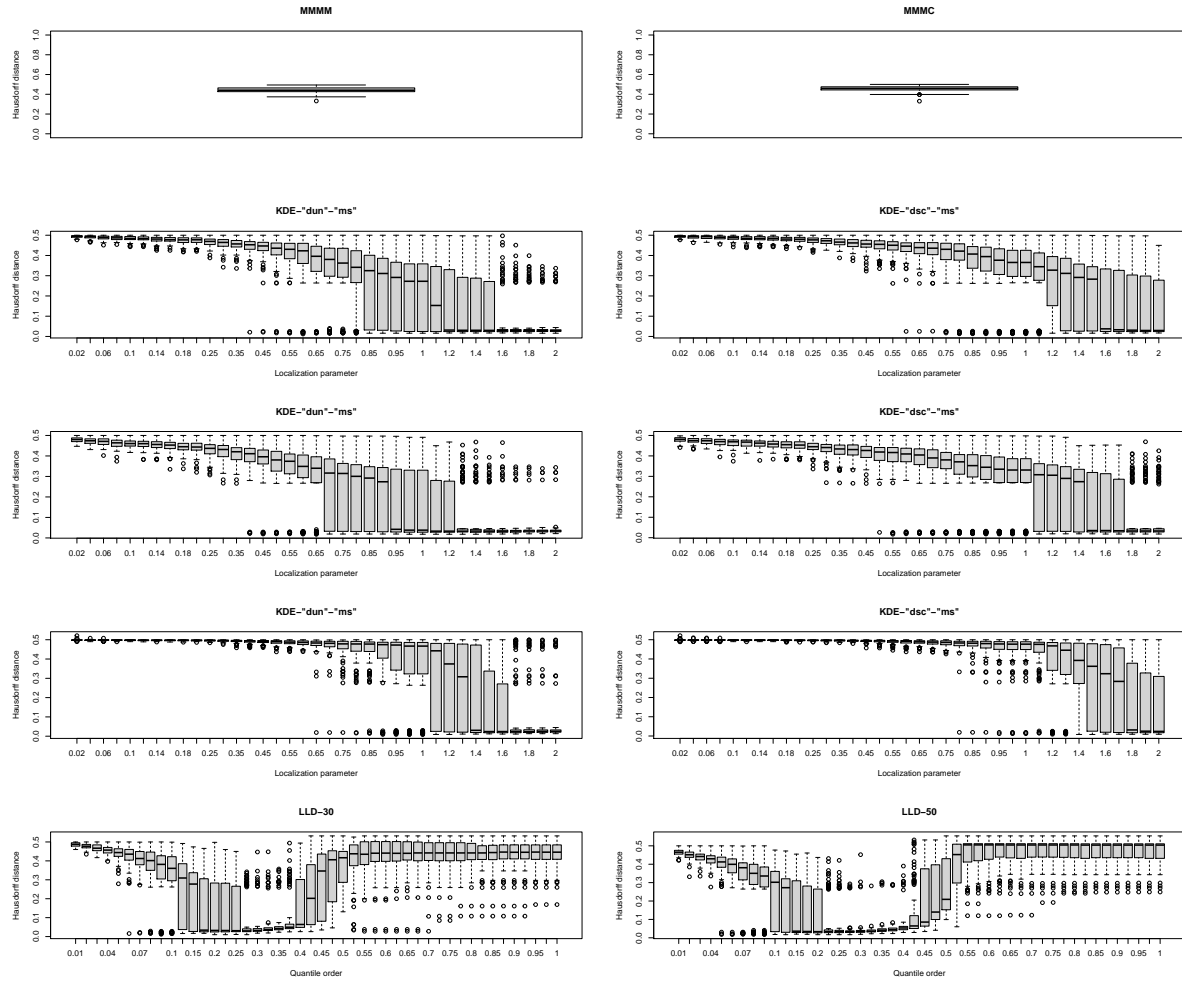


Figure 26: Boxplot of clustering errors based on Hausdorff distance over 100 replications with $n = 1000$ samples for the Circular Bimodal I density.

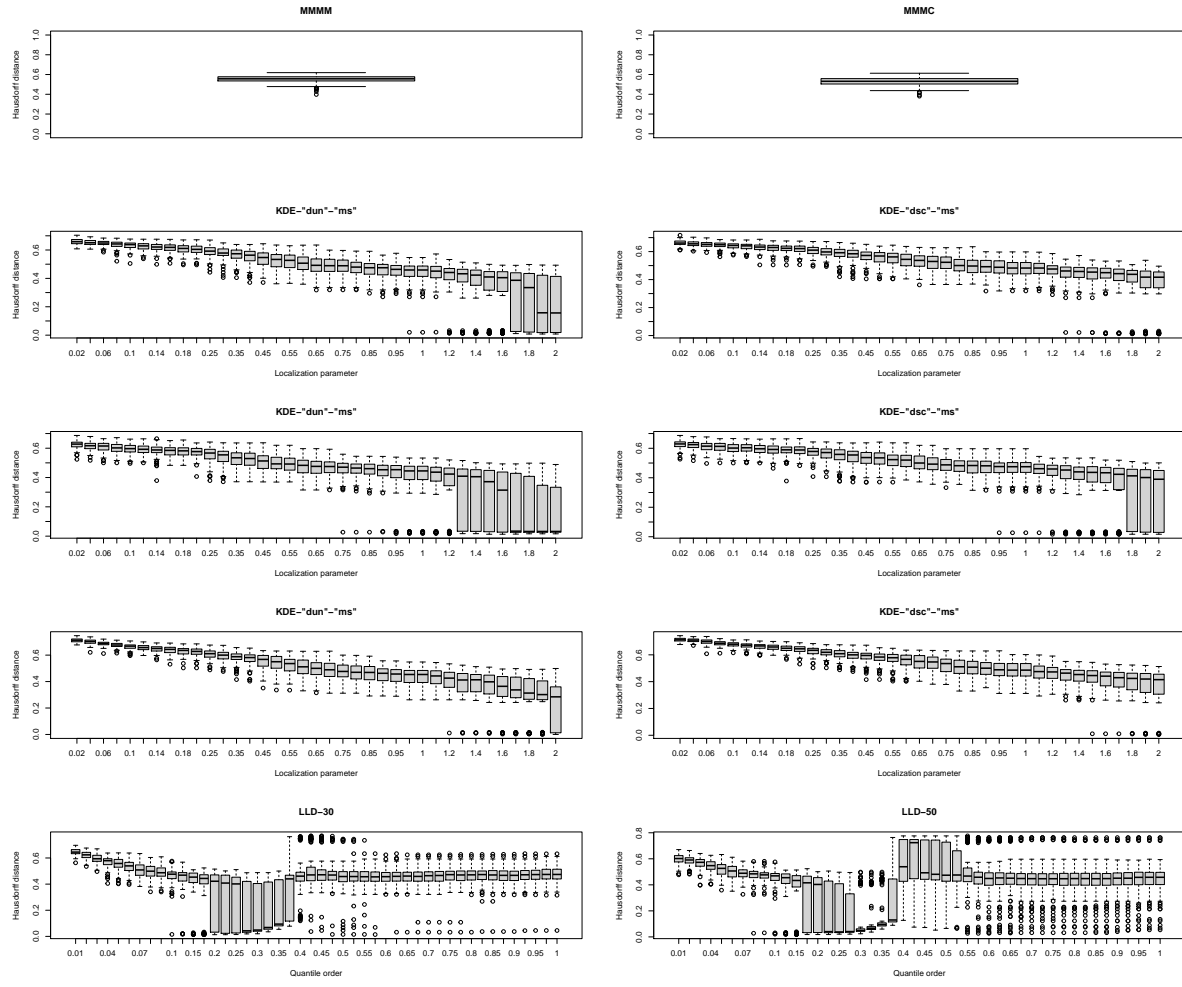


Figure 27: Boxplot of clustering errors based on Hausdorff distance over 100 replications with $n = 1000$ samples for the Circular Bimodal II density.

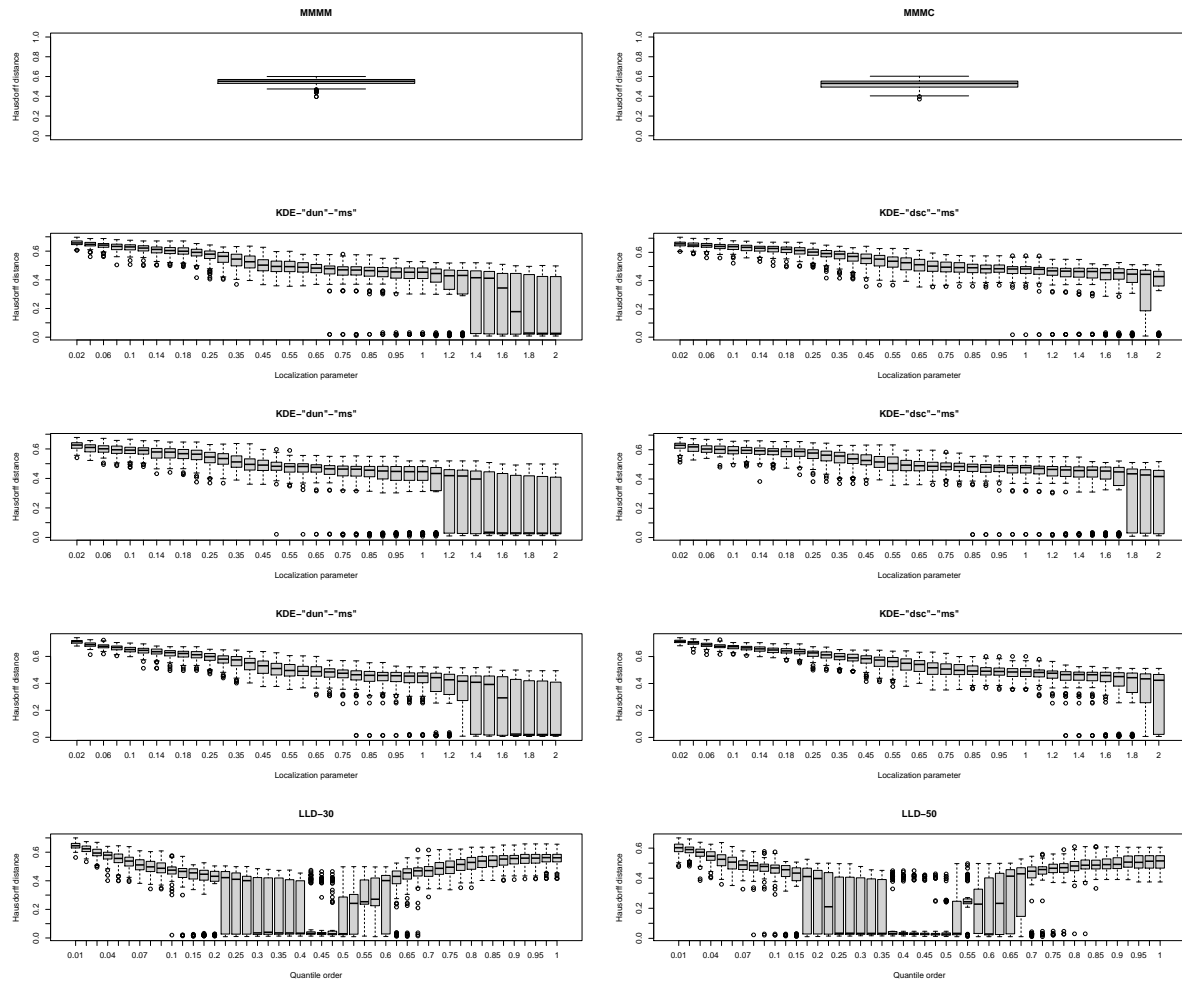


Figure 28: Boxplot of clustering errors based on Hausdorff distance over 100 replications with $n = 1000$ samples for the Circular Bimodal III density.

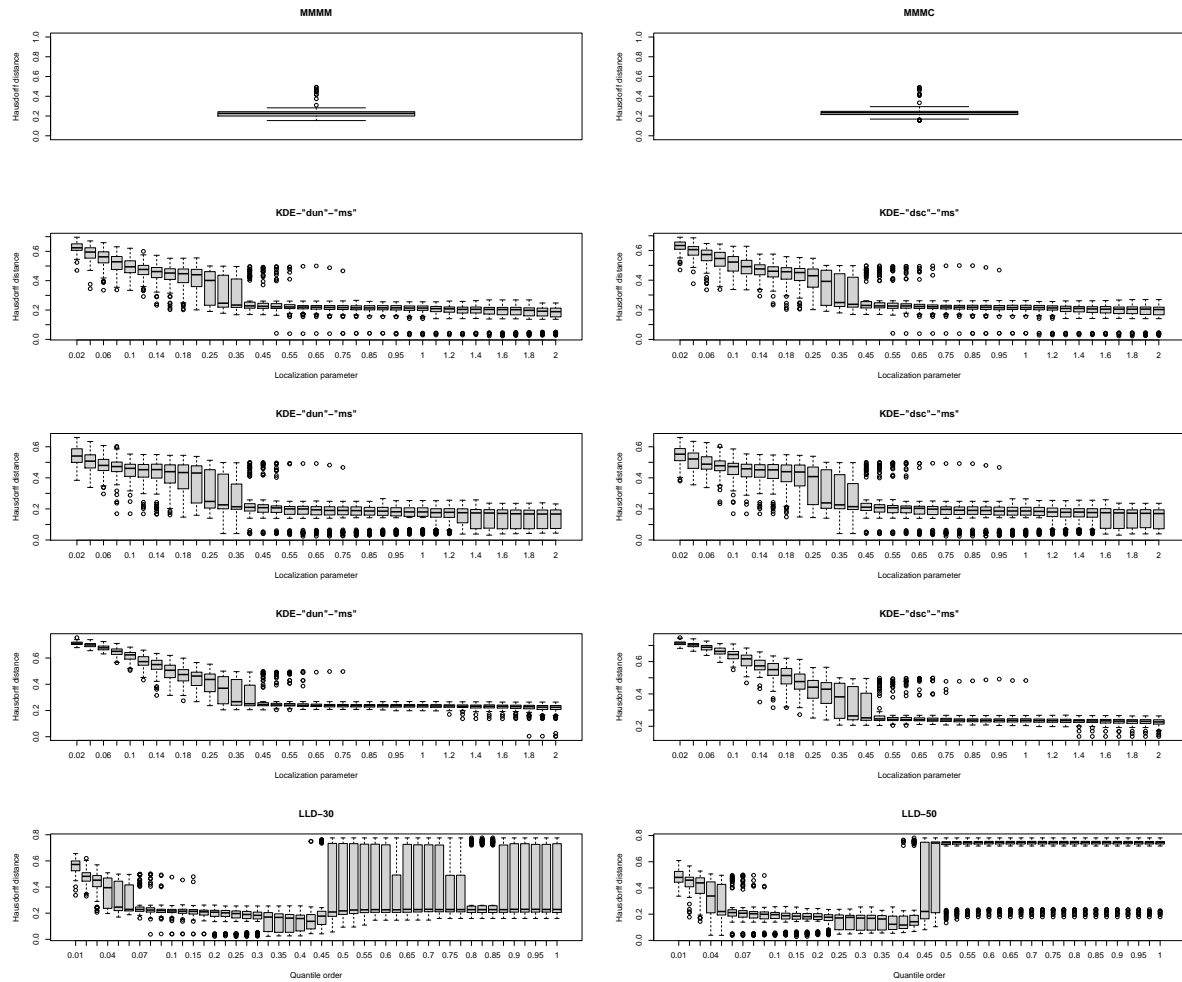


Figure 29: Boxplot of clustering errors based on Hausdorff distance over 100 replications with $n = 1000$ samples for the Circular Bimodal IV density.

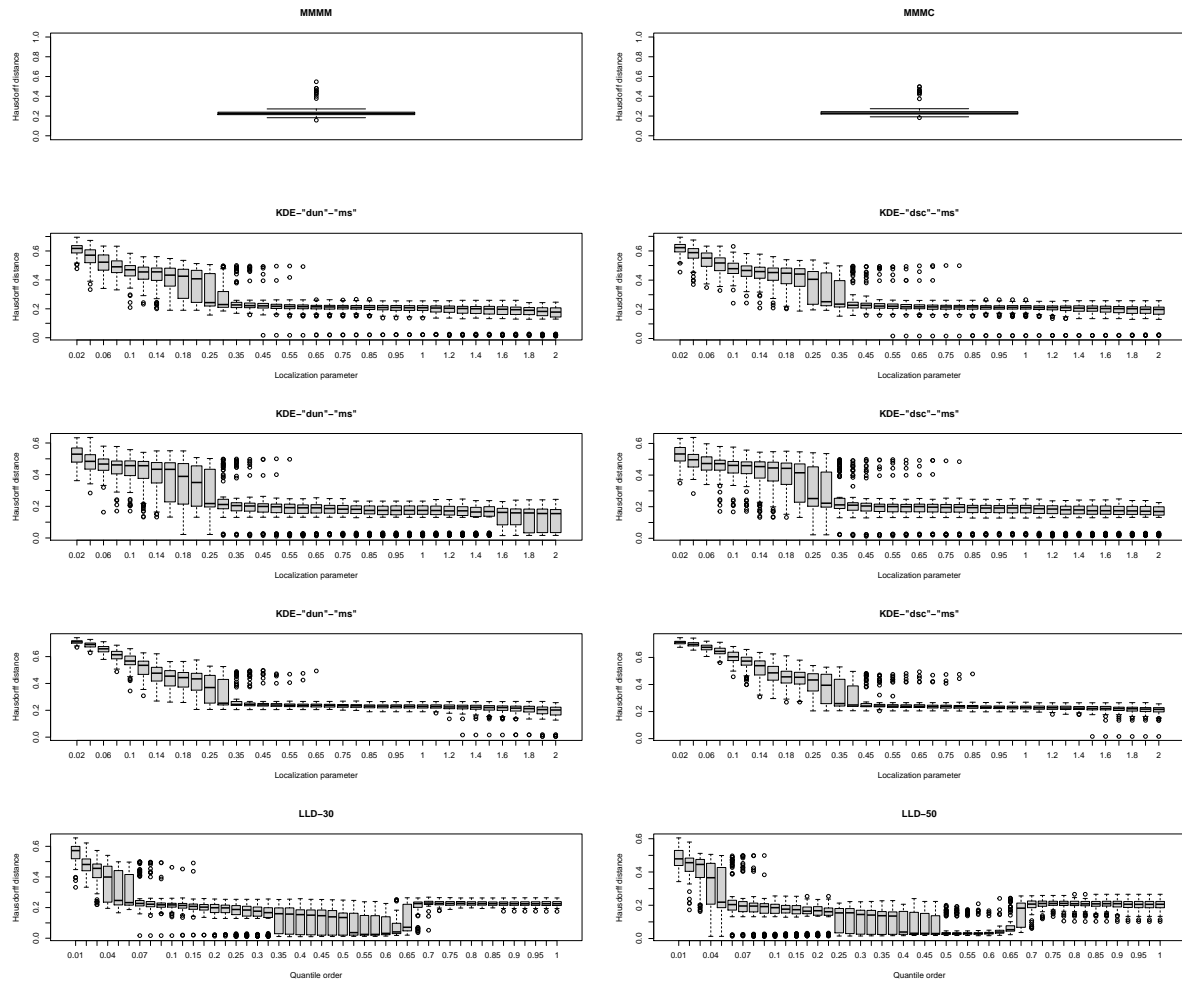


Figure 30: Boxplot of clustering errors based on Hausdorff distance over 100 replications with $n = 1000$ samples for the Circular Bimodal V density.

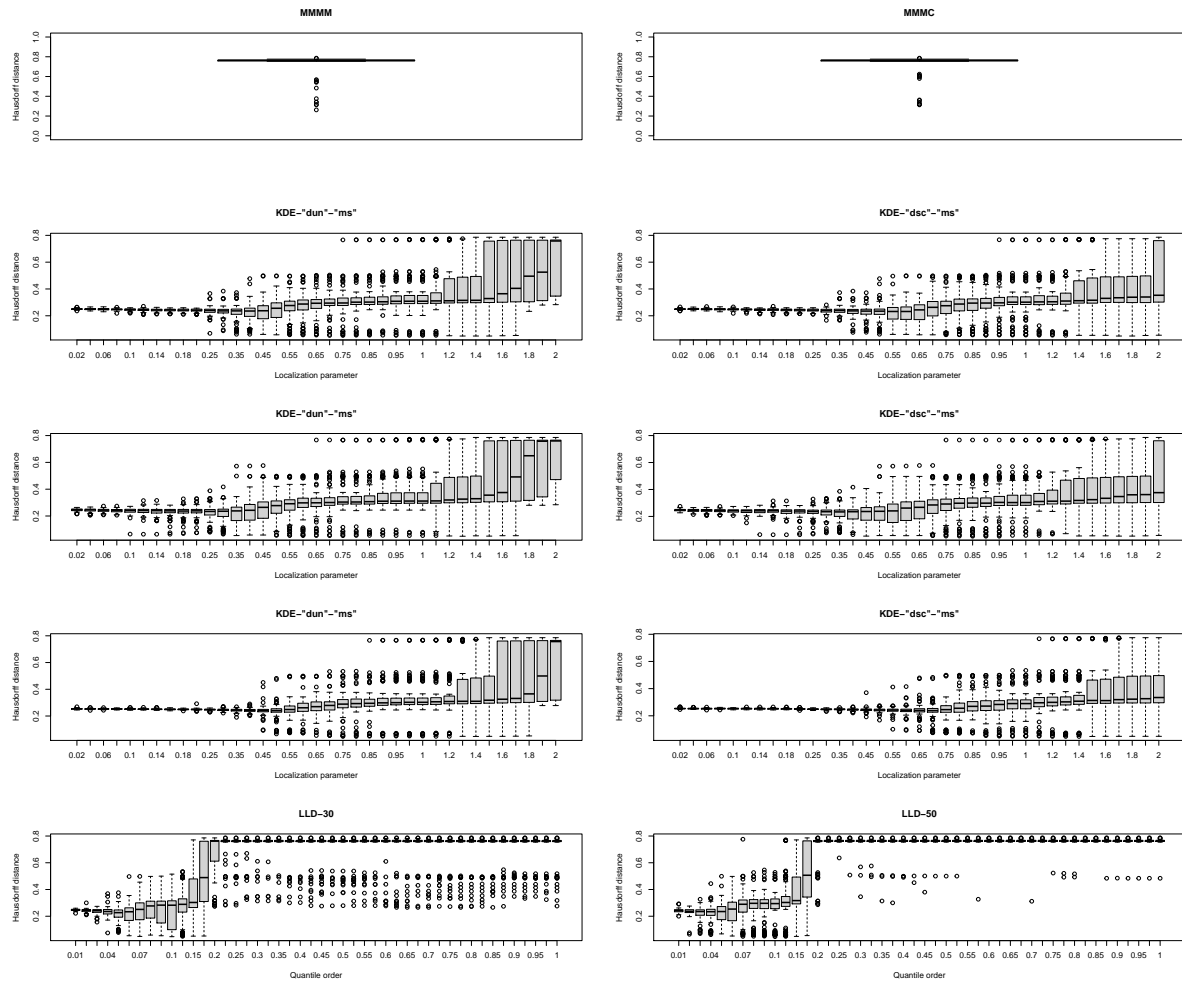


Figure 31: Boxplot of clustering errors based on Hausdorff distance over 100 replications with $n = 1000$ samples for the Circular Quadrimodal I density.

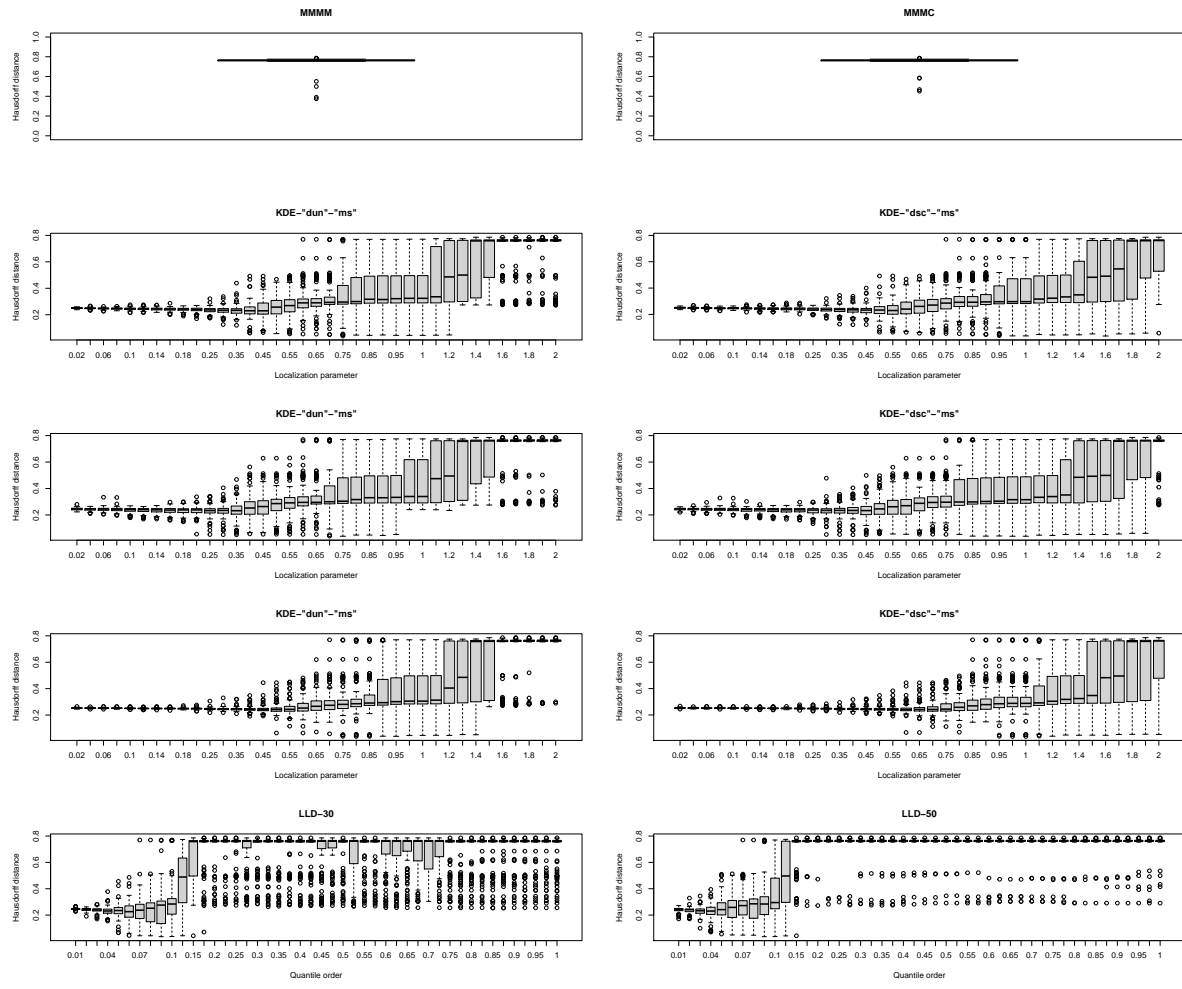


Figure 32: Boxplot of clustering errors based on Hausdorff distance over 100 replications with $n = 1000$ samples for the Circular Quadrinomodal II density.

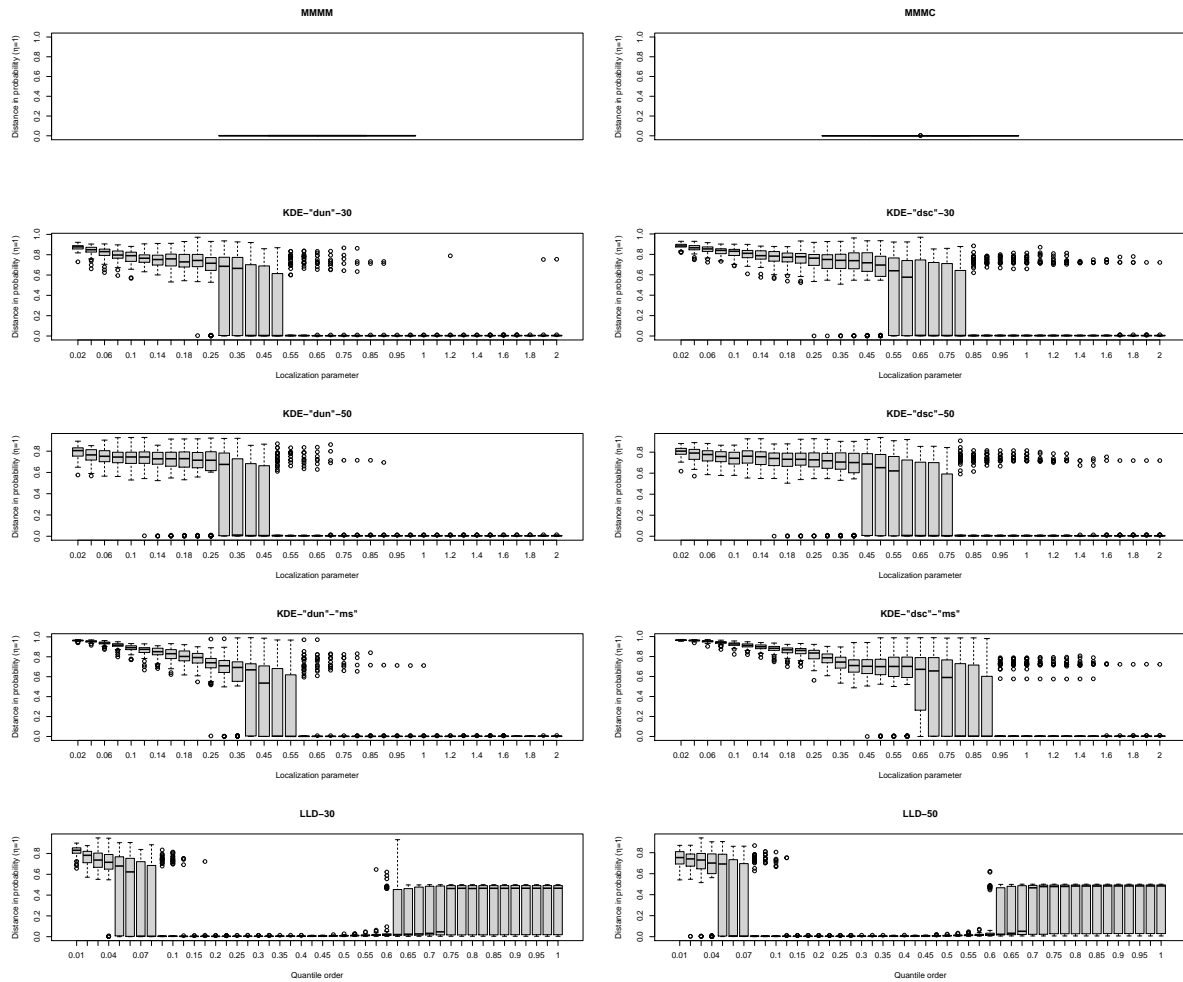


Figure 33: Boxplot of clustering errors based on distance in probability over 100 replications with $n = 1000$ samples for the (H) Bimodal IV density.

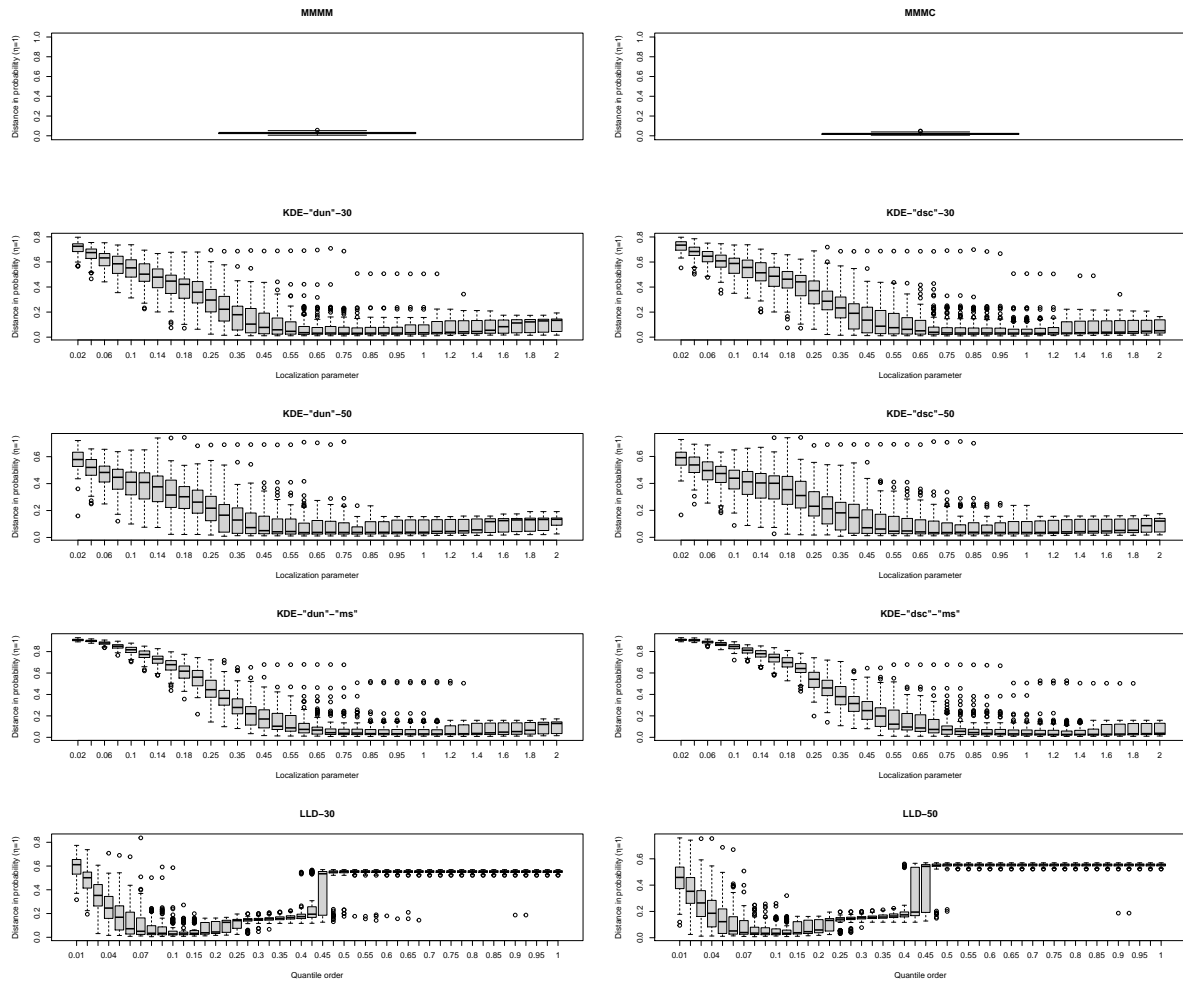


Figure 34: Boxplot of clustering errors based on distance in probability over 100 replications with $n = 1000$ samples for the (K) Trimodal III density.

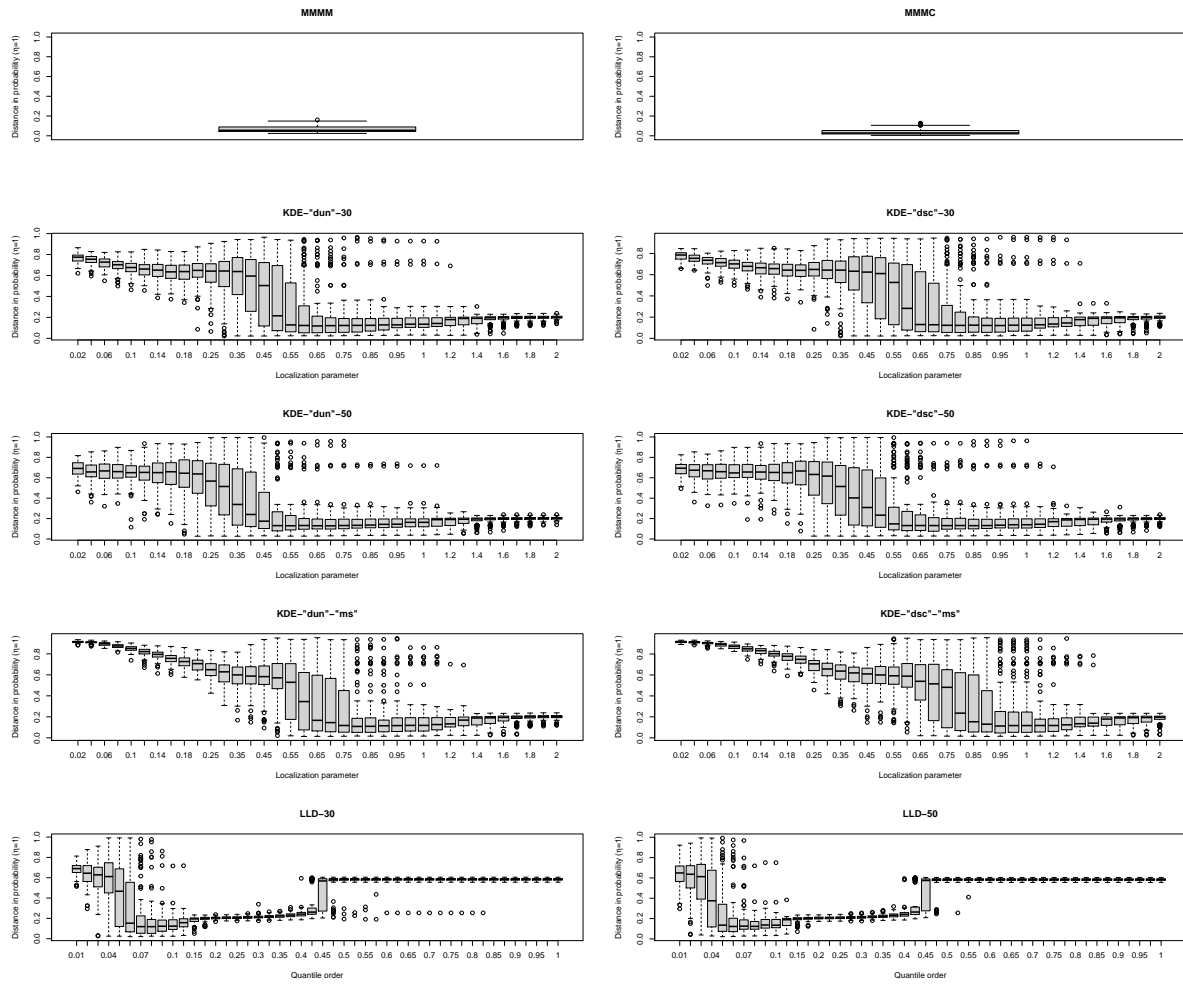


Figure 35: Boxplot of clustering errors based on distance in probability over 100 replications with $n = 1000$ samples for the (L) Quadrimodal density.

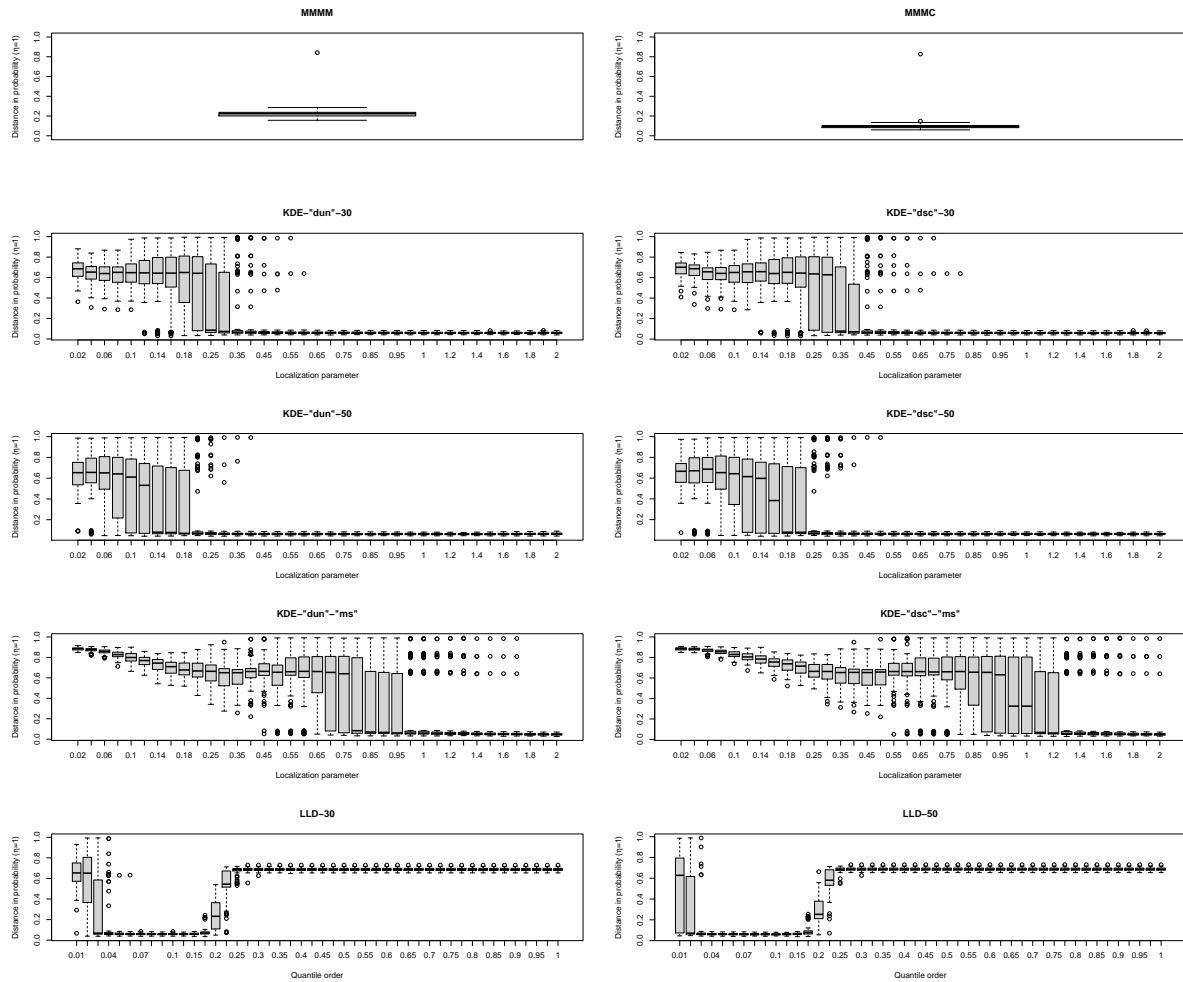


Figure 36: Boxplot of clustering errors based on distance in probability over 100 replications with $n = 1000$ samples for the #10 fountain density.

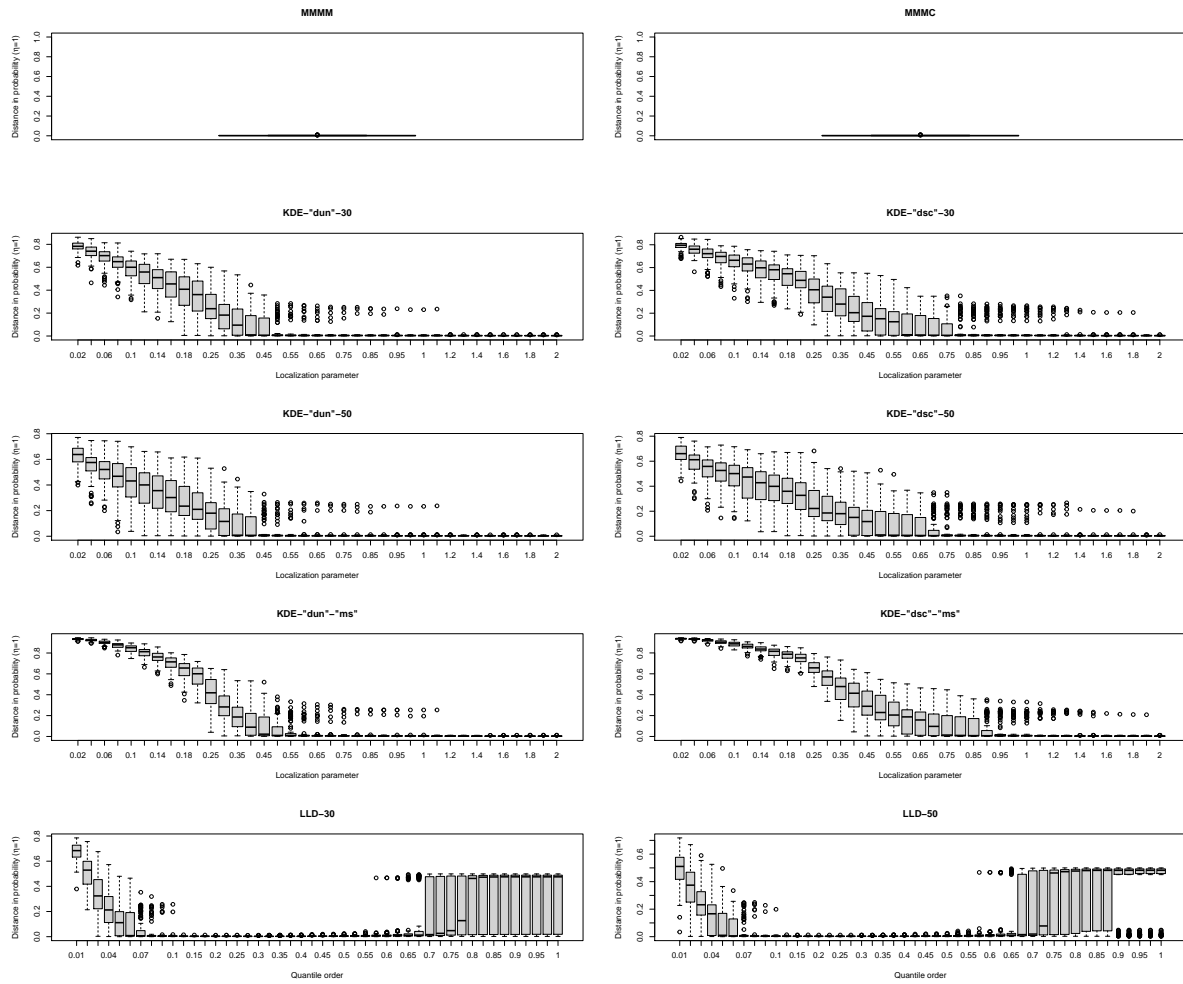


Figure 37: Boxplot of clustering errors based on distance in probability over 100 replications with $n = 1000$ samples for the Bimodal density.

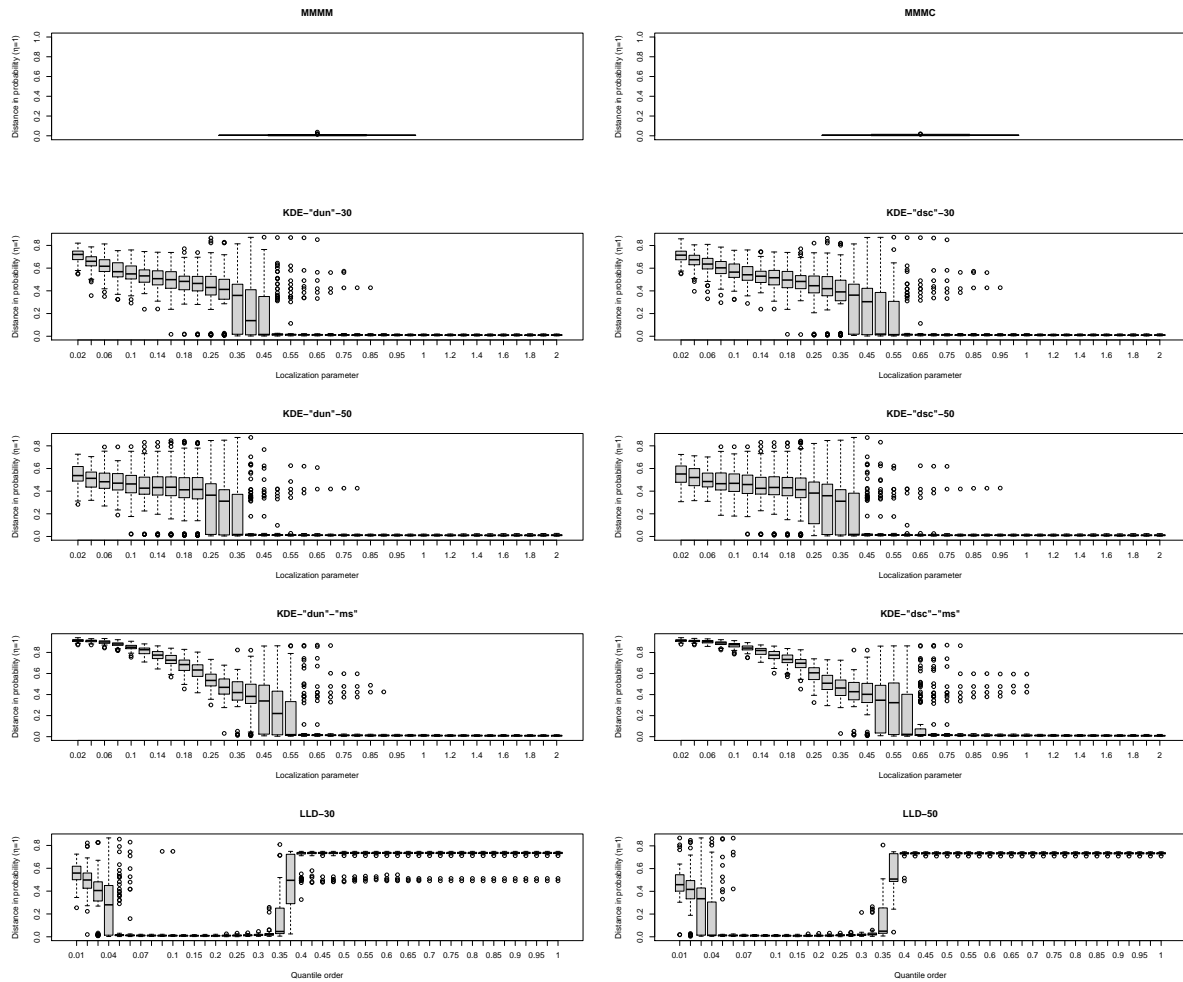


Figure 38: Boxplot of clustering errors based on distance in probability over 100 replications with $n = 1000$ samples for the Quadrimodal density.

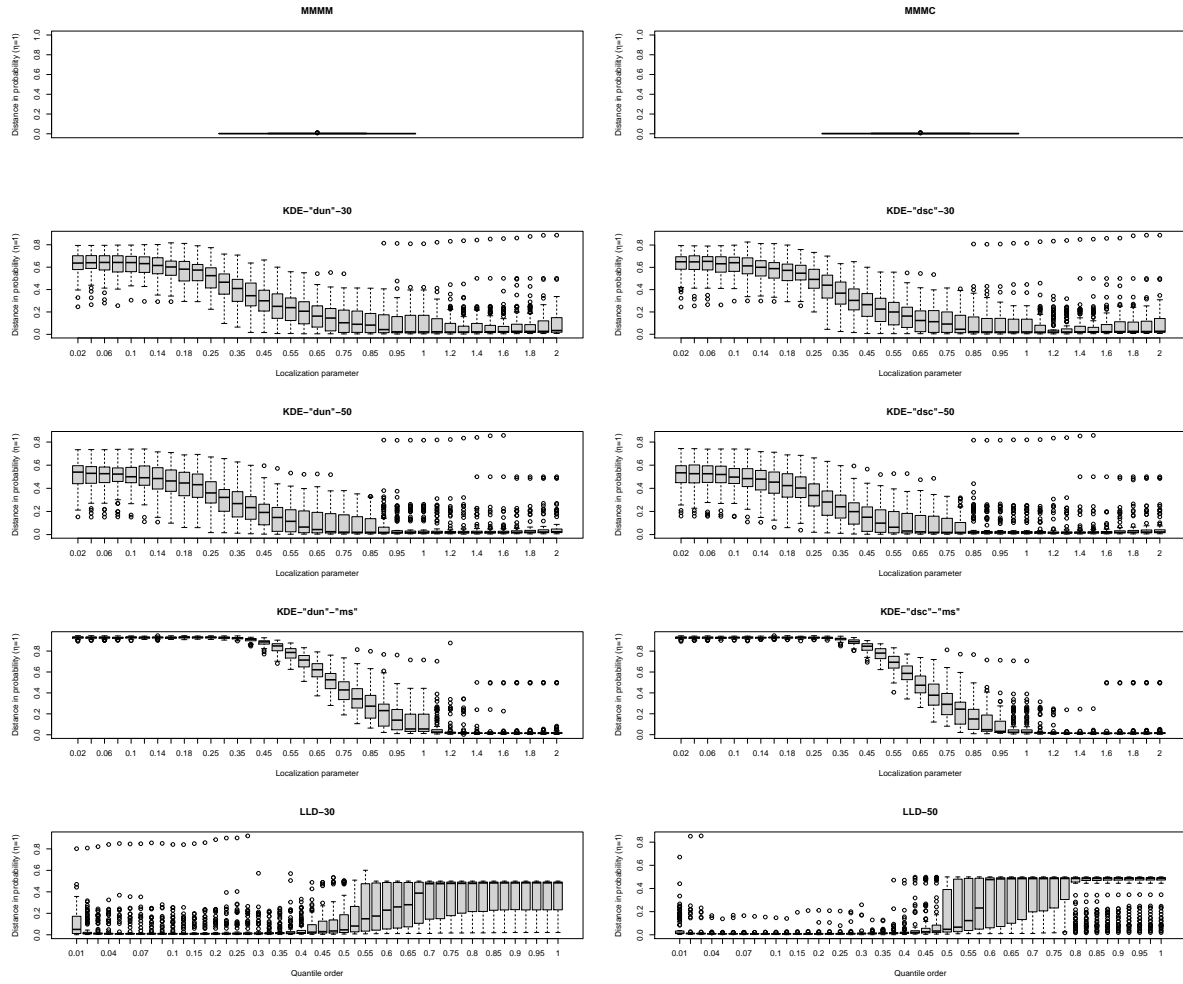


Figure 39: Boxplot of clustering errors based on distance in probability over 100 replications with $n = 1000$ samples for the Mult. Bimodal density.

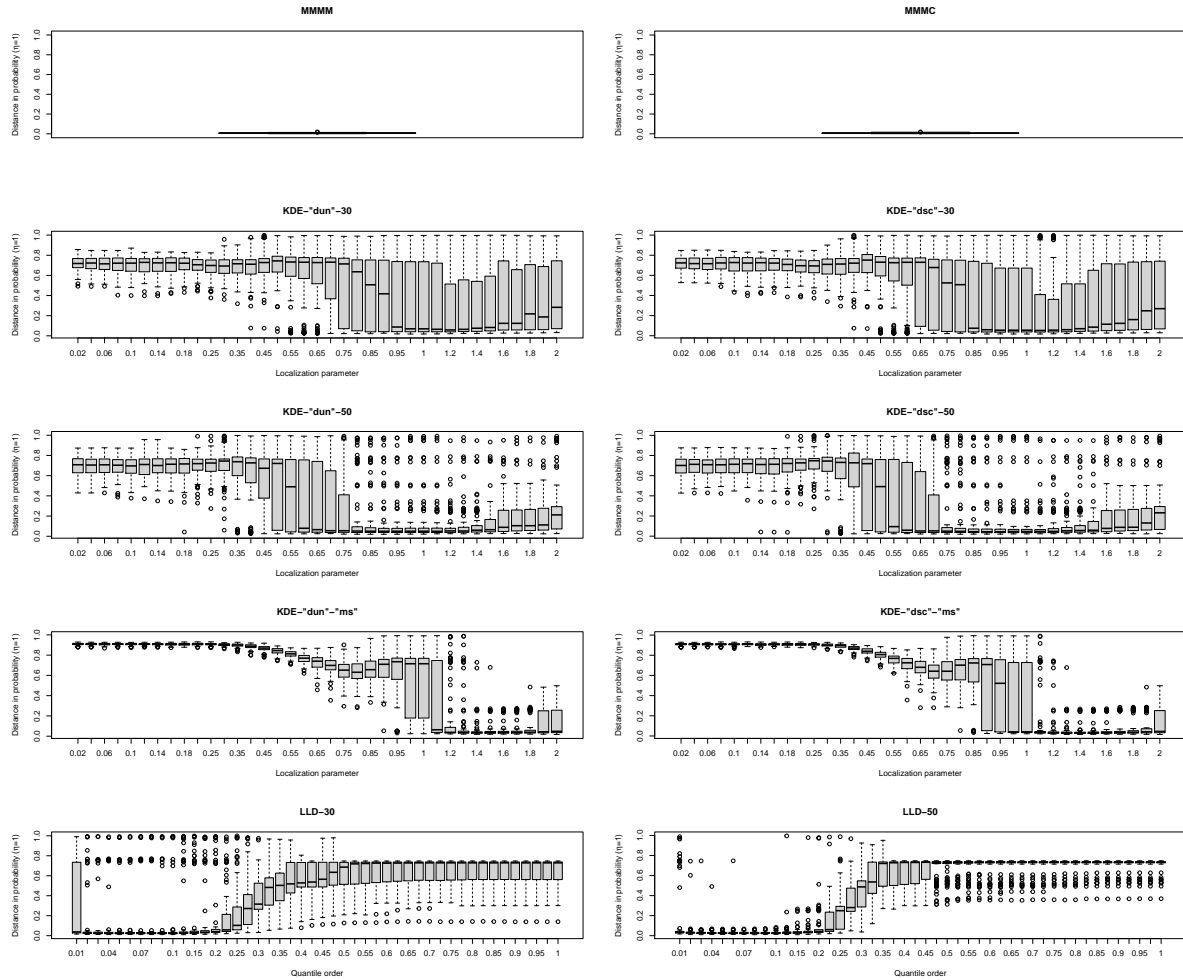


Figure 40: Boxplot of clustering errors based on distance in probability over 100 replications with $n = 1000$ samples for the Mult. Quadrinodal density.

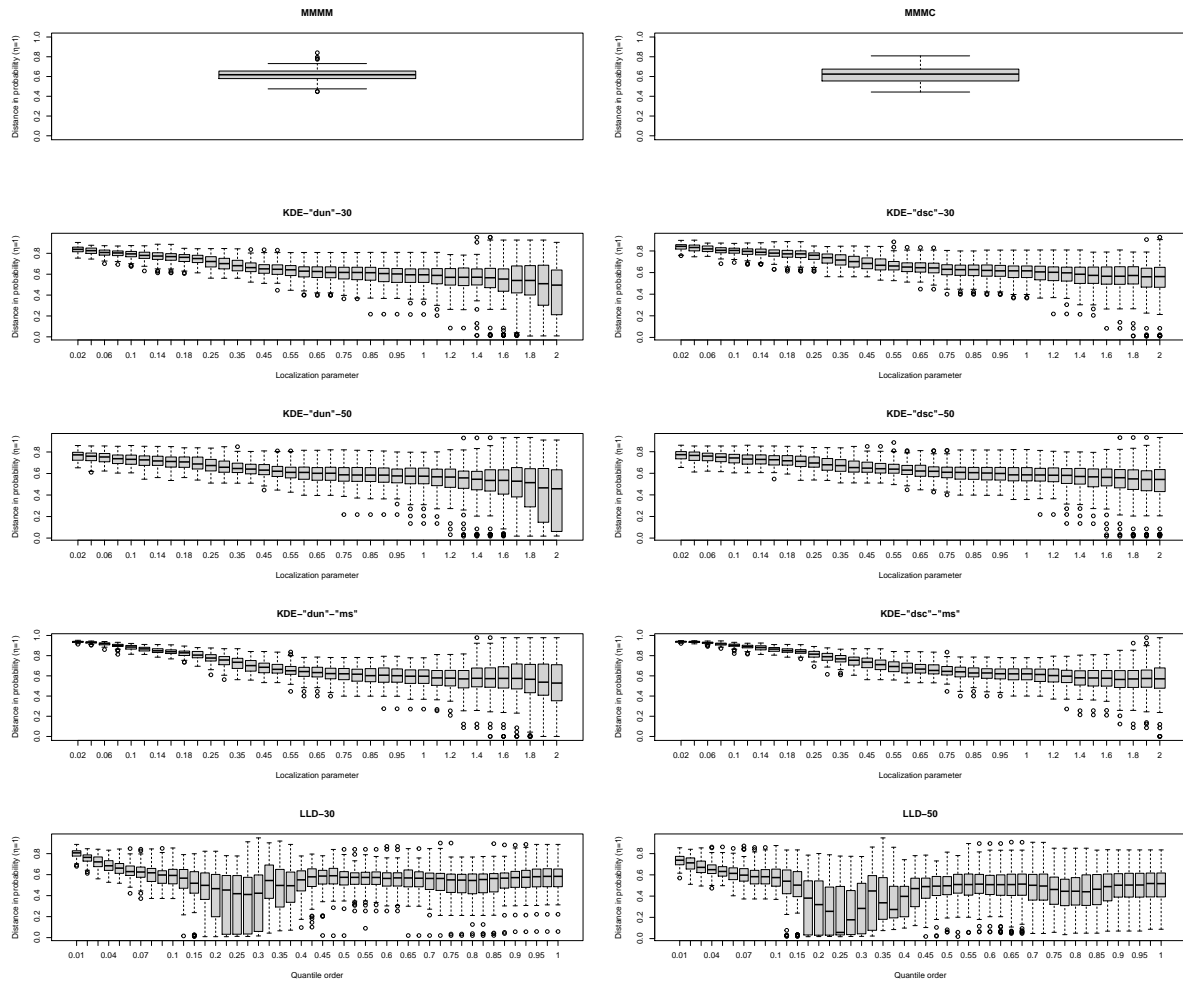


Figure 41: Boxplot of clustering errors based on distance in probability over 100 replicates with $n = 1000$ samples for the Circular 2 density.

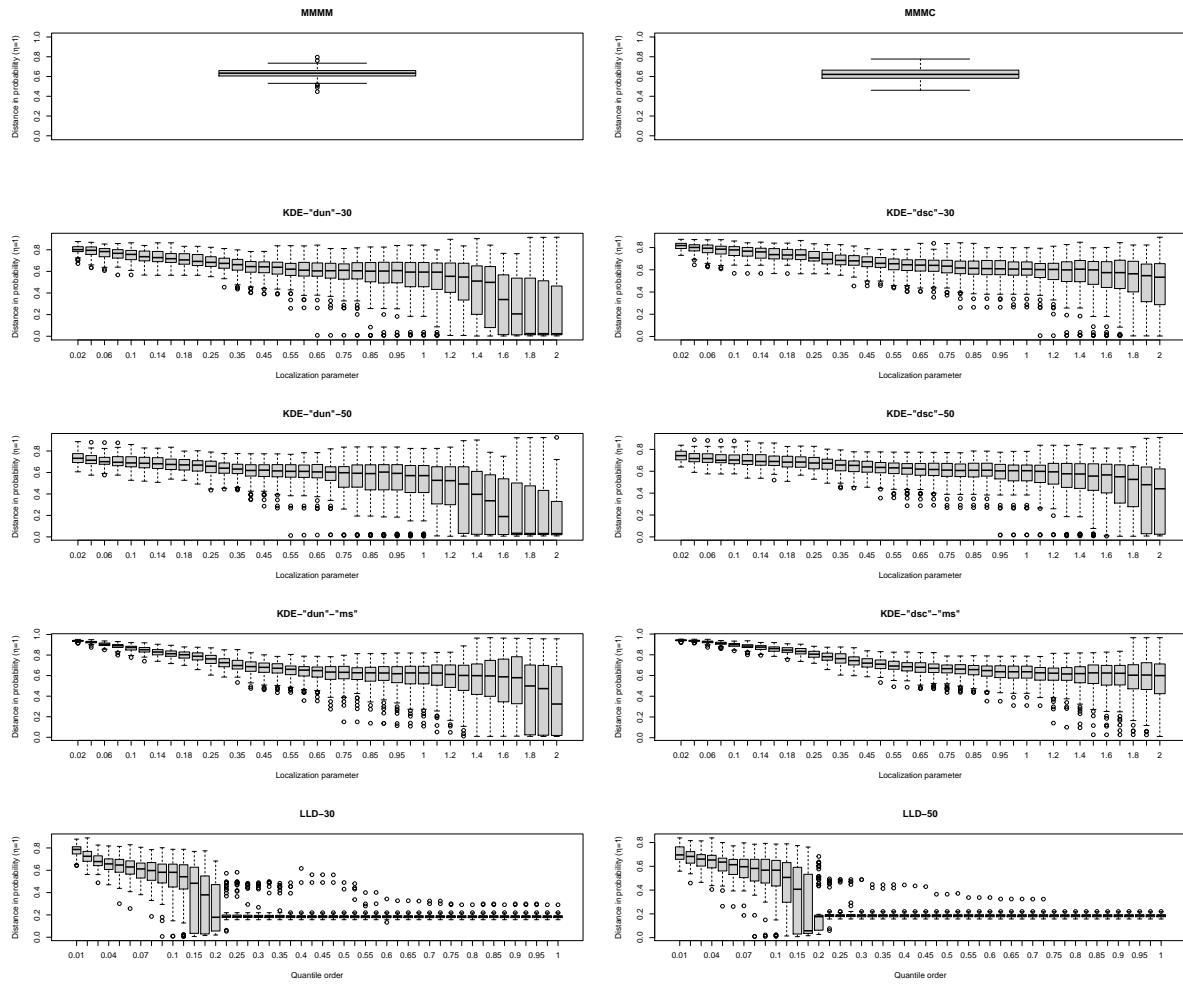


Figure 42: Boxplot of clustering errors based on distance in probability over 100 replications with $n = 1000$ samples for the Circular 2 Cauchy density.

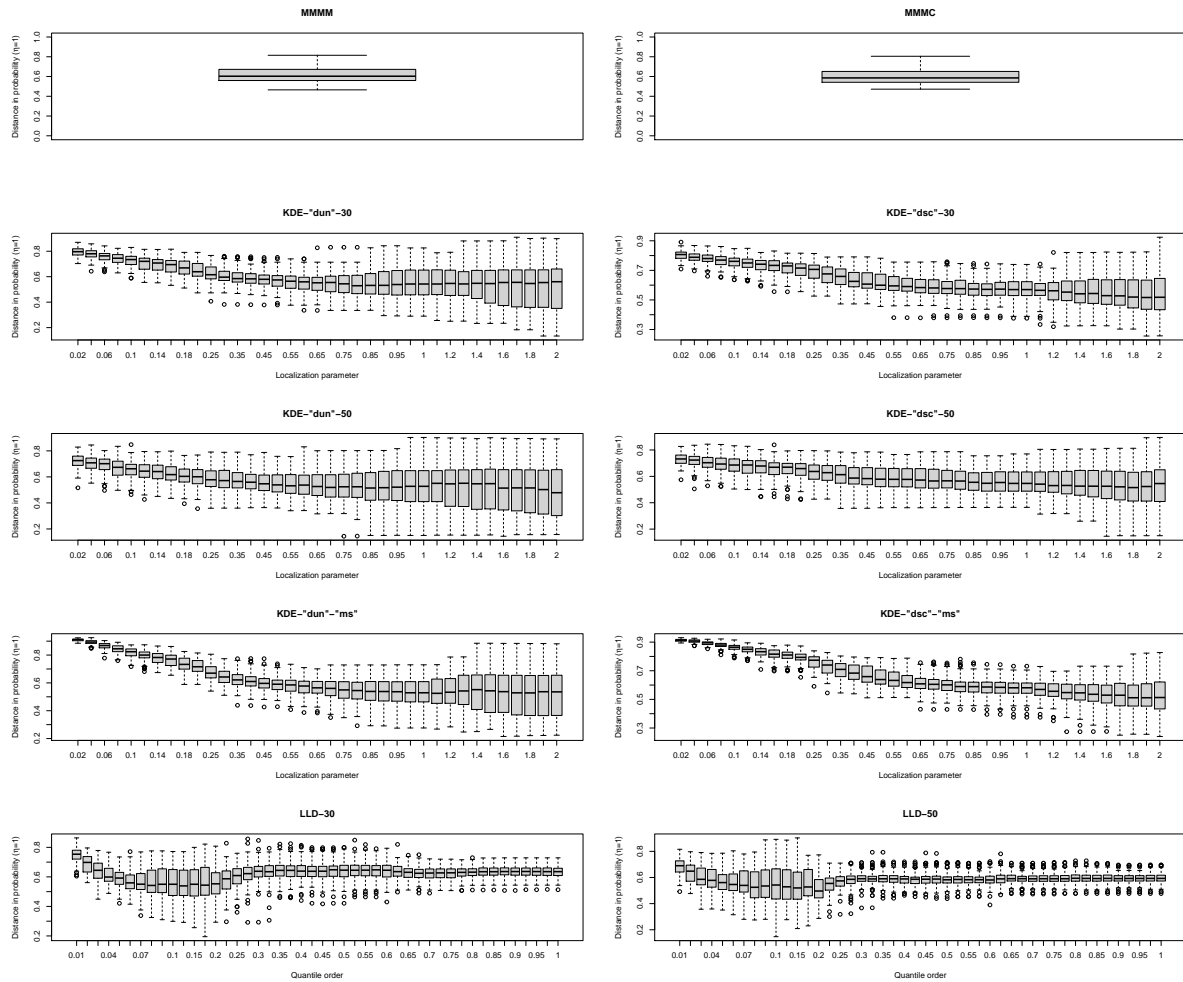


Figure 43: Boxplot of clustering errors based on distance in probability over 100 replications with $n = 1000$ samples for the Circular 3 density.

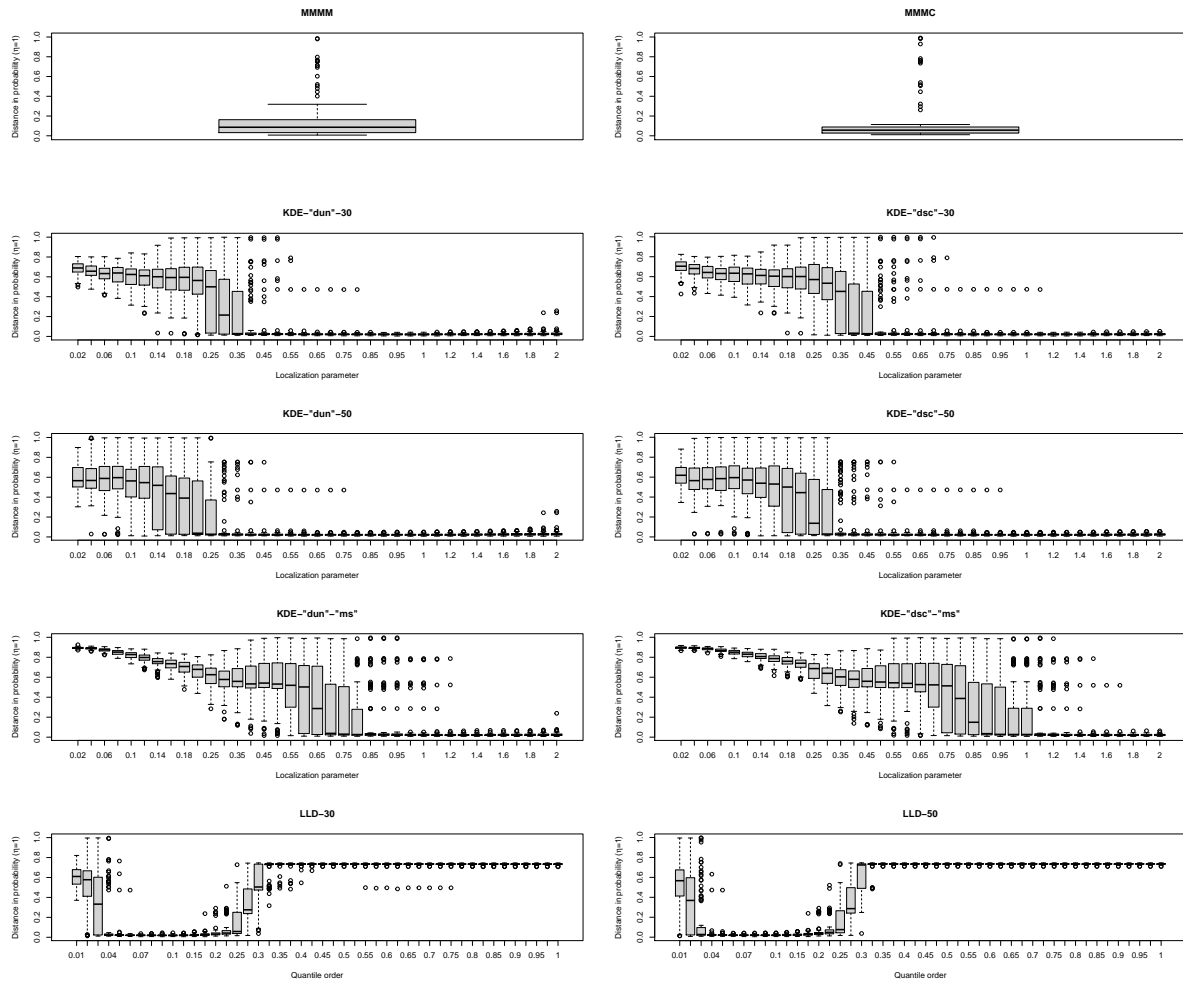


Figure 44: Boxplot of clustering errors based on distance in probability over 100 replications with $n = 1000$ samples for the Circular 4 Cauchy density.

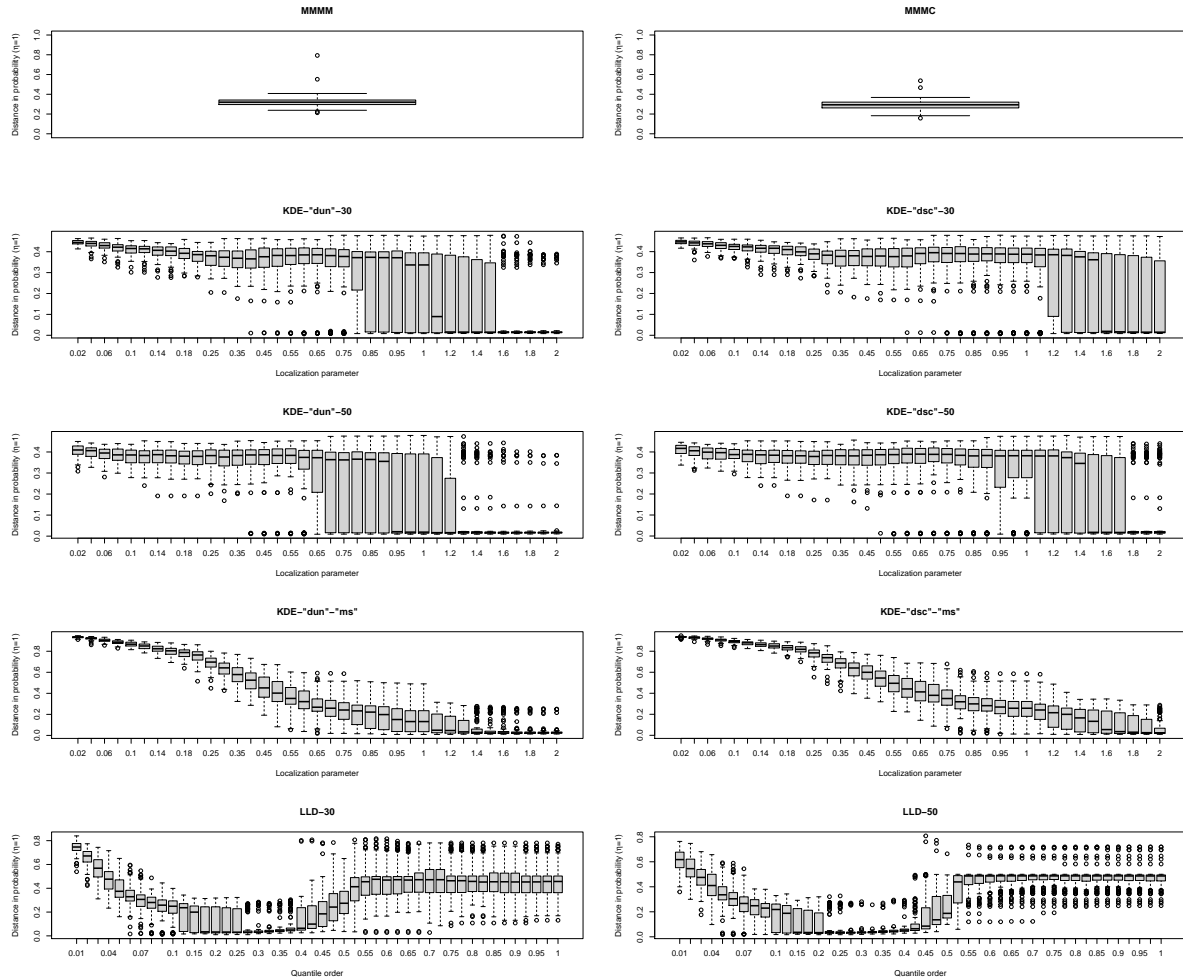


Figure 45: Boxplot of clustering errors based on distance in probability over 100 replications with $n = 1000$ samples for the Circular Bimodal I density.

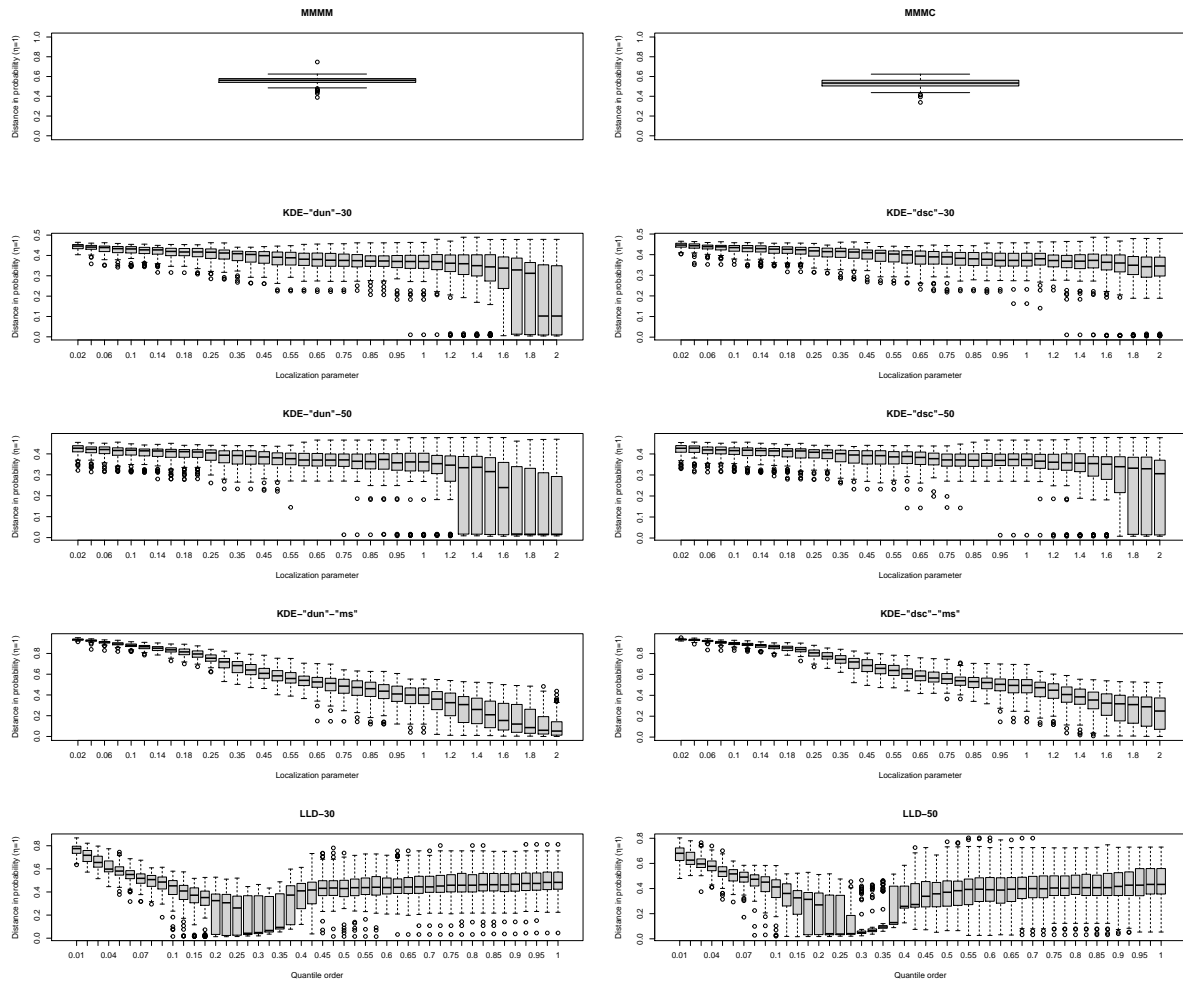


Figure 46: Boxplot of clustering errors based on distance in probability over 100 replications with $n = 1000$ samples for the Circular Bimodal II density.

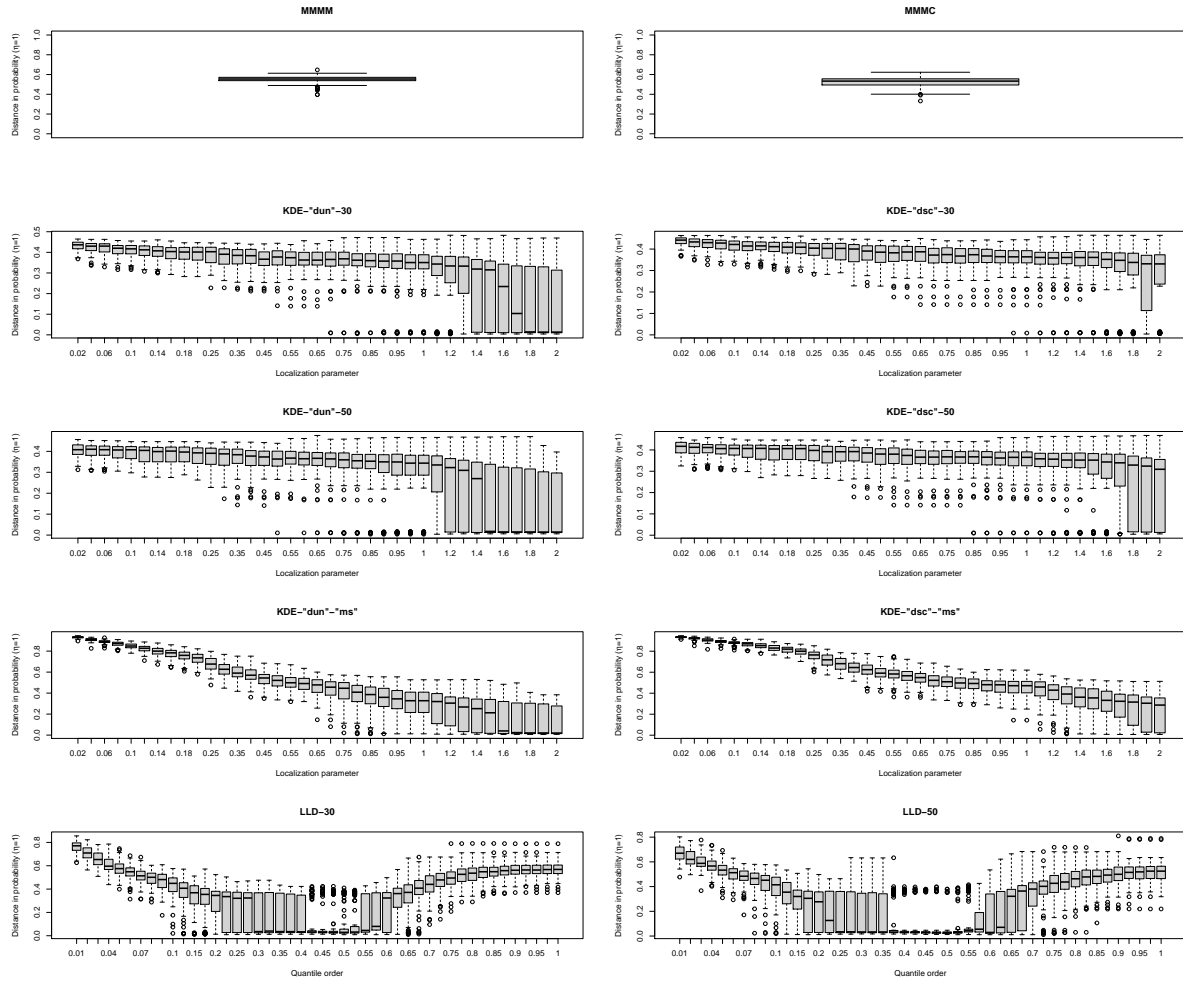


Figure 47: Boxplot of clustering errors based on distance in probability over 100 replications with $n = 1000$ samples for the Circular Bimodal III density.

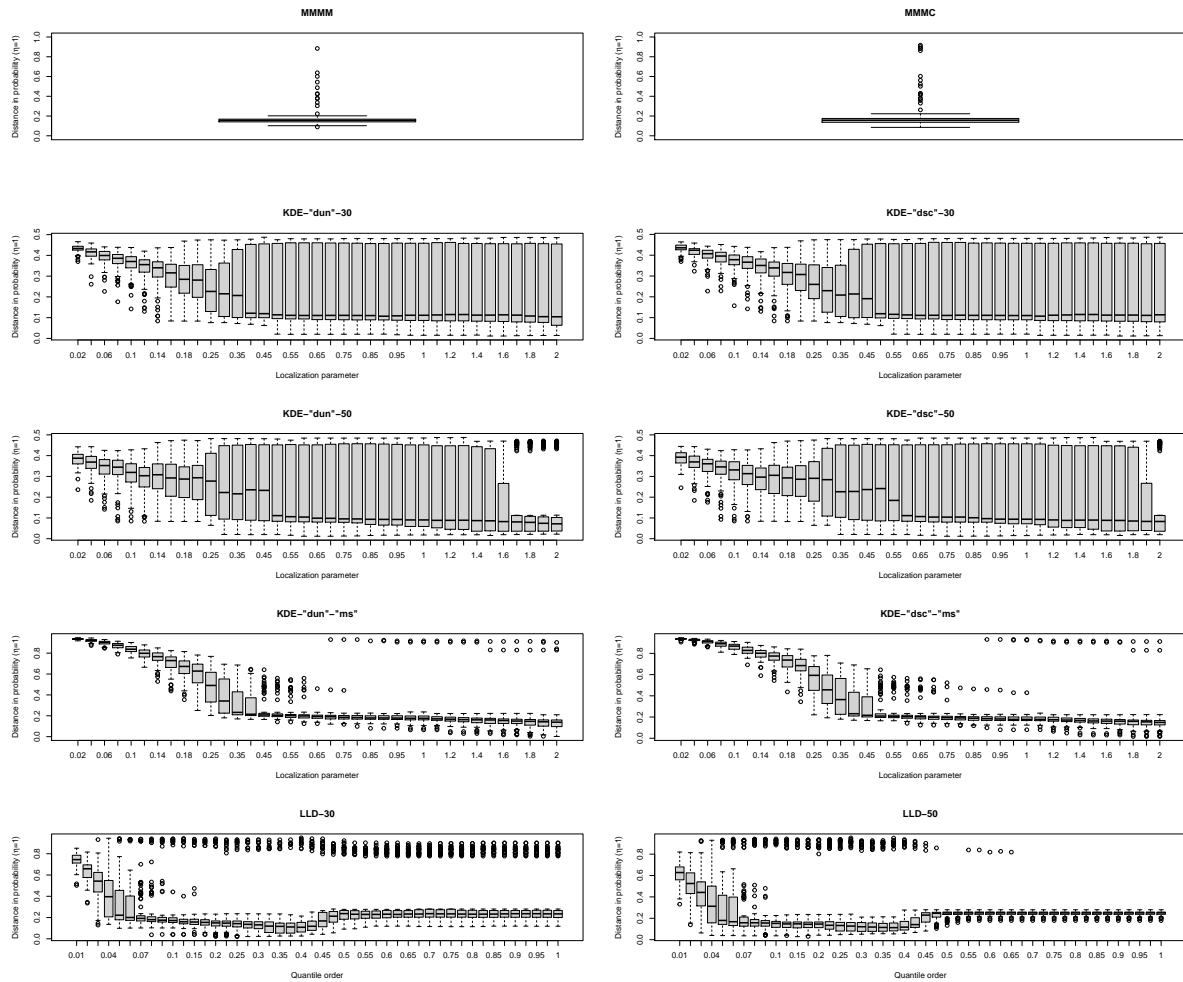


Figure 48: Boxplot of clustering errors based on distance in probability over 100 replications with $n = 1000$ samples for the Circular Bimodal IV density.

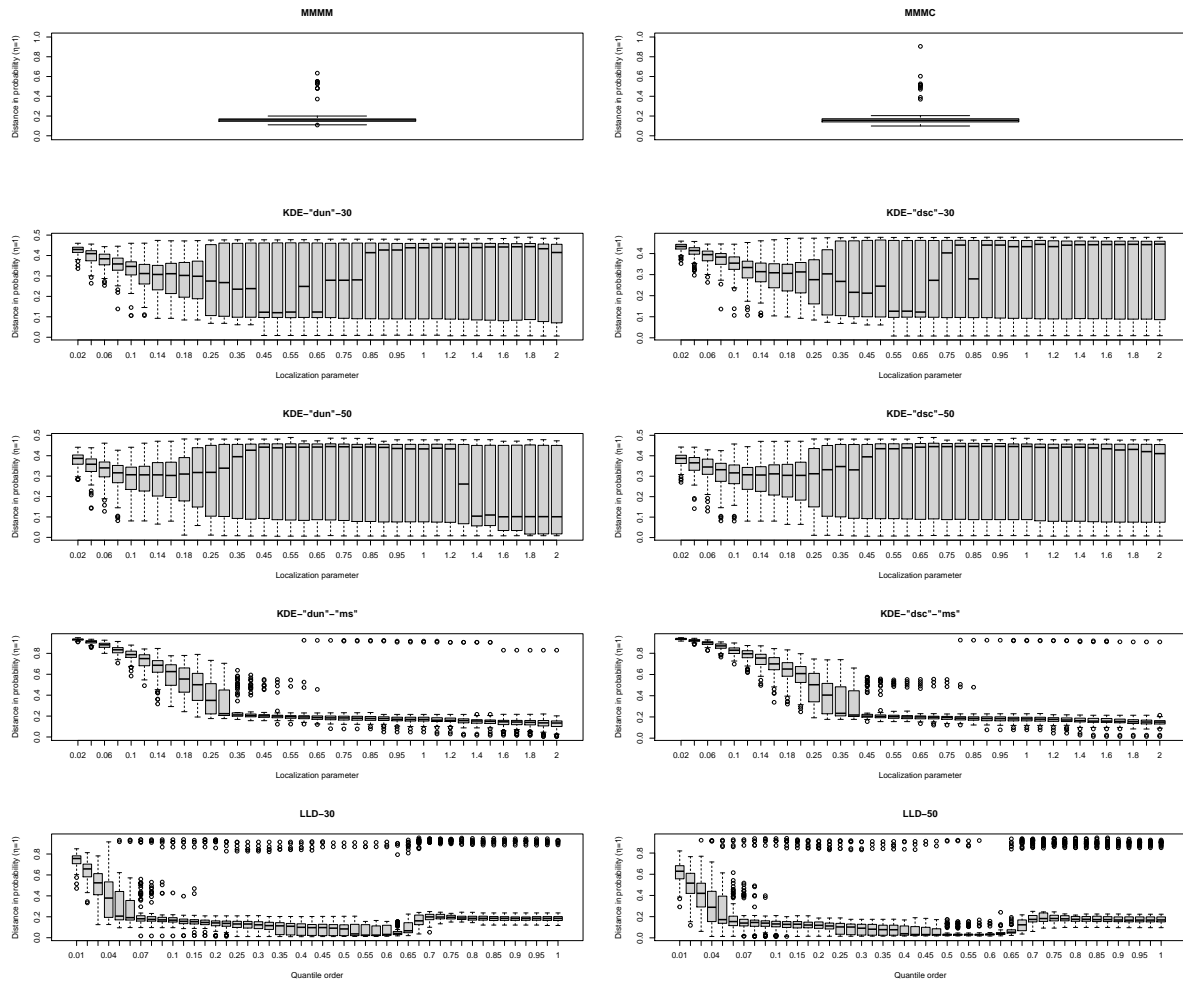


Figure 49: Boxplot of clustering errors based on distance in probability over 100 replications with $n = 1000$ samples for the Circular Bimodal V density.

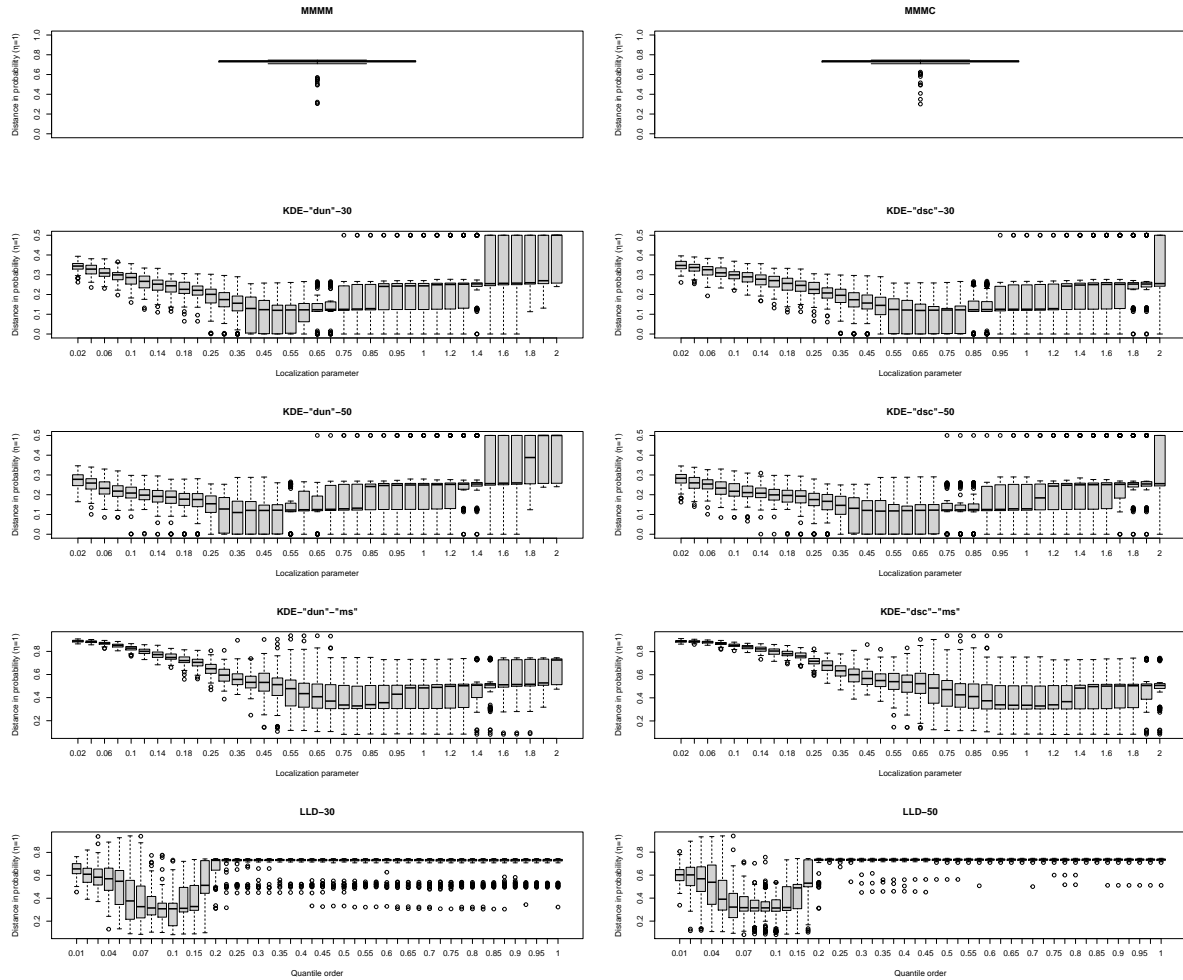


Figure 50: Boxplot of clustering errors based on distance in probability over 100 replications with $n = 1000$ samples for the Circular Quadrimodal I density.

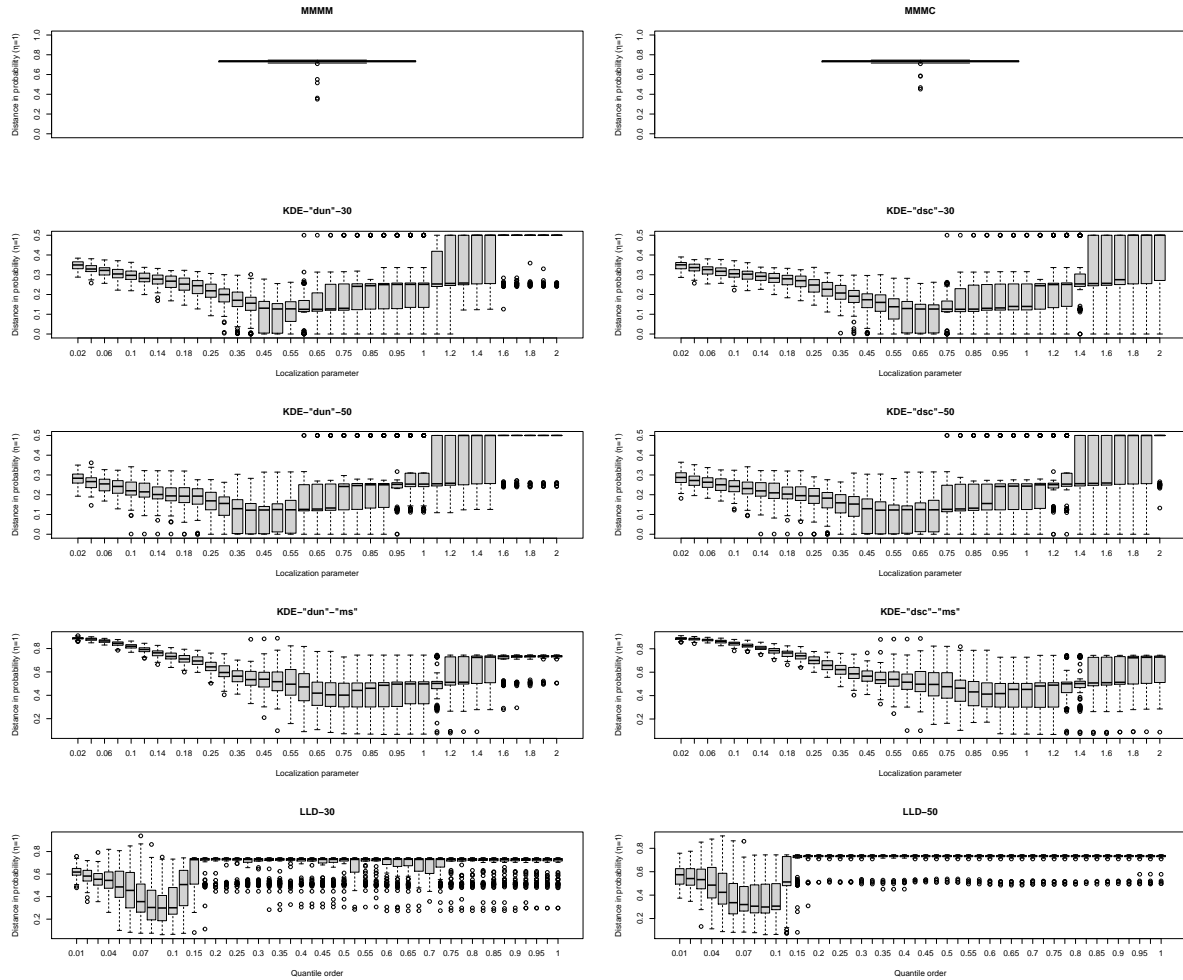


Figure 51: Boxplot of clustering errors based on distance in probability over 100 replications with $n = 1000$ samples for the Circular Quadrimodal II density.

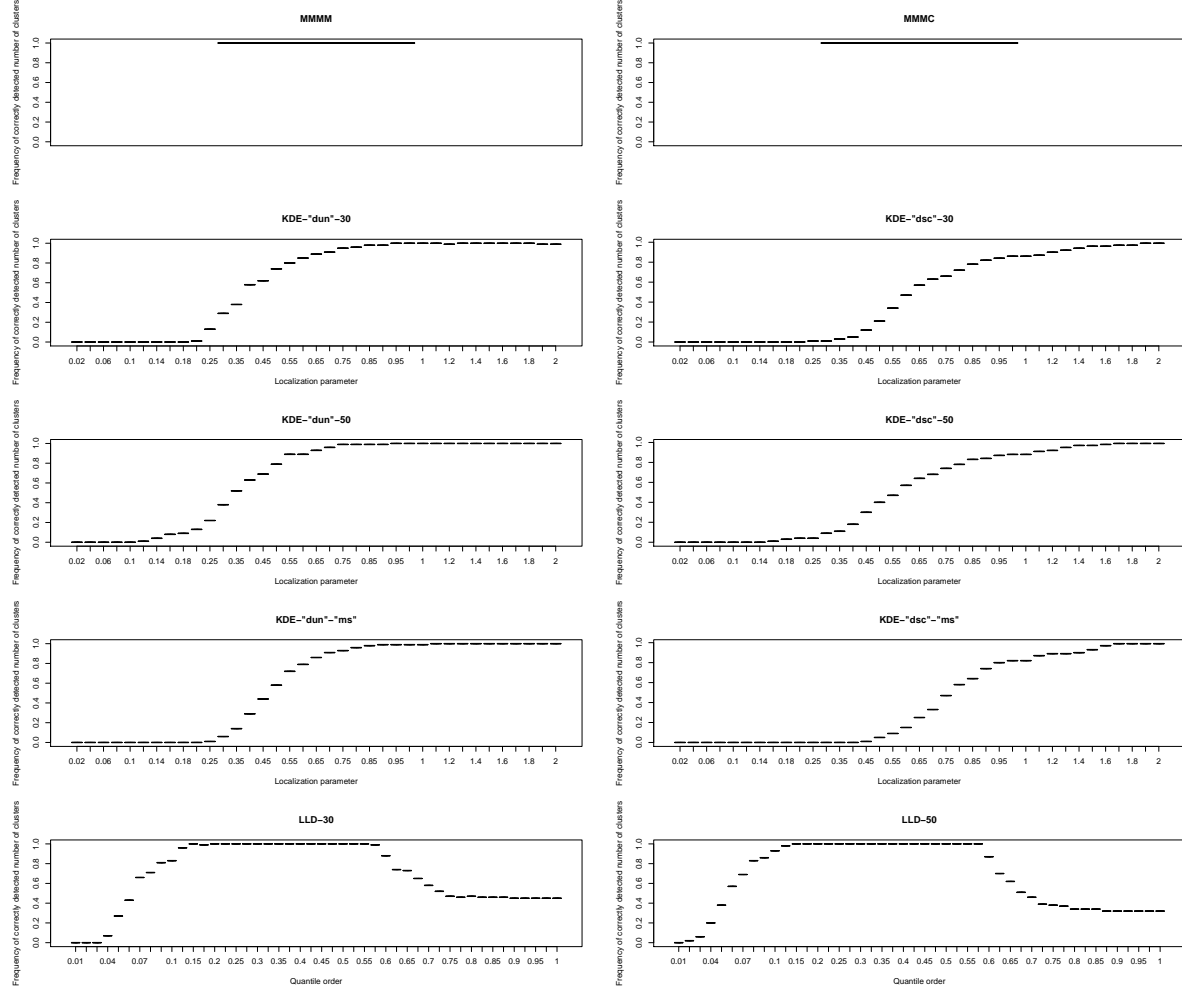


Figure 52: Boxplot of frequency of correctly detected number of clusters over 100 replications with $n = 1000$ samples for the (H) Bimodal IV density.

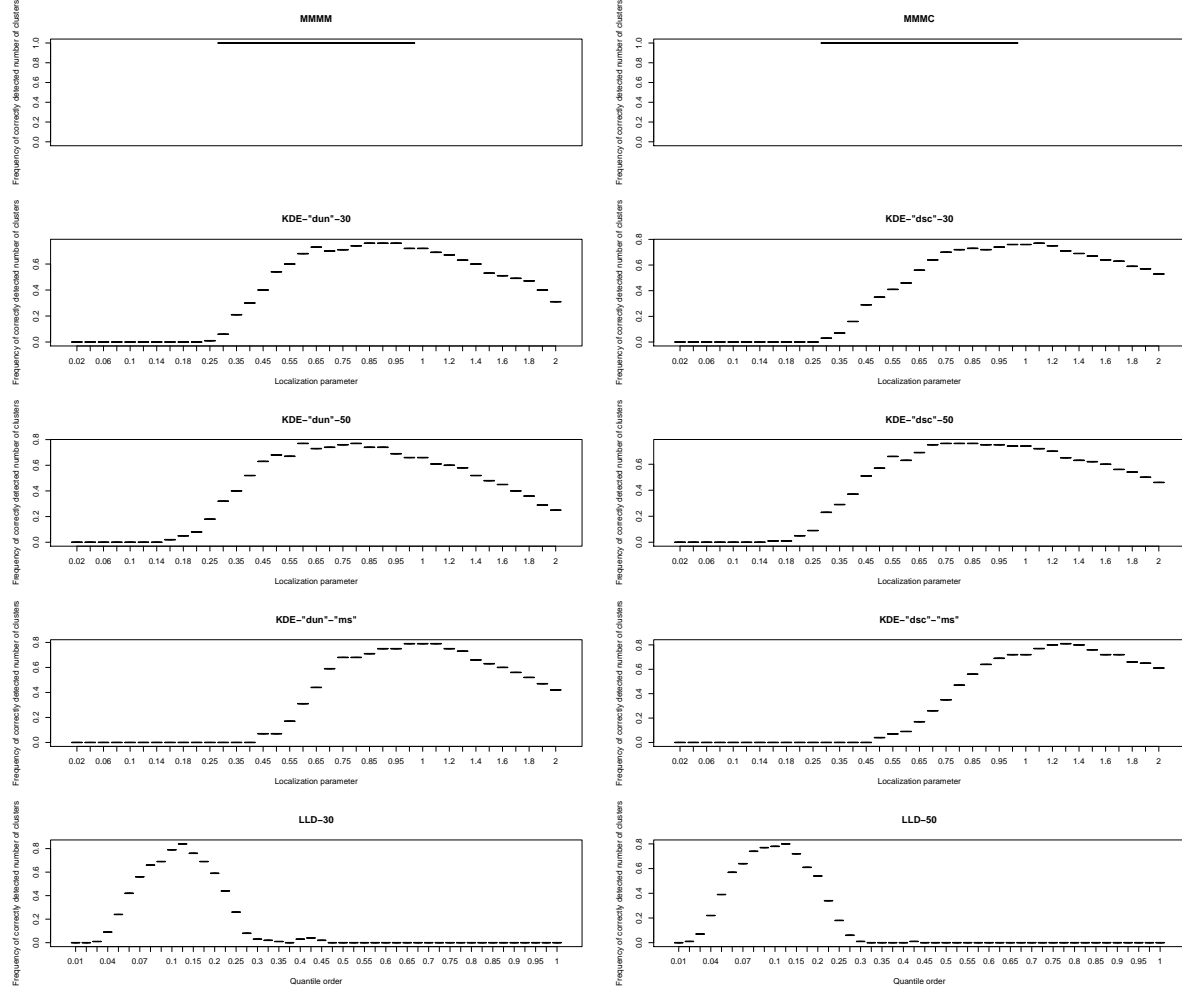


Figure 53: Boxplot of frequency of correctly detected number of clusters over 100 replications with $n = 1000$ samples for the (K) Trimodal III density.

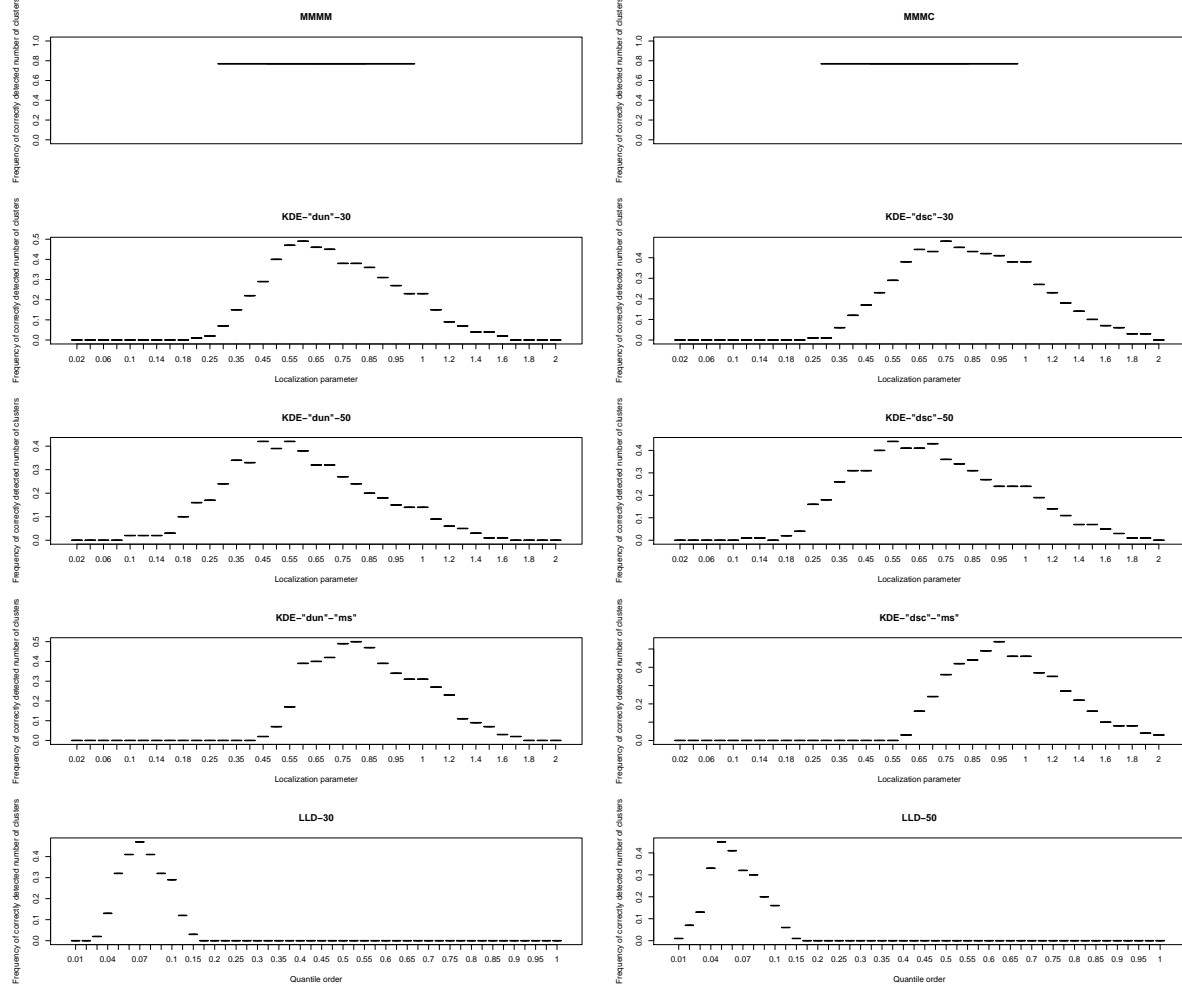


Figure 54: Boxplot of frequency of correctly detected number of clusters over 100 replications with $n = 1000$ samples for the (L) Quadrimodal density.

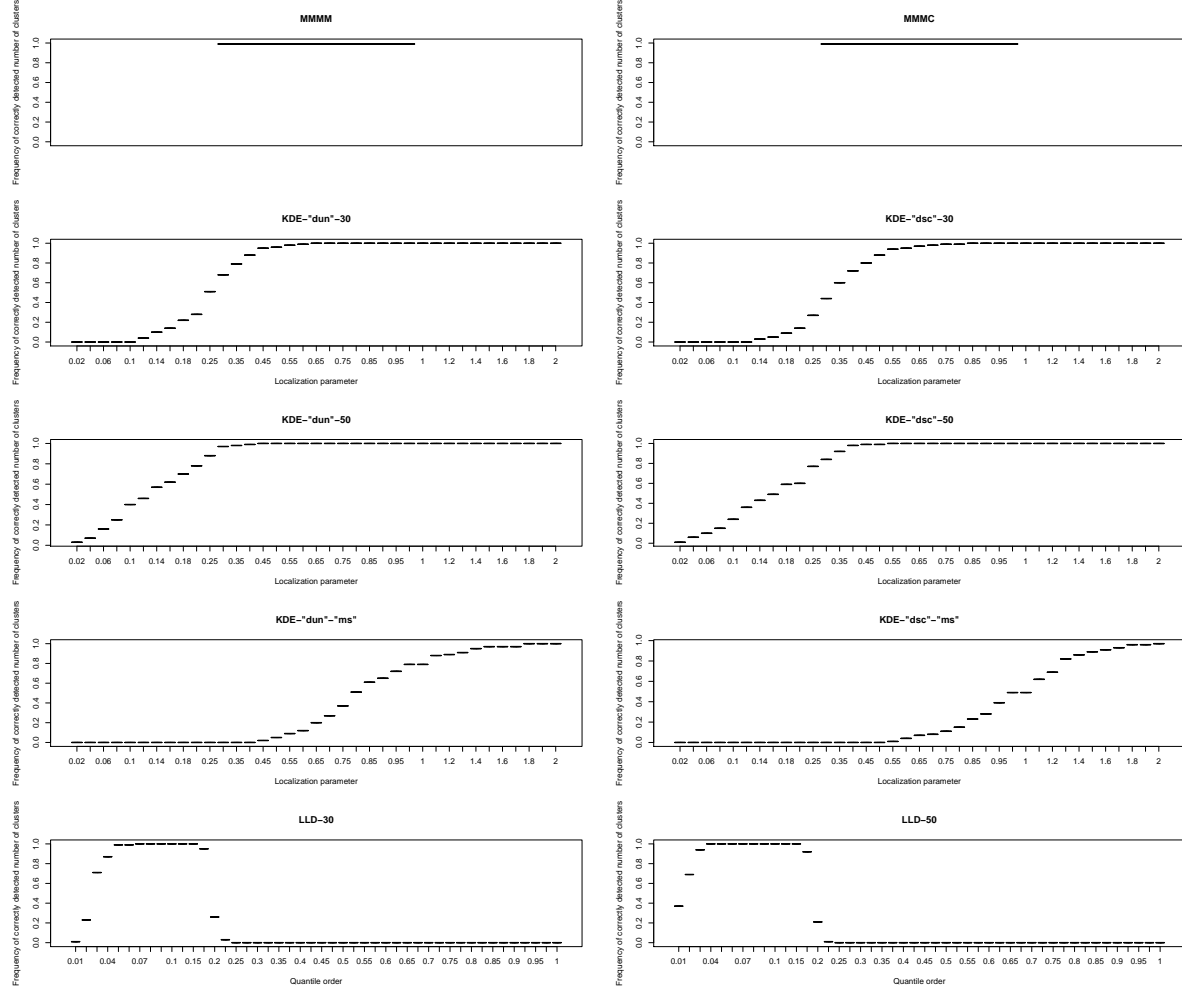


Figure 55: Boxplot of frequency of correctly detected number of clusters over 100 replications with $n = 1000$ samples for the #10 fountain density.

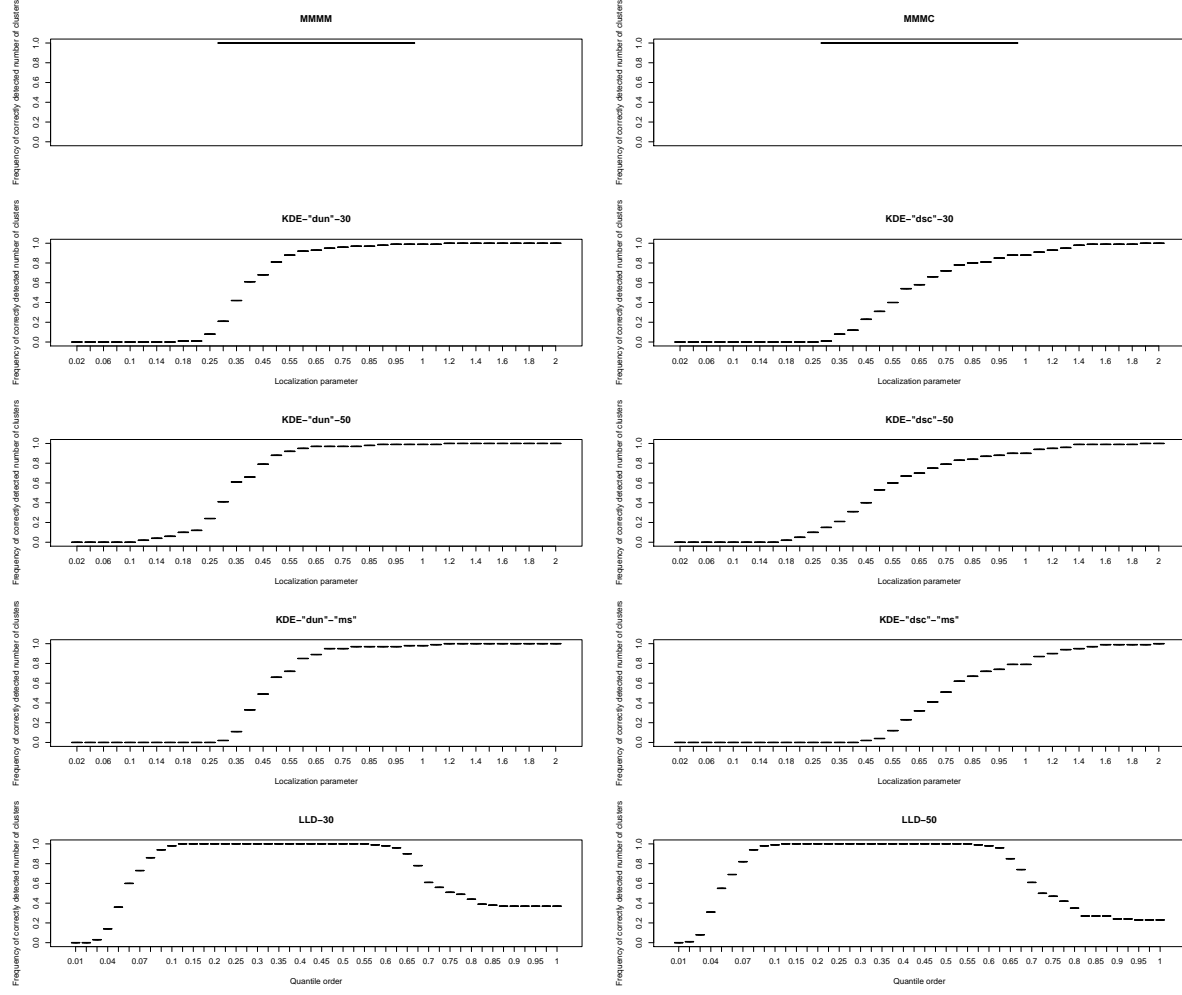


Figure 56: Boxplot of frequency of correctly detected number of clusters over 100 replications with $n = 1000$ samples for the Bimodal density.

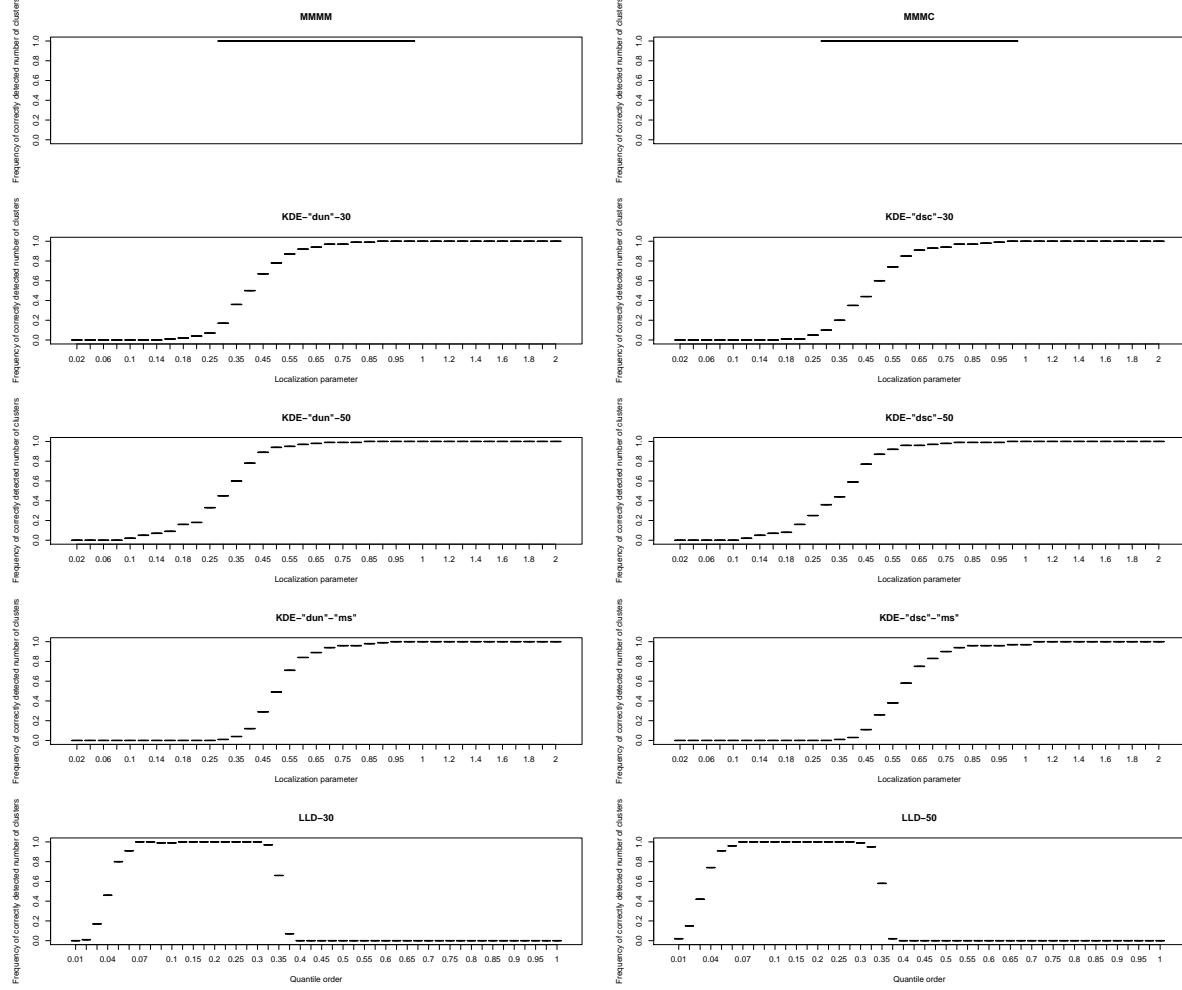


Figure 57: Boxplot of frequency of correctly detected number of clusters over 100 replications with $n = 1000$ samples for the Quadrimodal density.

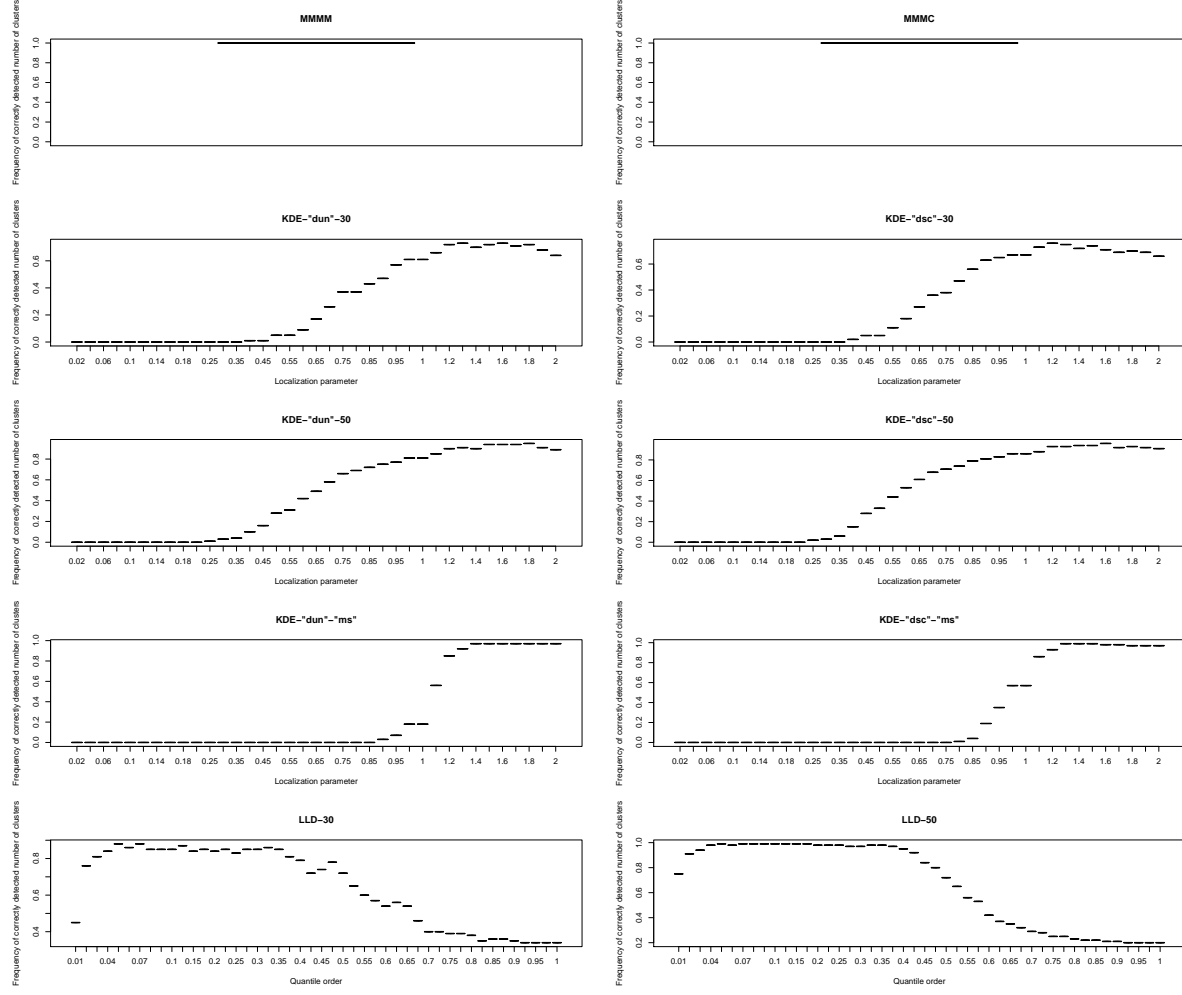


Figure 58: Boxplot of frequency of correctly detected number of clusters over 100 replications with $n = 1000$ samples for the Mult. Bimodal density.

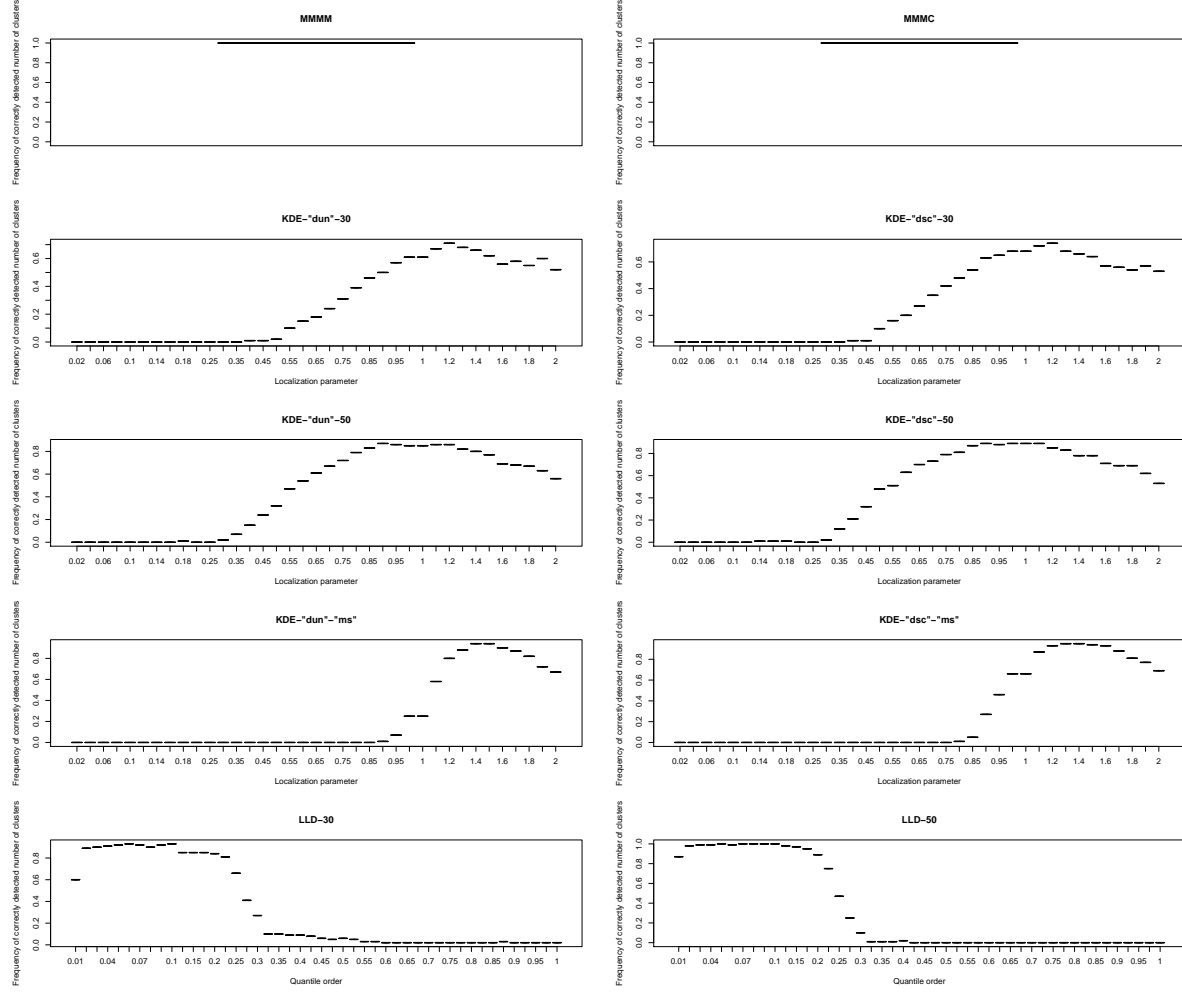


Figure 59: Boxplot of frequency of correctly detected number of clusters over 100 replications with $n = 1000$ samples for the Mult. Quadrimodal density.

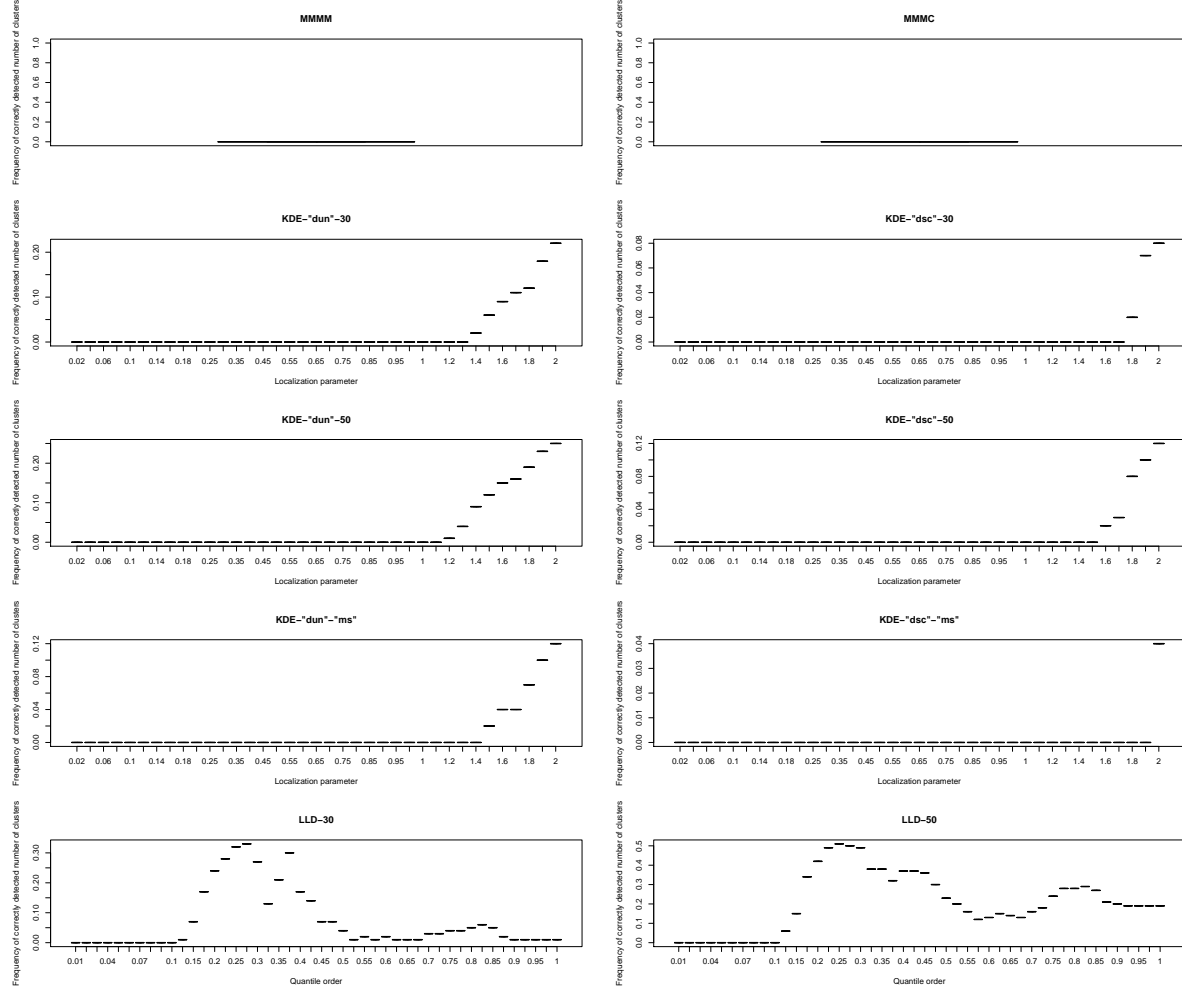


Figure 60: Boxplot of frequency of correctly detected number of clusters over 100 replications with $n = 1000$ samples for the Circular 2 density.

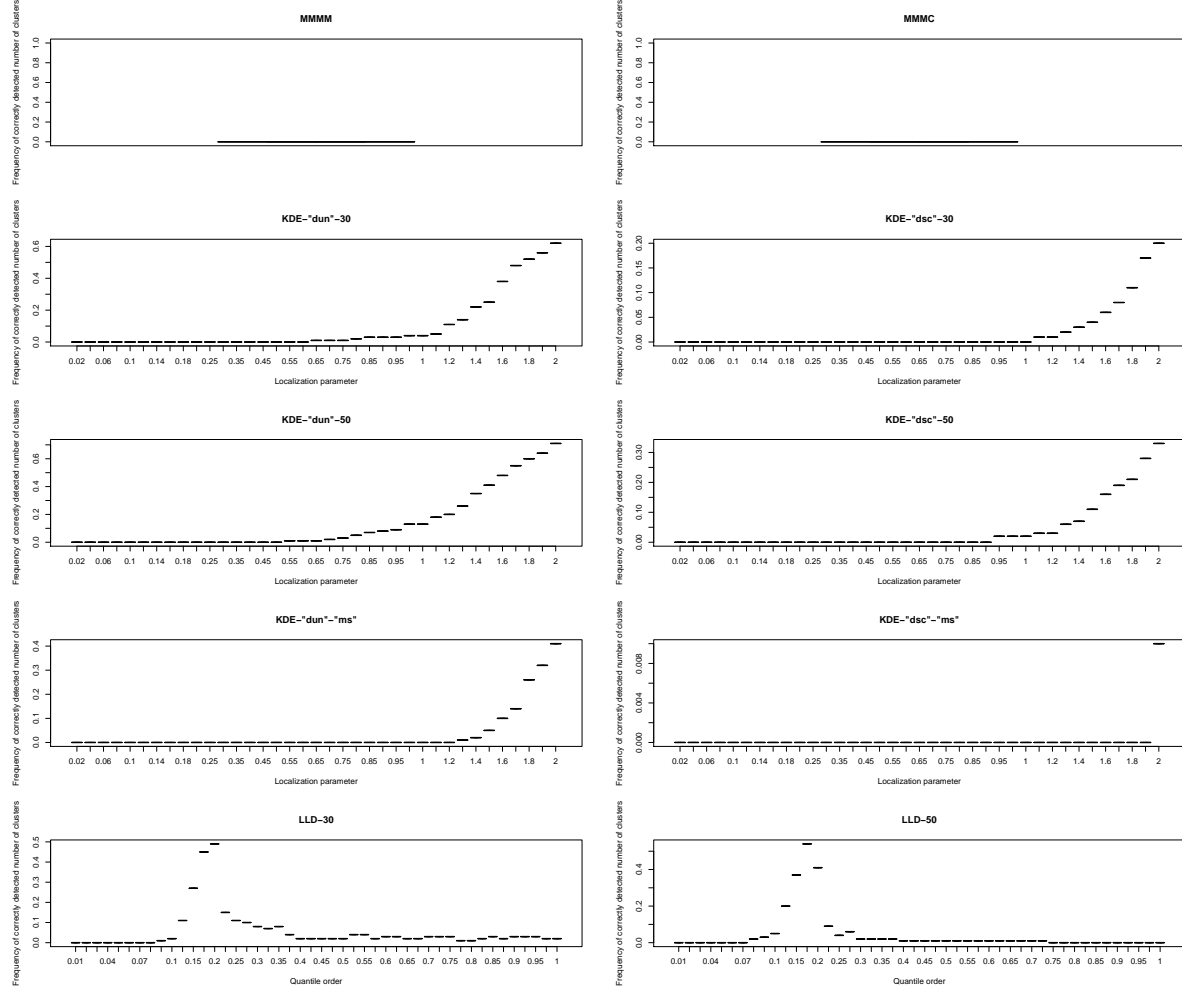


Figure 61: Boxplot of frequency of correctly detected number of clusters over 100 replications with $n = 1000$ samples for the Circular 2 Cauchy density.

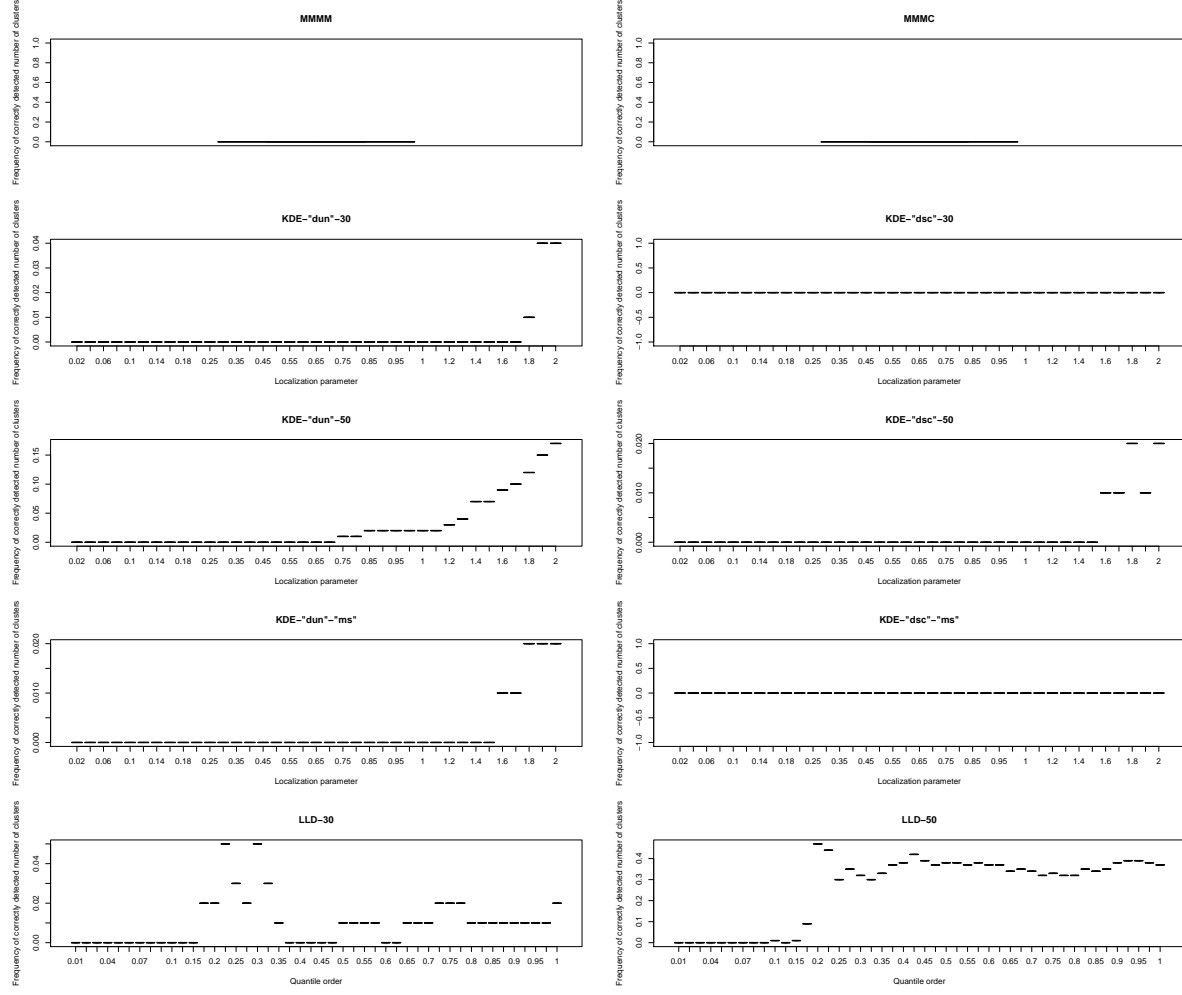


Figure 62: Boxplot of frequency of correctly detected number of clusters over 100 replications with $n = 1000$ samples for the Circular 3 density.

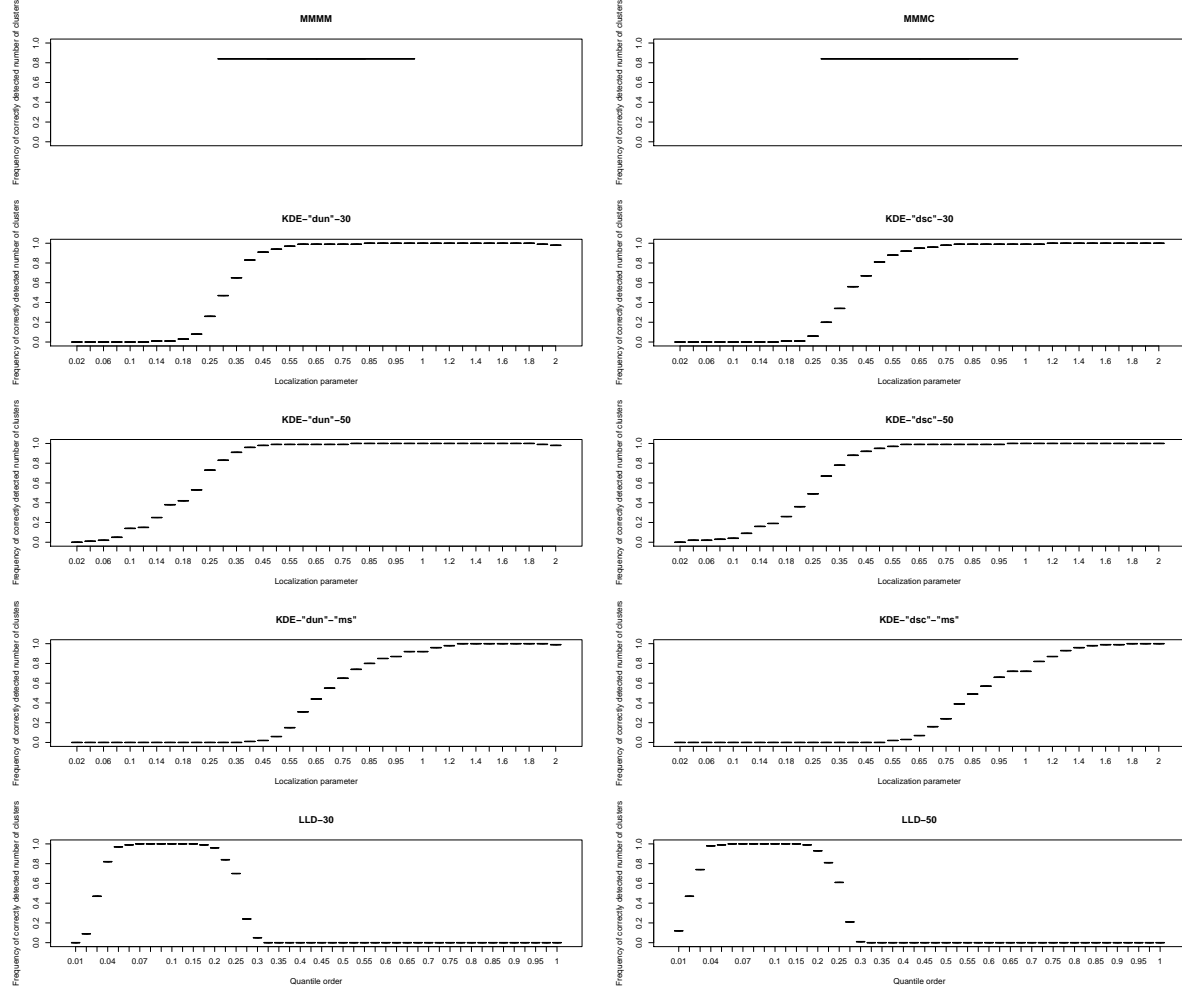


Figure 63: Boxplot of frequency of correctly detected number of clusters over 100 replications with $n = 1000$ samples for the Circular 4 Cauchy density.

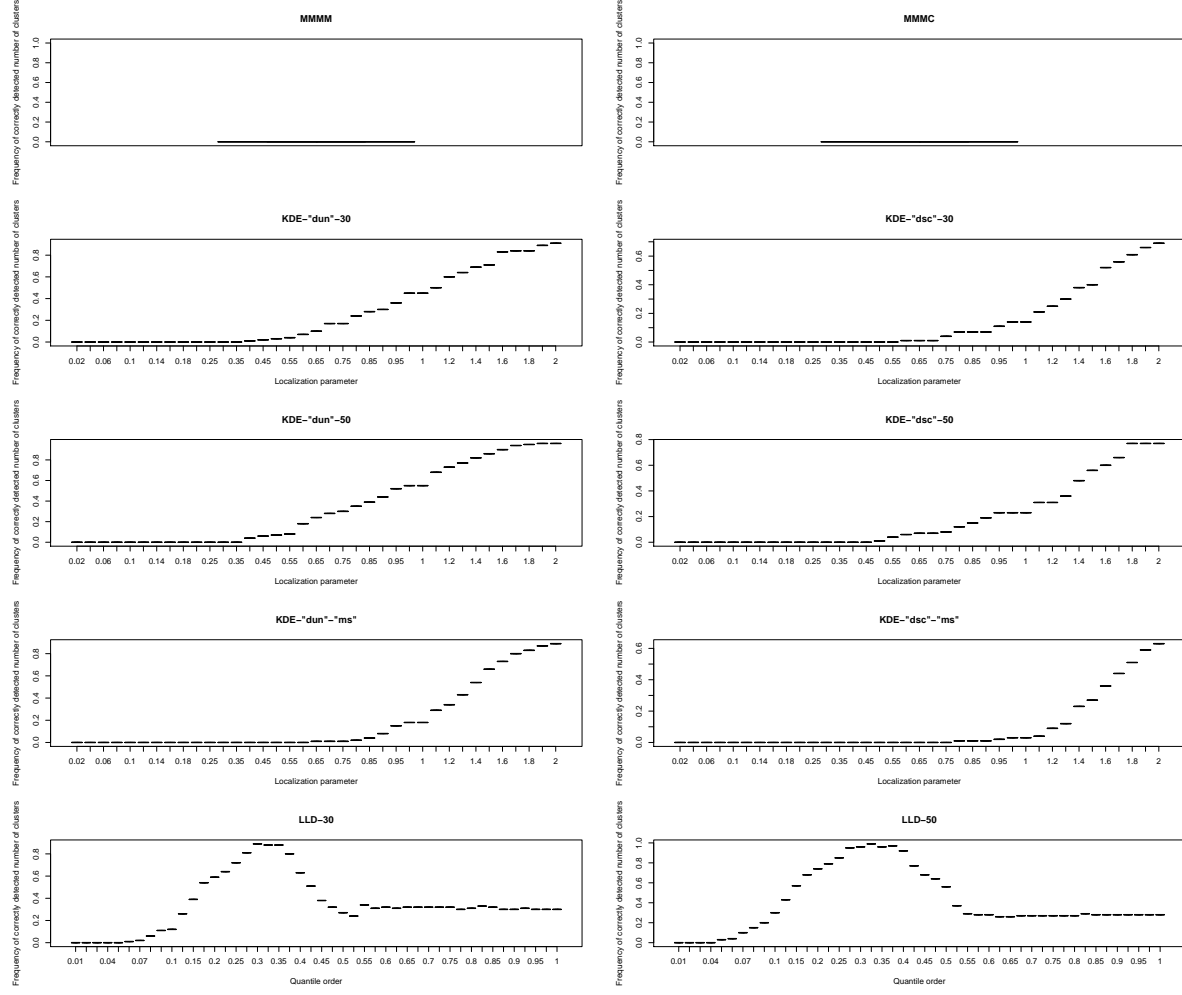


Figure 64: Boxplot of frequency of correctly detected number of clusters over 100 replications with $n = 1000$ samples for the Circular Bimodal I density.

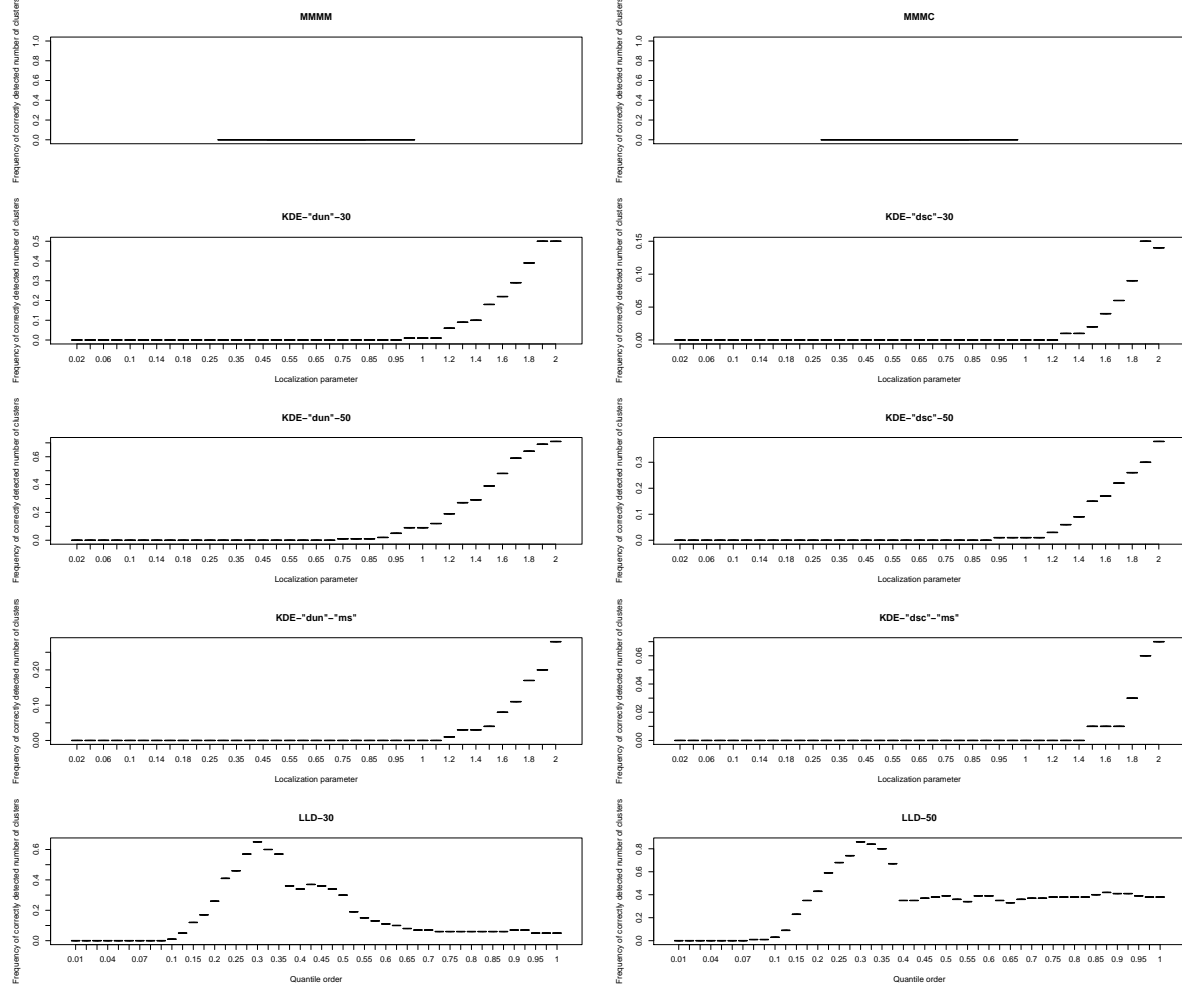


Figure 65: Boxplot of frequency of correctly detected number of clusters over 100 replications with $n = 1000$ samples for the Circular Bimodal II density.

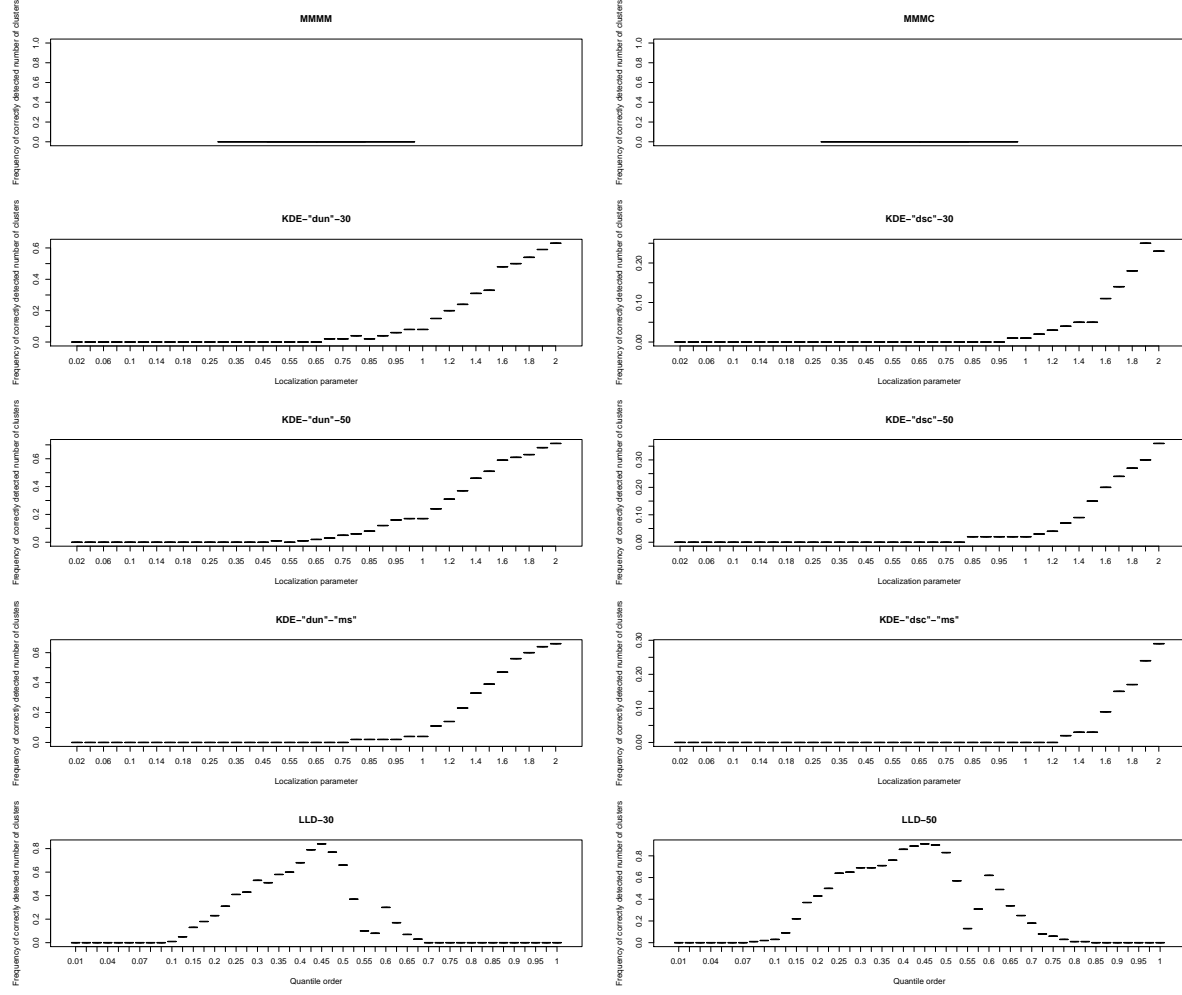


Figure 66: Boxplot of frequency of correctly detected number of clusters over 100 replications with $n = 1000$ samples for the Circular Bimodal III density.

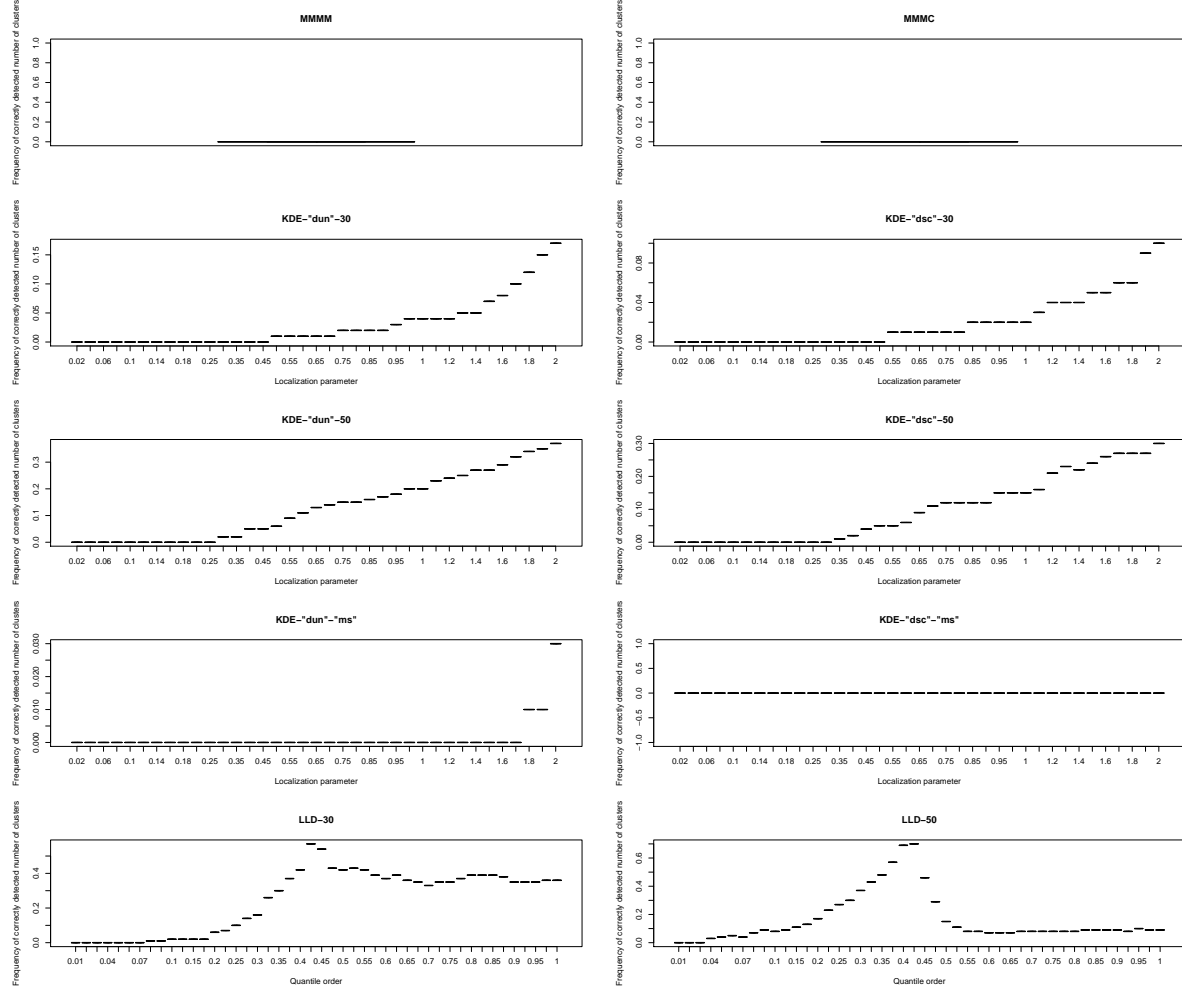


Figure 67: Boxplot of frequency of correctly detected number of clusters over 100 replications with $n = 1000$ samples for the Circular Bimodal IV density.

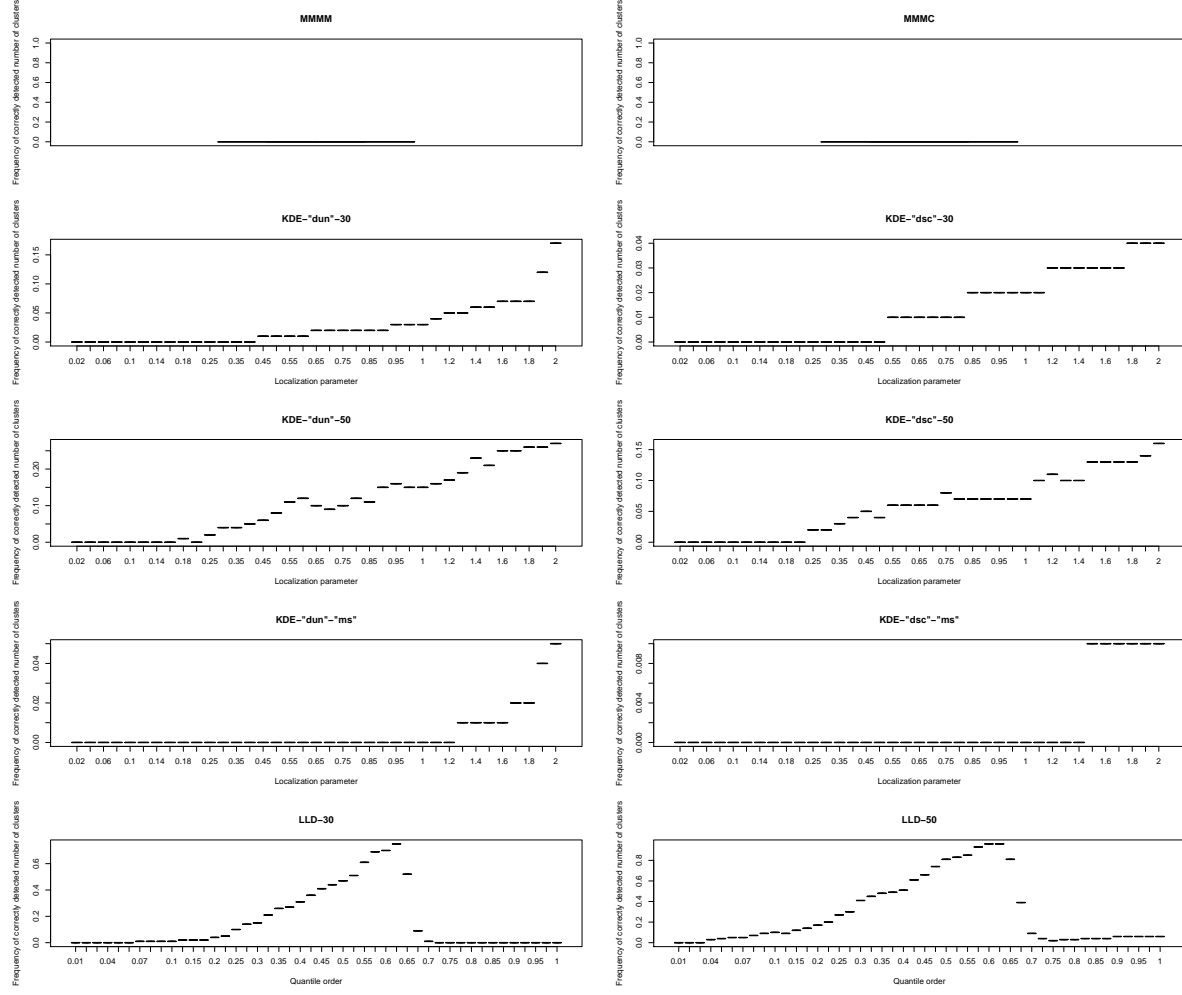


Figure 68: Boxplot of frequency of correctly detected number of clusters over 100 replications with $n = 1000$ samples for the Circular Bimodal V density.

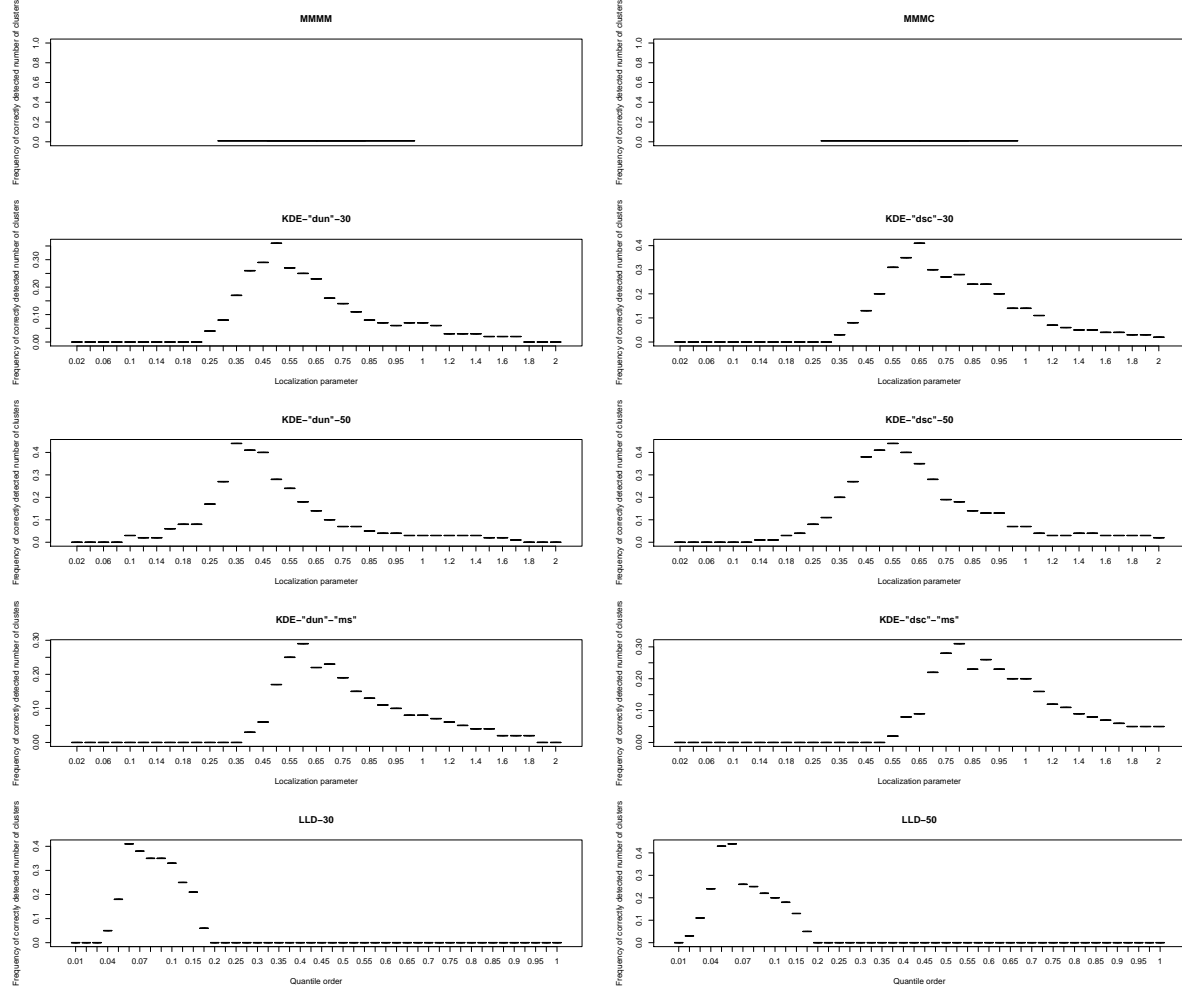


Figure 69: Boxplot of frequency of correctly detected number of clusters over 100 replications with $n = 1000$ samples for the Circular Quadrimodal I density.

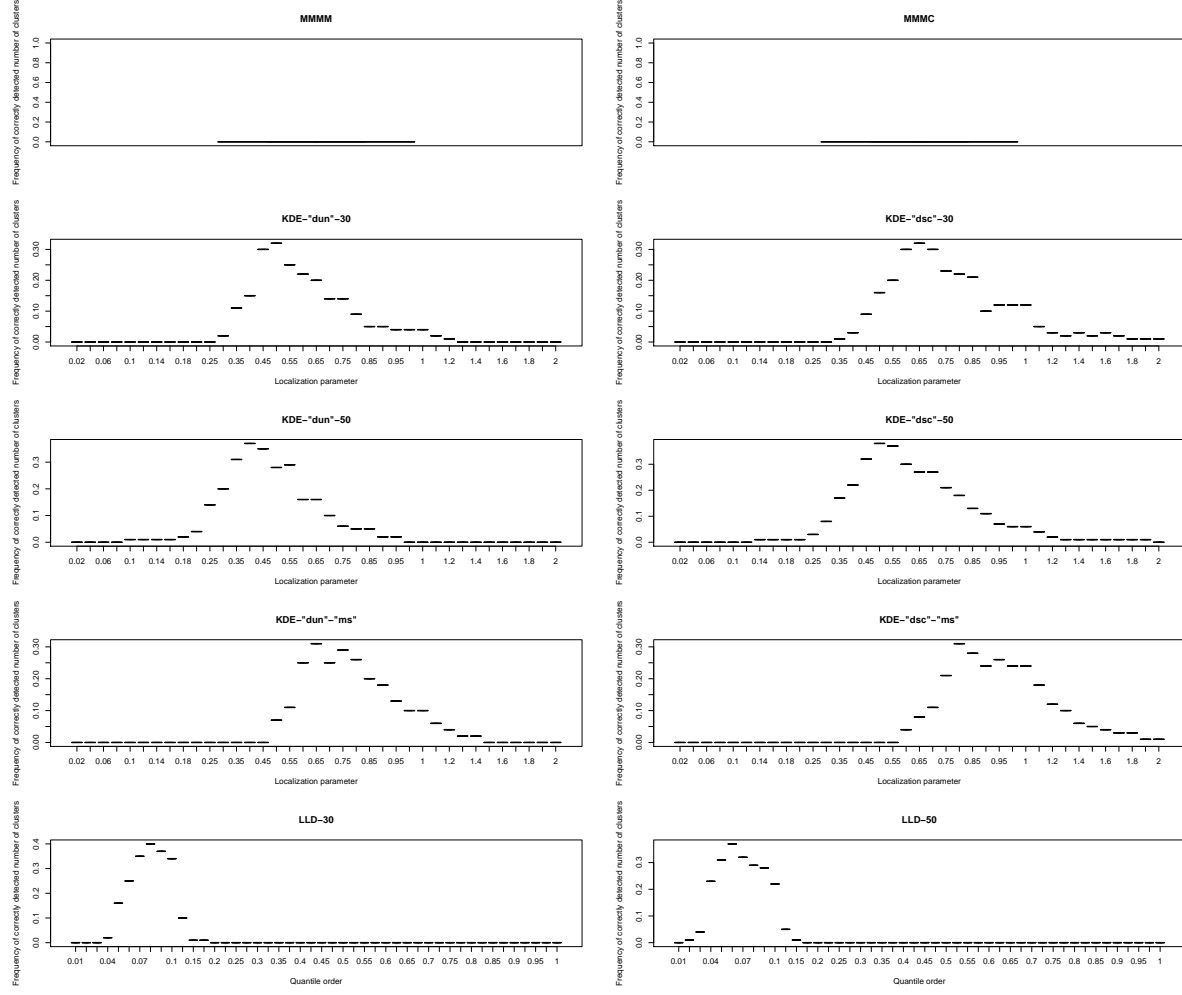


Figure 70: Boxplot of frequency of correctly detected number of clusters over 100 replications with $n = 1000$ samples for the Circular Quadrimodal II density.

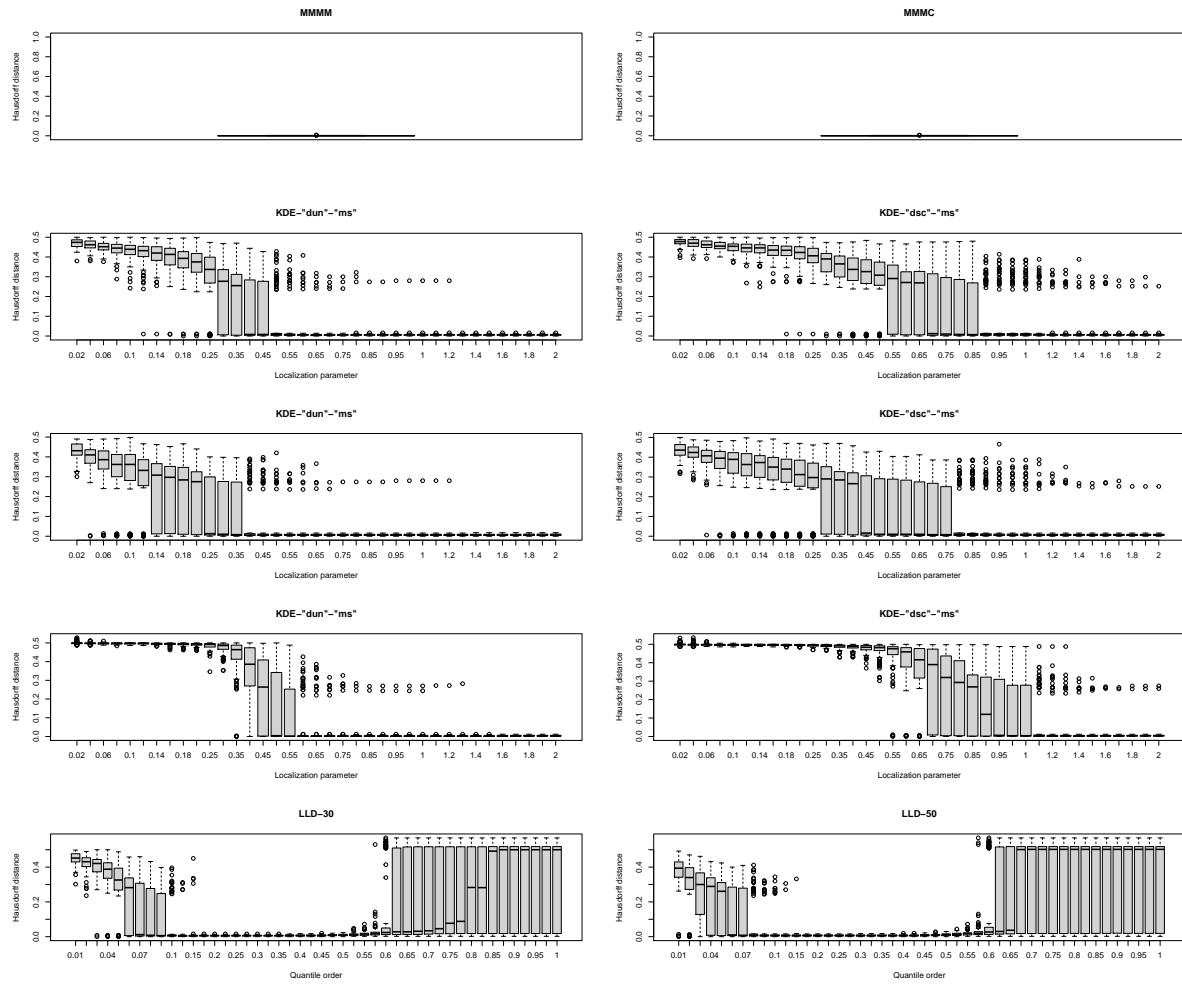


Figure 71: Boxplot of clustering errors based on Hausdorff distance over 100 replications with $n = 500$ samples for the (H) Bimodal IV density.

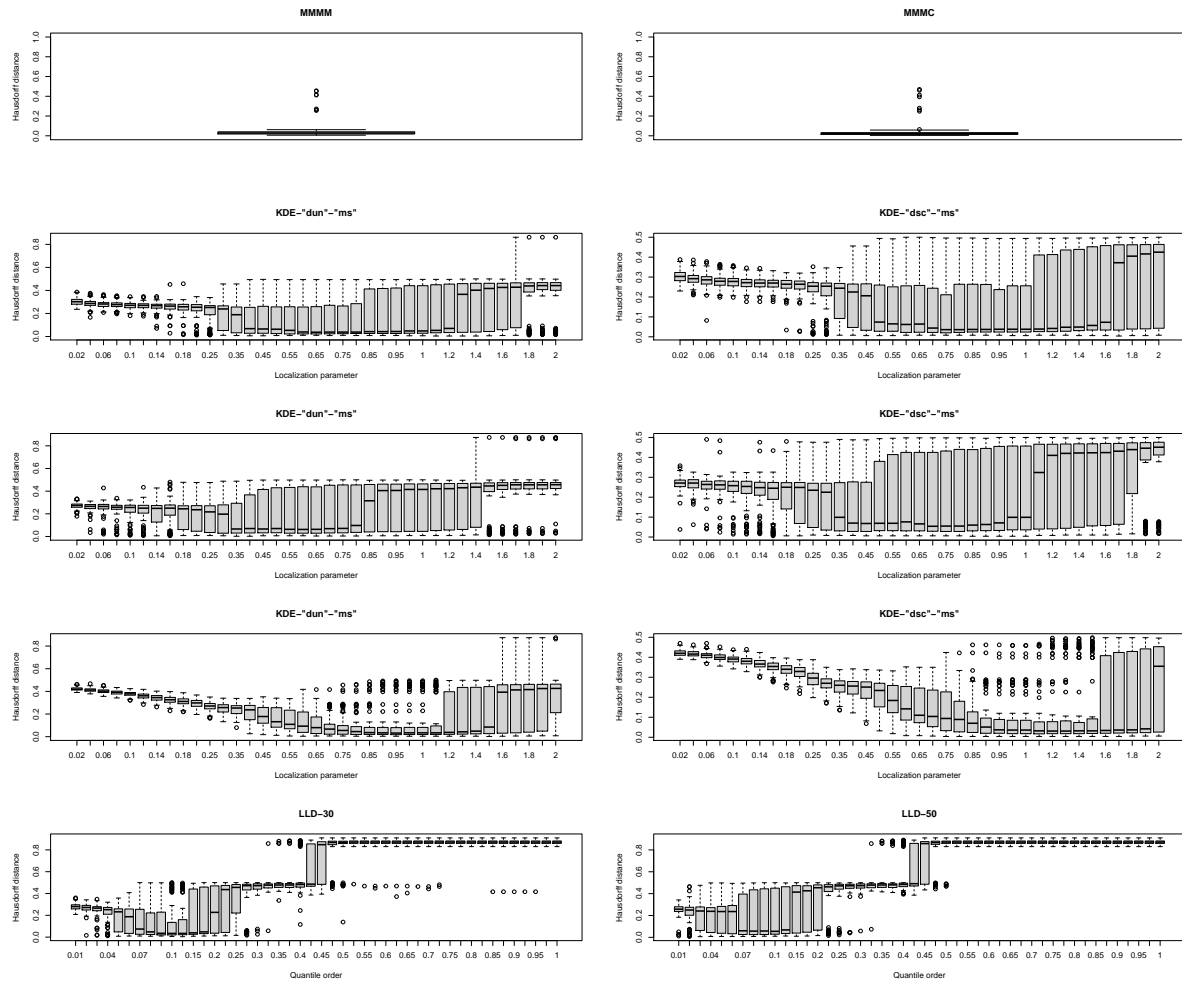


Figure 72: Boxplot of clustering errors based on Hausdorff distance over 100 replications with $n = 500$ samples for the (K) Trimodal III density.

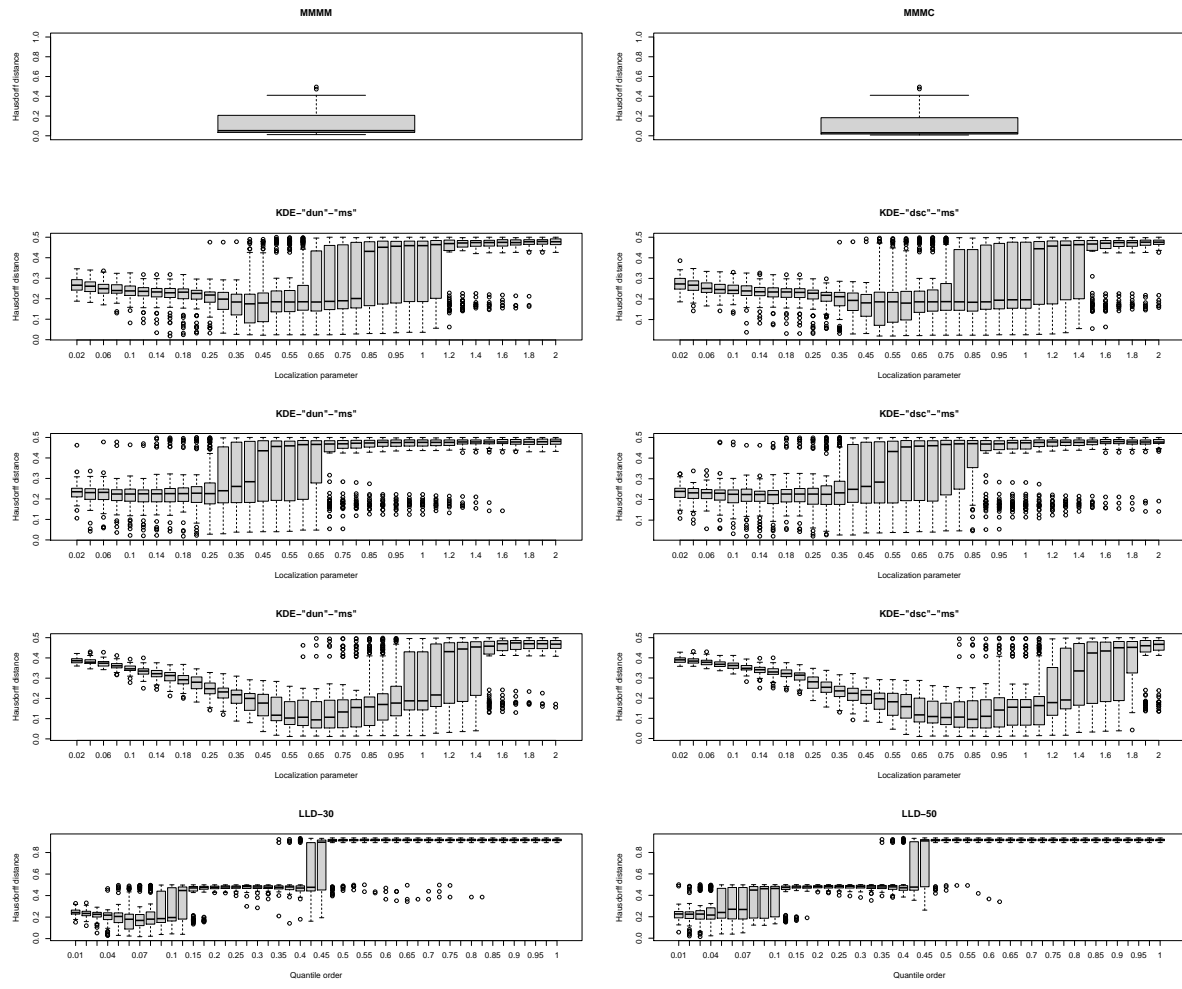


Figure 73: Boxplot of clustering errors based on Hausdorff distance over 100 replications with $n = 500$ samples for the (L) Quadrimodal density.

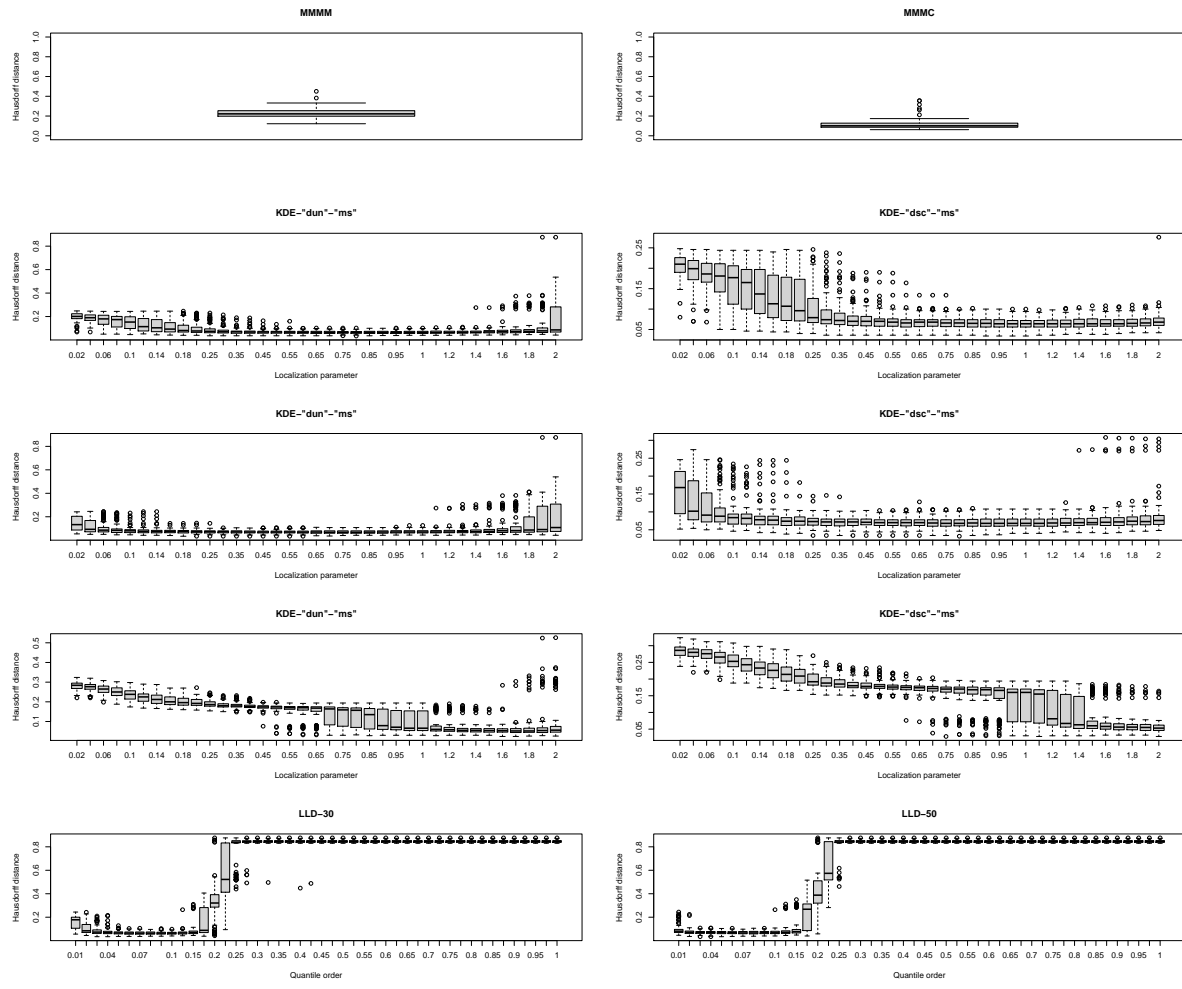


Figure 74: Boxplot of clustering errors based on Hausdorff distance over 100 replications with $n = 500$ samples for the #10 fountain density.

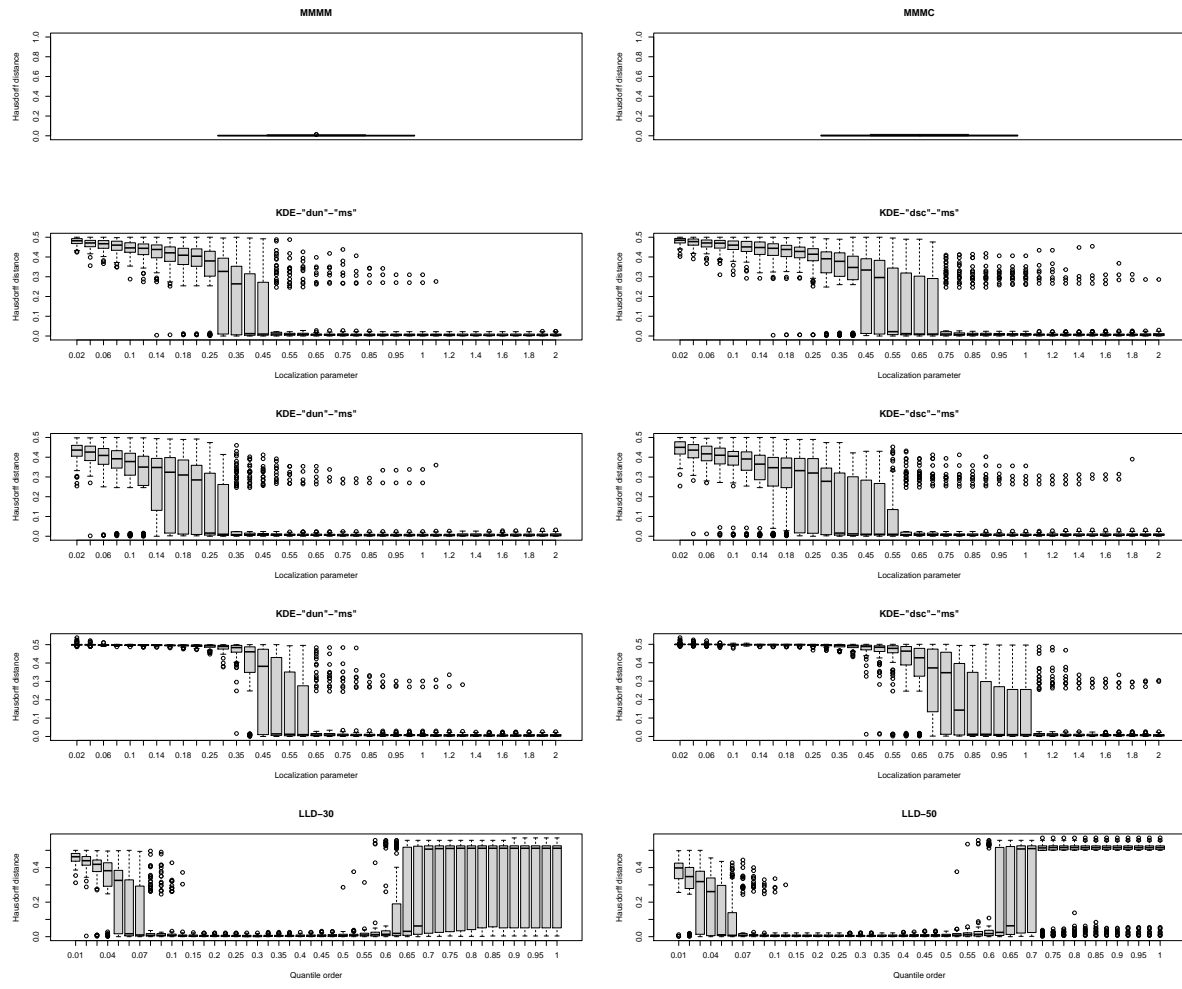


Figure 75: Boxplot of clustering errors based on Hausdorff distance over 100 replications with $n = 500$ samples for the Bimodal density.

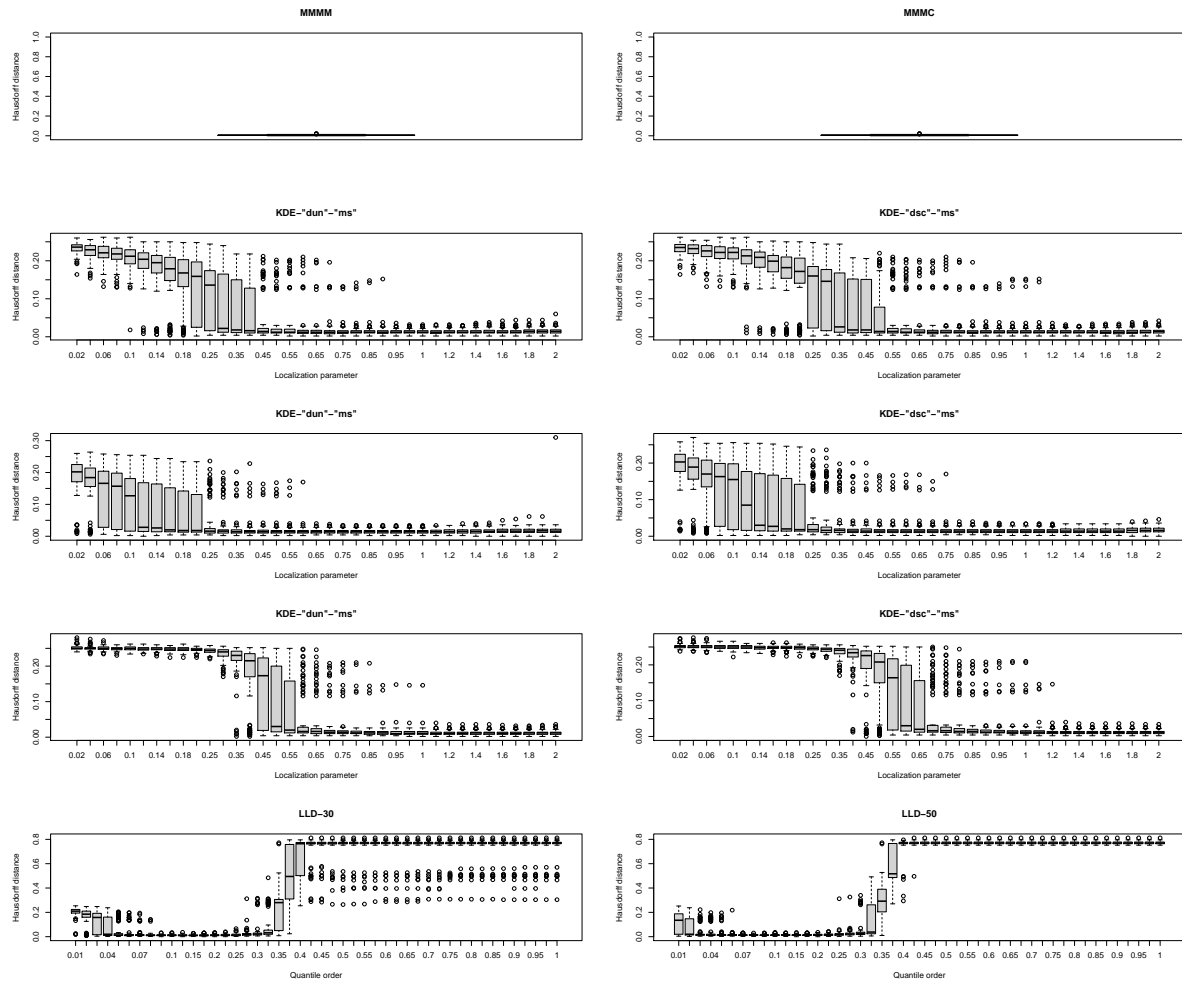


Figure 76: Boxplot of clustering errors based on Hausdorff distance over 100 replications with $n = 500$ samples for the Quadrimodal density.

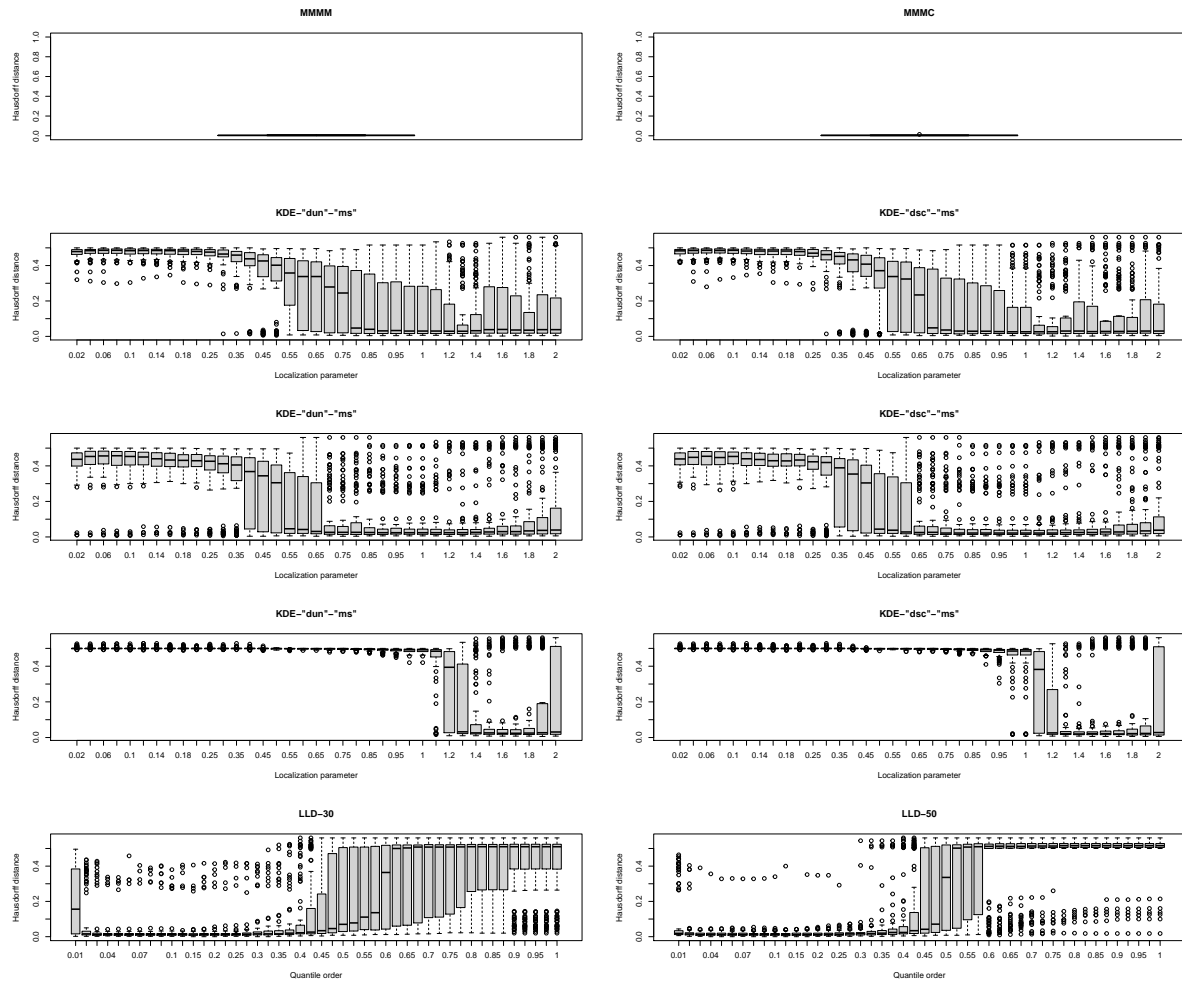


Figure 77: Boxplot of clustering errors based on Hausdorff distance over 100 replications with $n = 500$ samples for the Mult. Bimodal density.

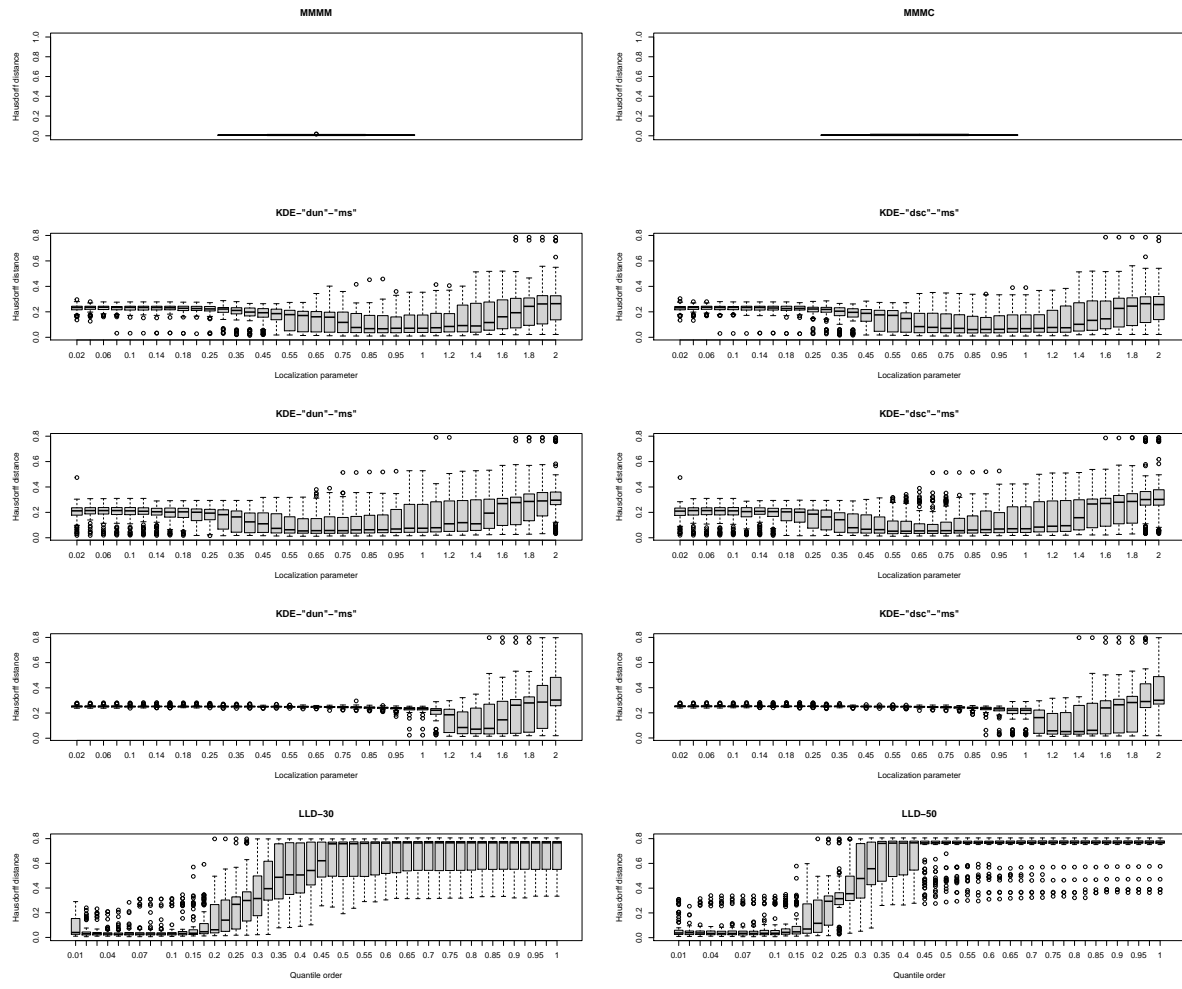


Figure 78: Boxplot of clustering errors based on Hausdorff distance over 100 replications with $n = 500$ samples for the Mult. Quadrimodal density.

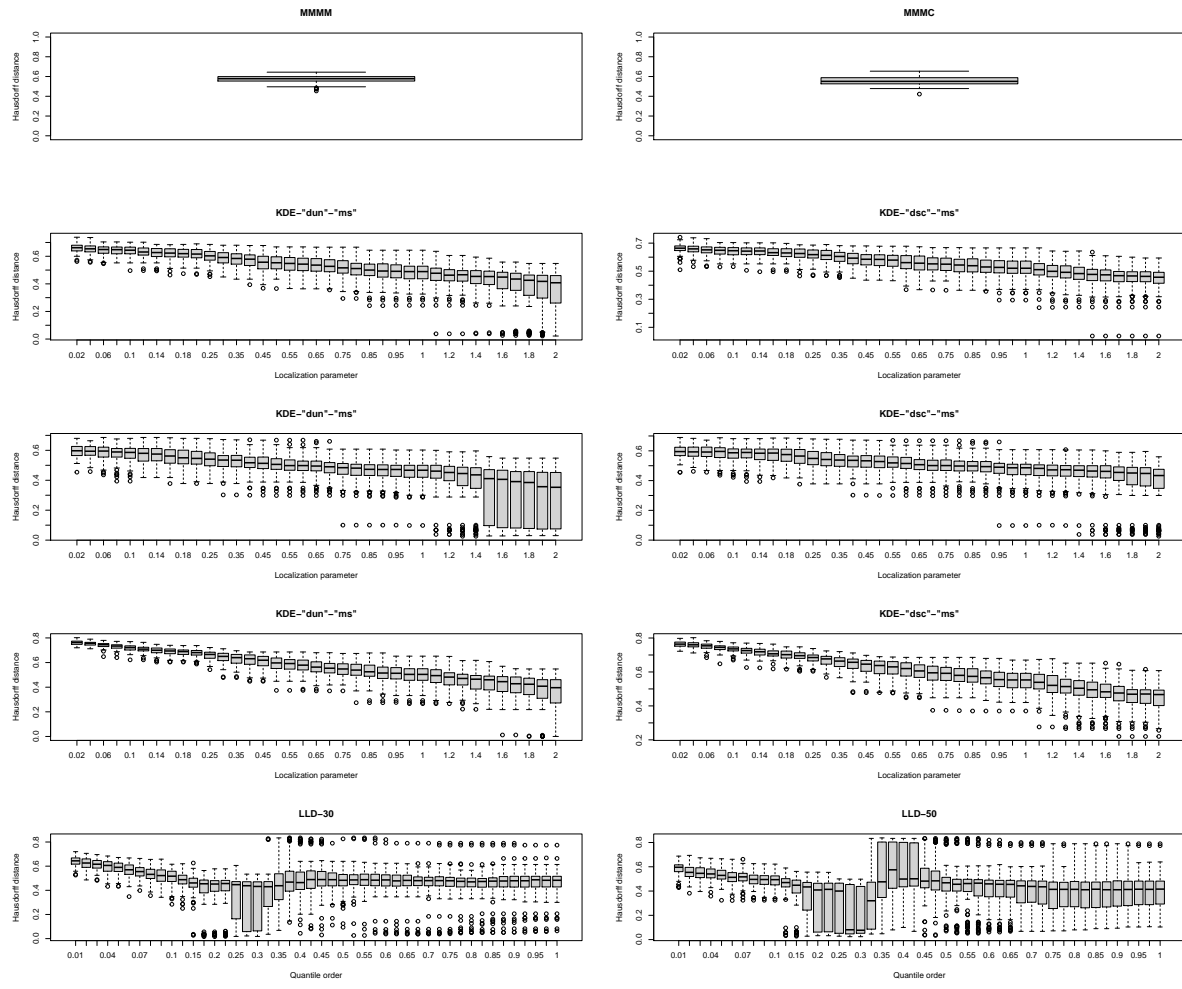


Figure 79: Boxplot of clustering errors based on Hausdorff distance over 100 replications with $n = 500$ samples for the Circular 2 density.

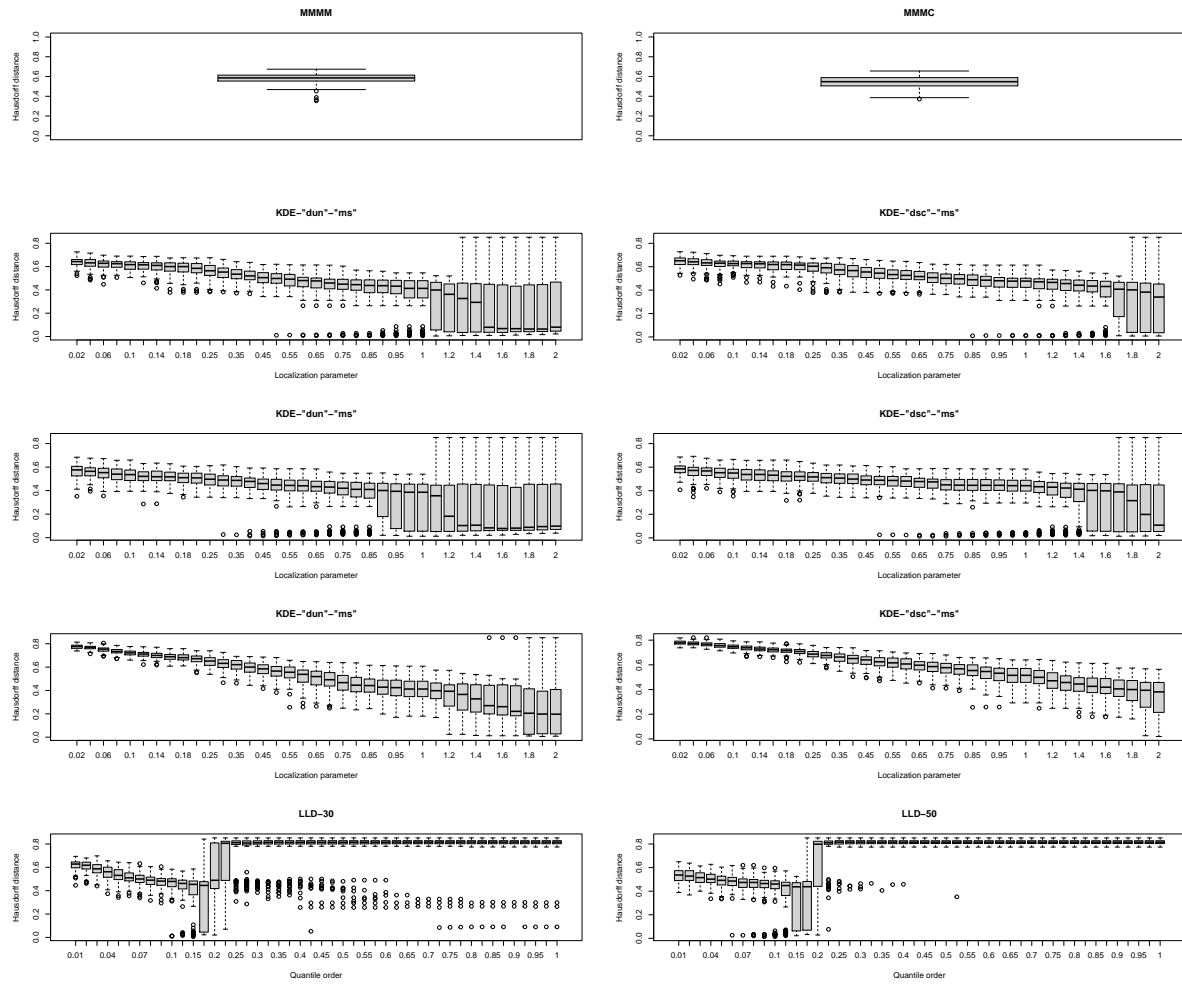


Figure 80: Boxplot of clustering errors based on Hausdorff distance over 100 replications with $n = 500$ samples for the Circular 2 Cauchy density.

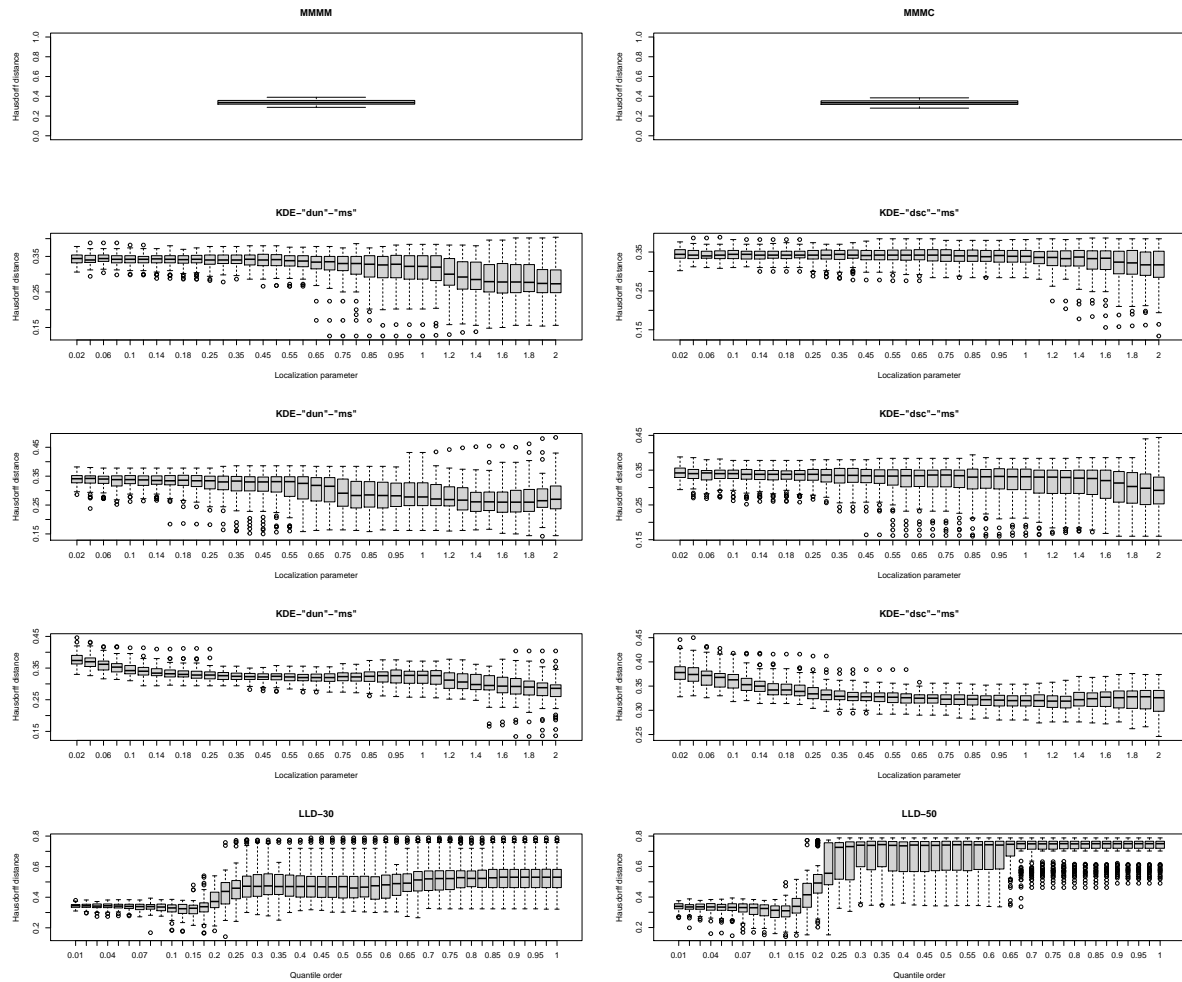


Figure 81: Boxplot of clustering errors based on Hausdorff distance over 100 replications with $n = 500$ samples for the Circular 3 density.

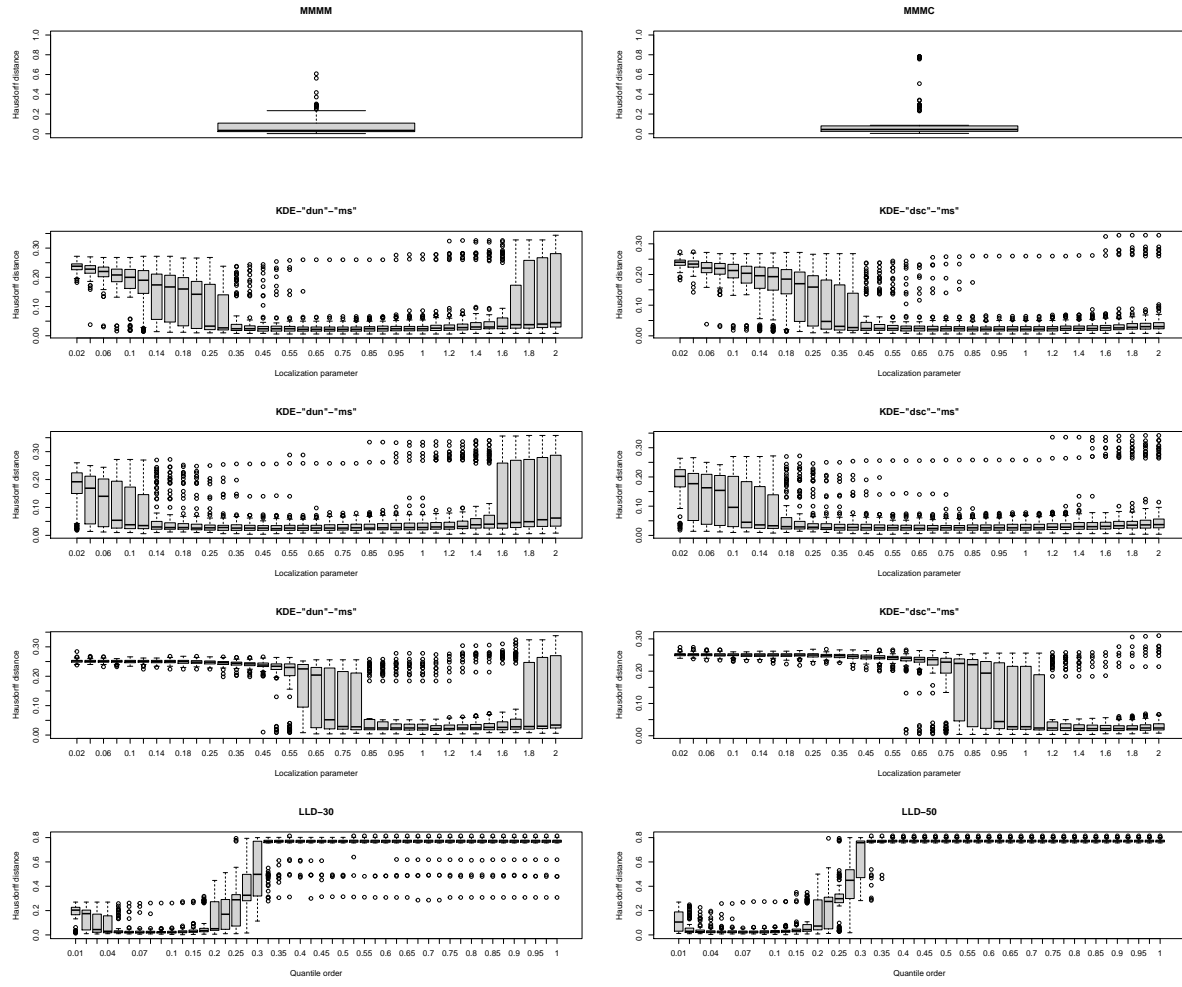


Figure 82: Boxplot of clustering errors based on Hausdorff distance over 100 replications with $n = 500$ samples for the Circular 4 Cauchy density.

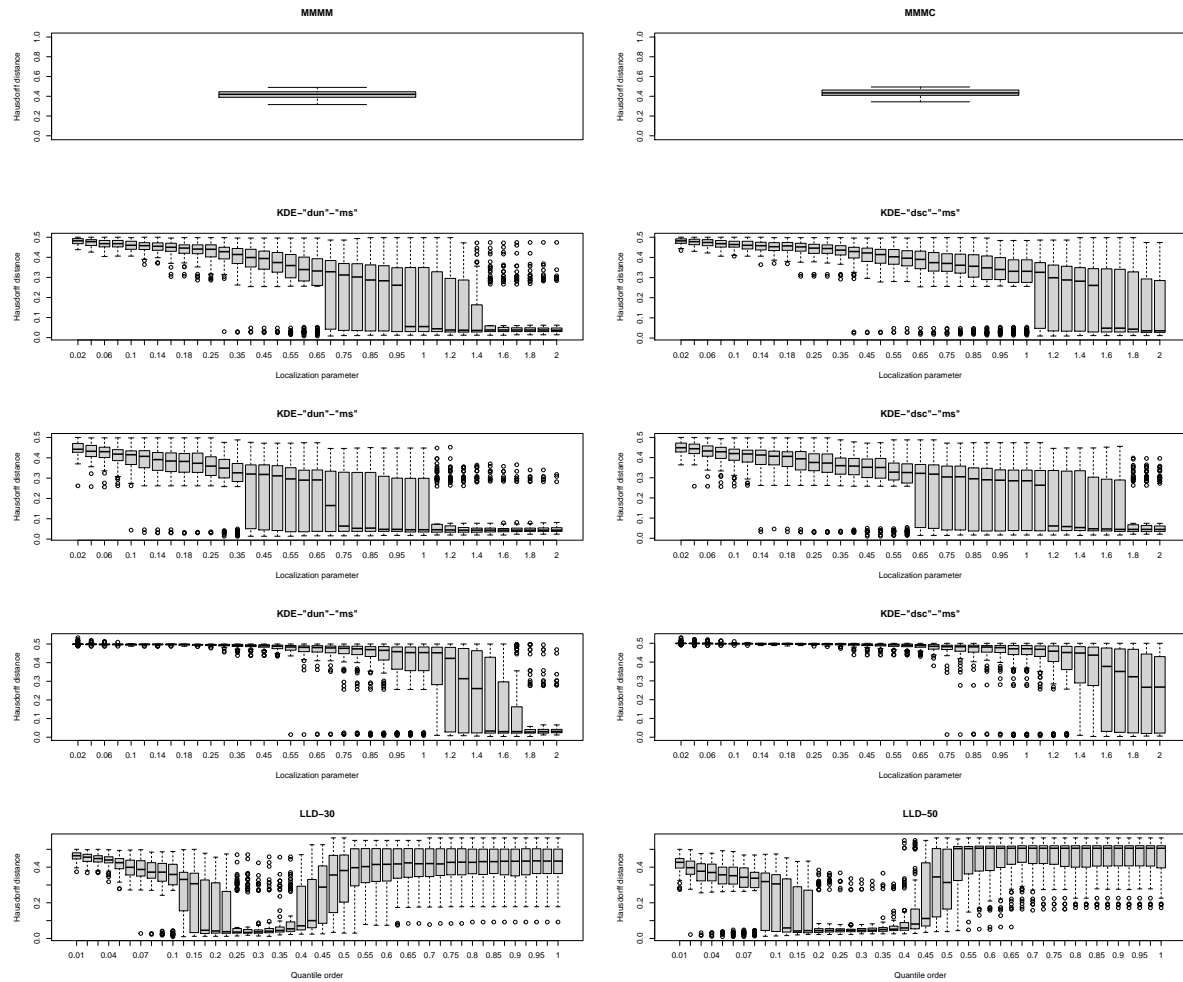


Figure 83: Boxplot of clustering errors based on Hausdorff distance over 100 replications with $n = 500$ samples for the Circular Bimodal I density.

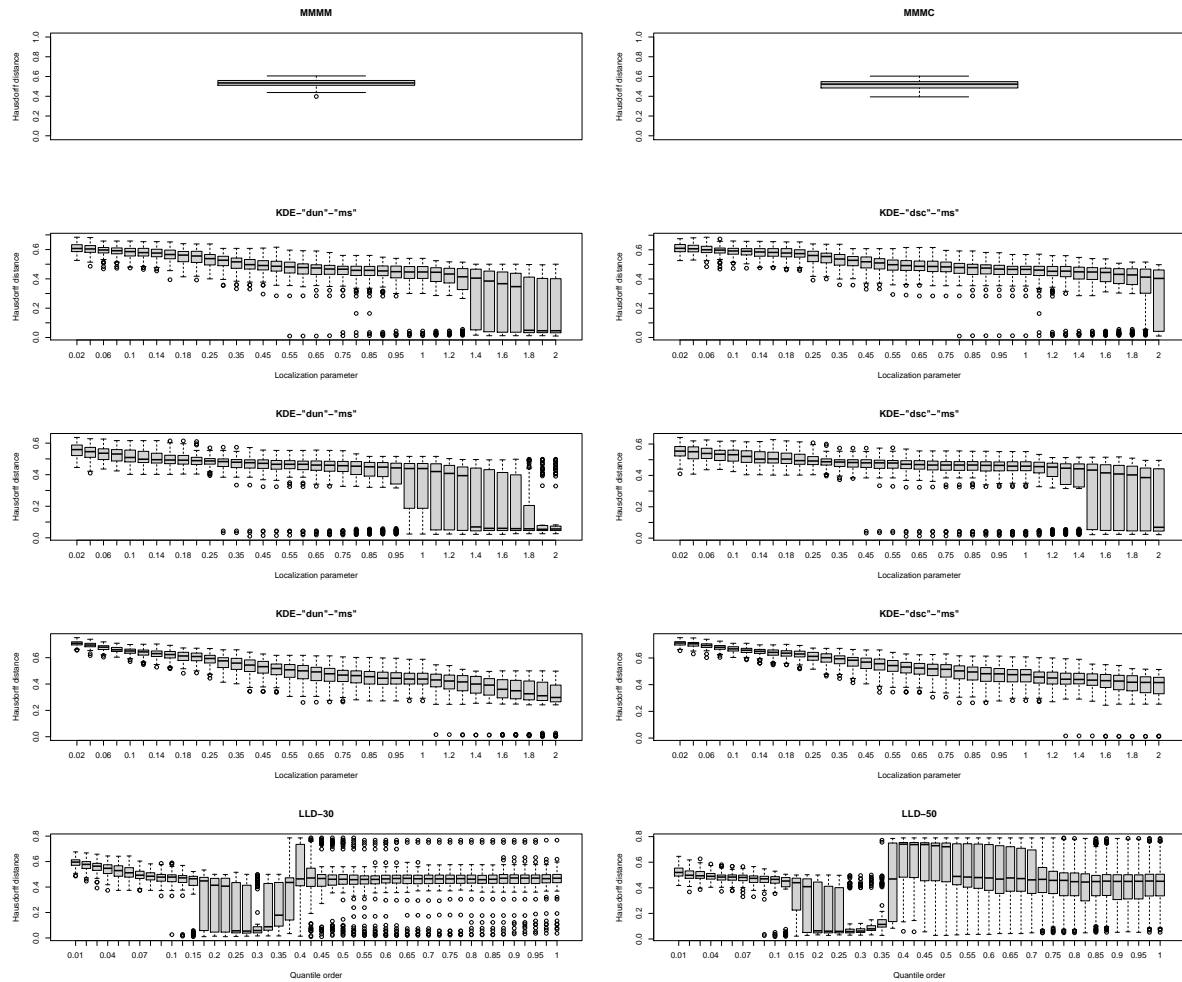


Figure 84: Boxplot of clustering errors based on Hausdorff distance over 100 replications with $n = 500$ samples for the Circular Bimodal II density.

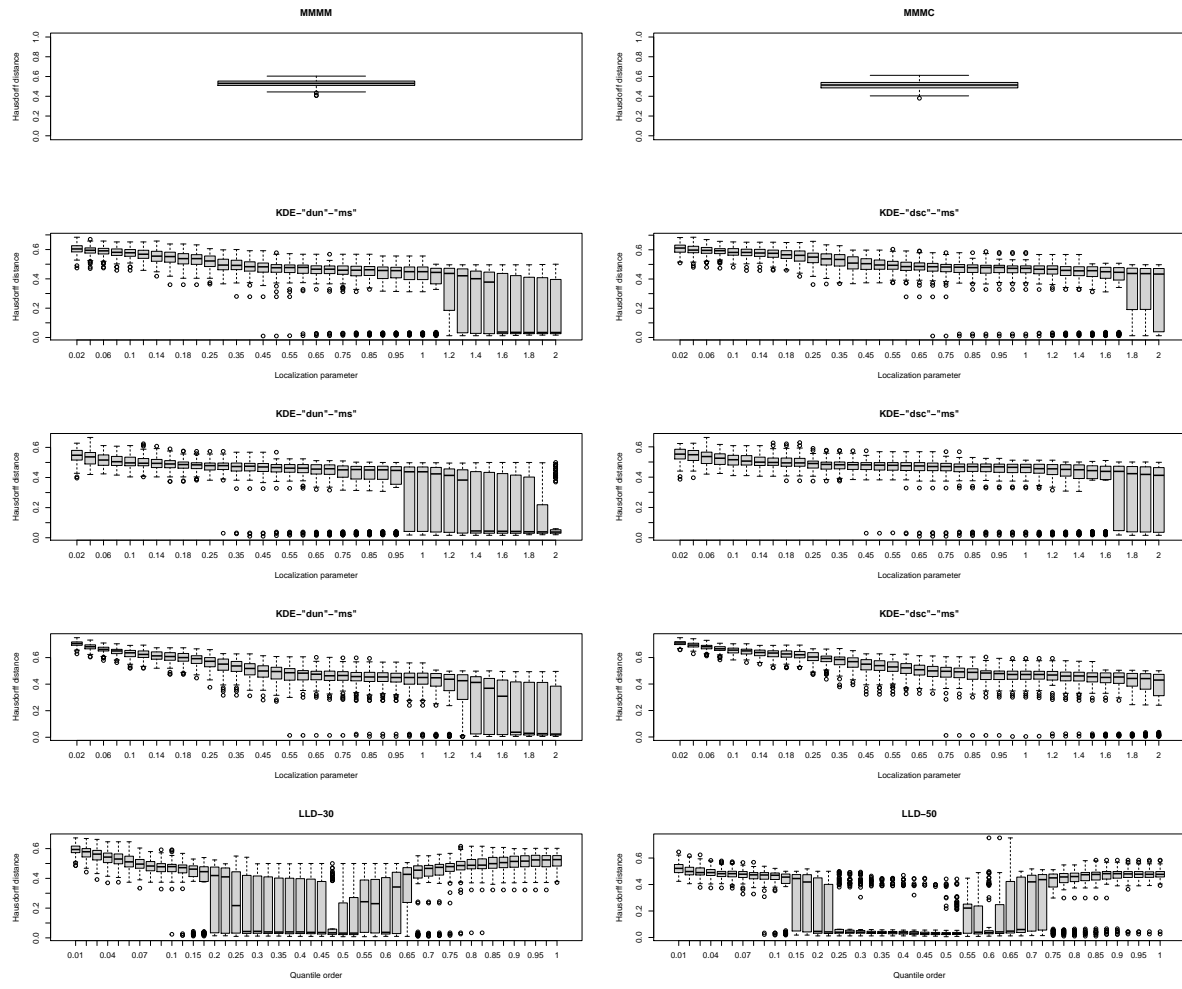


Figure 85: Boxplot of clustering errors based on Hausdorff distance over 100 replications with $n = 500$ samples for the Circular Bimodal III density.

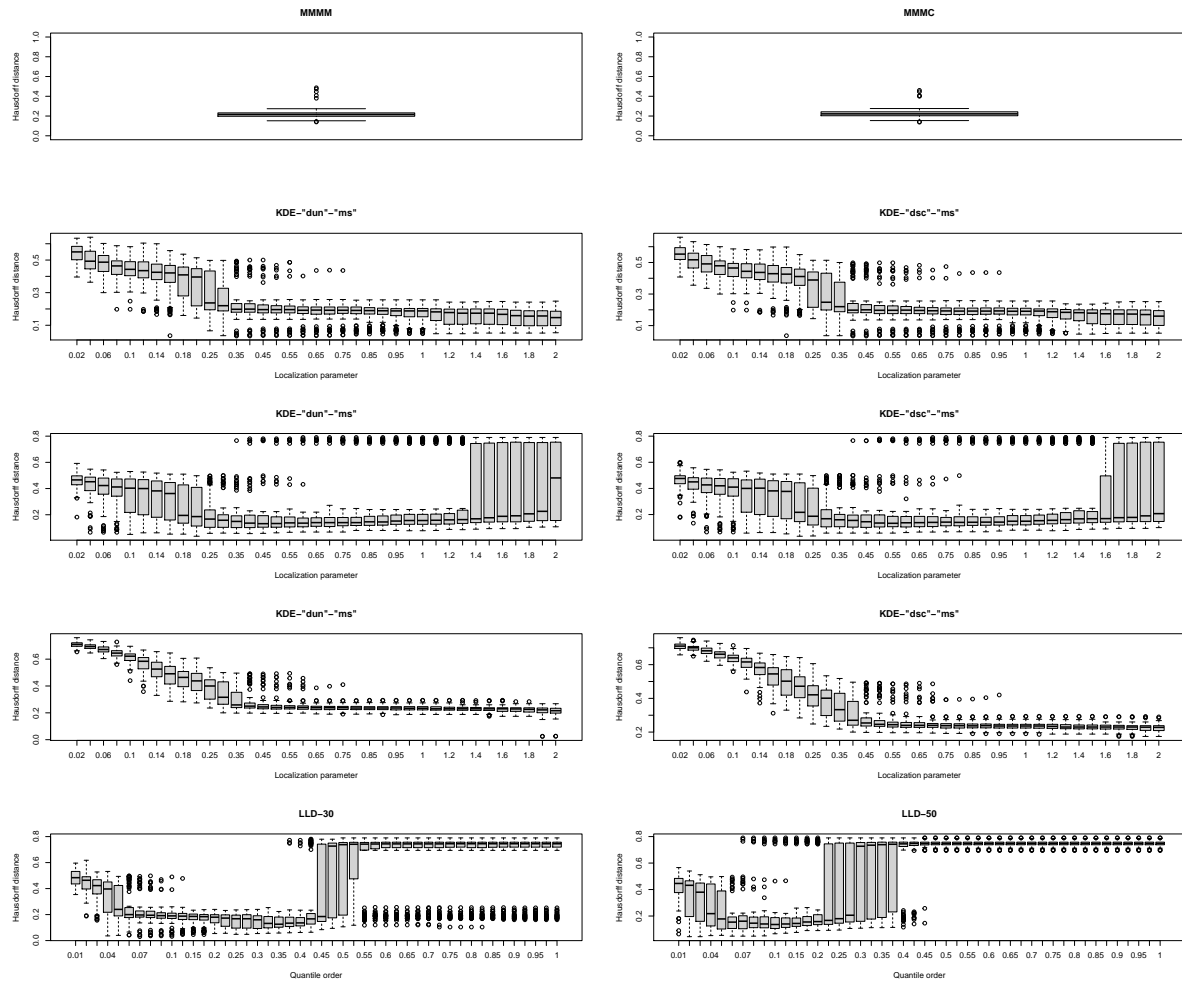


Figure 86: Boxplot of clustering errors based on Hausdorff distance over 100 replications with $n = 500$ samples for the Circular Bimodal IV density.

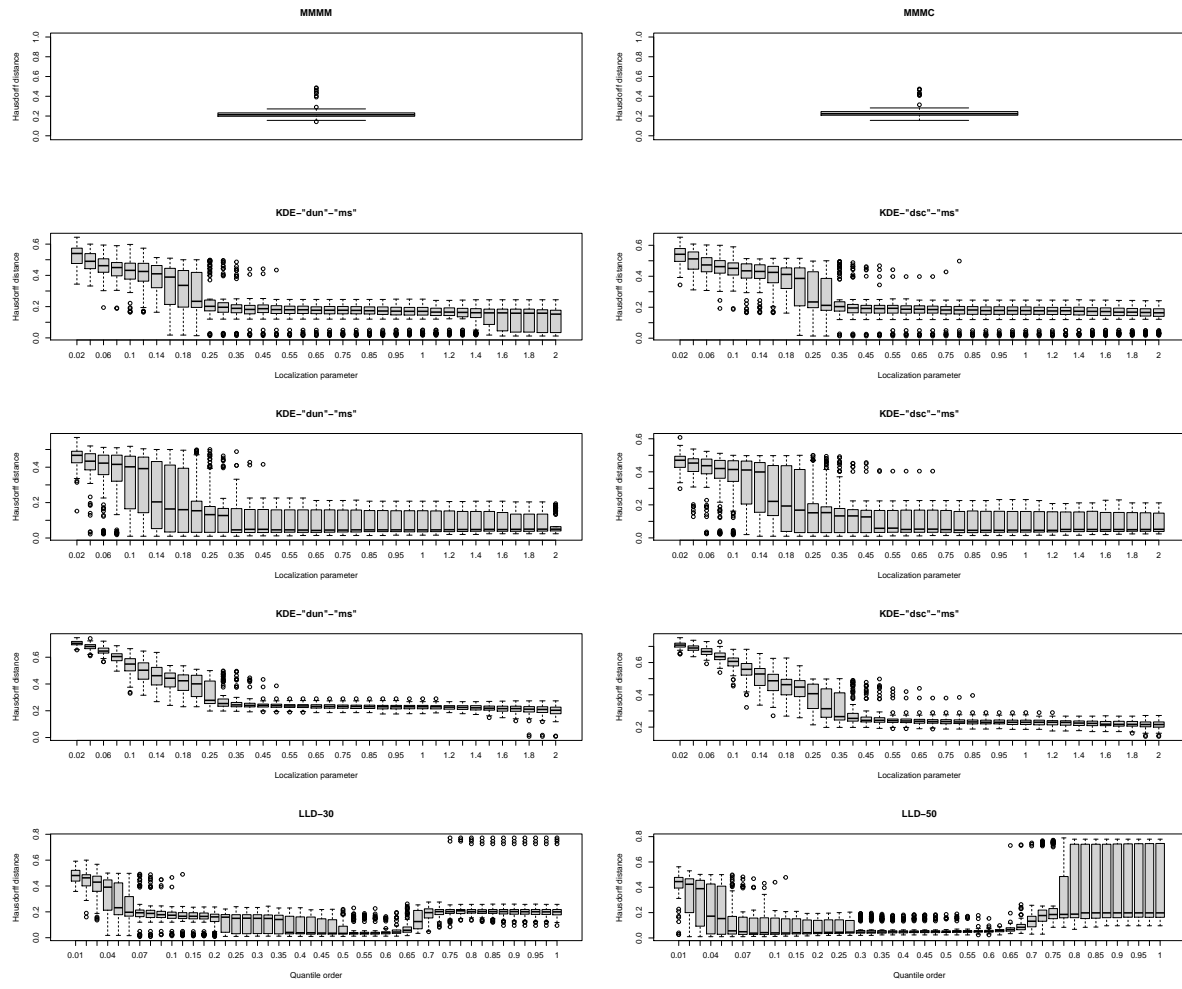


Figure 87: Boxplot of clustering errors based on Hausdorff distance over 100 replications with $n = 500$ samples for the Circular Bimodal V density.

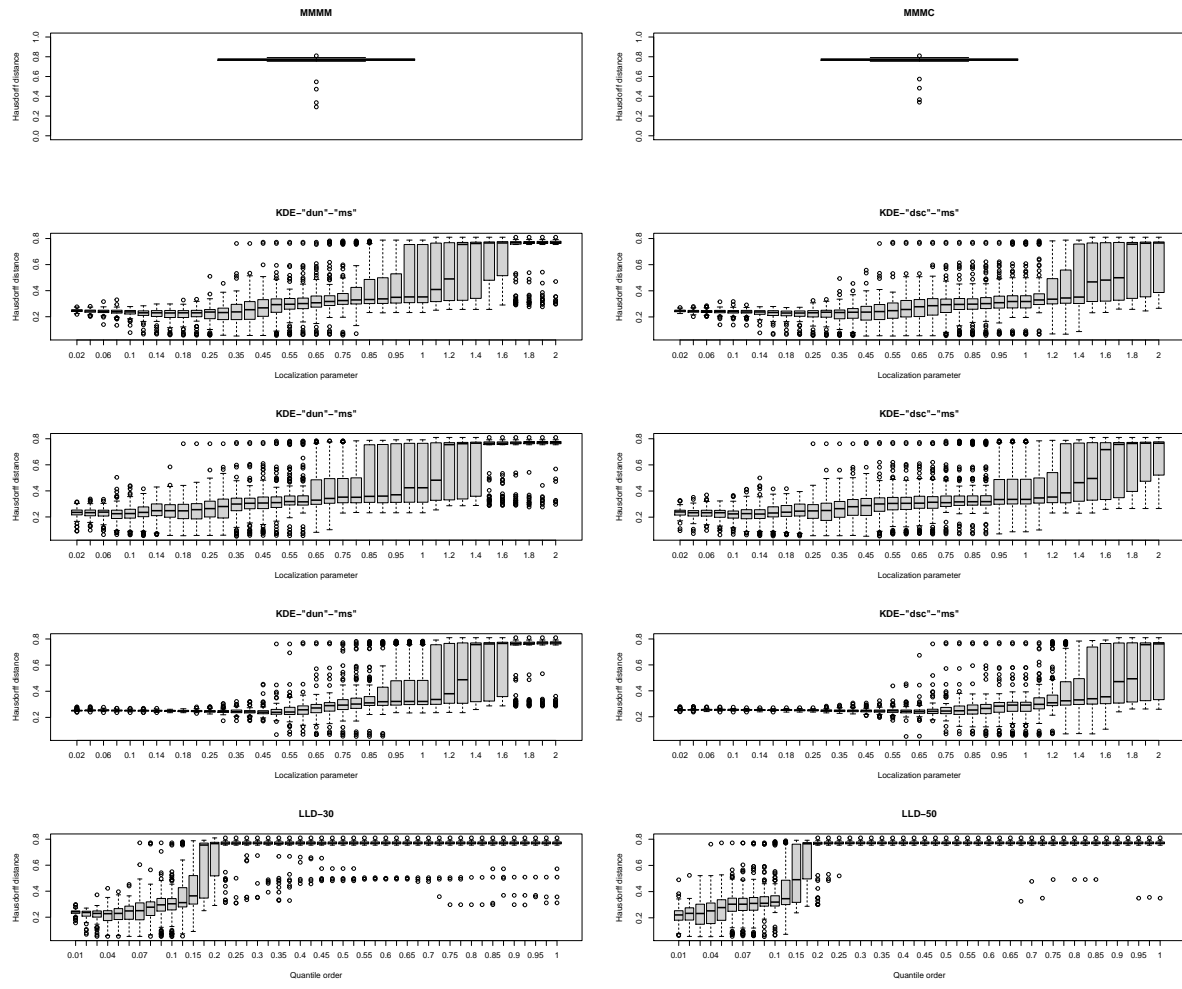


Figure 88: Boxplot of clustering errors based on Hausdorff distance over 100 replications with $n = 500$ samples for the Circular Quadrimodal I density.

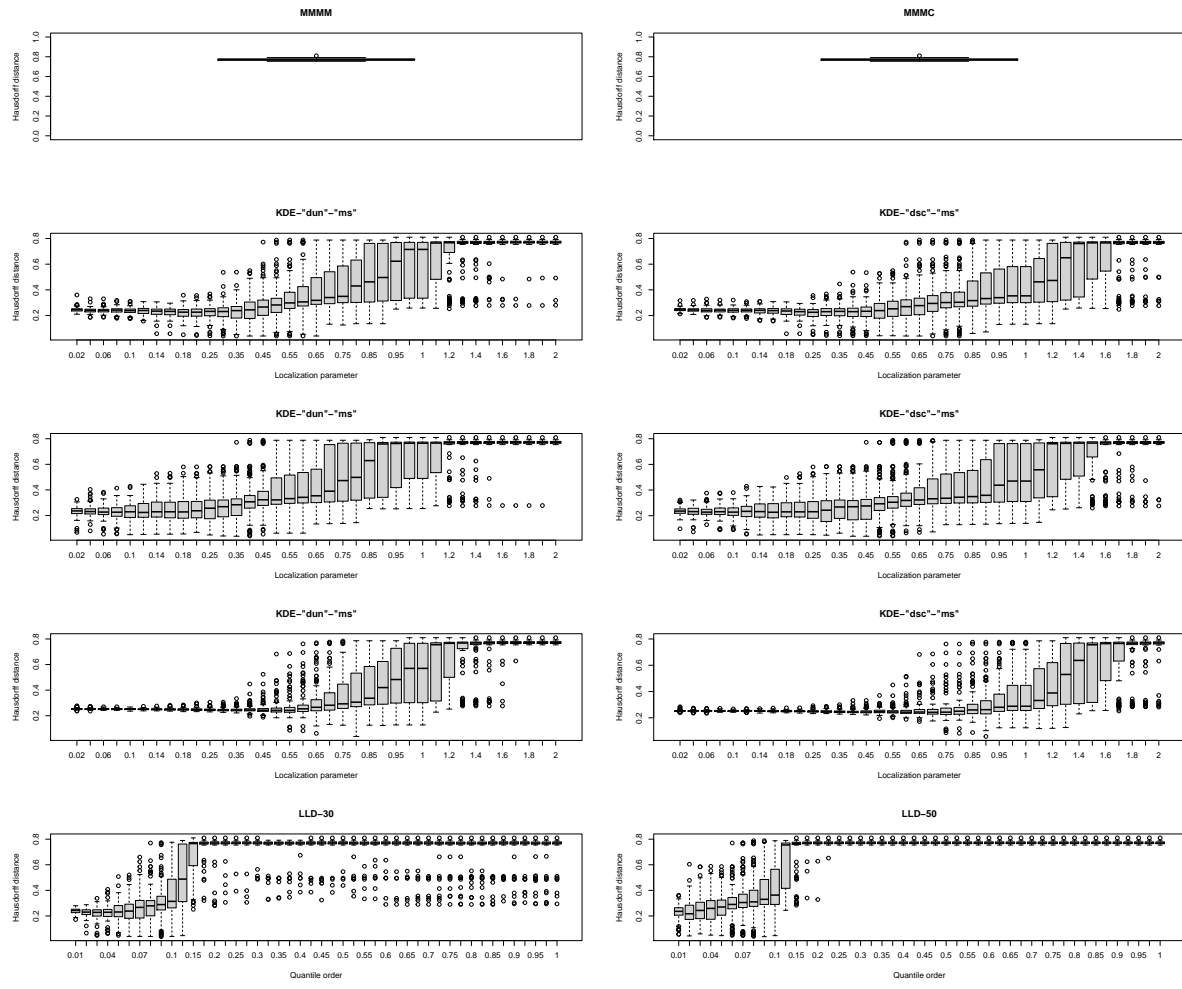


Figure 89: Boxplot of clustering errors based on Hausdorff distance over 100 replications with $n = 500$ samples for the Circular Quadrimodal II density.

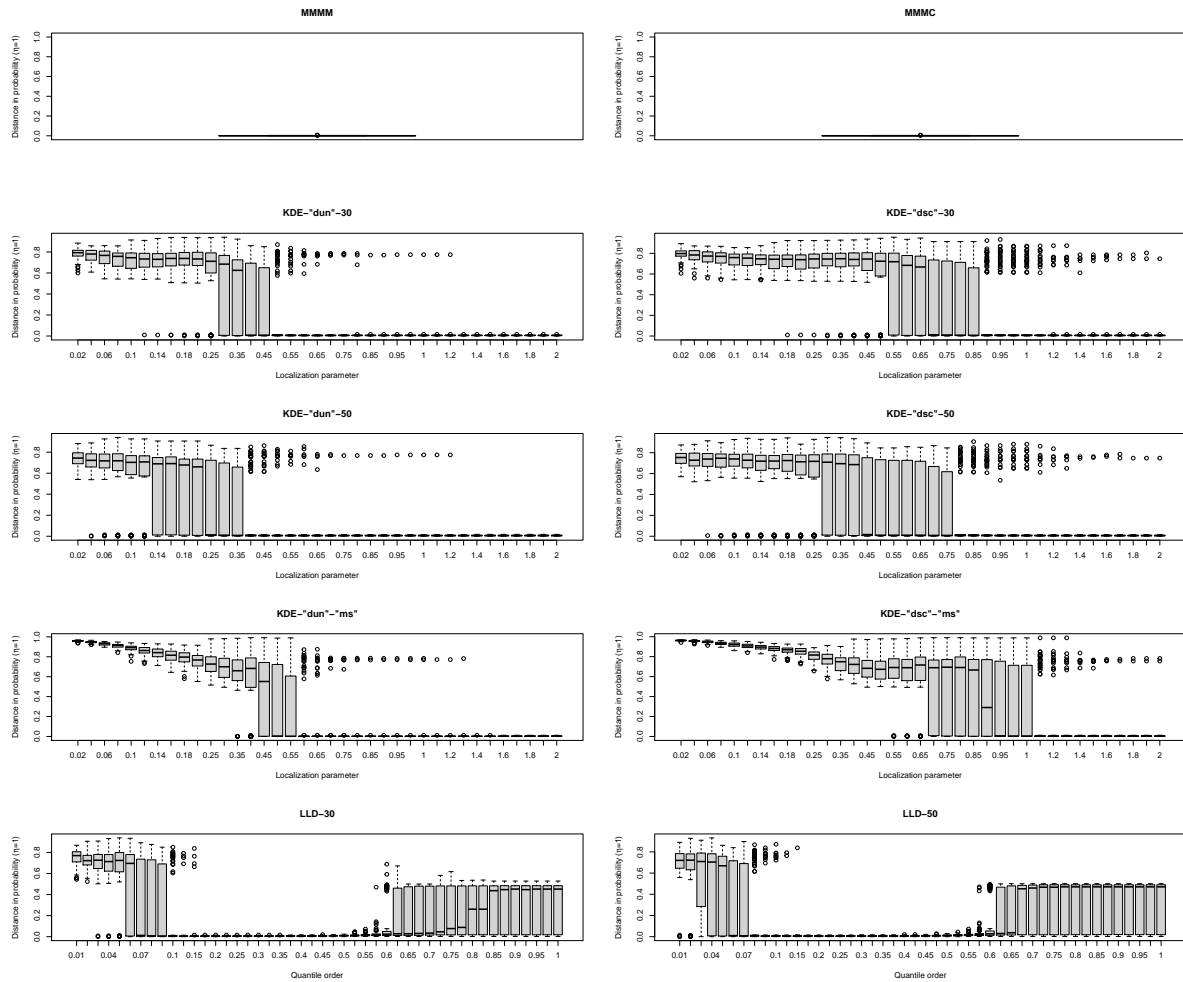


Figure 90: Boxplot of clustering errors based on distance in probability over 100 replications with $n = 500$ samples for the (H) Bimodal IV density.

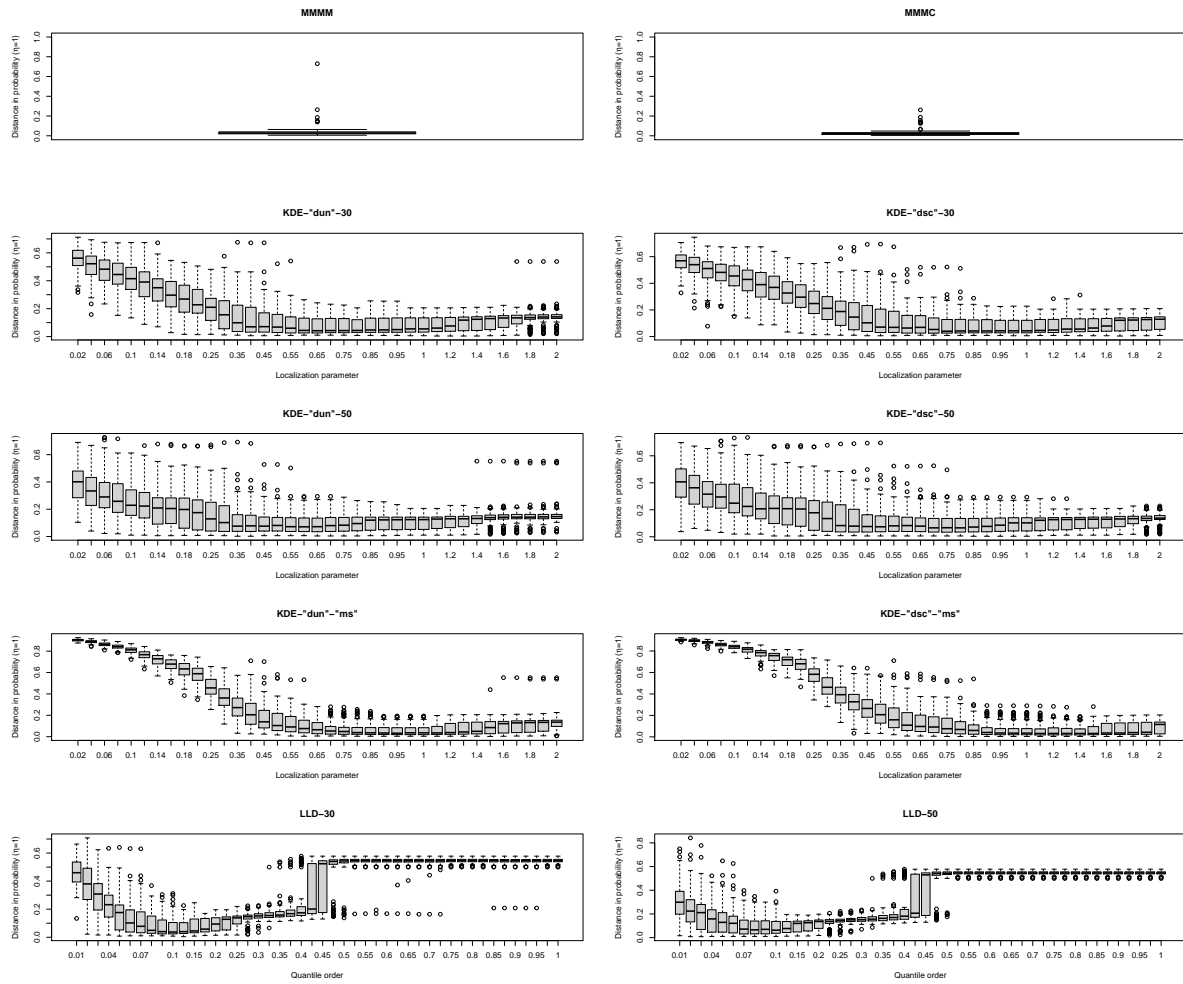


Figure 91: Boxplot of clustering errors based on distance in probability over 100 replications with $n = 500$ samples for the (K) Trimodal III density.

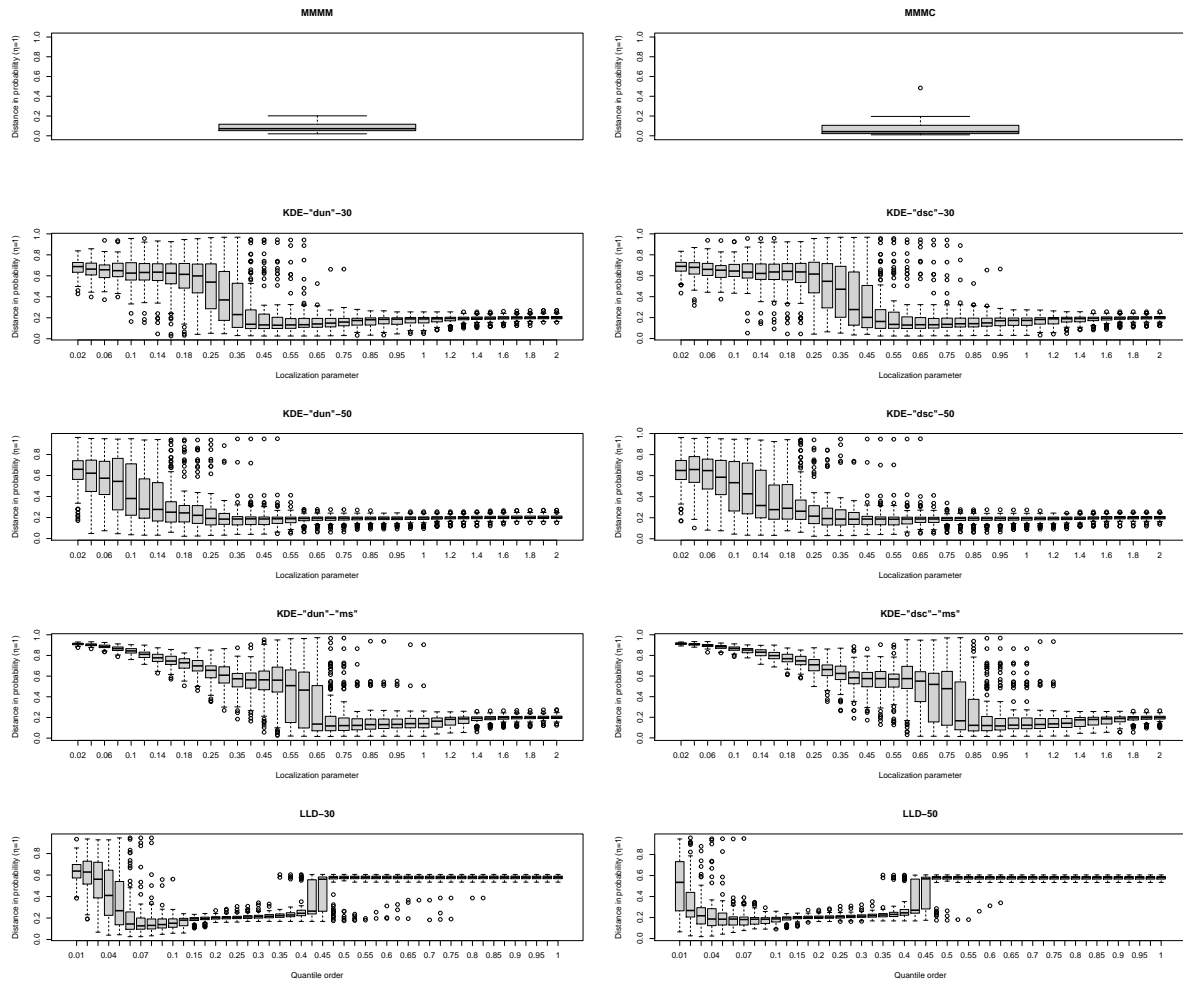


Figure 92: Boxplot of clustering errors based on distance in probability over 100 replications with $n = 500$ samples for the (L) Quadrimodal density.

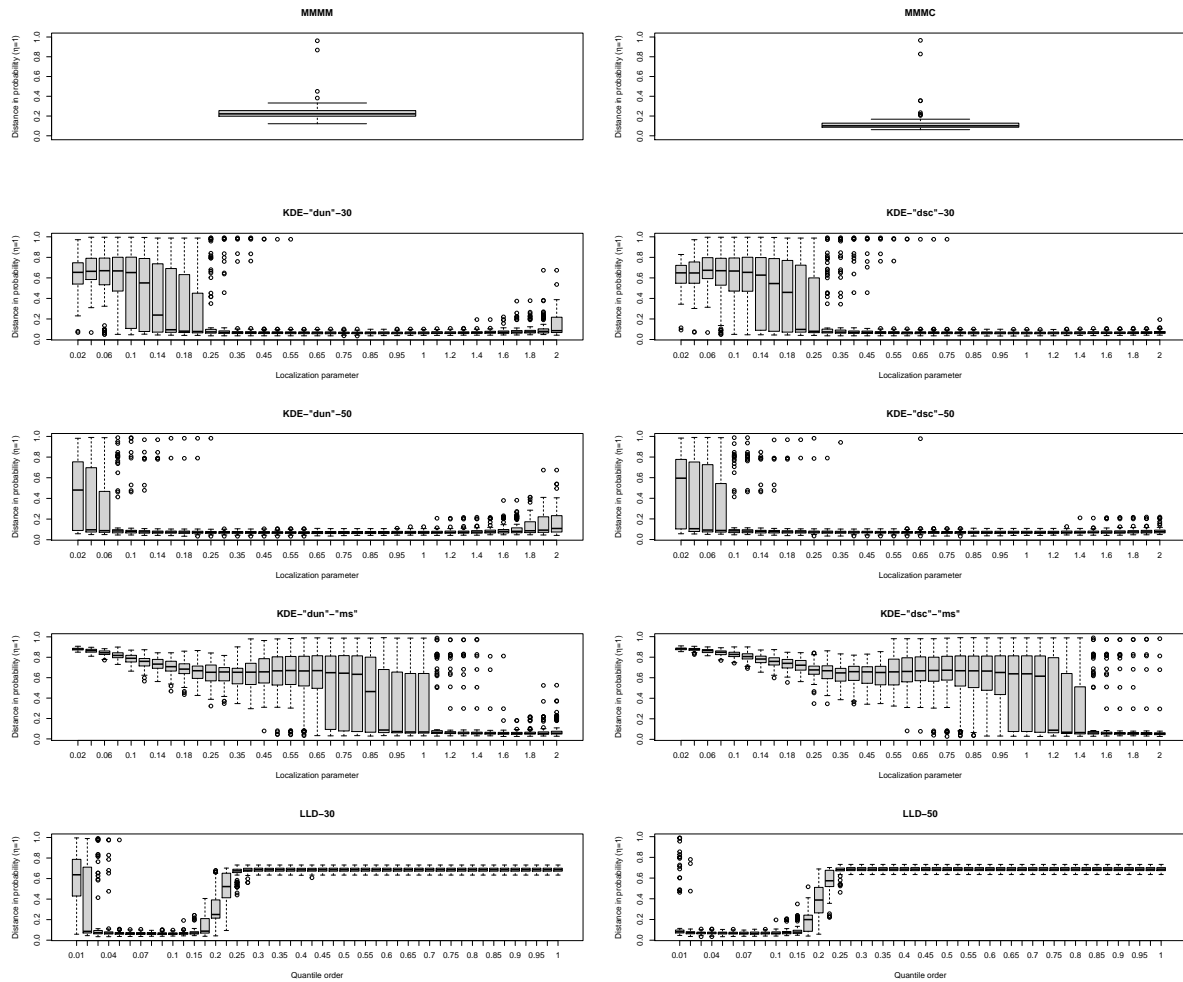


Figure 93: Boxplot of clustering errors based on distance in probability over 100 replications with $n = 500$ samples for the #10 fountain density.

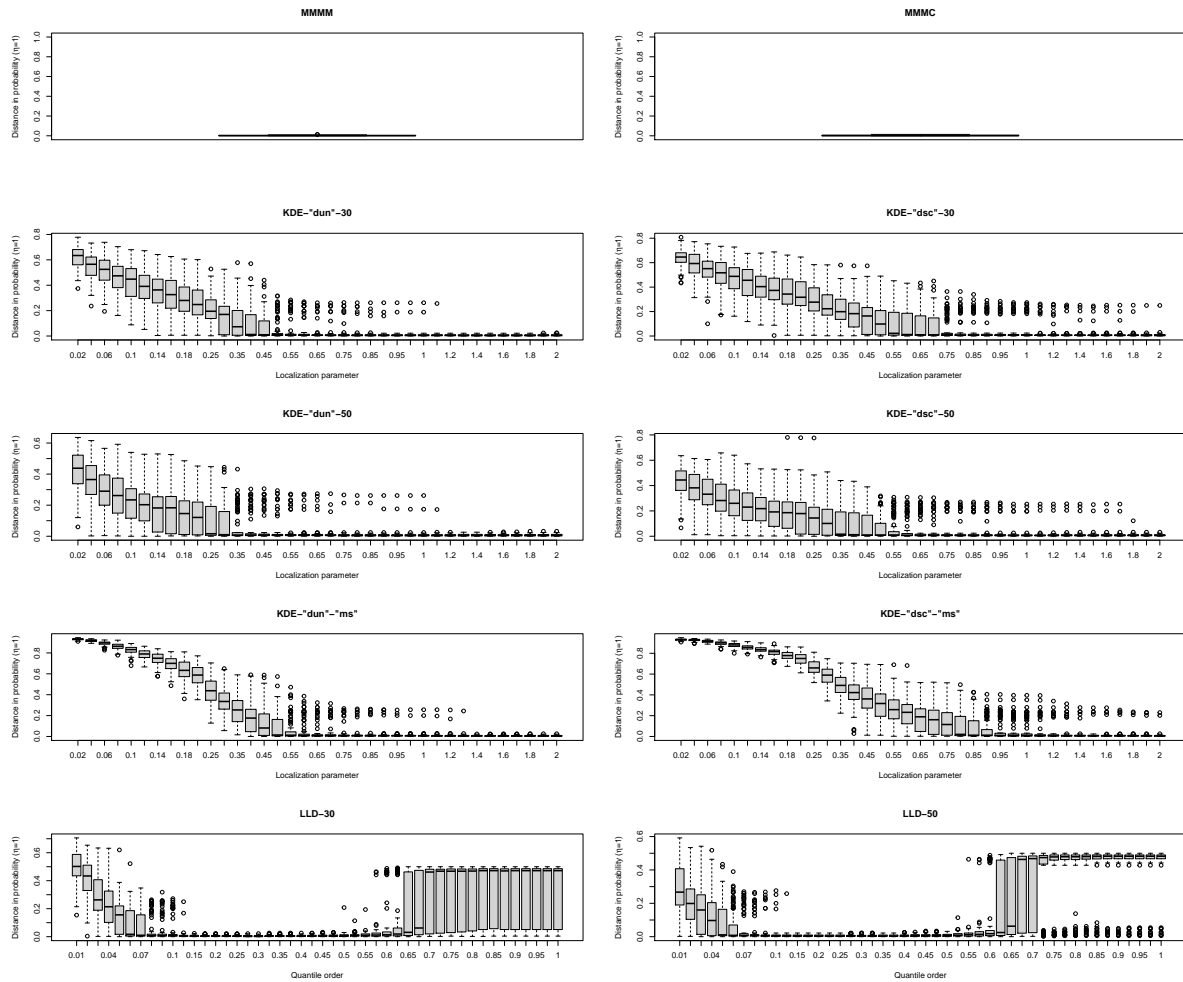


Figure 94: Boxplot of clustering errors based on distance in probability over 100 replications with $n = 500$ samples for the Bimodal density.

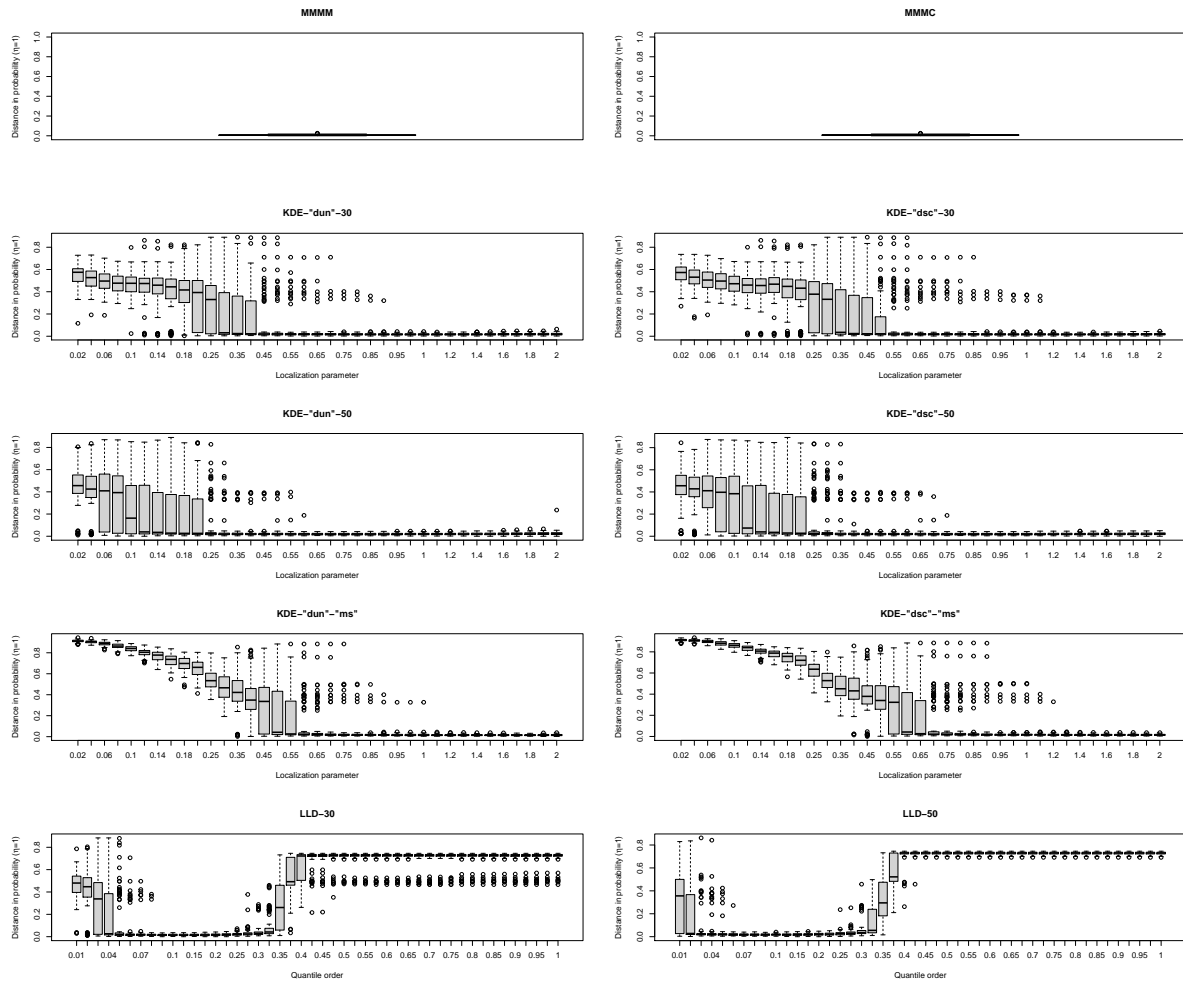


Figure 95: Boxplot of clustering errors based on distance in probability over 100 replications with $n = 500$ samples for the Quadrimodal density.

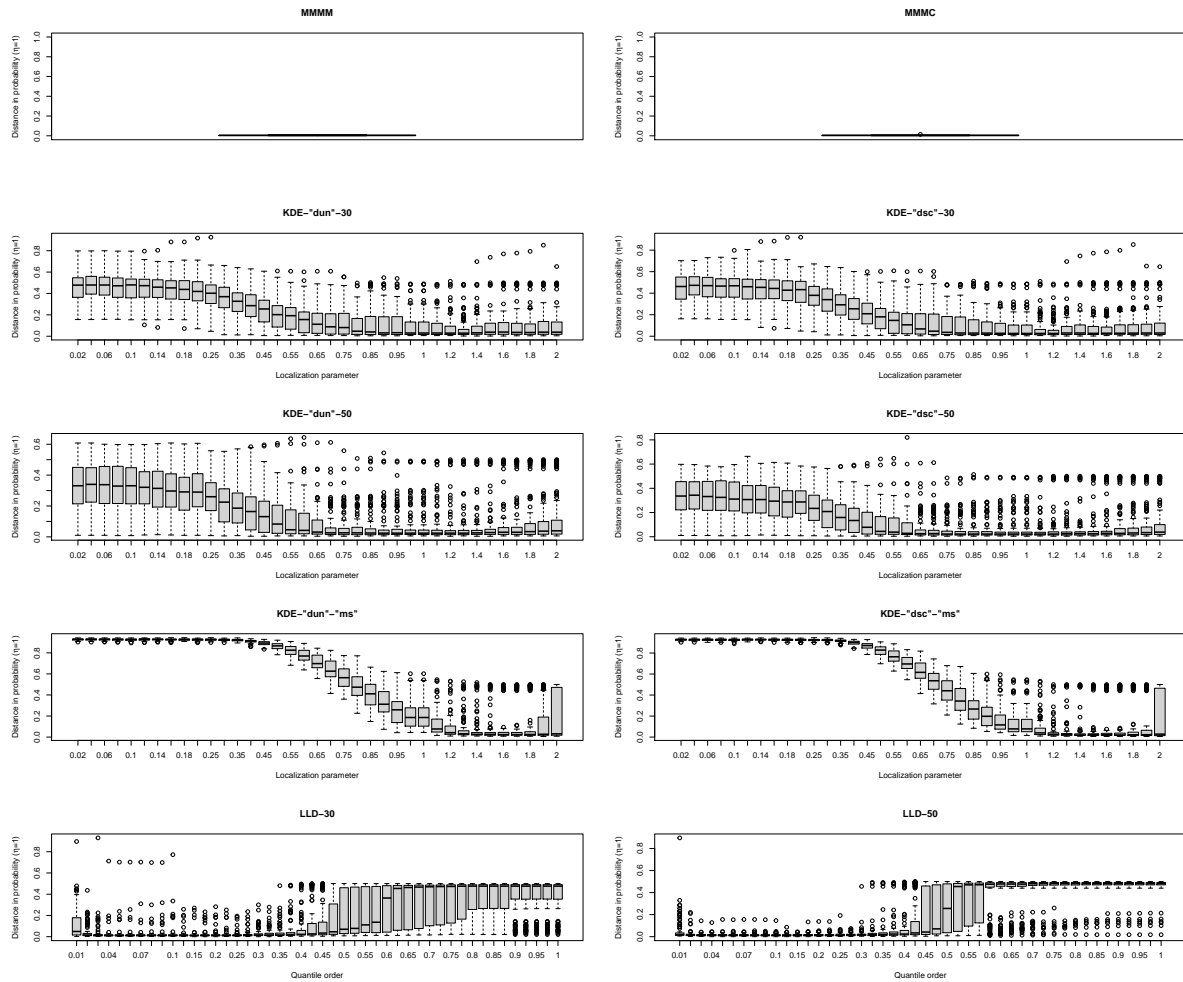


Figure 96: Boxplot of clustering errors based on distance in probability over 100 replications with $n = 500$ samples for the Mult. Bimodal density.

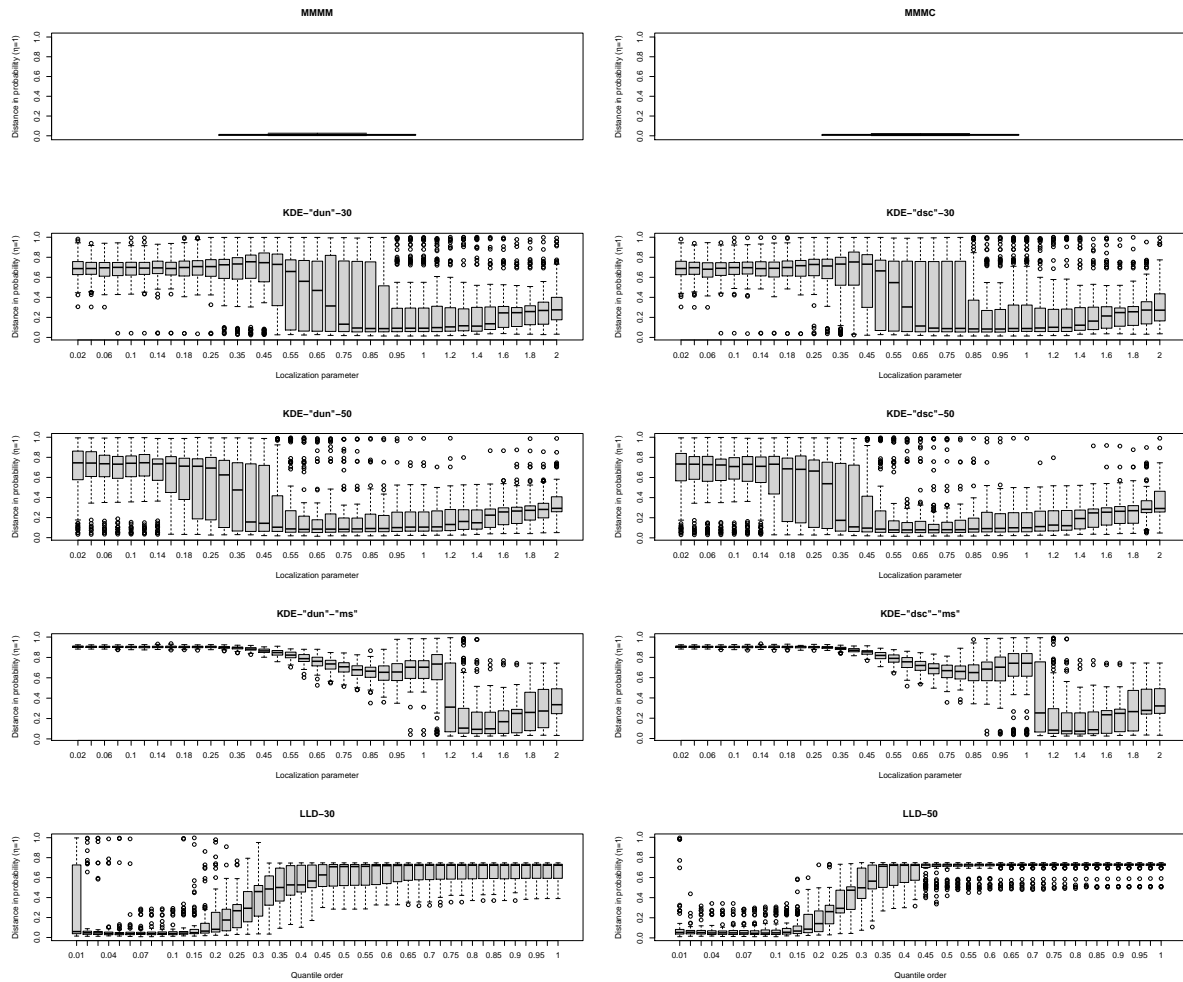


Figure 97: Boxplot of clustering errors based on distance in probability over 100 replications with $n = 500$ samples for the Mult. Quadrimodal density.

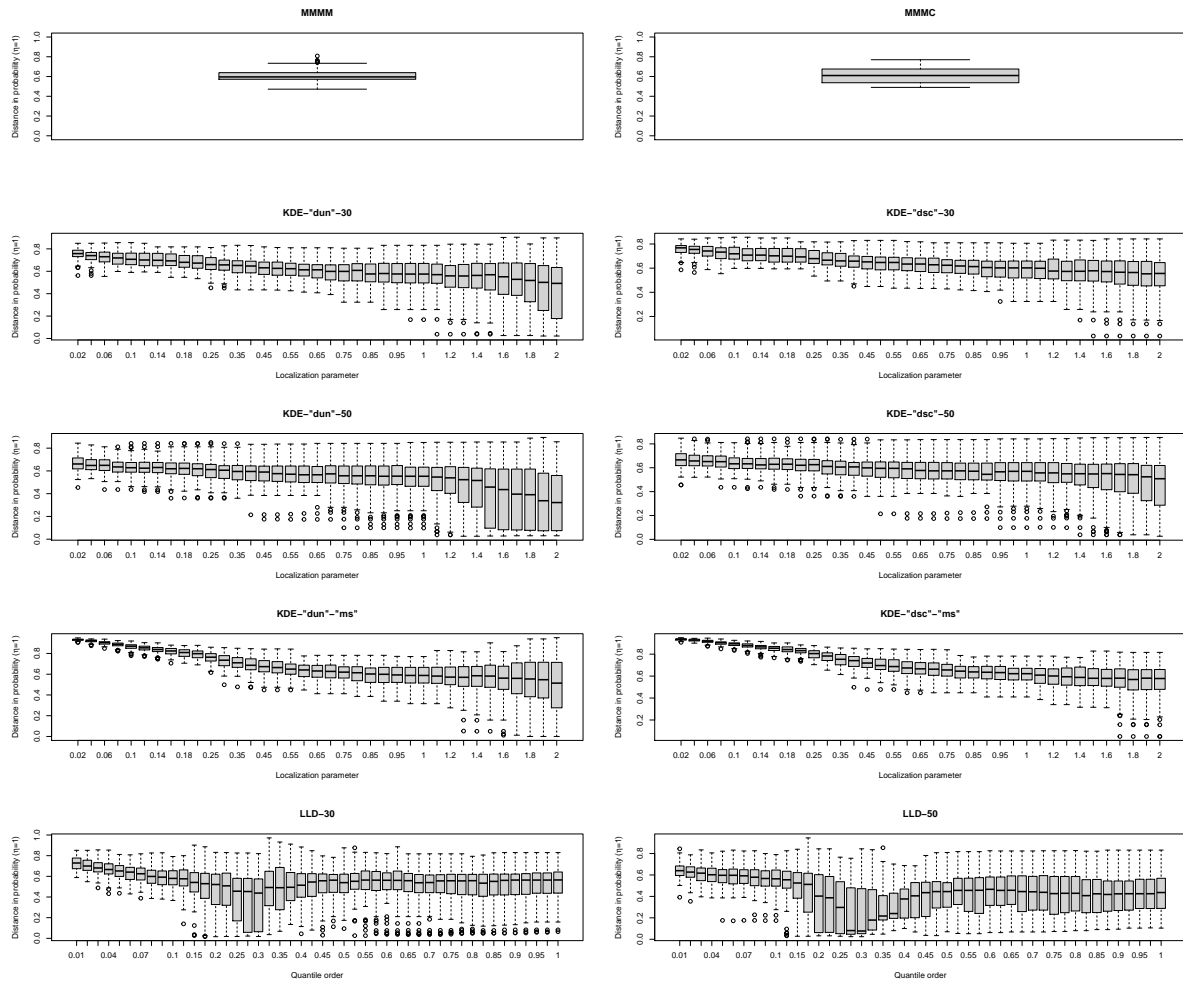


Figure 98: Boxplot of clustering errors based on distance in probability over 100 replications with $n = 500$ samples for the Circular 2 density.

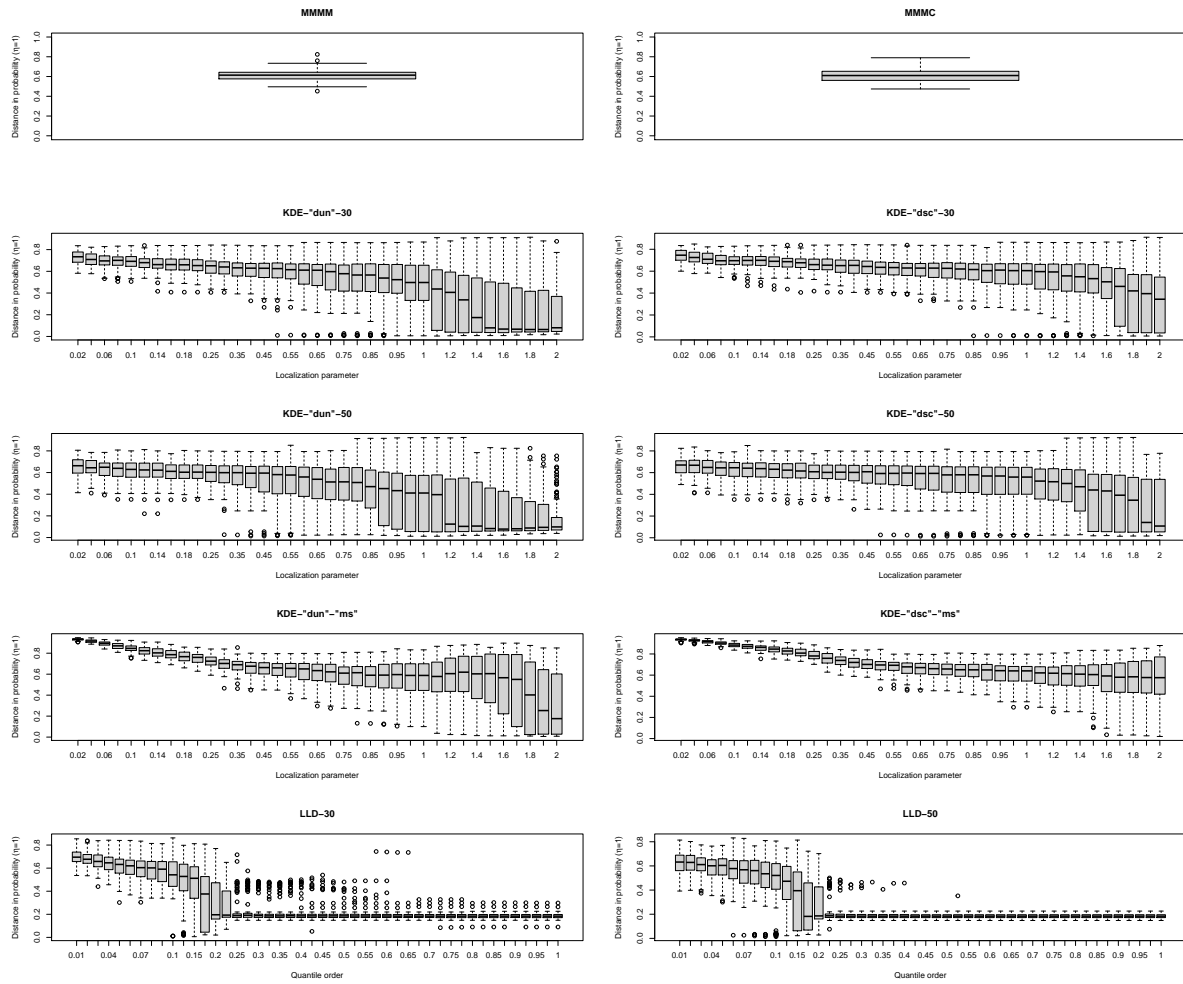


Figure 99: Boxplot of clustering errors based on distance in probability over 100 replicates with $n = 500$ samples for the Circular 2 Cauchy density.

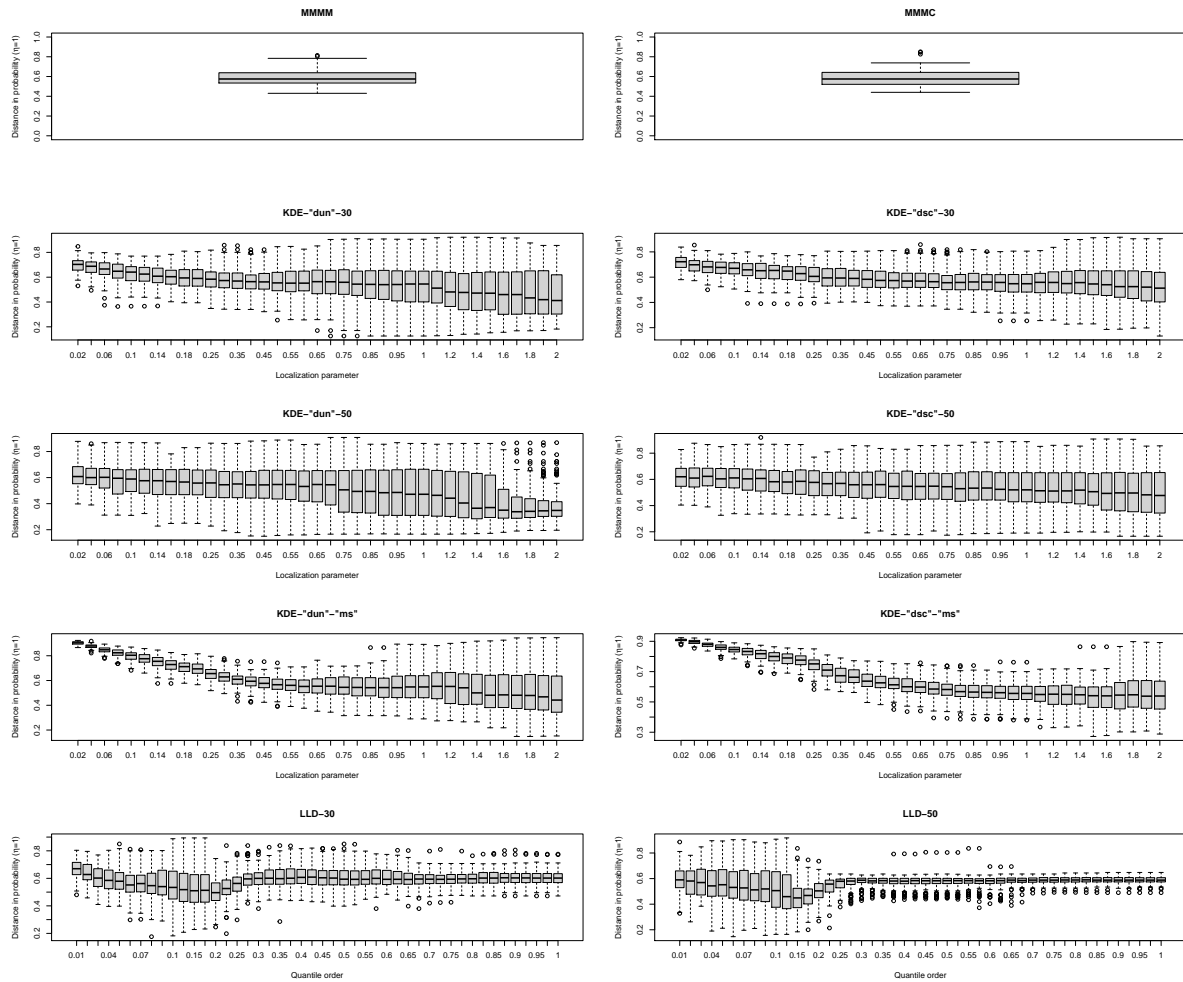


Figure 100: Boxplot of clustering errors based on distance in probability over 100 replications with $n = 500$ samples for the Circular 3 density.

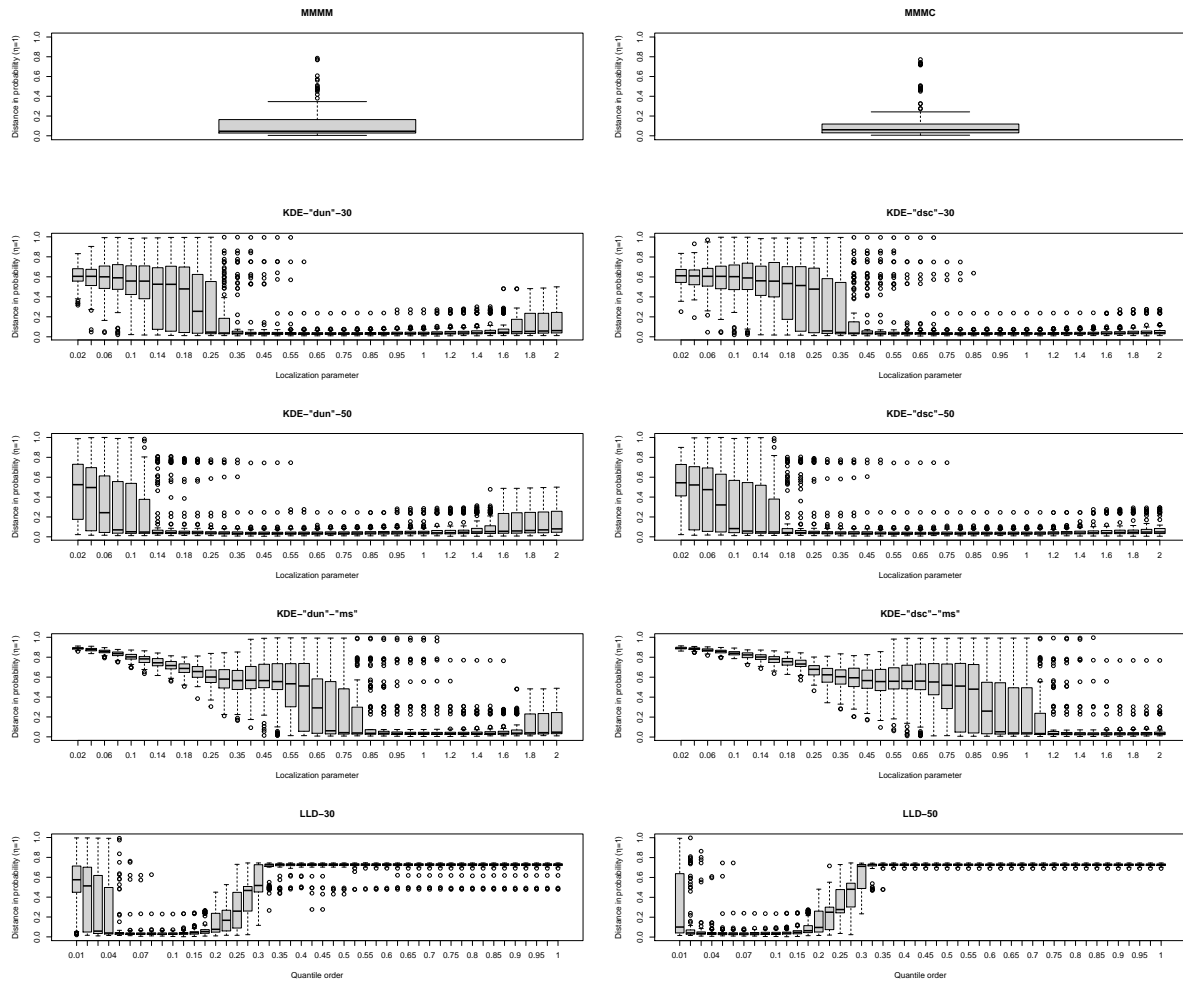


Figure 101: Boxplot of clustering errors based on distance in probability over 100 replications with $n = 500$ samples for the Circular 4 Cauchy density.

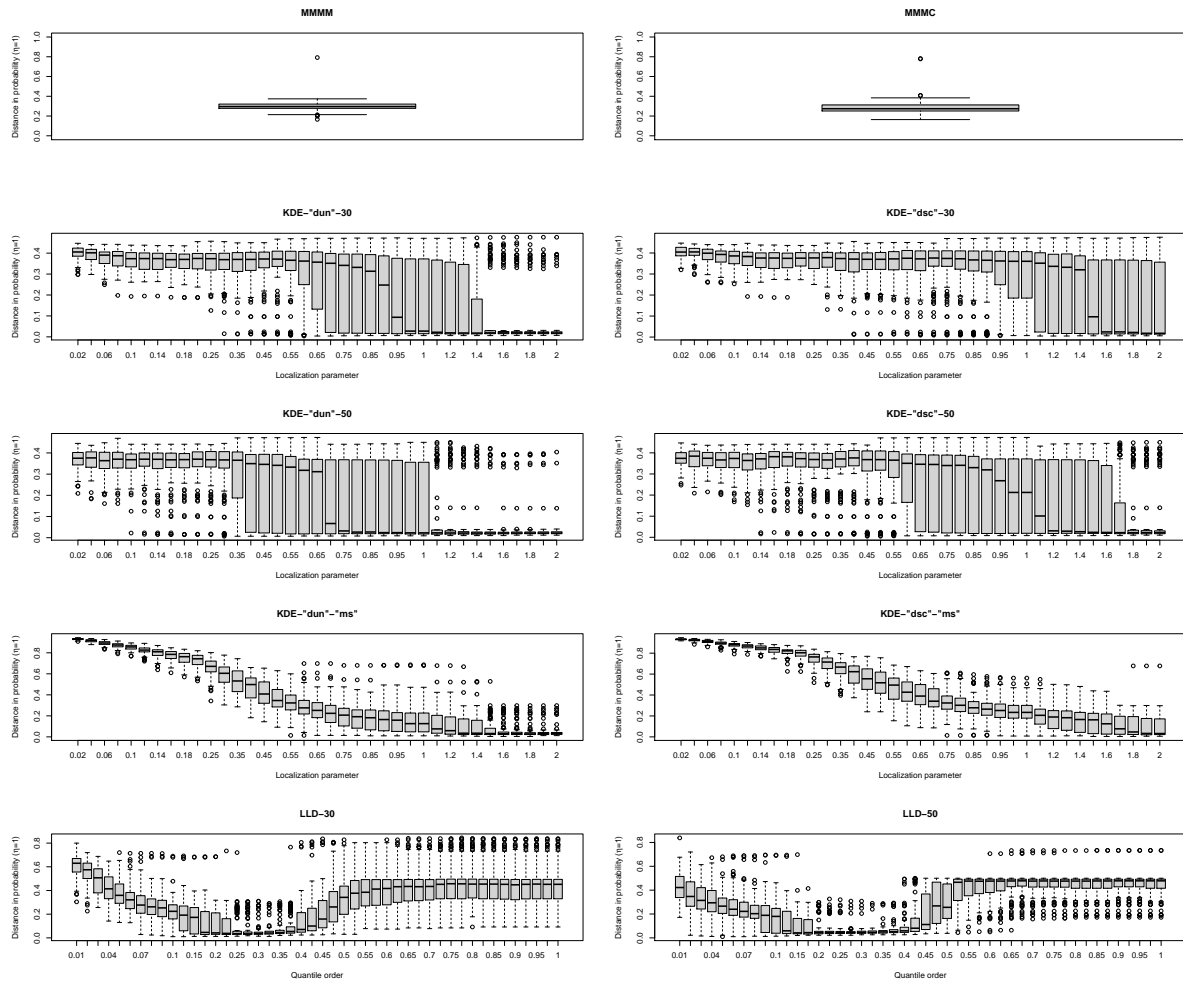


Figure 102: Boxplot of clustering errors based on distance in probability over 100 replications with $n = 500$ samples for the Circular Bimodal I density.

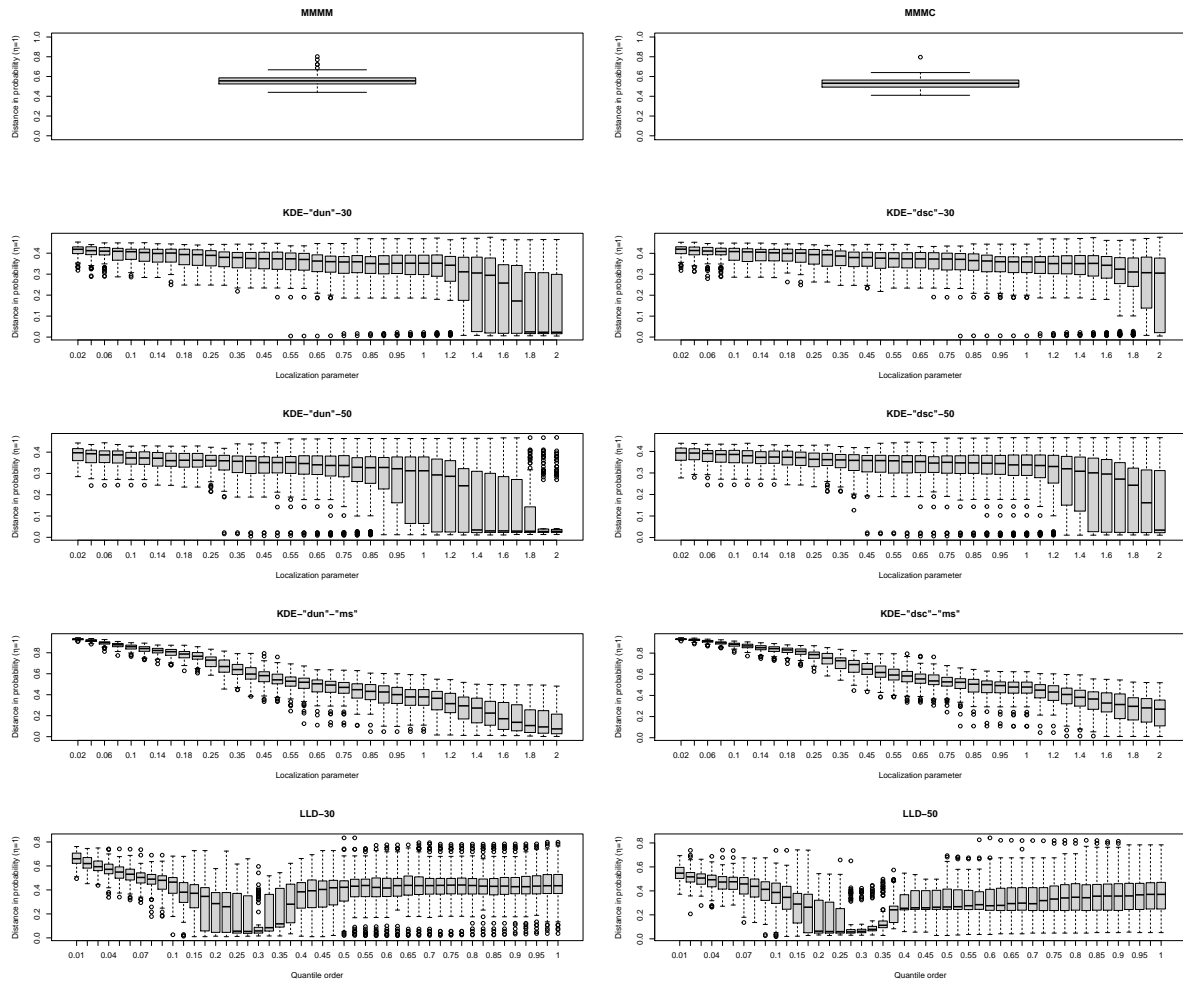


Figure 103: Boxplot of clustering errors based on distance in probability over 100 replications with $n = 500$ samples for the Circular Bimodal II density.

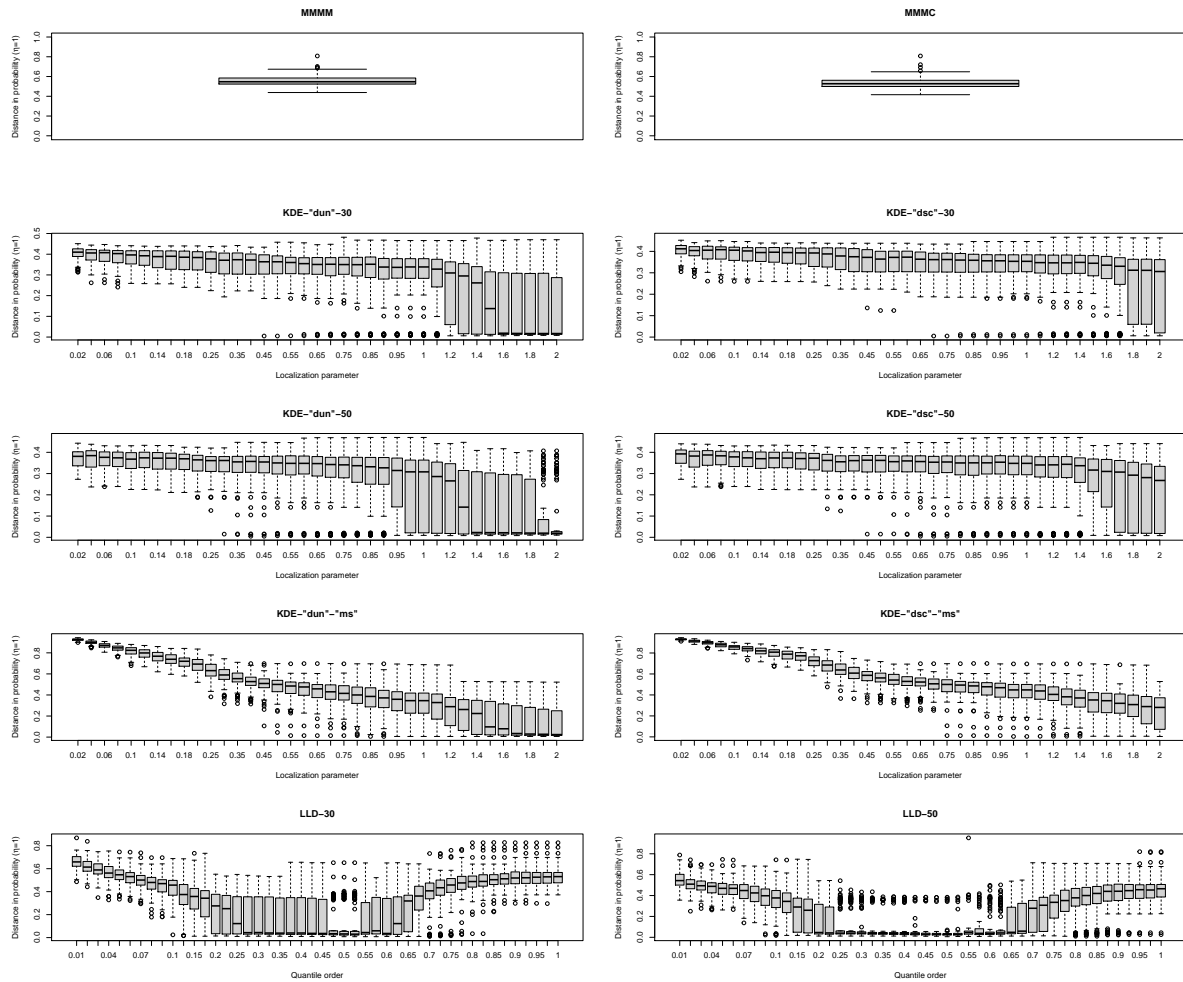


Figure 104: Boxplot of clustering errors based on distance in probability over 100 replications with $n = 500$ samples for the Circular Bimodal III density.

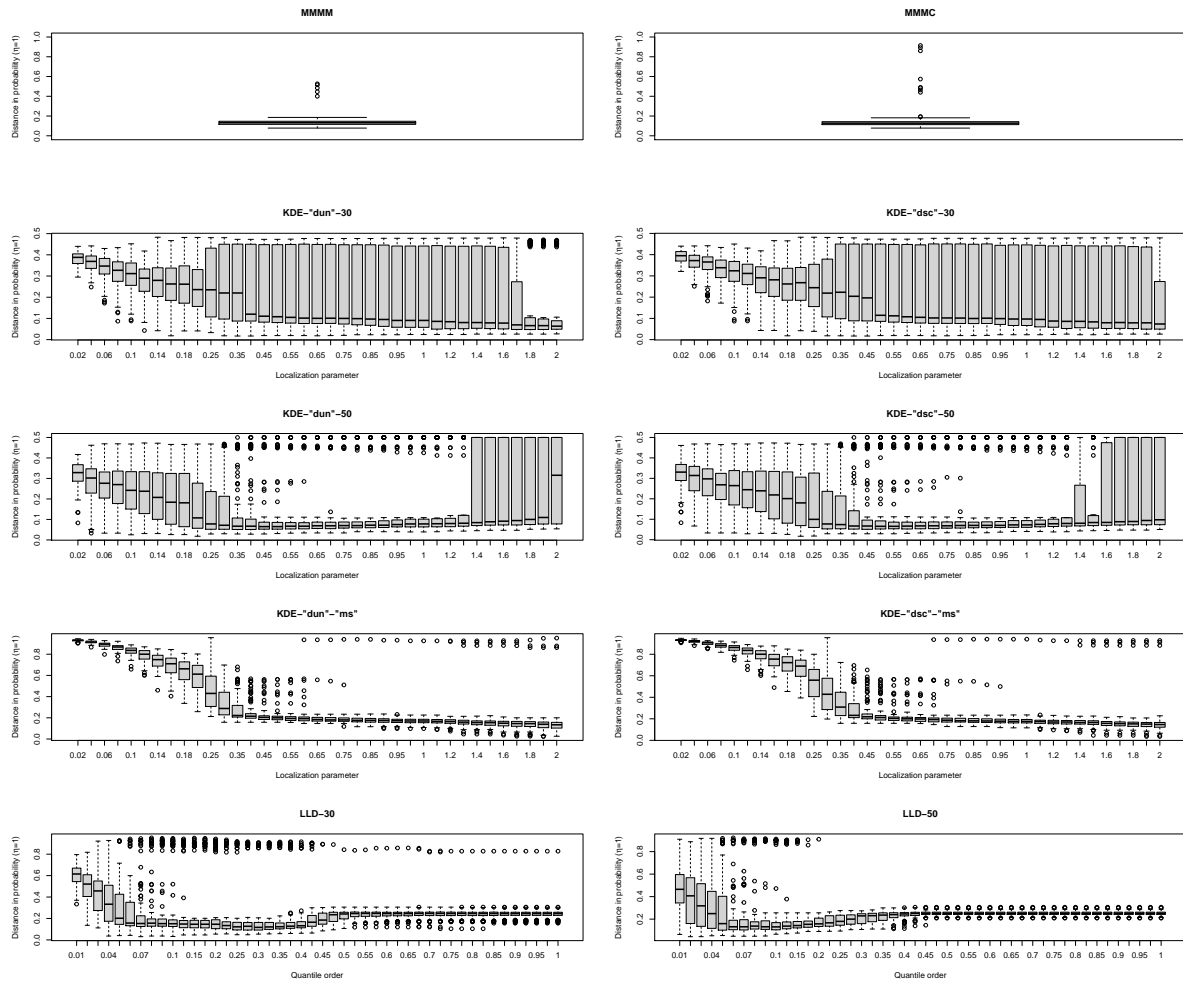


Figure 105: Boxplot of clustering errors based on distance in probability over 100 replications with $n = 500$ samples for the Circular Bimodal IV density.

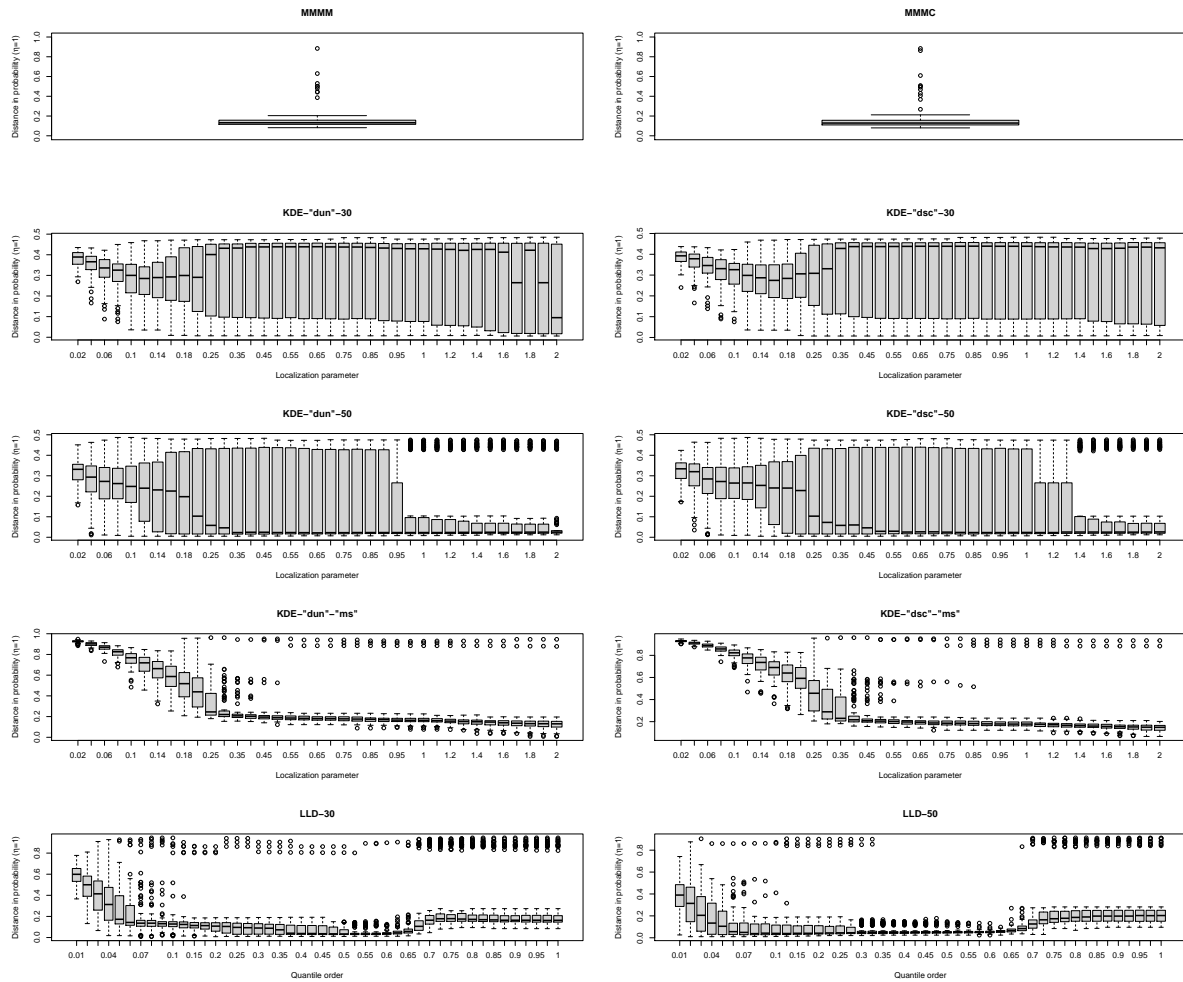


Figure 106: Boxplot of clustering errors based on distance in probability over 100 replications with $n = 500$ samples for the Circular Bimodal V density.

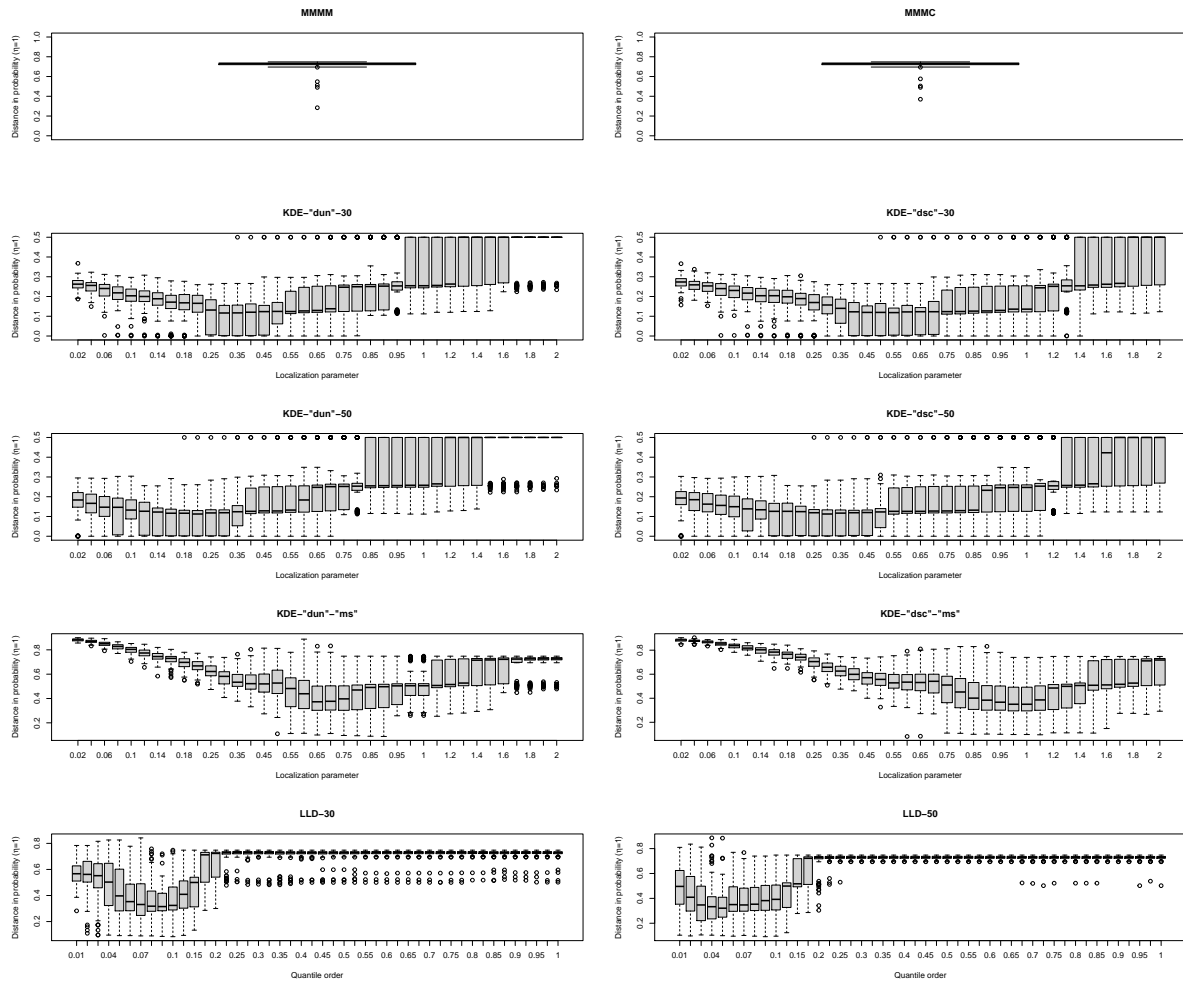


Figure 107: Boxplot of clustering errors based on distance in probability over 100 replications with $n = 500$ samples for the Circular Quadrinodal I density.

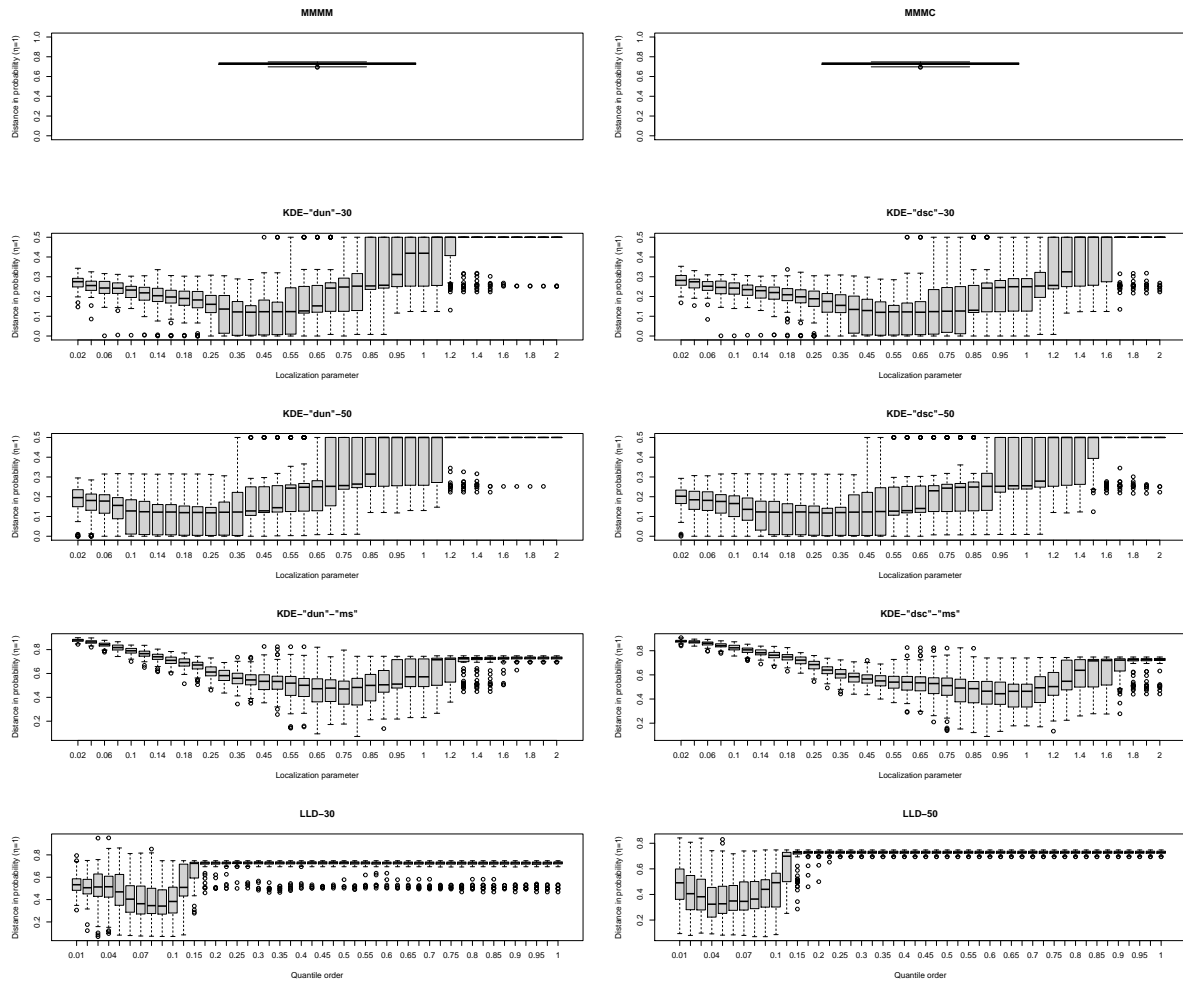


Figure 108: Boxplot of clustering errors based on distance in probability over 100 replications with $n = 500$ samples for the Circular Quadrinodal II density.

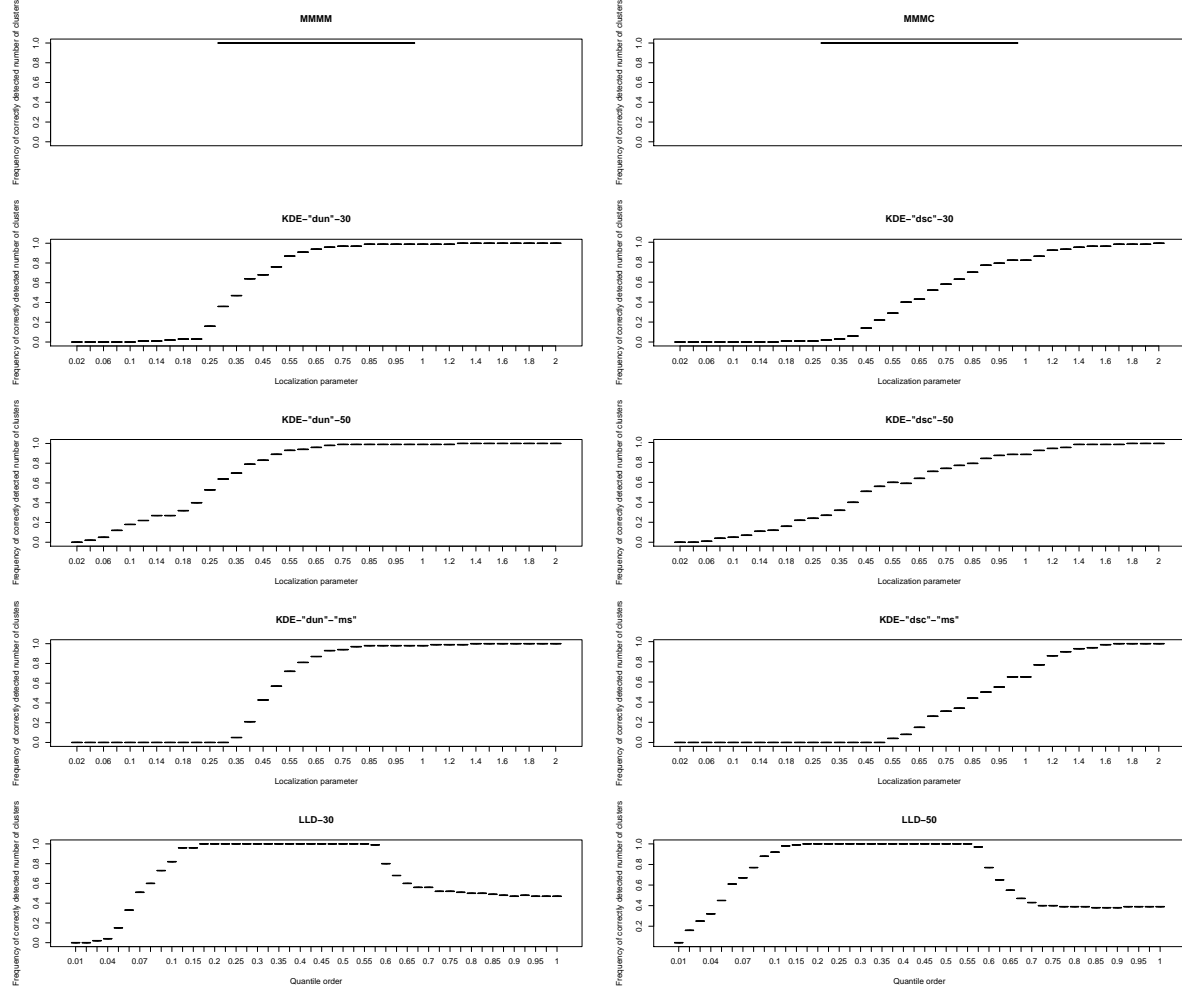


Figure 109: Boxplot of frequency of correctly detected number of clusters over 100 replications with $n = 500$ samples for the (H) Bimodal IV density.

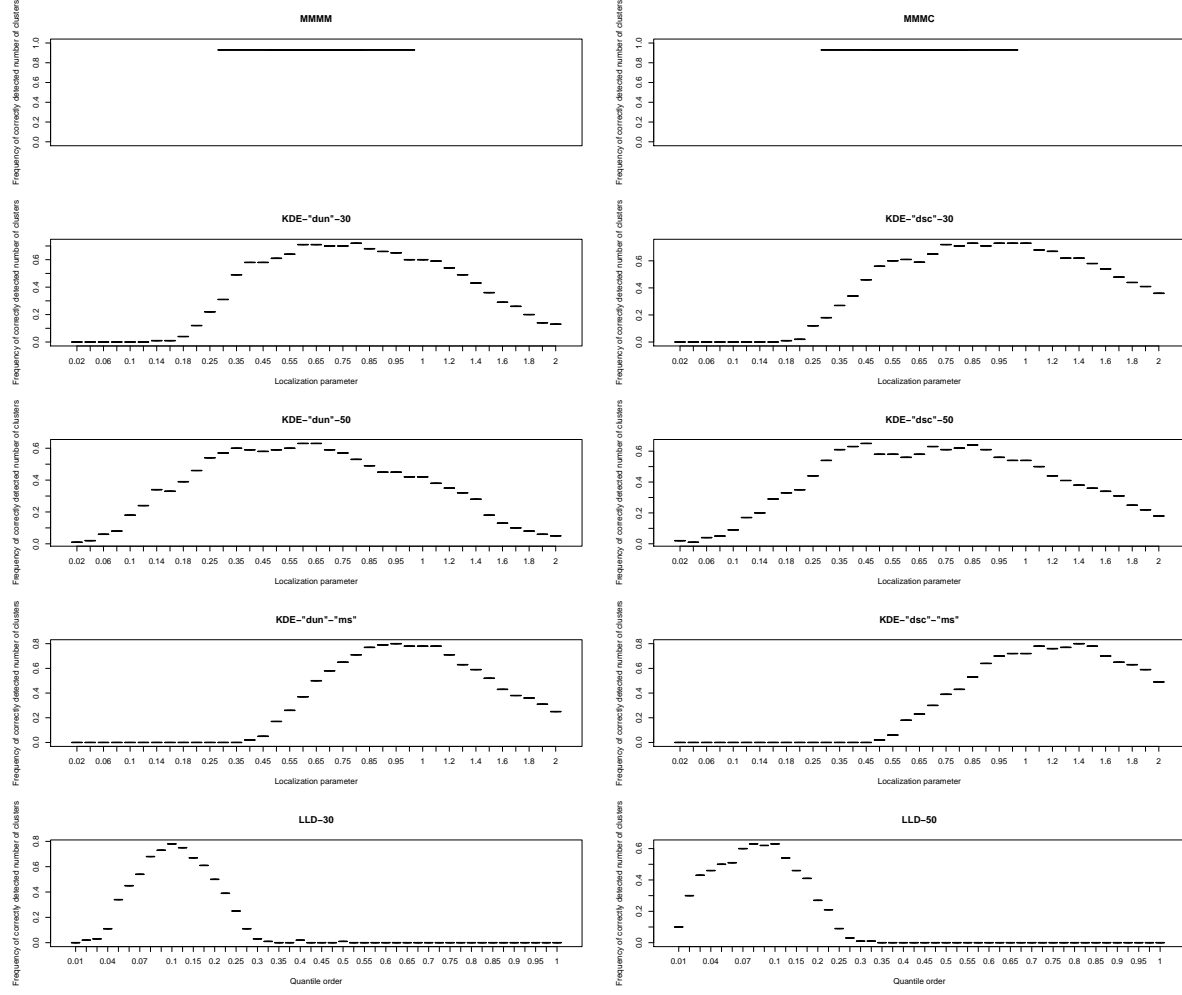


Figure 110: Boxplot of frequency of correctly detected number of clusters over 100 replications with $n = 500$ samples for the (K) Trimodal III density.

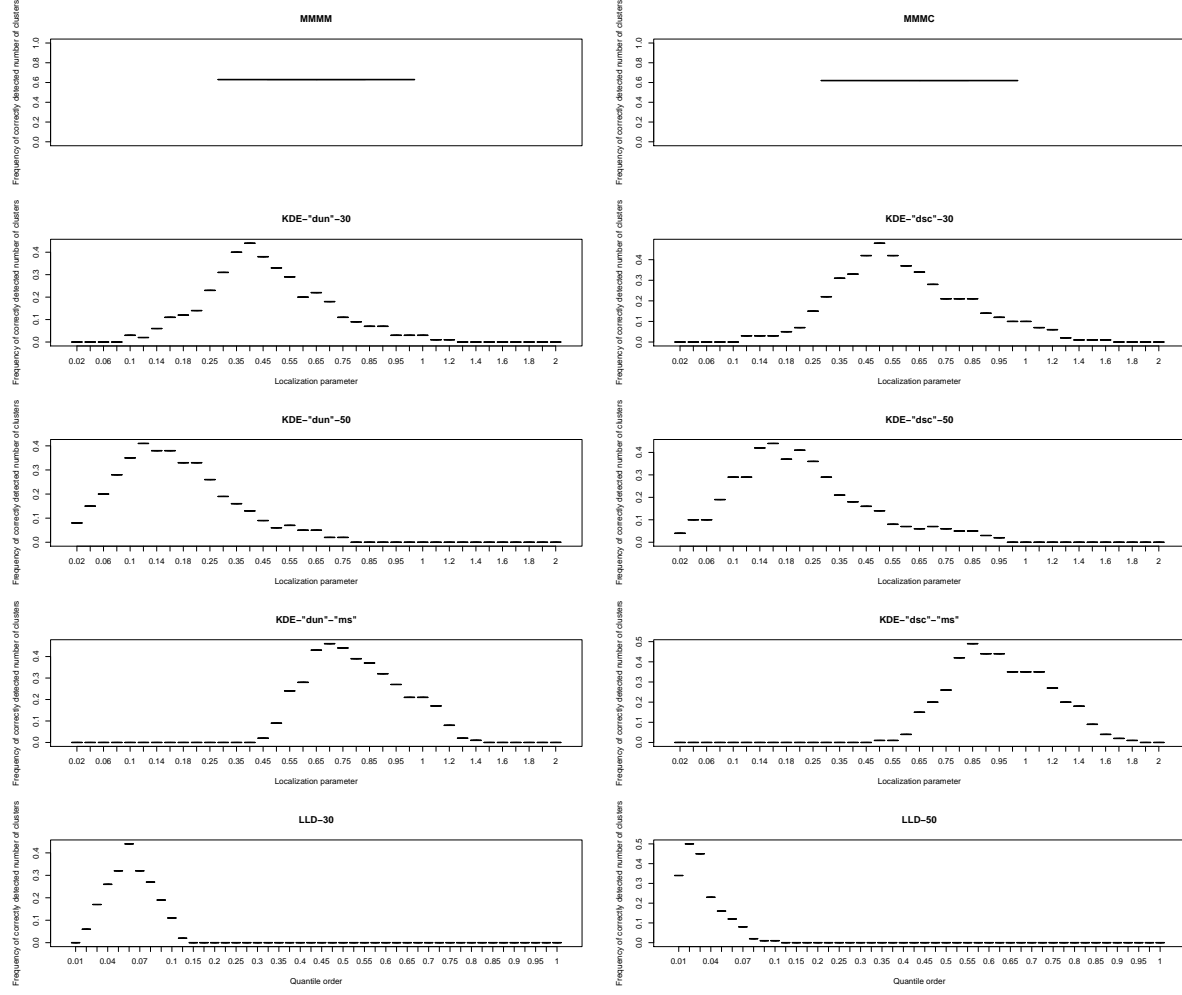


Figure 111: Boxplot of frequency of correctly detected number of clusters over 100 replications with $n = 500$ samples for the (L) Quadrinomodal density.

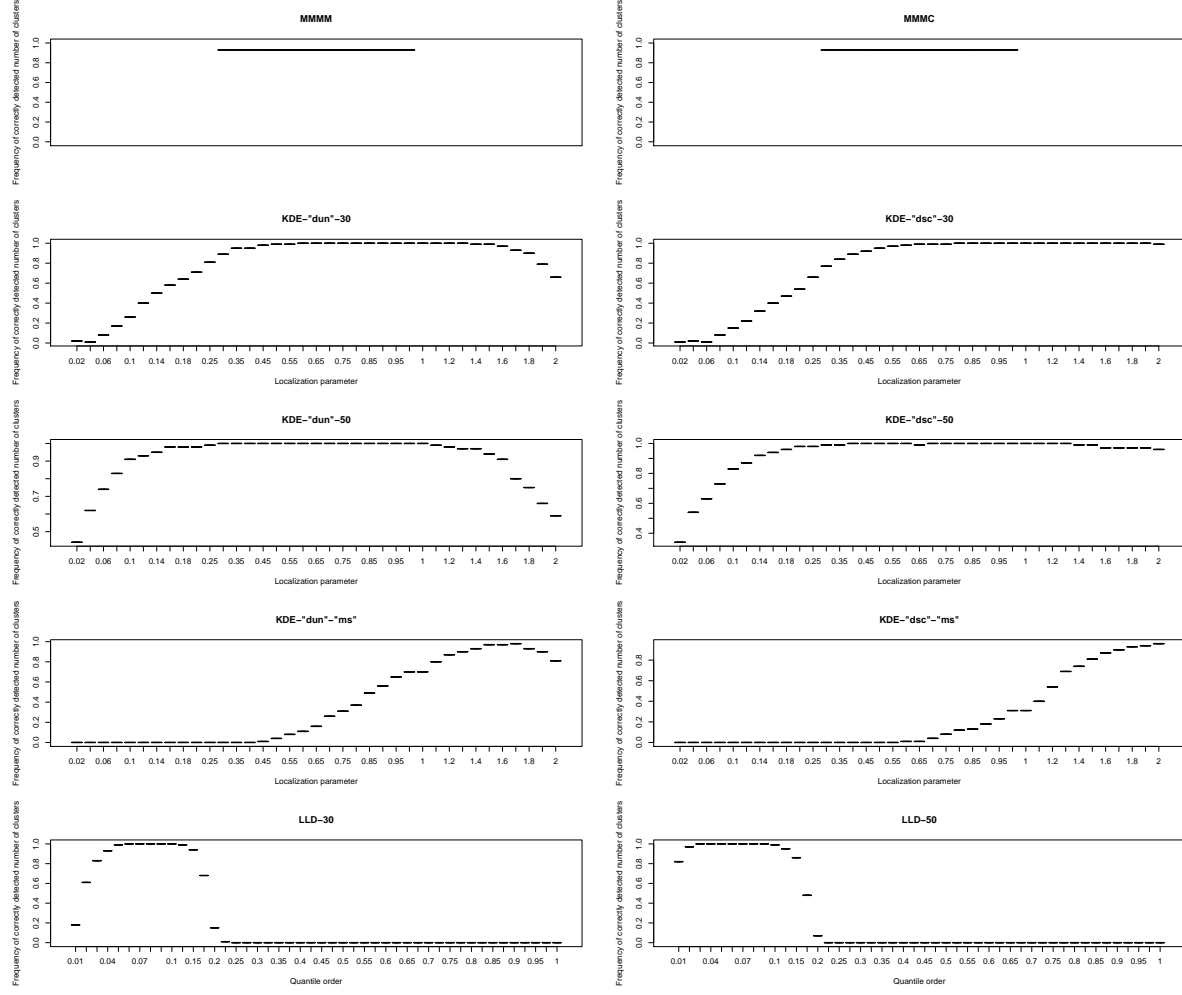


Figure 112: Boxplot of frequency of correctly detected number of clusters over 100 replications with $n = 500$ samples for the #10 fountain density.

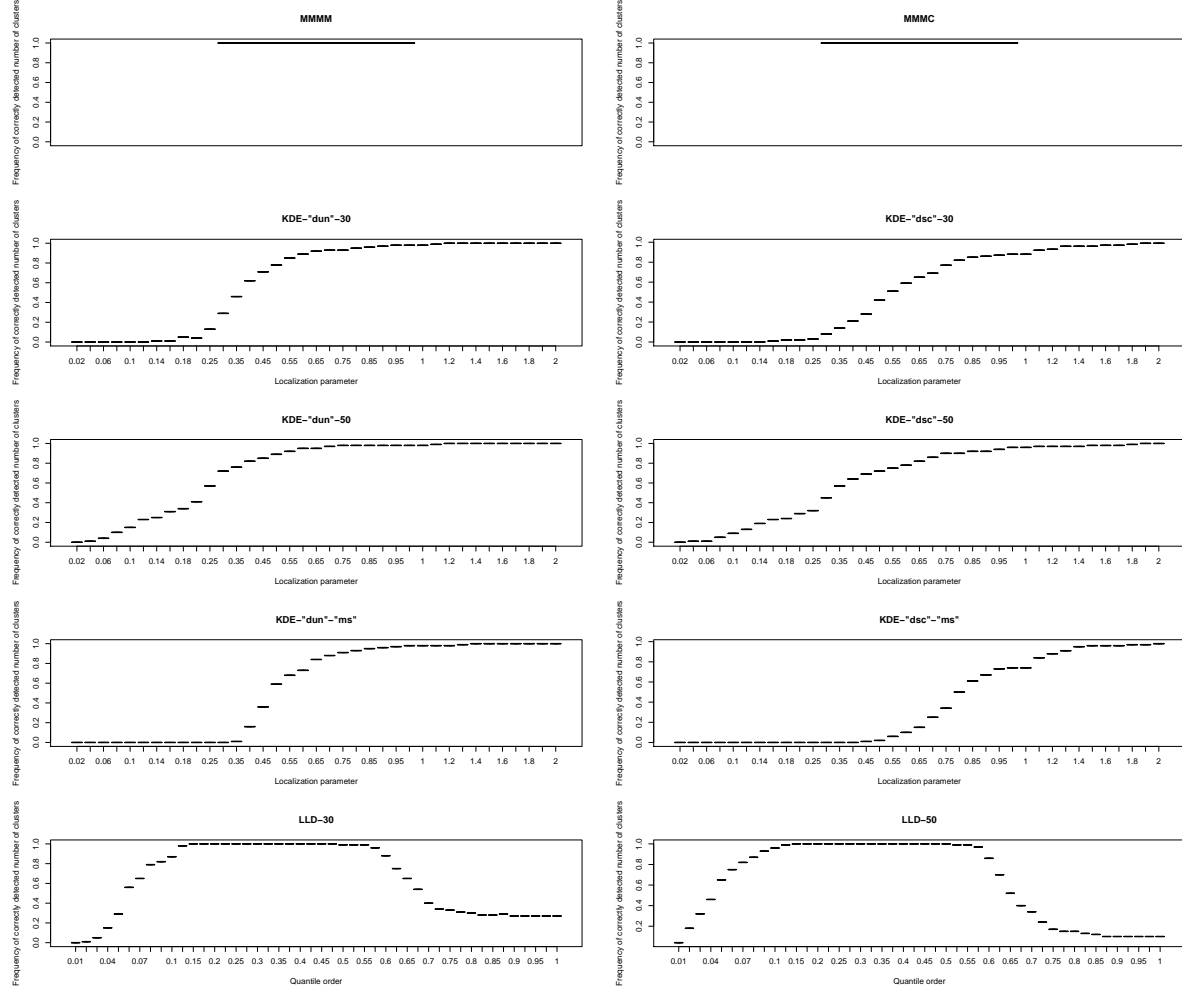


Figure 113: Boxplot of frequency of correctly detected number of clusters over 100 replications with $n = 500$ samples for the Bimodal density.

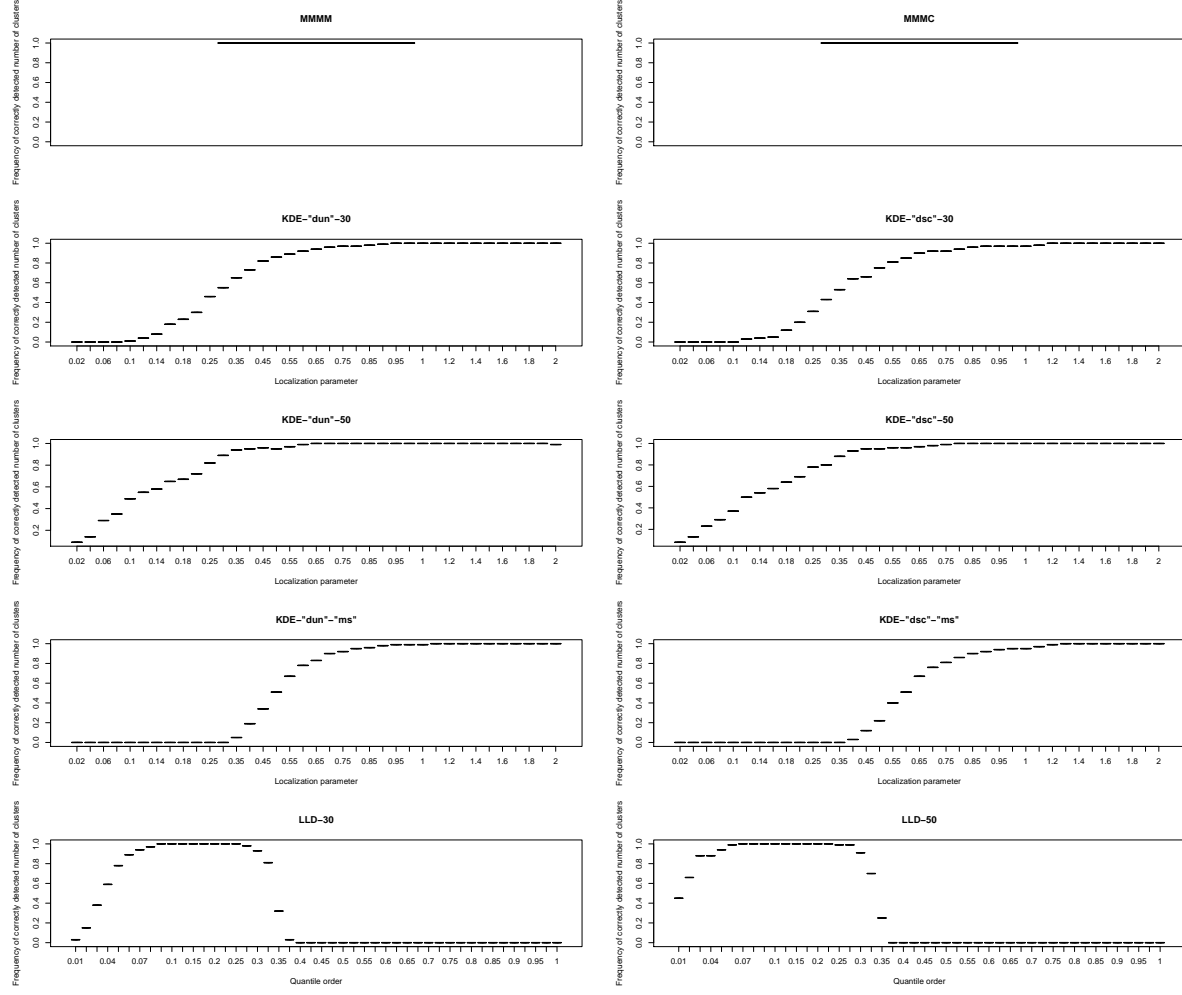


Figure 114: Boxplot of frequency of correctly detected number of clusters over 100 replications with $n = 500$ samples for the Quadrimodal density.

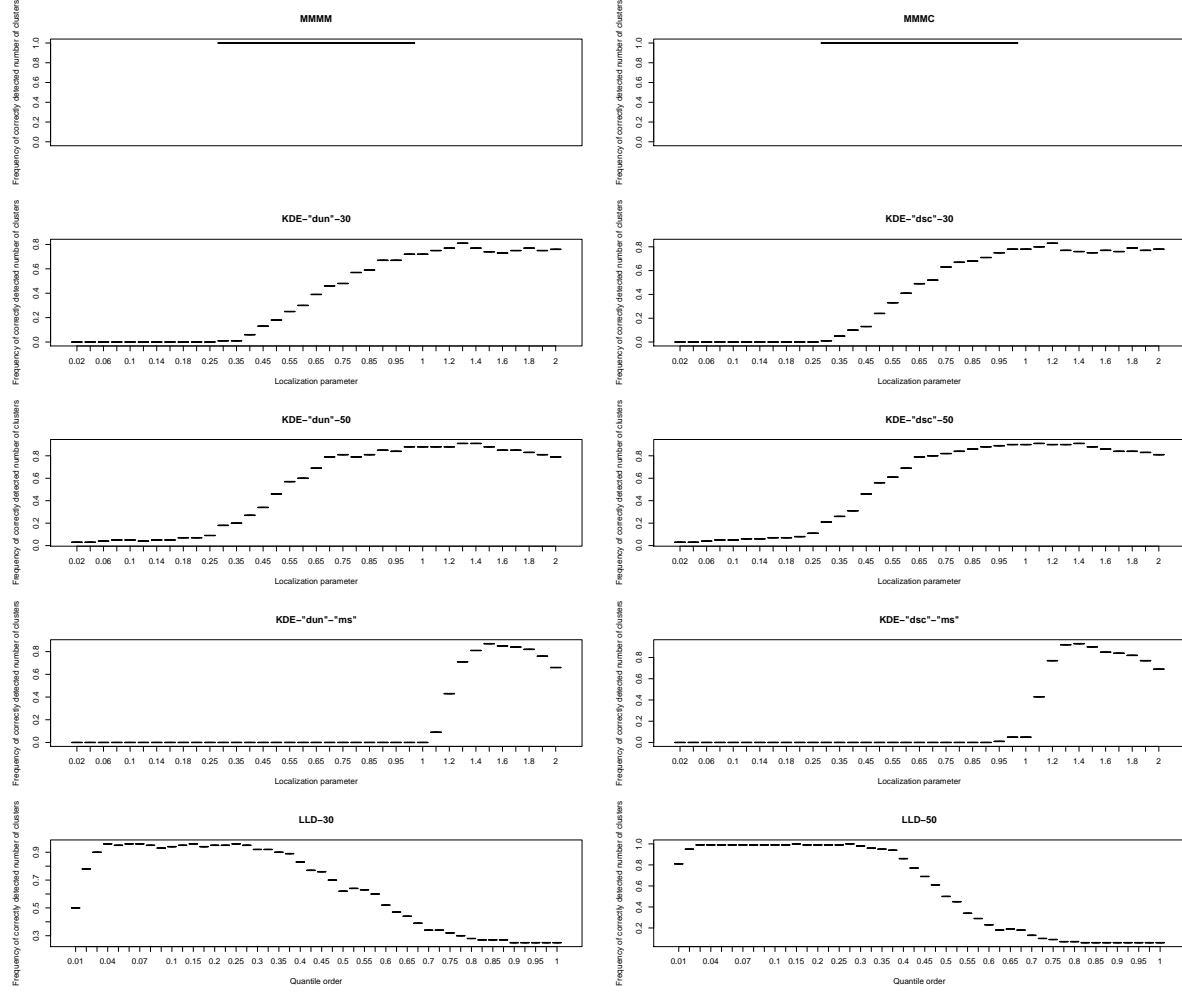


Figure 115: Boxplot of frequency of correctly detected number of clusters over 100 replications with $n = 500$ samples for the Mult. Bimodal density.

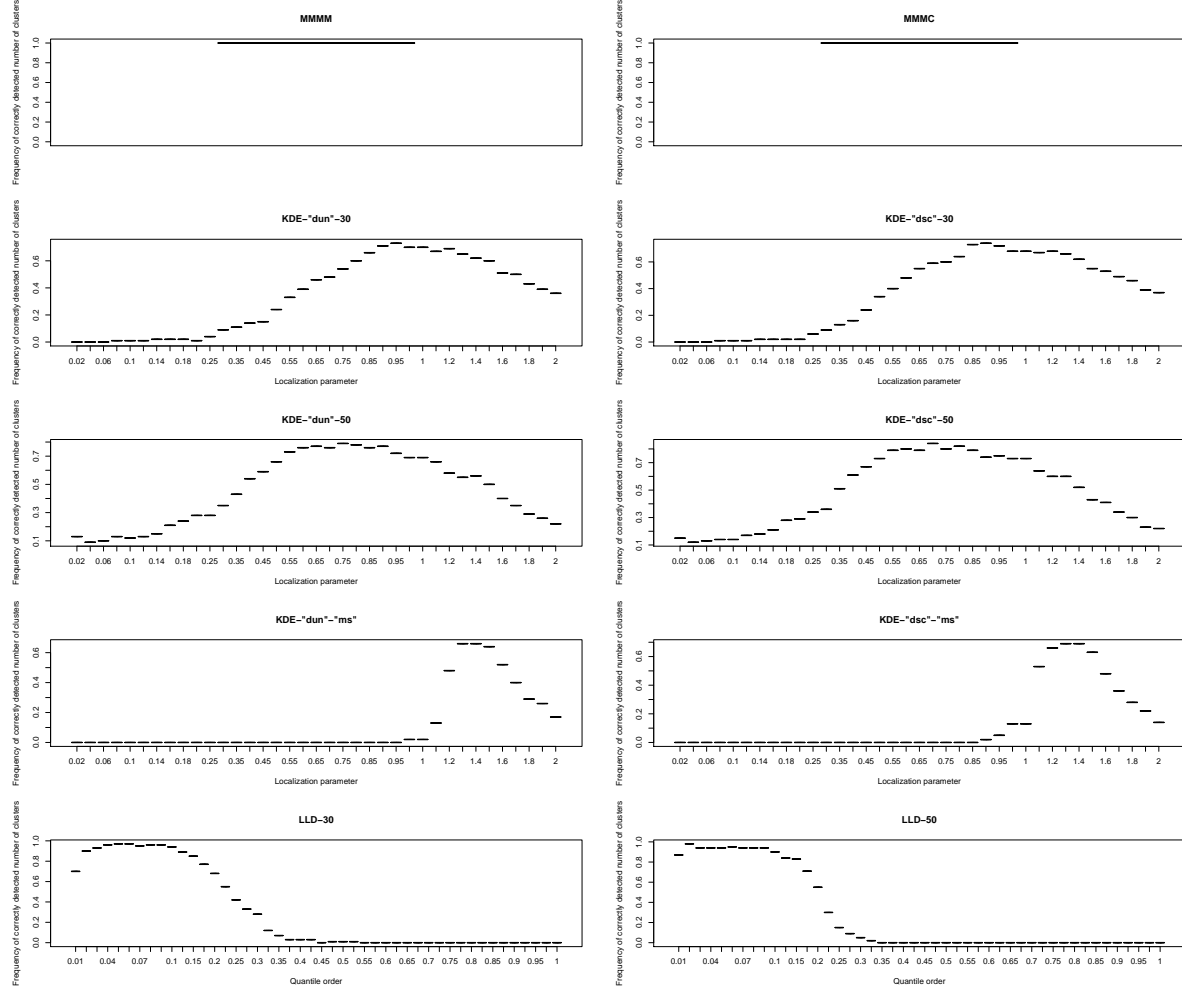


Figure 116: Boxplot of frequency of correctly detected number of clusters over 100 replications with $n = 500$ samples for the Mult. Quadrinodal density.

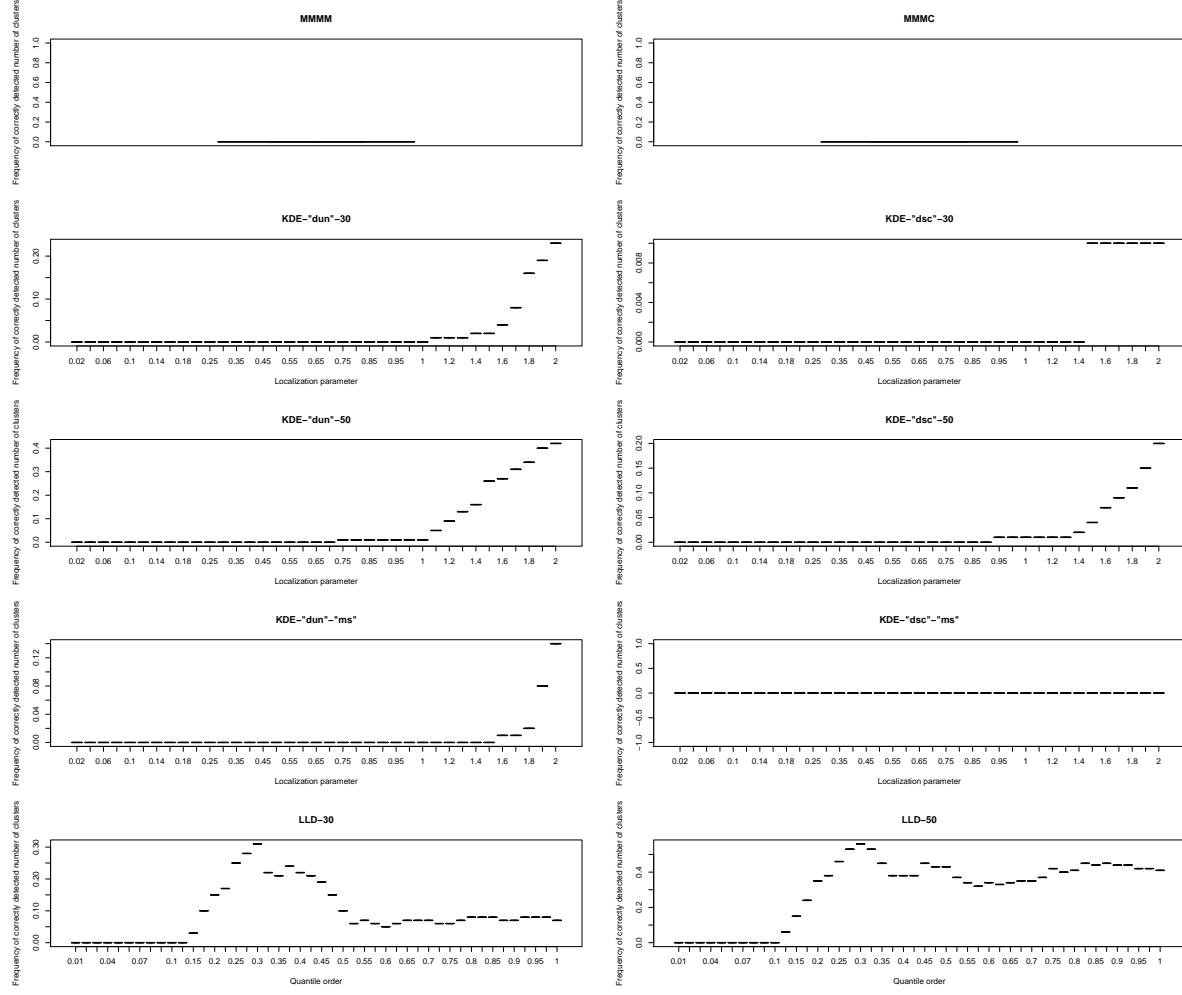


Figure 117: Boxplot of frequency of correctly detected number of clusters over 100 replications with $n = 500$ samples for the Circular 2 density.

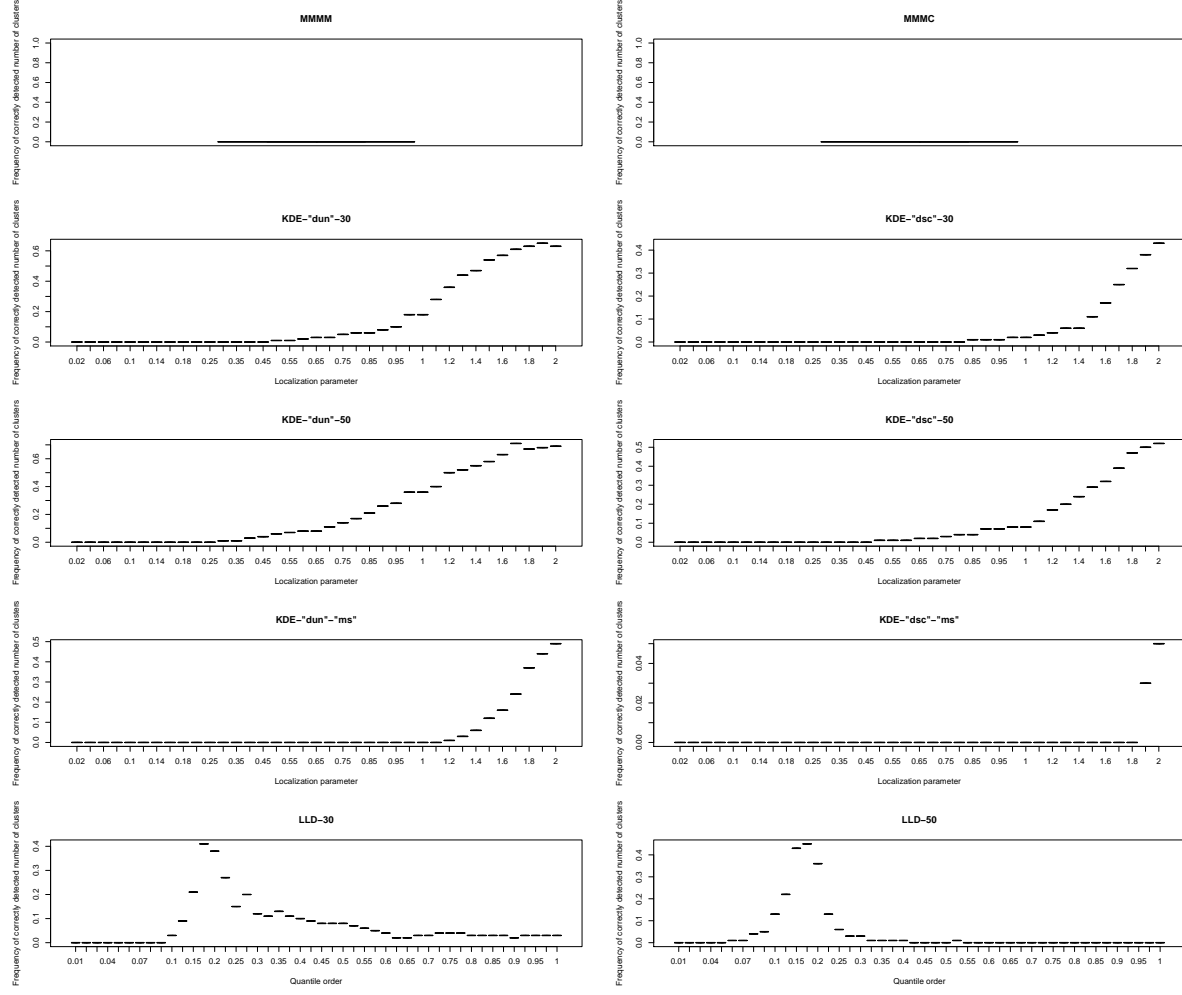


Figure 118: Boxplot of frequency of correctly detected number of clusters over 100 replications with $n = 500$ samples for the Circular 2 Cauchy density.

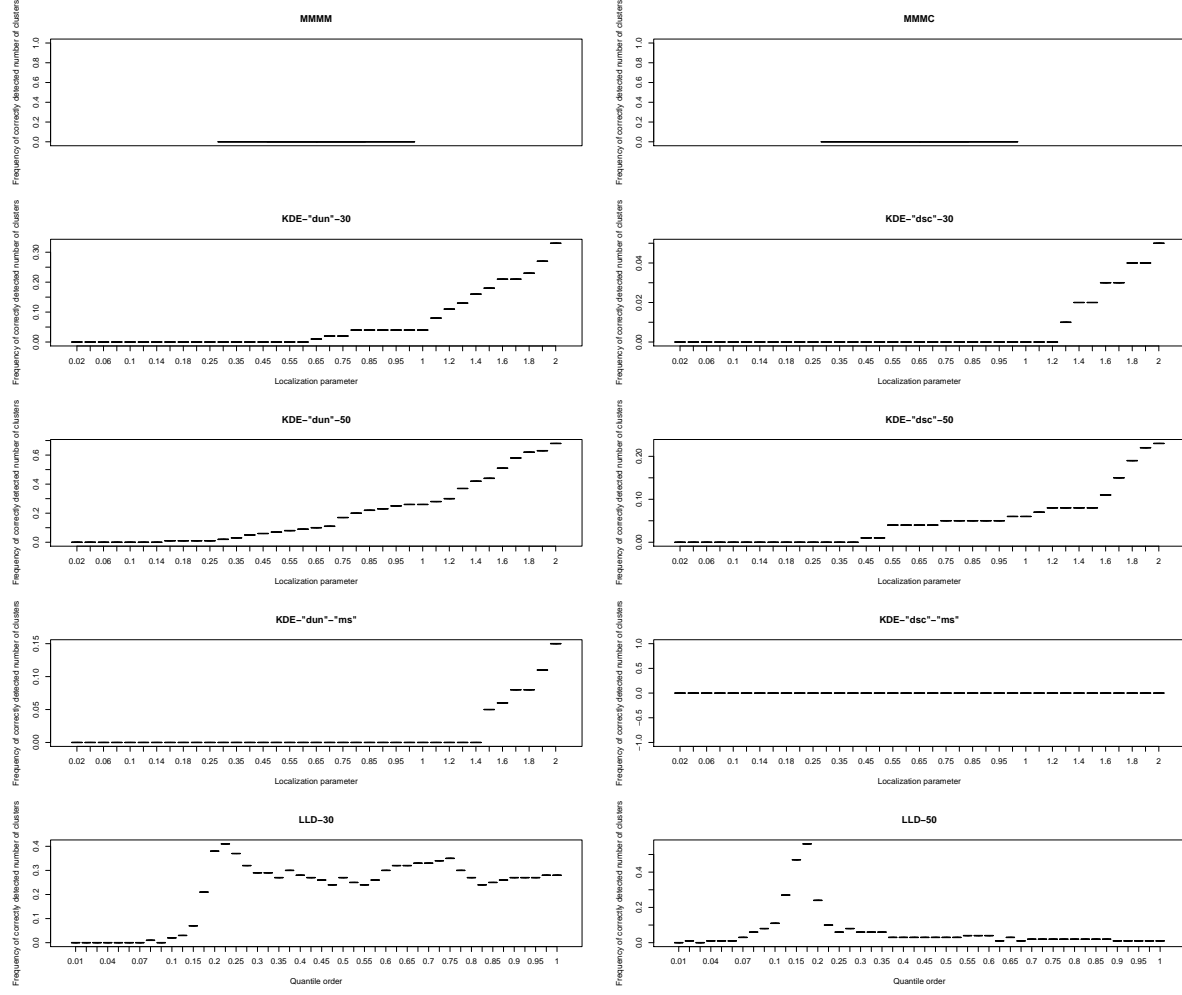


Figure 119: Boxplot of frequency of correctly detected number of clusters over 100 replications with $n = 500$ samples for the Circular 3 density.

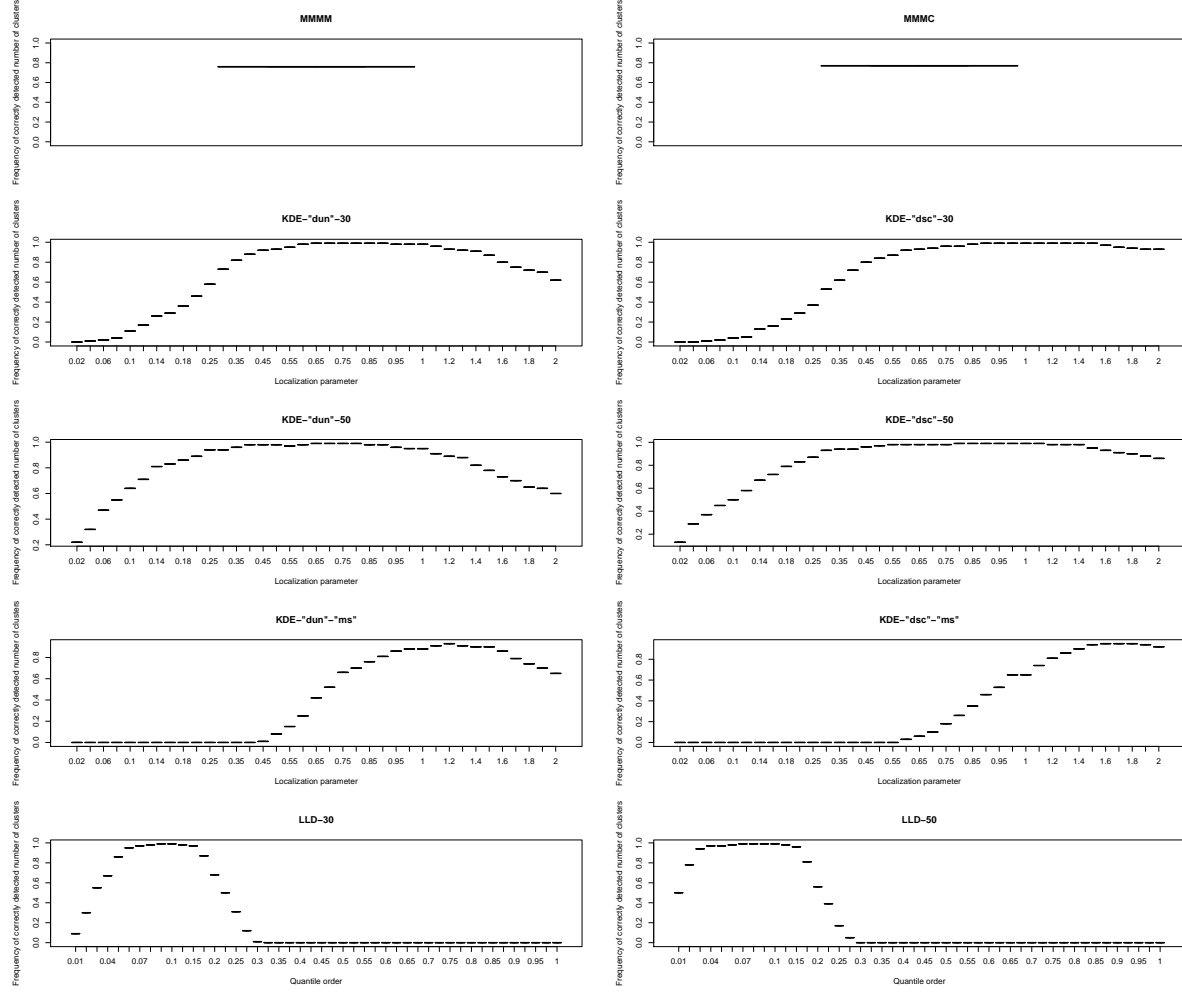


Figure 120: Boxplot of frequency of correctly detected number of clusters over 100 replications with $n = 500$ samples for the Circular 4 Cauchy density.

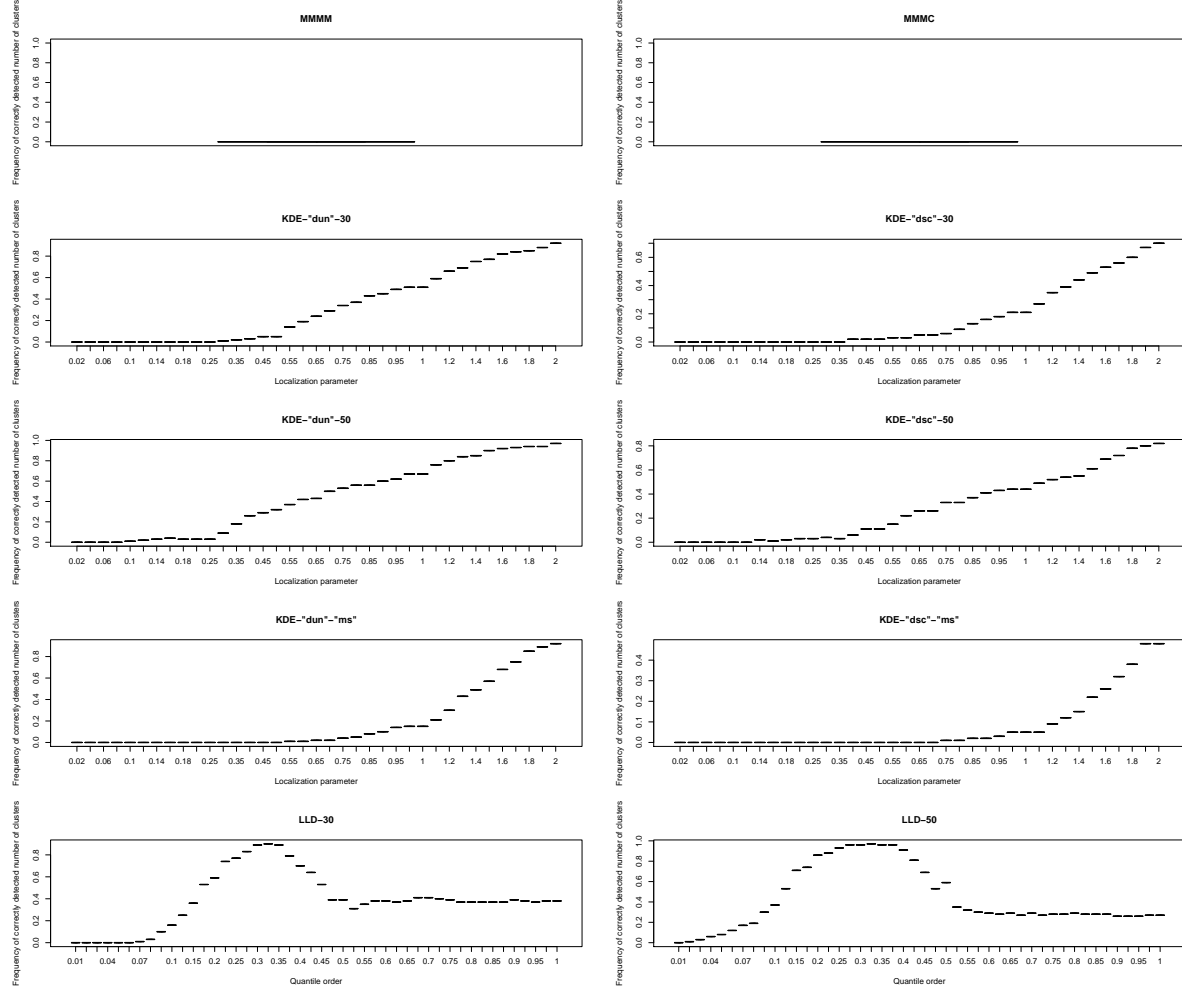


Figure 121: Boxplot of frequency of correctly detected number of clusters over 100 replications with $n = 500$ samples for the Circular Bimodal I density.

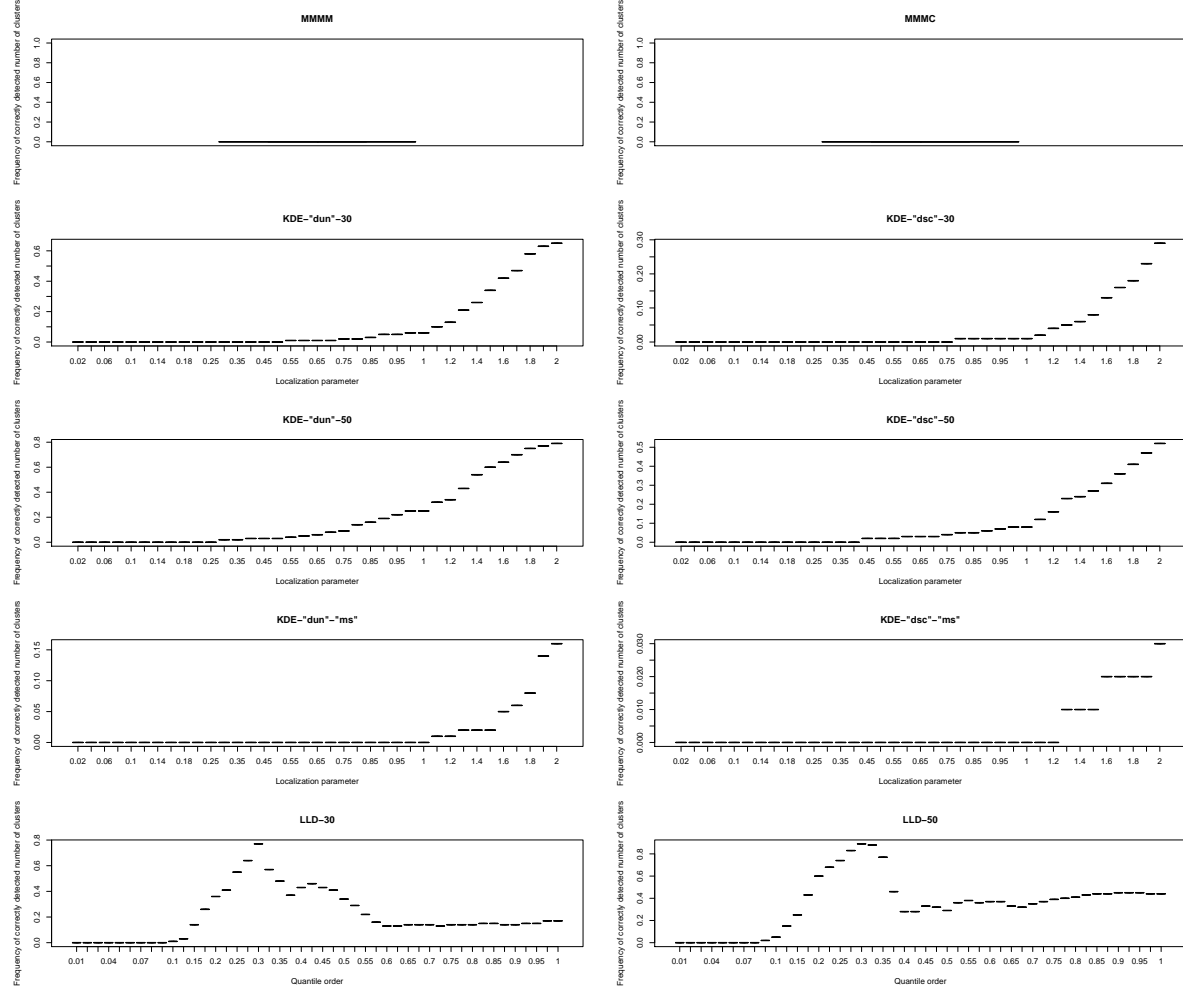


Figure 122: Boxplot of frequency of correctly detected number of clusters over 100 replications with $n = 500$ samples for the Circular Bimodal II density.

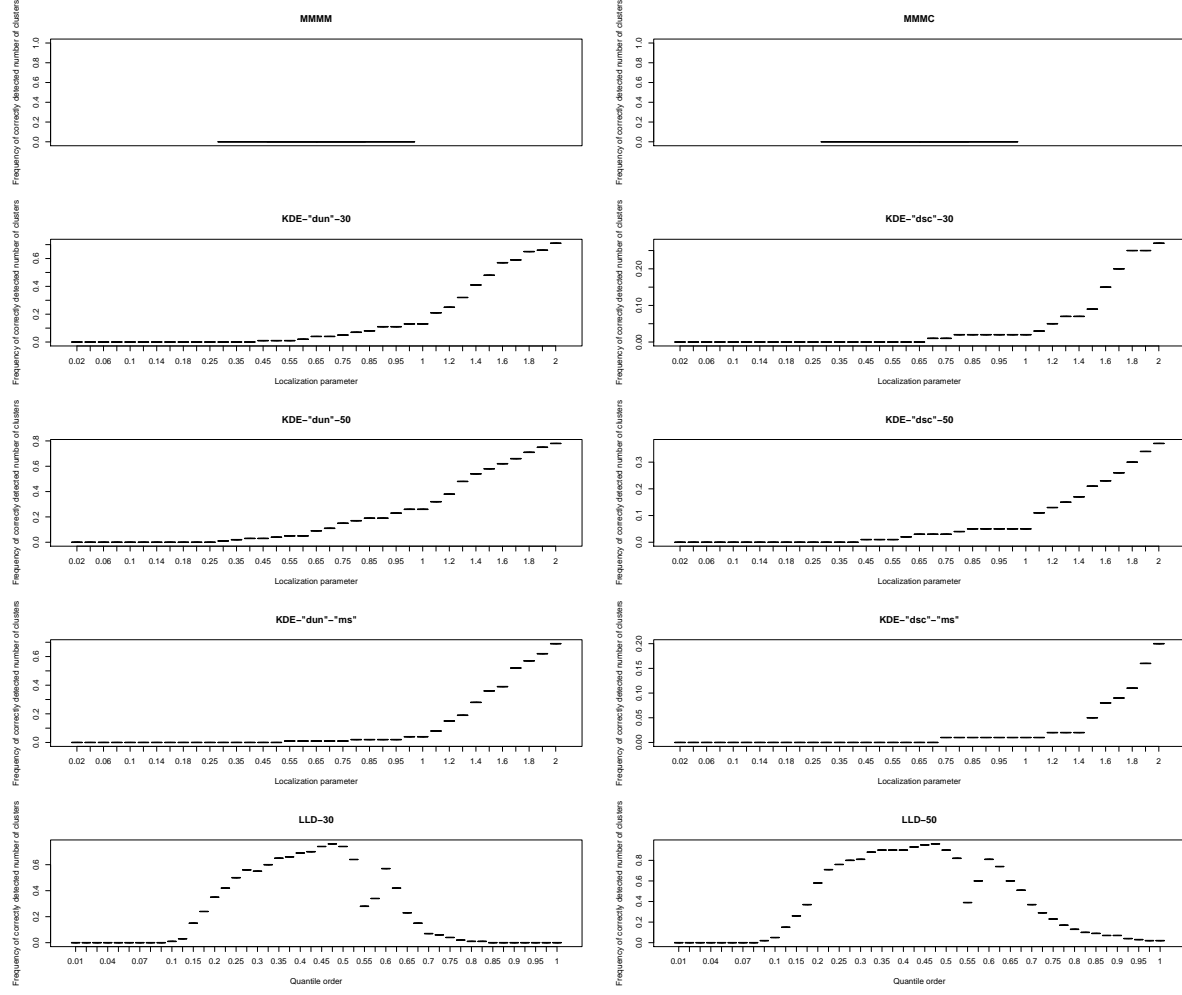


Figure 123: Boxplot of frequency of correctly detected number of clusters over 100 replications with $n = 500$ samples for the Circular Bimodal III density.

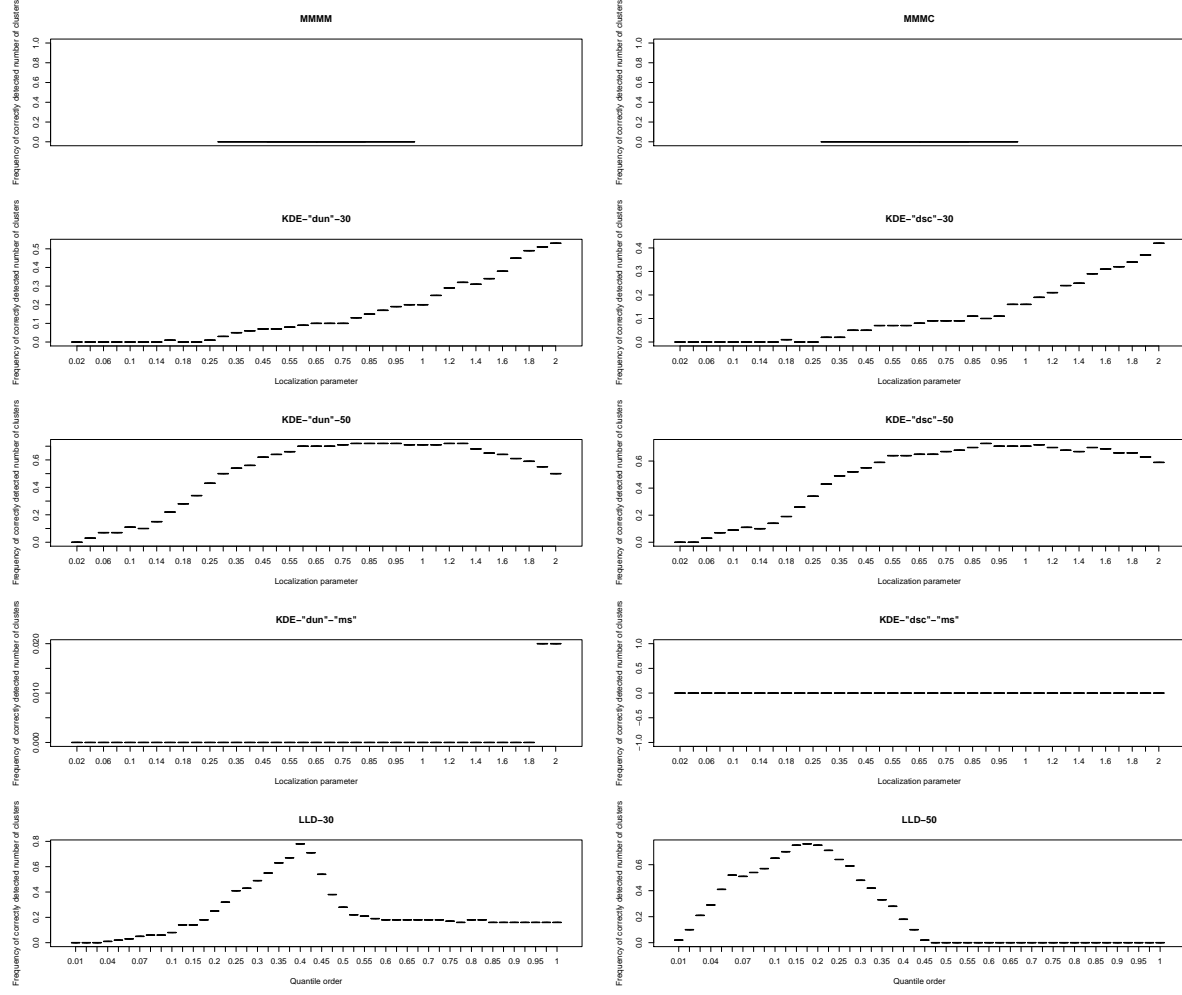


Figure 124: Boxplot of frequency of correctly detected number of clusters over 100 replications with $n = 500$ samples for the Circular Bimodal IV density.

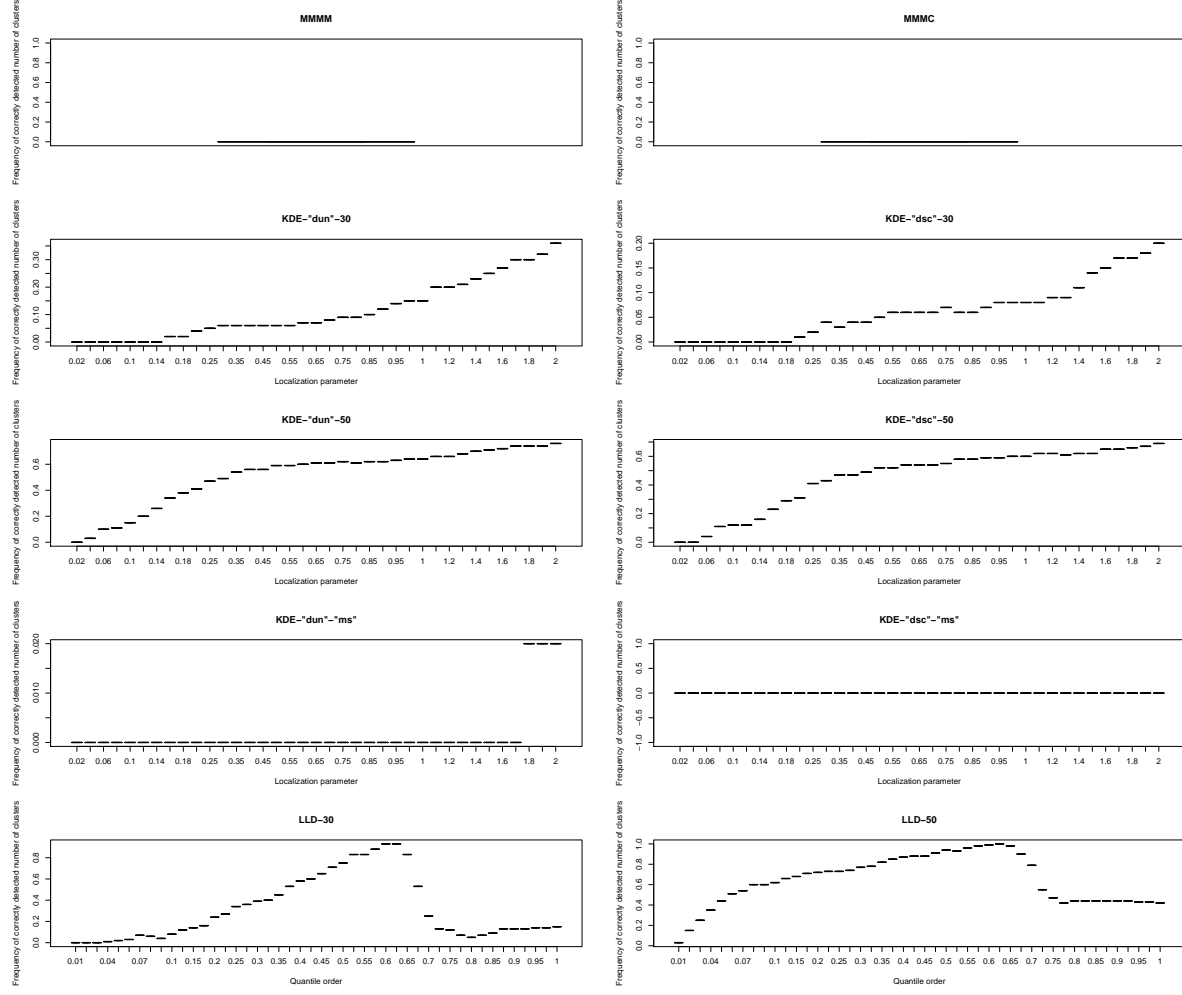


Figure 125: Boxplot of frequency of correctly detected number of clusters over 100 replications with $n = 500$ samples for the Circular Bimodal V density.

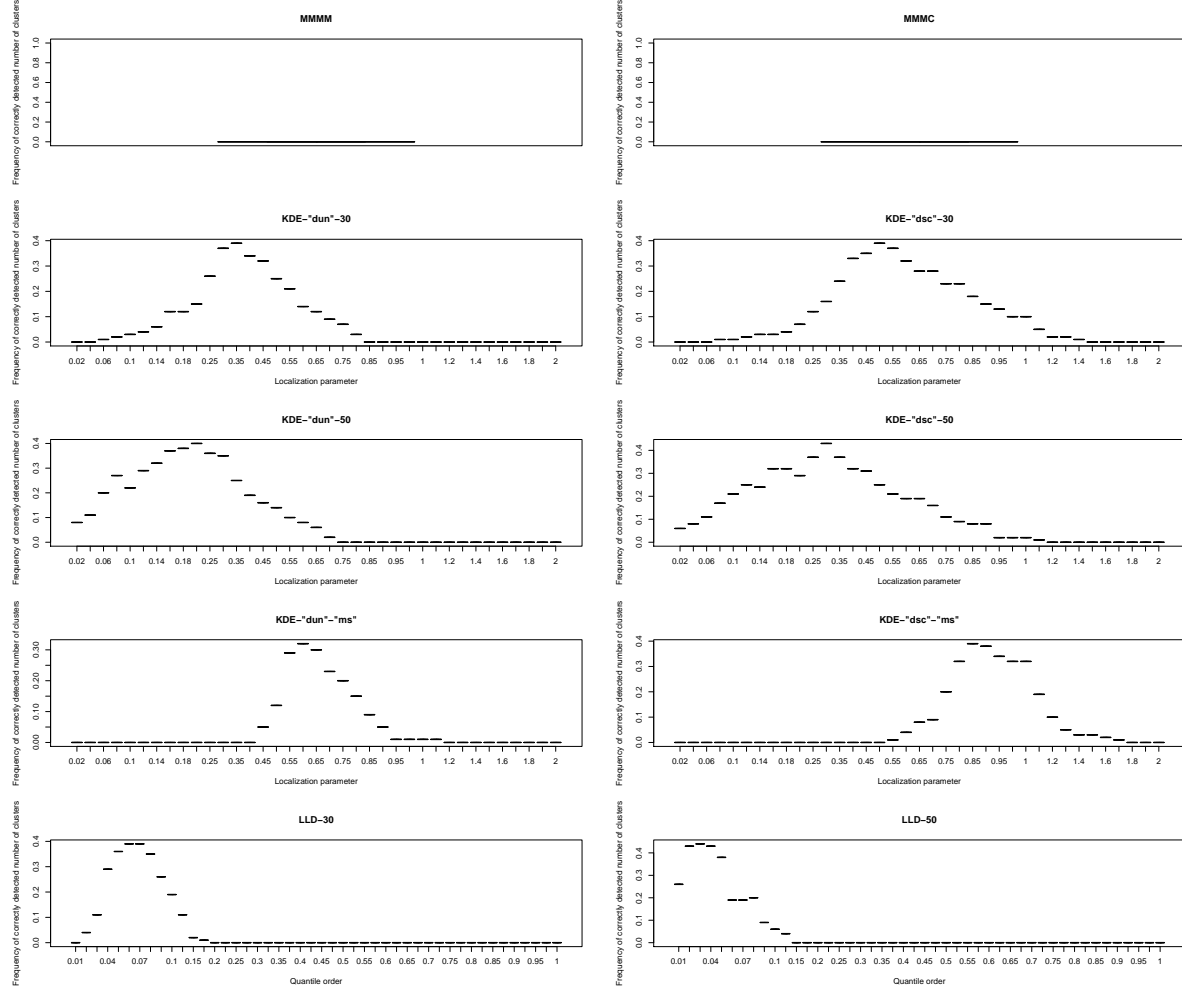


Figure 126: Boxplot of frequency of correctly detected number of clusters over 100 replications with $n = 500$ samples for the Circular Quadrinodal I density.

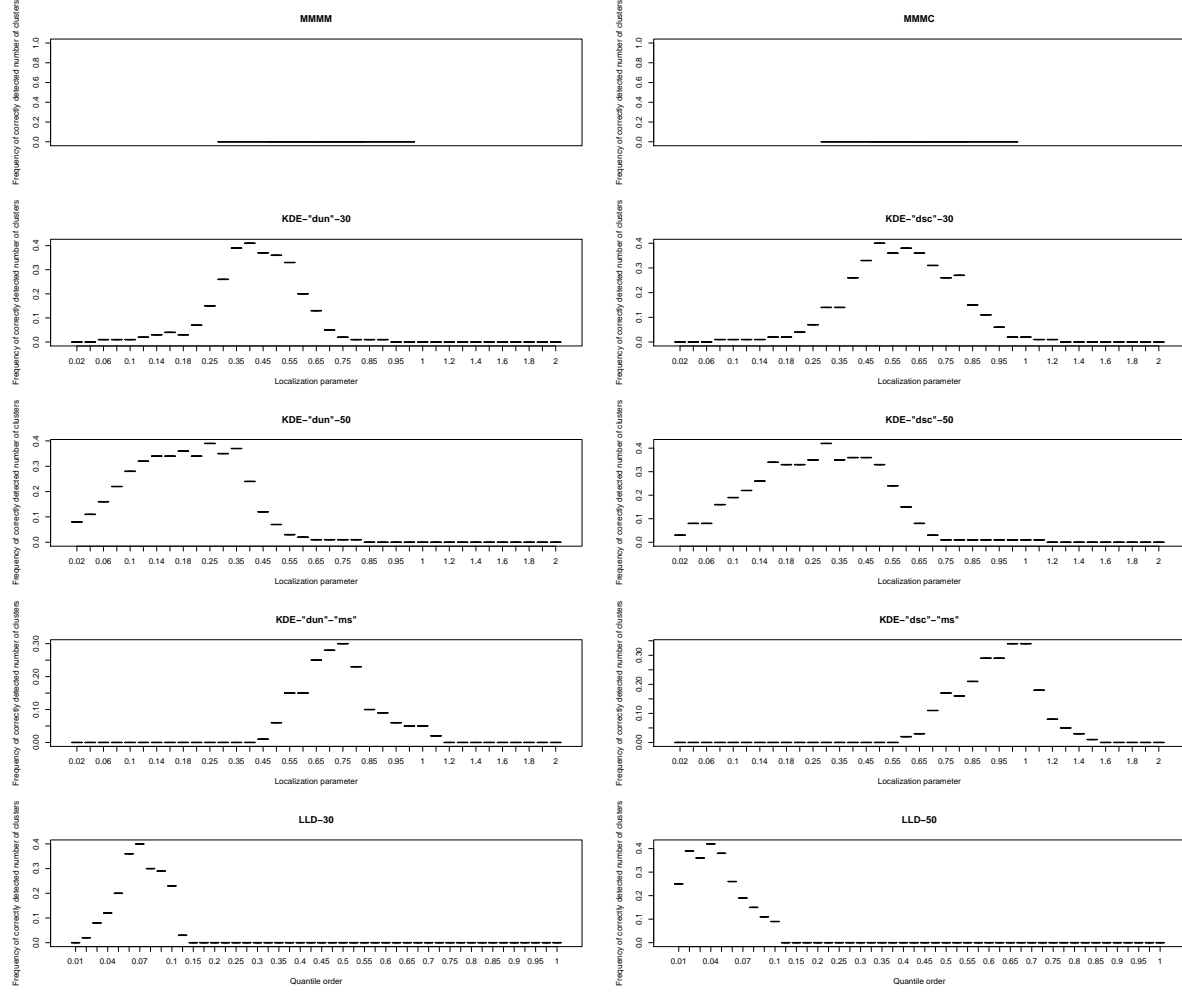


Figure 127: Boxplot of frequency of correctly detected number of clusters over 100 replications with $n = 500$ samples for the Circular Quadrinodal II density.

In particular, if $A = \lim_{n \rightarrow \infty} A_n$ and $B = \lim_{n \rightarrow \infty} B_n$ exist, then

$$(v) \quad \lim_{n \rightarrow \infty} (A_n \cap B_n) = A \cap B \text{ and } (vi) \quad \lim_{n \rightarrow \infty} (A_n \cup B_n) = A \cup B.$$

Proof of Lemma L.1. We begin by proving (i). It holds that

$$\begin{aligned} x \in \liminf_{n \rightarrow \infty} (A_n \cap B_n) &\Leftrightarrow \exists n^* \in \mathbb{N} : x \in \bigcap_{n=n^*}^{\infty} (A_n \cap B_n) \\ &\Leftrightarrow \exists n^* \in \mathbb{N} : x \in (A_n \cap B_n) \forall n \geq n^* \\ &\Leftrightarrow \exists n_A, n_B \in \mathbb{N} : x \in A_n \forall n \geq n_A \text{ and } x \in B_n \forall n \geq n_B \\ &\Leftrightarrow \exists n_A, n_B \in \mathbb{N} : x \in \bigcap_{n=n_A}^{\infty} A_n \text{ and } x \in \bigcap_{n=n_B}^{\infty} B_n \\ &\Leftrightarrow x \in \liminf_{n \rightarrow \infty} A_n \text{ and } x \in \liminf_{n \rightarrow \infty} B_n \\ &\Leftrightarrow x \in (\liminf_{n \rightarrow \infty} A_n) \cap (\liminf_{n \rightarrow \infty} B_n). \end{aligned}$$

For (ii), we have that

$$\begin{aligned} x \in \limsup_{n \rightarrow \infty} (A_n \cap B_n) &\Leftrightarrow \forall n^* \in \mathbb{N} x \in \bigcup_{n=n^*}^{\infty} (A_n \cap B_n) \\ &\Leftrightarrow \forall n^* \in \mathbb{N} \exists \tilde{n}^* \geq n^* : x \in (A_{\tilde{n}^*} \cap B_{\tilde{n}^*}) \\ &\Leftrightarrow \forall n^* \in \mathbb{N} \exists \tilde{n}^* \geq n^* : x \in A_{\tilde{n}^*} \text{ and } x \in B_{\tilde{n}^*} \\ &\Rightarrow \forall n_A, n_B \in \mathbb{N} \exists \tilde{n}_A \geq n_A \text{ and } \tilde{n}_B \geq n_B : x \in A_{\tilde{n}_A} \text{ and } x \in B_{\tilde{n}_B} \\ &\Leftrightarrow \forall n_A, n_B \in \mathbb{N} x \in \bigcup_{n=n_A}^{\infty} A_n \text{ and } x \in \bigcup_{n=n_B}^{\infty} B_n \\ &\Leftrightarrow x \in \limsup_{n \rightarrow \infty} A_n \text{ and } x \in \limsup_{n \rightarrow \infty} B_n \\ &\Leftrightarrow x \in (\limsup_{n \rightarrow \infty} A_n) \cap (\limsup_{n \rightarrow \infty} B_n). \end{aligned}$$

We now prove (iii). We have that

$$\begin{aligned} x \in \liminf_{n \rightarrow \infty} (A_n \cup B_n) &\Leftrightarrow \exists n^* \in \mathbb{N} : x \in \bigcap_{n=n^*}^{\infty} (A_n \cup B_n) \\ &\Leftrightarrow \exists n^* \in \mathbb{N} : x \in (A_n \cup B_n) \forall n \geq n^* \\ &\Leftrightarrow \exists n_A \in \mathbb{N} : x \in A_n \forall n \geq n_A \text{ or } \exists n_B \in \mathbb{N} : x \in B_n \forall n \geq n_B \\ &\Leftrightarrow \exists n_A \in \mathbb{N} : x \in \bigcap_{n=n_A}^{\infty} A_n \text{ or } \exists n_B \in \mathbb{N} : x \in \bigcap_{n=n_B}^{\infty} B_n \\ &\Leftrightarrow x \in \liminf_{n \rightarrow \infty} A_n \text{ or } x \in \liminf_{n \rightarrow \infty} B_n \\ &\Leftrightarrow x \in (\liminf_{n \rightarrow \infty} A_n) \cup (\liminf_{n \rightarrow \infty} B_n). \end{aligned}$$

For (iv), we notice that

$$\begin{aligned}
x \in \limsup_{n \rightarrow \infty} (A_n \cup B_n) &\Leftrightarrow \forall n^* \in \mathbb{N} \ x \in \bigcup_{n=n^*}^{\infty} (A_n \cup B_n) \\
&\Leftrightarrow \forall n^* \in \mathbb{N} \ \exists \tilde{n}^* \geq n^* : x \in (A_{\tilde{n}^*} \cup B_{\tilde{n}^*}) \\
&\Leftrightarrow \forall n^* \in \mathbb{N} \ \exists \tilde{n}^* \geq n^* : x \in A_{\tilde{n}^*} \text{ or } x \in B_{\tilde{n}^*} \\
&\Leftrightarrow \forall n_A \in \mathbb{N} \ \exists \tilde{n}_A \geq n_A : x \in A_{\tilde{n}_A} \text{ or } \forall n_B \in \mathbb{N} \ \exists \tilde{n}_B \geq n_B : x \in B_{\tilde{n}_B} \\
&\Leftrightarrow \forall n_A \in \mathbb{N} \ x \in \bigcup_{n=n_A}^{\infty} A_n \text{ or } \forall n_B \in \mathbb{N} \ x \in \bigcup_{n=n_B}^{\infty} B_n \\
&\Leftrightarrow x \in \limsup_{n \rightarrow \infty} A_n \text{ or } x \in \limsup_{n \rightarrow \infty} B_n \\
&\Leftrightarrow x \in (\limsup_{n \rightarrow \infty} A_n) \cup (\limsup_{n \rightarrow \infty} B_n).
\end{aligned}$$

Finally, using that $A = \liminf_{n \rightarrow \infty} A_n = \limsup_{n \rightarrow \infty} A_n$ and $B = \liminf_{n \rightarrow \infty} B_n = \limsup_{n \rightarrow \infty} B_n$, (v) follows from (i) and (ii) and (vi) follows from (iii) and (iv). \blacksquare

Corollary L.1 Let $\{A_n\}_{n=1}^{\infty}$ be a sequence of sets in \mathbb{R}^p and $B \subset \mathbb{R}^p$. Then, it holds that

- (i) $\liminf_{n \rightarrow \infty} (A_n \cap B) = (\liminf_{n \rightarrow \infty} A_n) \cap B$
- (ii) $\limsup_{n \rightarrow \infty} (A_n \cap B) = (\limsup_{n \rightarrow \infty} A_n) \cap B$,
- (iii) $\liminf_{n \rightarrow \infty} (A_n \cup B) = (\liminf_{n \rightarrow \infty} A_n) \cup B$, and
- (iv) $\limsup_{n \rightarrow \infty} (A_n \cup B) = (\limsup_{n \rightarrow \infty} A_n) \cup B$.

In particular, if $A = \lim_{n \rightarrow \infty} A_n$ exists, then

$$(v) \ \lim_{n \rightarrow \infty} (A_n \cap B) = A \cap B \text{ and } (vi) \ \lim_{n \rightarrow \infty} (A_n \cup B) = A \cup B.$$

Proof of Corollary L.1. (i),(iv),(v) and (vi) follow directly from Lemma L.1 (i),(iv),(v) and (vi) with $B_n = B$ for all $n \in \mathbb{N}$. We now prove (ii). It holds that

$$\begin{aligned}
x \in \limsup_{n \rightarrow \infty} (A_n \cap B) &\Leftrightarrow \forall n^* \in \mathbb{N} \ x \in \bigcup_{n=n^*}^{\infty} (A_n \cap B) \\
&\Leftrightarrow \forall n^* \in \mathbb{N} \ \exists \tilde{n}^* \geq n^* : x \in (A_{\tilde{n}^*} \cap B) \\
&\Leftrightarrow \forall n^* \in \mathbb{N} \ \exists \tilde{n}^* \geq n^* : x \in A_{\tilde{n}^*} \text{ and } x \in B \\
&\Leftrightarrow \forall n^* \in \mathbb{N} \ x \in \bigcup_{n=n^*}^{\infty} A_n \text{ and } x \in B \\
&\Leftrightarrow x \in \limsup_{n \rightarrow \infty} A_n \text{ and } x \in B \\
&\Leftrightarrow x \in (\limsup_{n \rightarrow \infty} A_n) \cap B.
\end{aligned}$$

For (iii), we have that

$$\begin{aligned}
x \in \liminf_{n \rightarrow \infty} (A_n \cup B_n) &\Leftrightarrow \exists n^* \in \mathbb{N} : x \in \cap_{n=n^*}^{\infty} (A_n \cup B) \\
&\Leftrightarrow \exists n^* \in \mathbb{N} : x \in (A_n \cup B) \forall n \geq n^* \\
&\Leftrightarrow \exists n^* \in \mathbb{N} : \forall n \geq n^* x \in A_n \text{ or } x \in B \\
&\Leftrightarrow \exists n^* \in \mathbb{N} : x \in \cap_{n=n^*}^{\infty} A_n \text{ or } x \in B \\
&\Leftrightarrow x \in \liminf_{n \rightarrow \infty} A_n \text{ or } x \in B \\
&\Leftrightarrow x \in (\liminf_{n \rightarrow \infty} A_n) \cup B.
\end{aligned}$$

■

Lemma L.2 Let $\{A_n\}_{n=1}^{\infty}$ be a sequence of sets in \mathbb{R}^p and $B \subset \mathbb{R}^p$. Then

$$\liminf_{n \rightarrow \infty} (B \setminus A_n) = B \setminus (\limsup_{n \rightarrow \infty} A_n) \text{ and } \limsup_{n \rightarrow \infty} (B \setminus A_n) = B \setminus (\liminf_{n \rightarrow \infty} A_n).$$

In particular, if $A = \lim_{n \rightarrow \infty} A_n$ exists, then

$$\lim_{n \rightarrow \infty} (\mathbb{R}^p \setminus A_n) = \mathbb{R}^p \setminus A.$$

Proof of Lemma L.2. We use that, for a sequence of sets $\{C_n\}_{n=1}^{\infty}$ in \mathbb{R}^p and $D \subset \mathbb{R}^p$, it holds that $D \setminus (\cup_{n=1}^{\infty} C_n) = \cap_{n=1}^{\infty} (D \setminus C_n)$ and $D \setminus (\cap_{n=1}^{\infty} C_n) = \cup_{n=1}^{\infty} (D \setminus C_n)$. Then, we have that

$$\begin{aligned}
\liminf_{n \rightarrow \infty} (B \setminus A_n) &= \cup_{n=1}^{\infty} (B \setminus (\cup_{l=n}^{\infty} A_l)) = B \setminus (\limsup_{n \rightarrow \infty} A_n), \text{ and} \\
\limsup_{n \rightarrow \infty} (B \setminus A_n) &= \cap_{n=1}^{\infty} (B \setminus (\cap_{l=n}^{\infty} A_l)) = B \setminus (\liminf_{n \rightarrow \infty} A_n).
\end{aligned}$$

Finally, the last part follows from $A = \liminf_{n \rightarrow \infty} A_n = \limsup_{n \rightarrow \infty} A_n$. ■

Lemma L.3 Let $\{A_n\}_{n=1}^{\infty}$ be a sequence of sets in \mathbb{R}^p and $A \subset \mathbb{R}^p$. Then, $\lim_{n \rightarrow \infty} A_n = A$ if and only if $\lim_{n \rightarrow \infty} (A_n \Delta A) = \emptyset$.

Proof of Lemma L.3. First, suppose that $\lim_{n \rightarrow \infty} A_n = A$. Using Lemma L.2 and Corollary L.1 (v)-(vi), we have that

$$\begin{aligned}
\emptyset &= (A \cap (\mathbb{R}^p \setminus A)) \cup ((\mathbb{R}^p \setminus A) \cap A) \\
&= ((\lim_{n \rightarrow \infty} A_n) \cap (\mathbb{R}^p \setminus A)) \cup ((\lim_{n \rightarrow \infty} (\mathbb{R}^p \setminus A_n)) \cap A) \\
&= (\lim_{n \rightarrow \infty} (A_n \cap (\mathbb{R}^p \setminus A))) \cup (\lim_{n \rightarrow \infty} ((\mathbb{R}^p \setminus A_n) \cap A)) \\
&= \lim_{n \rightarrow \infty} ((A_n \cap (\mathbb{R}^p \setminus A)) \cup ((\mathbb{R}^p \setminus A_n) \cap A)) = \lim_{n \rightarrow \infty} (A_n \Delta A).
\end{aligned}$$

Second, suppose that $\lim_{n \rightarrow \infty} (A_n \Delta A) = \emptyset$. Then, by Lemma L.1 (iv), Corollary L.1 (ii), and Lemma L.2, it holds that

$$\begin{aligned}\emptyset &= \limsup_{n \rightarrow \infty} (A_n \Delta A) = \limsup_{n \rightarrow \infty} ((A_n \cap (\mathbb{R}^p \setminus A)) \cup ((\mathbb{R}^p \setminus A_n) \cap A)) \\ &= (\limsup_{n \rightarrow \infty} (A_n \cap (\mathbb{R}^p \setminus A))) \cup (\limsup_{n \rightarrow \infty} ((\mathbb{R}^p \setminus A_n) \cap A)) \\ &= ((\limsup_{n \rightarrow \infty} A_n) \cap (\mathbb{R}^p \setminus A)) \cup ((\limsup_{n \rightarrow \infty} (\mathbb{R}^p \setminus A_n)) \cap A) \\ &= ((\limsup_{n \rightarrow \infty} A_n) \cap (\mathbb{R}^p \setminus A)) \cup ((\mathbb{R}^p \setminus (\liminf_{n \rightarrow \infty} A_n)) \cap A).\end{aligned}$$

Therefore, $(\limsup_{n \rightarrow \infty} A_n) \cap (\mathbb{R}^p \setminus A) = \emptyset$ and $(\mathbb{R}^p \setminus (\liminf_{n \rightarrow \infty} A_n)) \cap A = \emptyset$, which imply that $\limsup_{n \rightarrow \infty} A_n \subset A$ and $A \subset \liminf_{n \rightarrow \infty} A_n$. Hence, $\lim_{n \rightarrow \infty} A_n = A$. ■

Lemma L.4 *Let $\{A_n\}_{n=1}^\infty$ be a sequence of sets in \mathbb{R}^p and $\xi \geq 0$. Then,*

$$(\liminf_{n \rightarrow \infty} A_n)^{+\xi} \subset \liminf_{n \rightarrow \infty} (A_n)^{+\xi} \subset \limsup_{n \rightarrow \infty} (A_n)^{+\xi} \subset (\limsup_{n \rightarrow \infty} A_n)^{+\xi}.$$

In particular, if $A := \lim_{n \rightarrow \infty} A_n$ exists, then $\lim_{n \rightarrow \infty} (A_n)^{+\xi} = (A)^{+\xi}$ and $\lim_{n \rightarrow \infty} \overline{A_n} = \overline{A}$. Finally, if A_n and A are open, then $\lim_{n \rightarrow \infty} \partial A_n = \partial A$.

Proof of Lemma L.4. For the first part, it is enough to show the first and third inclusion. With this aim, let $x \in (\liminf_{n \rightarrow \infty} A_n)^{+\xi}$. Hence, $\text{dist}(\{x\}, \bigcup_{j=1}^\infty \cap_{n=j}^\infty A_n) \leq \xi$. Therefore, there exists a sequence $\{y_l\}_{l=1}^\infty$ in $\bigcup_{j=1}^\infty \cap_{n=j}^\infty A_n$ such that $\lim_{l \rightarrow \infty} \|x - y_l\| \leq \xi$. Then, for some $n^* \in \mathbb{N}$, the sequence $\{y_l\}_{l=1}^\infty$ is in $\cap_{n=n^*}^\infty A_n$, that is, $\{y_l\}_{l=1}^\infty$ is in A_n for all $n \geq n^*$. It follows that, for all $n \geq n^*$, $\text{dist}(\{x\}, A_n) \leq \lim_{l \rightarrow \infty} \|x - y_l\| \leq \xi$. Hence, for all $n \geq n^*$, $x \in (A_n)^{+\xi}$, that is, $x \in \cap_{n=n^*}^\infty (A_n)^{+\xi} \subset \liminf_{n \rightarrow \infty} (A_n)^{+\xi}$. We now prove the third inclusion. To this end, let $x \in \limsup_{n \rightarrow \infty} (A_n)^{+\xi}$. Then, for all $j \in \mathbb{N}$, there exists a constant $n \geq j$ such that $x \in (A_n)^{+\xi}$, that is, $\text{dist}(\{x\}, A_n) \leq \xi$. It follows that $\text{dist}(\{x\}, \bigcup_{k=j}^\infty A_k) \leq \text{dist}(\{x\}, A_n) \leq \xi$. Hence, $x \in (\bigcup_{k=j}^\infty A_k)^{+\xi} = (\bigcap_{l=1}^j \bigcup_{k=l}^\infty A_k)^{+\xi}$, for all $j \in \mathbb{N}$, which implies that $x \in (\limsup_{k \rightarrow \infty} A_k)^{+\xi}$. For the second part, notice that, by definition of limit of sets, $A = \liminf_{n \rightarrow \infty} A_n = \limsup_{n \rightarrow \infty} A_n$. It follows from the first part that $\liminf_{n \rightarrow \infty} (A_n)^{+\xi} = \limsup_{n \rightarrow \infty} (A_n)^{+\xi} = (A)^{+\xi}$. Next, notice that, for all $\emptyset \neq B \subset \mathbb{R}^p$, $x \in \overline{B}$ if and only if $\text{dist}(\{x\}, B) = 0$. In particular, $\overline{B} = (B)^{+0}$. Hence, $\lim_{n \rightarrow \infty} \overline{A_n} = \overline{A}$. Finally, if A_n and A are open, then, using Lemma L.1 (v) and Lemma L.2, we have that

$$\lim_{n \rightarrow \infty} \partial A_n = \lim_{n \rightarrow \infty} (\overline{A_n} \cap (\mathbb{R}^p \setminus A_n)) = (\lim_{n \rightarrow \infty} \overline{A_n}) \cap (\lim_{n \rightarrow \infty} (\mathbb{R}^p \setminus A_n)) = \overline{A} \cap (\mathbb{R}^p \setminus A) = \partial A.$$

■

Lemma L.5 Let $\{A_n\}_{n=1}^{\infty}$ be a sequence of sets in \mathbb{R}^p and $\xi > 0$. If $\lim_{n \rightarrow \infty} A_n = A$, then there exists $n^*(\xi) \in \mathbb{N}$ such that, for all $n \geq n^*(\xi)$, $A_n^{+\xi} \subset A$ and $A_n \subset (A)^{+\xi}$.

Proof of Lemma L.5. Since $\lim_{n \rightarrow \infty} \cup_{j=n}^{\infty} A_j = A \subset (A)^{+\xi}$, there exists $n_1^*(\epsilon) \in \mathbb{N}$ such that $\cup_{n=n^*}^{\infty} A_n \subset (A)^{+\xi}$. Hence $A_n \subset (A)^{+\xi}$, for all $n \geq n_1^*(\xi)$. On the other hand, by Lemma L.4, we have that $\lim_{n \rightarrow \infty} \cap_{j=n}^{\infty} (A_j)^{+\xi} = (A)^{+\xi} \supset A$. Hence, there is $n_2^*(\xi)$ such that $\cap_{n=n^*}^{\infty} (A_n)^{+\xi} \supset A$, which implies that $(A_n)^{+\xi} \supset A$, for all $n \geq n_2^*(\xi)$. ■

References

- Alberto Abbondandolo and Majer Pietro. On the global stable manifold. *Studia Mathematica*, 177:113–131, 2006.
- Ratan Prakash Agarwal and V. Lakshmikantham. *Uniqueness and nonuniqueness criteria for ordinary differential equations*, volume 6. World Scientific, 1993.
- Claudio Agostinelli and Mario Romanazzi. Local depth of multidimensional data. Working Paper 3, Ca' Foscari University of Venice, 2008.
- Miguel A. Arcones and Evarist Giné. Limit theorems for U-processes. *The Annals of Probability*, 21(3):1494–1542, 1993.
- Kendall Atkinson, Weimin Han, and David Stewart. *Numerical solution of ordinary differential equations*. John Wiley & Sons, 2009.
- Adelchi Azzalini and Antonella Capitanio. Statistical applications of the multivariate skew normal distribution. *Journal of the Royal Statistical Society: Series B (Statistical Methodology)*, 61(3):579–602, 1999.
- Ayanendranath Basu, Hiroyuki Shioya, and Chanseok Park. *Statistical inference: the minimum distance approach*. Chapman and Hall/CRC, 2019.
- Rudolf Beran. Minimum hellinger distance estimates for parametric models. *The annals of Statistics*, 5(3):445–463, 1977.
- Patrick Billingsley. *Convergence of Probability Measures*. John Wiley & Sons, 1999.
- Patrick Billingsley. *Probability and Measure*, volume 939. John Wiley & Sons, 2012.

- José E. Chacón. Data-driven choice of the smoothing parametrization for kernel density estimators. *Canadian Journal of Statistics*, 37(2):249–265, 2009.
- José E. Chacón. A population background for nonparametric density-based clustering. *Statistical Science*, 30(4):518–532, 2015.
- José E. Chacón. Mixture model modal clustering. *Adv. Data Anal. Classif.*, 13(2):379–404, 2019.
- José E. Chacón and Tarn Duong. *Multivariate kernel smoothing and its applications*. Chapman and Hall/CRC, 2018.
- Frédéric Chazal, Leonidas J. Guibas, Steve Y. Oudot, and Primoz Skraba. Persistence-based clustering in riemannian manifolds. *Journal of the ACM*, 60(6), 2013.
- Antonio Cuevas, Manuel Febrero, and Ricardo Fraiman. Robust estimation and classification for functional data via projection-based depth notions. *Computational Statistics*, 22:481–496, 2007.
- Luc Devroye and László Györfi. *Nonparametric Density Estimation: The L1 View*. Wiley & Sons, 1985.
- Richard M. Dudley. Balls in \mathbb{R}^k do not cut all subsets of $k + 2$ points. *Advances in Mathematics*, 31(3):306 – 308, 1979.
- Tarn Duong. *ks: kernel smoothing*, 2018. R package version 1.11.3.
- Gerald Edgar. *Measure, topology, and fractal geometry*. Springer Science & Business Media, 2007.
- Stanley C. Eisenstat and Ilse C. F. Ipsen. Three absolute perturbation bounds for matrix eigenvalues imply relative bounds. *SIAM Journal on Matrix Analysis and Applications*, 20(1):149–158, 1998.
- Chris Fraley and Adrian E. Raftery. Model-based clustering, discriminant analysis, and density estimation. *Journal of the American Statistical Association*, 97(458):611–631, 2002.
- Keinosuke Fukunaga and Larry Hostetler. The estimation of the gradient of a density function, with applications in pattern recognition. *IEEE Transactions on information theory*, 21(1):32–40, 1975.

- Evarist Giné and Richard Nickl. *Mathematical foundations of infinite-dimensional statistical models*, volume 40. Cambridge University Press, 2016.
- Jack K. Hale. *Ordinary differential equations*, volume 21. Dover Publications Inc., 1980.
- Michael Hardy. Combinatorics of partial derivatives. *The electronic journal of combinatorics*, 13(R1), 2006.
- Morris W. Hirsch, Robert L. Devaney, and Stephen Smale. *Differential equations, dynamical systems, and linear algebra*, volume 60. Academic press, 1974.
- John M. Holte. Discrete gronwall lemma and applications. In *MAA-NCS meeting at the University of North Dakota*, 2009.
- Jürgen Jost. *Riemannian geometry and geometric analysis*. Springer, 2005.
- Matthäus Kleindessner and Ulrike Von Luxburg. Lens depth function and k-relative neighborhood graph: versatile tools for ordinal data analysis. *The Journal of Machine Learning Research*, 18(1):1889–1940, 2017.
- Vladimir S. Korolyuk and Yu V. Borovskich. *Theory of U-statistics*, volume 273. Springer Science & Business Media, 2013.
- Shengqiao Li. Concise formulas for the area and volume of a hyperspherical cap. *Asian Journal of Mathematics and Statistics*, 4(1):66–70, 2011.
- Bruce G. Lindsay. Efficiency versus robustness: The case for minimum hellinger distance and related methods. *The Annals of Statistics*, 22(2):1081–1114, 1994.
- Giovanna Menardi. A review on modal clustering. *International Statistical Review*, 84(3): 413–433, 2016.
- Lawrence Perko. *Differential equations and dynamical systems*, volume 7. Springer Science & Business Media, 2013.
- Walter Rudin. *Principles of mathematical analysis*, volume 3. McGraw-hill New York, 1976.
- Hans Sagan. *Space-filling curves*. Springer, 1994.
- Wilhelm Schneemeier. Weak convergence and Glivenko-Cantelli results for empirical processes of U-statistic structure. *Stochastic processes and their applications*, 33(2):325–334, 1989.

Luca Scrucca, Michael Fop, T. Brendan Murphy, and Adrian E Raftery. mclust 5: clustering, classification and density estimation using Gaussian finite mixture models. *The R Journal*, 8(1):289–317, 2016.

Roy N. Tamura and Dennis D. Boos. Minimum hellinger distance estimation for multivariate location and covariance. *Journal of the American Statistical Association*, 81 (393):223–229, 1986.

Gerald Teschl. *Ordinary differential equations and dynamical systems*, volume 140. American Mathematical Society, 2012.

Alberto Torchinsky. *Real variables*. Chapman and Hall/CRC, 1995.

Loring W. Tu. An introduction to manifolds., 2011.

Matt P. Wand and M. Chris Jones. Comparison of smoothing parameterizations in bivariate kernel density estimation. *Journal of the American Statistical Association*, 88 (422):520–528, 1993.

Richard L. Wheeden and Antoni Zygmund. *Measure and integral: an introduction to real analysis*. Chapman and Hall/CRC, 2015.

Y. Zuo. *Contributions to the theory and applications of statistical depth*. PhD thesis, The University of Texas at Dallas, 1998. URL http://www.stt.msu.edu/~zuo/papers_html/main.pdf.

Yijun Zuo and Robert Serfling. General notions of statistical depth function. *Annals of statistics*, pages 461–482, 2000a.